Springer Proceedings in Mathematics & Statistics

Alfonso García-Parrado
Filipe C. Mena
Filipe Moura
Estelita Vaz *Editors*

# Progress in Mathematical Relativity, Gravitation and Cosmology

Springer

# Springer Proceedings in Mathematics and Statistics

Volume 60

For further volumes:
http://www.springer.com/series/10533

# Springer Proceedings in Mathematics and Statistics

This book series features volumes composed of selected contributions from workshops and conferences in all areas of current research in mathematics and statistics, including OR and optimization. In addition to an overall evaluation of the interest, scientific quality, and timeliness of each proposal at the hands of the publisher, individual contributions are all refereed to the high quality standards of leading journals in the field. Thus, this series provides the research community with well-edited, authoritative reports on developments in the most exciting areas of mathematical and statistical research today.

Alfonso García-Parrado • Filipe C. Mena
Filipe Moura • Estelita Vaz
Editors

# Progress in Mathematical Relativity, Gravitation and Cosmology

Proceedings of the Spanish Relativity Meeting ERE2012, University of Minho, Guimarães, Portugal, September 3-7, 2012

Springer

*Editors*
Alfonso García-Parrado
Filipe C. Mena
Filipe Moura
Estelita Vaz
Centre of Mathematics
University of Minho
Campus de Gualtar
Braga, Portugal

*Photo on page V*: By courtesy of Joaquim Lopes, Momentos Únicos Fotografia, Guimarães, Portugal

ISSN 2194-1009 ISSN 2194-1017 (electronic)
ISBN 978-3-642-40156-5 ISBN 978-3-642-40157-2 (eBook)
DOI 10.1007/978-3-642-40157-2
Springer Heidelberg New York Dordrecht London

Library of Congress Control Number: 2013952967

Mathematics Subject Classification (2010): 83Cxx, 83-XX, 81Txx, 53-XX



Printed on acid-free paper

Springer is part of Springer Science+Business Media (www.springer.com)


ESCOLA DE CIÊNCIAS

# Preface

The Spanish Relativity Meeting (ERE) is a well-established meeting devoted to General Relativity and Gravitation, and it has been organized in Spain for more than 30 years. However, in 2012, the Relativity group at the University of Minho in Portugal, took the challenge of the Spanish Society of Gravitation and Relativity (SEGRE), and organized the meeting in Portugal, for the first time. The meeting was organized in Guimarães, a world heritage site, and European Capital of Culture in 2012.

The ERE2012 was organized under the title "Progress in Mathematical Relativity, Gravitation and Cosmology", and we were pleased to host an excellent panel of invited speakers on topics which ranged from mathematical cosmology, numerical relativity and black holes to string theory and quantum gravity. We were also very glad to have an exceptional international list of over a 100 participants from the 5 continents and over 40 countries.

The conference opening, on September 3rd, had the presence of both the Dean of the School of Sciences of Minho University, Prof. Estelita Vaz, who, luckily, was one of the meetings' organizers, and the Secretary of the SEGRE society, Prof. Jaume Carot. Nineteen plenary lectures took place in the mornings while the afternoons included 81 talks in 10 parallel sessions as well as 7 poster presentations.

Following the tradition of previous meetings, there were also several social events, from the memorable Public Lecture by Carlos Herdeiro at "Centro de Artes e Espetáculos São Mamede" and the cocktail at "Escola de Ciências" to the guided visit to Porto and the closing dinner at Guimarães historical centre, with the Rector of Minho University, Prof. António Cunha.

We thank all the participants for creating a very pleasant atmosphere and hope that our first step can encourage future editions of the ERE in Portugal.

Braga, Portugal
June 2013

Alfonso García-Parrado, Estelita Vaz,
Filipe Mena, Filipe Moura

# Acknowledgements

We would like to warmly thank our sponsors whose help was crucial to the success of the meeting: Universidade do Minho (UM); Escola de Ciências (ECUM); Centro de Matemática (CMAT), including FEDER Funds through Programa Operacional Factores de Competitividade—COMPETE and Portuguese Funds through Fundação para a Ciência e a Tecnologia (FCT) within the Project PEst-C/MAT/UI0013/2011; FCT projects CERN/FP/123609/2011 and PTDC/MAT/108921/2008; Project DFRH/WIIA/28/2011, co-sponsored by FCT and Marie Curie Cofund, within the Program People of the 7th Frame Program of the European Commission; The Spanish Society of Gravitation and Relativity (SEGRE); The journal "Classical and Quantum Gravity", from the Institute of Physics Publishing, UK; Guimarães 2012—European Capital of Culture.

# Sponsors

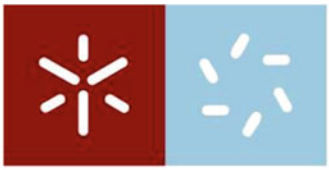

**Universidade do Minho**
Escola de Ciências

Centro de Matemática

SEARE

FCT Fundação para a Ciência e a Tecnologia
MINISTÉRIO DA EDUCAÇÃO E CIÊNCIA

## Invited Speakers

| | |
|---|---|
| Vítor Cardoso | *IST, Lisbon, Portugal* |
| Óscar Dias | *CEA, Saclay, France* |
| Peter Dunsby | *University of Cape Town, South Africa* |
| José Edelstein | *University of Santiago de Compostela, Spain* |
| George Ellis | *University of Cape Town, South Africa* |
| Pedro Ferreira | *University of Oxford, UK* |
| Pau Figueras | *University of Cambridge, UK* |
| Jörg Frauendiener | *Otago University, New Zealand* |
| Gabriel Lopes-Cardoso | *IST, Lisbon, Portugal* |
| Marc Mars | *University of Salamanca, Spain* |
| Alan Rendall | *Albert Einstein Institut, Golm, Germany* |
| László Szabados | *Hungarian Academy of Sciences, Budapest, Hungary* |
| Paul Tod | *University of Oxford, UK* |
| Claes Uggla | *Karstad University, Sweden* |
| Juan Antonio Valiente Kroon | *Queen Mary, University of London, UK* |

## Scientific Committee

| | |
|---|---|
| Miguel Alcubierre | *ICN, Universidad Nacional Autónoma de México, México* |
| Abbay Ashtekar | *Penn State University, USA* |
| Robert Beig | *Institute of Theoretical Physics, University of Vienna, Austria* |
| Thibault Damour | *Institut des Hautes Études Scientifiques, Paris, France* |
| Roy Maartens | *Institute of Cosmology and Gravitation, University of Portsmouth, UK* |
| Fernando Quevedo | *DAMTP, University of Cambridge, UK* |
| Matt Visser | *Victoria University of Wellington, New Zealand* |

## Session Convenors

| | |
|---|---|
| José P. S. Lemos | *IST, Lisbon, Portugal* |
| José Mimoso | *Universidade de Lisboa, Portugal* |
| Paulo Moniz | *Universidade da Beira Interior, Covilhã Portugal* |
| José Natário | *IST, Lisbon, Portugal* |

## Local Organising Committee

Irene Brito
Viktor Czinner
Alfonso García-Parrado
Filipe Mena
Filipe Moura
Maria Ramos
Estelita Vaz

# Contents

**Part I Plenary Sessions**

**Linearized Gravitational Waves Near Space-Like and Null Infinity** ..... 3
Florian Beyer, George Doulis, Jörg Frauendiener, and Ben Whale

**Lovelock Theory, Black Holes and Holography** ..... 19
José D. Edelstein

**Braneworld Black Holes** ..... 37
Pau Figueras

**BPS Black Holes in String Theory** ..... 55
Gabriel Lopes Cardoso

**Geometry of General Hypersurfaces, Constraint Equations and Applications to Shells** ..... 67
Marc Mars

**Cosmological Gravitational Waves and Einstein–Straus Voids** ..... 85
Marc Mars, Filipe C. Mena, and Raül Vera

**Construction of Oscillatory Singularities** ..... 95
Alan D. Rendall

**Inverse Scattering Construction of Dipole Black Rings** ..... 107
Jorge V. Rocha, Maria J. Rodriguez, Oscar Varela, and Amitabh Virmani

**Quantum Cosmology: Meeting SUSY** ..... 117
Paulo Vargas Moniz

**Part II Parallel Sessions**

**Avoiding the Trans-Planckian Problem in Black Hole Physics** ..... 129
Carlos Barceló, Luis C. Barbado, Luis J. Garay, and Gil Jannes

**A 2D Field Theory Equivalent to 3D Gravity with No Cosmological Constant** ..... 135
Glenn Barnich, Andrés Gomberoff, and Hernán A. González

**The Holographic Ricci Dark Energy and Its Possible Doomsdays** ..... 139
Moulay-Hicham Belkacemi, Mariam Bouhmadi-López, Ahmed Errahmani, and Taoufiq Ouali

**Black-Hole Lattices** ..... 143
Eloisa Bentivegna

**Axial Quasi-normal Modes of Neutron Stars with Exotic Matter** ..... 147
J.L. Blázquez-Salcedo, L.M. González-Romero, and Francisco Navarro-Lérida

**The Quantum Scalar Field in Spherically Symmetric Loop Quantum Gravity** ..... 153
Enrique F. Borja, Iñaki Garay, and Eckhard Strobel

**The Spectrum of Gravitational Waves in an $f(R)$ Model with a Bounce** ..... 157
Mariam Bouhmadi-López, João Morais, and Alfredo B. Henriques

**On the Isotropization of a 3-Brane in an Extra-Dimensional Tolman–Bondi Universe** ..... 161
Philippe Brax, José Pedro Mimoso, and Nelson Nunes

**Phase Transitions in General Gravity Theories** ..... 167
Xián O. Camanho

**Concordance Cosmology with Particle Creation** ..... 173
Saulo Carneiro

**Quasinormal Modes from a Naked Singularity** ..... 179
Cecilia Chirenti, Alberto Saa, and Jozef Skákala

**$n$-DBI Gravity: A Short Overview** ..... 185
Flávio S. Coelho, Carlos Herdeiro, Shinji Hirano, and Yuki Sato

**Radiation from a D-Dimensional Collision of Shock Waves: A Summary of the First Order Results** ..... 189
Flávio S. Coelho, Carlos Herdeiro, Carmen Rebelo, and Marco O.P. Sampaio

**Radiation from a D-Dimensional Collision of Shock Waves: Numerics and a Charged Case** ..... 193
Flávio. S. Coelho, Carlos Herdeiro, Carmen Rebelo, and Marco O.P. Sampaio

**Relativistic Positioning Systems in Flat Space-Time: The Location Problem** ..... 199
Bartolomé Coll, Joan Josep Ferrando, and Juan Antonio Morales-Lladosa

**BSSN Equations in Spherical Coordinates Without Regularization** ..... 205
Isabel Cordero-Carrión and Pedro J. Montero

**Hidden Momentum in the Framework of Gravitoelectromagnetism** ..... 211
L. Filipe O. Costa

**Comparing Results for a Global Metric from Analytical Perturbation Theory and a Numerical Code** ..... 217
J.E. Cuchí, A. Molina, and E. Ruiz

**Thick Dirac–Nambu–Goto Branes on Black Hole Backgrounds** ..... 223
Viktor G. Czinner

**Cosmological Applications of Extended Electromagnetism** ..... 227
Roberto Dale and Diego Sáez

**General Relativistic Simulations of the Collapsar Scenario** ..... 231
Nicolas de Brye, Pablo Cerdá-Durán, Miguel Ángel Aloy, and José Antonio Font

**Cleaning Up a Tiny Part of the Exact Solution's Augean Stable** ..... 237
Liselotte De Groote

**Towards Degeneracy Problem Breaking by Large Scale Structures Methods** ..... 243
Álvaro de la Cruz Dombriz

**Geometric and Thermodynamic Aspects of Charged Black Holes in Nonlinear Electrodynamics** ..... 249
Joaquín Díaz-Alonso and Diego Rubiera-García

**Properties of Holographic Dark Energy at the Hubble Length** ..... 255
Ivan Duran and Luca Parisi

**Complete Quantization of Scalar Cosmological Perturbations** ..... 261
Mikel Fernández-Méndez, Guillermo A. Mena Marugán, and Javier Olmedo

**Null Geodesics of Black Holes in String Theory** ..... 267
Sharmanthie Fernando

**The Causal Boundary of Spacetimes Isocausal to Standard Stationary Ones** ..... 271
José L. Flores

**A New Numerical Approach to Estimate the Sunyaev–Zel'dovich Effect** ..... 277
Màrius Josep Fullana i Alfonso, Josep Vicent Arnau i Córdoba, Robert J. Thacker, Hugh M.P. Couchman, and Diego P. Sáez Milán

**Hawking Radiation for a Proca Field: Numerical Strategy** ..... 283
Carlos Herdeiro, Marco O.P. Sampaio, and Mengjie Wang

**Perturbations of Kantowski–Sachs Models with a Cosmological Constant** ..... 289
Z. Keresztes, M. Forsberg, M. Bradley, P.K.S. Dunsby, and L.Á. Gergely

**On the Uniqueness of the Energy and Momenta of an Asymptotically Minkowskian Space-Time: The Case of the Schwarzschild Metric** ..... 295
Ramon Lapiedra and Juan Antonio Morales-Lladosa

**Matter and Ricci Collineations** ..... 301
Josep Llosa

**Self-Gravitating Newtonian Disks Revisited** ..... 305
Patryk Mach, Edward Malec, and Walter Simon

**Weyl Curvature Hypothesis in Terms of Spacetime Thermodynamics** .... 311
Takuya Maki and Masaaki Morita

**On the Properties of Exact Solutions Endowed with Negative Mass** ..... 317
Vladimir S. Manko

**On the Bergqvist Approach to the Penrose Inequality** ..... 321
Marc Mars and Alberto Soria

**Inhomogeneous Loop Quantum Cosmology: Hybrid Quantization and Approximated Solutions** ..... 327
Daniel Martín-de Blas, Mercedes Martín-Benito, and Guillermo A. Mena Marugán

**Black Holes in Extended Gravity Theories in Palatini Formalism** ..... 333
Jesús Martínez-Asencio, Gonzalo J. Olmo, and Diego Rubiera-García

**What Is a Reasonable Spacetime? Some Remarks on the Hole-Free Condition** ..... 339
Ettore Minguzzi

**Optimal Time Travel in the Gödel Universe** ..... 345
José Natário

**Diagonal Future of Some Non-diagonal Bianchi A Spacetimes with Matter of Vlasov Type** ..... 349
Ernesto Nungesser

**Stability of the Einstein Static Universe in Massive Gravity** ..... 355
Luca Parisi, Ninfa Radicella, and Gaetano Vilasi

**Tilted Lemaître Model and the Dark Flow** ..... 361
Julio J. Fernández and José-F. Pascual-Sánchez

**Accelerating $f(T)$ Gravity Models Constrained by Recent Cosmological Data** ..... 367
Ninfa Radicella, Vincenzo F. Cardone, and Stefano Camera

**Kasner Solution in Brans–Dicke Theory and Its Corresponding Reduced Cosmology** ..... 371
Seyed M.M. Rasouli

**Revisiting Hartle's Model for Relativistic Rotating Stars** ..... 377
Borja Reina and Raül Vera

**Is General Relativity a $v/c \to 0$ Limit of a Finsler Geometry?** ..... 383
Martin Rivas

**Phenomenology of Unified Dark Matter Models with Fast Transition** ..... 387
Alberto Rozas-Fernández, Marco Bruni, and Ruth Lazkoz

**Locating Objects Away from Earth Surface: Positioning Accuracy** ..... 391
Diego Sáez and Neus Puchades

**SN and BAO Constraints on (New) Polynomial Dark Energy Parametrizations** ..... 397
Irene Sendra and Ruth Lazkoz

**Remarks on the Stability Operator for MOTS** ..... 403
José M.M. Senovilla

**CMB Anisotropies by Collapsing Textures** ..... 409
Kepa Sousa and Jon Urrestilla

**Relative Motions of Free Test Particles in Robinson–Trautman Spacetimes of Any Dimension** ..... 415
Robert Švarc and Jiří Podolský

**Connection Between Horizons and Algebraic Type** ..... 421
Otakar Svítek

**Dynamics of Apparent Horizons in Quantum Gravitational Collapse** ..... 427
Yaser Tavakoli, Andrea Dapor, and João Marto

**Thermodynamical Inequivalence of Stress-Energy and Spin Tensors** ..... 433
Leonardo Tinti

**Wormholes and Off-Diagonal Solutions in f(R,T), Einstein and Finsler Gravity Theories** ..... 439
Sergiu I. Vacaru

**Conformally Reducible Perfect Fluids with 2-Spaces of Constant Curvature** ..... 445
Norbert Van den Bergh

**Head-On Collisions of Charged Black Holes from Rest** ..... 452
Miguel Zilhão, Vitor Cardoso, Carlos Herdeiro, Luis Lehner, and Ulrich Sperhake

**Velocity-of-Light Surfaces in Kerr and Extreme Kerr** ..... 457
Jan E. Åman and Helgi Freyr Rúnarsson

**Part III Poster Presentations**

**The Spin-2 Equation on Minkowski Background** ..... 465
Florian Beyer, George Doulis, Jörg Frauendiener, and Ben Whale

**Matching the Linet–Tian Spacetime with Conformally Flat Cylindrically Symmetric Sources** ..... 469
Irene Brito, Maria de Fátima A. da Silva, Filipe C. Mena, and Nilton O. Santos

**Phase Structure of Black Di-ring in Five-Dimensional Asymptotically Flat Vacuum Gravity** ..... 475
Hideo Iguchi

**Spectrum from an Initially Anisotropic Universe** ..... 481
Hyeong-Chan Kim and Masato Minamitsuji

# Contributors

**Miguel Ángel Aloy** Departamento de Astronomía y Astrofísica, Universidad de Valencia, Burjassot (Valencia), Spain

**Maria de Fátima Alves da Silva** Departamento de Física Teórica, Instituto de Física, Universidade do Estado do Rio de Janeiro, Rio de Janeiro, Brazil

**Jan E. Åman** Department of Physics, Stockholm University, Stockholm, Sweden

**Carlos Barceló** Instituto de Astrofísica de Andalucía, Glorieta de la Astronomía, Granada, Spain

**Luis C. Barbado** Instituto de Astrofísica de Andalucía (CSIC), Glorieta de la Astronomía, Granada, Spain

**Glenn Barnich** Physique Théorique et Mathématique, Université Libre de Bruxelles and International Solvay Institutes, Bruxelles, Belgium

**Moulay-Hicham Belkacemi** Laboratory of Physics of Matter and Radiation, Mohammed I University, Oujda, Morocco

**Eloisa Bentivegna** Max-Planck-Institut für Gravitationphysik, Golm, Germany

**Florian Beyer** Department of Mathematics and Statistics, University of Otago, Dunedin, New Zealand

**José Luis Blázquez Salcedo** Depto. Física Teórica II, Facultad de Ciencias Físicas, Universidad Complutense de Madrid, Madrid, Spain

**Enrique F. Borja** Laboratoire de Physique, ENS Lyon, Lyon, France

**Mariam Bouhmadi-López** Instituto de Estructura de la Materia, IEM-CSIC, Serrano, Madrid, Spain

**Michael Bradley** Department of Physics, Umeå University, Umeå, Sweden

**Philippe Brax** Institut de Physique Theorique, CEA, IPhT, CNRS, Cedex, France

**Irene Brito** Centro de Matemática, Departamento de Matemática e Aplicações, Universidade do Minho, Guimarães, Portugal

**Marco Bruni** Institute of Cosmology and Gravitation, University of Portsmouth, Portsmouth, UK

**Xián O. Camanho** Department of Particle Physics and IGFAE, University of Santiago de Compostela, Santiago de Compostela, Spain

**Stefano Camera** CENTRA, Instituto Superior Técnico, Universidade Técnica de Lisboa, Lisboa, Portugal

**Vincenzo F. Cardone** I.N.A.F. - Osservatorio Astronomico di Roma, Monte Porzio Catone (Roma), Italy

**Vítor Cardoso** Centro Multidisciplinar de Astrofísica—CENTRA, Departamento de Física, Instituto Superior Técnico—IST, Lisboa, Portugal

**Saulo Carneiro** Instituto de Física, Universidade Federal da Bahia, Salvador, Brazil

**Pablo Cerdá-Durán** Departamento de Astronomía y Astrofísica, Universidad de Valencia, Burjassot (Valencia), Spain

**Cecilia Chirenti** Centro de Matemática, Computação e Cognição UFABC, Santo André, Brazil

**Flávio S. Coelho** Department de Física da Universidade de Aveiro and I3N, Aveiro, Portugal

**Bartolomé Coll** Department d'Astronomia i Astrofísica, Universitat de València, Burjassot, València, Spain

**Isabel Cordero-Carrión** Max-Planck-Institute for Astrophysics, Garching, Germany

**Josep Vicent Arnau i Córdoba** DMA, Universitat de València, Burjassot, Spain

**Filipe O. Costa** Centro de Física do Porto, Rua do Campo Alegre, Porto, Portugal

**Hugh M.P. Couchman** DPA, McMaster University, Hamilton, ON, Canada

**Javier E. Cuchí** Department of Física Fundamental, Universidad de Salamanca, Edificio Trilíngüe, Salamanca, Spain

**Viktor G. Czinner** Centro de Matemática, Universidade do Minho, Braga, Portugal

**Roberto Dale** Departament d'Estadística, Matemàtiques i Informàtica, Universitat Miguel Hernàndez, Alacant, Spain

**Andrea Dapor** Instytut Fizyki Teoretycznej, Uniwersytet Warszawski, Warsaw, Poland

**Nicolas de Brye** Dpto. de Astronomía y Astrofísica, Universidad de Valencia, Burjasssot, Valencia, Spain

**Liselotte De Groote** Ghent University, Ghent, Belgium

**Álvaro de la Cruz Dombriz** Astronomy, Cosmology and Gravity Center (ACGC), University of Cape Town, Rondebosch, South Africa

**Joaquín Díaz-Alonso** LUTH, Observatoire de Paris, CNRS, Université Paris Diderot. 5 Place Jules Janssen, Meudon, France

**George Doulis** Department of Mathematics and Statistics, University of Otago, Dunedin, New Zealand

**Peter K.S. Dunsby** Department of Mathematics and Applied Mathematics, University of Cape Town, South Africa

**Iván Durán** Departamento de Física, Universitat Autònoma de Barcelona, Bellaterra, Spain

**José D. Edelstein** Department of Particle Physics, University of Santiago de Compostela, Santiago de Compostela, Spain

**Ahmed Errahmani** Laboratory of Physics of Matter and Radiation, Mohammed I University, Oujda, Morocco

**Julio J. Fernández** Dept. Fisica Teórica, Facultad de Ciencias, Universidad de Valladolid, Valladolid, Spain

**Mikel Fernández-Méndez** Instituto de Estructura de la Materia, IEM-CSIC, Madrid, Spain

**Sharmanthie Fernando** Northern Kentucky University, Highland Heights, KY, USA

**Joan Josep Ferrando** Departament d'Astronomia i Astrofísica, Universitat de València, Burjassot, València, Spain

**Pau Figueras** DAMTP, Centre for Mathematical Sciences, Cambridge, UK

**José Luis Flores** Dept. de Álgebra, Geometría y Topología, Universidad de Málaga, Málaga, Spain

**José Antonio Font** Departamento de Astronomía y Astrofísica, Universidad de Valencia, Burjassot (Valencia), Spain

**Mats Forsberg** Department of Physics, Umeå University, Umeå, Sweden

**Jörg Frauendiener** Department of Mathematics and Statistics, University of Otago, Dunedin, New Zealand

**Helgi Freyr Rúnarsson** Physics Department Aveiro University, Campus de Santiago, Aveiro, Portugal

**Màrius Josep Fullana i Alfonso** IMM, Universitat Politècnica de València, València, Spain

**Iñaki Garay** Dpto. de Física Teórica, Universidad del País Vasco, Bilbao, Spain

**László Á. Gergely** Department of Theoretical Physics and Department of Experimental Physics, University of Szeged, Szeged, Hungary

**Andrés Gomberoff** Dept. de Ciencias Físicas, Universidad Andrés Bello, Av. República, Santiago, Chile

**Hernán A. González** Departamento de Física, P. Universidad Católica de Chile, Santiago, Chile

**Luis Manuel González-Romero** Depto. Física Teórica II, Facultad de Ciencias Físicas, Universidad Complutense de Madrid, Madrid, Spain

**Alfredo B. Henriques** CENTRA, Dept. de Física, Instituto Superior Técnico, Lisboa, Portugal

**Carlos Herdeiro** Departamento de Física da Universidade de Aveiro and I3N, Aveiro, Portugal

**Shinji Hirano** Department of Physics, Nagoya University, Nagoya, Japan

**Hideo Iguchi** College of Science and Technology, Nihon University, Narashinodai, Funabashi, Chiba, Japan

**Gil Jannes** Low Temperature Laboratory, Aalto University School of Science, Aalto, Finland

**Zoltán Keresztes** Department of Theoretical Physics and Department of Experimental Physics, University of Szeged, Szeged, Hungary

**Hyeong-Chan Kim** School of Liberal Arts and Sciences, Korea National University of Transportation, Chungju, Korea

**Ramon Lapiedra** Departament d'Astronomia i Astrofísica, Universitat de València, Burjassot, València, Spain

**Ruth Lazkoz** Fisika Teorikoa, Zientzia eta Teknologia Fakultatea, Euskal Herriko Unibertsitatea UPV/EHU, Bilbao, Spain

**Luis Lehner** Perimeter Institute for Theoretical Physics, Waterloo, ON, Canada

**Josep Llosa** Dept. Física Fonamental and Institut de Ciències del Cosmos (ICCUB), Universitat de Barcelona, Spain

**Gabriel Lopes Cardoso** CAMGSD, Departamento de Matemática, Instituto Superior Técnico, Lisboa, Portugal

**Patryk Mach** M. Smoluchowski Institute of Physics, Jagiellonian University, Kraków, Poland

**Takuya Maki** Japan Women's College of Physical Education, Nikaido-gakuen, Setagaya, Tokyo, Japan

**Edward Malec** M. Smoluchowski Institute of Physics, Jagiellonian University, Kraków, Poland

**Vladimir S. Manko** Departamento de Física, Centro de Investigación y de Estudios Avanzados del IPN, México

**Marc Mars** Dept. Física Fundamental, Universidad de Salamanca, Salamanca, Spain

**Mercedes Martín-Benito** Perimeter Institute, Waterloo, ON, Canada

**Daniel Martín-de Blas** Instituto de Estructura de la Materia, IEM-CSIC, Madrid, Spain

**Jesús Martínez-Asencio** Departamento de Física Teórica and IFIC, Universidad de Valencia-CSIC, Facultad de Física, Burjassot, Valencia, Spain

**João Marto** Departamento de Física, Universidade da Beira Interior, Portugal

**Filipe C. Mena** Centro de Matemática, Universidade do Minho, Campus de Gualtar, Braga, Portugal

**Guillermo A. Mena Marugán** Instituto de Estructura de la Materia, IEM-CSIC, Serrano, Madrid, Spain

**José Pedro Mimoso** Departamento de Física and Centro de Astronomia e Astrofísica da Universidade de Lisboa, Faculdade de Ciências, Campo Grande, Lisboa, Portugal

**Masato Minamitsuji** Yukawa Institute for Theoretical Physics, Kyoto University, Kyoto, Japan

**Alfred Molina** Departamento de Física Fonamental, Universitat de Barcelona, Barcelona, Spain

**Paulo Vargas Moniz** Departamento de Física, Universidade da Beira Interior, Rua Marquês d'Avila e Bolama, Covilhã, Portugal

**João Morais** CENTRA, Dept. de Física, Instituto Superior Técnico, Lisboa, Portugal

**Juan Antonio Morales-Lladosa** Departament d'Astronomia i Astrofísica, Universitat de València, Burjassot, València, Spain

**Masaaki Morita** Okinawa National College of Technology, Nago, Okinawa, Japan

**José Natário** Departamento de Matemática, Instituto Superior Técnico, Lisboa, Portugal

**Francisco Navarro-Lérida** Depto. Física Átomica, Molecular y Nuclear, Facultad de Ciencias Físicas, Universidad Complutense de Madrid, Madrid, Spain

**Nelson Nunes** Centro de Astronomia e Astrofísica da Universidade de Lisboa, Faculdade de Ciências, Lisboa, Portugal

**Ernesto Nungesser** KTH Royal Institute of Technology, Stockholm, Sweden

**Javier Olmedo** Instituto de Física, Facultad de Ciencias, Montevideo, Uruguay

**Gonzalo J. Olmo** Departamento de Física Teórica and IFIC, Universidad de Valencia-CSIC, Facultad de Física, Burjassot, Valencia, Spain

**Taoufiq Ouali** Laboratory of Physics of Matter and Radiation, Mohammed I University, Oujda, Morocco

**Luca Parisi** Dipartimento di Fisica "E.R.Caianiello", Università degli Studi di Salerno, Fisciano (Sa), Italy

**José-Fernando Pascual-Sánchez** Dept. Matemática Aplicada, Universidad de Valladolid, Valladolid, Spain

**Jiří Podolský** Institute of Theoretical Physics, Faculty of Mathematics and Physics, Charles University in Prague, Prague, Czech Republic

**Neus Puchades** Departamento de Astronomía y Astrofísica, Universidad de Valencia, Burjassot, Valencia, Spain

**Ninfa Radicella** Dipartimento di Fisica, Università degli Studi di Salerno INFN sez. Napoli, Italy

**Seyed M. M. Rasouli** Departamento de Física, Universidade da Beira Interior, Covilhã, Portugal

**Carmen Rebelo** Departamento de Física da Universidade de Aveiro and I3N, Campus de Santiago, Aveiro, Portugal

**Borja Reina** Física Teórica e Hist. de la Ciencia, UPV/EHU, Bilbao, Basque Country, Spain

**Alan D. Rendall** Max Planck Institute for Gravitational Physics, Potsdam, Germany

**Martin Rivas** Theoretical Physics Department, University of the Basque Country, Bilbao, Spain

**Jorge V. Rocha** Centro Multidisciplinar de Astrofísica, Dept. de Física, Instituto Superior Técnico, Technical University of Lisbon, Lisboa, Portugal

**Maria J. Rodriguez** Center for the Fundamental Laws of Nature, Harvard University, Cambridge, MA, USA

**Alberto Rozas-Fernández** Institute of Cosmology and Gravitation, University of Portsmouth, Porsmouth, UK

**Diego Rubiera-García** Departamento de Física, Universidad de Oviedo, Oviedo, Asturias, Spain

**Eduardo Ruiz** Departamento de Física Fundamental, Universidad de Salamanca, Salamanca, Spain

**Alberto Saa** Departamento de Matemática Aplicada, Universidade Estadual de Campinas, Campinas, SP, Brazil

**Diego Sáez** Departamento de Astronomía y Astrofísica, Universidad de Valencia, Burjassot, Valencia, Spain

**Marco O.P. Sampaio** Departamento de Física da Universidade de Aveiro and I3N, Campus de Santiago, Aveiro, Portugal

**Nilton Óscar Santos** School of Mathematical Sciences, Queen Mary, University of London, London, UK

**Yuki Sato** Department of Physics, Nagoya University, Nagoya, Japan

**Irene Sendra** Fisika Teorikoa, Zientzia eta Teknologia Fakultatea, Euskal Herriko Unibertsitatea UPV/EHU, Bilbao, Spain

**José M.M. Senovilla** Física Teórica, Universidad del País Vasco, Bilbao, Spain

**Walter Simon** Gravitational Physics, Faculty of Physics, Vienna University, Vienna, Austria

**Jozef Skákala** Centro de Matemática, Computação e Cognição, UFABC, Santo André, SP, Brazil

**Alberto Soria** Dept. Física Fundamental, Univ. de Salamanca, Salamanca, Spain

**Kepa Sousa** School of Engineering and Science, Jacobs University Bremen, Bremen, Germany

**Ulrich Sperhake** Department of Applied Mathematics and Theoretical Physics, Centre for Mathematical Sciences, University of Cambridge, Cambridge, UK

**Eckhard Strobel** ICRA, Piazzale della Repubblica 10, Pescara, Italy

**Robert Švarc** Department of Physics, Faculty of Science, J. E. Purkinje University in Ústí nad Labem, České mládeže 8, Ústí nad Labem, Czech Republic

**Otakar Svítek** Institute of Theoretical Physics, Faculty of Mathematics and Physics, Charles University in Prague, Praha, Czech Republic

**Yaser Tavakoli** Departamento de Física, Universidade da Beira Interior, Covilhã, Portugal

**Robert J. Thacker** DAP, St. Mary's University, Halifax, NS, Canada

**Leonardo Tinti** Università di Firenze and INFN Sezione di Firenze, Florence, Italy

**Jon Urrestilla** Department of Theoretical Physics, University of the Basque Country UPV/EHU, Bilbao, Spain

**Sergiu Vacaru** Alexandru Ioan Cuza University, Iaşi, Romania

**Norbert Van den Bergh** Department of Mathematical Analysis, Ghent University Galglaan, Gent, Belgium

**Oscar Varela** Institute for Theoretical Physics and Spinoza Institute, Utrecht University, TD Utrecht, The Netherlands

**Raül Vera** Física Teórica e Hist. de la Ciencia, UPV/EHU, Bilbao, Basque Country, Spain

**Gaetano Vilasi** Dipartimento di Fisica “E.R.Caianiello”, Università degli Studi di Salerno, Fisciano (Sa), Italy

**Amitabh Virmani** Institute of Physics, Sachivalaya Marg, Bhubaneswar, Odisha, India

**Mengjie Wang** Departamento de Física da Universidade de Aveiro and I3N, Campus de Santiago, Aveiro, Portugal

**Ben Whale** Department of Mathematics and Statistics, University of Otago, Dunedin, New Zealand

**Miguel Zilhão** Departamento de Física da Universidade de Aveiro and I3N, Campus de Santiago, Aveiro, Portugal

# Part I
# Plenary Sessions

# Linearized Gravitational Waves Near Space-Like and Null Infinity

**Florian Beyer, George Doulis, Jörg Frauendiener, and Ben Whale**

**Abstract** Linear perturbations on Minkowski space are used to probe numerically the remote region of an asymptotically flat space-time close to spatial infinity. The study is undertaken within the framework of Friedrich's conformal field equations and the corresponding conformal representation of spatial infinity as a cylinder. The system under consideration is the (linear) zero-rest-mass equation for a spin-2 field. The spherical symmetry of the underlying background is used to decompose the field into separate non-interacting multipoles. It is demonstrated that it is possible to reach null-infinity from initial data on an asymptotically Euclidean hyper-surface and that the physically important radiation field can be extracted accurately on $\mathscr{I}^+$.

## 1 Introduction

Asymptotically simple space-times as defined by Penrose [21] are distinguished by their qualitatively completely different structure at infinity. Depending on the sign of the cosmological constant $\lambda$ their conformal boundary is time-like, space-like or null. These space-times have been studied extensively from the point of view of the initial (boundary) value problem and a lot is known about their properties. In particular, space-times which are asymptotically de Sitter ($\lambda > 0$) are known to exist globally for small initial data. The same is true for asymptotically flat space-times ($\lambda = 0$) while for asymptotically anti-de Sitter space-times we only have short-time existence results for the initial boundary value problem. On the contrary, initiated by an important paper by Bizoń and Rostrowroski [2] and based on numerical and

F. Beyer · G. Doulis (✉) · J. Frauendiener · B. Whale
Department of Mathematics and Statistics, University of Otago, P.O. Box 56,
Dunedin 9010, New Zealand
e-mail: fbeyer@maths.otago.ac.nz; gdoulis@maths.otago.ac.nz; joergf@maths.otago.ac.nz;
bwhale@maths.otago.ac.nz

A. García-Parrado et al. (eds.), *Progress in Mathematical Relativity, Gravitation and Cosmology*, Springer Proceedings in Mathematics & Statistics 60,
DOI 10.1007/978-3-642-40157-2_1, © Springer-Verlag Berlin Heidelberg 2014

perturbative methods, there are now strong hints that these space-times are in fact non-linearly unstable.

In the present paper we want to focus on asymptotically flat space-times. As we already mentioned these space-times exist globally for small enough initial data. However, it is still not completely understood in detail, how to characterize the admissible initial data from a geometrical or physical point of view. The reason lies in the fact that in every space-time with a non-vanishing ADM-mass spatial infinity is necessarily singular for the four-dimensional conformal structure.

In a seminal paper [10], Friedrich shows how to set up a particular gauge near space-like infinity which exhibits explicitly the structure of the space-time near space-like and null-infinity. The so called "conformal Gauß gauge" is based entirely on the conformal structure of the space-time fixing simultaneously a coordinate system, an orthogonal frame and a general Weyl connection compatible with the conformal structure. The detailed description of this gauge is beyond the scope of this paper and we need to refer the reader to the existing literature [8–10, 16]. Suffice it to say that the conformal Gauß gauge is based on a congruence of time-like conformal geodesics emanating orthogonally from an initial space-like hyper-surface. The coordinate system, tetrad and Weyl connection are defined initially on that hyper-surface and are dragged along the congruence of conformal geodesics so that they are defined everywhere.

It turns out that in this gauge the space-time region near space-like infinity has a boundary consisting of future and past null-infinity $\mathscr{I}^{\pm}$ together with a three-dimensional "cylindrical" hyper-surface $I$ connecting them. In a certain sense, in Minkowski space-time, this cylinder is a blow-up of the (regular) point $i^0$. The "general conformal field equations" (GCFE) express the fact that the conformal class of the space-time contains an Einstein metric. They are a set of geometric partial differential equations (PDEs) generalizing the standard Einstein equations with cosmological constant. When split into evolution and constraint equations within the conformal Gauß gauge the evolution equations take a particularly simple form and it turns out that the cylinder $I$ becomes a *total characteristic*. This means that the evolution equations reduce to an intrinsic system of PDEs on $I$, i.e., they contain no derivatives transverse to $I$. The intrinsic equations are symmetric hyperbolic on $I$ except for the locations $I^{\pm} := I \cap \mathscr{I}^{\pm}$, the 2-spheres where $I$ meets future or past null-infinity. There, the equations loose hyperbolicity. It is this feature which is responsible for the singular behavior of the conformal structure near space-like infinity.

In a series of papers [10,12–14], Friedrich has analyzed the behavior of the fields, in particular of the Weyl tensor components and their transverse derivatives, along the cylinder $I$. He has shown that generic initial data lead to singularities at $I^{\pm}$. The singularities can be avoided if the initial data satisfy certain conditions, one of them being the geometric condition that the Cotton tensor of the induced geometry on the initial hyper-surface and all its symmetric trace-free derivatives vanish at the intersection of $I$ and the initial hyper-surface. It is still not completely clear what is the correct geometric classification of those space-times which satisfy Friedrich's conditions (however, see [12, 14, 15]).

Here, we want to discuss these issues from the numerical point of view. It is clear, that the fact that the evolution equations extracted from the GCFE cease to be hyperbolic is a troublesome feature in a numerical evolution scheme. We want to see how it manifests itself in the simplest scenario we can think of: linearized gravitational fields on Minkowski space. If we could not control this situation then the use of the GCFE for numerical purposes would not be possible.

The plan of the paper is as follows: in Sects. 2 and 3 we give brief summaries of the basic analytical and numerical results. In Sect. 4 we discuss ways to overcome the singular behavior at $I^+$ while in Sect. 5 we show how we can reach future null-infinity. The conventions we use and much of the background can be found in [22].

## 2 The Spin-2 Zero-Rest-Mass Equations

It is well known [22] that perturbations of the Weyl tensor $C_{abc}{}^{d}$ or, equivalently, the Weyl spinor $\Psi_{ABCD}$ satisfy the equations for a field with spin 2 and vanishing rest-mass:

$$\nabla^{A}{}_{A'}\phi_{ABCD} = 0. \tag{1}$$

It is also known [22] that this system of equations suffers from Buchdahl conditions, algebraic conditions relating the conformal curvature $\Psi_{ABCD}$ of the underlying background geometry with the field

$$\Psi_{ABC(D}\phi^{ABC}{}_{E)} = 0$$

which severely restrict the possible perturbations in any conformally curved space-time, rendering (1) inconsistent.

Therefore, we choose flat Minkowski space-time as our background so that $\phi_{ABCD}$ describes small amplitude gravitational waves propagating in an otherwise empty space-time. For a detailed discussion and derivation of the explicit form of the spin-2 equations in the present context we refer to [1]. Here, we focus only on the relevant points. Starting with the standard Minkowski metric in Cartesian coordinates $X^{\mathbf{a}}$

$$\tilde{g} = \eta_{\mathbf{ab}}\mathrm{d}X^{\mathbf{a}}\mathrm{d}X^{\mathbf{b}} \tag{2}$$

where $\eta_{\mathbf{ab}} = \mathrm{diag}(1, -1, -1, -1)$, and performing an inversion at the null-cone of the origin

$$X^{\mathbf{a}} = -\frac{x^{\mathbf{a}}}{x \cdot x}, \qquad x \cdot x := \eta_{\mathbf{ab}}x^{\mathbf{a}}x^{\mathbf{b}} = \frac{1}{(X \cdot X)}$$

puts the metric into the form

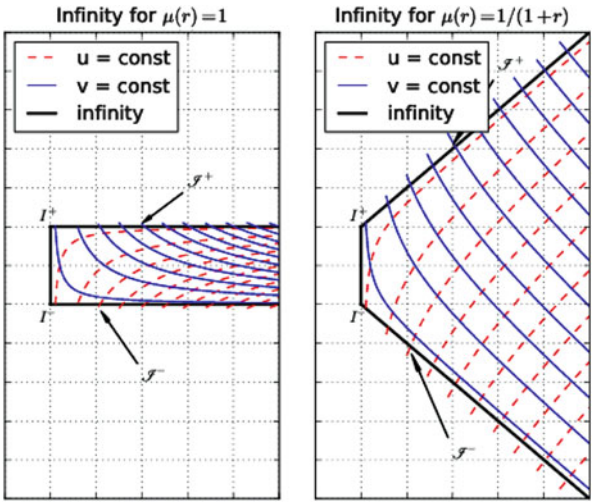


**Fig. 1** The neighborhood of space-like infinity in two different $(t, r)$-coordinate representations corresponding to $\mu(r) = 1$ and $\mu(r) = 1/(1 + r)$

$$\tilde{g} = \frac{\eta_{\mathbf{ab}} \mathrm{d}x^{\mathbf{a}} \mathrm{d}x^{\mathbf{b}}}{(x \cdot x)^2}. \tag{3}$$

This metric is singular whenever $x \cdot x = 0$, i.e., on the null-cone at infinity. So we define a conformally related metric

$$g' = \Omega^2 \tilde{g} = \eta_{\mathbf{ab}} \mathrm{d}x^{\mathbf{a}} \mathrm{d}x^{\mathbf{b}}, \qquad \Omega = -(x \cdot x) \tag{4}$$

which extends smoothly to the null-cone of infinity. Note, that space-like infinity is represented in this metric as the point $x^{\mathbf{a}} = 0$. In order to exhibit the cylindrical structure referred to above we perform a further rescaling of the metric using a function $\kappa(r) = r\mu(r)$, where $r^2 = (x^1)^2 + (x^2)^2 + (x^3)^2$ and $\mu$ is a smooth function with $\mu(0) = 1$. Furthermore, we introduce a new time coordinate by defining $x^0 = t\kappa(r)$. These steps give the final form of the metric

$$g = \frac{1}{\kappa^2} \left( \kappa^2 \mathrm{d}t^2 + 2t\kappa\kappa' \mathrm{d}t\mathrm{d}r - (1 - t^2\kappa'^2)\mathrm{d}r^2 - r^2 \mathrm{d}\omega^2 \right). \tag{5}$$

Here, we have denoted the metric on the unit sphere by $\mathrm{d}\omega^2$. Note, that the metric $g$ is spherically symmetric.

The function $\mu(r)$ determines the "shape" of $\mathscr{I}^{\pm}$ in the $(t, r)$-coordinate system. We have chosen the two possibilities $\mu(r) = 1/(1 + nr)$ with either $n = 0$ or $n = 1$ with the consequence that $\mathscr{I}^{\pm}$ are represented as either a horizontal ($n = 0$) or diagonal ($n = 1$) line in a $(t, r)$ diagram, see Fig. 1. They meet the cylinder $I$ in the spheres $I^{\pm}$ at $(t, r) = (\pm 1, 0)$. We introduce the double null-coordinates $(u, v)$ by

$$u = \kappa t - r, \qquad v = \kappa t + r, \tag{6}$$

which puts the metric into the form

$$g = \frac{1}{\kappa^2}\mathrm{d}u\mathrm{d}v - \frac{1}{\mu^2}\mathrm{d}\omega^2.$$

Null-infinity is characterized by the vanishing of one of the null coordinates, the other one being non-zero ($u = 0$, $v \neq 0$ on $\mathscr{I}^+$ and $u \neq 0$, $v = 0$ on $\mathscr{I}^-$). Both coordinates vanish on the cylinder $I$. In Fig. 1 we also display the lines of constant $u$ and $v$, corresponding to radial null geodesics. There are two families of null geodesics, one leaving the space-time through $\mathscr{I}^+$, the other entering it through $\mathscr{I}^-$.

Since the null coordinates are adapted to the conformal structure, we can see clearly that the cylinder is "invisible" from the point of view of the conformal structure. This structure is exactly the same as the representation of space-like infinity in the coordinates $x^{\mathbf{a}}$, it appears like a point. However, the differentiable structures defined by the $(u, v)$ and the $(t, r)$ coordinates are completely different near the boundary $r = 0$ from the one defined by the $x^{\mathbf{a}}$ coordinates.

In order to derive the spin-2 equations explicitly we introduce a complex null tetrad $(l^a, n^a, m^a, \bar{m}^a)$ adapted to the spherical symmetry, i.e.,

$$l^a\partial_a = \frac{1}{\sqrt{2}}\left(\left(1 - t\kappa'\right)\partial_t + \kappa\partial_r\right), \qquad n^a\partial_a = \frac{1}{\sqrt{2}}\left(\left(1 + t\kappa'\right)\partial_t - \kappa\partial_r\right),$$

and $m^a$ tangent to the spheres of symmetry. Writing the spin-2 equation in the NP formalism, computing the spin-coefficients and finally introducing the "eth" operator $\eth$ (see [17,20,22]) on the unit sphere puts (1) into the form of eight coupled equations

$$\begin{aligned}(1 - t\kappa')\partial_t\phi_k + \kappa\partial_r\phi_k - (3\kappa' - (5-k)\mu)\phi_k &= \mu\eth'\phi_{k-1}, \quad k = 1:4,\\ (1 + t\kappa')\partial_t\phi_k - \kappa\partial_r\phi_k + (3\kappa' + (k+1)\mu)\phi_k &= \mu\eth\phi_{k+1}, \quad k = 0:3\end{aligned} \tag{7}$$

for the five complex components of the spin-2 field $\phi_{ABCD}$, see e.g. [22]. We exploit the spherical symmetry of the background Minkowski space-time even further by decomposing the field components $\phi_k(t, r, \theta, \phi)$ into different multipole moments using the spin-weighted spherical harmonics ${}_sY_{lm}$

$$\phi_k(t, r, \theta, \phi) = \sum_{l\geq 2-k}\sum_{m=-l}^{l}\phi_k^{lm}(t, r)\ {}_{2-k}Y_{lm}(\theta, \phi). \tag{8}$$

Inserting this expansion into (7) and using the action of $\eth$ and $\eth'$ on the spin-weighted spherical harmonics [22] the system decouples into a countable family of $1 + 1$ systems indexed by admissible pairs of integers $(l, m)$. We find that each mode $\phi_k^{lm}$ propagates along radial null geodesics, the "inner" modes $\phi_1^{lm}$, $\phi_2^{lm}$, $\phi_3^{lm}$ propagate in both directions while the "outer" modes $\phi_0^{lm}$ and $\phi_4^{lm}$ only propagate along one null direction.

The final step in the preparation of the equations is the split into constraint and evolution equations, which leads to a system of five evolution equations

$$\begin{aligned}
(1+t\kappa')\partial_t\phi_0 - \kappa\partial_r\phi_0 &= -(3\kappa'-\mu)\phi_0 - \mu\alpha_2\phi_1,\\
\partial_t\phi_1 &= -\mu\phi_1 + \frac{1}{2}\mu\alpha_2\phi_0 - \frac{1}{2}\mu\alpha_0\phi_2,\\
\partial_t\phi_2 &= \frac{1}{2}\mu\alpha_0\phi_1 - \frac{1}{2}\mu\alpha_0\phi_3,\\
\partial_t\phi_3 &= \mu\phi_3 + \frac{1}{2}\mu\alpha_0\phi_2 - \frac{1}{2}\mu\alpha_2\phi_4,\\
(1-t\kappa')\partial_t\phi_4 + \kappa\partial_r\phi_4 &= (3\kappa'-\mu)\phi_4 + \mu\alpha_2\phi_3
\end{aligned} \tag{9}$$

and three constraint equations

$$\begin{aligned}
-2\kappa\partial_r\phi_1 + 6r\mu'\phi_1 - 2t\kappa'\mu\phi_1 + \alpha_0\mu(1-t\kappa')\phi_2 + \alpha_2\mu(1+t\kappa')\phi_0 &= 0,\\
-2\kappa\partial_r\phi_2 + 6r\mu'\phi_2 + \alpha_0\mu(1-t\kappa')\phi_3 + \alpha_0\mu(1+t\kappa')\phi_1 &= 0,\\
-2\kappa\partial_r\phi_3 + 6r\mu'\phi_3 + 2t\kappa'\mu\phi_3 + \alpha_0\mu(1+t\kappa')\phi_2 + \alpha_2\mu(1-t\kappa')\phi_4 &= 0.
\end{aligned} \tag{10}$$

Note that we have dropped here the superscripts from $\phi_k^{lm}$ and we introduced the quantities $\alpha_0 = \sqrt{l(l+1)}$ and $\alpha_2 = \sqrt{l(l+1)-2}$. Since $\kappa(0) = 0$ it is obvious that the evolution equations reduce to a system intrinsic to $I$. Since on $I$ also $\kappa'(0) = 1$, it follows that the coefficients in front of the time derivatives of $\phi_0$ (respectively $\phi_4$) vanish when $t = -1$ (respectively when $t = 1$).

In Fig. 2 we show again the neighbourhood of $I$ and $\mathscr{I}^+$ for $\mu(r) = 1/(1+r)$. This time we show the characteristics also in the unphysical part of the diagram. The non-shaded region bounded partly by the thick broken line is the domain of hyperbolicity of the evolution equations, i.e., the domain where $t < \pm|\kappa'(r)|$. Notice that every neighborhood of $I^+$ contains regions where the hyperbolicity breaks down. Apart from the fact that one cannot hope to get existence and uniqueness of solutions beyond that region its presence also makes the numerical evolution challenging. For instance, setting up an initial boundary value problem with the left boundary at negative values of $r$ does not make sense if the evolution is to reach up to $I^+$. Even with the left boundary on $I$ it is not possible to go beyond $I^+$ since the evolution hits the non-hyperbolicity region.

## 3 Numerical Methods and Tests

Again, we give a brief summary and refer to [1] for further details. We have different equations for different values of the multipole index $l$. Here, we focus only on the case $l = 2$ without mentioning it any further. We have done evolutions with other

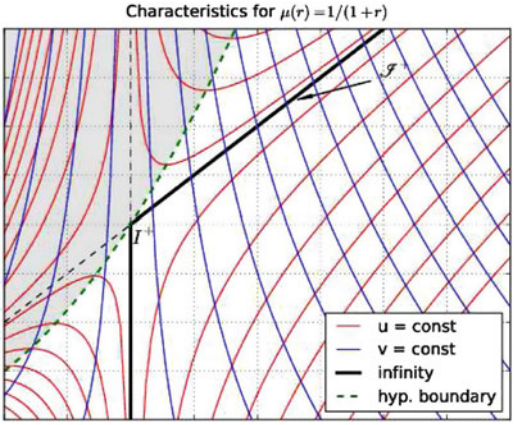


**Fig. 2** The characteristics of the evolution equations in a neighborhood of $I^+$ in the diagonal representation. The *shaded region* is the domain where the equations fail to be hyperbolic, i.e., where $t < \kappa'(r)$. The corresponding neighborhood of $I^-$ is obtained by reflection at the lower border of the diagram accompanied by an interchange of $u$ and $v$. The *thick* (*green*) *broken line* indicates the boundary of the domain of non-hyperbolicity

values of $l$ which lead to very similar results. The evolution equations (9) are solved on a spatial interval $0 \leq r \leq 1$ as an initial boundary value problem. We use the method of lines constructing the spatial discretisation using a 4th order accurate finite difference scheme. The initial data are obtained either from exact solutions or by solving the constraint equations (10) explicitly in terms of two free functions. The boundary at $r = 0$ is a characteristic so we do not need to specify any free functions there, while the boundary at $r = 1$ is an artificial boundary, which needs exactly one free function for the component $\phi_0$ that propagates through this boundary into the computational domain. The boundary conditions are implemented using SBP operators [6, 18, 24] and the SAT penalty method [3, 4, 19, 23]. The semi-discrete system of ODEs is solved using the standard 4th order Runge–Kutta method.

This code stably propagates the initial data from $t = 0$ up to any value of $t < 1$, independently of whether we use the diagonal or the horizontal representation of $\mathscr{I}$. The code converges to 4th order, the constraints propagate and the constraint violations remain bounded. However, the two representations behave differently when we attempt to reach $t = 1$.

In the diagonal case we can reach $t = 1$ exactly and the code converges in 4th order, indicating that the numerical problem is still well-posed. With any fixed time-step $\tau$ we can also step beyond $t = 1$ to $t = 1 + \tau$. However, the code fails to converge at $t = 1 + \tau$ for every $\tau > 0$. Clearly, the loss of hyperbolicity at $t = 1$ is also responsible for the lack of well-posedness of the numerical problem. Referring back to Fig. 2 it is clear that there will always be a sufficiently high resolution in time and space which will detect the domain of non-hyperbolicity of the evolution equations beyond $I^+$.

In the horizontal case the situation is apparently worse. In this case, it is *principally impossible* to reach $t = 1$ simply because the propagation speed of $\phi_4$ becomes infinite and so stability is lost not only at the point $I^+$ but at the entire time-slice $t = 1$ which coincides with $\mathscr{I}^+$, a characteristic hyper-surface, in this representation.

However, *in principle* we can come arbitrarily close to $t = 1$ (within numerical accuracy) if at every time we choose the next time-step small enough so that the CFL criterion—the numerical domain of dependence includes the analytical domain of dependence—is satisfied. Such an adaptive time-stepping scheme has been implemented and we have in fact demonstrated that we can come very close to $t = 1$ without loosing convergence. However, since the time-steps decrease to zero exponentially with the number of steps the simulation takes arbitrarily long.

## 4 Beyond $I^+$?

Given that we can reach $t = 1$ in a stable fashion in the diagonal representation we may ask the question as to whether it is possible to continue beyond $I^+$? Clearly, for the reasons discussed above we cannot simply continue the computation because we run into the non-hyperbolicity region near $I^+$. Referring back to Fig. 2 we see that one family of the characteristics—corresponding to the field component $\phi_4$—asymptotes to the cylinder and, subsequently, to $\mathscr{I}^+$ in a non-uniform way. This non-uniformity is due to the fact that the coefficient in front of the time derivative of $\phi_4$ in the evolution system vanishes at $t = 1$, causing the loss of hyperbolicity of the system. Can we avoid this problem? There are a few possibilities which come to mind:

- Chop the computational domain by dropping points outside $\mathscr{I}^+$ from the left.
- Change the radial coordinate so that $\mathscr{I}^+$ becomes the left boundary of the computational domain. This is a form of $\mathscr{I}$-freezing (see [7]).
- Change the time coordinate so that the (space-like) time-slices tilt upwards towards $\mathscr{I}^+$.

We have considered the first two possibilities. These two methods are complementary to each other in the sense that in the first case we change the computational domain but not the system, while in the second case we change the equations but not the computational domain.

Figure 2 shows the behavior of the characteristics for $\phi_0$ and $\phi_4$ as well as the region in which hyperbolicity fails. The surfaces that we are evolving our data on are horizontal and to the right of the vertical solid and broken black lines. Note that for $t > 1$ these surfaces are guaranteed to intersect the region in which hyperbolicity fails. In addition, for surfaces with $t > 1$ a new boundary condition for $\phi_4$, on the "left" of the grid is required. However, since $\mathscr{I}^+$ is one of the characteristics for $\phi_4$ this boundary condition cannot influence the physical region to the right of $\mathscr{I}^+$.

**Table 1** Absolute error $\Delta$ compared to an exact solution

| Grid points | $\phi_0$ $\log_2(\|\|\Delta\|\|_2)$ | Rate | $\phi_4$ $\log_2(\|\|\Delta\|\|_2)$ | Rate |
|---|---|---|---|---|
| 100 | −28.38 | | −5.93 | |
| 200 | −31.75 | 3.37 | −5.98 | 0.05 |
| 400 | −35.21 | 3.46 | −6.07 | 0.10 |
| 800 | −38.71 | 3.50 | −8.41 | 2.34 |

$L^2$ norm and convergence rates at time $t = 1.1$ for $\phi_0, \phi_4$. The calculation was done with a fixed time-step

To solve both of these problems we set the values of $\phi_0, \ldots, \phi_4$ to zero after some predetermined grid point that is beyond future null infinity, but before the region in which hyperbolicity fails. That is, between the broken green line and $\mathscr{I}^+$. The equation for the broken green line is

$$1 - \frac{t}{(r+1)^2} = 0$$

and the equation for future null infinity, where $t \geq 1$, is

$$1 - \frac{t}{r+1} = 0.$$

We chose, after some experimentation, that the "cut off" point, after which all data values would be set to zero would be 10 % of all grid points beyond $\mathscr{I}^+$. That is, the values of $\phi_0, \ldots, \phi_4$ would be set to zero on the 90 % of grid points between $r = 0$ and $\mathscr{I}^+$. This condition, of setting values to zero, allows us to numerically provide the necessary boundary condition for $\phi_4$ and cope with the lack of hyperbolicity in the region of the grid to the left of the broken green line.

Other than this technicality, the same evolution scheme, with the same fixed step size was used to evaluate the initial data up to $t = 1.1$. We evolved an exact solution and estimated the error at $t = 1.1$ by comparing the values of $\phi_0, \ldots, \phi_4$, on the "physical" portion of the grid to the exact solution. The $L_2$ measure of the error is presented in Table 1. We only give the error for the $\phi_0$ and $\phi_4$ components. The convergence rates for $\phi_1, \phi_2$ and $\phi_3$ are, roughly, a linear interpolation between those for $\phi_0$ and $\phi_4$. Note, that the error in $\phi_0$ is of the order of $10^{-11}$ while the error in $\phi_4$ is roughly $10^{-2}$.

In the second case we change the $r$-coordinate in a very simple minded way using the coordinate transformation

$$r \mapsto \bar{r} = r - t + 1, \qquad t \mapsto \bar{t} = t, \qquad \text{for } t \geq 1.$$

This has the effect that $\mathscr{I}^+$ is given as the locus $\{\bar{r} = 0\}$. Note, that the coordinate transformation is only continuous and not even $\mathscr{C}^1$. Since the partial derivatives transform according to

$$\partial_t = \partial_{\bar{t}} - \partial_{\bar{r}}, \qquad \partial_r = \partial_{\bar{r}}$$

we still have the problem that the coefficient in front of the time derivative of $\phi_4$ vanishes at $t = 1$. Clearly, we cannot make the system regular at $t = 1$ by a coordinate transformation. We can try to avoid the evaluation at $t = 1$ by arranging the time stepping to "straddle" $t = 1$ so that we never actually hit it exactly. However, this has the consequence that the "kink" that we obtain due to the non-smoothness of the coordinate transformation induces oscillations at the right boundary. We would probably be able to avoid those if we used a smoother coordinate transformation. However, this would change the equations in much more complicated ways and we have not pursued this any further.

The third possibility mentioned above—changing the time coordinate—has the effect that the time-slices globally approach $\mathscr{I}^+$ which is exactly the feature that we see in the horizontal representation. This prompted us to look at the relationships between the different conformal representations in more detail.

The two representations are related by a conformal rescaling and a coordinate transformation. We can derive the corresponding relationships for the field components as follows. Let $\mu_n(r) = 1/(1 + nr)$ and define $\Theta = \mu_1/\mu_0$. Let $g_0$ and $g_1$ be the metrics corresponding to the horizontal and diagonal representations, then we have

$$g_1 = \frac{\mu_1^2}{\mu_0^2}\, g_0 = \Theta^2 g_0. \tag{11}$$

Furthermore, the two time coordinates $t_0$ and $t_1$ in the two representations are related by

$$x^0 = r\mu_0 t_0 = r\mu_1 t_1 \implies t_1 = \Theta^{-1} t_0. \tag{12}$$

The spin-2 field has conformal weight $-1$ under conformal rescalings. This implies that with (11) we also have

$$\phi^1_{ABCD} = \Theta^{-1} \phi^0_{ABCD}. \tag{13}$$

In order to get the behavior of the field components under conformal rescalings we observe that (11) implies that the tetrad vectors rescale as

$$l^a_1 = \Theta^{-1} l^a_0, \quad \text{etc} \tag{14}$$

and the spin-frame correspondingly rescales with $\Theta^{-1/2}$. Taken altogether, these transformation properties imply that

$$\phi^1_k(t_1, r) = \Theta^{-3} \phi^0_k(\Theta^{-1} t_0, r). \tag{15}$$

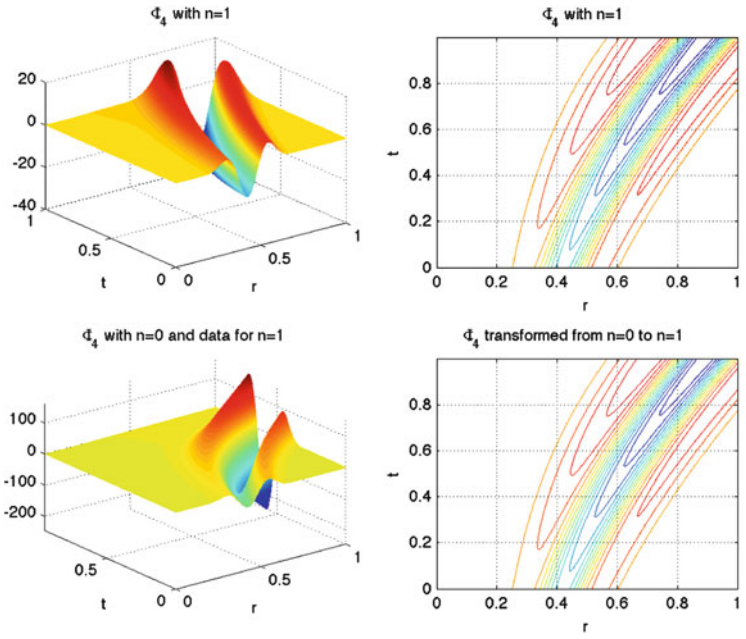


**Fig. 3** Comparison between the two representations. For detailed explanation see text

We can now make use of these relationships in the following way. Suppose we want to evolve initial data in the diagonal representation. We rescale the data on the initial hyper-surface $t_1 = 0 = t_0$ using (15) into initial data for the horizontal representation and evolve them with the system for the horizontal representation up to a time $t \approx 1$. Then we undo the rescaling with (15) and obtain the solution in the diagonal representation. In Fig. 3 we present the results of these operations. The surface plot in the upper left shows the component $\phi_4$ evolved with the diagonal representation $n = 1$, while the plot on the lower left shows $\phi_4$ obtained in the horizontal representation using the same data as for the case $n = 1$ but rescaled according to (15). The contour plots on the right show the obtained solutions. Above is the solution directly obtained in the diagonal representation while below is the solution obtained after rescaling back from the horizontal representation. The contour plots agree visually. Note, that the $t$ coordinates in the two surface plots are not the same. They refer to $t_0$ in the lower plot and to $t_1$ in the other.

In the horizontal representation we come arbitrarily close to $t = 1$. Hence, we can "almost" compute the entire space-time (at least in this simple set-up). In this sense the horizontal representation is much more efficient than the diagonal one. In Fig. 4 we show the contour plots of the rescaled solution in the diagonal representation. Clearly, it extends way over the $t = 1$ time-slice reaching $\mathscr{I}^+$ to within the graphical resolution.

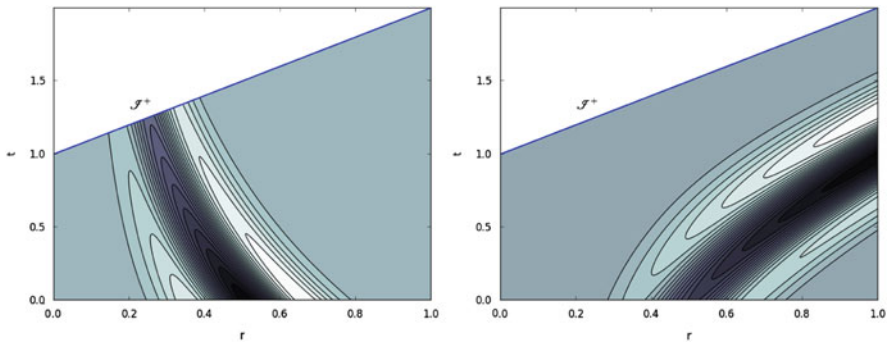


**Fig. 4** Contour plots of $\phi_0$ (*left*) and $\phi_4$ (*right*) computed with $n = 0$ but rescaled to the diagonal representation

## 5 Reaching Null-Infinity

Since the horizontal representation allows us to almost reach null-infinity one may wonder whether it might be possible to extend the computation to $\mathscr{I}^+$ from the last time-level at $t = \bar{t}$, say? To answer this question we refer back to Fig. 1 where we showed the space-time in the horizontal representation together with the two families of characteristics. The "outgoing" characteristics (those intersecting $\mathscr{I}^+$) are well-behaved while the other family asymptotes to $I \cup \mathscr{I}^+$ in a non-uniform way. Referring to (7) we see that all components except for $\phi_4$ propagate along the well-behaved characteristics. This suggests that we use those four propagation equations to estimate the values of $\phi_0, \phi_1, \phi_2, \phi_3$ on $\mathscr{I}^+$. Since we cannot use any values of $\phi_4$ beyond $t = \bar{t}$ we are forced to use an Euler step to get to $t = 1$.

As for $\phi_4$ we observe that its propagation equation reduces to an intrinsic equation on $\mathscr{I}^+$, which we could integrate if we had initial conditions for $\phi_4$ at $r = 0$, once we know the values of the other components on $\mathscr{I}^+$. The equation for $\phi_4$ on $\mathscr{I}^+$ reduces to

$$r\partial_r\phi_4 - 2\phi_4 = \alpha_2\phi_3. \tag{16}$$

This equation is singular at $r = 0$ and the requirement that $\phi_4$ and its derivative be bounded forces the initial condition

$$\phi_4(1,0) = -\frac{\alpha_2}{2}\phi_3(1,0).$$

So we see that we can perform the last step to $\mathscr{I}^+$, albeit only with a first order method.

We tested this approach by evolving compactly supported initial data obtained by explicitly solving the constraints (the same ones as in Sect. 4). The error at $t = 1$ was estimated by comparing the values produced in some simulation to the

**Table 2** Absolute error $\Delta$ compared to a 6,400 grid point simulation using the $L^2$ norm and convergence rates at time $t = 1$ for $\phi_0, \phi_4$ for compactly supported data in the $n = 0$ space-time

| | $\phi_0$ | | $\phi_4$ | |
|---|---|---|---|---|
| Grid points | $\log_2(\|\|\Delta\|\|_2)$ | Rate | $\log_2(\|\|\Delta\|\|_2)$ | Rate |
| 200 | −7.99 | | 0.082 | |
| 400 | −11.48 | 3.49 | −0.44 | 0.52 |
| 800 | −14.98 | 3.49 | −1.02 | 0.57 |
| 1,600 | −18.48 | 3.50 | −1.73 | 0.71 |
| 3,200 | −22.07 | 3.58 | −2.81 | 1.08 |

values produced in the highest resolution simulation with 6,400 grid points. The $L_2$ measure of the error is presented in Table 2. Since the $\phi_0$ and $\phi_4$ components mark the extreme cases, we do not present the error convergence rates for $\phi_1, \phi_2, \phi_3$. Their convergence rates are comparable to $\phi_0$. Remarkably, the convergence rate for $\phi_0$ is close to 4th order, while for $\phi_0$ we get the expected first order convergence. The accuracy in the radiation component is roughly $10^{-7}$ while for $\phi_4$ it is not good, only $\approx 10\,\%$. This low accuracy is due to the singular behavior of the propagation equation (16) for $\phi_4$ at $r = 0$, which we might not have taken care of appropriately. There is still room for improvement because we could use the intrinsic transport equations (see [1, 11]) along the cylinder—mentioned in the introduction—to drag along as many derivatives of $\phi_4$ as we please. These could be used to construct a Taylor approximation for $\phi_4$ near $r = 0$ to get the integration process started more smoothly.

## 6 Conclusion

In this paper we have presented a study of the spin-2 equation in the neighborhood of spatial infinity in Minkowski space-time. Since the perturbations of the Weyl curvature on flat space obey this equation we can interpret this system as a model for small amplitude gravitational waves. We used this model to study the asymptotic properties of the fields—and, hence, to some extent also of the perturbed space-time—close to spatial infinity. This region is still not completely understood and we hope that our work will ultimately contribute to the complete understanding of this issue.

We have shown here that it is possible to generate a complete evolution from initial data on an asymptotically Euclidean hyper-surface to the asymptotic regime including null-infinity even though the equations show a certain degeneracy at the cylinder which represents spatial infinity in Friedrich's conformal Gauß gauge. Using the horizontal representation as described in Sects. 4 and 5 we can get the radiation field $\phi_0$ quite accurately on $\mathscr{I}^+$. The drop in convergence for the component $\phi_4$ is akin to the loss of smoothness of null-infinity in the first result on the global stability of Minkowski space by Christodoulou and Klainerman [5]. This was caused by the loss of peeling in the corresponding component of the Weyl tensor.

Of course, we deal here with a highly simplified system and the fact that we can make things work here does not immediately imply that it will also work in the physically relevant 3D cases. However, this toy system does provide valuable insights into the possibilities of and the restrictions imposed by the structure of spatial infinity. We should point out that the structure of the fully non-linear general conformal field equations is very similar to the linear spin-2 system. This is essentially due to the fact that the spin-2 system results from the Bianchi equations obeyed by the rescaled Weyl spinor.

Our next steps will be the removal of the artificial boundary at $r = 1$. This will allow us to perform an entirely global evolution of the mode decomposed spin-2 field. The challenge here is to get the centre under control because due to the spherical symmetry this will be a singular point for the equations. Then, we intend to remove the mode decomposition and look at the linearized system in three spatial dimensions.

**Acknowledgements** This research was supported in part by Marsden grant UOO0922 from the Royal Society of New Zealand. JF wishes to thank the organizers of the ERE2012 meeting in Guimarães for their support.

## References

1. Beyer, F., Doulis, G., Frauendiener, J.: Numerical space-times near space-like and null infinity. The spin-2 system on Minkowski space. Classical and Quantum Gravity **29**(24), 245,013 (2012)
2. Bizoń, P., Rostworowski, A.: On weakly turbulent instability of anti-de Sitter space. Phys. Rev. Lett. **107** (2011)
3. Carpenter, M.H., Gottlieb, D., Abarbanel, S.: Time-stable boundary conditions for finite-difference schemes solving hyperbolic systems: methodology and application to high-order compact schemes. J. Comp. Phys. **111**(2), 220–236 (1994)
4. Carpenter, M.H., Nordström, J., Gottlieb, D.: A stable and conservative interface treatment of arbitrary spatial accuracy. J. Comp. Phys. **148**(2), 341–365 (1999)
5. Christodoulou, D., Klainerman, S.: The global nonlinear stability of the Minkowski space, vol. 41. Princeton University Press, Princeton (1993)
6. Diener, P., Dorband, E., Schnetter, E., Tiglio, M.: Optimized high-order derivative and dissipation operators satisfying summation by parts, and applications in three-dimensional multi-block evolutions. J Sci Comput **32**(1), 109–145 (2007)
7. Frauendiener, J.: Numerical treatment of the hyperboloidal initial value problem for the vacuum Einstein equations. II. The evolution equations. Phys Rev D **58**(6), 064,003 (1998)
8. Frauendiener, J.: Conformal infinity. Living Rev. Relativity **7**, 2004–1, 82 pp. (electronic) (2004)
9. Friedrich, H.: Einstein equations and conformal structure: Existence of anti-de Sitter-type space-times. J. Geom. Phys. **17**, 125–184 (1995)
10. Friedrich, H.: Gravitational fields near space-like and null infinity. J. Geom. Phys. **24**, 83–163 (1998)
11. Friedrich, H.: Spin-2 fields on Minkowski space near spacelike and null infinity. Classical and Quantum Gravity **20**(1), 101 (2003)

12. Friedrich, H.: Static Vacuum Solutions from Convergent Null Data Expansions at Space-Like Infinity. Annales de l'IHP A (2007)
13. Friedrich, H.: Conformal classes of asymptotically flat, static vacuum data. Classical and Quantum Gravity **25**(6), 065,012 (2008)
14. Friedrich, H.: One-parameter families of conformally related asymptotically flat, static vacuum data. Classical and Quantum Gravity (2008)
15. Friedrich, H.: Conformal structures of static vacuum data. arXiv **gr-qc** (2012)
16. Friedrich, H., Schmidt, B.G.: Conformal Geodesics in General Relativity. Proc. Roy. Soc. A (1987)
17. Goldberg, J.N., Macfarlane, A., Newman, E.T.: Spin-s Spherical Harmonics and Eth. J Math Phys (1967)
18. Gustafsson, B., Kreiss, H.O., Oliger, S.: Time-dependent problems and difference methods. A Wiley-Interscience Publication (1995)
19. Lehner, L., Reula, O., Tiglio, M.: Multi-block simulations in general relativity: high-order discretizations, numerical stability and applications. Classical and Quantum Gravity **22**(24), 5283 (2005)
20. Newman, E.T., Penrose, R.: New conservation laws for zero rest-mass fields in asymptotically flat space-time. Proc. Roy. Soc. A **305**(1482), 175–204 (1968)
21. Penrose, R.: Zero rest-mass fields including gravitation: asymptotic behaviour. Proc. Roy. Soc. London A **284**, 159–203 (1965)
22. Penrose, R., Rindler, W.: Spinors and Spacetime: Two-spinor calculus and relativistic fields, vol. 1. Cambridge University Press, Cambridge (1984)
23. Schnetter, E., Diener, P., Dorband, E.N., Tiglio, M.: A multi-block infrastructure for three-dimensional time-dependent numerical relativity. Classical and Quantum Gravity **23**(16), S553–S578 (2006)
24. Strand, B.: Summation by Parts for Finite Difference Approximations for d/dx. J. Comp. Phys. **110**(1), 47–67 (1994)

# Lovelock Theory, Black Holes and Holography

**José D. Edelstein**

**Abstract** Lovelock theory is the natural extension of general relativity to higher dimensions. It can be also thought of as a toy model for ghost-free higher curvature gravity. It admits a family of AdS vacua, most (but not all) of them supporting black holes that display interesting features. This provides an appealing arena to explore different holographic aspects in the context of the AdS/CFT correspondence.

## 1 Lovelock Theory

While classical gravity seems well-described by the Einstein–Hilbert action, quantum corrections generically involve higher curvature terms. This is the case, for instance, of $\alpha'$ corrections in string theory. On general grounds, higher curvature terms arise in Wilsonian low-energy effective descriptions of gravity.

The inclusion of higher curvature corrections customarily leads to higher order equations of motion. They are consequently argued to be plagued of ghosts. Despite that, David Lovelock tackled the problem some four decades ago finding the most general situation leading to second order Euler–Lagrange equations [1]. He showed that, whereas in four dimensions General Relativity is the natural answer, higher dimensional scenarios lead to the appearance of higher curvature contributions to the action, on equal footing with the Einstein–Hilbert term. The action of Lovelock theory is given, in $d$ space-time dimensions, by a sum of $K \leq [\frac{d-1}{2}]$ terms,

J.D. Edelstein (✉)
Department of Particle Physics and IGFAE, University of Santiago de Compostela, 15782 Santiago de Compostela, Spain

Centro de Estudios Científicos CECs, Av. Arturo Prat 514, Valdivia, Chile
e-mail: jose.edelstein@usc.es

A. García-Parrado et al. (eds.), *Progress in Mathematical Relativity, Gravitation and Cosmology*, Springer Proceedings in Mathematics & Statistics 60,
DOI 10.1007/978-3-642-40157-2_2, 

$$\mathscr{I} = \sum_{k=0}^{K} \frac{c_k}{d-2k}\, \mathscr{I}_k, \tag{1}$$

which admit a compact expression in terms of differential forms

$$\mathscr{I}_k = \int \epsilon_{a_1 \cdots a_d}\; R^{a_1 a_2} \wedge \cdots \wedge R^{a_{2k-1} a_{2k}} \wedge e^{a_{2k+1}} \wedge \cdots \wedge e^{a_d}, \tag{2}$$

where $\epsilon_{a_1 \cdots a_d}$ is the anti-symmetric symbol, $R^{ab} := d\omega^{ab} + \omega^a{}_c \wedge \omega^{cb}$ is the Riemann curvature 2-form, computed from the spin connection 1-form $\omega^{ab}$, and $e^a$ is the vierbein 1-form. By construction, Lovelock theories are intrinsically higher dimensional.

It is easy to see that the first two terms (most general up to $d = 4$) are quite familiar; $\mathscr{I}_0$ gives the cosmological term while $\mathscr{I}_1$ is nothing but the Einstein–Hilbert (EH) action. Their normalization is fixed along this talk as

$$L^2 c_0 = c_1 = 1, \tag{3}$$

or, in terms of the more familiar dimensionfull quantities of General Relativity,

$$\Lambda = -\frac{(d-1)(d-2)}{2L^2}, \quad 16\pi (d-3)!\, G_N = 1, \tag{4}$$

$G_N$ being the Newton constant. For $d \geq 5$, for instance, we have the Lanczos–Gauss–Bonnet (LGB) term [2] ($c_2 = \lambda\, L^2$),

$$\mathscr{I}_2 \simeq d^d x\, \sqrt{-g}\, \left( R^2 - 4 R_{\mu\nu} R^{\mu\nu} + R_{\mu\nu\rho\sigma} R^{\mu\nu\rho\sigma} \right), \tag{5}$$

while for $d \geq 7$, we introduce the cubic Lovelock Lagrangian ($c_3 = \mu\, L^4$),

$$\begin{aligned} \mathscr{I}_3 \simeq d^d x\, \sqrt{-g}\, \big( & R^3 + 3 R R^{\mu\nu\alpha\beta} R_{\alpha\beta\mu\nu} - 12 R R^{\mu\nu} R_{\mu\nu} \\ & + 24 R^{\mu\nu\alpha\beta} R_{\alpha\mu} R_{\beta\nu} + 16 R^{\mu\nu} R_{\nu\alpha} R_{\mu}{}^{\alpha} + 24 R^{\mu\nu\alpha\beta} R_{\alpha\beta\nu\rho} R_{\mu}{}^{\rho} \\ & + 8 R^{\mu\nu}{}_{\alpha\rho} R^{\alpha\beta}{}_{\nu\sigma} R^{\rho\sigma}{}_{\mu\beta} + 2 R_{\alpha\beta\rho\sigma} R^{\mu\nu\alpha\beta} R^{\rho\sigma}{}_{\mu\nu} \big). \end{aligned} \tag{6}$$

By simple comparison of (2) and, say, (6), the advantages of the so-called first order formalism become manifest. The equations of motion are obtained by varying independently with respect to the vierbein and the spin connection. The latter can be solved by simply setting the torsion $T^a := de^a + \omega^a_{\ b} \wedge e^b$ to zero. This is not the most general solution, but the one we will consider along this talk, since it allows us to make contact with the second order metric formulation of gravity.

The equations of motion, when varying the vierbein, can be cast into the form

$$\epsilon_{aa_1\cdots a_{d-1}}\ \mathscr{F}^{a_1a_2}_{(1)}\wedge\cdots\wedge\mathscr{F}^{a_{2K-1}a_{2K}}_{(K)}\wedge e^{a_{2K+1}}\wedge\ldots\wedge e^{a_{d-1}}=0, \tag{7}$$

which neatly displays the fact that these theories admit (up to) $K$ constant curvature maximally symmetric *vacua*,

$$\mathscr{F}^{ab}_{(i)}:=R^{ab}-\Lambda_i\, e^a\wedge e^b=0. \tag{8}$$

The *effective* cosmological constants turn out to be the (real) roots of the characteristic polynomial $\Upsilon[\Lambda]$,

$$\Upsilon[\Lambda]:=\sum_{k=0}^{K}c_k\,\Lambda^k=c_K\prod_{i=1}^{K}(\Lambda-\Lambda_i)\,. \tag{9}$$

We will see that many important features of these theories and their black hole solutions are governed by this polynomial. Degeneracies arise when its discriminant, $\Delta:=\prod_{i<j}(\Lambda_i-\Lambda_j)^2$, vanishes. This is typically associated with symmetry enhancement and/or the emergence of non-generic features of Lovelock theory. Even though they can be fairly interesting (see [3] for a recent example), we will mostly deal with the $\Delta\neq 0$ case throughout this presentation.

For the sake of clarity, let us briefly consider the $K=2$ case. This amounts to the inclusion of the LGB term which, for instance, arises in superstring theory [4–6]. Being quadratic, the roots of the polynomial $\Upsilon[\Lambda]$ can be explicitly sorted out:

$$\Lambda_\pm=-\frac{1\pm\sqrt{1-4\lambda}}{2\lambda\,L^2}\qquad\text{then}\qquad\Delta=0\quad\Leftrightarrow\quad\lambda=\lambda_{\rm CS}:=\frac{1}{4}. \tag{10}$$

The CS subscript in $\lambda_{\rm CS}$ amounts for Chern–Simons, since that is the critical value of $\lambda$ for which the theory acquires an extra symmetry (in $d=5$) becoming a gauge theory for the AdS group [7]. For $0<\lambda<\lambda_{\rm CS}$ the theory has two AdS vacua[1]; $\Lambda_+$ is known to be unstable [8]. For $\lambda>\lambda_{\rm CS}$ there is no AdS vacuum.

The branch corresponding to $\Lambda_-$ is called the EH-branch, since it is continuously connected to the solution of General Relativity when $\lambda\to 0$. It has $\Upsilon'[\Lambda_-]>0$, which amounts to a positive effective Newton constant. In fact, each vacuum $\Lambda_i$ has a different *effective* Newton constant, $G_N^i\sim 1/\Upsilon'[\Lambda_i]$, whose sign coincides with that of $\Upsilon'[\Lambda_i]$. Thus, a given root of Lovelock gravity, $\Lambda_\star$, must satisfy

$$\Upsilon'[\Lambda_\star]>0, \tag{11}$$

[1] If $\lambda<0$, there is no a priori lower bound for it and it is clear that $\Lambda_+$ becomes positive.

in order to correspond to a vacuum that hosts gravitons propagating with the right sign of the kinetic term. Else, if $\Upsilon'[\Lambda_\star]$ is negative, we say that the corresponding vacuum is affected by Boulware–Deser (BD) instabilities.

On top of the maximally symmetric vacua, we are interested in shockwave backgrounds of Lovelock theory. We want to show that in the presence of a shockwave there is room for causality violation [9]. This will raise the question whether all possible values of Lovelock's couplings, $c_k$, lead to physically sensible theories of gravity. The shockwave solution on AdS, with cosmological constant $\Lambda_\star$, reads [9]

$$ds^2_{\text{AdS},sw} = \frac{L_\star^2}{z^2}\left(-du\,dv + d\mathbf{x}^2 + dz^2\right) + F(u)\,\varpi(\mathbf{x},z)\,du^2, \tag{12}$$

where $z = L_\star^2/r$ is the Poincaré radial direction, $u, v = x^0 \pm x^{d-1}$ are light-cone coordinates, and $\mathbf{x}$ are the remaining $d-3$ spatial directions. $L_\star$ is the AdS radius corresponding to the branch on top of which we construct the shockwave, $L_\star \sim (-\Lambda_\star)^{-1/2}$. We should think of $F(u)$ as a distribution with support in $u = 0$, which we will finally identify as a Dirac delta function, $F(u) = \delta(u)$.

The shock wave is parameterized by the function $\varpi(\mathbf{x}, z)$, obeying

$$2(d-3)\varpi + (d-6)z\partial_z\varpi - z^2(\partial_z^2 + \nabla_\perp^2)\varpi = 0, \tag{13}$$

where $\nabla_\perp^2$ is the Laplacian in the $\mathbf{x}$-space. This equation admits the following solutions, whose holographic counterpart will be briefly addressed later. The simplest profile

$$\varpi = \varpi_0\, z^{d-3}, \tag{14}$$

on the one hand, and the $\mathbf{x}$-dependent solution

$$\varpi = \varpi_0\,\frac{z^{d-3}}{\left(z^2 + (\mathbf{x}-\mathbf{x}_0)^2\right)^{d-2}}, \qquad \mathbf{x}_0 = \frac{\mathbf{n}}{1+|\mathbf{n}|^{d-2}}, \tag{15}$$

where $\mathbf{n}$ is a unit vector. We will use these shockwave profiles below.

## 2 Black Holes

The black holes of Lovelock theory were exhaustively studied in [10]. In this talk we will just discuss some salient features that are instrumental to their holographic applications. The solutions can be obtained from the ansatz [8, 11, 12]

$$ds^2 = -f(r)\,dt^2 + \frac{dr^2}{f(r)} + \frac{r^2}{L^2}\,d\Sigma^2_{\sigma,d-2}, \tag{16}$$

where $d\Sigma_{\sigma,d-2}$ is the metric of a $(d-2)$-dimensional manifold, $\mathscr{M}$, of negative, zero or positive constant curvature ($\sigma = -1, 0, 1$ parametrizing the different horizon topologies). A natural frame is given by

$$e^0 = \sqrt{f(r)}\, dt, \qquad e^1 = \frac{1}{\sqrt{f(r)}}\, dr, \qquad e^a = \frac{r}{L}\, \tilde{e}^a, \tag{17}$$

where $a = 2, \ldots, d-1$, and $\tilde{R}^{ab} = \sigma\, \tilde{e}^a \wedge \tilde{e}^b$. The Riemann 2-form reads

$$\begin{aligned} R^{01} &= -\frac{1}{2}\, f''(r)\, e^0 \wedge e^1, & R^{0a} &= -\frac{f'(r)}{2r}\, e^0 \wedge e^a, \\ R^{1a} &= -\frac{f'(r)}{2r}\, e^1 \wedge e^a, & R^{ab} &= -\frac{f(r)-\sigma}{r^2}\, e^a \wedge e^b. \end{aligned} \tag{18}$$

Strikingly enough, if we insert these expressions into the equations of motion, we get after some manipulations a quite simple ordinary differential equation—not for $f(r)$ but for $\Upsilon[g(r)]$,

$$\left[\frac{d}{d\log r} + (d-1)\right]\left(\sum_{k=0}^{K} c_k\, g^k\right) = 0, \tag{19}$$

where $g(r) := \frac{\sigma - f(r)}{r^2}$. It can be straightforwardly solved as

$$\Upsilon[g] = \mathrm{V}_{d-2}\, \frac{M}{r^{d-1}}, \tag{20}$$

where the integration constant, through the Hamiltonian formalism [13], can be seen to be the space-time mass $M$ times the volume $\mathrm{V}_{d-2}$ of the unit constant curvature manifold $\mathscr{M}$. The black hole solutions are implicitly (and analytically!) given by this polynomial equation. The variation of $r$ translates the $y$-intercept of $\Upsilon[g]$ rigidly, upwards. This leads to $K$ branches, $g_i(r)$, corresponding to the monotonous sections of $\Upsilon[g]$, associated with each $\Lambda_i$: $g_i(r \to \infty) = \Lambda_i$.

The existence of a black hole horizon requires $g_+ = 0$ for planar black holes, and, since $g_+ = \sigma / r_+^2$,

$$\Upsilon[g_+] = \mathrm{V}_{d-2}\, M\, |g_+|^{(d-1)/2}, \tag{21}$$

for spherical or hyperbolic black holes. In the case of non-planar black holes, the curve (21) can intersect the polynomial at different points. Several branches can display black holes with the same mass or temperature. This entails the possibility of a rich phase diagram, provided that the free energy or entropy of these solutions differ, which turns out to be the case [14–16].

The plethora of vacua and possibilities for the local behavior of the polynomial $\Upsilon[g]$ lead to a bestiary of black hole solutions that has been analyzed in depth [10].

We will just review some features of black holes belonging to the EH branch,[2] which are a sort of distorted Schwarzschild-AdS black holes. When real, the effective cosmological constant associated with this branch, $\Lambda_\star$, is negative and so the spacetime is asymptotically AdS, regardless of the sign of the cosmological constant appearing in the original Lagrangian.

Even though the EH-branch is just a deformation of the usual Schwarzschild-AdS black hole, it can be a quite dramatic one. For instance, it may happen that the polynomial has a minimum at $g_{\rm min} < 0$, such that $\Upsilon[g_{\rm min}] > 0$. Now, by derivation of (20) with respect to the radial variable,

$$g' = -(d-1)\,\mathrm{V}_{d-2}\,\frac{M}{r^d}\,\Upsilon'[g]^{-1}. \tag{22}$$

making clear that the metric is regular everywhere except at $r = 0$ and at points where $\Upsilon'[g] = 0$. A naked singularity would arise at large radius, $r_{\rm naked}$, where $g(r_{\rm naked}) = g_{\rm min}$. This case was first discussed in [17, 18] for third order Lovelock theory and planar topology, but the same applies in the general case for a vast region of the space of parameters that we call the *excluded region* (see Fig. 1). We will assume in what follows that the Lovelock couplings do not belong to the excluded region (in the LGB case, this simply means $\lambda \leq 1/4$).

For *hyperbolic* or *planar* topology, as this branch always crosses $g = 0$ with positive slope, it has always a horizon hiding the singularity of the geometry which is located either at $r = 0$ [(a) type] or at the value $r_\star$ corresponding to a maximum of $\Upsilon[g]$ [(b) type] for which $g(r_\star) = g_{\rm max} > 0$. Hyperbolic black holes can have a negative mass above a critical value that is nothing but an extremal solution.

The *spherical* case is quite more involved. For high enough mass, the existence of the horizon is ensured, but this is not the case in general. For the (a) type EH-branch the existence of the horizon is certain for arbitrarily low masses if $d > 2K+1$. The *critical* case, $d = 2K+1$, is more subtle. There will be a minimal mass $M_{\rm crit}$ related to the gravitational coupling $c_K$ below which a naked singularity appears [10]. For high enough orders of the Lovelock polynomial, *multi-horizon black holes* can exist but for the critical case, at some point, all of them disappear.

The case of a (b) type branch is simpler. There is a critical value of the mass, $M_\star$, for which the horizon coincides with the singularity, $r_+ = r_\star$. Below that mass a naked singularity forms. The simplest example is LGB gravity with $\lambda < 0$, where the EH branch has a maximum at $g_{\rm max} > 0$. This is a singularity at finite $r$ that may or may not be naked depending on the value of the mass in relation to $M_\star$,

$$M_\star = \frac{(-2\lambda L^2)^{(d-3)/2}}{2\,\mathrm{V}_{d-2}}(1-4\lambda). \tag{23}$$

[2] Recall that it is the branch crossing $g = 0$ with slope $\Upsilon'[0] = 1$.

For bigger masses we have a well defined horizon while below this bound the singularity is naked.

Some aspects of Lovelock black holes *thermodynamics* have been considered in [19]. The (outermost) event horizon has a well defined (positive) temperature

$$T = \frac{f'(r_+)}{4\pi} = \frac{r_+}{4\pi}\left[(d-1)\,\frac{\Upsilon[g_+]}{\Upsilon'[g_+]} - 2\,g_+\right]. \tag{24}$$

It is easy to see that large black holes have $M \sim \mathrm{V}_{d-2}\ T^{d-1}$. Then, $dM/dT > 0$ and they can be put in equilibrium with a thermal bath. They are locally thermodynamically stable. In general, this will not happen for small black holes, pointing towards the occurrence of Hawking-Page phase transitions, which have been already studied in the case of LGB gravity [20, 21]. One important feature regarding the classical stability of these black holes is that

$$\frac{dS}{dr_+} = \frac{1}{T}\frac{dM}{dr_+} \simeq r_+^{d-3}\ \Upsilon'\left[g_+\right], \tag{25}$$

and, as long as we are in a branch free from BD instabilities, both the radial derivative of the mass and the entropy are positive. This is necessary to discuss classical instability, since the heat capacity reads

$$C = \frac{dM}{dT} = \frac{dM}{dr_+}\frac{dr_+}{dT}, \tag{26}$$

and then the only factor that can be negative leading to an instability is

$$\frac{dT}{dr_+} = -\frac{g_+}{2\pi}\left[(d-2) - \frac{d-1}{2}\,\frac{\Upsilon[g_+]}{g_+\Upsilon'[g_+]}\left(1 + 2g_+\frac{\Upsilon''[g_+]}{\Upsilon'[g_+]}\right)\right]. \tag{27}$$

It is not easy to check classical stability in full generality for non-planar black holes, but in the regimes of *high* and *low* masses. In the simplest case of planar black holes, the thermodynamic variables do not receive any correction from the higher curvature terms in the action and the expression reduces to the usual formula

$$\frac{dT}{dr_+} = \frac{d-1}{4\pi L^2}. \tag{28}$$

This expression is manifestly positive. Therefore, these black holes are locally thermodynamically stable for all values of the mass. This is also the case for maximally degenerated Lovelock theories that admit a single (EH-)branch of black holes [22]. The entropy can be easily obtained by integrating (25),

$$S \simeq r_+^{d-2}\left(1 + \sum_{k=2}^{K} k\,c_k\,\frac{d-2}{d-2k}\,g_+^{k-1}\right), \tag{29}$$

and it coincides with the prescription obtained by other means such as the Wald entropy [23] or the euclideanized on-shell action [24]. For planar horizons this formula reproduces the proportionality of the entropy and the area of the event horizon, $S \simeq r_+^{d-2}$, whereas it gets corrections for other topologies. From these quantities we can now compute any other thermodynamic potential such as the Helmholtz free energy, $F = M - TS$,

$$F \simeq \frac{r_+^{d-1}}{\Upsilon'[g_+]} \sum_{k,m=0}^{K} \frac{2m-2k+1}{d-2k}\, k\, c_k\, c_m\, g_+^{k+m-1}. \tag{30}$$

This magnitude is relevant to analyze the global stability of the solutions for processes at constant temperature. As a function of $g_+$, it has a polynomial of degree $2K-1$ in the numerator. This is the maximal number of zeros that may eventually correspond to Hawking-Page-like phase transitions. Moreover, taking into account that (30) is a sum involving the whole set of branches of the theory, phase transitions involving jumps between different branches are expected [14–16].

## 3 Holography

The main motivation of our work in Lovelock theory is gaining a better understanding of some aspects of the AdS/CFT correspondence. Since the groundbreaking paper of Juan Maldacena [25], evidence has been accumulating towards the validity of the following bold statement: a theory of quantum gravity in AdS space-time is equal to a corresponding (dual) CFT living at the boundary. The relation between both descriptions of the same physical system is holographic.

A key ingredient of this highly nontrivial statement is given by the recipe to compute holographically correlation functions in the CFT [26,27]. Restricted to the stress–energy tensor, $T_{ab}(\mathbf{x})$, it reads

$$\mathscr{Z}\left[g_{\mu\nu}\right] \approx \exp\left(-\mathscr{I}[g_{\mu\nu}]\right) = \left\langle \exp\left( \int d\mathbf{x}\, \eta^{ab}(\mathbf{x})\, T_{ab}(\mathbf{x}) \right) \right\rangle_{\text{CFT}}, \tag{31}$$

where $\mathscr{Z}\left[g_{\mu\nu}\right]$ is the partition function of quantum gravity, and $g_{\mu\nu} = g_{\mu\nu}(z,\mathbf{x})$ such that $g_{ab}(0,\mathbf{x}) = \eta_{ab}(\mathbf{x})$. From this expression, correlators of the stress–energy tensor can be obtained by performing functional derivatives of the gravity action with respect to the boundary metric. This, in turn, is simply given by considering gravitational fluctuations around an asymptotically AdS configuration of the theory.

In the remainder of this presentation, we will investigate the uses of this framework in the case of Lovelock theory and extract some of its consequences.

### 3.1 CFT Unitarity and 2-Point Functions

Consider a CFT$_{d-1}$. The leading singularity of the 2-point function is fully characterized by the central charge $C_T$ [28]

$$\langle T_{ab}(\mathbf{x})\, T_{cd}(\mathbf{0})\rangle = \frac{C_T}{\mathbf{x}^{2(d-1)}}\, \mathscr{I}_{ab,cd}(\mathbf{x}), \tag{32}$$

where

$$\mathscr{I}_{ab,cd}(\mathbf{x}) = \frac{1}{2}\left( I_{ac}(\mathbf{x})\, I_{bd}(\mathbf{x}) + I_{ad}(\mathbf{x})\, I_{bc}(\mathbf{x}) - \frac{1}{d-1}\, \eta_{ab}\, \eta_{cd} \right), \tag{33}$$

whereas $I_{ab}(\mathbf{x}) = \eta_{ab} - 2\, x_a\, x_b/\mathbf{x}^2$. For instance, $C_T$ is proportional in a CFT$_4$ to the standard central charge $c$ that multiplies the (Weyl)$^2$ term in the trace anomaly, $C_T = 40\, c/\pi^4$.

The holographic computation of $C_T$ was performed in [29] for LGB, and in [30] for Lovelock theory. According to the AdS/CFT dictionary, it is sufficient[3] to take a metric fluctuation $h_{xy}(z, \mathbf{x}) := L_\star^2/z^2\ \phi(z, \mathbf{x})$ about empty AdS with cosmological constant $\Lambda_\star$. Expanding (1) to quadratic order in $\phi$, and evaluating it on-shell,

$$\mathscr{I}_{\text{quad}} = \frac{\Upsilon'[\Lambda_\star]}{2(-\Lambda_\star)^{d/2}} \int d\mathbf{x}\, z^{2-d}\, (\phi\, \partial_z \phi)\,. \tag{34}$$

Imposing the boundary conditions $\phi(0, \mathbf{x}) = \hat{\phi}(\mathbf{x})$, the full bulk solution reads

$$\phi(z, \mathbf{x}) = \frac{d}{d-2} \frac{\Gamma[d]}{\pi^{\frac{d-1}{2}}\, \Gamma\left[\frac{d-1}{2}\right]} \int d\mathbf{y}\, \frac{z^{d-1}}{(z^2 + |\mathbf{x}-\mathbf{y}|^2)^{d-1}}\, \mathscr{I}_{ab,cd}(\mathbf{x}-\mathbf{y})\, \hat{\phi}(\mathbf{y}). \tag{35}$$

Plugging this expression into $\mathscr{I}_{\text{quad}}$, we obtain

$$\mathscr{I}_{\text{quad}} = \frac{C_T}{2} \int d\mathbf{x} \int d\mathbf{y}\, \frac{\hat{\phi}(\mathbf{x})\, \mathscr{I}_{ab,cd}(\mathbf{x}-\mathbf{y})\, \hat{\phi}(\mathbf{y})}{|\mathbf{x}-\mathbf{y}|^{2(d-1)}}, \tag{36}$$

where $C_T$ is the central charge of the dual CFT$_{d-1}$,

$$C_T = \frac{d}{d-2} \frac{\Gamma[d]}{\pi^{\frac{d-1}{2}}\, \Gamma\left[\frac{d-1}{2}\right]} \frac{\Upsilon'[\Lambda_\star]}{(-\Lambda_\star)^{d/2}}. \tag{37}$$

[3] Other components of the metric fluctuations must be considered as well, but they are irrelevant for our current discussion.

The upshot of this computation in an AdS vacuum, $\Lambda_\star < 0$, is thought-provoking:

$$C_T > 0 \qquad \Longleftrightarrow \qquad \Upsilon'[\Lambda_\star] > 0. \tag{38}$$

The latter inequality, in the gravity side, corresponded to the generalized BD condition preventing ghost gravitons in the branch corresponding to the AdS vacuum with cosmological constant $\Lambda_\star$. Thereby, unitarity of the CFT and the absence of ghosts gravitons in AdS, seem to be the two faces of the same holographic coin.

## 3.2 Positivity of the Energy and 3-Point Functions

The form of the 3-point function of the stress-tensor in a $\text{CFT}_{d-1}$ is highly constrained. In [28, 31], it was shown that it can always be written in the form

$$\langle T_{ab}(\mathbf{x})\, T_{cd}(\mathbf{y})\, T_{ef}(\mathbf{z})\rangle = \frac{\left(\mathscr{A}\, \mathscr{I}^{(1)}_{ab,cd,ef} + \mathscr{B}\, \mathscr{I}^{(2)}_{ab,cd,ef} + \mathscr{C}\, \mathscr{I}^{(3)}_{ab,cd,ef}\right)}{|\mathbf{x}-\mathbf{y}|^{d-1}\, |\mathbf{y}-\mathbf{z}|^{d-1}\, |\mathbf{z}-\mathbf{x}|^{d-1}}, \tag{39}$$

where the specific form of the tensor structures $\mathscr{I}^{(i)}_{ab,cd,ef}$ is irrelevant for us. Ward identities relate 2-point and 3-point correlation functions, which means that the central charge $C_T$ can be written in terms of the parameters $\mathscr{A}$, $\mathscr{B}$ and $\mathscr{C}$,

$$C_T = \frac{\pi^{\frac{d-1}{2}}}{\Gamma\left[\frac{d-1}{2}\right]} \frac{(d-2)(d+1)\mathscr{A} - 2\mathscr{B} - 4d\,\mathscr{C}}{(d-1)(d+1)}. \tag{40}$$

Nicely enough, an holographic computation of the parameters entering the above formula can be tackled. It is certainly more intricate than that of $C_T$; thus we omit the details. The result is [18]

$$\mathscr{A} = \frac{\Gamma[d]}{\pi^{d-1}} \left( a_1(d) \frac{\Upsilon'[\Lambda_\star]}{(-\Lambda_\star)^{d/2}} - a_2(d) \frac{\Upsilon''[\Lambda_\star]}{(-\Lambda_\star)^{d/2-1}} \right), \tag{41}$$

and analogous expressions for $\mathscr{B}$ and $\mathscr{C}$, where $a_i(d)$ are rational functions of $d$, the space-time dimensionality.

A convenient parametrization of the 3-point function of the stress–energy tensor was introduced in [32]. The idea is to consider a localized insertion of the form[4] $\int d\omega\, e^{-i\omega t}\, \epsilon_{jk}\, T^{jk}(\mathbf{x})$, and to measure the energy flux at light-like future infinity along a certain direction $\mathbf{n}$,

[4] Notice that we are splitting time and space indices and, thus, from now on vectors are understood as $(d-2)$ dimensional objects.

$$\mathscr{E}(\mathbf{n}) = \lim_{r\to\infty} r^{d-2}\int_{-\infty}^{\infty} dt \;\; \mathbf{n}^i \; T^{\,0}_{\,i}(t, r\,\mathbf{n}). \tag{42}$$

Given a state created by a local gauge invariant operator $\mathscr{O} = \epsilon_{ij}\, T_{ij}$, since $\epsilon_{ij}$ is a symmetric and traceless polarization tensor, the final answer for the energy flux is fully constrained by conformal symmetry to be [29, 33]

$$\langle \mathscr{E}(\mathbf{n})\rangle = \frac{E}{\Omega_{d-3}}\left[1 + t_2\left(\frac{|\mathbf{n}\cdot\boldsymbol{\epsilon}|^2}{|\epsilon|^2} - \frac{1}{d-2}\right) + t_4\left(\frac{|\mathbf{n}\cdot\boldsymbol{\epsilon}\cdot\mathbf{n}|^2}{|\epsilon|^2} - \frac{2}{d(d-2)}\right)\right], \tag{43}$$

where $E$ is the total energy of the insertion, $\mathbf{n}\cdot\boldsymbol{\epsilon} = n_i\,\epsilon_{ik}$, $\mathbf{n}\cdot\boldsymbol{\epsilon}\cdot\mathbf{n} = n_i n_j \epsilon_{ij}$, and $|\epsilon|^2 = \epsilon^*_{ik}\epsilon_{ik}$, while $\Omega_{d-3}$ is the volume of a unit $(d-3)$-sphere. For any $\text{CFT}_{d-1}$, it is characterized by the two parameters $t_2$ and $t_4$. Being the quotient of 3-point and 2-point correlators, $\langle \mathscr{E}(\mathbf{n})\rangle$ is fully determined by the parameters $\mathscr{A}$, $\mathscr{B}$ and $\mathscr{C}$. In particular [29],

$$t_2 = \frac{2d}{d-1}\,\frac{d(d-3)(d+1)\,\mathscr{A} + 3(d-1)^2\,\mathscr{B} - 4(d-1)(2d-1)\,\mathscr{C}}{(d-2)(d+1)\,\mathscr{A} - 2\,\mathscr{B} - 4d\,\mathscr{C}}, \tag{44}$$

and a similar expression for $t_4$. We do not care about the latter for the following reason. If the $\text{CFT}_{d-1}$ is supersymmetric, $t_4$ vanishes [32, 34]. On the other hand, even though there is no proof in the literature showing that Lovelock theories admit a supersymmetric extension, it turns out that the holographic computation suggests that a $\text{CFT}_{d-1}$ with a weakly curved gravitational dual whose dynamics is governed by Lovelock theory has a null value of $t_4$ [18],

$$t_4 = 0 \qquad \Rightarrow \qquad \langle \mathscr{E}(\mathbf{n})\rangle = \frac{E}{\Omega_{d-3}}\left[1 + t_2\left(\frac{|\mathbf{n}\cdot\boldsymbol{\epsilon}|^2}{|\epsilon|^2} - \frac{1}{d-2}\right)\right]. \tag{45}$$

The existence of a minus sign in (45) leads to interesting constraints on $t_2$, by demanding that the energy flux be positive for any direction $\mathbf{n}$ and polarization $\epsilon_{ij}$. For the tensor, vector and scalar channels, we obtain, respectively,

$$t_2 \le d-2, \qquad t_2 \ge -\frac{2(d-2)}{d-4}, \qquad t_2 \ge -\frac{d-2}{d-4}. \tag{46}$$

The vector channel constraint is irrelevant. In any supersymmetric $\text{CFT}_{d-1}$, therefore, the parameter $t_2$ has to take values within the window

$$-\frac{d-2}{d-4} \le t_2 \le d-2, \tag{47}$$

if the energy flux at infinity is constrained to be positive. For instance, any $\mathscr{N} = 1$ supersymmetric $\text{CFT}_4$ has $|t_2| \le 3$, with

$$t_2 = 6\,\frac{c-a}{c} \qquad \Rightarrow \qquad \frac{1}{2} \leq \frac{a}{c} \leq \frac{3}{2}. \tag{48}$$

where $a$ and $c$ are the parameters entering the trace anomaly formula, the bound being saturated for free theories [32].

We can holographically compute $t_2$ by inserting a shockwave on AdS, which sources the field theory insertion, and considering a metric fluctuation $h_{xy}(z,\mathbf{x}) := L_\star^2/z^2\ \phi(z,\mathbf{x})$ about this background. The 3-point function follows from evaluating on-shell the effective action for the field $\phi$ on a particular shockwave solution. The relevant shockwave profile is given by (15), as discussed in [32]. Up to an overall factor, the cubic vertex is [29]

$$\mathscr{I}_{\text{cubic}} \sim C_T \int d\mathbf{x}\, du\, dv\ \sqrt{-g}\ \phi\ \partial_v^2\phi\ \varpi\ \left(1 - \frac{\Lambda_\star\, \Upsilon''(\Lambda_\star)}{\Upsilon'(\Lambda_\star)}\,\frac{T_2}{(d-3)(d-4)}\right), \tag{49}$$

where

$$T_2 = \frac{z^2(\partial_x^2\varpi + \partial_y^2\varpi) - 2z\partial_z\varpi - 4\varpi}{\varpi}. \tag{50}$$

The relevant graviton profile [29]

$$\phi(u=0,v,\mathbf{x},z) \sim e^{-iEv}\,\delta(\mathbf{x})\,\delta(z-1), \tag{51}$$

allows us to impose $\mathbf{x} = \mathbf{0}$ and $z = 1$ in (50), this yielding the result

$$T_2 = 2(d-1)(d-2)\left(\frac{n_x^2+n_y^2}{2} - \frac{1}{d-2}\right). \tag{52}$$

We therefore read off, by plugging (52) into (49) and comparing against the expression for $\langle\mathscr{E}(\mathbf{n})\rangle$ in (45), the holographic prescription for $t_2$ in Lovelock theory:

$$t_2 = -\frac{2(d-1)(d-2)}{(d-3)(d-4)}\,\frac{\Lambda_\star\,\Upsilon''[\Lambda_\star]}{\Upsilon'[\Lambda_\star]}, \tag{53}$$

and $t_4 = 0$. Needless to say, this is the same expression we would have gotten by simply plugging the holographic formulas of the parameters $\mathscr{A}$, $\mathscr{B}$ and $\mathscr{C}$ (41) into (44). Combining (47) and (53), we obtain [17, 18],

$$-\frac{d-2}{d-4} \leq -\frac{2(d-1)(d-2)}{(d-3)(d-4)}\,\frac{\Lambda_\star\,\Upsilon''[\Lambda_\star]}{\Upsilon'[\Lambda_\star]} \leq d-2. \tag{54}$$

For instance, Fig. 1 displays the two curves that establish the upper ($t_2 = 5$) and lower ($t_2 = -5/3$) limits of the allowed window for the case of cubic Lovelock theory in $d = 7$. It enables us to appreciate how tight this restriction is in terms of

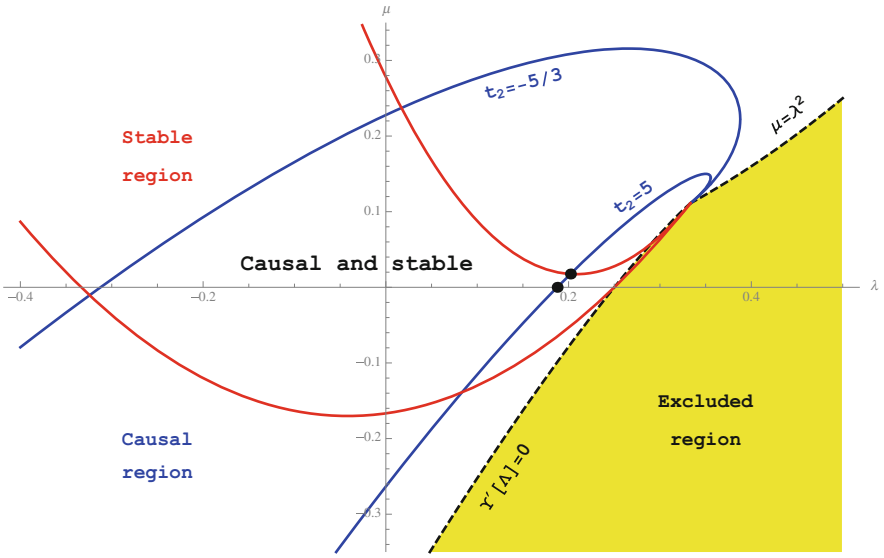


**Fig. 1** The allowed region of gravitational couplings by causality and stability for cubic Lovelock theory in $d = 7$ is displayed. The *black points* are the maximal values of $\lambda$ that can be attained in LGB [33, 36] and cubic Lovelock [17, 18] gravities, that are related to the lowest possible value of $\eta/s$ in a dual CFT$_6$ strongly coupled plasma [30]

the acceptable Lovelock couplings. In the $d = 5$ case, $-3 \leq t_2 \leq 3$, which together with the dependence of $t_2$ on the LGB coupling leads to [9, 35]

$$t_2 = 12\left(\frac{1}{\sqrt{1-4\lambda}} - 1\right) \qquad \Rightarrow \qquad -\frac{7}{36} \leq \lambda \leq \frac{9}{100}. \tag{55}$$

Notice, in particular, from (48), that $a = c$ corresponds to vanishing $t_2$ and $\lambda$. This suggests that higher curvature corrections are mandatory to study, for instance, four dimensional strongly coupled CFTs with $a \neq c$ under the light of the gauge/gravity correspondence.

## 3.3 *Gravitons Thrown onto Shock Waves Must Age Properly*

Consider a shock wave with profile given in (14) in AdS with cosmological constant $\Lambda_\star$. We would like to analyze the following process. A highly energetic tensor graviton will be thrown from the boundary $z = 0$ towards the shock wave.[5] This

[5]The same computation can be carried out with vector and scalar gravitons, and the result in these two cases will be obvious from the present analysis.

amounts to perturbing the relevant metric up to quadratic order and keeping only those terms involving derivatives like $\partial_u^2$, $\partial_v^2$ and $\partial_u\partial_v$ acting on the perturbation $\phi$:

$$\partial_u\partial_v\phi + \varpi_0\, L^2\left(1+\frac{2(d-1)}{(d-3)(d-4)}\frac{\Lambda_\star\,\Upsilon''[\Lambda_\star]}{\Upsilon'[\Lambda_\star]}\right)\delta(u)\, z^{d-1}\,\partial_v^2\phi = 0, \tag{56}$$

assuming $\Upsilon'[\Lambda_\star] \neq 0$, which means that the vacuum we are dealing with is non-degenerated. Causality problems arise when the coefficient of $\partial_v^2\phi$ becomes negative. In fact, notice that (56) is a free wave equation except at the locus $u = 0$. We must only care about the discontinuity of $P_z$ for a graviton colliding the shock wave [9, 30]

$$\Delta P_z = \frac{(d-1)}{z}|P_v|\left(\frac{z}{L}\right)^2 z^{d-3}\left(1+\frac{2(d-1)}{(d-3)(d-4)}\frac{\Lambda_\star\,\Upsilon''[\Lambda_\star]}{\Upsilon'[\Lambda_\star]}\right), \tag{57}$$

while the shift in the light-like time is [18]

$$\Delta v = \left(\frac{z}{L}\right)^2 z^{d-3}\left(1+\frac{2(d-1)}{(d-3)(d-4)}\frac{\Lambda_\star\,\Upsilon''[\Lambda_\star]}{\Upsilon'[\Lambda_\star]}\right). \tag{58}$$

Thus, if the quantity in parenthesis is negative, a graviton thrown into the bulk from the AdS boundary, bounces back, landing outside its own light-cone! This is understood as a signal of causality violation. If we repeat this computation for vector and scalar polarizations, we end up with the constant

$$-\frac{d-2}{d-4} \leq -\frac{2(d-1)(d-2)}{(d-3)(d-4)}\frac{\Lambda_\star\,\Upsilon''[\Lambda_\star]}{\Upsilon'[\Lambda_\star]} \leq d-2. \tag{59}$$

These are exactly the allowed values for $t_2$—once the holographic dictionary has been put into work, that ensure positivity of the energy in the dual CFT. This ends up, once again, in an alluring match between gravity and gauge theory.

### 3.4 Black Holes and Plasma Instabilities

We could have obtained the results of the previous subsection following a different approach. Consider Lovelock black holes and study the potentials felt by high momentum gravitons exploring the bulk. Close to the boundary, $z\ell^2 z_+$, for the different helicities [17, 18]

$$c^2_{\text{tensor}} \approx 1 + \frac{1}{L_\star^2\Lambda_\star}\frac{z^{d-1}}{z_+^{d-1}}\left[1+\frac{2(d-1)}{(d-3)(d-4)}\frac{\Lambda_\star\,\Upsilon''[\Lambda_\star]}{\Upsilon'[\Lambda_\star]}\right], \tag{60}$$

$$c^2_{\text{vector}} \approx 1 + \frac{1}{L^2_\star \Lambda_\star} \frac{z^{d-1}}{z_+^{d-1}} \left[ 1 - \frac{(d-1)}{(d-3)} \frac{\Lambda_\star \Upsilon''[\Lambda_\star]}{\Upsilon'[\Lambda_\star]} \right], \tag{61}$$

$$c^2_{\text{scalar}} \approx 1 + \frac{1}{L^2_\star \Lambda_\star} \frac{z^{d-1}}{z_+^{d-1}} \left[ 1 - \frac{2(d-1)}{(d-3)} \frac{\Lambda_\star \Upsilon''[\Lambda_\star]}{\Upsilon'[\Lambda_\star]} \right]. \tag{62}$$

The argument proceeds as follows [37]. Notice that the potentials are normalized in such a way that their boundary value is 1, while they need to vanish at the black hole horizon. These potentials can be understood as the square of the local speed of gravitons with the corresponding polarization. Even though there is no problem with a graviton whose local speed surpass that of light measured at the boundary, any excess would entail the existence of a local maximum.

Therefore, the graviton energy can be fine-tuned in such a way that it stays an arbitrarily large period of time at the top of the potential. Without the need of an explicit knowledge of the geodesic, it is clear that the average speed of the graviton will be bigger than the speed of light at the boundary. Since the graviton bounces back into the boundary, it means that there would be a corresponding excitation in the dual gauge theory that becomes superluminal. This should be forbidden in any sensible theory that respects the principle of relativity.

The conditions $c^2_{\text{tensor}}, c^2_{\text{scalar}} \leq 1$ in the vicinity of the boundary lead to the same constraints found before. We can argue that this is due to the fact that the shockwave analysis is related to the current one through a Penrose limit. A more physical interpretation would be that causality violation is not linked to the existence of a black hole solution since it is not due to thermal effects.

Once we consider the current setup, there is a second source for pathologies. If any of the squared potentials becomes negative anywhere, either close to the black hole horizon or deep into the bulk, an imaginary local speed of light will reflect an instability of the system. This ceases to exist in the absence of a black hole. Thus, it seems natural to identify it with a thermal feature of the CFT. They should correspond to plasma instabilities [29]. Analogously to what happens with the restrictions coming from the window of allowed values for $t_2$, these restrictions further constrain the values that Lovelock couplings can take in a sensible theory [30]. This is explicitly shown in Fig. 1 for the case of cubic Lovelock theory in $d = 7$. There, the region of Lovelock couplings leading to causal and stable physics is given by a connected and compact vicinity of the EH-point ($\lambda = \mu = 0$).

## 4 Final Comments

The study of higher curvature gravity in the context of the AdS/CFT correspondence appears, at the least, as a territory worth exploring. It allows to further understand how profound concepts of quantum field theory might be linked, holographically,

to comparable deep concepts in the realm of gravity. Some examples were briefly presented above, such as the relation between positivity of the energy in the CFT and a certain kind of causality violation in the dual gravitational theory. We have not discussed, although they exist [30], other sources of causality violation occurring in the bulk, which do not seem to be related to pathologies inherited from the 3-point stress–energy tensor correlators in the dual CFT.

Lovelock theories are remarkable in that lots of physically relevant information is encoded in the polynomial $\Upsilon[g]$. BD instabilities, for instance, can be simply written as $\Upsilon'[\Lambda_\star] < 0$, which has a beautiful counterpart telling us that the central charge of the dual CFT, $C_T$, has to be positive. This is unitarity. Now, $\Upsilon'[\Lambda_\star]$ is the asymptotic value of the quantity $\Upsilon'[g]$, the latter being meaningful in the interior of the geometry, and positive along the corresponding branch. Recalling that naked singularities take place at extremal points of $\Upsilon[g]$ further suggests that $\Upsilon'[g]$ might be a meaningful entry in the holographic dictionary (see [38] for related ideas).

In spite of the higher dimensional nature of Lovelock theory, it is important to mention that there are lower dimensional gravities, dubbed *quasi-topological*, whose black hole solutions are alike those discussed in this talk. Many of the results presented above are pertinent in those "more physical" setups of AdS/CFT [39].

**Acknowledgements** I am very pleased to thank Xián Camanho, Gastón Giribet, Andy Gomberoff and Miguel Paulos for collaboration on this subject and most interesting discussions held throughout the last few years. I would also like to thank the organizers of the Spanish Relativity Meeting in Portugal (ERE2012) for the invitation to present my work and for the nice scientific and friendly atmosphere that prevailed during my stay in Guimarães. This work is supported in part by MICINN and FEDER (grant FPA2011-22594), by Xunta de Galicia (Consellería de Educación and grant PGIDIT10PXIB206075PR), and by the Spanish Consolider-Ingenio 2010 Programme CPAN (CSD2007-00042). The Centro de Estudios Científicos (CECs) is funded by the Chilean Government through the Centers of Excellence Base Financing Program of Conicyt.

## References

1. D. Lovelock: The Einstein tensor and its generalizations. J. Math. Phys. **12**, 498 (1971).
2. C. Lanczos: A Remarkable property of the Riemann-Christoffel tensor in four dimensions. Annals Math. **39**, 842 (1938).
3. G. Giribet: The large D limit of dimensionally continued gravity. arXiv:1303.1982 [gr-qc].
4. C. P. Bachas, P. Bain and M. B. Green: Curvature terms in D-brane actions and their M theory origin. JHEP **9905**, 011 (1999) [hep-th/9903210].
5. Y. Kats and P. Petrov: Effect of curvature squared corrections in AdS on the viscosity of the dual gauge theory. JHEP **0901**, 044 (2009) [arXiv:0712.0743 [hep-th]].
6. A. Buchel, R. C. Myers and A. Sinha: Beyond $\eta/s = 1/4\pi$. JHEP **0903**, 084 (2009) [arXiv:0812.2521 [hep-th]].
7. A. H. Chamseddine: Topological gauge theory of gravity in five-dimensions and all odd dimensions. Phys. Lett. B **233**, 291 (1989).
8. D. Boulware and S. Deser: String generated gravity models. Phys. Rev. Lett. **55**, 2656 (1985).
9. D. M. Hofman: Higher derivative gravity, causality and positivity of energy in a UV complete QFT. Nucl. Phys. B **823**, 174 (2009) [arXiv:0907.1625 [hep-th]].

10. X. O. Camanho and J. D. Edelstein, A Lovelock black hole bestiary. Class. Quant. Grav. **30**, 035009 (2013) [arXiv:1103.3669 [hep-th]].
11. J. T. Wheeler: Symmetric solutions to the Gauss-Bonnet extended Einstein equations. Nucl. Phys. B **268**, 737 (1986).
12. J. T. Wheeler: Symmetric solutions to the maximally Gauss-bonnet extended Einstein equations. Nucl. Phys. B **273**, 732 (1986).
13. D. Kastor, S. Ray and J. Traschen: Mass and Free Energy of Lovelock Black Holes. Class. Quant. Grav. **28**, 195022 (2011) [arXiv:1106.2764 [hep-th]].
14. X. O. Camanho, J. D. Edelstein, G. Giribet and A. Gomberoff: New type of phase transition in gravitational theories. Phys. Rev. D **86**, 124048 (2012) [arXiv:1204.6737 [hep-th]].
15. X. O. Camanho, J. D. Edelstein, G. Giribet and A. Gomberoff: Generalized phase transitions in Lovelock theory. To appear (2013).
16. X. O. Camanho: Phase transitions in general gravity theories. These Proceedings (2013).
17. J. de Boer, M. Kulaxizi and A. Parnachev: Holographic Lovelock gravities and black holes. JHEP **1006**, 008 (2010) [arXiv:0912.1877 [hep-th]].
18. X. O. Camanho and J. D. Edelstein: Causality in AdS/CFT and Lovelock theory. JHEP **1006**, 099 (2010) [arXiv:0912.1944 [hep-th]].
19. R. -G. Cai: A Note on thermodynamics of black holes in Lovelock gravity. Phys. Lett. B **582**, 237 (2004) [hep-th/0311240].
20. S. 'i. Nojiri and S. D. Odintsov: Anti-de Sitter black hole thermodynamics in higher derivative gravity and new confining deconfining phases in dual CFT. Phys. Lett. B **521**, 87 (2001) [Erratum-ibid. B **542**, 301 (2002)] [hep-th/0109122].
21. Y. M. Cho and I. P. Neupane: Anti-de Sitter black holes, thermal phase transition and holography in higher curvature gravity. Phys. Rev. D **66**, 024044 (2002) [hep-th/0202140].
22. J. Crisostomo, R. Troncoso and J. Zanelli: Black hole scan. Phys. Rev. D **62**, 084013 (2000) [hep-th/0003271].
23. T. Jacobson and R. C. Myers: Black hole entropy and higher curvature interactions. Phys. Rev. Lett. **70**, 3684 (1993) [hep-th/9305016].
24. R. C. Myers and J. Z. Simon: Black hole thermodynamics in Lovelock gravity. Phys. Rev. D **38**, 2434 (1988).
25. J. M. Maldacena: The Large N limit of superconformal field theories and supergravity. Adv. Theor. Math. Phys. **2**, 231 (1998) [hep-th/9711200].
26. S. S. Gubser, I. R. Klebanov and A. M. Polyakov: Gauge theory correlators from noncritical string theory. Phys. Lett. B **428**, 105 (1998) [hep-th/9802109].
27. E. Witten: Anti-de Sitter space and holography. Adv. Theor. Math. Phys. **2**, 253 (1998) [hep-th/9802150].
28. H. Osborn and A. C. Petkou: Implications of conformal invariance in field theories for general dimensions. Annals Phys. **231**, 311 (1994) [hep-th/9307010].
29. A. Buchel, J. Escobedo, R. C. Myers, M. F. Paulos, A. Sinha and M. Smolkin: Holographic GB gravity in arbitrary dimensions. JHEP **1003**, 111 (2010) [arXiv:0911.4257 [hep-th]].
30. X. O. Camanho, J. D. Edelstein and M. F. Paulos: Lovelock theories, holography and the fate of the viscosity bound. JHEP **1105**, 127 (2011) [arXiv:1010.1682 [hep-th]].
31. J. Erdmenger and H. Osborn: Conserved currents and the energy momentum tensor in conformally invariant theories for general dimensions. Nucl. Phys. B **483**, 431 (1997) [hep-th/9605009].
32. D. M. Hofman and J. Maldacena: Conformal collider physics: Energy and charge correlations. JHEP **0805**, 012 (2008) [arXiv:0803.1467 [hep-th]].
33. X. O. Camanho and J. D. Edelstein: Causality constraints in AdS/CFT from conformal collider physics and Gauss-Bonnet gravity. JHEP **1004**, 007 (2010) [arXiv:0911.3160 [hep-th]].
34. M. Kulaxizi and A. Parnachev: Supersymmetry constraints in holographic gravities. Phys. Rev. D **82**, 066001 (2010) [arXiv:0912.4244 [hep-th]].
35. A. Buchel and R. C. Myers: Causality of holographic hydrodynamics. JHEP **0908**, 016 (2009) [arXiv:0906.2922 [hep-th]].

36. J. de Boer, M. Kulaxizi and A. Parnachev: $AdS_7/CFT_6$, Gauss-Bonnet gravity, and viscosity bound. JHEP **1003**, 087 (2010) [arXiv:0910.5347 [hep-th]].
37. M. Brigante, H. Liu, R. C. Myers, S. Shenker and S. Yaida: The viscosity bound and causality violation. Phys. Rev. Lett. **100**, 191601 (2008) [arXiv:0802.3318 [hep-th]].
38. M. F. Paulos: Holographic phase space: $c$-functions and black holes as renormalization group flows. JHEP **1105**, 043 (2011) [arXiv:1101.5993 [hep-th]].
39. R. C. Myers, M. F. Paulos and A. Sinha. Holographic studies of quasi-topological gravity. JHEP **1008**, 035 (2010) [arXiv:1004.2055 [hep-th]].

# Braneworld Black Holes

**Pau Figueras**

**Abstract** In this article we review the present status of the numerical construction of black holes in the Randall–Sundrum II braneworld model. After reviewing the new numerical methods to solve the elliptic Einstein equations, we numerically construct a black hole solution in five-dimensional anti-de Sitter ($AdS_5$) space whose boundary geometry is conformal to the four-dimensional Schwarzschild solution. We argue that such a solution can be viewed as the infinite radius limit of a braneworld black hole, and we provide convincing evidence for its existence. By deforming this solution in AdS we can then construct braneworld black holes of various sizes. We find that standard $4d$ gravity on the brane is recovered when the radius of the black hole on the brane is much larger than the radius of the bulk AdS space.

## 1 Introduction

String theory is the best candidate for a theory of quantum gravity but its mathematical consistency requires the existence of extra spatial dimensions beyond the three that we observe. Almost a century ago Kaluza and Klein (KK) offered an attractive way of dealing with these extra (and yet unobserved) dimensions and obtain an effective theory at low energies which is compatible with observations: if these extra dimensions are compact and sufficiently small (naturally of the Planck radius, $\ell_P \sim 10^{-33}$ cm) then, in four dimensions, they should manifest in experiments as a tower of massive particles with masses $\sim 1/\ell_P$ and therefore not detectable in present day particle accelerators.

P. Figueras (✉)
DAMTP, Centre for Mathematical Sciences, Wilberforce Rd., Cambridge CB3 0WA, UK
e-mail: p.figueras@damtp.cam.ac.uk

A. García-Parrado et al. (eds.), *Progress in Mathematical Relativity, Gravitation and Cosmology*, Springer Proceedings in Mathematics & Statistics 60,
DOI 10.1007/978-3-642-40157-2_3, 

In [1,2] Randall and Sundrum proposed a remarkable alternative to KK compactification in which the extra dimensions are non-compact. In the Randall–Sundrum infinite braneworld model (henceforth RSII) [2] one takes two copies of $AdS_5$ and glues them together along a common boundary, the brane. This hypersurface (the brane) represents our $4d$ world and all Standard Model particles are pinned there, except for gravity which can propagate in all dimensions. This model provides a natural solution to the hierarchy problem since gravity is dissolved in the extra dimension. This construction is motivated by String Theory, where dynamical $(d+1)$-dimensional objects, known as $d$-branes, with gauge fields living on their worldvolume, are fundamental objects in the theory.

Considering small fluctuations of the metric around the aforementioned background, Randall and Sundrum showed that there exists a zero mode of the graviton localised on the brane, together with continuum of *massive* KK modes. Moreover, it was shown [3, 4] that in the linearised regime, an observer living on the brane would experiment standard $4d$ gravity plus power law corrections, as opposed to the exponential corrections that arise in standard KK theory.

However, to validate the RSII model as viable description of our universe, one has to consider the strong field regime. In particular, one would like to check if there exist black holes in this model and, if so, understand their properties and compare them to astrophysical observations. Chamblin et al. [5] was the first one to consider black holes in RSII, but their solutions are singular and therefore unphysical. On the other hand, Emparan et al. [6] constructed an explicit (and regular) braneworld black hole solution in $3+1$ bulk dimensions and verified that standard $3d$ gravity is recovered on the brane. The phenomenologically more interesting case of a $4+1$ braneworld black hole remained elusive to analytical methods and numerical techniques were used to construct such solutions. However, the works of Kudoh et al. [7–10] did not succeed to numerically construct black holes on branes in the phenomenologically interesting regime. In fact, Yoshino [9] even conjectured that no non-extremal braneworld black holes of any size should exist.

Braneworld black holes can be understood using the AdS/CFT correspondence as quantum corrected black holes [11]. Using free field theory intuition and motivated by the previous unsuccessful attempts to numerically construct static braneworld black holes, Emparan et al. [11] conjectured that no large (compared to the size of the parent AdS space) static non-extremal braneworld black holes could exist since they would Hawking radiate and therefore be dynamical. However, Fitzpatrick et al. [12] provided counterarguments. We should point of that authors of [13–15] constructed the near horizon geometry of extremal braneworld black holes of any size. These black holes evade the non-existence conjecture because being extremal they do not Hawking radiate in the first place.

This was the status of braneworld black holes before the work of Figueras et al. [16, 17]. In this article, we will review and improve these works, which show that not only large braneworld black holes exist, but also that $4d$ gravity on the brane is recovered. Recently, Abdolrahimi et al. [18] appeared (see also [19]) which uses a different numerical method than that of [16, 17]. Furthermore, their results

support those of [16,17], which is rather non-trivial. Therefore, the present evidence suggests that the RSII model seems to provide a viable description of our universe even in the strong gravity regime.

## 2 The Harmonic Einstein Equations

In this section we review the numerical method that we used to construct the braneworld black holes. This method was first proposed in [20] to construct static spacetimes containing black holes and then extended in [21] to the stationary case (see [22] for review). Recently the method has been further extended to construct stationary spacetimes with non-Killing horizons [23] (see also [24]).

For simplicity, we start considering the Einstein vacuum equations in $D$-dimensions:

$$R_{ab} = 0. \tag{1}$$

As we shall see shortly, adding a cosmological constant (positive or negative) and/or matter is straightforward. Furthermore, in this article we will only consider *static* spacetimes $(\mathscr{M}, g)$.

Naively, it appears that in (1) there are as many equations as metric components and hence one would be tempted to think that they completely determine the metric. However, closer inspection reveals that this is not the case; the reason is that because of the underlying diffeomorphism invariance of the the theory, for *any* metric the corresponding Ricci tensor satisfies the Bianchi identity. In the general situation, the Bianchi identity contains $D$ equations, and hence in (1) there are only $D(D-1)/2$ non-trivial equations, rendering the problem for the metric underdetermined. The difficulty with (1) is that this is not an elliptic equation for the metric. More precisely, (1) is only an elliptic equation for the dynamical degrees of freedom but pure gauge modes are annihilated by the principle symbol of the operator. Therefore, we have to fix the gauge in order to turn (1) into an elliptic equation that can be solved numerically. The proposal of [20] is just one particular choice of gauge, but as we shall see shortly, it has great advantages as far as the numerical implementation is concerned.

The proposal of [20] is as follows. Instead of considering (1) on $(\mathscr{M}, g)$, we consider a modified set of equations known as the "harmonic" or "DeTurck" Einstein equations:

$$R_{ab} - \nabla_{(a}\xi_{b)} = 0, \qquad \xi^a = g^{bc}(\Gamma^a_{\ bc} - \bar{\Gamma}^a_{\ bc}), \tag{2}$$

where $\bar{\Gamma}$ is a fixed reference connection on $\mathscr{M}$, which for simplicity we take to be the Levi–Civita connection of a reference metric $\bar{g}$ on $\mathscr{M}$. The virtue of (2) is that the principle symbol of the operator is simply $P = -\frac{1}{2}g^{ab}\partial_a\partial_b$ and hence, for any

*Riemannian* metric $g$, (2) is a manifestly elliptic equation for the metric components and, as such, can be solved as a standard boundary value problem.

Clearly (2) is equivalent to (1) iff $\xi^a = 0$ everywhere on the spacetime manifold $\mathscr{M}$.[1] This is precisely the gauge condition that we shall be imposing and it provides $D$ local equations for the spacetime coordinates. More precisely, $\xi^a = 0$ is equivalent to $\Delta_g x^a = H^a$, where $\Delta_g$ is the scalar Laplacian and the source $H^a$ is specified in terms of the reference metric $\bar{g}$ as $H^a = -g^{bc}\bar{\Gamma}^a_{\ bc}$. Therefore, the gauge choice that we are implementing is closely related to the celebrated generalised harmonic gauge [25–28]. There is, however, an important difference: whilst in generalised harmonic gauge one prescribes the sources $H^a$, which in general are not tensors on $\mathscr{M}$, in our method the sources depend on both the metric $g$ and the reference metric $\bar{g}$.

Whilst a solution to the Einstein equations (1) in our gauge $\xi^a = 0$ solves the harmonic Einstein equations (2), the converse is not true. In fact, there can exist solutions to (2) with $\xi^a \neq 0$ and these are known as Ricci solitons. Since our ultimate goal is to solve (2) as a boundary value problem and find Einstein metrics instead of Ricci solitons, we have to supplement (2) with boundary conditions compatible with $\xi^a = 0$ at the boundary whilst preserving the ellipticity of the problem.[2] We will come back to this point when we consider the concrete problem of numerically constructing braneworld black holes. Having specified suitable boundary conditions, the existence of Ricci solitons on $\mathscr{M}$ is constrained by the fact that $\xi^a$ has to satisfy the following manifestly elliptic equation:

$$\nabla^2 \xi^a + R^a_{\ b}\xi^b = 0. \tag{3}$$

This is a well-posed boundary value problem for $\xi^a$ and, for boundary conditions compatible with $\xi^a = 0|_{\partial\mathscr{M}}$, it always admits the zero solution.

Before we continue the discussion about the existence of Ricci solitons, we note that adding a cosmological constant term to the Einstein equations (1) does not change the character of the equations because such a term has no derivatives of the metric. Obviously the same is true for the harmonic Einstein equations (2). Therefore, from now on we will consider the harmonic Einstein equations augmented with a cosmological constant term, since these are the equations that we will have to solve for finding black holes on branes:

$$R^H_{ab} \equiv R_{ab} - \Lambda\, g_{ab} - \nabla_{(a}\xi_{b)} = 0. \tag{4}$$

[1] In this discussion we are implicitly assuming that $\xi^a$ is not a Killing vector.

[2] In Riemannian manifolds with boundaries, Anderson [29] has shown that imposing $\xi^a = 0$ and Dirichlet or Neumann conditions for the induced metric on an given boundary gives rise to an ill posed problem.

It turns out that in favourable circumstances and for suitable boundary conditions one can prove that no Ricci solitons exist on $\mathscr{M}$. For instance, Bourguignon [30] proved that there are no Ricci solitons on a compact manifold without boundaries for any choice of gauge fixing vector $\xi^a$. More recently, Figueras et al. [16] proved a similar statement for non-compact and *static* spacetimes with different asymptotics of interest (flat, Kaluza-Klein and AdS). Their argument is as follows. Contracting (3) with $\xi_a$ and using (4) one finds

$$\nabla^2\phi + \xi^a\partial_a\phi = -2\,\Lambda\,\phi + 2\,(\nabla^a\xi^b)(\nabla_a\xi_b), \qquad \phi = \xi^a\xi_a. \tag{5}$$

For static spacetimes with a non-positive cosmological constant ($\Lambda \leq 0$), the right hand side of this equation is non-negative and its solutions are governed by a maximum principle. Therefore, if $\phi$ is non-constant, its maximum must be attained at the boundary and the normal outer gradient there must be positive. Then, imposing suitable regularity conditions and for flat, Kaluza-Klein or AdS asymptotic boundary conditions, one shows that $\phi = 0$ at $\partial\mathscr{M}$, from which it follows that $\phi = 0$ everywhere. From this and the fact that the metric is static, one then deduces that $\xi^a = 0$ everywhere on $\mathscr{M}$.

As we shall see later in the context of the numerical construction of braneworld black holes, the result of Figueras et al. [16] does not apply for the boundary conditions that one has to impose on the brane and in this case the existence of Ricci solitons cannot be ruled out a priori. However, because (4) is elliptic, then for fixed boundary conditions there exists a locally (in the space of solutions) unique solution. Therefore, it should always be possible to tell an Einstein metric from a Ricci soliton. In practice, a posteriori we can check whether $\xi^a \to 0$ in the continuum limit. Needless to say, in the numerical results that we will present later we found no evidence of Ricci solitons.

## 2.1 Methods for Solving the Harmonic Einstein Equations

In this subsection we will briefly review two general algorithms for solving the harmonic Einstein equations (2). The first one is based on relaxation whilst the second one is based on a root finding algorithm.

A standard algorithm to solve a non-linear elliptic equation is to simulate the associated diffusion equation; then, fixed points of the diffusion equation are solutions to the original elliptic equation. In the present context of solving the harmonic Einstein equations (4), the metric is evolved according to the diffusion equation

$$\frac{\partial}{\partial\lambda}\,g_{ab}(\lambda) = -2\,R^H_{ab}, \tag{6}$$

where $\lambda$ is the diffusion time. In the mathematics literature, (6) is known as the Ricci–DeTurck equation and it is diffeomorphic to Hamilton's famous Ricci flow equation. It is worth noting we want to solve (2) to find static (or stationary) spacetimes containing a black hole, and therefore the metric $g$ Lorentzian. However, because (2) is elliptic then (6) is a well-posed parabolic equation.

The great advantage of this algorithm is that it is very easy to implement and, because it is diffeomorphic to Ricci flow, it does not depend on the choice of reference metric. However, as discussed in [20], some black hole spacetimes may be unstable fixed points of Ricci flow. The stability of a fixed point under the Ricci–DeTurck flow is determined by the spectrum of the Lichnerowicz operator, $\Delta_L$, about the fixed point. If $\Delta_L$ admits negative modes, then small perturbations about the fixed point grow exponentially with the diffusion time and any initial data that does not coincide with the fixed point metric will be diverted away from the latter. It is well known that for some black hole spacetimes, $\Delta_L$ admits negative modes [31]. Even in this situation one may still use (6) to find Einstein metrics, but the initial data has to be suitably fine-tuned so that the flow happens on a hypersurface (in the space of geometries) orthogonal to the negative modes. See [20] for more details.

The other standard algorithm to solve (2) (or (4)), is Newton's method. This algorithm is more difficult to implement in practice than Ricci flow and its basin of attraction depends on the choice of reference metric. On the other hand, it is insensitive to the presence of negative modes and it converges much faster to the fixed point. In this method, one starts with an initial guess $g^{(old)}$ that does not solve (2) and then iteratively corrects it:

$$g_{ab}^{(new)} = g_{ab}^{(old)} + \epsilon\, h_{ab}, \qquad (\Delta_H h)_{ab} = -R^H_{ab}[g^{(old)}], \tag{7}$$

where $\Delta_H$ is the linearisation of $R^H_{ab}$ around a given background metric (not necessarily Einstein) and $\epsilon$ is a parameter (generically between 0 and 1) that controls the size of the correction. Newton's method is basically a root finding algorithm and if the initial guess is sufficiently close to the actual solution, Newton's method will converge to it. The performance of Newton's method is not affected by the presence of positive or negative modes of $\Delta_H$; only zero modes could cause problems, but because the problem is elliptic, boundary conditions should remove all of them (in fact, this is how an elliptic problem is defined).

## 3 An Aside: AdS/CFT on Black Hole Backgrounds

In this section we will use AdS/CFT to construct the gravitational dual of $\mathcal{N} = 4$ super Yang-Mills (SYM) on the background of the $4d$ Schwarzschild black hole in a certain vacuum state. At this stage such a solution may seem unrelated to the problem of constructing braneworld black holes, but as we shall see later, large braneworld black holes can be understood as perturbations of this solution.

### 3.1 Setup

We want to find a static solution to the Einstein equations in five dimensions with a negative cosmological constant that is asymptotically locally AdS, with a metric on the conformal boundary in the same conformal class as $4d$ Schwarzschild. Furthermore, far from the conformal boundary we want the spacetime to approach the Poincare horizon of AdS. With these assumptions, the isometry group of the spacetime is $R \times SO(3)$, and the most general metric with this symmetry (which is closed under diffeomorphisms that preserve it) is given by

$$ds^2 = \frac{\ell^2}{f(x)^2}\Big( -4\, r^2\, f(r)^2\, dt^2 + x^2\, g(x)\, e^S\, d\Omega_{(2)}^2 + \frac{4}{f(r)^2}\, e^{T+r^2 A}\, dr^2 + \frac{4}{g(x)}\, e^{S+x^2 B}\, dx^2 + \frac{2\, r\, x\, F}{f(r)}\, dr\, dx\Big), \tag{8}$$

where $f(\xi) = 1 - \xi^2$ and $g(x) = 2 - x^2$, and the range of the coordinates is $r, x \in [0, 1]$. The functions $X = \{T, S, A, B, F\}$ are assumed to be smooth functions of $r$ and $x$, and they are the unknowns. With our choice of coordinates, $r = 0$ and $x = 0$ correspond to location of the horizon of the black hole and the axis of symmetry respectively, and smoothness there requires that all functions $X$ have to satisfy Neumann boundary conditions. $r = 1$ is the Poincare horizon and we impose a Dirichlet boundary condition $X = 0$ there so that the metric reduces to that of the Poincare horizon of $AdS_5$. Finally, $x = 1$ corresponds to the conformal boundary of AdS and we impose $X = 0$ there so that the induced metric is conformal to that of $4d$ Schwarzschild.

Finally, in order to solve the Einstein–DeTurck equation (4) we have to specify a reference metric. In the original work of Figueras et al. [16], the background metric was taken to be (9) with $X = 0$. However, one can show that in this gauge, the solution near the boundary of AdS ($x = 1$) has logs (and therefore it is not smooth), which leads to a poor convergence of the spectral code at sufficiently high resolution. In order to cure this deficiency, in the present work we take the reference metric to be (9) with $T = S = A = 0$, $B = -\frac{18}{5} f(r)^2 f(x)^2$ and $F = -\frac{6}{5} f(r)^2 f(x)^3$. One can show that in this gauge there are no logs at the order that affected [16] but we cannot rule out the presence of logs at higher orders.

Henceforth we set the radius of AdS to be one, $\ell = 1$. In addition, note that because in AdS/CFT we only have to specify a representative of the conformal class of boundary metrics, we can set, without loss of generality, the radius of the boundary Schwarzschild solution to be one.

### 3.2 Results

In this subsection we briefly summarise our results for this AdS/CFT solution. Firstly we present the numerical solution. As we shall see later in the discussion

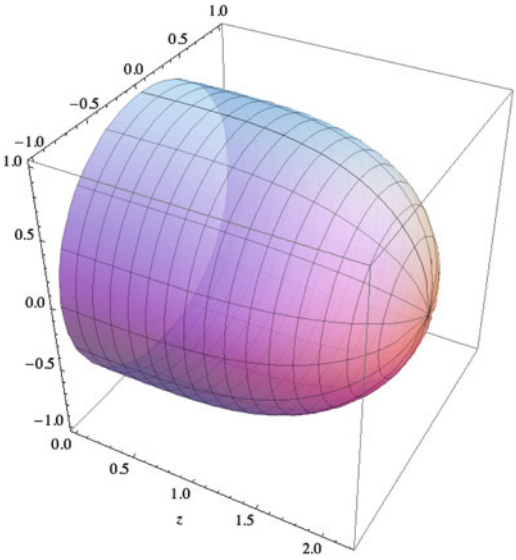


**Fig. 1** Embedding of the horizon of the AdS/CFT solution as a surface of revolution into four-dimensional hyperbolic space $\mathbf{H}_4$, $ds^2(\mathbf{H}_4) = \frac{1}{z^2}(dz^2 + dR^2 + R^2\, d\Omega^2_{(2)})$. Here $z$ is the standard Poincare coordinate so that $z = 0$ is the boundary of $\mathbf{H}_4$, which coincides with the boundary of AdS

of braneworld black holes, it is important to show that this AdS/CFT solution exists and it is smooth. Secondly we will consider the dual stress tensor.

We have solved (4) numerically using a pseudospectral collocation approximation and Newton's algorithm as described in Sect. 2.1. We have performed convergence tests and our numerical solution convergences exponentially (with the number of grid points) to the continuum, at least as far as we were able to check. This is the expected behaviour if a smooth solution exists. Moreover, for the data presented here, the maximal fractional error in the Einstein equations is better than $10^{-9}$, so these are extremely accurate numerical solutions.

In Fig. 1 we present the embedding of the horizon, as a surface of revolution, into four-dimensional hyperbolic space, $\mathbf{H}_4$. As this figure shows, at $z = 0$ (i.e., the boundary of AdS) the horizon has radius one, as it should since the boundary black hole has radius one by our choice of boundary conditions. In addition, one can see that the horizon extends from the boundary into to the bulk, and at some finite value of $z$ the 2-sphere shrinks to zero size smoothly.

One can use the standard holographic renormalisation prescription [32] to extract the boundary stress tensor. The details of the calculation can be found in [16] and the result is:

$$\langle T_i{}^j \rangle = \frac{N_c^2}{2\pi^2 R^4}\mathrm{diag}\Big\{ \frac{3\,R_0}{4\,R}\Big(1 - \frac{7\,R_0}{12\,R} - \frac{R_0^2}{2\,R^2}\Big) + t_4(R),$$
$$\frac{357\,R_0^2}{80\,R^2}\Big(1 - \frac{18\,R_0^2}{17\,R}\Big) - \big(t_4(R) + 2\,s_4(R)\big), -\frac{3\,R_0}{8\,R}\Big(1 + \frac{161\,R_0}{30\,R} - \frac{34\,R_0^2}{5\,R^2}\Big) + s_4(R),$$
$$-\frac{3\,R_0}{8\,R}\Big(1 + \frac{161\,R_0}{30\,R} - \frac{34\,R_0^2}{5\,R^2}\Big) + s_4(R)\Big\}, \tag{9}$$

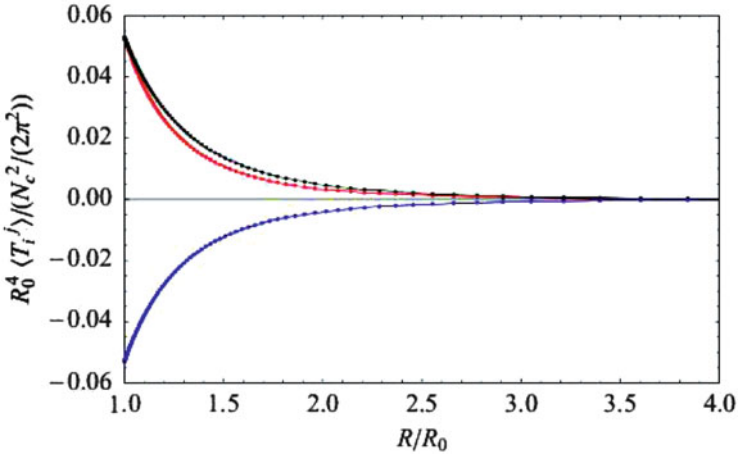


**Fig. 2** $\langle T_t^t \rangle$ (*black*), $\langle T_R^R \rangle$ (*red*) and $\langle T_\Omega^\Omega \rangle$ (*blue*) components of the stress tensor as functions of the Schwarzschild radial coordinate $R$. The *dots* correspond to the values of our interpolated data and the *solid lines* simply serve to guide the eye. Note that $\langle T_t^t \rangle = \langle T_R^R \rangle$ at $R = R_0$ (the horizon) which is necessary and sufficient for the regularity of the stress tensor there. For $R \to \infty$ the various components of $\langle T_i^{\ j} \rangle$ decay as $\sim R^{-5}$

where $R$ is the standard Schwarzschild radial coordinate[3] and $t_4$ and $s_4$ can be extracted from the near boundary ($x \to 1$) expansion of the metric:

$$T \approx \frac{1}{5}\left(4 - 13r^2 + 9r^4\right)\left(1 - x^2\right)^2 - \frac{18}{11}\left(1 - r^2\right)^2\left(1 - x^2\right)^3 + \left(1 - x^2\right)^4 t_4(r) + \ldots,$$

$$S \approx \frac{1}{10}\left(23 - 41r^2 + 18r^4\right)\left(1 - x^2\right)^2 - \frac{18}{11}\left(1 - r^2\right)^2\left(1 - x^2\right)^3 + \left(1 - x^2\right)^4 s_4(r) + \ldots,$$

where here $t_4$ and $s_4$ should be viewed as functions of the compact radial coordinate $r$ used in (9). We want to emphasise that with our choice of gauge, terms in the expansions above up to 5th order do *not* contain logs. The same is true for the remaining metric coefficients (not shown here).

Note that the stress tensor (9) is traceless and conserved as consequence of the bulk Einstein equations. Therefore, $t_4$ and $s_4$ are not independent; they are related by a differential equation which expresses nothing but the conservation of (9). In Fig. 2 we plot the various components of the stress tensor of the dual field theory. First it is worth noting that the stress tensor is static, finite and regular everywhere in our domain. This is non-trivial since, as we now explain, it corresponds to the expectation value of the stress tensor of $\mathcal{N} = 4$ SYM in the background of the $4d$ Schwarzschild black in the Unruh state. Note that our boundary conditions are such that the bulk solution far from the black hole horizon approaches the Poincare

[3]The Schwarzschild radial coordinate $R$ is related to the compact radial coordinate $r$ as $R = \frac{R_0}{1-r^2}$.

horizon of $AdS_5$. From the boundary point of view, this corresponds to the vacuum of the theory (i.e., zero temperature) and not a thermal state. The latter is given by the Hartle-Hawking vacuum and from the bulk point of view, it can be obtained by putting a finite temperature horizon in the IR. The so called static "black funnel" provides an example of a field theory in a black hole background in the Hartle-Hawking state and it has been recently constructed in [33]. With our boundary conditions, the stress tensor is regular on both the future and past event horizons and hence it cannot correspond to the Boulware state either since in the latter case, the dual stress tensor should be singular [34]. Therefore, we conclude that our stress tensor should correspond to the Unruh vacuum. This may seem puzzling at first sight because one usually associates the Unruh state to an evaporating black hole and therefore to a dynamical (as opposed to static) situation. The reason why our stress tensor is static is that our computation, which uses classical gravity in the bulk, only captures the leading order $O(N_c^2)$ piece of the stress tensor, not the full quantum stress tensor. Time-dependence should only show up as an $O(1)$ effect and it can only be detected including 1-loop graviton corrections in the bulk.

This AdS/CFT solution explicitly shows that strong coupling effects significantly alter the behaviour of quantum fields in black hole backgrounds. In particular, the arguments of Emparan et al. [11] against the existence of braneworld black holes should apply to this situation as well and this example shows that they are incorrect. Therefore, there is no reason why braneworld black holes should not exist.

## 4 Braneworld Black Holes

In this section we consider the numerical construction of braneworld black holes. The results in this section will be discussed in detail in a forthcoming paper [35]. In Sect. 4.1 we will argue that large braneworld black holes can be understood as perturbations of the AdS/CFT solution presented in Sect. 3. In Sect. 4.2 we present the details of our numerical construction of braneworld black holes and compare them to the previous results of [17]. In Sect. 4.3 we present our main results.

### *4.1 Large Braneworld Black Holes from AdS/CFT*

Consider the AdS/CFT solution presented in Sect. 3 in Fefferman-Graham coordinates. In the near boundary expansion ($z \to 0$), one has

$$ds^2 = \frac{1}{z^2}(dz^2 + \tilde{g}(z,x)\,dx^\mu dx^\nu), \qquad \tilde{g}_{\mu\nu}(z,x) = g^{(0)}_{\mu\nu}(x)$$
$$+\frac{z^2}{2}\left(R^{(0)}_{\mu\nu}(x) - \frac{1}{6}\,g^{(0)}_{\mu\nu}(x)R^{(0)}(x)\right) + z^4\left(g^{(4)}_{\mu\nu}(x) + t_{\mu\nu}(x)\right) + 2\,z^4\,\log z\; h^{(4)}_{\mu\nu}(x)$$
$$+O(z^6).$$

Here $g^{(0)}_{\mu\nu}$ is the boundary metric and $R^{(0)}_{\mu\nu}$ and $R^{(0)}$ are the associated Ricci tensor and Ricci scalar respectively. $t_{\mu\nu}$ is related to the vev of the stress tensor of the dual CFT by $\langle T^{CFT}_{\mu\nu}\rangle = t_{\mu\nu}/(4\pi\, G_5)$ and the expressions for $g^{(4)}_{\mu\nu}$ and $h^{(4)}_{\mu\nu}$ can be found in [32]. In our setting $g^{(0)}_{\mu\nu}$ is the metric of the $4d$ Schwarzschild solution $g^{Schw}_{\mu\nu}$, which implies that $R^{(0)}_{\mu\nu} = 0$, $R^{(0)} = 0$ and $h^{(4)}_{\mu\nu} = 0$.

Now assume that there exists a solution in AdS such that its boundary metric is given by the $4d$ Schwarzschild solution plus a small perturbation, $g^{(0)}_{\mu\nu} = g^{Schw}_{\mu\nu} + \epsilon^2\, h_{\mu\nu}$ where $\epsilon$ is a small parameter.[4] In addition, as in Sect. 3, far from the horizon the solution should asymptote to the Poincare horizon of $AdS_5$. In this set up, we now slice the spacetime with an infinitely thin brane (as in the RSII model) located at $z = \epsilon$. de Haro et al. [36] (see also [17]) showed that in order for this be possible, such a perturbation has to satisfy the induced Einstein equations on the brane with a source given by the expectation value of the CFT stress tensor obtained in Sect. 3:

$$\delta G_{\mu\nu}[h] = 16\,\pi G_4 \langle T^{CFT}_{\mu\nu}\rangle. \tag{10}$$

Moreover, the induced metric on the brane is given by the Schwarzschild geometry, with a radius which is parametrically larger than the radius of the bulk AdS spacetime $\ell$ plus a small perturbation:

$$\gamma_{\mu\nu} = \frac{\ell^2}{\epsilon^2}(g^{Schw}_{\mu\nu} + \epsilon^2\, h_{\mu\nu}). \tag{11}$$

Therefore, if such a perturbation exists, then one can construct arbitrarily large braneworld black holes. In the next subsection we shall see how this can be done numerically.

## 4.2 Numerical Construction

In the previous subsection we have argued that large braneworld black holes can be viewed as perturbations of the AdS/CFT solution constructed in Sect. 3. Therefore, in order to numerically construct the braneworld black holes we shall use a metric ansatz which is close to (9):

$$ds^2 = \frac{\ell^2}{\Delta(r,x)^2}\Big( -4\,r^2\, f(r)^2\, e^T\, dt^2 + x^2 g(x)\, e^S\, d\Omega^2_{(2)} + \frac{4}{f(r)^2}\, e^{T+r^2 f(r) A} dr^2 + \frac{4}{g(x)}\, e^{S+x^2 B}\, dx^2 + \frac{2\,r\,x}{f(r)}\, F\, dr\, dx\Big), \tag{12}$$

[4] For a well-posed elliptic problem, as is our case, one should expect that such a solution exists and it is close to the solution in Sect. 3.

where $\Delta(r,x) = (1-x^2)+\epsilon(1-r^2)$. Here $\epsilon$ is a parameter that effectively measures the ratio between the radius of $AdS_5$ and the radius of the black hole on the brane. Hence, taking $\epsilon \to 0$ in (12) corresponds to having an infinitely large braneworld black hole and we recover the AdS/CFT solution, (9).

Using the ansatz (12) we numerically solve the equations of motion (4) subject to suitable boundary conditions. As a reference metric we took (12) with $X = 0$. The boundary conditions are as in Sect. 3 except at $x = 1$, where we impose the Israel junction conditions, $K_{\mu\nu} = \frac{1}{\ell}\gamma_{\mu\nu}$. This imposes conditions on $T, S, A$. In addition we fix $F = 0$ and $\xi^x = 0$. These boundary conditions give rise to a regular elliptic problem and in particular they imply $\partial_n \xi_r = \frac{2}{\ell}\xi_r$ on the brane (where $\partial_n$ denotes the normal derivative), which is compatible with obtaining an Einstein solution with $\xi^a = 0$ everywhere on $\mathscr{M}$. We note that with these boundary conditions the soliton non-existence result of [16] does not apply and a posteriori we have to check that our solution is an Einstein metric and not a Ricci soliton. We have performed such checks and found no evidence of Ricci solitons.

### 4.3 Results

Following [17] we solved the equations of motion numerically using pseudospectral collocation approximation (using Newton's method) and taking the same number of grid points $N$ in the $r$ and $x$ directions. To characterise the numerical errors we consider the maximum value of $|R/20 + 1|$ in the whole domain, including the brane. This quantity should be exactly zero for an Einstein metric and hence it tells us about the vanishing of both $\xi^a$ and its gradients in the continuum limit. In Fig. 3 we show two representative plots for the $\epsilon = 0.5, 1$ solutions, which roughly correspond to black holes of size $\sim 2$ and $\sim 1$ respectively. As these plots show, $|R/20 + 1|_{max}$ does not vanish in the continuum limit and therefore our numerical solutions do *not* approximate a continuum solution and should be discarded. Moreover, the smaller the value of $\epsilon$ (i.e., the larger the black hole on the brane), the higher the resolution that is needed in order to see this lack of convergence. Note that depending on the size of the black hole on the brane, $|R/20+1|_{max}$ exhibits a spike at a certain value of $N$. One can see that this is due to the appearance of a numerical non-smooth near zero mode; it would be interesting to understand if our boundary conditions can be improved in order to get rid off these unphysical modes.

By plotting $R/20 + 1$ over the whole domain one sees that this lack of convergence is due to some oscillations that appear to be localised on the brane and do not go away in the continuum limit. Such a phenomenon is known as the Gibbs phenomenon and it is known to occur when one tries to approximate a non-smooth function with smooth polynomials, as in a pseudospectral collocation approximation. Since in Sect. 3 we convincingly showed the existence of the

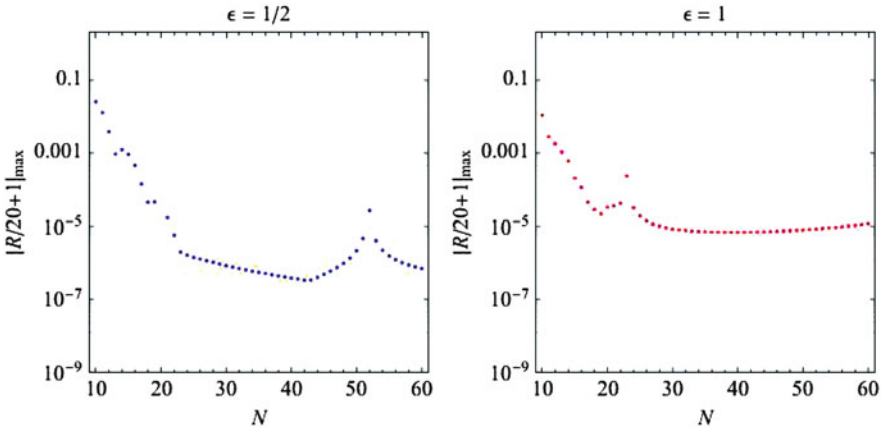


**Fig. 3** Maximum (absolute) value of the normalised Ricci scalar over the whole domain (including the brane) as a function of the number of grid points for the $\epsilon = 0.5, 1$ solutions obtained with pseudospectral methods. This quantity should vanish in the continuum limit but the plots show that it does not

AdS/CFT solution, from which large braneworld black holes can be perturbatively constructed, we believe that this lack of convergence is just due to a poor choice of gauge. One might think that this lack of smoothness comes from the presence of logs near the brane, but this does not seem to be case. Indeed, we have performed the same calculation but choosing the same reference metric as in Sect. 3 (which has smoother near boundary behaviour) or in $d = 6$ (where no logs are expected) and found similar results. It would be interesting to understand in detail where this lack of smoothness comes from.

Since spectral methods seem to fail because of the lack of smoothness of the solutions, we have constructed braneworld black holes in $d = 5, 6$ using 3rd and 4th order finite differences respectively. In either case we have found good convergence (see Fig. 4 for the $5d$ results) to the continuum and, more importantly, the finite difference code is able to find solutions in a region of parameter space (i.e., small black holes) where the spectral code fails. Moreover, for the highest resolution solutions that we have constructed, the numerical errors of the finite difference solutions are smaller than those of the spectral solutions. However, higher order finite difference methods do not converge, which suggests that in our gauge the $d = 5(6)$ solutions are only $C^3(C^4)$.[5] Summarising, our finite difference solutions converge to the continuum according the order of the approximation, therefore providing good evidence that the continuum solutions do exist. However, in our

[5]Recall that a classical solution to the Einstein equations need only be $C^2$.

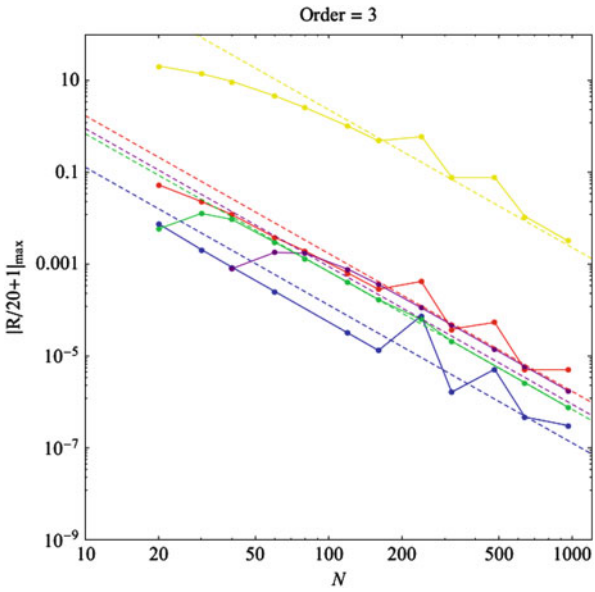


**Fig. 4** $|R/20+1|_{max}$ against the number of grid points for the $\epsilon = 0.01$ (*purple*), 0.1 (*green*), 1 (*blue*), 10 (*red*) and 100 (*yellow*) solutions, together with the fits (*dashed*) assuming exact third order convergence. As this plot shows, we have good third order convergence for braneworld black holes of all sizes

gauge they do not appear to be very smooth and hence the spectral approximation fails.

There are various reasons why [17] could not observe this lack of convergence. First, the metric ansatz used in this other paper is different from ours, and therefore the gauge is different. As we have argued above, this lack of convergence should be a gauge issue and therefore different gauges should give rise to different convergence properties of the numerical solutions. Secondly, and perhaps more fundamentally, the resolutions used in [17] were quite modest and as we have seen above, the lack of convergence only becomes apparent at sufficiently large $N$. Finally, Figueras and Wiseman [17] monitored $\phi = \xi^a \xi_a$ to estimate the numerical error and one can see that this quantity is better behaved than $|R/20+1|$.

Finally, in Fig. 5 we display the area of the horizon of the full five-dimensional black hole as a function of the radius of the black hole on the brane. On this plot we also display the behaviour of the area as a function of the horizon radius for the $5d$ asymptotically flat Schwarzschild solution (in red) and the $4d$ asymptotically flat Schwarzschild solution times one AdS radius. As one can see from this plot, the geometry of the braneworld black holes smoothly interpolates between the $5d$ behaviour for small black holes ($R_4 \ell^2 \ell$) and the $4d$ behaviour for large black holes ($R_4 \gg \ell$). Therefore, we confirm that standard $4d$ gravity on the brane is recovered for large black holes and that the latter can indeed be seen as small deformations of the $4d$ asymptotically flat Schwarzschild solution.

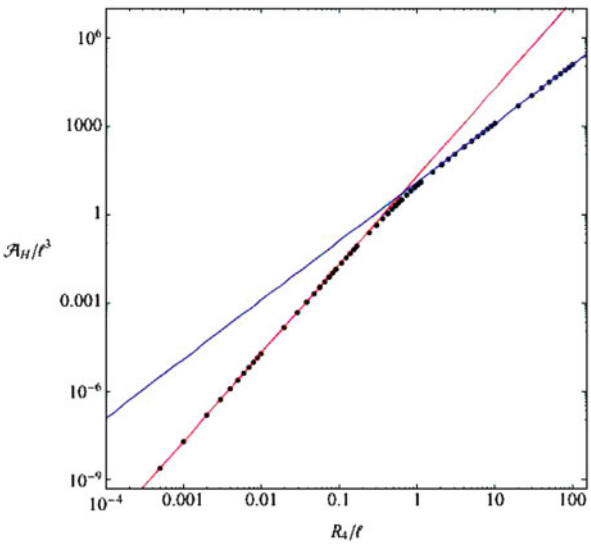


**Fig. 5** $\mathscr{A}_H/\ell^3$ vs. $R_4/\ell$ in a log–log plot. For small braneworld black holes, the area function approaches that of the $5d$ asymptotically flat Schwarzschild solution (in *red*). For large braneworld black holes it approaches of a $4d$ Schwarzschild solution which extends one AdS length into the bulk (in *blue*)

## 5 Summary and Conclusions

In Sect. 2 we have briefly reviewed a new method for casting the Einstein equations into a manifestly elliptic form which is amenable for numerics. We have also reviewed two standard algorithms for solving the equations numerically, namely the Ricci–DeTurck flow and Newton's method.

Using this machinery, in Sect. 3 we have numerically constructed a static black hole solution in (the Poincare patch of) AdS whose boundary metric is conformal to the $4d$ asymptotically flat Schwarzschild solution. Using AdS/CFT we have identified this solution as the gravitational dual of $\mathcal{N} = 4$ SYM in the background of Schwarzschild in the Unruh vacuum. Interestingly, for this solution the Lichnerowicz operator $\Delta_L$ is positive definite which implies that it is a stable fixed point of Ricci flow [16].

Naive arguments [11] would have suggested that such a black hole cannot be static. However, our construction shows that this is not the case, and the leading $O(N_c^2)$ solution is both smooth and static. We have also argued that one can perturb this black hole by deforming the boundary metric and construct an arbitrarily large braneworld black hole.

In Sect. 4 we have numerically constructed braneworld black holes of various sizes. Rather surprisingly, we have found that, at least in our gauge, the solutions do not appear to be very smooth. It would be interesting to understand in detail why this is so. Using our numerical solutions we have checked that $4d$ gravity on the brane is recovered for braneworld black holes which are large compared to the radius of AdS. Therefore, the RSII model can be in agreement with astrophysical observations.

One can check that for all braneworld black holes that we have constructed $\Delta_L$ has one, and only one, negative mode. Moreover, for large black holes, the negative mode that we find approaches the celebrated negative mode of $4d$ Schwarzschild. These results suggest that braneworld black holes should be stable under gravitational perturbations. Further evidence for this has been noted recently by Abdolrahimi et al. [18, 19], who have shown that braneworld black holes have greater entropy than a $4d$ Schwarzschild black hole with the same mass.

**Acknowledgements** It is a great pleasure to acknowledge the contributions of my collaborators J. Lucietti and especially T. Wiseman, without whom this work would not have been possible. I would also like to thank the organisers of the ERE2012 meeting in Guimarães (Portugal) for the invitation and for such a successful and enjoyable event. I am supported by an EPSRC postdoctoral fellowship [EP/H027106/1].

## References

1. L. Randall and R. Sundrum, Phys. Rev. Lett. **83**, 3370 (1999) [hep-ph/9905221].
2. L. Randall and R. Sundrum, Phys. Rev. Lett. **83** (1999) 4690 [hep-th/9906064].
3. J. Garriga and T. Tanaka, Phys. Rev. Lett. **84** (2000) 2778 [hep-th/9911055].
4. S. B. Giddings, E. Katz and L. Randall, JHEP **0003** (2000) 023 [hep-th/0002091].
5. A. Chamblin, S. W. Hawking and H. S. Reall, Phys. Rev. D **61** (2000) 065007 [hep-th/9909205].
6. R. Emparan, G. T. Horowitz and R. C. Myers, JHEP **0001** (2000) 007 [hep-th/9911043].
7. H. Kudoh, T. Tanaka and T. Nakamura, Phys. Rev. D **68** (2003) 024035 [gr-qc/0301089].
8. H. Kudoh, Phys. Rev. D **69** (2004) 104019 [Erratum-ibid. D **70** (2004) 029901] [hep-th/0401229].
9. H. Yoshino, JHEP **0901** (2009) 068 [arXiv:0812.0465 [gr-qc]].
10. B. Kleihaus, J. Kunz, E. Radu and D. Senkbeil, Phys. Rev. D **83** (2011) 104050 [arXiv:1103.4758 [gr-qc]].
11. R. Emparan, A. Fabbri and N. Kaloper, JHEP **0208** (2002) 043 [hep-th/0206155].
12. A. L. Fitzpatrick, L. Randall and T. Wiseman, JHEP **0611** (2006) 033 [hep-th/0608208].
13. A. Kaus and H. S. Reall, JHEP **0905** (2009) 032 [arXiv:0901.4236 [hep-th]].
14. R. Suzuki, T. Shiromizu and N. Tanahashi, Phys. Rev. D **82** (2010) 085029 [arXiv:1007.1820 [hep-th]].
15. A. Kaus, arXiv:1105.4739 [hep-th].
16. P. Figueras, J. Lucietti and T. Wiseman, Class. Quant. Grav. **28** (2011) 215018 [arXiv:1104.4489 [hep-th]].
17. P. Figueras and T. Wiseman, Phys. Rev. Lett. **107** (2011) 081101 [arXiv:1105.2558 [hep-th]].
18. S. Abdolrahimi, C. Cattoen, D. N. Page and S. Yaghoobpour-Tari, arXiv:1206.0708 [hep-th].
19. S. Abdolrahimi, C. Cattoen, D. N. Page and S. Yaghoobpour-Tari, arXiv:1212.5623 [hep-th].
20. M. Headrick, S. Kitchen and T. Wiseman, Class. Quant. Grav. **27** (2010) 035002 [arXiv:0905.1822 [gr-qc]].
21. A. Adam, S. Kitchen and T. Wiseman, Class. Quant. Grav. **29** (2012) 165002 [arXiv:1105.6347 [gr-qc]].
22. T. Wiseman, arXiv:1107.5513 [gr-qc].
23. P. Figueras and T. Wiseman, Phys. Rev. Lett. **110** (2013) 171602 [arXiv:1212.4498 [hep-th]].
24. S. Fischetti, D. Marolf and J. Santos, arXiv:1212.4820 [hep-th].
25. Y. Choquet-Bruhat, Acta. Math. **88** (1952), 141–225.
26. D. Garfinkle, Phys. Rev. D **65** (2002) 044029 [gr-qc/0110013].

27. F. Pretorius, Class. Quant. Grav. **22** (2005) 425 [gr-qc/0407110].
28. F. Pretorius, Phys. Rev. Lett. **95** (2005) 121101 [gr-qc/0507014].
29. M. T. Anderson Geom. Topol. **12** 2009–45 [math/0612647].
30. J. P. Bourguignon, In Global differential geometry and global analysis (Berlin, 1979), vol. 838 of Lecture notes in Math. pp 42–63, Springer, Berlin 1981.
31. D. J. Gross, M. J. Perry and L. G. Yaffe, Phys. Rev. D **25** (1982) 330.
32. S. de Haro, S. N. Solodukhin and K. Skenderis, Commun. Math. Phys. **217** (2001) 595 [hep-th/0002230].
33. J. E. Santos and B. Way, JHEP **1212** (2012) 060 [arXiv:1208.6291 [hep-th]].
34. D. Marolf, *private communication*.
35. P. Figueras and T. Wiseman, *to appear.*
36. S. de Haro, K. Skenderis and S. N. Solodukhin, Class. Quant. Grav. **18** (2001) 3171 [hep-th/0011230].

# BPS Black Holes in String Theory

**Gabriel Lopes Cardoso**

**Abstract** We give an overview of four-dimensional BPS black holes in supergravity and string theory from both a macroscopic and a microscopic perspective.

## 1 Introduction

Black holes play an important role for testing theories of quantum gravity. Classically, they are solutions of the equations of motion of General Relativity that have an event horizon shielding a space-time singularity. When taking quantum effects into account, a black hole turns out to have a temperature, the so-called Hawking temperature. A black hole is therefore a thermodynamical system with a thermodynamic entropy. Entropy is also a measure for the number of microstates of the system. Therefore, an essential requirement for any quantum theory of gravity is that it has to be able to derive the thermodynamics of black holes by identifying and counting microstates. String theory, a mathematically consistent theory of quantum gravity, is capable of providing an answer to this question [1, 2].

In string theory, the class of black holes for which there has been a detailed study of the matching of the thermodynamic entropy with the counting of microstates is the class of supersymmetric black holes, also called BPS black holes. In this review, we shall focus on BPS black holes in four dimensions. These are black holes that are asymptotically flat, charged and extremal. BPS solutions may be single-centered or have multiple centers. At the two-derivative level, single-center BPS solutions are static. Thus, they are distinct from the near-extremal spinning black holes, such as the near-extremal Kerr black hole GRS 1915 + 105 [3], whose existence has been confirmed by astrophysical measurements. A conjecture for the microscopic

G.L. Cardoso (✉)
CAMGSD, Departamento de Matemática, Instituto Superior Técnico, Av. Rovisco Pais, 1049-001 Lisboa, Portugal
e-mail: gcardoso@math.ist.utl.pt

A. García-Parrado et al. (eds.), *Progress in Mathematical Relativity, Gravitation and Cosmology*, Springer Proceedings in Mathematics & Statistics 60,
DOI 10.1007/978-3-642-40157-2_4, 

description of extremal Kerr black holes has been proposed in [4] in terms of two-dimensional chiral conformal field theories. We refer to [5] for a review of this subject. Here, we will mainly focus on single-center static black holes.

Charged black holes arise as solutions of gravity coupled to abelian gauge fields and neutral scalar fields. In four dimensions, they may, in general, carry both electric and magnetic charges with respect to these gauge fields (we allow for the presence of various such Maxwell fields). Extremal black holes are charged black holes that carry the minimum mass possible for a given set of charges, and their mass is uniquely fixed in terms of the charges and the asymptotic values of the scalar fields. These black holes have zero temperature and a very high entropy. BPS black holes constitute a subset of extremal black holes, and it is for BPS black holes in string models with a high amount of supersymmetry that there exist exact formulae for the number of microstates in terms of the charges carried by the BPS black hole. This is the case for string models with $N = 4$ supersymmetry [6–9] and with $N = 8$ supersymmetry [10].

The role of supersymmetry in the successful matching of the thermodynamic entropy with the microscopic entropy based on state counting in string theory can be understood as follows. String theory has a length scale $\alpha' = l_s^2$ and a string coupling constant $g_s$. In string theory, Newton's constant $G_N$ is a derived quantity given by $G_N \sim g_s^2 \alpha'$. Let us consider an extremal Reissner–Nordstrom black hole solution to the equations of motion of the Einstein–Maxwell theory. Its thermodynamic entropy, computed by the area law of Bekenstein and Hawking, is given by (in units $k_B = c = \hbar = 1$) $S_{\text{macro}} = A/4G_N = \pi Q^2$, where $Q$ denotes the electric charge carried by the black hole. Thus, its entropy is independent of $G_N$, and the same holds for BPS black holes in string theory. Therefore, the thermodynamic entropy of a supersymmetric black hole is independent of the string coupling constant $g_s$. In string theory, a charged black hole (carrying a number of Maxwell charges which we generically denote by $Q$) is a system with two different descriptions that hold in two different regimes [11]. The macroscopic regime, where the system is described by a gravitational solution (a black hole), corresponds to the regime where $|Q|\, g_s >> 1$. In this regime, the entropy of the system is given by the thermodynamic entropy $S_{\text{macro}}(Q)$ of the black hole. $S_{\text{macro}}(Q)$ is determined in terms of the charges $Q$ carried by the black hole, and is independent of $g_s$. The microscopic description of the system corresponds to the opposite regime $|Q|\, g_s << 1$. In this regime, the system is described in terms of a boundstate of excited strings and branes [1], and it is possible to count microstates (excitations) of this system. This, in turn, defines a microscopic entropy $S_{\text{micro}}(Q)$. Supersymmetry gives rise to various non-renormalization theorems. Due to these theorems, the entropy of a supersymmetric black hole is independent of $g_s$, and therefore one may compare the entropy calculation in the macroscopic regime with the entropy calculation in the microscopic regime, and check whether the microscopic picture (based on strings and branes) gives results in agreement with the macroscopic description. This is what has been achieved for BPS black holes in string models with a high degree of supersymmetry.

In addition, the power of supersymmetry also helps in determining the precise form of the low-energy effective actions of these string models, and this in turn results in a precision calculation of the macroscopic entropy which, for large charges, has the following expansion (schematically),

$$S_{\text{macro}}(Q) = a_0\, A(Q) + a_1 \ln A(Q) + \frac{a_2}{A(Q)} + \ldots + \mathrm{e}^{-c_0\, A(Q)} + \ldots \quad (1)$$

For large charges, the leading term (proportional to $a_0$) describes the area law of Bekenstein and Hawking. The subleading terms include a power series expansion in $A(Q)$, logarithmic corrections as well as non-perturbative corrections. On the other hand, supersymmetry also allows for the exact determination of the spectrum of boundstates of strings and branes in certain string models, resulting in a precision calculation of the microscopic entropy which, for large charges $Q$, takes a form that is similar to (1),

$$S_{\text{micro}}(Q) = b_0\, A(Q) + b_1 \ln A(Q) + \frac{b_2}{A(Q)} + \ldots + \mathrm{e}^{-d_0\, A(Q)} + \ldots$$

Then, the matching of macroscopic and microscopic entropies requires checking whether $a_i = b_i$ and $c_i = d_i$ for $i = 0, 1, \ldots$, and this turns out to be the case in the string models for which a detailed comparison has been performed, namely models with $N = 4, 8$ supersymmetry, as mentioned above. A detailed account of these precision tests can be found in [12, 13].

## 2 Macroscopic Aspects of BPS Black Holes

We focus on four-dimensional models derived from string theory with $N = 4$ supersymmetry. These models are obtained by compactifying superstring theory in ten dimensions down to four dimensions on suitably chosen six-dimensional manifolds $X$. The resulting low-energy effective action describes gravity coupled to a number of abelian gauge fields $F^I$ as well as neutral scalar fields $\phi^I$ ($I = 1, \ldots, n$). It also includes higher-derivative terms, in particular higher-curvature terms, that represent $\alpha'$-corrections to the two-derivative action. The associated equations of motion allow for single-center BPS black holes that are charged. These may be electrically charged, or they may be dyonic and carry electric/magnetic charges $(Q_I, P^I)$ associated with the $F^I$. The characteristic features of the dyonic solutions can be summarized as follows. They are supersymmetric solitons [14], i.e.

- they are static and have finite energy. Their mass satisfies the BPS bound;
- they have residual supersymmetry and interpolate between two maximally supersymmetric vacua, namely Minkowski spacetime at spatial infinity, and $AdS_2 \times S^2$ at the horizon;
- they are stable. They have vanishing temperature.

An important feature of these single-center BPS black holes is that they are supported by the neutral scalar fields. In the black hole background these scalar fields $\phi^I(r)$ vary radially as one moves from spatial infinity to the horizon of the black hole, and they get attracted to specific values at the horizon which are determined by the black hole charges $(Q_I, P^I)$. These values are independent of the asymptotic values of the fields at spatial infinity. This is the so-called attractor mechanism, which was first noted in the context of supergravity [15, 16] and then generalized to theories with higher-curvature terms in [17, 18]. The horizon values of the scalar fields are determined by extremising an entropy function , whose value at the extremum gives the macroscopic entropy $S_{\rm macro}(Q, P)$ [19, 20]. Thus, as a result of the attractor mechanism, the macroscopic entropy is entirely determined in terms of the black hole charges. We note that since the scalar fields parametrize the size and shape of the internal six-dimensional manifold $X$, the latter changes as one moves around in the black hole background.

In models with $N = 4$ supersymmetry, the macroscopic entropy of a single-center dyonic BPS black hole is invariant under electric–magnetic duality (also called S-duality), a property that has to be respected by any candidate microstate counting formula for these black holes [21].

As mentioned above, the low-energy (Wilsonian) action of a four-dimensional string model contains higher-curvature terms. These affect and modfiy the black hole solution. Moreover, in the presence of higher-curvature interactions, the macroscopic entropy $S_{\rm macro}$ is no longer given by the area law of Bekenstein and Hawking. Instead, one uses Wald's definition of black hole entropy based on a Noether surface charge [22], which ensures the validity of the First Law of black hole mechanics. For stationary black holes in local, generally covariant theories of gravity, such as the low-energy Wilsonian actions derived from string theory, $S_{\rm macro}$ is expressed as a local geometric density integrated over a space-like cross section of the event horizon [22],

$$S_{\rm macro} = 2\pi \int_{\rm Hor} d^2x \, \sqrt{h} \, Q^{\mu\nu} \, \epsilon_{\mu\nu}, \tag{2}$$

where $h_{\mu\nu}$ and $\epsilon_{\mu\nu}$ denote the induced metric and the binormal on the horizon, respectively, and $Q_{\mu\nu} = -Q_{\nu\mu}$ is the so-called Noether potential. Wald's definition of entropy

- is based on a Lorentzian signature derivation of the First Law of black hole mechanics,
- assumes a non-vanishing surface gravity,
- and assumes that the event horizon is a Killing horizon.

Thus, in order to define the entropy of an extremal black hole (which has vanishing temperature) one has to work slightly away from extremality, compute the entropy of the associated non-extremal black hole using Wald's formula and then send the extremality parameter to zero.

The Noether potential $Q$ which enters Wald's definition of entropy is related to diffeomorphisms under the Killing vector field associated with the horizon of the stationary black hole, as follows. Given a general covariant Lagrangian $L = L(\psi)$, one constructs a Noether current $J(\psi, \xi)$ associated with diffeomorphisms $x \to x + \xi$, which is conserved when the equations of motion are satisfied, $\nabla_\mu J^\mu = 0$. Then, it can be shown [22] that $J^\mu = \nabla_\nu \tilde{Q}^{\nu\mu}$ with $\tilde{Q}^{\mu\nu} = -\tilde{Q}^{\nu\mu}$ globally defined. This is the Noether potential. Now, consider identifying $\xi$ with the Killing vector field generating the Killing horizon, and define

$$Q^{\mu\nu} = \tilde{Q}^{\mu\nu}|_{\xi=0, \nabla_{[\mu}\xi_{\nu]}=\epsilon_{\mu\nu}}. \tag{3}$$

Observe that $Q$ only depends on the dynamical fields $\psi$ and on the binormal $\epsilon$, i.e. $Q^{\mu\nu} = Q^{\mu\nu}(\psi, \epsilon)$. Then, the surface integral at the horizon over $Q$ yields the entropy. Hence, black hole entropy is Noether charge [22].

We note that the power of Wald's definition of entropy lays in its generality. It applies to stationary black holes in any spacetime dimensions. When applied to BPS black holes, it yields a macroscopic entropy that is reproduced by microstate counting in string theory, as we will see.

Let us consider a low-energy Wilsonian action described by a Lagrangian $L = L(g_{\mu\nu}, R_{\mu\nu\rho\sigma}; \chi, \nabla_\mu \chi)$ which is allowed to depend on any number of powers of the Riemann curvature tensor $R_{\mu\nu\rho\sigma}$, but not on derivatives thereof. The fields $\chi$ denote matter fields. Then, the resulting black hole entropy is given by [23, 24]

$$Q^{\mu\nu} = \frac{\partial L}{\partial R_{\mu\nu\rho\sigma}} \epsilon_{\rho\sigma} \;\longrightarrow\; S_{\text{macro}} = 2\pi \int_{\text{Hor}} d^2x \, \sqrt{h} \, \frac{\partial L}{\partial R_{\mu\nu\rho\sigma}} \, \epsilon_{\rho\sigma} \, \epsilon_{\mu\nu}. \tag{4}$$

At the two-derivative level, this yields the area law of Bekenstein and Hawking. For a static black hole, the binormal is non-vanishing in the subspace orthogonal to the horizon associated with the time and the radial coordinates.

Let us now turn to the Wilsonian action of the four-dimensional string models under consideration. The higher-derivative terms arising in these actions correspond to either supersymmetric F-terms or supersymmetric D-terms. Not much is known about D-term contributions to these actions, but it is believed that they do not contribute to the entropy of BPS black holes. This has been explicitly confirmed recently for a class of D-terms that are quartic [25]. Thus, we will only be concerned with F-terms in the following. F-term contributions to the Wilsonian action have been extensively discussed in the supergravity and string literature [26, 27]. In the following, we will focus on a particular string model with $N = 4$ supersymmetry, for concreteness, namely heterotic string theory compactified on a six-torus $X = T^6$. At order $\alpha'$, the associated Wilsonian action is, schematically, given by

$$L = R + g_{IJ}(\phi) \partial_\mu \phi^I \partial_\mu \phi^J + f_{IJ}(\phi) \mathscr{F}^I_{\mu\nu} \mathscr{F}^J_{\mu\nu} + \alpha' \, F^{(1)}(\phi) \, C^2_{\mu\nu\rho\sigma}. \tag{5}$$

It contains an F-term proportional to the square of the Weyl tensor $C_{\mu\nu\rho\sigma}$.

As mentioned above, the associated equations of motion allow for both electrically charged and dyonic solutions. Let us first consider electrically charged solutions. At the two-derivative level, i.e. when switching off $\alpha'$-corrections, these solutions are singular: they have a null singularity, and there is no horizon to shield it. However, when including $\alpha'$-corrections, in particular when taking into account the term proportional to $F^{(1)}$, the singularity gets cloaked [28]. A horizon forms, with the near-horizon geometry of the modified solution given by $AdS_2 \times S^2$. The aforementioned attractor mechanism ensures that the near-horizon solution is entirely determined in terms of the electric charges carried by the black hole. To be specific, let us consider an electrically charged black hole carrying two electric charges, which we denote by $n$ and $w$. Then, after cloaking, the area of the two-sphere is given by $\frac{1}{4} A(S^2)/G_N = 2\pi\sqrt{nw}$. Using (4) one obtains for Wald's entropy,

$$S_{\text{macro}} = 4\pi\sqrt{nw} - 12\ln(nw). \tag{6}$$

The first term equals $\frac{1}{2} A(S^2)/G_N$, while the second term is of the form $\ln A(S^2)$, as in (1).

On the other hand, in the case of a dyonic black hole carrying electric/magnetic charges $(Q_I, P^I)$, the solution has a horizon at the two-derivative level, and the area of the horizon two-sphere is given by $\frac{1}{4} A(S^2)/G_N = \pi\sqrt{Q^2P^2 - (Q\cdot P)^2}$. This is invariant under the interchange of electric and magnetic charges, i.e. invariant under S-duality transformations. In the presence of $\alpha'$-corrections, such as the term proportional to $F^{(1)}$ in (5), the thermodynamic entropy ceases to be given by the area law. Using (4) to compute Wald's entropy, one obtains corrections to the area law that are subleading. These include the following logarithmic correction,

$$S_{\text{macro}} = \pi\sqrt{Q^2P^2 - (Q\cdot P)^2} - 12\ln[(Q^2P^2 - (Q\cdot P)^2)/P^2] + \dots \tag{7}$$

In the next section, we turn to the microscopic derivation of (6) and (7). This will require specifying the statistical ensemble that underlies the computation of the microscopic entropy.

So far, we focussed on single-center BPS black hole solutions. Multi-center solutions describing bound states can be constructed as well [29]. For instance, a BPS solution with total charge $(Q_I, P^I)$ and describing a two-center bound state with charges $(Q_I, 0)$ and $(0, P^I)$ each, is a stationary solution constructed in terms of harmonic functions

$$H^I = C^I + \frac{P^I}{|\vec{x} - \vec{x}_P|}, \qquad \tilde{H}_I = D_I + \frac{Q_I}{|\vec{x} - \vec{x}_Q|}. \tag{8}$$

Here, $(C^I, D_I)$ denote integration constants that parametrize the asymptotic moduli space. This boundstate carries intrinsic angular momentum $J = \frac{1}{2} Q\cdot P$. The distance $|\vec{x}_Q - \vec{x}_P|$ between the two centers is fixed and given by [29,30]

$$\frac{1}{|\vec{x}_Q - \vec{x}_P|} = -\frac{C \cdot Q}{Q \cdot P} = -\frac{D \cdot P}{Q \cdot P} > 0. \tag{9}$$

When changing the values of the parameters $(C^I, D_I)$, it may happen that $|\vec{x}_Q - \vec{x}_P| \to \infty$, in which case the two-center bound state will cease to exist. This happens at so-called walls of marginal stability in asymptotic moduli space [29–32].

## 3 Microscopic Aspects of BPS Black Holes

Let us begin by considering the microscopic description of the two-charge BPS black hole discussed in (6). As mentioned earlier, we work in the regime $|Q|g_s << 1$. At zero string coupling, the microstates are described by elementary string states, as follows [33,34]. Consider a fundamental heterotic string wrapped $w$ times around one circle in $X = T^6$, and add $n$ units of left-moving momentum along the string. For this to describe a BPS state, the string must oscillate in 24 transverse dimensions, with the total oscillator number $N$ satisfying $N - 1 = n\,w$. The number of distinct states that can be obtained in this way is given by $\Omega(n, w) = p_{24}(N)$, where $p_{24}(N)$ is the number of partitions of $N$ into the sum of 24 integers. The associated generating function is

$$\sum_{N=0}^{\infty} p_{24}(N)\, q^N = \left(\prod_{n=1}^{\infty}(1-q^n)\right)^{-1}. \tag{10}$$

The large $N$-expansion of $\Omega(n, w)$ is given by [35]

$$\Omega(n, w) = \sum_{c=1}^{\infty} c^{-14}\, KL(nw+1, -1; c)\, \hat{I}_{13}\left(\frac{4\pi}{c}\sqrt{nw}\right), \tag{11}$$

where $\hat{I}_{13}$ denotes a modified Bessel function, and where the KL are the so-called Kloosterman sums. Thus, for large values of $N = 1 + nw$, we obtain

$$\ln \Omega(n, w) \approx 4\pi\sqrt{nw} - \frac{27}{4}\ln(nw). \tag{12}$$

Comparing (12) with the thermodynamic entropy (6) shows that there is agreement at leading order, but also a mismatch at subleading order. This suggests that the microcanonical ensemble implied by (12) is not the correct statistical ensemble to consider in order to define the microscopic entropy of electrically charged BPS black holes. Instead, let us consider the grand canonical ensemble defined by [36]

$$e^{\mathcal{F}(\mu)} = \sum_{N=0}^{\infty} \Omega(N-1)\, e^{-\mu(N-1)}, \tag{13}$$

and define the microscopic entropy by the Legendre transform

$$S_{\text{micro}} = \mathscr{F}(\mu) + \mu\,(N-1), \tag{14}$$

with $\mu$ given by

$$\frac{\partial \mathscr{F}}{\partial \mu} + (N-1) = 0. \tag{15}$$

Evaluation of $S_{\text{micro}}$ then yields a result that is in agreement with (6). Thus, the correct statistical ensemble to use when dealing with electrically charged BPS black holes is the grand canonical ensemble.

Next, let us turn to the microscopic description of dyonic BPS black holes. The microstate degeneracy $\Omega(Q,P)$ of BPS dyons must, for large charges, reproduce the leading contribution to the macroscopic entropy (7). It must also be compatible with S-duality, which is a symmetry of heterotic string theory compactified on a six-torus $X = T^6$, as mentioned above. In addition, it must take into account that a single-center dyonic black hole with total charge $(Q,P)$ may fragment into a two-center black hole solution, where one center carries charge $(Q,0)$ and the other center carries charge $(0,P)$. This may happen at so-called walls of marginal stability, as mentioned below (9).

A proposal for the microstate degeneracy of $N = 4$ dyons satisfying these various requirements was put forward in [6], and is based on the unique automorphic form $\Phi_{10}$ of weight 10 under the genus two modular group $\mathrm{Sp}(2,\mathrm{Z})$,

$$\Omega(Q,P) = \int_C d\sigma d\rho dv\, \frac{\mathrm{e}^{i\pi(\sigma\, Q^2+\rho\, P^2+(2v-1)\, Q\cdot P)}}{\Phi_{10}(\sigma,\rho,v)} \tag{16}$$

where a shift of $v$ has been included, following [37]. Here, $(\rho,\sigma,v)$ parametrize the Siegel upper half-plane $\mathrm{Im}\sigma > 0, \mathrm{Im}\rho > 0, \mathrm{Im}\sigma\,\mathrm{Im}\rho - (\mathrm{Im}v)^2 > 0$, and the contour $C$ denotes a suitably chosen three real-dimensional subspace. $\Phi_{10}$ is invariant under S-duality transformations, which are the transformations that belong to the subgroup $\mathrm{SL}(2,Z) \subset \mathrm{Sp}(2,Z)$. The computation of (16) proceeds by evaluating residues associated with the zeroes of $\Phi_{10}$. These are double zeroes that are labelled by four independent integers, one of which is called $n_2 \geq 0$ [6].

The statistical ensemble that defines the microscopic entropy of dyonic BPS black holes is the microcanonical ensemble, $S_{\text{micro}} = \ln \Omega(Q,P)$. The leading contribution to $\ln \Omega(Q,P)$ comes from the double zero $n_2 = 1$, and precisely reproduces the macroscopic result (7) [38]. The double zeroes with $n_2 > 1$ contribute exponentially suppressed terms [39],

$$\ln \Omega(Q,P)_{\text{exp}} \approx \sum_{n_2>1} \pi \sqrt{Q^2P^2 - (Q\cdot P)^2}/n_2. \tag{17}$$

And finally, the contour $C$ may, or may not, encircle the double zero $n_2 = 0$. If it does, it produces a jump in $\Omega$ given by [30, 32]

$$\Delta\Omega(Q, P) = (-1)^{Q\cdot P+1} \, |Q \cdot P| \, \Omega(Q) \, \Omega(P). \tag{18}$$

The macroscopic interpretation of the contribution from the double zero $n_2 = 0$ is the one described in (9). It describes the jump in the entropy associated with the decay of a single-center BPS black hole into a two-center black hole system, with one center carrying the electric charges, and the other center carrying the magnetic charges. As already mentioned, the resulting boundstate carries intrinsic angular momentum $J = \frac{1}{2} Q\cdot P$ which, upon quantization, results in a $2J+1 = Q\cdot P$- fold degeneracy [29]. For large separations of the centers, one expects the jump in the degeneracy to be given by by the product of the individual degeneracies, multiplied by the angular momentum degeneracy, and this is precisely the contribution (18) stemming from the double zero $n_2 = 0$. Thus, we see that the exact degeneracy formula for $N = 4$ dyons encodes information about single-center BPS black holes as well as black hole bound states with total charge $(Q, P)$.

On the other hand, the macroscopic interpretation of the exponentially suppressed corrections steming from the zeroes with $n_2 > 1$ requires going beyond the framework of Wald's entropy. Wald's definition of entropy is based on a local action principle. The low-energy string effective action is, however, in general non-local due to quantum corrections. This requires going beyond Wald's formalism and introducing a generalization that correctly reduces to Wald's definition of entropy when dealing with local actions. Such a concept was introduced in [40] and is called the quantum entropy function. It assumes that the black hole is extremal (not necessarily supersymmetric), and that is has an $AdS_2$ type near horizon geometry. It is defined in terms of an Euclidean path integral over two-dimensional field configurations that asymptote to $AdS_2$, with a Wilson line insertion,

$$W(Q, P) = \langle \mathrm{e}^{-i\, Q_I \oint A^I_\theta \, d\theta} \rangle_{\mathrm{AdS}_2}, \tag{19}$$

where $\theta$ denotes Euclidean time. In this proposal, the asymptotic values of fields are specified by the near-horizon black hole solution which is determined in terms of the charges $(Q, P)$ by the aforementioned attractor mechanism. The path integral runs over all string modes. In the supersymmetric context, this complicated path integral can be evaluated using so-called localization techniques [41]. In the classical limit, the functional integral is dominated by the saddle point describing the near-horizon black hole solution, and $\ln W(Q, P)$ becomes Wald's entropy. Other saddle points contribute exponentially suppressed contributions, reproducing (17) in the case of $N = 4$ BPS black holes [39].

Summarizing, we appear to have a (very) good understanding of $N = 4$ black holes in four dimensions. BPS black holes arising in models with less supersymmetry, such as $N = 2$ supersymmetry, are far more complicated, and there are currently no exact microscopic degeneracy formulae available for these black holes. Clearly, much more work needs to be done to fully understand BPS black holes in $N = 2$ theories.

**Acknowledgements** This work is supported by by the Center for Mathematical Analysis, Geometry and Dynamical Systems (IST/Portugal) and by Fundação para a Ciência e a Tecnologia (FCT/Portugal).

## References

1. A. Strominger, C. Vafa, Phys. Lett. B **379**, 99–104 (1996) [hep-th/9601029].
2. J. M. Maldacena, A. Strominger, E. Witten, JHEP **9712**, 002 (1997) [hep-th/9711053].
3. J. E. McClintock, R. Shafee, R. Narayan, R. A. Remillard, S. W. Davis, et al., Astrophys. J. **652**, 518–539 (2006) [astro-ph/0606076].
4. M. Guica, T. Hartman, W. Song, A. Strominger, Phys. Rev. D **80**, 124008 (2009) [0809.4266].
5. I. Bredberg, C. Keeler, V. Lysov, A. Strominger, Nucl. Phys. Proc. Suppl. **216**, 194–210 (2011) [1103.2355].
6. R. Dijkgraaf, E. P. Verlinde, H. L. Verlinde, Nucl. Phys. B **484**, 543–561 (1997) [hep-th/9607026].
7. D. Shih, A. Strominger, X. Yin, JHEP **0610**, 087 (2006) [hep-th/0505094].
8. D. P. Jatkar, A. Sen, JHEP **0604**, 018 (2006) [hep-th/0510147].
9. A. Dabholkar, J. Gomes, S. Murthy, JHEP **1105**, 059 (2011) [0803.2692].
10. A. Sen, JHEP **0807**, 118 (2008) [0803.1014].
11. G. T. Horowitz, in Y. M. Cho (ed.), Gravitation and Cosmology, Pacific Conference, Seoul, Korea, February 1996 [gr-qc/9604051].
12. A. Sen, Gen. Rel. Grav. **40**, 2249–2431 (2008) [0708.1270].
13. A. Dabholkar, S. Nampuri, Lect. Notes Phys. **851**, 165–232 (2012) [1208.4814].
14. G. Gibbons, in H. de Vega, N. Sanchez (eds.), Field Theory, Quantum Gravity and Strings, 46–59 (1985).
15. S. Ferrara, R. Kallosh, Phys. Rev. D **54**, 1514–1524 (1996) [hep-th/9602136].
16. S. Ferrara, R. Kallosh, Phys. Rev. D **54**, 1525–1534 (1996) [hep-th/9603090].
17. G. L. Cardoso, B. de Wit, T. Mohaupt, Phys. Lett. B **451**, 309–316 (1999) [hep-th/9812082].
18. G. L. Cardoso, B. de Wit, J. Käppeli, T. Mohaupt, JHEP **0012**, 019 (2000) [hep-th/0009234].
19. K. Behrndt, G. L. Cardoso, B. de Wit, R. Kallosh, D. Lüst, T. Mohaupt, Nucl. Phys. B **488**, 236–260 (1997) [hep-th/9610105].
20. A. Sen, JHEP **0509**, 038 (2005) [hep-th/0506177].
21. A. Sen, Int. J. Mod. Phys. A **9**, 3707–3750 (1994) [hep-th/9402002].
22. R. M. Wald, Phys. Rev. D **48**, 3427–3431 (1993) [gr-qc/9307038].
23. T. Jacobson, G. Kang, R. C. Myers, Phys. Rev. D **49**, 6587–6598 (1994) [gr-qc/9312023].
24. V. Iyer, R. M. Wald, Phys. Rev. D **50**, 846–864 (1994) [gr-qc/9403028].
25. B. de Wit, S. Katmadas, M. van Zalk, JHEP **1101**, 007 (2011) [1010.2150].
26. I. Antoniadis, E. Gava, K. Narain, Nucl. Phys. **B383**, 93–109 (1992) [hep-th/9204030].
27. M. Bershadsky, S. Cecotti, H. Ooguri, C. Vafa, Commun. Math. Phys. **165**, 311–428 (1994) [hep-th/9309140].
28. A. Dabholkar, R. Kallosh, A. Maloney, JHEP **0412**, 059 (2004) [hep-th/0410076].
29. F. Denef, JHEP **0008**, 050 (2000) [hep-th/0005049].
30. M. C. Cheng, E. Verlinde, JHEP **0709**, 070 (2007) [0706.2363].
31. A. Sen, JHEP **0705**, 039 (2007) [hep-th/0702141].
32. A. Sen, JHEP **0709**, 045 (2007) [0705.3874].
33. A. Dabholkar, Phys. Rev. Lett. **94**, 241301 (2005) [hep-th/0409148].
34. L. Cornalba, M. S. Costa, J. Penedones, P. Vieira, JHEP **0612**, 023 (2006) [hep-th/0607083].

35. A. Dabholkar, F. Denef, G. W. Moore, B. Pioline, JHEP **0510**, 096 (2005) [hep-th/0507014].
36. A. Sen, JHEP **0507**, 063 (2005) [hep-th/0502126].
37. D. Shih and X. Yin, JHEP **0604**, 034 (2006) [hep-th/0508174].
38. G. L. Cardoso, B. de Wit, J. Käppeli, T. Mohaupt, JHEP **0412**, 075 (2004) [hep-th/0412287].
39. N. Banerjee, D. P. Jatkar, A. Sen, JHEP **0905**, 121 (2009) [0810.3472].
40. A. Sen, Int. J. Mod. Phys. A **24**, 4225–4244 (2009) [0809.3304].
41. A. Dabholkar, J. Gomes, S. Murthy, JHEP **1106**, 019 (2011) [1012.0265].

# Geometry of General Hypersurfaces, Constraint Equations and Applications to Shells

**Marc Mars**

**Abstract** The constraint equations are well-understood for hypersurfaces which are either everywhere non-null or null everywhere. The corresponding form of the equations is very different in both cases. In this paper, I discuss a general framework capable of analyzing the intrinsic and extrinsic geometry of general hypersurfaces of a spacetime. This framework is then applied to derive the form of the constraint equations in this general context. As an application, I will generalize the Israel equations for spacetime shells to the case when the shell is allowed to have varying causal character.

## 1 Introduction

The evolution problem in General Relativity (and many other geometric theories of gravity) consists in prescribing suitable initial data for the metric and determining the spacetime metric from this data. This requires a splitting of the spacetime so that it makes sense to talk about "evolution". The most widely used splitting consists in foliating the spacetime into a one-parameter family of spacelike hypersurfaces. The initial data are then fields defined on one such hypersurface (taken as the initial one), and the field equations become partial differential equations once a suitable coordinate system (or, alternatively, evolution direction) has been chosen. The initial data on the hypersurface takes different forms depending on the particular choice of fields in which the evolution equations are written. However, in all cases, this data is not free but subject to the so-called constraint equations. The specific form of the constraints obviously depends on the choice of fields, but, in one way or another, it always involves the induced metric on the hypersurface and

M. Mars (✉)
Dept. Física Fundamental, Universidad de Salamanca, Plaza de la Merzed s/n, 37008, Salamanca, Spain
e-mail: marc@usal.es

A. García-Parrado et al. (eds.), *Progress in Mathematical Relativity, Gravitation and Cosmology*, Springer Proceedings in Mathematics & Statistics 60,
DOI 10.1007/978-3-642-40157-2_5, © Springer-Verlag Berlin Heidelberg 2014

its time derivative. In more geometric terms, let $\Sigma$ be a spacelike hypersurface embedded in a spacetime $(\mathscr{M}, g)$ of arbitrary dimension $m+1$ ($m \geq 2$) and let $\boldsymbol{n}$ be the unit, future directed one-form orthogonal to the hypersurface. Spacetime tensors will carry Greek indices $(\alpha, \beta, \cdots = 0, \cdots, m)$ which will be raised and lowered with the spacetime metric and its inverse. If we denote by $\Phi : \Sigma \to \mathscr{M}$ the embedding of $\Sigma$ into the spacetime, $\Sigma$ inherits a first fundamental form $\gamma \stackrel{\text{def}}{=} \Phi^\star(g)$ and a second fundamental form $K \stackrel{\text{def}}{=} \Phi^\star(\nabla \boldsymbol{n})$, where $\nabla$ is the Levi–Civita covariant derivative of $(\mathscr{M}, g)$ and $\boldsymbol{n}$ has been extended arbitrarily off $\Sigma$. Tensors on $\Sigma$ will carry Latin indices $(a, b, \cdots = 1, \cdots m)$.

The Gauss and Codazzi identities relate suitable components of the Riemann tensor of the ambient spacetime (evaluated on $\Sigma$) to $\gamma$ and $K$ and their derivatives. Taking traces of these identities, the ambient geometry terms become expressions involving the Einstein tensor $G$ of $(\mathscr{M}, g)$ as follows (see e.g. [23])

$$2\rho := 2G_{\alpha\beta} n^\alpha n^\beta|_\Sigma = R(\gamma) - K_{ab}K^{ab} + K^2, \qquad K := \gamma^{ab} K_{ab}, \tag{1}$$

$$-J_a := G_{\alpha\beta} e^\alpha_a n^\beta|_\Sigma = D_b \left(K^b_{\ a} - K\delta^b_{\ a}\right) \tag{2}$$

where $D$ is the Levi–Civita covariant derivative of $(\Sigma, \gamma)$ and $R(\gamma)$ its curvature scalar. The constraint equations determine the normal–normal component ($\rho$) and the normal–tangential component ($J_a$) of the Einstein tensor.

Given a matter model, the Einstein field equations provide expressions for $\rho$ and $J_a$ in terms of the matter variables (e.g. in vacuum $\rho = 0, J_a = 0$) and hence, identities (1)–(2) become a set of partial differential equations for $\gamma_{ab}$, $K_{ab}$ and the matter variables. These are the constraint equations of General Relativity in the spacelike case. The constraint equations, although obtained via geometric identities for submanifolds, become equations intrinsic to $\Sigma$. This is important for the initial value problem since it detaches the initial data from the spacetime. This is accomplished by defining an initial data set as an abstract $m$-dimensional manifold $\Sigma$ endowed with a positive definite metric $\gamma_{ab}$, a symmetric tensor $K_{ab}$, a scalar $\rho$ and a one-form $J_a$ (typically given in terms of other fields on $\Sigma$ which, possibly, satisfy their own equations) such that (1)–(2) are satisfied. The five-tuple $\{\Sigma, \gamma_{ab}, K_{ab}, \rho, J_a\}$ is called an **initial data set**. The connection with the spacetime comes via a well-posedness theorem, which states that, given appropriate matter fields (e.g. vacuum), then an initial data set generates a spacetime (maximally unique) satisfying the Einstein field equations in which the data can be embedded. Embedded here means not only that there exists an embedding $\Phi : \Sigma \to \mathscr{M}$ but also that (a) the corresponding induced metric and second fundamental form defined by this embedding agree respectively with $\gamma_{ab}$, $K_{ab}$ and (b) $G_{\alpha\beta} n^\alpha n^\beta \stackrel{\Sigma}{=} \rho, G_{\alpha\beta} e^\alpha_a n^\beta \stackrel{\Sigma}{=} -J_a$.

Initial value problems arise not only in the spacelike context. A useful alternative is the characteristic initial value problem, where initial data is given on two null hypersurfaces which intersect transversally on a spacelike, codimension-two surface. Without going into details, the constraint equations in this setting are

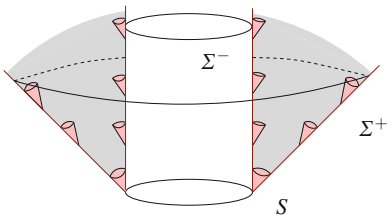


**Fig. 1** Schematic figure for the well-posedness of the characteristic initial value problem

essentially (see e.g. [19]) a hierarchical set of ODEs along the null direction tangent to each hypersurface. The formulation of the constraints typically requires a $2+1$ splitting of the null hypersurfaces. Thus, the constraints in this setting take a completely different form than in the spacelike case. However, such characteristic initial data also gives rise to a well-posed evolution problem [20] (see Fig. 1).

The limiting case where there is only one null hypersurface with a conical singularity (representing the future null cone of a point) has been dealt with recently [6] and both the constraint equations and the well-posedness of the evolution problem has been established in this case. The last situation I am aware of where the initial value problem has been set up and solved is the so-called Cauchy-characteristic initial value problem [24], where the initial configuration consists of suitable fields defined on two hypersurfaces, one spacelike and one null, intersecting on a codimension-two surface.

Despite the very different nature of the constraint equations (and of the evolution problem) in the settings described above, a natural question that arises is whether there is any framework which is capable of dealing with all cases at once. More generally, one would like to know how do the constraint equations look like in completely general hypersurfaces, with no restriction whatsoever on their causal character (note that a general hypersurface may perfectly have portions where it is spacelike, portions where it is timelike and portions—or subsets—where the first fundamental form degenerates). The motivation for doing so is not only in order to have a common framework for all the cases described above, but also as a tool to generalize well-posedness results to more general settings. For example, by causality arguments it is reasonable to expect that appropriate initial data prescribed on a hypersurface with everywhere positive semidefinite first fundamental form should define a well-posed evolution problem (see Fig. 2).

Besides its unifying power, this problem is relevant also from a more practical point of view because hypersurfaces of varying causal character with physical relevance are much more common that one may think at first sight. One example are the so-called marginally outer trapped tubes (also called trapping horizons [10], and dynamical/isolated horizons [3] with slight variations in their definitions). These are hypersurfaces foliated by codimension-two spacelike surfaces with one of its null expansions identically vanishing. A priori, these hypersurfaces may have any causal character. Under appropriate stability and energy conditions, no timelike

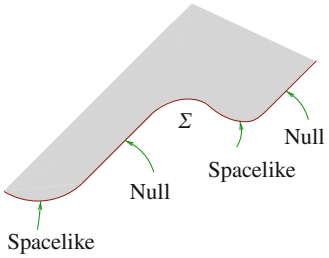


**Fig. 2** Representation of a hypersurface $\Sigma$ for which initial data satisfying the constraint equations are expected to produce a unique maximal spacetime (the portion to the future is shown in *grey* in the figure) satisfying the Einstein field equations

portion may exist [1, 2] but they can still vary their causal character from spacelike to null. Marginally outer trapped tubes are physically very relevant since they are suitable quasi-local replacements for black hole event horizons, and are analyzed routinely in any numerical evolution of "black hole" mergers of in any collapsing process. Other examples of physically relevant hypersurfaces of varying causal character can be found in the introduction of [17] where the geometry or arbitrary hypersurfaces in the spacetime was studied. The developments of that paper were focused in generalizing the matching conditions from the case of constant causal character (well-developed both in the spacelike and timelike cases [8, 15, 22] and in the null case [4]) to the arbitrary case of varying causal character and this required a better understanding of the geometry of general hypersurfaces in a spacetime.

In this work I will report recent work where the geometry of general hypersurfaces is developed further with the aim of writing down the constraint equations for arbitrary hypersurfaces. As an application, the field equations for thin shells will be derived as a simple consequence. Here, only a summary of results will be given. Details will be given elsewhere [16]. The plan of the paper is as follows. In Sect. 2, I will recall some fundamental notions for the geometry of general hypersurfaces [17] and I will identify the intrinsic information on the hypersurface that can be extracted from this construction. This will lead us to the notion of hypersurface data, that will play a central role in the rest of the paper. In Sect. 3, I will describe how the constraint equations may be derived and I will present the explicit expression they take in the case of general hypersurfaces. Finally, in Sect. 4, I will describe briefly the matching theory between two spacetimes and I will explain how the Israel equations for thin shells can be derived in the arbitrary causal character case (even changing one) as a simple consequence of the constraint equations obtained in the previous section.

## 2 Geometry of General Hypersurfaces in a Spacetime

Our setup for discussing the geometry of hypersurfaces consists on an $(m+1)$-dimensional spacetime $(\mathscr{M}, g)$, i.e. a smooth manifold $\mathscr{M}$ of dimension $m+1$ with $m \geq 2$ endowed with a smooth metric $g$ of Lorentzian signature.[1] We assume the spacetime to be oriented and time oriented. The covariant derivative associated to the spacetime metric is denoted by $\nabla$. The term "hypersurface" stands for smooth, embedded and orientable submanifold of codimension one (embedding is in the sense of injective immersion such the image of any open set is open in the subset topology of the image). The manifold will be denoted by $\Sigma$ and the embedding by $\Phi : \Sigma \longrightarrow \mathscr{M}$. Since $\Sigma$ is a homeomorphic with its image, it is safe to identify $\Sigma$ and $\Phi(\Sigma)$. We will therefore use $\Sigma$ for both objects and let the context determine the precise meaning that is intended.

As before, $\Sigma$ inherits a first fundamental form $\gamma \stackrel{\text{def}}{=} \Phi^\star(g)$. $\Sigma$ being orientable, its normal bundle admits global, nowhere vanishing, sections. Let $\boldsymbol{n}$ be any such section. This defines a "normal one-form" to $\Sigma$. Obviously, two normal one-forms $\boldsymbol{n}$ and $\boldsymbol{n'}$ are necessarily related by a smooth, nowhere zero function $F$ by $\boldsymbol{n'} = F\boldsymbol{n}$. For general hypersurfaces there is no canonical way of choosing a representative for "normal one-form". In the everywhere spacelike case $\boldsymbol{n}$ can be uniquely selected by making it unit and future directed. Already in the null case $\boldsymbol{n}$ has a built-in scaling freedom that cannot be fixed and this obviously remains true in the general case. A second fundamental form is associated to each choice of normal one-form, according to the same definition as before

$$K^n \stackrel{\text{def}}{=} \Phi^\star(\nabla \boldsymbol{n}),$$

where $\boldsymbol{n}$ in the right-hand side is any smooth extension of the normal one-form to a neighbourhood on $\Sigma$. All the second fundamental forms contain the same information, given the transformation law $K^{Fn} = FK^n$. However, given the absence of a canonical choice, we add a superscript $n$ in order to identify the normal one-form to which the second fundamental is attached.

In the general case, the first fundamental form is not a metric (it may degenerate on a non-empty subset) and its signature is not constant. This means, in particular, that $\Sigma$ inherits no canonical connection from the ambient manifold. It is well-known that $\gamma$ is degenerate precisely at those points where $\boldsymbol{n}$ is null, i.e. $g^\flat(\boldsymbol{n}, \boldsymbol{n}) = 0$. We will call them "null points". At null points, the vector $n$ (obtained by raising the index to $\boldsymbol{n}$ with the spacetime metric) is both normal and tangential to $\Sigma$. As a consequence, at null points, $K^n$ does not measure "extrinsic" properties of $\Sigma$ in $(\mathscr{M}, g)$ and hence loses all relationship with a transversal derivative of the first fundamental form.

[1] In fact, with only minor changes, everything below would apply equally well to Riemannian manifolds of arbitrary (non-degenerate) signature. We work with Lorentzian signature for definiteness and because it is the most interesting case in the context of gravitation.

It is clear that additional structure is required on $\Sigma$ to encode the extrinsic part of the geometry. The fundamental idea is due to Schouten [21] and consists in assigning to each point $p \in \Sigma$ a vector which is transverse to $T_pN$. It can be proven that, irrespective of the causal character of $\Sigma$, this choice of transverse vector can be made smoothly on $\Sigma$ (for this, it is crucial that $\Sigma$ is orientable). This transverse vector field is called "rigging". The formal definition is as follows.

**Definition 2.1 (Rigging vector [21]).** A rigging $\ell$ is a vector field along $\Sigma$ satisfying $\ell|_p \notin T_p\Sigma$ for all $p \in \Sigma$.

Alternatively, a rigging can be defined as a vector field along $\Sigma$ satisfying $\boldsymbol{n}(\ell) \neq 0$ everywhere for one (and hence any) choice of normal one-form $\boldsymbol{n}$. It is clear that the choice of rigging is highly non-unique and everything we say concerning the geometry of $\Sigma$ will have to take this fact into account. The rigging $\ell|_p$ being transversal to $\Sigma$ implies $T_p\mathscr{M} = \langle \ell|_p \rangle \oplus T_p\Sigma$, where $\langle \ell|_p \rangle$ is the one-dimensional vector space generated by $\ell|_p$. This fact can be stated equivalently as follows. Choose any basis $\{\hat{e}_a|_p\}$ $(a = 1, \cdots, m)$ of vectors of $T_p\Sigma$. These vectors can be pushed forward to the ambient spacetime to define a set of $m$ linearly independent vectors $e_a|_p$ of $T_p\mathscr{M}$ tangent to $\Sigma$. Adding the rigging, we have a basis $\{e_a|_p, \ell|_p\}$ of $T_p\mathscr{M}$. From now on, let us assume that we have chosen a set of $m$ vector fields $\{\hat{e}_a\}$ on $\Sigma$ which are linearly independent at each point. If such choice does not exist globally, then the basis should be selected on each open set of a suitable open cover of $\Sigma$. This adds no complications to the discussion except for the need of a more cumbersome notation.

Given a rigging, the choice of normal one-form $\boldsymbol{n}$ can be fixed uniquely and unambiguously by the condition $\boldsymbol{n}(\ell) = 1$. Obviously, this does not remove the intrinsic freedom in the choice of normal. It simply shifts it to the choice of rigging vector. The normalization $\boldsymbol{n}(\ell) = 1$ will be assumed from now on.

As briefly explained above in the spacelike case, it is necessary to define the data on an abstract manifold without reference to any spacetime. The first step is to encode the spacetime metric along $\Sigma$ in this abstract manner. In the spacelike case, all this information lies in the induced metric (this is because the normal vector can be chosen to be unit). In the general case, we need to transform the spacetime metric along $\Sigma$ in terms of objects defined on $\Sigma$. To that aim, let us define a one-form $\ell_a$ and a scalar $\ell^2$ on $\Sigma$ by

$$\ell_a \stackrel{\text{def}}{=} g(\ell, e_a), \qquad \ell^2 \stackrel{\text{def}}{=} g(\ell, \ell).$$

It is clear that the collection $\{\gamma_{ab}, \ell_a, \ell^2\}$ corresponds to the tensor representation of $g$ in the basis $\{e_a, \ell\}$ and, hence, it contains the same information as $g$ on $\Sigma$. Since the signature of $g$ is Lorentzian at every point (and no other restriction, except for smoothness, is required in order to define a spacetime metric along $\Sigma$), this leads to the following definition.

**Definition 2.2 (Hypersurface metric data).** Let $\Sigma$ be a smooth $m$-dimensional orientable manifold. Let $\gamma_{ab}$ be a symmetric tensor field, $\ell_a$ a one-form and $\ell^2$ a

scalar on $\Sigma$. The four-tuple $\{\Sigma, \gamma_{ab}, \ell_a, \ell^2\}$ define a **hypersurface metric data set** provided the square $(m+1)$-matrix

$$\begin{bmatrix} \gamma_{ab} & \ell_b \\ \ell_a & \ell^2 \end{bmatrix}$$

has Lorentzian signature at every point.

Note that a similar definition can be given for any other signature of the ambient metric by simply replacing "Lorentzian" in the definition by the new choice of signature. I also emphasize that $\ell^2$ in this definition is a scalar on its own and not the square of any quantity (the definition is given at the abstract level on $\Sigma$ and hence requires no embedding, nor rigging).

Given hypersurface metric data, we can define immediately a symmetric tensor $P^{ab}$, a vector $n^a$ and a scalar $n^2$ on $\Sigma$ by the following definition.

$$\begin{bmatrix} P^{ab} & n^b \\ n^a & n^2 \end{bmatrix} \stackrel{\text{def}}{=} \begin{bmatrix} \gamma_{ab} & \ell_b \\ \ell_a & \ell^2 \end{bmatrix}^{-1}. \tag{3}$$

It is obvious that all these objects are tensorial on $\Sigma$. Given hypersurface metric data we will always define $P^{ab}$, $n^a$ and $n^2$ according to this definition.

In order to make contact from the abstract level to the spacetime level, we need a definition that states under which conditions metric hypersurface data corresponds to a spacetime hypersurface endowed with a rigging vector. The definition is natural and reads

**Definition 2.3.** A metric hypersurface data $\{\Sigma, \gamma_{ab}, \ell_a, \ell^2\}$ is **embedded** in a spacetime $(\mathscr{M}, g)$ if there exists an embedding $\Phi : \Sigma \to \mathscr{M}$ and a rigging vector $\ell$ such that

$$\gamma = \Phi^\star(g), \qquad \ell_a = \Phi^\star(\boldsymbol{\ell})_a, \qquad \ell^2 = \Phi^\star(g(\ell, \ell)),$$

where $\boldsymbol{\ell}$ is obtained by lowering the index to $\ell$ with the spacetime metric $g$.

Assume that we are given metric hypersurface data $(\Sigma, \gamma, \ell_a, \ell^2)$ with embedding $\Phi$ and rigging $\ell$. Let $\{\boldsymbol{\omega^a}, \boldsymbol{n}\}$ be the dual basis of $\{e_a, \ell\}$. We can lower the indices to $\{e_a, \ell\}$ to define $m+1$ one-forms $\{\boldsymbol{e_a}, \boldsymbol{\ell}\}$ and raise the indices to $\{\boldsymbol{\omega^a}, \boldsymbol{n}\}$ to define $m+1$ vectors $\{\omega^a, n\}$. Then the following expressions hold

$$n = n^a e_a + n^2 \ell, \tag{4}$$

$$\boldsymbol{\ell} = \ell_a \boldsymbol{\omega^a} + \ell^2 \boldsymbol{n}, \tag{5}$$

$$\boldsymbol{e_a} = \gamma_{ab} \boldsymbol{\omega^b} + \ell_a \boldsymbol{n}, \tag{6}$$

$$\omega^a = P^{ab} e_b + n^a \ell. \tag{7}$$

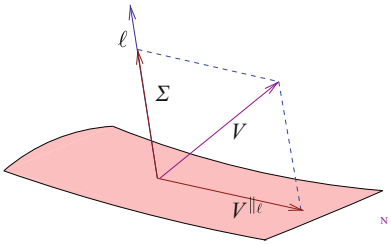


**Fig. 3** Decomposition of a vector $V$ into a transversal component $V^{\perp_\ell}\ell$ and a tangential component $V^{\parallel_\ell}$. This decomposition obviously depends on the choice of rigging

Consequently, $n^2$ (which we have defined by (3)) happens to be in the embedded case the square norm of the normal vector $n$, $n^2 = g(n,n)$. In addition $n^a$ has the spacetime interpretation of being the tangential component of the vector $n$. Indeed, the direct sum decomposition $T_p\mathscr{M} = \langle \ell|_p \rangle \oplus T_p\Sigma$ allows us to decompose any vector $V \in T_p\mathscr{M}$ as $V = V^{\perp_\ell}\ell + V^{\parallel_\ell}$, where $V^{\perp_\ell}\ell$ is the *transversal* part and $V^{\parallel_\ell}$ is the parallel part of $V$ (see Fig. 3).

As a consequence of (4) we have $n^{\parallel_\ell} = n^a e_a$. For notational simplicity we will denote this tangential vector as $\hat{n}$ from now on. Note that the decomposition of a vector $V$ into transversal and tangential parts depends strongly on the choice of rigging. However, when $n$ is null, then $\hat{n}$ is independent of the rigging (see (4)). This is just a consequence of the fact that a null normal is tangent to the hypersurface and hence defined intrinsically. In any other case $n^a$ is a vector that depends on the choice of rigging.

A rigging allows us not only to encode the spacetime metric along $\Sigma$ in terms of hypersurface data, but also to define a natural connection on the hypersurface.

**Proposition 2.4 (Rigging connection [17, 21]).** *Let $(\mathscr{M}, g)$ be a spacetime and $\Sigma$ a hypersurface. Given $X, Y$ vector fields tangent to $\Sigma$ define $\overline{\nabla}_X Y \stackrel{def}{=} (\nabla_X Y)^{\parallel}$. Then $\overline{\nabla}$ is a torsion-free covariant derivative on $\Sigma$.*

We will denote by $\overline{\Gamma}^a_{bc}$ the Christoffel symbols of $\overline{\nabla}$ in a basis $\{\hat{e}_a\}$. From the definition of second fundamental form, we have [17]

$$\nabla_{e_a} e_b = -K^n_{ab}\,\ell + \overline{\Gamma}^c_{ba}\, e_c .$$

Decomposing $\nabla_{e_a}\ell$ in transversal and tangential components defines two tensor fields $\varphi_a$, $\Psi^a_{\ b}$ on $\Sigma$ by [17]

$$\nabla_{e_a}\ell = \varphi_a\,\ell + \Psi^b_{\ a}\, e_b . \tag{8}$$

These tensors are not independent from each other and must satisfy appropriate equations, which follow from the condition that the spacetime connection is metric. As an example, we compute the directional derivative of the first fundamental form along $\hat{e}_a$,

$$\hat{e}_a(\gamma_{bc}) = \nabla_{e_a}\langle e_b, e_c\rangle = g(\nabla_{e_a}e_b, e_c) + g(e_b, \nabla_{e_a}e_c) =$$
$$= -K^n_{ab}\ell_c - K^n_{ac}\ell_b + \overline{\Gamma}^d_{ab}\gamma_{dc} + \overline{\Gamma}^d_{ac}\gamma_{db}.$$

A similar computation on $\ell_a$ and $\ell^2$ leads to the following set of compatibility equations for the unknowns $\{\overline{\Gamma}^b_{ab}, K^n_{ab}, \Psi^b{}_a, \varphi_a\}$.

$$\overline{\nabla}_a\gamma_{bc} + \left(\ell_b K^n_{ac} + \ell_c K^n_{ab}\right) = 0, \tag{9}$$

$$\overline{\nabla}_a\ell_b - \varphi_a\ell_b + \ell^2 K^n_{ab} - \gamma_{bc}\Psi^c{}_a = 0, \tag{10}$$

$$\frac{1}{2}\overline{\nabla}_a\ell^2 - \ell^2\varphi_a - \Psi^b{}_a\ell_b = 0. \tag{11}$$

The following result provides the general solution of these equations in terms of free data on $\Sigma$ (see [16] for the proof).

**Proposition 2.5.** *Let $\{\Sigma, \gamma_{ab}, \ell_a, \ell^2\}$ be hypersurface metric data and $Y_{ab}$ an arbitrary symmetric tensor. Define $F_{ab}$ as the two-form $F_{ab} \overset{\text{def}}{=} \frac{1}{2}(\partial_a\ell_b - \partial_b\ell_a)$. Choose a coordinate basis $\{\hat{e}_a\}$ and let*

$$\overline{\Gamma}^c_{ab} \overset{\text{def}}{=} \frac{1}{2}P^{cd}\left(\partial_a\gamma_{bd} + \partial_b\gamma_{ad} - \partial_d\gamma_{ab}\right) + n^c\left(-Y_{ab} + \frac{1}{2}\left(\partial_a\ell_b + \partial_b\ell_a\right)\right), \tag{12}$$

$$K^n_{ab} \overset{\text{def}}{=} n^2 Y_{ab} + \frac{1}{2}\mathscr{L}_{\hat{n}}\gamma_{ab} + \frac{1}{2}\left(\ell_a\partial_b n^2 + \ell_b\partial_a n^2\right), \tag{13}$$

$$\varphi_a \overset{\text{def}}{=} \frac{1}{2}n^2\partial_a\ell^2 + n^b\left(Y_{ab} + F_{ab}\right), \tag{14}$$

$$\Psi^b{}_a \overset{\text{def}}{=} P^{bc}\left(Y_{ac} + F_{ac}\right) + \frac{1}{2}n^b\partial_a\ell^2. \tag{15}$$

*Then $\overline{\Gamma}^b_{ab}$ defines a torsion-free connection on $\Sigma$ and $\{\overline{\Gamma}^b_{ab}, K^n_{ab}, \Psi^b{}_a, \varphi_a\}$ solves the compatibility equations (9)–(11).*

*Conversely, any solution of these equations can be written in this form for some symmetric tensor $Y_{ab}$.*

Given hypersurface data, we will always associate to it a linear connection with connection coefficients $\overline{\Gamma}^a_{bc}$ (in a coordinate basis) given by (12) and tensors $K^n_{ab}$, $\varphi_a$ and $\Psi^b{}_a$ by the expressions (13)–(15).

Having obtained the general solution of the compatibility equations, it makes sense to define abstract data, independently of any spacetime or choice of rigging.

**Definition 2.6 (Hypersurface data).** A five-tuple $\{\Sigma, \gamma_{ab}, \ell_a, \ell^2, Y_{ab}\}$ is called **hypersurface data** provided $\{\Sigma, \gamma_{ab}, \ell_a, \ell^2\}$ is metric hypersurface data and $Y_{ab}$ is a symmetric tensor on $\Sigma$.

Similarly as before, a notion of embedding of hypersurface data becomes natural.

**Definition 2.7 (Embedding of hypersurface data).** Let $\{\Sigma, \gamma_{ab}, \ell_a, \ell^2, Y_{ab}\}$ be hypersurface data. We will say that this data is embedded in a spacetime $(\mathscr{M}, g)$ if there exists an embedding $\Phi : \Sigma \longrightarrow \mathscr{M}$ and a choice of rigging $\ell$ such that

$$\Phi^\star(g) = \gamma, \quad \Phi^\star(\boldsymbol{\ell})_a = \ell_a, \quad \Phi^\star(g(\ell,\ell)) = \ell^2, \quad \tfrac{1}{2}\Phi^\star(\mathscr{L}_\ell\, g) = Y.$$

For this definition to make sense it is necessary to check that $\Phi^\star(\mathscr{L}_\ell\, g) = Y$ is a consistent requirement. This follows easily because from the expressions in Proposition 2.5, the following identity on $\Sigma$ holds

$$Y_{ab} = \frac{1}{2}\left(\overline{\nabla}_a \ell_b + \overline{\nabla}_b \ell_a\right) + \ell^2 K^n_{ab}.$$

Once the data is embedded in a spacetime, it is immediate to check that the right hand side of this expression equals $\Phi^\star(\mathscr{L}_\ell\, g)$.

As we have already mentioned, general hypersurfaces admit no canonical choice of rigging. We can deal with this freedom by introducing a gauge transformation on the initial data. Assume first that the hypersurface data is embedded, consider a change of rigging and evaluate the changes that it induces in the data. The last step is to ignore the process and simply define the final result as gauge transformation of the data. Two rigging vectors $\ell$, $\ell'$ are necessarily related by $\ell' = u\ell + v$, where $u$ is a positive function on $\Sigma$ and $v$ is a vector field tangent to $\Sigma$. The process above leads to the following definition [16].

**Definition 2.8 (Gauge transformation).** Two hypersurface data $\{\Sigma, \gamma_{ab}, \ell_a, \ell^2, Y_{ab}\}$ and $\{\Sigma, \gamma_{ab}, \ell'_a, \ell^{2\prime}, Y'_{ab}\}$ are related by a gauge transformation if there exists a scalar $u$ and a vector $v^a$ on $\Sigma$ such that

$$\begin{aligned}
\ell'_a &= u(\ell_a + v^b\gamma_{ab}),\\
\ell^{2\prime} &= u^2(\ell^2 + 2v^a\ell_a + v^a v^b\gamma_{ab}),\\
Y'_{ab} &= uY_{ab} + \tfrac{1}{2}\mathscr{L}_{uv}\gamma_{ab} + \tfrac{1}{2}\left(\ell_a\overline{\nabla}_b u + \ell_b\overline{\nabla}_a u\right).
\end{aligned}$$

## 3 Constraint Equations for General Hypersurfaces

With the geometric considerations of the previous section, we are ready to obtain the constraint equations on general hypersurfaces. Let us start noting that, given hypersurface data embedded in a spacetime, all the tangential derivatives $\nabla_{e_a}\ell$, $\nabla_{e_a}e_b$ can be computed. On the other hand, from the definition of the Riemann tensor of the ambient spacetime

$$\nabla_X\nabla_Y Z - \nabla_Y\nabla_X Z - \nabla_{[X,Y]}Z = \mathbf{R}(X,Y)Z,$$

it follows that, along $\Sigma$, the components of the Riemann tensor of the type $\mathrm{R}^{\alpha}{}_{\beta\gamma\delta}e_a^{\gamma}e_b^{\delta}$ can be computed in terms of hypersurface data. The question is, hence, whether the knowledge of these components is sufficient or not to determine the components $G_{\alpha\beta}n^{\beta}$ of the Einstein tensor in terms of hypersurface data. The answer turns out to be yes, and the relationship is given by the following identities (see [16] for the proof)

$$\mathrm{G}^{\alpha}_{\beta}n_{\alpha}\ell^{\beta} = -\mathrm{R}_{\alpha\beta\gamma\delta}\ell^{\alpha}e_b^{\beta}e_c^{\gamma}e_d^{\delta}n^c P^{bd} - \tfrac{1}{2}\mathrm{R}_{\alpha\beta\gamma\delta}e_a^{\alpha}e_b^{\beta}e_c^{\gamma}e_d^{\delta}P^{ac}P^{bd}, \tag{16}$$

$$\mathrm{G}^{\alpha}_{\beta}n_{\alpha}e_c^{\beta} = \mathrm{R}_{\alpha\beta\gamma\delta}\ell^{\alpha}e_b^{\beta}e_c^{\gamma}e_d^{\delta}\left(n^2P^{bd} - n^bn^d\right) + \mathrm{R}_{\alpha\beta\gamma\delta}e_a^{\alpha}e_b^{\beta}e_c^{\gamma}e_d^{\delta}n^aP^{bd}. \tag{17}$$

In order to make contact with the constraint equations in the spacelike case, let us define a scalar $\rho_\ell$ and a one-form $J_a$ on $\Sigma$ by

$$\rho_\ell \overset{\text{def}}{=} -\mathrm{G}^{\alpha}_{\beta}n_{\alpha}\ell^{\beta}, \qquad J_a \overset{\text{def}}{=} -\mathrm{G}^{\alpha}_{\beta}n_{\alpha}e_a^{\beta}. \tag{18}$$

To motivate these definitions, we note that in the case of a spacelike hypersurface, the natural choice of rigging is along the normal direction. If we let $n$ to be the future directed unit vector orthogonal to $\Sigma$, then the condition $g(\ell, n) = 1$ (which we have imposed all along) together with the choice that $\ell$ is parallel to $n$ force the relationship $\ell = -n$. As a consequence $\ell_a = 0$, $n^a = 0$, $P^{ab}$ is the inverse of $\gamma_{ab}$ and the rigging connection is simply the Levi–Civita connection of the positive definite metric $\gamma$ (see (12)). Hence, in this case, $\rho_\ell$ as defined in (18) matches exactly the definition of energy density in the spacelike case (this explains the choice of sign we have made in (18)). For general hypersurfaces we call $\rho_\ell$ the "energy along $\ell$", although in physical terms it does not correspond to the energy of any observer. Similarly, we will call $J_a$ the "energy flux along $n$". Note that $J_a$ is independent of the choice of rigging. Nevertheless, the name is not intended to mean that $J_a$ is any physical energy flux for a spacetime observer. The names are simply adequate for a decomposition of the one-form $\mathrm{G}_{\alpha\beta}n^{\beta}$ in terms of transversal and tangential components.

Inserting the expressions for $R_{\alpha\beta\gamma\delta}e_a^{\gamma}e_b^{\delta}$ into (16)–(17), the following theorem can be proved [16].

**Theorem 3.1 (Constraint equations).** *Let $\{\Sigma, \gamma_{ab}, \ell_a, \ell^2, Y_{ab}\}$ be hypersurface data embedded into a spacetime $(\mathscr{M}, g)$. Then the following identities hold:*

*"Hamiltonian" constraint:*

$$2\rho_\ell = P^{ab}\Big[n^c\left(\overline{\nabla}_b\left(\ell^2K^n_{ac}\right) - \overline{\nabla}_c\left(\ell^2K^n_{ab}\right) + \ell_d\overline{R}^d{}_{acb}\right) + \overline{R}^c{}_{acb}$$

$$+P^{cd}\left(K^n_{ac}Y_{bd} - K^n_{ab}Y_{cd}\right)\Big].$$

*"Momentum" constraint:*

$$-J_a = \left(P^{bd} - \ell^2n^bn^d\right)\left(\overline{\nabla}_dK^n_{ab} - \overline{\nabla}_aK^n_{bd}\right) - n^bn^d\ell_c\overline{R}^c{}_{bad}$$

$$+\tfrac{1}{2}\left(n^2P^{bd}-n^bn^d\right)\times$$
$$\times\left(K^n_{ab}\overline{\nabla}_d\ell^2-K^n_{bd}\overline{\nabla}_a\ell^2\right)+P^{bd}n^c\left[K^n_{ba}\left(\overline{\nabla}_d\ell_c+\ell^2K^n_{dc}\right)\right.$$
$$\left.-K^n_{bd}\left(\overline{\nabla}_a\ell_c+\ell^2K^n_{ac}\right)\right].$$

When $\Sigma$ is spacelike and the rigging is chosen as $\ell=-n$ (with $n$ future directed and unit, as before), these identities become the standard constraint equations (1)–(2) after simply setting $n^a=\ell_a=0, n^2=1$ and $P^{ab}=\gamma^{-1\,ab}$. We emphasize, however, that even in the spacelike case, there is no need to choose the rigging as $\ell=-n$. It is perfectly possible that, in certain circumstances, a different choice of rigging may be more convenient. Thus, the general and unified framework developed above may be useful not only in order to deal with general hypersurfaces, but also to look at the standard constraint equations in the spacelike case from a different, and probably useful, new perspective.

## 4 An Application: Barrabès–Israel Equations for Arbitrary Shells

An important method to build physically interesting spacetimes consists in the matching of two spacetimes with boundary. This theory is useful to describe many physical systems composed of several parts with intrinsically distinct properties (e.g. a vacuum region outside a matter region which ends sharply on some hypersurface). This theory was developed first for the case when the boundaries of the spacetimes to be matched were spacelike or timelike. The main contributions here are due to Darmois [8], Lichnerowicz [15] and O'Brien–Synge [22]. Their proposals were different but a close relationship between them could be established [5]. There is now consensus that the matching conditions to be imposed in the spacelike (or timelike) case are the Darmois matching conditions which demand that the boundaries to be matched are diffeomorphic to each other and that the diffeomorphism transforms the first and second fundamental forms of one boundary onto the corresponding fundamental forms of the other boundary (with the restriction that the second fundamental forms are computed with respect to unit normals with, for one spacetime points inwards and for the other spacetime points outwards). When the matching is such that there is energy and/or matter concentrated on the matching hypersurface, then the second fundamental forms jump across the matching hypersurface a certain amount related to the energy-momentum tensor on the shell. This are the so-called Israel conditions [11–13]. By performing a suitable limit of these conditions from the spacelike to the lightlike case, Barrabès and Israel were able to derive the shell equations for null hypersurfaces (and hence also the matching conditions across null hypersurfaces by simply setting the energy-momentum tensor on the shell equal to zero). In all works quoted above, the

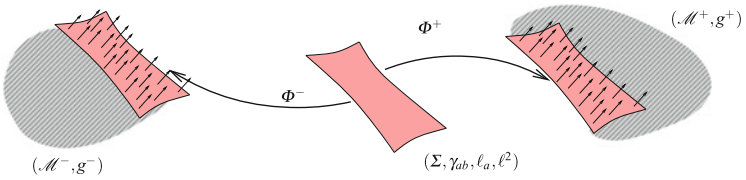


**Fig. 4** The matching of two spacetimes has as basic ingredient that the boundaries are diffeomorphic to each other and that each boundary admits a choice of rigging such that the hypersurface metric data they define on the abstract manifold $\Sigma$ are the same. Moreover, the choice of riggings must be such that it points inwards in one spacetime and outwards in the other

necessity of imposing the continuity of the first fundamental form was always added as a requirement. A firm basis for this came from the work of Clarke and Dray [7], who showed that this condition is necessary and sufficient for the existence of a matched spacetime with continuous metric in a suitable atlas. The work by Clarke and Dray was performed in the case of constant signature (including null). However, the arguments could be generalized to the arbitrary signature case [17]. The precise statement (see Fig. 4 for a schematic representation) can be written as follows (we adapt the statement to the notions introduced above).

**Theorem 4.1 ([7, 17, 18]).** *Consider two* $(m+1)$*-dimensional spacetimes* $(\mathscr{M}^\pm, g^\pm)$ *with boundaries* $\partial\mathscr{M}^\pm$*. They can be matched across their boundaries to produce a spacetime* $(\mathscr{M}, g)$ *with continuous metric (in a suitable differentiable atlas) if and only if:*

*(i) There exists metric hypersurface data* $(\Sigma, \gamma_{ab}, \ell_a, \ell^2)$ *which can be embedded both in* $(\mathscr{M}^+, g^+)$ *and in* $(\mathscr{M}^-, g^-)$ *with respective embedding and riggings* $\Phi^\pm$ *and* $\ell^\pm$*. Moreover, the embeddings satisfy* $\Phi^\pm(\Sigma) = \partial\mathscr{M}^\pm$*.*
*(ii) The rigging vectors* $\ell^\pm$ *point, respectively, inside and outside of* $\mathscr{M}^\pm$*.*

The original statements in [7,17] demanded only that the first fundamental forms on $\Sigma$ induced by the two embeddings were the same. It was taken for granted that under these circumstances, the existence of suitable riggings satisfying (i) and (ii) always exist. This is indeed true for nowhere degenerate hypersurfaces (timelike or spacelike everywhere), but it need not be true when the hypersurface has null points. This was first realized in [18]. Hence the necessity of stating the theorem in terms of existence of suitable riggings on each boundary.

In order to discuss the shell equations (or, in particular, the Darmois matching conditions) in the general case let us consider two spacetimes $(\mathscr{M}^\pm, g^\pm)$ that can be matched across $\partial\mathscr{M}^+ \simeq \partial\mathscr{M}^- \simeq \Sigma$ to produce a spacetime with continuous metric. We can extract two hypersurface data on $\Sigma$, one from each embedding which, according to Theorem 4.1, are of the form $\{\Sigma, \gamma_{ab}, \ell_a, \ell^2, Y_a^\pm\}$. For any quantity $A(Y)$ depending on $Y$ let us define $[A] \stackrel{\text{def}}{=} A(Y^+) - A(Y^-)$.

In the nowhere null case, let $\epsilon = g(n,n) = \pm 1$, depending on whether the hypersurface is timelike or spacelike. For any choice of rigging $\ell$, it follows

from (13) that $[K_{ab}] = \epsilon[Y_{ab}]$. The Darmois matching conditions require the "continuity" of the second fundamental forms i.e. $[K_{ab}] = 0$ (or equivalently $[Y_{ab}] = 0$). Then, it follows that there is a subatlas of $(\mathscr{M}, g)$ in which the metric is in fact $C^1$ [5, 11]. The Riemann tensor of $(\mathscr{M}, g)$ may be discontinuous at $\Sigma$ but it is otherwise regular everywhere. This is interpreted physically as saying that there is no matter-energy, or gravitational field concentrated on the matching hypersurface.

On the other hand, if $[K_{ab}] \neq 0$, then the Riemann tensor (viewed as a tensor distribution in $(\mathscr{M}, g)$, see [9, 14, 15, 17] for details on how to define and use tensor distributions in this setting) has a Dirac delta function supported on $\Sigma$. In physical terms, this means that the hypersurface $\Sigma$ carries energy and momentum and hence should be interpreted as a thin shell (also called "surface layer") of matter-energy. It turns out that the Dirac delta part of the Einstein tensor is (still in the nowhere null case)

$$\mathscr{G}^{\mu\nu} = \tau^{ab} e_a^\mu e_b^\nu \delta_{\mathscr{N}} \quad \text{with} \quad \tau_{ab} = -\left([K_{ab}] - [K]\gamma_{ab}\right), \quad \delta_{\mathscr{N}} : \text{ Dirac delta on } (\Sigma, \gamma).$$

The (distributional) conservation equations $\nabla_\mu G^\mu{}_\nu = 0$ imply

$$(K^+_{ab} + K^-_{ab})\tau^{ab} = 2[G_{\mu\nu} n^\mu n^\mu], \qquad \overline{\nabla}_b \tau^b{}_a = [J_a], \tag{19}$$

which are field equations for the shell. We note that these equations can be derived directly from the constraint equations (1)–(2) by simply taking the difference of both equations at each side of the matching hypersurface, and using the fact that the metric and the connection do not jump across the shell. As already mentioned, these field equations were extended to the null case by Barrabès and Israel [4] with an argument based on taking limits where the spacelike/timelike matching hypersurface becomes null.

Regarding general hypersurfaces, the Darmois matching conditions (which demand that the Riemann tensor has no singular distribution on the matching hypersurface) were extended to this case in [17], the main result being that the necessary and sufficient conditions for the matched spacetime $(\mathscr{M}, g)$ to admit a $C^1$ atlas (which happens to be equivalent to the absence of Dirac delta part in the distributional Riemann tensor) is that $[Y_{ab}] = 0$ (this was written differently in [17], but it is easy to check that $[Y_{ab}] = 0$ gives an equivalent formulation of the conditions). This result was derived by first obtaining an explicit form of the Dirac delta part of the distributional Riemann tensor in the atlas where the matched spacetime metric is continuous. It turned out that this Dirac delta part vanishes identically if and only if $[Y_{ab}] = 0$. We note that, as a by-product of the analysis in [17], an explicit form of the Dirac delta part of the Einstein tensor was obtained.

At this point, two natural questions arise. The first one is what is the expression for the singular part of the Einstein tensor in terms of hypersurface data and the second, what are the field equations for thin shells or arbitrary causal character. These two questions could be addressed using distributions, as done in the nowhere

null case (recall that the null case was obtained as a limiting case of those). However, we noticed before that the shell equations in the nowhere null case can also be derived directly and easily from the constraint equations (1)–(2). Having obtained general expressions for the constraint equations in arbitrary hypersurfaces it makes sense to try and derive the shell equations from them. This method is, on the one hand, simpler than the previous one because there is no need to introduce spacetime distributions nor specific atlas in the matched spacetime in order to perform the calculation. But even more, it does not even need to assume that a spacetime exists. This may seem spurious, but it is not so. The initial data on a hypersurface does not immediately generate a spacetime. A well-posed problem is required for that, and in some cases such a result is not yet available (or even expected). Nevertheless, jump discontinuities on the data may still be considered and the field equations that they need to satisfy can be derived from the constraint equations. This makes all the sense already at the initial data level, and may be used for several things, ranging from studying shell equations on their own (i.e. detached from the spacetime) to more practical purposes like obtaining new solutions of the constraint equations from a seed solution and a solution of the shell equations.

Let us therefore try and find the shell equations from the expressions in Theorem 3.1. Assume we are given two hypersurface data $\{\Sigma, \gamma_{ab}, \ell_a, \ell^2, Y^{\pm}_{ab}\}$ and let us define $V_{ab} \stackrel{\text{def}}{=} [Y_{ab}]$. We first give the answer to the first question posed above (details will be given in [16]).

**Definition 4.2 (Energy-momentum of the shell).** The energy-momentum tensor on the shell $\tau^{ab}$ is defined as

$$\tau^{ab} \stackrel{\text{def}}{=} \left(n^a P^{bc} + n^b P^{ac}\right) n^d V_{cd} - \left(n^2 P^{ac} P^{bd} + P^{ab} n^c n^d\right) V_{cd} + \left(n^2 P^{ab} - n^a n^b\right) P^{cd} V_{cd}.$$

Although the final motivation for this definition comes from the distributional part of the Einstein tensor in a matched spacetime, there are several indications at the initial data level which makes this definition adequate. First of all the definition is intrinsic to the initial data, and there is no need to invoke any spacetime to write it down. Moreover, the following are properties that can be checked directly from the definition:

(a) The energy-momentum tensor is symmetric, $\tau^{ab} = \tau^{ba}$.
(b) At any point $p \in \Sigma$ where $n^2(p) \neq 0$, $\tau^{fa}$ vanishes if and only if $V_{ab} = 0$. At any point where $n^2(p) = 0$, $\tau^{fa}$ vanishes if and only if $V_{ab} n^b = 0$ and $P^{ab} V_{ab} = 0$.
(c) Under a gauge transformation defined by $(u, v)$ one has

$$V'_{ab} = u V_{ab}, \qquad \tau'^{ab} = \frac{1}{u} \tau^{ab}.$$

It is clear that the jump $V_{ab} = [Y_{ab}]$ induces jumps on other quantities, for instance on the connection coefficient or on the second fundamental form, which satisfy

$$[\overline{\Gamma}^{c}_{ab}] = -n^c V_{ab}, \qquad [K^n_{ab}] = n^2 V_{ab}.$$

The first expressions implies that we need to choose which connection should be used in order to write down the equations. One possibility is to use as connection coefficients the semi-sum of the previous two, i.e.

$$\overline{\Gamma}^{a}_{bc} = \frac{1}{2}\left(\Gamma^{-a}_{bc} + \Gamma^{+a}_{bc}\right).$$

This was the choice made by Barrabès and Israel [4] to derive the shell equations in the null case. However, this choice has the inconvenience that the unknown $V_{ab}$ appears in the covariant derivative itself, and this obscures the meaning of the equations. Since we have explicit expressions for the connection coefficients in terms of the hypersurface metric data, a direct inspection suggests the following choice of connection, which depends *only* on the hypersurface metric data (i.e. it is completely independent of $Y_{ab}$),

$$\overset{\circ}{\Gamma}{}^{c}_{ab} \overset{\text{def}}{=} \tfrac{1}{2}P^{cd}\left(\partial_a\gamma_{bd} + \partial_b\gamma_{ad} - \partial_d\gamma_{ab}\right) + n^c\partial_{(a}\ell_{b)} \quad \Longleftrightarrow \quad \overline{\Gamma}^{a}_{bc} = \overset{\circ}{\Gamma}{}^{c}_{ab} - n^c Y_{ab}.$$

Its corresponding covariant derivative will be denoted by $\overset{\circ}{\nabla}$. It is now a matter of simple subtraction (we first need to transform the $\overline{\nabla}$ covariant derivatives into $\overset{\circ}{\nabla}$ covariant derivatives) in Theorem 3.1 to obtain the field equations on arbitrary shells. The result is [16].

**Theorem 4.3 (Field equations for shells).** *The jump $V_{ab}$ satisfies the following identities:*

$$\begin{aligned}
&\overset{\circ}{\nabla}_a\left(\tau^{ab}\ell_b\right) - \tfrac{1}{2}\tau^{ab}\left(Y^+_{ab} + Y^-_{ab}\right) + \tfrac{1}{2}\left(n^2\overset{\circ}{\nabla}_a\ell^2 + n^d\left[\overset{\circ}{\nabla}_a\ell_d - \overset{\circ}{\nabla}_d\ell_a\right]\right)\times\\
&\quad\times\tau^{ab}\ell_b = [\rho_\ell],\\
&\overset{\circ}{\nabla}_b\tau^{b}_{\ a} + \tfrac{1}{2}\left(n^2\overset{\circ}{\nabla}_b\ell^2 + n^c\left[\overset{\circ}{\nabla}_b\ell_c - \overset{\circ}{\nabla}_c\ell_b\right]\right)\tau^{b}_{\ a} + \left(\tfrac{1}{2}\mathscr{L}_{\hat{n}}\gamma_{ab} + \ell_{(a}\overset{\circ}{\nabla}_{b)}n^2\right)\times\\
&\quad\times\tau^{bc}\ell_c = [J_a],
\end{aligned}$$

*where* $\tau^{a}_{\ b} \overset{\text{def}}{=} \tau^{ac}\gamma_{cb}$.

It is straightforward to check that, in the spacelike (or timelike case), these equations become exactly the Israel equations (19).

**Acknowledgements** Financial support under the projects FIS2009-07238, FIS2012-30926 (Spanish MICINN) and P09-FQM-4496 (Junta de Andalucía and FEDER funds).

## References


1. Andersson, L., Mars, M., Simon, W.: Local existence of dynamical and trapping horizons. Phys. Rev. Lett. **95**, 111102 (4 pp.) (2005)
2. Andersson, L., Mars, M., Simon, W.: Stability of marginally outer trapped surfaces and existence of marginally outer trapped tubes. Adv. Theor. Math. Phys. **12**, 853–888 (2008)
3. Ashtekar, A. Krishnan, B.: Isolated and Dynamical Horizons and Their Applications. Living Rev. Relativity **7**, 10 (2004), URL (cited on 31 January 2013): http://www.livingreviews.org/lrr-2004-10
4. Barrabès. C., Israel, W.: Thin shells in general relativity and cosmology: The lightlike limit. Phys. Rev. D **43**, 1129–1142 (1991)
5. Bonnor, W.B., Vickers, P.A.: Junction conditions in General Relativity. Gen. Rel. Grav. **13**, 29–36 (1981)
6. Choquet-Bruhat, Y., Chruściel P.T., Martín-García J.M.: The Cauchy problem on a characteristic cone for the Einstein equations in arbitrary dimensions. Annales Henri Poincaré **12**, 419–482 (2011)
7. Clarke, C.J.S., Dray, T.: Junction conditions for null hypersurfaces. Class Quantum Grav. **4**, 265–275 (1987)
8. Darmois, G.: Les équations de la gravitation einstenienne. Mémorial des Sciences Mathématiques, Fascicule XXV (Paris, Gauthier-Villars) (1927)
9. Geroch, R., Traschen, J.: Strings and other distributional sources in general relativity. Phys. Rev. D **36**, 1017–1031 (1987)
10. Hayward, S.A.: General Laws of Black-Hole Dynamics. Phys. Rev. D. **49**, 6467–6474 (1994)
11. Israel, W.: Singular hypersurfaces and thin shells in general relativity. Nuovo Cimento **B44**, 1–14 (erratum B48 463) (1967)
12. Lanczos, K.: Bemerkungen zur de Sitterschen Welt. Physikalische Zeitschrift **23**, 539–547 (1922)
13. Lanczos, K.: Flächenhafte verteiliung der Materie in der Einsteinschen Gravitationstheorie. Annalen der Physik (Leipzig) **74**, 518–540 (1924)
14. LeFloch, P.G., Mardare, C.: Definition and weak stability of spacetimes with distributional curvature. Port. Math. **64**, 535–573 (2007)
15. Lichnerowicz A.: Théories Relativistes de la Gravitation et de l'Electromagnétisme. (Paris, Masson) (1955)
16. Mars, M.: Constraint equations for general hypersurfaces and applications to shells. Gen. Relat. Gravit. **45**, 2175–2221 (2013)
17. Mars, M., Senovilla, J.M.M.: Geometry of general hypersurfaces in spacetime: junction conditions. Class. Quantum Grav. **10**, 1865–1897 (1993)
18. Mars, M., Senovilla, J.M.M., Vera, R.: Lorentzian and signature changing branes. Phys. Rev. D **76**, 044029 (22 pp.)2007
19. Nicolò, F.: The characteristic problem for the Einstein vacuum equations. Il Nuovo Cimento B **119**, 749–771 (2004)
20. Rendall, A.D.: Reduction of the characteristic initial value problem to the Cauchy problem and its applications for the Einstein equations. Proc. Roy. Soc. London A **427**, 221–239 (1990)
21. Schouten, J.A.: Ricci Calculus. (Springer, Berlin) (1954)
22. O'Brien, S., Synge, J.L.: Jump conditions at discontinuities in general relativity. Commun. Dublin Institite Adv. Studies A **9**, (1952)
23. Wald, R.M.: General Relativity. (The University of Chicago Press, Chicago) (1984)
24. Winicour, J.: Characteristic Evolution and Matching. Living Rev. Relativity **1**, 5 (1998), URL (cited on 31 January 2013): http://www.livingreviews.org/lrr-1998-5

# Cosmological Gravitational Waves and Einstein–Straus Voids

**Marc Mars, Filipe C. Mena, and Raül Vera**

**Abstract** The Einstein–Straus model results from the embedding of a Schwarzschild spherically symmetric region on a FLRW dust spacetime. It constituted the first, and most widely accepted, model to answer the question of the influence of large scale (cosmological) dynamics on local systems. The conclusion drawn by the model was that there is no influence from the cosmic background, since the spherical vacuole is static. However, apart from being highly inflexible, the model has been proved to be remarkably reluctant to admit non-spherical generalizations. This led us to consider the problem of the linearised perturbations of the Einstein–Straus model, first from a purely geometrical point of view. We now concentrate on imposing the Einstein field equations and in understanding the mixing between vector and tensor modes in the FLRW side, which arises as a consequence of the existence of an inner boundary. In particular, we analyse the relationship between exterior gravitational waves and the stationary and axial vacuum perturbations inside.

M. Mars
Instituto de Fisica Fundamental y Matematicas (IUFFyM), Universidad de Salamanca, Plaza de la Merced s/n 37008, Salamanca, Spain
e-mail: marc@usal.es

F.C. Mena
Centro de Matemática, Universidade do Minho, Campus de Gualtar, 4710-057 Braga, Portugal

R. Vera (✉)
Física Teórica e Hist. de la Ciencia, UPV/EHU, Apt. 644, 48080 Bilbao, Basque Country, Spain
e-mail: raul.vera@ehu.es

A. García-Parrado et al. (eds.), *Progress in Mathematical Relativity, Gravitation and Cosmology*, Springer Proceedings in Mathematics & Statistics 60,
DOI 10.1007/978-3-642-40157-2_6, 

## 1 Introduction

The historical starting point is the long standing question in Cosmology that concerns the influence of the dynamics of the Universe on local systems. Related to this lies the problem of the relationship between the large scale "macroscopic" gravitational cosmology and the "microscopic" gravitational physics, and in fact, of understanding the scales of their applicability.

While the large scale dynamics is taken to be described by a Friedman–Lemaître–Robertson–Walker (FLRW) cosmological model, or perturbations thereof, at smaller scales the surroundings of astrophysical objects—planetary orbits, galaxies, clusters, voids, etc.—are many times modelled by nearly vacuum and stationary regions, since the most common view is that the cosmic dynamics does not affect the local physics. The main argument supporting this conclusion is based on the Einstein–Straus (ES) model, which consists of a vacuum spherical—and hence static—cavity, i.e. Schwarzschild, embedded in an expanding (dust) FLRW model. The local physics would take place inside the Schwarzschild static cavity, not perceiving any effect of the cosmological expansion.

Although the ES model provides a clear physical interpretation, it presents serious problems and involves a number of idealisations. Indeed, more sophisticated models have been constructed by using Lemaître–Tolman–Bondi regions for the cosmological part and other type of cavities (see [5]). However, all those models are spherically symmetric. An important question was whether the Einstein–Straus conclusion is robust with respect to non-spherically symmetric generalisations.

The first conclusive discussion of different metrics and shapes of the static region [16] showed that a *locally* cylindrically symmetric static region cannot match an expanding FLRW model, irrespective of the matter content. A subsequent detailed analysis decided that the assumption of spherical symmetry of the static region was a fundamental ingredient for the models: in two steps, [6, 7], it was shown that a static region matched to a FRLW cosmological model is forced to be spherically symmetric under very weak conditions on the matter content which, in particular, allow for vacuum. As a result, *the only static vacuum region that can be matched to a non-static FLRW is a spherically shaped region of Schwarzschild*.

Regarding the assumption of staticity, it was then shown [15] that if a stationary and axially symmetric region is to be matched to a FLRW preserving the axial symmetry, then the stationary region must be static. Thence, by the results in [6, 7], *the only stationary and axisymmetric vacuum region that can be matched to FLRW is a spherically shaped region of Schwarzschild.*

Summarising, the ES model, thought of as the embedding of a static vacuole in FLRW, does not allow any non-spherical generalisation, and it is thus "unstable", and it does not admit a stationary rotation in an axisymmetric vacuole either.

One is thus faced with the necessity of going beyond FLRW. Taking the "exact" approach, it was found in [13] that there is no reasonable evolving spatially homogeneous (LRS) spacetimes surrounding a locally cylindrically symmetric static compact region, and vacuum is never possible. The other possibility is to

study non-spherical, completely general inhomogeneous, perturbations of the whole model. With that aim, we presented in [9] an initial framework to study the linear perturbations of the ES model, consisting of stationary and axisymmetric perturbations of Schwarzschild in the cavity and arbitrary perturbations (scalar, vector and tensor modes) in the FLRW region, matched through a general perturbation of the sphere.

Apart from the inherent interest of studying the perturbed ES, from the point of view of mathematical cosmology it is also relevant to ascertain how the usual scalar, vector and tensor decomposition transforms due to the existence of spacetime boundaries. Note that the usual decomposition relies on the non existence of boundaries and convenient boundedness and decay of the FLRW perturbations, which ensure the uniqueness of the decomposition and also imply the decoupling of the Einstein equations for a perfect fluid for each type of mode. However, in order to describe the existence of voids or, more generally, underdense regions with a different dynamical regime, it seems necessary to introduce certain kind of boundaries. By studying the linearised ES model we consider an (arbitrary) boundary shared with a stationary axisymmetric (vacuum or not) region and explore the consequences.

Perturbed scenarios closely related to the present work have been already considered in the literature. Chamorro presented the first order matching of a Kerr cavity in an expanding perturbed FLRW [2]. The linearised matching conditions around spherical symmetry in terms of gauge invariants was introduced by Gerlach and Sengupta (GS) [4], (see also [12]). A matching perturbation theory in general relativity has been developed in full generality for first order perturbations in [1,14] and to second order in [8]. A critical review about the study of linear perturbations of matched spacetimes including gauge problems has been recently presented in [9].

Another interesting approach has been followed in [3], studying slowly rotating voids in cosmology with a model consisting on an interior Minkowskian void, a matter shell between the void and the cosmological model and a FLRW universe with a particular type of perturbation describing rotation. We emphasise that we focus on generalisations of the ES model without surface layers of matter, and we do not restrict the FLRW perturbations in any way.

The usual way of exploiting the underlying spherical symmetry of the background configuration has been by resorting to decompositions of all objects in terms of scalar, vector and tensor harmonics on the sphere. Instead, we have preferred to use an alternative method based on the Hodge decomposition of all tensor objects on the sphere in terms of scalars. The two approaches are obviously related to each other. However, by working with Hodge scalars, although depending on three coordinates, allows us to avoid the need to deal with infinite series of objects (one for each $l$ and $m$ in the spherical harmonic decomposition).

Before entering into the linearised ES model we devote a couple of sections to introduce the tools used in its present derivation: the theory of linearised matching and the Hodge dual decomposition, which we complement now with an analogous to the GS $2+2$ formalism [4]. Although the use of gauge invariants is not necessary [9], it is a suitable choice. For now, we concentrate on the odd sector of the

perturbations. After presenting the equations that govern the linearised ES model, and in the form of conclusions, we discuss the possible generation of gravitational waves in the perturbed FLRW region due to the matching to stationary vacuoles, which is still work in progress.

Indices $i, j, \ldots = 1, 2, 3$ refer to objects on constant cosmic time hypersurfaces in FLRW, $a, b, \ldots = 1, 2, 3$ on the matching hypersurface, $A, B, \ldots = 2, 3$ on the sphere while $I, J, \ldots = 0, 1$ on the surfaces orthogonal to the spheres. Greek indices $\alpha, \beta, \ldots = 0, 1, 2, 3$ refer to general spacetime objects.

## 2 Linearised Matching Theory in Short

Perturbing a matching involves perturbing a background which is already given by the matching of two regions with boundary, say $(M^+, g^+)$ and $(M^-, g^-)$ with corresponding boundaries $\Sigma^\pm$. The "gluing" of the boundaries amounts to the fact that they are diffeomorphic to each other (thence identified as the matching hypersurface $\Sigma$). This amounts to write down two embeddings $\Phi_\pm : \Sigma \longrightarrow M^\pm$ such that $\Phi_\pm(\Sigma) = \Sigma^\pm$. The identification is thus given through $\Phi_+ \circ \Phi_-^{-1}$. The preliminary junction conditions demand the equality of the first fundamental forms $q^\pm_{ab} \equiv \Phi^*_\pm g^\pm_{\alpha\beta}$ so that $\Sigma$ is endowed with a metric $q_{ab} \equiv q^+_{ab} = q^-_{ab}$. Assuming $\Sigma^\pm$ not to be null at any point, there is a unique up to orientation unit normal vector $n^\alpha_\pm$. The orientation of one of the normals can be chosen arbitrarily but the other must be chosen accordingly so that both point to the same region after the matching, allowing for its eventual identification. The second fundamental forms $K^\pm_{ab} = \Phi^*_\pm \nabla^\pm_\alpha n^\pm_\beta$ can then be constructed. The second matching conditions, $K^+_{ab} = K^-_{ab}$, are the necessary and sufficient conditions so that the Riemann tensor of the matched spacetime, which can be defined in a distributional sense, does not have a term with support on $\Sigma$ (i.e. a Dirac delta term).

The first order perturbation of the matching is defined by the following ingredients defined on both $M^\pm$: the perturbed metric tensors, $g^{(1)\pm}_{\alpha\beta}$, and the perturbation vectors of $\Sigma$, $Z^\alpha_\pm = Q_\pm n^\alpha + T^\alpha_\pm|_\Sigma$, with corresponding quantities defined on $\Sigma$ given by $Q_\pm \equiv \Phi^* Q_\pm$ and $T^\alpha_\pm = \Phi_*(T^a_\pm)$. With these quantities at hand, as shown in [1, 8, 14], one constructs the first and second perturbed fundamental forms

$$
\begin{aligned}
q^{(1)}_{ab} &= \mathscr{L}_T q_{ab} + 2QK_{ab} + \Phi^*_{ab}(g^{(1)}_{\alpha\beta}) \\
K^{(1)}_{ab} &= \mathscr{L}_T K_{ab} - D_a D_b Q + Q(\Phi^*_{ab}(n^\mu n^\nu R_{\alpha\mu\beta\nu}) + K_{ac}K^c{}_b) \\
&\quad + \frac{1}{2}\Phi^*(g^{(1)}_{\alpha\beta} n^\alpha n^\beta) K_{ab} - \Phi^*_{ab}(n_\mu S^{(1)\mu}_{\alpha\beta})
\end{aligned}
$$

where $2S^{(1)\alpha}_{\beta\gamma} \equiv \nabla_\beta g^{(1)\alpha}{}_\gamma + \nabla_\gamma g^{(1)\alpha}{}_\beta - \nabla^\alpha g^{(1)}{}_{\beta\gamma}$, and the perturbed matching conditions read

$$
q^{(1)+}_{ab} = q^{(1)-}_{ab}, \qquad K^{(1)+}_{ab} = K^{(1)-}_{ab}. \tag{1}
$$

Let us insist that it is important to note that these conditions concern quantities defined on $\Sigma$, and are therefore independent of the coordinates used in $M^+$ and $M^-$ for their computation. As a result, these conditions are (spacetime) gauge independent by construction. This makes unnecessary the use of gauge independent quantities in order to establish the perturbed matching conditions, although they turn out to be convenient in the end.

## 3 Spherical Symmetry: GS Formalism and Hodge Decomposition

Consider the round unit metric $\Omega_{AB}dx^A dx^B = d\vartheta^2 + \sin^2\vartheta d\varphi^2$, with $\eta_{AB}$ and $D_A$ denoting the corresponding volume form and covariant derivative respectively, and $(\star dG)_A = \eta^C{}_A D_C G$ the Hodge dual with respect to $\Omega_{AB}$. The usual Hodge decomposition on $S^2$ states that any one-form $V_A$ can be canonically decomposed as $V_A = D_A F + (\star dG)_A$, where $F$ and $G$ are functions on $S^2$, and any symmetric tensor $T_{AB}$ as $T_{AB} = D_A U_B + D_B U_A + H\Omega_{AB}$, for some $U_A$, which can be in turn decomposed in terms of scalars as before.

It is convenient to define the following two functionals. Given three scalars $\mathscr{X}_{tr}$, $\mathscr{X}_1$ and $\mathscr{X}_2$ on $(S^2, \Omega_{AB})$ we define the functional one form $V_A(\mathscr{X}_1, \mathscr{X}_2)$ as

$$V_A(\mathscr{X}_1, \mathscr{X}_2) = D_A \mathscr{X}_1 + (\star d\, \mathscr{X}_2)_A,$$

and the functional symmetric tensor $T_{AB}(\mathscr{X}_{tr}, \mathscr{X}_1, \mathscr{X}_2)$ as

$$T_{AB}(\mathscr{X}_{tr}, \mathscr{X}_1, \mathscr{X}_2) = D_A V_B(\mathscr{X}_1, \mathscr{X}_2) + D_B V_A(\mathscr{X}_1, \mathscr{X}_2) + \mathscr{X}_{tr}\Omega_{AB}.$$

Let us recall that the decomposition defines these $\mathscr{X}$'s on $S^2$ up to the kernels of the operators $V_A$ and $T_{AB}$. To fix the decomposition uniquely we define a *canonical dual decomposition*. by demanding that $V_A(\mathscr{X}_1, \mathscr{X}_2)$ applies to functions $\mathscr{X}_1$, $\mathscr{X}_2$ orthogonal (in the $L^2$ sense on $S^2$) to 1, and $T_A(\mathscr{X}_{tr}, \mathscr{X}_1, \mathscr{X}_2)$ applies to $\mathscr{X}_1$, $\mathscr{X}_2$ orthogonal to 1 and to the $l = 1$ spherical harmonics. Schematically we may use $W_A \overset{S^2}{\to} \mathscr{X}_1, \mathscr{X}_2$ to indicate $W_A = V_A(\mathscr{X}_1, \mathscr{X}_2)$, and $W_{AB} \overset{S^2}{\to} \mathscr{X}_{tr}, \mathscr{X}_1, \mathscr{X}_2$ when $W_{AB} = T_{AB}(\mathscr{X}_{tr}, \mathscr{X}_1, \mathscr{X}_2)$. The scalars with subscripts 1 and *tr* remain unchanged under reflection, and are typically called longitudinal, even or polar quantities, while those with subscripts 2 change sign, and correspond to the transversal, odd or axial quantities.

Let us consider now the general spherically symmetric spacetime $M = M^2 \times S^2$ with metric $g_{\alpha\beta} = \omega_{IJ} \oplus r^2\Omega_{AB}$, so that $(M^2, \omega_{IJ})$ is a 2-dimensional Lorentzian space and $r > 0$ a function on $M^2$, and an orthonormal basis $\{u_I, m_I\}$: $\omega_{IJ} = -u_I u_J + m_I m_J$. The dual in $(M^2, \omega_{IJ})$ will be indicated by $*$ and the covariant derivative by $\nabla$.

We can now decompose the metric perturbation tensor $g^{(1)}_{\alpha\beta}$ using $g^{(1)}_{IJ} = \mathscr{Z}_{IJ}$, $g^{(1)}_{IA} \overset{S^2}{\to} \mathscr{Z}_{I1}, \mathscr{Z}_{I2}$, $g^{(1)}_{AB} \overset{S^2}{\to} \mathscr{Z}^{S_2}_{tr}, \mathscr{Z}^{S_2}_1, \mathscr{Z}^{S_2}_2$ and the deformation vector by $Z_\alpha \to \{Z_I \to Q, T\} \oplus \{Z_A \overset{S^2}{\to} \mathscr{T}_1, \mathscr{T}_2\}$, this is, the part of $Z_\alpha$ orthogonal to the spheres gets decomposed, in turn, onto the normal and tangential parts to $\Sigma$, $Q$ and $T$ respectively. The deformation of $\Sigma$ gets encoded in $Q$.

Let us now concentrate on the odd (axial) sector. Odd (axial) gauge invariant quantities are encoded in the vector [11] (c.f. [4])

$$\mathscr{K}_I \equiv \mathscr{Z}_{I2} - \nabla_I \mathscr{Z}^{S_2}_2 + 2\mathscr{Z}^{S_2}_2 r^{-1} \nabla_I r.$$

Note that $\mathscr{K}_I$ as defined above contains $l = 1$ harmonics, from $\mathscr{Z}_{I2}$, but only the $l \geq 2$ sector is gauge invariant. After decomposing the equations of the perturbed matching (1), and once the orthonormal basis $\{u_I, m_I\}$ has been identified at both sides, the linearised matching (odd sector) is found to be equivalent to [11] (c.f. [4])

$$\mathscr{K}^+_m \overset{\Sigma}{=} \mathscr{K}^-_m, \quad \mathscr{K}^+_u \overset{\Sigma}{=} \mathscr{K}^-_u, \quad *\, d(r^{-2}\mathscr{K}^+) \overset{\Sigma}{=} *d(r^{-2}\mathscr{K}^-) \tag{2}$$

together with an equation for $\mathscr{T}^+_2 - \mathscr{T}^-_2$.

## 4 Linearised ES Model: Matching Conditions for the Odd Sector

Consider the linearised matching of the perturbed Schwarzschild and FLRW spacetimes. Take the FLRW geometry $g^+ = a^2(\tau)\left(-d\tau^2 + \gamma_{ij}dx^i dx^j\right)$ where $\gamma_{ij}dx^i dx^j = dR^2 + f^2(R,\epsilon)(d\theta^2 + \sin^2\theta d\phi^2)$ with $f = \sinh R, R, \sin R$ for $\epsilon = -1, 0, 1$ respectively. The background matching hypersurface $\Sigma$ is found to be necessarily $\Sigma^+ : \{\tau = \lambda, R = R_c, \theta = \vartheta, \phi = \varphi\}$. The orthonormal basis is formed by $u_\alpha = ad\tau$, $m_\alpha = adR$. Let us define $f_c \equiv f(R_c, \epsilon)$, $a_\Sigma \equiv a(\lambda)$. Dots and primes will indicate differentiation with respect to $\lambda$ and $R$ respectively.

Take the first order perturbations of FLRW, in no specific gauge, formally decomposed into the usual scalar, vector and tensor (SVT) modes, i.e. $g^{(1)+}_{00} = -2a^2\Psi$, $g^{(1)+}_{0i} = a^2 W_i$, $g^{(1)+}_{ij} = a^2(-2\Phi\gamma_{ij} + \chi_{ij})$ with $W_i = \partial_i W + \tilde{W}_i$, $\chi_{ij} = (\nabla_i\nabla_j - \frac{1}{3}\gamma_{ij}\nabla^2)\chi + 2\nabla_{(i}Y_{j)} + \Pi_{ij}$ satisfying the constraints $\nabla^i Y_i = \Pi_i{}^i = 0$, $\nabla^i \Pi_{ij} = 0$, $\nabla^i \tilde{W}_i = 0$. The canonical Hodge decomposition is then used to encode the part tangent to the spheres into $S^2$ scalars in the following schematic way: *vector* $\tilde{W}_i \to \tilde{W}_R \oplus \{\tilde{W}_A \overset{S^2}{\to} \mathscr{W}_1, \mathscr{W}_2\}$, and $Y_i \to Y_R \oplus \{Y_A \overset{S^2}{\to} \mathscr{Y}_1, \mathscr{Y}_2\}$, *tensor* $\Pi_{RA} \overset{S^2}{\to} \mathscr{Q}_1, \mathscr{Q}_2$, $\Pi_{AB} \overset{S^2}{\to} \mathscr{H}, \mathscr{U}_1, \mathscr{U}_2$. All in all, encoding $g^{(1)+}$ using the SVT and the Hodge decomposition leaves us with 15 quantities, only 4 in the odd sector; **vector:** $\{\mathscr{W}_2, \mathscr{Y}_2\}$ **tensor:** $\{\mathscr{Q}_2, \mathscr{U}_2\}$, not all independent due to the previous constraints, and, on the other hand, not unique. The components of the gauge

invariant odd vector of the above construction, $\mathscr{K}_I^+$, in terms of the SVT-Hodge quantities read

$$\mathscr{K}_u^+ = a\left(\mathscr{W}_2 - (\dot{\mathscr{U}}_2 + \dot{\mathscr{V}}_2)\right), \qquad \mathscr{K}_m^+ = a\left(\mathscr{Q}_2 - \mathscr{U}_2' + 2\mathscr{U}_2 f' f^{-1}\right).$$

Regarding the Schwarzschild region, we consider the Schwarzschild metric of mass $M$ in standard coordinates, and stationary and axially symmetric vacuum perturbations in the Weyl gauge, so that they can be described in terms of two functions $U^{(1)}(r,\theta)$ and $A^{(1)}(r,\theta)$ (see [10]). The Schwarzschild/FLRW background matching implies $\Sigma^- = \{r = r_0(\lambda), t = t_0(\lambda), \theta = \vartheta, \phi = \varphi\}$ with $r_0 = f_c a_\Sigma$ and $\dot{t_0} = \frac{a_\Sigma^2 f_c f_c'}{f_c a_\Sigma - 2M}$. Moreover, the FLRW must be dust and the energy density obeys $\rho = \frac{6M}{f_c^3 a^3}$.

At first order only $A^{(1)}(r,\theta)$ enters the odd sector, and the Hodge decomposition leads to $A^{(1)} = \sin\theta\partial_\theta\mathscr{G}$, where $\mathscr{G} \equiv -\left(1-\frac{2M}{r}\right)^{-1}\mathscr{Z}_{t2}^-$ is a convenient redefinition. The odd gauge invariant vector $\mathscr{K}_I^-$ now reads $\mathscr{K}_r^- = 0$, $\mathscr{K}_t^- = -\left(1-\frac{2M}{r}\right)\mathscr{G}$. Equations (2) eventually read ($\vec{n}$ points towards the FLRW region)

$$\mathscr{K}_u^+ \overset{\Sigma}{=} -\mathscr{G} f_c', \quad \mathscr{K}_m^+ \overset{\Sigma}{=} -\mathscr{G} a_\Sigma^{-1}\dot{a}_\Sigma f_c, \quad \vec{n}(\mathscr{K}_u^+) \overset{\Sigma}{=} \mathscr{G}\frac{f_c^3 a_\Sigma \epsilon - 3M}{f_c^2 a_\Sigma^2} + \mathscr{G}_{,r}(f_c^2\epsilon - 1). \tag{3}$$

The first direct consequence of the above equations is that if the FLRW remains unperturbed then the stationary region must be static in the range of variation of $r_0(\lambda)$. This result generalises that in [15] because now the matching hypersurface does not necessarily keep the axial symmetry. Thus, *the only way of having a stationary and axisymmetric vacuum arbitrarily shaped (at the linear level) region in FLRW is to have the ES model.*

## 5 Conclusions: On Cosmological Gravitational Waves

From the previous set of equations we obtain, in particular, $\mathscr{K}_I^+\nabla^I(af) \overset{\Sigma}{=} 0$. This involves only quantities on FLRW, and thus constitutes a *constraint*. This constraint implies that if the perturbed FLRW contains vector modes with $l > 1$ harmonics on $\Sigma$, then it must contain also tensor modes there. Eventually, the existence of a rotation in the stationary region $\mathscr{G}$ implies [10] the existence of both vector and tensor modes on $\Sigma$.

This may indicate the existence of some kind of gravitational waves on FLRW near $\Sigma$. In order to analyse further this issue we now take the Einstein field equations (odd sector for now) into consideration. In FLRW, the dust perturbation is described by the first order perturbations of the dust 4-velocity $v_\mu$ and density $\rho$: $v_\mu^{(1)} = v_I \oplus \{v_A \overset{S^2}{\to} v_1, v_2\}$ and $\rho^{(1)}$, respectively. The odd equations read [11] (c.f.[4])

$$\nabla^I \mathscr{K}_I^+ = 0 \tag{4}$$

$$\nabla^I \nabla_I \left(\frac{1}{f}\mathscr{K}_m^+\right) + \left(\frac{1}{(af)^2}\triangle_{S^2} + \frac{\rho}{6}\right)\frac{1}{f}\mathscr{K}_m^+ = 0 \to \text{Wave equation}, \tag{5}$$

plus an equation for $v_2$, which is gauge invariant. The linearised matching conditions (3) together with (4) provide now the value of both $\mathscr{K}_m^+$ and $\vec{n}(\mathscr{K}_m)^+$ on $\Sigma$. Since $\Sigma$ is timelike, this leads to an overdetermined boundary value problem for a wave equation. Existence and uniqueness is hence a non-trivial problem that needs to be analysed.

*Exact Schwarzschild:* It can be proved that the trivial data implies $\mathscr{K}_m^+ = 0$, and therefore the only odd perturbation allowed is an arbitrary $\mathscr{K}_u^+(R)$ restricted to $\mathscr{K}_u^+ \overset{\Sigma}{=} \partial_R \mathscr{K}_u^+ \overset{\Sigma}{=} 0$. Thus, odd gravitational waves cannot exist. The complementary argument states that if gravitational waves are present, they must "enter" the vacuole somehow.

*Schwarzschild $l = 1$ modes perturbation:* One should obtain Chamorro's model [2] but, firstly, we find that it is not unique and, secondly, that the "freedom" in the FLRW part is pure gauge, so no waves are present. $\mathscr{G}$ satisfies a well known second order ODE, and we plan to study its general solution, including that branch diverging at $\infty$. That would provide us with a link between the FLRW perturbations and the inner dynamics of a local system being a simple implementation of Ellis' "finite infinity" which would generalise Hartle's model.

*Schwarzschild $l = 2$ modes perturbation:* The general solution for $\mathscr{G}$ is known, and the Cauchy data for FLRW can be written down. Although there are non-trivial solutions $\mathscr{K}_m^+/f$ to the wave equation it remains to be seen whether these can be interpreted as *gravitational waves*.

**Acknowledgements** MM acknowledges support from the projects FIS2009-07238, FIS2012-30926 (MICINN) and P09-FQM-4496 (Junta de Andalucía and FEDER funds). RV thanks support from project IT-221-07 of the Basque Government, and FIS2010-15492 from the MICINN. FM thanks CMAT, University of Minho, for support through FEDER Funds—"Programa COMPETE" and FCT Projects Est-C/MAT/UI0013/2011, PTDC/MAT/108921/2008 and CERN/FP/116377/2010.

## References

1. Battye R.A. and Carter B.: Gravitational Perturbations of Relativistic Membranes and Strings, Phys. Lett. **B357**, 29–35 (1995)
2. Chamorro A.: A Kerr cavity with a small rotation parameter embedded in Friedmann universes, Gen. Rel. Grav. **20**, 1309–1323 (1988)
3. Doležel T., Bičák J. and Deruelle N.: Slowly rotating voids in cosmology, Class. Quantum Grav. **17**, 2719–2737 (2000)

4. Gerlach U.H. and Sengupta U.K.: Junction conditions for odd-parity perturbations on most general spherically symmetric space-times, Phys. Rev. D **20**, 3009–3014 (1979); Gerlach U.H. and Sengupta U.K.: Even parity junction conditions for perturbations on most spherically symmetric space-times, J. Math. Phys. **20**, 2540–2546 (1979)
5. Krasiński A.: Inhomogeneus Cosmological Models, Cambridge University Press, Cambridge (1997) Bonnor W.B.: A generalization of the Einstein-Straus vacuole, Class. Quantum Grav. **17**, 2739–2748 (2000) ; Fayos F., Senovilla J.M.M., Torres R.: General matching of two spherically symmetric spacetimes, Phys. Rev. D **54**, 4862–4872 (1996)
6. Mars M.: Axially symmetric Einstein-Straus models, Phys. Rev. D **57**, 3389–3400 (1998)
7. Mars M.: On the uniqueness of the Einstein–Strauss model, Class. Quantum Grav. **18**, 3645–3663 (2001)
8. Mars M.: First and second order perturbations of hypersurfaces, Class. Quantum Grav. **22**, 3325–3347 (2005)
9. Mars M., Mena F.C. and Vera R.: Linear perturbations of matched spacetimes: the gauge problem and background symmetries, Class. Quantum Grav. **24**, 3673–3689 (2007)
10. Mars M., Mena F.C. and Vera R.: First order perturbations of the Einstein-Straus and Oppenheimer-Snyder models, Phys. Rev. D **78**, 084022–29 (2008)
11. Mars M., Mena F.C. and Vera R.: In preparation
12. Martín-García J.M. and Gundlach C.: Gauge-invariant and coordinate-independent perturbations of stellar collapse II: matching to the exterior, Phys. Rev. D **64**, 024012 (2001)
13. Mena F.C., Tavakol R. and Vera R.: Generalisation of Einstein-Straus models to anisotropic settings, Phys. Rev. D **66**, 044004 (2002)
14. Mukohyama S.: Perturbation of junction condition and doubly gauge-invariant variables, Class. Quantum Grav. **17**, 4777–4798 (2000)
15. Nolan B.C. and Vera R.: Axially symmetric equilibrium regions of Friedmann-Lemaitre-Robertson-Walker universes, Class. Quantum Grav. **22**, 4031–4050 (2005)
16. Senovilla J.M.M. and Vera R.: Impossibility of the cylindrically symmetric Einstein–Straus model, Phys. Rev. Lett. **78**, 2284–2287 (1997)

# Construction of Oscillatory Singularities

**Alan D. Rendall**

**Abstract** One way to understand more about spacetime singularities is to construct solutions of the Einstein equations containing singularities with prescribed properties. The heuristic ideas of the BKL picture suggest that oscillatory singularities should be very common and give a detailed picture of how these could look. The more straightforward case of singularities without oscillations is reviewed and existing results on that subject are surveyed. Then recent theorems proving the existence of spatially homogeneous solutions with oscillatory singularities of a specific type are presented. The proofs of these involve applications of some ideas concerning heteroclinic chains and their stability. Some necessary background from the theory of dynamical systems is explained. Finally some directions in which this research might be generalized in the future are pointed out.

## 1 Introduction

One of the characteristic features of general relativity is its prediction of spacetime singularities. These can already be observed in explicit solutions of the Einstein equations such as the Schwarzschild solution and the Friedman–Lemaitre–Robertson–Walker (FLRW) solutions. These explicit solutions have a high degree of symmetry. The question arose early whether the known singularities might be artefacts of symmetry. The work of Lifshitz and Khalatnikov [13] supported this idea. These authors made what they believed to be a general ansatz for the form of the geometry near the singularity and found that it could not accommodate the full number of free functions expected. They concluded that generic solutions of the Einstein equations do not develop singularities. The result was heuristic in nature.

A.D. Rendall (✉)
Max Planck Institute for Gravitational Physics, Am Mühlenberg 1, 14476 Potsdam, Germany
e-mail: rendall@aei.mpg.de

A. García-Parrado et al. (eds.), *Progress in Mathematical Relativity, Gravitation and Cosmology*, Springer Proceedings in Mathematics & Statistics 60,
DOI 10.1007/978-3-642-40157-2_7, 

The conclusions of [13] were shown to be invalid by the singularity theorems of Penrose and Hawking [5]. In contrast to the arguments in [13] the results of the singularity theorems were based on mathematical proofs. It was shown that singularities occur for open sets of solutions of the Einstein equations. More specifically, using the point of view of the initial value problem, they occur for the solutions arising from open sets of initial data. This means that the occurrence of singularities is stable in a certain precise sense. A positive feature of these theorems is that the hypotheses are relatively weak. On the other hand the conclusions are also relatively weak. What is proved is that the spacetimes to which the theorems apply are geodesically incomplete. Very little is said about the nature of the singularities. There is no information on whether the singularities are accompanied by large energy densities or tidal forces, as might be expected on the basis of physical intuition.

Later, Belinskii, Khalatnikov and Lifshitz (abbreviated in what follows by BKL) presented a more detailed picture of spacetime singularities [3]. Their arguments are heuristic. They are similar to the work of [13] with the important difference that this time the ansatz used is more complicated, including oscillatory behaviour. This allows the full number of free functions to be included. Some of the main assertions belonging to the BKL picture are:

1. the solutions of the partial differential equations are approximated by solutions of ordinary differential equations near the singularity
2. the approach to the singularity is oscillatory
3. solutions of the Einstein equations with matter are approximated by solutions of the vacuum equations near the singularity

The solutions of the ordinary differential equations in point (1) correspond to spatially homogeneous solutions of the Einstein equations. In the original work one of the most general classes of spatially homogeneous solutions, the Bianchi type IX solutions, played a central role. These solutions were also studied independently at about the same time by Misner [14] who called them the Mixmaster model. On the basis of heuristic and numerical work the conclusion was reached that these solutions show a highly oscillatory behaviour near the singularity. This statement is correct but, as will be discussed below, it took a long time to prove it. Here the connection to point (2) above can be seen. Moreover, the oscillations are observed in the vacuum case and this makes contact with point (3). From these remarks it follows that if the BKL picture is correct then spatially homogeneous solutions of the vacuum equations are very important in understanding singularities in solutions of the Einstein equations without symmetries and with quite general matter. Note, however, that after 40 years it is still not known whether the BKL picture is correct. At least there have been many studies of solutions with symmetries which give good agreement with the conclusions obtained by specializing the general BKL picture to symmetric cases.

Since the general case is very complicated to treat it makes sense to start looking for a better understanding of the question of the validity of the BKL picture by concentrating on the spatially homogeneous case. This is especially true due to

the fact that the wider significance of the homogeneous case is intimately related to the main claims of the BKL picture. This leads to the study of certain systems of ordinary differential equations. A concept from the theory of ODE which turns out to be of particular relevance in this context is that of heteroclinic chains. They will be discussed in Sect. 4. In special cases the dynamics near the singularity is convergent rather than oscillatory and in this easier case there do exist results for inhomogeneous spacetimes. Since these are relevant for the conceptual approach used in the case of oscillatory asymptotics they will be discussed in Sect. 3. In order to even define the concepts "monotone" and "oscillatory" being used it is necessary to introduce some basic notation and terminology and this is the subject of Sect. 2.

## 2 Notation and Terminology

Let $M$ be a four-dimensional manifold and $g_{\alpha\beta}$ a Lorentzian metric on $M$. Let $S_t$ be a foliation by spacelike hypersurfaces whose leaves are parametrized by $t$. Let $g_{ab}(t)$ and $k_{ab}(t)$ be the induced metric and the second fundamental form of the leaves of the foliation. Define the Hubble parameter as $H = -\frac{1}{3}g^{ab}k_{ab}$. It is possible to do a $3+1$ decomposition of the Einstein equations for the metric $g_{\alpha\beta}$ based on the foliation $S_t$ which brings in a lapse function and a shift vector. This can of course be done in the presence of matter and also in a closely analogous way in other dimensions.

Let $\lambda_i$ be the eigenvalues of $k_{ab}$ with respect to $g_{ab}$, i.e. the solutions of $k_{ab}X^b = \lambda_i g_{ab}X^b$ for some vector $X^b$. For a well-behaved foliation approaching the singularity towards the past $H > 0$ in a neighbourhood of the singularity. Hence the quantities $p_i = -\lambda_i/3H$, the generalized Kasner exponents, are well-defined functions of $t$ and $x$, where $x$ denotes a point on one of the leaves of the foliation. It follows from the definition that $\sum_i p_i = 1$ so that only two of the $p_i$ are independent. The way in which different leaves are identified with each other depends on the choice of the shift vector. Suppose that the limit $t \to 0$ corresponds to the approach to a singularity. Fix a point $x_0$ and consider the functions $p_i(t, x_0)$. A function $p_i$ is said to be oscillatory near the singularity if $\liminf_{t\to 0} p_i(t) < \limsup_{t\to 0} p_i(t)$. It is said to be convergent near the singularity if $\liminf_{t\to 0} p_i(t) = \limsup_{t\to 0} p_i(t)$, in other words if $p_i$ tends to a limit as $t \to 0$. Similar definitions can be made for other geometric quantities. Informally, a singularity is said to be oscillatory or convergent if some important geometric quantities have the corresponding properties. It is important that the quantities concerned are dimensionless, since otherwise they could be expected to diverge as the singularity is approached.

These definitions depend a lot on the choice of $3+1$ decomposition. Things are simpler in the case of spatially homogeneous spacetimes. There it is natural to choose the foliation to consist of level hypersurfaces of a Gaussian time coordinate based on a hypersurface of homogeneity. Then geometric quantities such as $p_i$ depend only on $t$.

## 3 The Convergent Case

Points (2) and (3) listed above as parts of the BKL picture are only supposed to hold in this form with certain restrictions on the type of matter which is coupled to the Einstein equations. Assuming the validity of point (1) this is directly related to the behaviour of homogeneous models with that type of matter. Two related types of matter which are known to be exceptional from this point of view are the scalar field and the stiff fluid. Here we will concentrate on the second. Consider a perfect fluid with linear equation of state $p = (\gamma - 1)\rho$ for a constant $\gamma$. An extreme case of this from the point of view of ordinary physics is $\gamma = 2$. This is the stiff fluid where the velocity of sound of the fluid $\sqrt{\gamma - 1}$ is equal to the velocity of light. (We use geometrical units.) It is also possible to consider ultrastiff fluids with $\gamma > 2$. These very exotic matter models have been considered in certain scenarios for the early universe. According to the BKL picture the generalized Kasner exponents in a general spatially homogeneous solution of the Einstein–Euler equations with a linear equation of state are oscillatory near the singularity in the case $1 \leq \gamma < 2$ and convergent for $2 \leq \gamma$. (The case $\gamma < 1$ will not be considered in what follows.) In fact for $\gamma > 2$ the $p_i$ all converge to the limit $\frac{1}{3}$. These limiting values agree with the values of these quantities in the FLRW solutions and correspond to isotropization. In the case $\gamma = 2$, on the other hand, the $p_i$ may converge to different limits in different solutions and at different spatial points in a single inhomogeneous solution.

What kind of mathematical results could count as a rigorous version of these expectations? It would be desirable to prove that an open neighbourhood with respect to some reasonable topology of the FLRW data leads to solutions which have the predicted asymptotics. This may be called a forwards result since it goes from the data to the asymptotics. Unfortunately this kind of result is hard to obtain. What is sometimes easier is to get a backwards result which goes from the asymptotics to the solution. The solutions with the predicted asymptotics can be parametrized by certain free functions. (Here we ignore complications arising from the Einstein constraints.) Call these functions the asymptotic data. The idea is then to ask whether for asymptotic data belonging to a large class there exists a solution with the correct asymptotics and exactly those free functions. A theorem of this kind was proved for stiff fluids in [1] and for ultrastiff fluids in [6]. In this work the notion of "large class" was defined to mean containing as many free functions as the general solution. It was only proved in the case that these functions are analytic ($C^\omega$). Until very recently the forwards problem was unsolved, even in the stiff case, but a theorem of this kind has been announced by Rodnianski and Speck [20].

For comparison it is of interest to quote what is known in a case with symmetry, that of the Gowdy solutions. Note that for the Gowdy solutions the BKL picture does not predict oscillations and indeed none are found. In this case the backwards problem was solved in [7] for the analytic case and in [16] for the smooth case. The forwards problem for Gowdy was solved in [19]. The aim of this section was to exhibit the backwards problem as a route to obtaining rigorous results and to show

that at least in some cases it can open the way to obtaining results of the type which are most desirable.

Just as some matter models such as the stiff fluid can suppress oscillations others can stimulate them. For instance a Maxwell field can produce BKL type oscillations within Bianchi types where there are no oscillations in the vacuum case. An example is discussed in Sect. 6. The BKL picture can be applied in higher dimensions and gives different results in that case. It says, for instance, that in the case of the Einstein vacuum equations generic oscillations disappear when the spacetime dimension is at least eleven but are present in all lower dimensions. The higher dimensional models come up in the context of string theory and there it is typical that there are other matter fields present. There is the dilaton which, as a scalar field, tends to suppress oscillations and the $p$-forms which, as generalizations of the Maxwell field, encourage them. Many of the conclusions of the heuristic analysis which lead to the conclusion that the singularity is convergent can be made rigorous using techniques generalizing those of [1]. For more information on this the reader is referred to [4]. To conclude it should be noted that there is not a single rigorous result which treats solutions which are both inhomogeneous and oscillatory.

## 4 Heteroclinic Chains

Consider a system of $k$ ordinary differential equations. This can be thought of as being defined by a vector field defined on an open subset of $\mathbf{R}^k$, a geometrical formulation which corresponds to the point of view of dynamical systems. A stationary (i.e. time-independent) solution of the ODE system corresponds to a fixed point of the vector field. A solution of the ODE system which is time-dependent corresponds to an integral curve of the vector field, an orbit of the dynamical system. An orbit which tends to a stationary solution $p$ as $t \to -\infty$ and a stationary point $q \neq p$ as $t \to +\infty$ is called a heteroclinic orbit. An orbit which tends to $p$ as $t \to -\infty$ and as $t \to +\infty$, but is not itself stationary, is called a homoclinic orbit.

Suppose now that $p_i$ is a sequence of points, finite or infinite, such that for each $i$ there is a heteroclinic orbit from $p_i$ to $p_{i+1}$. This configuration is called a heteroclinic chain. If the chain is finite and comes back to its starting point then it is called a heteroclinic cycle. It turns out that homoclinic orbits and heteroclinic cycles are not robust in the sense that a sufficiently general small perturbation of the vector field will destroy them. It is therefore perhaps surprising that they are found in models for many phenomena in nature. Given that all physical measurements only have finite precision it seems difficult to be able to rule out small perturbations in mathematical models for real phenomena. The answer to this question appears to be that there is some absolute element in the system whose presence is not subject to uncertainty and which therefore cannot be perturbed. In the case of spacetime singularities it is the singularity itself which appears to play this role. These considerations are admittedly rather vague and it would be desirable to understand issues of this type more precisely. In any case, heteroclinic cycles do

seem to be widespread in models for the dynamics of solutions of the Einstein equations near their singularities.

Coming back to more general dynamical systems, it is of interest to have criteria for the stability properties of heteroclinic chains. In other words, the aim is to find out under what conditions solutions which start close to a heteroclinic chain approach it as $t \to \infty$. The case of most interest is not that where a solution approaches one of the stationary points belonging to the heteroclinic chain (call them vertices) but the case where the solution follows successive heteroclinic orbits within the chain. When the chain is a cycle this means that the solutions exhibit oscillatory behaviour, repeatedly approaching the vertices of the cycle. In the next section it is shown that this is exactly what happens in the context of the BKL picture.

A solution which is converging to a heteroclinic chain spends most of its time near the vertices. Since the vector field vanishes at the vertices it is small near them and the solution moves slowly there. This suggests that the behaviour of the solution while it is near the vertices could have strong influence on the stability of the cycle. A way of studying the local flow near a vertex is to linearize there and examine the eigenvalues of the linearization. It turns out that this can give valuable information about the stability of the cycle.

## 5 Bianchi Models

A spatially homogeneous solution of the Einstein equations is one which admits a symmetry group whose orbits are spacelike hypersurfaces. The only case where the group cannot be assumed to be three-dimensional is the class of Kantowski–Sachs spacetimes. They are not discussed further in this paper. All the rest are the Bianchi models. In that case it can be assumed without loss of generality that the spatial manifold is simply connected and then it can be identified with the Lie group itself. The reason for this is that the dynamics on the universal covering manifold is the same as that on the original manifold. Thus in Bianchi models it can be assumed that $M = I \times G$ where $I$ is an interval and $G$ is a simply connected three-dimensional Lie group. These Lie groups are in one to one correspondence with their Lie algebras and the three-dimensional Lie algebras were classified by Bianchi into types I–IX. The metric can be written in the form

$$-dt^2 + \sum g_{ij}(t)\theta^i \otimes \theta^j \tag{1}$$

where $\theta^i$ is a basis of left invariant one-forms on $G$. Let $e_i$ be the dual basis of vector fields. The evolution equations depend on the Lie group chosen through the structure constants defined by $[e_i, e_j] = c_{ij}^k e_k$. It is customary to distinguish between Class A models where $c_{kj}^k = 0$ and Class B models which are the rest.

There are many ways in which the evolution equations for Bianchi models can be written as a system of ordinary differential equations. Consider for simplicity the vacuum models of Class A. In that case it can be shown that there is a basis of the Lie algebra with the property that diagonal initial data give rise to diagonal solutions. This is still true when the matter is described by a perfect fluid but it does not hold for general matter. A form of the equations for Class A models which has turned out to be particularly useful for proving theorems is the Wainwright–Hsu system [21]. The basic variables are called $\Sigma_+$, $\Sigma_-$, $N_1, N_2, N_3$. The first two are certain linear combinations of the generalized Kasner exponents. The quantity $N_1$ is given in the Bianchi type IX case by $\frac{1}{H}\sqrt{\frac{g_{11}}{g_{22}g_{33}}}$ and the other two $N_i$ are related to this by cyclic permutations. The Gaussian time coordinate $t$ is replaced by a coordinate $\tau$ which satisfies $\frac{d\tau}{dt} = H$. In this time coordinate the singularity is approached as $\tau \to -\infty$. Two important related features of this system is that the variables are dimensionless and that their evolution equations form a closed system, not depending on $H$. They must satisfy one algebraic condition which is the Hamiltonian constraint in the 3+1 formalism. There results a four-dimensional dynamical system. Stationary solutions of this system correspond to self-similar spacetimes. When a solution of the Wainwright–Hsu system is given the quantities $H$ and $t$ can be determined by integration.

The different Bianchi types are represented by subsets of the state space of the Wainwright–Hsu system where the $N_i$ have certain combinations of signs (positive, negative or zero). The simplest Bianchi type is Bianchi type I, the Abelian Lie algebra. The vacuum solutions of this type are the Kasner solutions. They are self-similar and form a circle in the state space, the Kasner circle $\mathscr{K}$. Let $\mathscr{T}$ be the equilateral triangle circumscribing the Kasner circle which is symmetric under reversal of $\Sigma_-$. It is tangential to $\mathscr{K}$ at three points $T_i$, the Taub points. They correspond to flat spacetimes. Each solution of Bianchi type II is a heteroclinic orbit joining two Kasner solutions. Its projection to the $(\Sigma_+, \Sigma_-)$-plane is a straight line which passes through a corner of $\mathscr{T}$. Concatenating Bianchi type II solutions gives rise to many heteroclinic chains. Given a point of $\mathscr{K}$ which is not one of the Taub points consider the straight line joining it to the closest corner of the triangle $\mathscr{T}$. The part of this straight line inside $\mathscr{K}$ is the projection of an orbit of type II and it intersects $\mathscr{K}$ in exactly one other point. In this way it is possible to define a continuous map from $\mathscr{K}$ to itself, the BKL map. (The map is defined to be the identity at the Taub points.) The two most general Bianchi types of Class A are type VIII and type IX, corresponding to the Lie algebras $sl(2, R)$ and $su(2)$. As already mentioned BKL concentrated on type IX. Type VIII shows many of the same features but may be even more complicated.

When specialized to the Bianchi Class A case the BKL picture suggests that as the singularity is approached in a Bianchi type IX solution the dynamics should be approximated by a heteroclinic chain of Bianchi type II solutions, successive vertices of which are generated by the BKL map. In particular the solution is oscillatory in the sense that the $\alpha$-limit set of a solution of this kind should consist of more than one point. (The $\alpha$-limit set consists of those points $x$ such there

is a sequence of times tending to $-\infty$ along which the value of the solution converges to $x$.) In fact there should be three non-collinear points in the $\alpha$-limit set. This implies that both $\Sigma_+$ and $\Sigma_-$ are oscillatory in the approach to the singularity. This statement about the $\alpha$-limit set was proved in fundamental work of Ringström [17]. He showed that there are at least three non-Taub points in the $\alpha$-limit set of a generic Bianchi IX solution. (He also described the exceptions explicitly.) In addition Ringström showed that the entire $\alpha$-limit set of a Bianchi type IX solution is contained in the union of the points of type I and II [18]. This means that in some sense the type IX solution is approximated by solutions of types I and II. The question of whether the corresponding statement holds for solutions of Bianchi type VIII is still open.

After the results just discussed it still took a long time before theorems about convergence to heteroclinic cycles were published. There is a heteroclinic cycle of Bianchi II solutions which comes back to its starting point after three steps. Let us call this particularly simple example "the triangle". It turns out that there is a codimension one manifold with the property that any Bianchi type IX solution which starts on this manifold converges to the triangle in the past time direction [11]. This result extends to a much larger class of heteroclinic chains generated by iterating the BKL map. The essential condition is that the vertices of the chain should remain outside an open neighborhood of the Taub points. The manifold constructed in [11], which may referred to as the unstable manifold of the triangle (unstable towards the future and hence stable towards the past), is only proved to be Lipschitz continuous. An alternative approach to this problem was given in [2]. It has the advantage that the stable manifold is shown to be continuously differentiable. On the other hand it cannot treat all the heteroclinic chains covered by the results of [11]. In particular, it does not cover heteroclinic cycles such as the triangle. The reason for this restriction is the need to avoid resonances, certain linear relations between the eigenvalues with integer coefficients. When this extra condition is satisfied it can be shown, using a theorem of Takens, that the flow near any vertex of the chain is equivalent to the linearized flow by a diffeomorphism. Some investigations of the case of chains which may approach the Taub points have been carried out in [15].

## 6 Construction of Solutions Converging to the Triangle

The construction of Bianchi type IX solutions converging to heteroclinic chains of Bianchi type II solutions in the approach to the initial singularity will be illustrated by the case of the triangle. The scenario being considered here is related to that described for more general dynamical systems in Sect. 4 by time reversal. As indicated in Sect. 4 the stability of heteroclinic chains is related to the eigenvalues of the linearization about the vertices. Since a vertex of the triangle lies on the Kasner circle and $\mathscr{K}$ consists of stationary points the linearization automatically has a zero eigenvalue. Of the three other eigenvalues one is negative, call it $-\mu$, and

two are positive, call them $\lambda_1$ and $\lambda_2$. The two positive eigenvalues are distinct and we adopt the convention that $\lambda_1 < \lambda_2$. The eigendirection corresponding to $\lambda_2$ is tangent to the triangle. The proofs of [11] are dependent on the fact that $\mu$ is smaller than both positive eigenvalues.

A solution which converges to the triangle repeatedly passes the vertices. Consider a point on the triangle which is close to a vertex and on an orbit approaching it. Let $S$ be a manifold passing through the point which is transverse to the heteroclinic orbit. Call this an incoming section. Similarly we can consider an outgoing section close to the vertex and passing through the orbit leaving it. A solution which starts on the incoming section sufficiently close to the heteroclinic cycle also intersects the outgoing section. Taking the first point of intersection defines a local mapping from the incoming section to the outgoing section, the local passage. There is a similar local mapping from the outgoing section of one vertex to the incoming section of the next in the cycle. This is called an excursion. Composing three passages and three excursions gives a mapping from the incoming section of a vertex to itself. It is important for the proof of [11] that this mapping is Lipschitz and that by restricting the domain of the mapping to a small enough neighbourhood of the triangle the Lipschitz constant can be made as small as desired. The norm used to define the Lipschitz property is that determined by the flat metric $dx^2 + dy^2 + dz^2$, where $(x, y, z)$ are some regular coordinates on the section. The mapping from a small local section to itself is a contraction. The excursions are expanding mappings but the expansion factor is bounded. The passages are contractions which can be made arbitrarily strong and which can therefore dominate the effect of the excursions. Once the contraction has been obtained the manifold being sought can be constructed in a similar way to the stable manifold of a stationary solution.

A system similar to the Wainwright–Hsu system can be obtained for solutions of Bianchi type $\mathrm{VI}_0$ with a magnetic field [10]. It also includes certain solutions of Bianchi types I and II with magnetic fields and the vacuum solutions of types I, II and $\mathrm{VI}_0$. It uses variables $\Sigma_+$ and $\Sigma_-$ which have the same geometrical interpretation as in the vacuum case. The Kasner circle can be considered as a subset of the state space for the magnetic system. It has been proved that solutions of this system are oscillatory [22]. There are two families of heteroclinic orbits defined by vacuum solutions of type II. The third family in the vacuum case is replaced by heteroclinic orbits defined by Bianchi type I solutions with magnetic field. The projections of these heteroclinic orbits onto the $(\Sigma_+, \Sigma_-)$-plane are the same straight lines as are obtained from heteroclinic orbits in the vacuum case. Thus the exactly the same heteroclinic chains are present. However their stability properties might be different. Now the stability of the triangle will be considered in the case with magnetic field, following [12]. The result is very similar to that in the vacuum case—there is a one-dimensional unstable manifold—but the proof is a lot more subtle. The reason that the method of proof of [11] does not apply directly is that the eigenvalue configuration is different. Compared to the vacuum case one of the eigenvalues is halved. Then it can happen that the negative eigenvalue is larger in modulus than one of the positive eigenvalues.

A problem which results from the different eigenvalue configuration is that the return map is no longer Lipschitz. More precisely it no longer has this property with respect to the Euclidean metric $dx^2 + dy^2 + dz^2$. It does, however, have the desired Lipschitz property with respect to the singular metric $\frac{x^2+y^2}{x^2}dx^2 + \frac{x^2+y^2}{y^2}dy^2 + dz^2$ and this observation allows the proof of [11] to be generalized to the case with magnetic field. It is important to know that the properties of eigenvalues and eigenvectors alone are not enough to make this proof work. It is also necessary to use the existence of certain invariant manifolds which follows form the geometric background of the problem. At this point it is necessary to remember that we are not just dealing with a heteroclinic cycle in an arbitrary dynamical system but with one in a system with very special properties.

It turns out that the difficulties just discussed can be avoided by a clever but elementary device which comes down to replacing the variable representing the magnetic field by its square. Although this provides a very simple way of studying the heteroclinic chains in the Bianchi $\mathrm{VI}_0$ model with magnetic field it cannot be expected that this kind of trick will apply to more general matter models. By contrast the new method is potentially much more generally applicable. There is one case where it is already known to give new results, as will now be explained. In addition to the results obtained on vacuum models results on models with a perfect fluid with linear equation of state $p = (\gamma - 1)\rho$ were obtained in [11]. It turns out, however, that the techniques of [11] only work under an assumption on $\gamma$ which has no physical interpretation. In the case of the triangle the condition is $\gamma < \frac{5-\sqrt{5}}{2} \sim 1.38$. For other chains other inequalities are obtained. These arise because the linearization has another positive eigenvalue coming from the fluid and it must be ensured that this eigenvalue is greater than $\mu$. With the method of [12] this restriction can be replaced by the inequality $\gamma < 2$, saying that the speed of sound in the fluid is smaller than the speed of light.

## 7 Future Challenges

This section discusses some directions in which the known results on the construction of oscillatory singularities might be extended in the future. There are dynamical systems describing Bianchi models of types I and II with magnetic fields which are not just special cases of those included in the system describing models of type $\mathrm{VI}_0$ [8, 9]. The reason for this is that the Maxwell constraints become less restrictive in the more special Bianchi types. It is possible to choose the basis so that the magnetic field only has one non-vanishing component but the price to be payed is that the metric becomes non-diagonal in that basis. In the dynamical systems describing solutions of types I and II the already familiar heteroclinic chains are still found. There are, however, additional heteroclinic orbits corresponding to the off-diagonal elements of the metric. This means that, in contrast to the models analysed up to now, the stable manifold of a point on the Kasner circle may be of dimension greater

than one. This means that when it is desired to continue a heteroclinic chain towards the past there is not a unique choice any more. New ideas are required to solve this type of problem.

Similar difficulties are met in Bianchi models of Class B. There it is believed on the basis of heuristic considerations that there is precisely one type, $\mathrm{VI}_{-\frac{1}{9}}$, which shows oscillatory behaviour similar to that found in types VIII and IX. There are no rigorous results on Class B comparable to the results of Ringström on models of Class A. In this case too the stable manifold of a Kasner solution may have dimension greater than one. It can also not be expected that invariant manifolds of the type exploited in [12] will exist.

Perhaps the most exciting challenge in this field is to construct inhomogeneous spacetimes with oscillatory singularities. The simplest class of inhomogeneous vacuum spacetimes where oscillations are expected are the $T^2$ models. These have a two-dimensional isometry group acting on spacelike hypersurfaces and so are effectively inhomogeneous in just one space dimension. They include the Gowdy spacetimes as a subset but it is believed that generic $T^2$-symmetric vacuum spacetimes have a much more complicated oscillatory behaviour near the singularity. The models of Bianchi type $\mathrm{VI}_{-\frac{1}{9}}$ are locally isometric to $T^2$ models but not locally isometric to Gowdy models. Thus understanding more about Bianchi models of Class B appears a very natural first step towards a better understanding of the inhomogeneous case.

## References


1. Andersson, L. and Rendall, A. D.: Quiescent cosmological singularities. Commun. Math. Phys. **218**, 479–511 (2001).
2. Béguin, F.: Aperiodic oscillatory asymptotic behaviour for some Bianchi spacetimes. Class. Quantum Grav. **27**, 185005 (2010).
3. Belinskii, V. A., Khalatnikov, I. M. and Lifshitz, E. M.: Oscillatory approach to a singular point in the relativistic cosmology. Adv. Phys. **19**, 525–573 (1970).
4. Damour, T., Henneaux, M., Rendall, A. D. and Weaver, M.: Kasner-like behaviour for subcritical Einstein–matter systems. Ann. H. Poincaré **3**, 1049–1111 (2002).
5. Hawking, S. W. and Ellis, G. F. R. The large scale structure of space-time. Cambridge University Press. Cambridge (1973).
6. Heinzle, J. M. and Sandin, P.: The initial singularity of ultrastiff perfect fluid spacetimes without symmetries. Commun. Math. Phys. **313**, 385–403 (2012).
7. Kichenassamy, S. and Rendall, A. D.: Analytic description of singularities in Gowdy spacetimes. Class. Quantum Grav. **15**, 1339–1355 (1998).
8. Leblanc, V. G.: Asymptotic states of magnetic Bianchi I cosmologies. Class. Quantum Grav. **14**, 2281–2301 (1997).
9. Leblanc, V. G.: Bianchi II magnetic cosmologies. Class. Quantum Grav. **15**, 1607–1626 (1998).
10. Leblanc, V. G., Kerr, D. and Wainwright, J.: Asymptotic states of magnetic Bianchi $\mathrm{VI}_0$ cosmologies. Class. Quantum Grav. **12**, 513–541 (1995).
11. Liebscher, S., Härterich, J., Webster, K. and Georgi, M.: Ancient dynamics in Bianchi models: approach to periodic cycles. Commun. Math. Phys. **305**, 59–83 (2011).

12. Liebscher, S., Rendall, A. D. and Tchapnda, S. B.: Oscillatory singularities in Bianchi models with magnetic fields. Preprint arXiv:1207.2655 (2012).
13. Lifshitz, E. M. and Khalatnikov, I. M.: Investigations in relativistic cosmology. Adv. Phys. **12**, 185–249 (1963).
14. Misner, C. W.: Mixmaster universe. Phys. Rev. **22**, 1071–1074 (1969).
15. Reiterer, M. and Trubowitz, E.: The BKL conjectures for spatially homogeneous spacetimes. Preprint arXiv:1005.4908 (2010).
16. Rendall, A. D.: Fuchsian analysis of singularities in Gowdy spacetimes beyond analyticity. Class. Quantum Grav. **17**, 3305–3316 (2000).
17. Ringström, H.: Curvature blow up in Bianchi VIII and IX vacuum spacetimes. Class. Quantum Grav. **17**, 713–731 (2000).
18. Ringström, H.: The Bianchi IX attractor. Ann. H. Poincaré **2**, 405–500 (2001).
19. Ringström, H.: Asymptotic expansions close to the singularity in Gowdy spacetimes. Class. Quantum Grav. **21**, S305–S322 (2004).
20. Rodnianski, I. and Speck, J.: Talk at Oberwolfach, August 2012.
21. Wainwright, J. and Hsu, L.: A dynamical systems approach to Bianchi cosmologies: orthogonal models of class A. Class. Quantum Grav. **6**, 1409–1431 (1989).
22. Weaver, M.: Dynamics of magnetic Bianchi type $VI_0$ cosmologies. Class. Quantum Grav. **17**, 421–434 (2000).

# Inverse Scattering Construction of Dipole Black Rings

**Jorge V. Rocha, Maria J. Rodriguez, Oscar Varela, and Amitabh Virmani**

**Abstract** We describe an approach to systematically generate regular and asymptotically flat dipole black rings in a 5D Einstein–Maxwell-dilaton theory obtained from 6D vacuum gravity by Kaluza–Klein reduction. Our construction employs the inverse scattering method in six dimensions. We illustrate the scheme with the explicit construction of the singly-spinning dipole ring. These techniques can also be used to generate more general five-dimensional black ring solutions, displaying rotation along the two orthogonal planes, electric charge and magnetic dipole charge.

## 1 Introduction

Gravity in higher dimensions is a proficuous subject that has attracted a lot of attention in the past couple of decades [6]. Its richness, compared to 4D gravity, is highlighted by some novel features including more than one independent rotation

J.V. Rocha (✉)
Centro Multidisciplinar de Astrofísica, Dept. de Física, Instituto Superior Técnico, Technical University of Lisbon, Av. Rovisco Pais 1, 1049-001 Lisboa, Portugal
e-mail: jorge.v.rocha@ist.utl.pt

M.J. Rodriguez
Center for the Fundamental Laws of Nature, Harvard University, Cambridge, MA 02138, USA
e-mail: mjrodri@harvard.physics.edu

O. Varela
Institute for Theoretical Physics and Spinoza Institute, Utrecht University, 3508 TD Utrecht, The Netherlands
e-mail: o.varela@uu.nl

A. Virmani
Institute of Physics, Sachivalaya Marg, Bhubaneswar, Odisha, India - 751005
e-mail: virmani@iopb.res.in

A. García-Parrado et al. (eds.), *Progress in Mathematical Relativity, Gravitation and Cosmology*, Springer Proceedings in Mathematics & Statistics 60,
DOI 10.1007/978-3-642-40157-2_8, © Springer-Verlag Berlin Heidelberg 2014

plane, black hole event horizons with non-spherical topology, non-uniqueness and the possibility of non-conserved dipole charges, when coupling gravity to gauge fields. Considerable amount of guesswork has usually been involved in the discovery of many higher-dimensional black holes but whenever solution-generating techniques are available quicker progress has been achieved.

The problem of finding the most general asymptotically flat black ring in a simple 5D supergravity theory is technically involved. Such a solution—carrying mass, two angular momenta, electric charge and magnetic dipole charge—was conjectured [3] to exist in minimal supergravity and its counterpart in 5D Einstein–Maxwell-dilaton theory was expected to exist as well. Until recently all known solutions possessed three independent parameters at most and there were no methods available that could handle dipole charge and multiple rotations simultaneously.

Black rings with a single rotation along the $S^1$ and with dipole charge but no electric charge were first constructed by Emparan [4] in the theory (1) below with arbitrary dilation coupling $a$ by educated guesswork. Rocha et al. [11] demonstrated how to systematically construct such solutions for a specific coupling constant, applying the inverse scattering method (ISM) of Belinsky and Zakharov [1] in six dimensions. These methods have been extended in [2, 7, 10] to generate a second rotation along the $S^2$ and electric charge as well, yielding the most general family of black ring solutions of this theory. Here we describe this systematic approach to obtain charged black ring solutions of five-dimensional Einstein–Maxwell-dilaton theory with Kaluza–Klein dilation coupling, following [10, 11].

## 2 Applying the ISM to Einstein–Maxwell-Dilaton Theory

We will be concerned with finding charged black ring solutions of five-dimensional Einstein–Maxwell-dilaton (EMd) theory,

$$S = \frac{1}{16\pi G_5}\int d^5x\sqrt{-g}\left(R - \frac{1}{2}\partial_\mu\Phi\,\partial^\mu\Phi - \frac{1}{4}e^{-a\Phi}F_{\mu\nu}F^{\mu\nu}\right), \tag{1}$$

with specific dilaton coupling $a = 2\sqrt{2/3}$. For this special value the theory can be obtained by dimensionally reducing 6D *vacuum* gravity on a circle by means of the standard Kaluza–Klein (KK) ansatz,

$$ds_6^2 = e^{\frac{\Phi}{\sqrt{6}}}\,ds_5^2 + e^{-\frac{\sqrt{3}\Phi}{\sqrt{2}}}(dw + A)^2. \tag{2}$$

Here, the metric $ds_5^2$, the dilatonic scalar $\Phi$ and the one-form $A$ constitute the fields of the five-dimensional theory. The internal KK circle is parametrized by $w$, and we denote by $F = dA$ the Abelian two-form field strength of $A$.

For our purposes, we can then employ the ISM in *six* dimensions, since the uplift of a (black ring) solution in 5D EMd is Ricci flat. A six-dimensional solution

of vacuum gravity with four commuting Killing vector fields—the amount of symmetry required by the ISM—necessarily features KK asymptotics [5] but this is desirable because ultimately we want to dimensionally reduce to five dimensions. The 5D black rings we obtain are asymptotically flat.

## 3 Inverse Scattering Construction of Dipole Ring Solutions

The ISM [1] is a powerful solution generating technique that, upon assumption of $D-2$ commuting isometries,[1] allows to generate solutions of vacuum gravity by *dressing* a known *seed* solution. When the seed is static and the dressing procedure is restricted to the class of solitonic transformations the whole prescription is purely algebraic. We refer the reader to [6, 9] for concise accounts of this method.

We take as our seed solution the six-dimensional metric corresponding to the rod configuration shown in Fig. 1. Note we assume the ordering $a_0 \leq a_1 \leq a_2 \leq a_4 \leq a_3$ for the rod endpoints. The rod in the $t$ direction is identified with the horizon. The negative density rod represented by the dashed line in Fig. 1 is included in the seed to facilitate adding the $S^1$ angular momentum to the ring. The finite rod along the $w$ direction allows the addition of dipole charge. When $a_0 = a_1$ and $a_4 = a_2$, the negative density rod and the rod in the $w$ direction disappear and the solution describes a neutral static black ring times a flat direction $w$.

The seed metric corresponding to the rod configuration of Fig. 1 is given in Weyl coordinates $(\rho, z)$ by

$$ds_6^2 = (G_0)_{ab}\, dx^a dx^b + e^{2\nu_0}(d\rho^2 + dz^2), \tag{3}$$

where

$$G_0 = \mathtt{diag}\left\{-\frac{\mu_0}{\mu_2}, \frac{\rho^2\mu_4}{\mu_1\mu_3}, \frac{\mu_1\mu_3}{\mu_0}, \frac{\mu_2}{\mu_4}\right\}, \qquad \det G_0 = -\rho^2, \tag{4}$$

and the conformal factor of the seed is

$$e^{2\nu_0} = k^2 \frac{\mu_1\,\mu_3}{\mu_0} \frac{Z_{01}\,Z_{02}\,Z_{03}\,Z_{14}\,Z_{24}\,Z_{34}}{Z_{13}^2\,\prod_{i=0}^4 Z_{ii}}, \qquad Z_{ij} \equiv (\mu_i\mu_j + \rho^2). \tag{5}$$

The integration constant $k$ is determined later by the requirement of asymptotic flatness. Our ordering of coordinates is $x^a = (t, \phi, \psi, w)$, with $t$ corresponding to the timelike coordinate, $\phi$ describing the azimuthal angle on the $S^2$ and $\psi$ being

[1] Any solution of the vacuum Einstein equations in $D$ dimensions possessing $D-2$ commuting isometries can be written in the form (3), with $G_0$ and $\nu_0$ only depending on $(\rho, z)$ and with the constraint $\det G_0 = -\rho^2$ [5, 8].

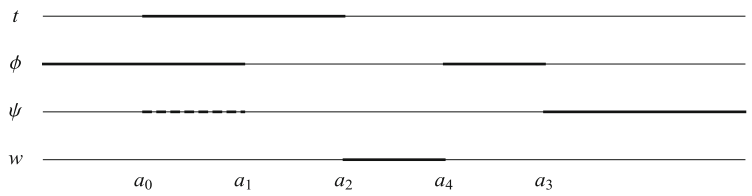


**Fig. 1** Rod diagram corresponding to the seed metric $G_0$. *Solid rods* have positive density and the *dashed rod* has negative density

the angle along the $S^1$ component of the ring. The $\mu_i$'s are commonly referred to as solitons and they are explicitly given by $\mu_i = \sqrt{\rho^2 + (z-a_i)^2} - (z-a_i)$. It is also convenient to introduce anti-solitons, $\overline{\mu}_i = -\sqrt{\rho^2 + (z-a_i)^2} - (z-a_i)$, and they are such that $\mu_i \overline{\mu}_i = -\rho^2$. The interested reader is referred to [6] for further notational details.

The seed solution (3)–(5) is singular and not of direct physical interest itself. However, applying the ISM we can obtain regular solutions by dressing this seed metric. Specifically, the following steps allow to generate the (six-dimensional uplift of the) electrically charged doubly spinning dipole ring by a 4-soliton transformation (see [10] for more details):

1. Perform the following four transformations on the seed (4): remove solitons at $z = a_0, a_1, a_4$ with trivial Belinski–Zakharov (BZ) vectors $(0,0,1,0)$, $(0,1,0,0)$, $(0,0,0,1)$, respectively, and remove an anti-soliton at $z = a_2$ with trivial BZ vector $(0,1,0,0)$. For convenience, supplement all this with a rescaling of the metric by an overall factor $\zeta = \rho^2/(\mu_1\mu_4)$. The resulting metric is

$$G_0' = \mathtt{diag}\left\{-\frac{\mu_0\,\rho^2}{\mu_1\,\mu_2\,\mu_4}, \frac{\rho^4}{\mu_2^2\,\mu_3}, -\frac{\mu_0\,\mu_3}{\mu_4}, -\frac{\mu_2}{\mu_1}\right\}. \tag{6}$$

2. Taking (6) as a seed solution, perform now a 4-soliton transformation that re-adds the same solitons but with more general BZ vectors, and undo the rescaling. More precisely,

   (a) add a soliton at $z = a_0$ with BZ vector $(c_1, 0, 1, 0)$;
   (b) add a soliton at $z = a_1$ with BZ vector $(0, 1, b_1, 0)$;
   (c) add an anti-soliton at $z = a_2$ with BZ vector $(b_2, 1, 0, b_3)$;
   (d) add a soliton at $z = a_4$ with BZ vector $(0, c_2, 0, 1)$;

   and rescale by $\zeta^{-1}$. Denote the final metric by $G$. The final rescaling ensures that $\det G = -\rho^2$.
3. Compute the conformal factor of the new metric, given by $e^{2\nu} = e^{2\nu_0}\frac{\det \Gamma}{\det \Gamma_0}$, where the matrix $\Gamma$ implements the addition of solitons [6, 9] and $\Gamma_0 \equiv \Gamma|_{c_1,b_1,b_2,b_3,c_2=0}$.

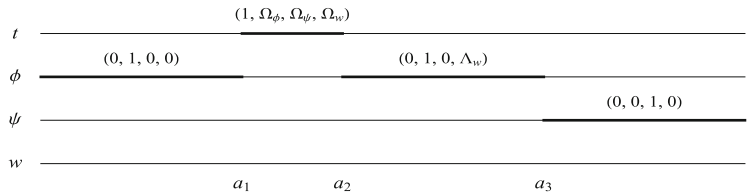


**Fig. 2** Rod diagram for the six-dimensional lift of the doubly spinning charged *black ring*. The direction of each rod is indicated

4. Make a coordinate transformation, $G \to \tilde{G} = S^T G\, S$ with $S \in SL(4, \mathbf{R})$, to ensure that the final metric has standard orientation, or equivalently, that it is asymptotically flat and has correct periodicities for the angular coordinates.

The pair $(\tilde{G}, e^{2\nu})$ determines the six-dimensional solution we seek. Considering a mixing matrix of the form

$$S = \begin{pmatrix} 1 & q_0 & p_0 & 0 \\ 0 & q_1 & p_1 & 0 \\ 0 & q_2 & p_2 & 0 \\ 0 & q_3 & p_3 & 1 \end{pmatrix} \tag{7}$$

a simple counting reveals that the solution depends on 18 parameters.[2] However, for general choices of the parameters the resulting five-dimensional black ring suffers from singularities in the domain of outer communications. Imposing asymptotic flatness fixes all components of the matrix $S$ and also the parameter $k$. In addition, requiring full regularity of the solution fixes the parameters $c_1$ and $c_2$. When considering finite BZ parameters $b_j$, a non-trivial constraint also arises from the requirement that the first three components of the direction of rod $[a_2, a_4]$ match those of rod $(-\infty, a_1]$; see Fig. 2. This is enforced so that $\phi = 0$ defines the axis of rotation both outside and inside the five-dimensional black ring. Finally, imposing that the solution is *balanced*, i.e., that there are no conical singularities along the disc bounded by the ring, introduces one further constraint, leaving only five free parameters for the most general solution. These are in correspondence with mass, two angular momenta, electric charge and magnetic dipole charge.

## *Example: Construction of the Singly-Spinning Dipole Ring*

In this section we illustrate the procedure outlined above for the singly-spinning dipole black ring. Its construction is simple enough so that we can present it in a

[2]The parameter counting is as follows: 4 from the rod endpoints (the solution is invariant under an overall shift in $z$ so we subtract 1), 5 from the BZ parameters $c_i$ and $b_j$, 8 from the coordinate mixing matrix $S$, and 1 from $k$.

concise manner, while retaining the non-trivial features that are common to every generation of black rings carrying dipole charge. Refer to [10, 11] for more details about the construction.

**6D Solution in Weyl Coordinates.** To obtain the singly-spinning dipole ring we take the steps described in Sect. 3 and set $b_1 = b_2 = b_3 = 0$.[3] This imposes the vanishing of the angular momentum associated with coordinate $\phi$ and of the electric charge. We obtain the following metric, written in Weyl coordinates $(\rho, z)$:

$$G_{tt} = -\frac{\mu_0\Big[\mu_2\,\mu_3\,Z_{01}^2 - c_1^2\,\mu_1\,Y_{02}^2\,Y_{03}^2\,\rho^4/\mu_0^2\Big]}{\mu_2\Big[\mu_2\,\mu_3\,Z_{01}^2 + c_1^2\,\mu_1\,Y_{02}^2\,Y_{03}^2\,\rho^2\Big]}, \tag{8}$$

$$G_{t\psi} = \frac{c_1\,\mu_1\,\mu_3\,Y_{02}\,Y_{03}\,Z_{00}\,Z_{01}}{\mu_0\Big[\mu_2\,\mu_3\,Z_{01}^2 + c_1^2\,\mu_1\,Y_{02}^2\,Y_{03}^2\,\rho^2\Big]}, \tag{9}$$

$$G_{\psi\psi} = \frac{\mu_1\,\mu_3\Big[\mu_2\,\mu_3\,Z_{01}^2 - c_1^2\,\mu_0^2\,\mu_1\,Y_{02}^2\,Y_{03}^2\Big]}{\mu_0\Big[\mu_2\,\mu_3\,Z_{01}^2 + c_1^2\,\mu_1\,Y_{02}^2\,Y_{03}^2\,\rho^2\Big]}, \tag{10}$$

$$G_{\phi\phi} = \frac{\rho^2\,\mu_4\Big[\mu_1\,\mu_2^3\,Y_{34}^4\,Z_{34}^6 + c_2^2\,\mu_3^5\,Y_{14}^2\,Y_{24}^4\,Z_{24}^2\,\rho^6/\mu_4^2\Big]}{\mu_1\,\mu_3\Big[\mu_1\,\mu_2^3\,Y_{34}^4\,Z_{34}^6 - c_2^2\,\mu_3^5\,Y_{14}^2\,Y_{24}^4\,Z_{24}^2\,\rho^4\Big]}, \tag{11}$$

$$G_{w\phi} = \frac{c_2\,\mu_2^2\,\mu_3^2\,Y_{14}\,Y_{24}^2\,Y_{34}^2\,Z_{24}\,Z_{34}^3\,Z_{44}\,\rho^2}{\mu_4\Big[\mu_1\,\mu_2^3\,Y_{34}^4\,Z_{34}^6 - c_2^2\,\mu_3^5\,Y_{14}^2\,Y_{24}^4\,Z_{24}^2\,\rho^4\Big]}, \tag{12}$$

$$G_{ww} = \frac{\mu_2\Big[\mu_1\,\mu_2^3\,Y_{34}^4\,Z_{34}^6 + c_2^2\,\mu_3^5\,\mu_4^2\,Y_{14}^2\,Y_{24}^4\,Z_{24}^2\,\rho^2\Big]}{\mu_4\Big[\mu_1\,\mu_2^3\,Y_{34}^4\,Z_{34}^6 - c_2^2\,\mu_3^5\,Y_{14}^2\,Y_{24}^4\,Z_{24}^2\,\rho^4\Big]}, \tag{13}$$

where we have introduced the notation $Y_{ij} \equiv \mu_i - \mu_j$ for convenience. The remaining components not related to these by symmetry vanish. The conformal factor of the solution generated is

$$e^{2v} = k^2\frac{Z_{02}\,Z_{03}\,Z_{14}\,Z_{24}}{\mu_0\,\mu_2^4\,Y_{34}^4\,Z_{01}\,Z_{13}^2\,Z_{34}^5\,\prod_{i=0}^4 Z_{ii}} \times\Big[\mu_2\,\mu_3\,Z_{01}^2 + c_1^2\,\mu_1\,Y_{02}^2\,Y_{03}^2\,\rho^2\Big]\Big[\mu_1\,\mu_2^3\,Y_{34}^4\,Z_{34}^6 - c_2^2\,\mu_3^5\,Y_{14}^2\,Y_{24}^4\,Z_{24}^2\,\rho^4\Big]. \tag{14}$$

[3] This particular case requires no coordinate mixing to display asymptotic flatness.

Regularity of the solution at the points $(\rho, z) = (0, a_0)$ and $(\rho, z) = (0, a_4)$ imposes two constraints [10]:

$$|c_1| = \sqrt{\frac{(a_1 - a_0)}{2(a_2 - a_0)(a_3 - a_0)}}, \qquad |c_2| = \sqrt{\frac{2(a_3 - a_4)^5}{(a_4 - a_1)(a_4 - a_2)^3}}. \tag{15}$$

**6D Solution in C-metric Coordinates.** The metric components simplify significantly when expressed in terms of so-called C-metric coordinates $(x, y)$, which are particularly well adapted for ring-like solutions. The coordinate transformation that accomplishes this is [8]

$$\rho = \frac{R^2\sqrt{-(1-x^2)(1+\nu x)(1-y^2)(1+\nu y)}}{(x-y)^2}, \quad z = \frac{R^2(1-xy)[2+\nu(x+y)]}{2(x-y)^2}. \tag{16}$$

Parametrizing the rod endpoints according to

$$a_0 = \frac{R^2}{2}\alpha, \quad a_1 = -\frac{R^2}{2}\nu, \quad a_2 = \frac{R^2}{2}\nu, \quad a_4 = \frac{R^2}{2}\beta, \quad a_3 = \frac{R^2}{2}, \tag{17}$$

where $R$ controls the overall length scale of the solution and

$$\alpha = \frac{\nu(1+\lambda) - 2\lambda}{(1-\lambda)}, \qquad \beta = \frac{\nu(1-\mu) + 2\mu}{(1+\mu)}, \tag{18}$$

the six-dimensional solution defined by (8)–(14) becomes [11]

$$\begin{aligned} ds_6^2 = &- \frac{F(y)}{F(x)}\left(dt + C\,R\frac{1+y}{F(y)}d\psi\right)^2 + \frac{H(x)}{H(y)}\left(dw + \tilde{C}\,R\frac{1+x}{H(x)}d\phi\right)^2 \\ &+ \frac{R^2F(x)H(y)}{(x-y)^2} \\ &\times\left[\frac{G(x)}{F(x)H(x)}d\phi^2 + \frac{(1-\nu)^2k^2}{(1+\mu)(1-\lambda)}\left(\frac{dx^2}{G(x)} - \frac{dy^2}{G(y)}\right) - \frac{G(y)}{F(y)H(y)}d\psi^2\right]. \end{aligned} \tag{19}$$

For convenience we introduced the following functions,

$$F(\xi) = 1 + \lambda\xi, \qquad G(\xi) = (1-\xi^2)(1+\nu\xi), \qquad H(\xi) = 1 - \mu\xi, \tag{20}$$

along with the quantities

$$C = \sqrt{\lambda(\lambda-\nu)\frac{1+\lambda}{1-\lambda}}, \qquad \tilde{C} = \sqrt{\mu(\mu+\nu)\frac{1-\mu}{1+\mu}}. \tag{21}$$

**From 6D to 5D.** Finally, we perform the dimensional reduction according to the KK ansatz (2). The resulting 5D line element, with the choice $k = \frac{\sqrt{(1+\mu)(1-\lambda)}}{(1-\nu)}$, is [4]

$$
\begin{aligned}
ds_5^2 = &-\frac{F(y)}{F(x)}\left(\frac{H(x)}{H(y)}\right)^{1/3}\left(dt + C\,R\frac{1+y}{F(y)}d\psi\right)^2 \\
&+\frac{R^2}{(x-y)^2}F(x)\left(H(x)H(y)^2\right)^{1/3} \\
&\times\left[-\frac{G(y)}{F(y)H(y)}d\psi^2 - \frac{dy^2}{G(y)} + \frac{dx^2}{G(x)} + \frac{G(x)}{F(x)H(x)}d\phi^2\right],
\end{aligned}
\tag{22}
$$

and the vector field $A$ and dilaton $\phi$ are given by

$$
A = \tilde{C}\,R\left(\frac{1+x}{H(x)}\right)d\phi, \qquad e^{-\phi} = \left(\frac{H(x)}{H(y)}\right)^{\sqrt{2/3}}. \tag{23}
$$

This solution precisely agrees with [4]. Furthermore, the ordering of the rod endpoints $a_i$, together with Eqs. (17), (18), implies that the parameters of the solution obey the bounds $0 < \nu \leq \lambda < 1$ and $0 \leq \mu < 1$, also in accordance with [4].[5]

## 4 Conclusions

In this contribution we described a systematic approach to construct black rings in five-dimensional Einstein–Maxwell-dilaton theory with Kaluza–Klein dilaton coupling. The procedure relies on the inverse scattering method in six dimensions and is sufficiently robust to generate solutions carrying two independent angular momenta, electric charge and magnetic dipole. In particular, this framework overcomes the difficulty of adding a dipole charge to neutral solutions—for the specific theory under consideration—putting it on the same footing as angular momentum. As an illustration of our method we presented an explicit construction of the singly-spinning dipole black ring.

[4] The angular coordinates have periodicity $\Delta\phi = \Delta\psi = 2\pi k$ so this choice does not yield canonically normalized angular variables. Nevertheless, we adopt this convention to more easily compare our results with [4].

[5] For general choices of parameters the solution (22), (23) is unbalanced. Avoidance of conical singularities is obtained by imposing a further constraint [4], yielding a final solution that is fully regular, balanced, and depending on three parameters, corresponding to mass, angular momentum and dipole charge.

**Acknowledgements** We thank the organizers and participants of the Spanish Relativity Meeting in Portugal, 3–7 September 2012, where this work was presented. J.V.R. is supported by *Fundação para a Ciência e Tecnologia* (FCT)-Portugal through contract no. SFRH/BPD/47332/2008. M.J.R. is supported by the European Commission—Marie Curie grant PIOF-GA 2010-275082. O.V. is supported in part by the Netherlands Organization for Scientific Research (NWO) under the VICI grant 680-47-603 and, at the time this work was done, by the Spanish Government research grant FIS2008-01980.

## References

1. Belinsky, V.A., Zakharov, V.E.: Stationary Gravitational Solitons with Axial Symmetry. Sov. Phys. JETP **50**, 1–9 (1979)
2. Chen, Y., Hong, K., Teo, E.: A doubly rotating black ring with dipole charge. JHEP **1206**, 148 (2012)
3. Elvang, H., Emparan, R., Figueras, P.: Non-supersymmetric black rings as thermally excited supertubes. JHEP **0502**, 031 (2005)
4. Emparan, R.: Rotating circular strings, and infinite nonuniqueness of black rings. JHEP **0403**, 064 (2004)
5. Emparan, R., Reall, H.S.: Generalized Weyl solutions. Phys. Rev. D **65**, 084025 (2002)
6. Emparan, R., Reall, H.S.: Black Holes in Higher Dimensions. Living Rev. Rel. **11**, 6 (2008)
7. Feldman, A.L., Pomeransky, A.A.: Charged black rings in supergravity with a single non-zero gauge field. JHEP **1207**, 141 (2012)
8. Harmark, T.: Stationary and axisymmetric solutions of higher-dimensional general relativity. Phys. Rev. D **70**, 124002 (2004)
9. Iguchi, H., Izumi, K., Mishima, T.: Systematic solution-generation of five-dimensional black holes. Prog. Theor. Phys. Suppl. **189**, 93–125 (2011)
10. Rocha, J.V., Rodriguez, M.J., Varela, O.: An electrically charged doubly spinning dipole black ring. JHEP **1212**, 121 (2012)
11. Rocha, J.V., Rodriguez, M.J., Virmani, A.: Inverse scattering construction of a dipole black ring. JHEP **1111**, 008 (2011)

# Quantum Cosmology: Meeting SUSY

**Paulo Vargas Moniz**

**Abstract** Some of the basics of supersymmetric quantum cosmology are briefly reviewed, pointing to promising lines of research to explore.

## 1 Motivation and *Justification*

I have been doing research on Supersymmetric Quantum Cosmology (SQC) for the past 20 years or so. My claim is that SQC [1–3] constitutes a most interesting and rewarding research topic. It provides the opportunity, on the one hand, to perform calculations that may be relevant for phenomenology and, on the other hand, it has a close connection to exciting new areas of fundamental research such as quantum gravity, M/string theory and theoretical high energy physics in general.

SQC vast research programme imports some of its guidelines from earlier investigations in quantum supergravity using canonical methods. It has been gradually enlarged, with many cosmological scenarios extensively reported in the published literature [1–3], with the following properties enhancing a significant motivation:

1. SQC subscribes to the idea that treating effects from quantum gravity and supersymmetry as both dominant, will bring forward an improved description of the very early universe. This contrasts with conventional quantum cosmology, where quantum gravity is present but *not* supersymmetry. In the SQC framework, we will therefore find a larger set of variables (bosonic and fermionic) as well as additional symmetries which increase the number of constraints, subsequently imposing a wider algebra.

P. Vargas Moniz (✉)
Departamento de Física, Universidade da Beira Interior Rua Marquês d'Avila e Bolama, Covilhã 6200, Portugal

CENTRA-IST, Av. Rovisco Pais, Lisboa, Portugal
e-mail: pmoniz@ubi.pt

A. García-Parrado et al. (eds.), *Progress in Mathematical Relativity, Gravitation and Cosmology*, Springer Proceedings in Mathematics & Statistics 60,
DOI 10.1007/978-3-642-40157-2_9, 

2. Moreover, $N = 1$ supergravity constitutes a natural "square-root" of gravity, in a Dirac-like manner: the analysis of a second order equation of the Klein–Gordon type (i.e., the Wheeler–DeWitt equation) could be substituted by that of a "supersymmetry induced" set of first order differential equations. This would then have profound consequences [1–3], regarding the dynamics of the wave function of the universe.

So far, to this date, no evidence in favor of supersymmetry has been found [4]. The more "energetic" efforts are the recent and forthcoming explorations at LHC [5]. If supersymmetry exists in nature (meaning it will be eventually detected), then, most possibly, it will also be present at the scales where gravity unifies with other interactions, playing therein an active role, in, e.g., supergravity. Let us hope (at least, I am) that a clear and unequivocal sign proving supersymmetry's existence will be the landmark result of the LHC operating years [5].

## 2 Introduction (*Somewhat Technical*)

Let us be more precise with respect to what SQC entails [1–3].

Following the Dirac procedure, the canonical representation is performed in the Hamiltonian formalism. More precisely, this means we find the Hamiltonian and the diffeomorphism constraint, $\mathscr{H}$ and $\mathscr{H}^i$, respectively, associated with general coordinate transformations, together with the supersymmetry constraints, $\mathscr{S}^A$, corresponding to supersymmetry transformations as well as the Lorentz constraints, $\mathscr{J}^{AB}$, for the Lorentz transformations. These constraints should then be satisfied by the physical states.

Then, from the form of the constraint algebra it may then be sufficient that only the Lorentz and supersymmetry constraints have to be solved. It is this exciting landscape (to explore and venture into) that makes SQC so interesting. In this context, SQC is usually (!...) retrieved from $N = 1$ supergravity theory by restricting it to spatial homogenous cosmologies:

- The usual dimensional reduction of the $N = 1$ supergravity action in four space-time dimensions to one-dimensional (time-dependent only) "mechanical" models. This can be made through suitable homogeneous ansätze integrating over the spatial hypersurfaces, leading to a cosmological minisuperspace characterized by a $N = 4$ local supersymmetry and time-invariance reparametrization. Friedmann–Robertson–Walker (FRW) models are the simplest to consider and have been widely investigated in this manner.
- Or, another procedure (not necessarily fully equivalent with the previous but also often employed within *diagonal* Bianchi models) can be used. It involves the use of the constraints of the full theory of supergravity. More precisely, the constraints are directly evaluated subject to the corresponding spatially homogenous ansatz on the supergravity physical variables

Regarding the subsequent quantization, the supersymmetric minisuperspace is characterized by the existence of second class constraints. These, when eliminated, replace the usual Poisson brackets by more complicated Dirac brackets. For the canonical momenta associated with bosonic variables, we can choose a differential operator representation and a similar procedure can be adopted for the conjugate momenta associated with the fermionic variables. This scheme has been widely employed with known results. Another possibility is to adopt a matrix representation for the fermions complying to the Dirac bracket algebra.

Once the quantum mechanical representation has been chosen for the fermionic momenta (matrix or differential operator), the next issue is the use of the quantum Lorentz and supersymmetry constraints (usually under the framework of a factor ordering prescription). When the Lorentz "annihilation" on the wave function has been performed, solving the corresponding equations, we get a set of expressions that must still satisfy the supersymmetry constraints. This is usually achieved by solving a subsequent set of (coupled) first-order differential equations (equivalent to a Dirac-like square root of the second order Wheeler–DeWitt equation in conventional quantum cosmology). This line of approach is usually designated as the metric representation point of view. Another important approach used instead Ashtekar (connection and loop) variables.

Other different formalisms have been employed in the literature, with the aim to approach SQC from alternative (perhaps more feasible) routes. They have had the merit of bringing contributions to still long standing open questions as well as allowing to formulate newly pertinent ones. In more detail, a superspace in a $N = 2$ conformal supersymmetry context has been explored, a $\sigma$-model approach from ($N = 2$) supersymmetric quantum mechanics has been introduced, while Darboux transformation and global supersymmetry were also explored. All the above approaches share some similarities but also have specific differences in method and results. A clear analysis establishing whether and how they are related (including if and how they can be equivalent) is yet to be achieved.

In the following sections we will attempt to describe, by means of specific applications, the main elements and some of the results within SQC. In Sect. 3, we will illustrate, using a FRW $N = 4$ supersymmetric setting, the metric and differential fermion operator approach. It is the simpler set up, but pedagogically useful to introduce some features. Bianchi and inhomogeneous models would convey more realistic appraisals for SQC, but they bring far more ingredients and technical difficulties [1,2]. We will add a few glimpses on the inhomogenous sector in Sect. 4, perhaps the (currently) more enticing and promising paths. In Sect. 5, we briefly make a summary and point to some useful references.

I apologize in advance for not being able to be as detailed and complete as it would be expected from an interested reader. A more complete overview is beyond the scope and range permitted in this article. In particular, if wanting to look at the difficulties which have hinder progress (and these surely still exist), the reader can investigate about them in [1–3]; All the readers that have either become interested

or got even more curious about SQC, are invited to embark in the route(s), some still waiting discovery and exploration, charted[1] in recent publications [1–3].

## 3 Metric and Differential Fermion Operator Approach (*Basics*)

Let us consider FRW geometries in pure $N = 1$ supergravity. The tetrad $e_{AA'\mu}$ and gravitino $\psi_{\mu}^{A}$ fields ought to be chosen accordingly. This *can only be possible* for a suitable combination of supersymmetry, Lorentz and local coordinate transformation. More precisely, closed FRW universes have $S^3$ spatial sections. A suitable ansatz reduces the number of degrees of freedom provided by $e_{AA'\mu}$. If supersymmetry invariance is to be retained, then we need an ansatz for ${\psi^{A}}_{\mu}$ and ${\bar{\psi}^{A'}}_{\mu}$, which reduces the number of fermionic degrees of freedom. We take ${\psi^{A}}_{0}$ and ${\bar{\psi}^{A'}}_{0}$ to be functions of time only. We further take

$$ {\psi^{A}}_{i} = {e^{AA'}}_{i}\bar{\psi}_{A'}, {\bar{\psi}^{A'}}_{i} = {e^{AA'}}_{i}\psi_{A}, \tag{1} $$

where we introduce the new spinors $\psi_A$ and $\bar{\psi}_{A'}$, which are functions of time only. This means we truncate the general decomposition ${\psi^{A}}_{BB'} = {e_{BB'}}^{i}{\psi^{A}}_{i}$ at the spin $\frac{1}{2}$ mode level. That is, with $\beta^A = \frac{3}{4}n^{AA'}\bar{\psi}_{A'} \sim \bar{\psi}^A$. This constitutes a direct consequence of assuming a FRW geometry and it is a necessary condition for supersymmetry invariance to be retained. It is also important to stress that auxiliary fields are also required to balance the number of fermionic and bosonic degrees of freedom. However, these auxiliary fields can be neglected in the end. The above ansätze preserves the form of the tetrad under a *suitable combination* of supersymmetry, Lorentz and local coordinate transformations.

Classically, the constraints vanish and this set of constraints forms an algebra. The constraints are functions of the basic dynamical variables. For the gravitino fields, their canonical momenta produce (second-class) constraints. These are eliminated when Dirac brackets are introduced instead of the original Poisson brackets.

Our constraints then take the simple form

$$ S_A = \psi_A\pi_a - 6ia\psi_a, \tag{2} $$

$$ H = -a^{-1}(\pi_a^2 + 36a^2), \tag{3} $$

$$ \bar{S}_{A'} = \bar{\psi}_{A'}\pi_a + 6ia\bar{\psi}_{A'}, \tag{4} $$

$$ J_{AB} = \psi_{(A}\bar{\psi}^{B'}n_{B)B'}. \tag{5} $$

[1] For conventions and notation, please consult [1, 2].

The presence of the free parameters $\rho_A$, $\bar{\rho}_{A'}$ shows that this minisuperspace model has $N = 4$ local supersymmetry.

Before solving the supersymmetry constraints $S_A, \bar{S}_{A'}$, note that $J^{AB}\Psi = 0$ implies that $\Psi$ can be written as $\Psi = A + B\psi_A\psi^A$, where $A$ and $B$ depend only on $a$. The quantum solutions from (2), (4) are then

$$\Psi = C\exp[-3a^2/\hbar] + D\exp[3a^2/\hbar]\psi_A\psi^A, \tag{6}$$

where $C$ and $D$ are independent of $a$ and $\psi^A$. The exponential factors have a *semi-classical* interpretation as $\exp(-I/\hbar)$, where $I$ is the Euclidean action for a classical solution outside or inside a three-sphere of radius $\frac{\kappa}{\sigma}a$ with a prescribed boundary value of $\psi^A$. That is, we get a Hartle–Hawking solution for $C = 0$.

Much more has been achieved regarding other more generic homogenous models and with other matter contents. For more details, in particular regarding methods and still existing obstacles to progress, please consult [1, 2]. The webpages [3] also attempt to contain updated and useful information for the interested researcher.

## 4 "Observational" SQC (*Not Basics, Anymore*)

Until the late 1990s, most of the research conducted in SQC was aimed at finding quantum states and overcome consistency problems [1, 2]. But it was crucial that progress would be made, to find *additional* quantum states, which would have a physical significance regarding (a) a period of evolution from supersymmetric quantum gravitational physics towards a semi-classical stage, together with (b) identifying the existence of any quantum state associated to structure formation, (c) followed by establishing how does conventional quantum cosmology harmonise into this picture, (d) and hence, determining if a path from supersymmetric quantum cosmology physics down to a classical level can be consistently established.

To be more precise, it remained to establish *if* and *how* the inclusion of supersymmetry in a quantum cosmological scenario could lead to a spectrum of density fluctuations compatible with today's observational data. By then constructing a model that describes perturbations about a supersymmetric FRW minisuperspace with complex scalar fields, SQC has been also directed towards an "observational context". But plenty of work remains to be done, please see [1, 2].

As far as the perturbations about the background minisuperspace are concerned, the scalar fields can be taken as

$$\Phi(x_i, t) = \phi(t) + \Sigma_{nlm} f_n^{lm}(t) Q_{lm}^n(x_i), \tag{7}$$

together with its complex conjugate, where the coefficients $f_n^{lm}$, $\bar{f}_n^{lm}$ are functions of the time coordinate $t$ and $Q_{lm}^n$ are standard scalar spherical harmonics on $S^3$, $x_i$

are coordinates on the three-sphere, and with $n = 1, 2, 3 \ldots$, $l = 0, \ldots, n-1$, $m = -l, \ldots, l$. The fermionic superpartners are expanded as:

$$\mathrm{X}_A(x_i, t) = \chi_A(t) + a^{-3/2} \Sigma_{mpq} \beta_m^{pq} \left[ s_{mp}(t) \rho_A^{nq}(x_i) + \bar{t}_{mp}(t) \bar{\tau}_A^{mq}(x_i) \right], \tag{8}$$

together with its Hermitian conjugate, with $m = 1, \ldots, \infty$, $p, q = 1, \ldots, (m+1)(m+2)$ and where $\rho_A^{mq}, \bar{\rho}_{A'}^{mq}, \tau_{A'}^{mq}, \bar{\tau}_A^{mq}$ are spinor hyperspherical harmonics on $S^3$. In addition, the time-dependent coefficients $t_{mp}, s_{mp}$ and their Hermitian conjugates are odd elements of a Grassmanian algebra, where the matrix $\beta_{pq}^n$ satisfy $\beta_{npq}^2 = 21_{\mathrm{n}}$.

Inserting now (7), (8) into the general action of $N = 1$ supergravity with scalar supermatter, we can obtain (after integration) a reduced action which includes an infinite sum of time-dependent harmonic and Fermi oscillators. After some suitable redefinitions of the $\psi^A$ and $\chi^A$ variables, the quantum supersymmetry constraints of the model can be constructed from the coefficients in $\psi_0^A, \bar{\psi}_0^{A'}$ in the Hamiltonian. They take the form $S_A = S_A^{(0)} + S_A^{(\mathrm{pertb.})}$, with [1,2]

$$\begin{aligned} S_A^{(0)} = & -i \chi_A \frac{\partial}{\partial \phi} - \frac{a \psi_A}{2\sqrt{3}} \frac{\partial}{\partial a} - \sqrt{3} a^2 \psi_A \\ & - \frac{i}{8} \bar{\phi} \chi^B \chi_B \frac{\partial}{\partial \chi^A} \\ & - \frac{i}{4} \bar{\phi} \chi_A \psi^B \frac{\partial}{\partial \psi^B} + \frac{3}{4\sqrt{3}} \psi_A \chi^B \frac{\partial}{\partial \chi^B} \\ & + \frac{\psi^B \psi_B}{8\sqrt{3}} \frac{\partial}{\partial \psi^A}, \end{aligned} \tag{9}$$

and

$$\begin{aligned} S_A^{(\mathrm{pertb.})} = & \frac{\psi_A}{\sqrt{3}} \Sigma_m \left[ s_{mp} \frac{\partial}{\partial s_{mp}} - t_{mp} \frac{\partial}{\partial t_{mp}} \right] \\ & + \frac{i}{2} \bar{\phi} \Sigma_m \left[ s_m \frac{\partial}{\partial s_m} - t_m \frac{\partial}{\partial t_m} \right] \chi_A \\ & - i \chi_A \Sigma_n \frac{\partial}{\partial f_n^{lm}} \\ & + 2ia^2 \Sigma_n \bar{f}_n^{lm} (n+1) \chi_A, \end{aligned} \tag{10}$$

together with their Hermitian conjugates, $\bar{S}_A = \bar{S}_A^{(0)} + \bar{S}_A^{(\mathrm{pertb.})}$. $S_A^{(0)}, \bar{S}_{A'}^{(0)}$ will denote the supersymmetry constraints of the unperturbed background, while $S_A^{(\mathrm{pertb.})}, \bar{S}_A^{(\mathrm{pertb.})}$ correspond to the perturbed sector. A significant point should be properly stressed at this point: *both* supersymmetry constraints are *linear* with

respect to the conjugate momenta of *any* bosonic variable. Hence, they determine that a set of coupled first-order differential equations are obtained [1,2].

This can be better understood if we introduce a natural ansatz for the wave function of the universe, which has the form

$$\begin{aligned}\Psi &= A + B\psi^C\psi_C + iC\psi^C\chi_C + D\chi^D\chi_D + \\ &\quad E\psi^C\psi_C\chi^D\chi_D \\ &= A^{(0)}\Pi_n A^{(n)}\Pi_m A^{(m)} \\ &+ B^{(0)}\Pi_n B^{(n)}\Pi_m B^{(m)}\psi^C\psi_C \\ &+ C^{(0)}\Pi_n C^{(n)}\Pi_m C^{(m)}\psi^C\chi_C \\ &+ D^{(0)}\Pi_n D^{(n)}\Pi_m D^{(m)}\chi^C\chi_C \\ &+ E^{(0)}\Pi_n E^{(n)}\Pi_m E^{(m)}\psi^C\psi_C\chi^D\chi_D, \end{aligned} \tag{11}$$

where the bosonic functionals $A^{(0)}, B^{(0)}, C^{(0)}, D^{(0)}, E^{(0)}$ depend on the minisuperspace variables $(a, \phi, \bar{\phi})$, while the bosonic amplitudes $A^{(n)}, \ldots, E^{(n)}$ and $A^{(m)}, \ldots E^{(m)}$ depend respectively also on the individual perturbation modes $f_n, \bar{f}_n$ or $s_m, t_m$. Expression (11) satisfies the Lorentz constraints associated with the unperturbed field variables $\psi_A, \bar{\psi}_{A'}, \chi_A$ and $\bar{\chi}_{A'}$: $J_{AB} = \psi_{(A}\bar{\psi}_{B)} - \chi_{(A}\bar{\chi}_{B)} = 0$. Now, let us substitute (11) into the supersymmetry constraint (9), (10) and their Hermitian conjugates. After having divided $S_A\Psi = 0$ and $\bar{S}_A\Psi = 0$ by $\Psi$ as given in (11), we then obtain the mentioned set of *first-order* differential equations. It is straightforward to obtain the following solutions [1,2]:

$$E^{(0)} = \hat{E}_0^{(0)} \frac{e^{3a^2+\phi(2\lambda_6-\Omega_5)-\Omega_5\bar{\phi}}}{a^{\Omega_6}} \tag{12}$$

$$\begin{aligned} E^{(n)} &= E_0^{(n)} e^{-\lambda_7\bar{\phi}+\phi(2\lambda_8-\lambda_7)} \\ &\quad e^{2\lambda_9\bar{f}_n+2a^2(n-1)f_n\bar{f}_n} \\ &\quad e^{-(\Omega_7-\lambda_9)f_n+(\Omega_7-\lambda_9)\bar{f}_n}, \end{aligned} \tag{13}$$

$$E^{(m)} = E_0^{(m)} e^{2\lambda_8\bar{\phi}-C_2\phi\bar{\phi}-\Omega_9\phi+\Omega_9\bar{\phi}}\tilde{E}, \tag{14}$$

where $\hat{E}_0^{(0)} = E_0^{(0)}e^{-3a^2}$. $E_0^{(n)}, E_0^{(m)}$ denote integration constants and $\tilde{E} \sim s_{mp}$ or $t_{mp}$. Let us emphasize the use of $\phi = \phi_1 + i\phi_2$ or $\phi = re^{i\theta}$ in the process of integration to decouple the physical degrees of freedom encompassed in $\phi, \bar{\phi}$. Notice as well that $\lambda_1, \lambda_2 \ldots$ and $C_1, C_2$ constitute further integration/separation constants. The quantities $\Omega_1, \Omega_2, \ldots$ represent back reactions of the scalar and fermionic perturbed modes in the homogenous modes and are assumed to be of a very small value.

Characteristic features of the no-boundary (Hartle–Hawking) solution are present in the bosonic coefficient $E$ (12)–(14). This state requires $|\Omega_6|\ell^2 1$ and the term

$e^{-na^2 f_n \bar{f}_n}$, $(n \gg 1)$ in (13) to dominate over the other remaining exponential terms. This is equivalent to assume that the corresponding separation/integration constants in (13), (14) to be very small [1,2]. It thus seems that the presence of supersymmetry *selects* a set of solutions, where the no-boundary (Hartle–Hawking) quantum state is mandatory. Concerning the $A, B, C, D$ coefficients, the corresponding equations lead to integral expressions.

In addition, the bosonic coefficient $E$ may lead to a satisfactory spectrum of density perturbations. It thus seems that supersymmetry in a quantum description of the very early universe intrisically contains the relevant seeds for structure formation [1, 2]. Finally, notice that each of the several bosonic amplitudes in (11) corresponds to a specific quantum scenario for the very early universe. Under the reasonable and desirable assumption that supersymmetry constitutes a mandatory component in any realistic analysis of a quantum universe, those several, surely possible, but quite specific scenarios of evolution, can be realistically considered and tested [1, 2].

## 5 Discussion and Outlook

SQC is, in this author's opinion, a most valid and worthy route for high energy physics exploration in the next decades. There are many open problems, as well as many others whose corresponding "solution" may still require novel attempts to address them properly. They are extensively discussed in [1–3], joined with summarized lists of research directions [1–3]. A pedagogical survey of the difficulties which have hindered progress (and these surely still exist) is also described in [1–3]. I do not think (neither feel it) to be realistic for this author to address all or even a small set of them. But "eager young minds" should and could consider to take these routes. Why not? If "yes", I surely would gladly like to read about it/them. My best wishes, indeed.

**Acknowledgements** It is indeed a great pleasure to thank the organizers of ERE-012 for the opportunity and privilege given me to present this lecture. This work has been partially supported by CERN/FP/116373/2010.

## References

1. P. Vargas Moniz, "Quantum cosmology: The supersymmetric perspective. Vol. 1," Lect. Notes Phys. **803** (1) (2010)
2. P. Vargas Moniz, "Quantum cosmology: The supersymmetric perspective. Vol. 2," Lect. Notes Phys. **804** (1) (2010)
3. http://www.facebook.com/pages/Supersymmetry-Quantum-Cosmology/275005232510942; https://plus.google.com/b/109093945032194560856/109093945032194560856/posts; http://www.dfis.ubi.pt/~pmoniz/

4. S. Akula, P. Nath and G. Peim, "Implications of the Higgs Boson Discovery for mSUGRA," Phys. Lett. B **717** (2012) 188 [arXiv:1207.1839 [hep-ph]];
P. Nath, "Higgs Physics and Supersymmetry," Int. J. Mod. Phys. A **27** (2012) 1230029 [arXiv:1210.0520 [hep-ph]];
http://profmattstrassler.com/articles-and-posts/some-speculative-theoretical-ideas-for-the-lhc/supersymmetry/where-stands-supersymmetry-as-of-42012/
5. http://lhc.web.cern.ch/lhc/; http://cms.web.cern.ch/; http://atlas.ch/.

# Part II
# Parallel Sessions

# Avoiding the Trans-Planckian Problem in Black Hole Physics

**Carlos Barceló, Luis C. Barbado, Luis J. Garay, and Gil Jannes**

**Abstract** We describe how the avoidance of the trans-Planckian problem of Hawking radiation can be used as a guiding principle in searching for a compelling scenario for the evaporation of black holes or black-hole-like objects. We argue that there exist only three possible scenarios, depending on whether the classical notion of long-lived horizon is preserved by high-energy physics and on whether the dark and compact astrophysical objects that we observe have long-lived horizons in the first place. Some specific findings along the way are (a) that a theory with high-energy superluminal signaling and a long-lived trapping horizon would be extremely unstable in astrophysical terms and (b) that stellar pulsations of objects hovering right outside, but extremely close to their gravitational radius, can result in a mechanism for Hawking emission.

## 1 The Trans-Planckian Problem

It is standardly assumed that the extremely dark and compact bodies existing in the cosmos are evaporating black holes: black holes, because without invoking still-uncertain quantum mechanisms, there are no stable stellar bodies with the

C. Barceló (✉) · L.C. Barbado
Instituto de Astrofísica de Andalucía (CSIC), Glorieta de la Astronomía, 18008 Granada, Spain
e-mail: carlos@iaa.es; luiscb@iaa.es

L.J. Garay
Departamento de Física Teórica II, Universidad Complutense de Madrid, 28040 Madrid, Spain

Instituto de Estructura de la Materia (CSIC), Serrano 121, 28006 Madrid, Spain
e-mail: luisj.garay@fis.ucm.es

G. Jannes
Low Temperature Laboratory, Aalto University School of Science, PO Box 15100, 00076 Aalto, Finland
e-mail: gil.jannes@gmail.com

A. García-Parrado et al. (eds.), *Progress in Mathematical Relativity, Gravitation and Cosmology*, Springer Proceedings in Mathematics & Statistics 60,
DOI 10.1007/978-3-642-40157-2_10, 

measured characteristics; evaporating, because even the most conservative quantum correction to classical black holes, based on quantum field theory in curved spacetimes, leads to the idea that these object should emit Hawking radiation [1]. The presence of Hawking emission would lead black holes to acquire some metabolism avoiding the "inert end point" character of classical black holes. When Hawking reached this conclusion it was soon realized that it was, however, not very trustable [2]. The original calculation seems to depend strongly on assumptions about the behaviour of fields at absurdly high energies: it invokes absurdly high trans-Planckian frequencies. Since then, after much work it has been realized that Hawking emission is quite robust to changes in the behaviour of high-energy physics: one recovers a Hawking-like emission under quite different high-energy assumptions and underlying mechanisms (see references in [3]).

These analyses are mostly based on adding modified dispersion relations at high energies. The modifications can be separated into subluminal and superluminal. The subluminal modifications avoid directly the trans-Planckian problem by introducing an effective cut-off to the maximum invoked frequency. The superluminal scenarios solve the trans-Planckian problem by recovering Hawking radiation independently of the details of the high-energy modifications. In this work (see the paper [3] for a more detailed presentation) we first point out collateral problems one might encounter in accepting any of these two scenarios. Then, we propose a third scenario able to solve the trans-Planckian problem by assuming in the first place the hypothesis that quantum effects make possible the existence of objects with surfaces hovering right outside the place where the horizon would have formed classically.

## 2 Subluminal Scenarios

Hawking-like radiation in these scenarios proceeds through a mode-conversion mechanism. To recover it, one only needs to assume, essentially, that the energy scale at which the modified dispersion shows up is much larger than the typical energy scale associated with the (low energy) surface gravity of the horizon.

If the quantum gravity theory underlying general relativity incorporated effective subluminal behaviours, then the existence of horizons (one-way membranes) would survive beyond its appearance in low-energy general relativity. Once a horizon is formed the theory would tend to form (close to) singular regions (of course, unless the modifications to the behaviour of matter lead it to violate some energy conditions). Again this tendency would not be ameliorated by the high-energy modifications as this would effectively narrow the light cones. A theory of this sort, in which even at high energies the transmission of information between the internal and external regions of the black hole is not possible, would have a severe information loss problem.

On the other hand, the evaporation of a stellar mass black hole would take $10^{56}$ times the current age of the universe. The existence in this scenario of long-lived trapping horizons enormously delays the time at which we will be able to have

experimental feedback about the real nature of the underlying high-energy theory. Therefore, in the absence of primordial black holes or microscopic black holes at the LHC, these scenarios do not allow an open positive exploration of the full nature of its underlying physics, at least not to the human race as we understand it. As physicists we find this idea, to say the least, disturbing.

## 3 Superluminal Scenarios

Hawking-like radiation in these scenarios proceeds also through a mode-conversion mechanism. To recover it, one needs to assume, essentially, that the energy scale at which the modified dispersion shows up is much larger than the typical energy scale associated with the (low energy) surface gravity of the horizon and that this surface gravity does not go to zero immediately after crossing the horizon [4]. In addition, is has been repeatedly acknowledged that the existence of Hawking-like radiation strongly depends on the boundary conditions imposed in the internal region, specifically on the place where the classical singularity is supposed to reside.

In these types of theories, the notion of horizon is just a low-energy notion. There are always high-energy signals able to escape from the interior of the black hole. Under this circumstance, it is not sensible to continue assuming that a system with a trapping horizon would tend to form a singular region in its interior. Instead, it is more reasonable to assume that the (quantum) high-energy behaviour would naturally regularize any potential singularity in the classical theory.

Now, taking this regularization as hypothesis, we have investigated the spectral characteristics of a black-hole-like configuration of this sort. Specifically, we consider a simple 1+1 spacetime geometry

$$ds^2 = -[1 - v(x)^2]dt^2 + 2v(x)dtdx + dx2, \tag{1}$$

with a step-like profile $v(x)$ such that $v(x) = 0$ for $x \in (0, +\infty)$ and $v(x) = v > 1$ for $x \in [-L, 0]$. On top of it we analyze the spectral properties of a scalar field with a quartic superluminal dispersion relation,

$$\left[\Box - (1/k_P^2)\nabla^4\right]\phi = 0, \tag{2}$$

under reflecting boundary conditions in the internal boundary $x = -L$. This is the place where the singularity would have been located in a standard black-hole configuration. Here, the regularity of the configuration can be seen in both the non-diverging character of the $v$ profile in the internal region and the reflecting boundary conditions imposed upon the scalar field. Qualitatively the results obtained do not depend on the simplifications used in our analysis.

Under these conditions we have found numerically that the system exhibits unstable modes. We have estimated the number of instabilities $n_{\text{inst}}$, as well as their maximal typical growth rates $\Gamma_{\max}$ and the real part $\omega_n$ of their frequencies, as

functions of $v$ and the size $L$ of the inner region. Overall, the qualitative behaviour of these quantities is

$$\Gamma_{\max} \sim 2(v-1)/L, \qquad n_{\text{inst}} \sim 2\omega_c/\Gamma_{\max}, \tag{3}$$

$$\omega_n \sim \pm\Gamma_{\max} n \quad (n = 1 \ldots n_{\text{inst}}/2), \tag{4}$$

where $\omega_c$ is the critical frequency (frequency above which there is no more mode mixing [4]). These results are in agreement with the numerical and analytical studies carried out for black-hole/white-hole configuration in [5, 6], where similar instabilities appear.

When inserting realistic astrophysical figures adapted from a one Solar-mass Schwarzschild black hole, we conclude that $\Gamma_{\max}$ would be of the order of microseconds. This means that a Solar mass black hole with superluminal dispersion would be extremely unstable in astrophysical terms and would tend to eliminate its horizon in microseconds. Thus, we see that if the singularity is smoothed away due to the presence of superluminal dispersion relations, black holes as such would be very unstable. In other words, this analysis suggests that any theory beyond classical general relativity that incorporates superluminal behaviour will avoid the formation of long-lived trapping horizons.

## 4 A Scenario Without Horizons

Finally, we propose a third scenario able to solve the trans-Planckian problem. Imagine as hypothesis that quantum effects were able to stabilize bodies with radia extremely close to their gravitational radia. What we have shown in [3] is that pulsations of such objects between two radia $r_{\text{out}} > r_{\text{in}}$, both very close to $r_g$, are able to produce Hawking-like radiation without invoking absurdly high frequencies. In this sense this mechanism does not ask for assumptions regarding ultra-high-energy physics. It is only necessary that the relativistic invariance is maintained up to a few orders of magnitude beyond Planck scale, something consistent with current experimental probes.

Objects of this kind, which we called black stars, will not encounter the problems associated with standard evaporating black holes. Most importantly, they will be open in principle to astrophysical exploration. Whether there are dynamical mechanisms able to produce these objects is a matter of on-going investigation.

## References

1. S. W. Hawking, "Particle Creation by Black Holes," Commun. Math. Phys. **43** 199–220 (1975) Erratum: ibid. **46** 206 (1976)
2. W. G. Unruh, "Notes on black hole evaporation," Phys. Rev. **D14** 870 (1976)

3. L. C. Barbado, C. Barcelo, L. J. Garay and G. Jannes, JHEP **1111**, 112 (2011) [arXiv:1109.3593 [gr-qc]].
4. J. Macher and R. Parentani, "Black/White hole radiation from dispersive theories," Phys. Rev. **D79** 124008 (2009) [arXiv:0903.2224 [hep-th]].
5. S. Finazzi and R. Parentani "Black hole lasers in Bose-Einstein condensates," New J. Phys. **12** 095015 (2010) [arXiv:1005.4024 [cond-mat.quant-gas]].
6. A. Coutant, R. Parentani, "Black hole lasers, a mode analysis," Phys. Rev. **D81** 084042 (2010) [arXiv:0912.2755 [hep-th]].

# A 2D Field Theory Equivalent to 3D Gravity with No Cosmological Constant

**Glenn Barnich, Andrés Gomberoff, and Hernán A. González**

**Abstract** In (2+1) space-time dimensions the Einstein theory of gravity has no local degrees of freedom. In fact, in the presence of a negative cosmological term, it is described by a (1+1) dimensional theory living on its boundary: Liouville theory. It is invariant under the action of the two-dimensional conformal group, which, in the gravitational context, corresponds to the asymptotic symmetries of asymptotically AdS geometries. In the flat case, when the cosmological term is turned off, a theory describing gravity at the boundary is absent. In this note we show that, in the Hamiltonian setup, such a theory may be constructed. The theory is $BMS_3$ invariant, as it should, corresponding to the asymptotic symmetry group of an asymptotically flat spacetime.

## 1 Introduction

In the last 30 years, gravitational theories in 2+1 spacetime dimensions have attracted much attention. A celebrated advance in this field is due to Brown and Henneaux in [1], where they found that asymptotically AdS spacetimes have more symmetries than one expects. Instead of being symmetric under the $SO(2,2)$ group as one may have guessed, they turned out to be invariant under the whole conformal

G. Barnich
Physique Théorique et Mathématique, Université Libre de Bruxelles and International Solvay Institutes, Campus Plaine C.P. 231, B-1050 Bruxelles, Belgium
e-mail: gbarnich@ulb.ac.be

A. Gomberoff (✉)
Departamento de Ciencias Físicas, Universidad Andres Bello, Av. República 252, Santiago, Chile
e-mail: agomberoff@unab.cl

H.A. González
Departamento de Física, P. Universidad Católica de Chile, Casilla 306, Santiago 22, Chile
e-mail: hdgonzal@uc.cl

A. García-Parrado et al. (eds.), *Progress in Mathematical Relativity, Gravitation and Cosmology*, Springer Proceedings in Mathematics & Statistics 60,
DOI 10.1007/978-3-642-40157-2_11, 

group in two dimensions, whose algebra gets centrally extended. This result is reminiscent from what was obtained in the study of asymptotically flat spacetimes where the group of asymptotic symmetries is much bigger than the Poincaré group one would expect. It is the infinite dimensional BMS group [2–5].

Ten years after it was shown that, in the presence of a negative cosmological term, Einstein–Hilbert gravity is described by Liouville theory [6], which is known to be conformally invariant (see, for instance [7]).

In the present talk, which is based on the work originally published in [8], we are going to show how we may take the limit of vanishing cosmological constant so that a field theory of asymptotically flat gravity is obtained. Although this procedure may appear to be trivial, it turns out that the limit is not well defined in the Lagrangian action when keeping a finite value of Newton's constant $G$. We will show, however, that in the Hamiltonian formulation a well defined limit may be taken for any value of $G$.

## 2 Liouville Theory and Gravity in 3D Spacetime

Liouville theory is defined by the action on the Minkowskian cylinder with time coordinate $t$, angular coordinate $\phi \in [0, 2\pi)$

$$I[\varphi] = \int dt d\phi \left( \frac{1}{2}\dot{\varphi}^2 - \frac{1}{2l^2}\varphi'^2 - \frac{\mu}{2\gamma^2} e^{\gamma\varphi} \right). \tag{1}$$

The action has three independent parameters, namely $\gamma$, $\mu$ and $l$. However, $\mu$ is irrelevant in the sense that with a redefinition of the field $\varphi \to \varphi+$const., its value may be shifted to any non-zero value. The theory is equivalent to (2+1)-dimensional gravity [6], when its constants are related to the gravitational ones by,

$$G = \frac{\gamma^2 l^2}{32\pi}, \quad \Lambda = -\frac{1}{l^2}, \tag{2}$$

where $\Lambda$ is the cosmological constant and $G$ is Newton's constant.

Liouville theory (1) is known to be invariant under the conformal group. Properly normalized, the corresponding Virasoro algebra gets a central extension [7],

$$c = \frac{48\pi}{\gamma^2 l}. \tag{3}$$

Written in terms of the gravitational parameters (2) this is precisely the Brown–Henneaux central charge, $c_{BH} = 3l/2G$.

It is clear, by inspection of (1), that the limit of vanishing cosmological constant is not immediate if one wishes to keep $G$ finite. Taking, $l \to \infty$ keeping $\gamma$ and $\mu$ finite one obtains

$$I[\varphi] = \int dtd\phi \left(\frac{1}{2}\dot{\varphi}^2 - \frac{\mu}{2\gamma^2}e^{\gamma\varphi}\right). \tag{4}$$

However this leads to $G \to \infty$ and a vanishing central charge $c = 0$. The resulting theory is invariant under $\text{bms}_3$ transformations, but it is not (2+1)-dimensional gravity. We will show in the next section how the limit may be taken using the Hamiltonian formulation keeping $G$ finite. We will also show why this limit may not be taken in the Lagrangian formulation.

## 3 Hamiltonian Formulation and the Flat Limit

The Hamiltonian action of Liouville theory is,

$$I[\varphi, \pi] = \int dtd\phi \left(\pi\dot{\varphi} - \frac{1}{2}\pi^2 - \frac{1}{2l^2}\varphi'^2 - \frac{\mu}{2\gamma^2}e^{\gamma\varphi}\right). \tag{5}$$

When minimizing the action with respect to the canonical momentum $\pi$ one obtains

$$\pi = \dot{\varphi}, \tag{6}$$

as expected. One may recover the Lagrangian action (1) by replacing the momentum (6) and putting it back in (5).

As is well-known, Liouville theory is invariant under two-dimensional conformal transformations[7]. In the Hamiltonian framework they are generated by charges satisfying a centrally extended conformal algebra, with a central charge given by (3). We are going to skip the derivation in this note. It is a well known result, and a derivation using the notation and normalizations used here may be found in [8].

We now study the limit $l \to \infty$ in the Hamiltonian version of the theory (5). We may first consider the limit discussed at the end of Sect. 2, which leads us to a theory of vanishing central charge, of no use for gravity unless one wishes to study some strong coupling limit in which $G \to \infty$ is relevant. Doing so, the third term of (5) drops out. Varying the action with respect to $\pi$ one again obtains (6), which once inserted back in the action, produces (4).

In the Hamiltonian version, however, there is a second way of proceeding with the flat limit, leading us to a theory which is equivalent to (2+1)-dimensional gravity for generic, finite $G$. We first rescale the field and its momentum through, $\varphi = l\Phi$, $\pi = \Pi/l$, and define $\beta = \gamma l$, $\nu = \mu l^2$. We obtain,

$$I[\Phi, \Pi] = \int dtd\phi \left(\Pi\dot{\Phi} - \frac{1}{2l^2}\Pi^2 - \frac{1}{2}\Phi'^2 - \frac{\nu}{2\beta^2}e^{\beta\Phi}\right). \tag{7}$$

Since the rescaling of variables is a canonical transformation, the Poisson algebra of the conformal group keeps its form and the central charge does not change. We now

take the limit $l \to \infty$ keeping $\beta$ and $\nu$ fixed. Note that the second term in the action is similar to that of a particle of mass $l$, so that the limit mimics the one of an ultra-massive particle,

$$I[\Phi, \Pi] = \int dtd\phi \left( \Pi \dot{\Phi} - \frac{1}{2}\Phi'^2 - \frac{\nu}{2\beta^2} e^{\beta\Phi} \right). \tag{8}$$

This action has no Lagrangian counterpart. Varying with respect to $\Pi$ gives no algebraic equation for it, and therefore the action cannot be reduced to a Lagrangian, second order form. The field $\Pi$ is now a Lagrangian multiplier. The constant $G$ is kept finite, because $\beta = \sqrt{32\pi G}$ is held fixed in the limit. The centrally extended Virasoro algebra becomes the centrally extended $\mathrm{BMS}_3$ algebra in the way it was first found in [5]. Note that here there is a subtlety. The generators of $\mathrm{BMS}_3$ must be properly rescaled before taking the limit, so that the central extension becomes proportional to $c/l$, which is finite in the limit as one may see from (3) (see also[8] for details).

The action (8), with $\beta = \sqrt{32\pi G}$ and arbitrary $\nu$ is equivalent to Einstein gravity with no cosmological constant in the same way Liouville theory is when the cosmological constant is turned on.[1] The theory is invariant under the $\mathrm{BMS}_3$ group, as it must be, because it is the asymptotic symmetry group of asymptotically flat three-dimensional gravity. The particular form the fields are transformed by the group may be found in [8].

**Acknowledgements** The work of G.B. is supported in part by the Fund for Scientific Research-FNRS (Belgium), by the Belgian Federal Science Policy Office through the Interuniversity Attraction Pole P6/11, by IISN-Belgium, by "Communauté française de Belgique—Actions de Recherche Concertées" and by Fondecyt Projects No. 1085322 and No. 1090753. The work of A.G. was partially supported by Fondecyt (Chile) Grant #1090753. H.G. thanks Conicyt for financial support.

## References

1. J.D. Brown, M. Henneaux, Commun. Math. Phys. **104**, 207 (1986).
2. R. Sachs, Phys.Rev. **128**, 2851 (1962).
3. H. Bondi, M. van der Burg, A. Metzner, Proc.Roy.Soc.Lond. **A269**, 21 (1962)
4. A. Ashtekar, J. Bicak, B.G. Schmidt, Phys.Rev. **D55**, 669 (1997).
5. G. Barnich, G. Compere, Class. Quant. Grav. **24**, F15 (2007)
6. O. Coussaert, M. Henneaux, P. van Driel, Class.Quant.Grav. **12**, 2961 (1995).
7. N. Seiberg, Prog.Theor.Phys.Suppl. **102**, 319 (1990).
8. G. Barnich, A. Gomberoff and H. A. Gonzalez, arXiv:1210.0731 [hep-th].
9. M. Henneaux, L. Maoz and A. Schwimmer, Annals Phys. **282** (2000) 31 [hep-th/9910013].

[1] Note however that, as discussed in [9], this equivalence generally holds only up to zero modes.

# The Holographic Ricci Dark Energy and Its Possible Doomsdays

**Moulay-Hicham Belkacemi, Mariam Bouhmadi-López, Ahmed Errahmani, and Taoufiq Ouali**

**Abstract** It is well known that the holographic Ricci dark energy can induce some future doomsdays in the evolution of the universe. Here we analyse the possible avoidance of those doomsdays by invoking a modification to general relativity on the form of curvature effects.

## 1 Introduction

A possible approach to explain the current acceleration of the universe is based on the holographic dark energy [1, 2]. Such a phenomenological model is based on the idea that the energy density of a given system is bounded by a magnitude proportional to the inverse square of a length characterising the system [3, 4]. When this principle is applied to the universe as a whole, we obtain the holographic dark energy [1, 2]. It turns out that there are many different ways of characterising the size of the universe and one of them is related to the inverse of the Ricci curvature of the universe. When the size of the universe is characterised in such a way, we end up with the holographic Ricci dark energy (RDE) model [5], whose energy density reads:

$$\rho_{\mathrm{H}} = 3\beta M_P^2 \left( \frac{1}{2} \frac{dH^2}{dx} + 2H^2 \right), \tag{1}$$

M.-H. Belkacemi · A. Errahmani · T. Ouali
Laboratory of Physics of Matter and Radiation, Mohammed I University, BP 717, Oujda, Morocco
e-mail: hicham.belkacemi@gmail.com; ahmederrahmani1@yahoo.fr; ouali_ta@yahoo.fr

M. Bouhmadi-López (✉)
Instituto de Estructura de la Materia, IEM-CSIC, Serrano 121, 28006 Madrid, Spain
e-mail: mariam.bouhmadi@iem.cfmac.csic.es

A. García-Parrado et al. (eds.), *Progress in Mathematical Relativity, Gravitation and Cosmology*, Springer Proceedings in Mathematics & Statistics 60,
DOI 10.1007/978-3-642-40157-2_12, 

where $M_P$ is the Planck mass, $x = -\ln(z+1) = \ln(a)$, $z$ is the redshift and $\beta$ is a dimensionless parameter that measures the strength of the holographic component.

A spatially flat Friedmann–Lemaître–Robertson–Walker (FLRW) universe filled with this kind of matter accelerates and therefore the RDE can play the role of dark energy on the Universe. It turns our that the asymptotic behaviour of the Universe depends crutially on the value acquired by $\beta$: (a) if $\beta \leq 1/2$ the universe is asymptotically de Sitter, otherwise (b) the universe faces a big rip singularity [6] in its future evolution.

Our main purpose in this paper is to see if we can appease the big rip appearing in some cases on the RDE by invoking some infra-red and ultra-violet curvature corrections. This two corrections can be quite important to remove the big rip singularity which takes place on the future and at high energy. The curvature corrections will be modeled within a five-dimensional brane-world model with an induced gravity (IG) term on the brane and a Gauss–Bonnet term in the bulk [7].

## 2 The RDE Model with Curvature Corrections

We consider a DGP brane-world model, where the bulk action contains a GB curvature term. The bulk corresponds to two symmetric pieces of a five-dimensional (5d) Minkowski space-time. The brane is spatially flat and its action contains an IG term. We assume that the brane is filled with matter and RDE. Then, the modified Friedmann equation reads [7]:

$$H^2 = \frac{1}{3M_P^2}\rho + \frac{\epsilon}{r_c}\left(1 + \frac{8\alpha}{3}H^2\right)H, \tag{2}$$

where $H$ is the brane Hubble parameter, $\rho = \rho_{\rm m} + \rho_{\rm H}$ is the total cosmic fluid energy density of the brane which can be described through a cold dark matter component (CDM) with energy density $\rho_{\rm m}$ and an holographic Ricci dark energy component with energy density $\rho_{\rm H}$. The parameters $r_c$ and $\alpha$ correspond to the cross over scale and the GB parameter, respectively, both of them being positive. The parameter $\epsilon$ in (2) can take two values: $\epsilon = 1$, corresponding to the self-accelerating branch in the absence of any kind of dark energy [7]; and $\epsilon = -1$, corresponding to the normal branch which requires a dark energy component to accelerate at late-time (see for example [8–10]). For simplicity, we will keep the terminology: (a) self-accelerating branch when $\epsilon = 1$ and (b) normal branch when $\epsilon = -1$.

The modified Friedmann equation (2) can be rewritten as

$$\frac{dE}{dx} = -\frac{\Omega_m e^{-3x} + (2\beta - 1)\,E^2 + 2\epsilon\sqrt{\Omega_{r_c}}(1 + \Omega_\alpha E^2)E}{\beta E}, \tag{3}$$

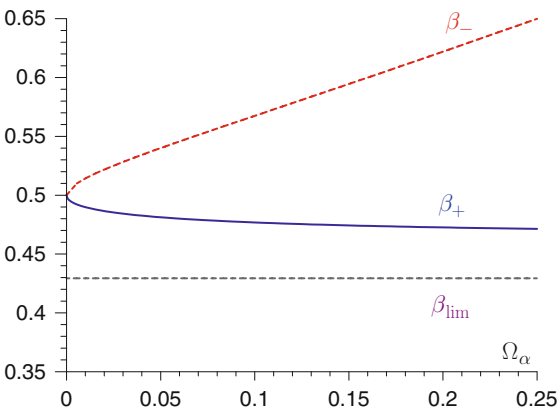


**Fig. 1** Plot of the parameters $\beta_\pm$ and $\beta_{\rm lim}$, defined in (7) and (6), respectively, versus the parameter $\Omega_\alpha$. We have used the values $q_0 \sim -0.7$, and $\Omega_m \sim 0.27$. The parameter $\beta_{\rm lim}$ defines the *border line* between the normal branch ($\beta_{\rm lim} < \beta$) and the self-accelerating branch ($\beta < \beta_{\rm lim}$)

where $E(z) = H/H_0$ and

$$\Omega_m = \frac{\rho_{m_0}}{3M_P^2 H_0^2}, \quad \Omega_{r_c} = \frac{1}{4r_c^2 H_0^2}, \text{ and } \Omega_\alpha = \frac{8}{3}\alpha H_0^2 \tag{4}$$

are the usual convenient dimensionless parameters and the subscripts 0 denotes the present value (we will follow the same notation as in [8, 10, 11]). By evaluating the modified Friedmann equation at present and imposing that the brane is currently accelerating, we obtain a constraint on the parameter $\beta$ which depends on the chosen brane

$$\begin{cases} \beta < \beta_{\rm lim} \text{ for } \epsilon = +1, \\ \beta > \beta_{\rm lim} \text{ for } \epsilon = -1, \end{cases} \tag{5}$$

where

$$\beta_{\rm lim} = \frac{1 - \Omega_m}{1 - q_0}. \tag{6}$$

An estimation of $\beta_{\rm lim}$ can be obtained as follows: the brane would behave roughly (to be consistent with the present observations) as the $\Lambda$CDM leading to $\beta_{\rm lim} \sim 0.43$.

Even though the modified Friedmann equation (3) cannot be solved analytically, we can obtain the future asymptotic behaviour of the brane which reads: (a) If $\beta < \beta_{\rm lim}$ or $\beta_- \leq \beta$, the brane is asymptotically de Sitter. (b) If $\beta_{\rm lim} < \beta < \beta_-$, the brane faces a big freeze singularity in its future [12], where (see also Fig. 1)

$$\beta_\pm = \frac{1 + \Omega_\alpha \pm 2\sqrt{\Omega_\alpha}(1 - \Omega_m)}{2\left[1 + \Omega_\alpha \pm \sqrt{\Omega_\alpha}(1 - q_0)\right]}. \tag{7}$$

We have completed and confirmed those results by solving numerically the cosmological evolution of the brane. We refer the reader to [11] for more details. Our

analysis shows that even though the infra-red and ultra-violet effect can appease the big rip appearing on the RDE model, it cannot remove them completely. We would like as well to point out that when the GB term is switched off a little rip event [13] can show up which is much milder that a big rip or a big freeze. The little rip has been previously found on brane-world model [14].

## 3 Conclusions

We present an HRD energy brane-world model of the Dvali–Gabadadze–Porrati scenario with a GB term in the bulk. The reason for invoking curvature corrections, for example through a brane-world scenario, is to try to smooth the doomdays present on a standard four-dimensional HRD energy model. It turns out that the model presented here can only partially remove those doomsdays.

**Acknowledgements** M.B.L. is supported by the Spanish Agency CSIC through JAEDOC064. A.E. and T.O. are supported by CNRST, through the fellowship URAC 07/214410. This work was supported by the Portuguese Agency FCT through PTDC/FIS/111032/2009.

## References

1. M. Li, Phys. Lett. B **603**, 1 (2004) [arXiv:hep-th/0403127].
2. S. D. H. Hsu, Phys. Lett. B **594**, 13 (2004) [arXiv:hep-th/0403052].
3. L. Susskind, J. Math. Phys. **36**, 6377 (1995) [arXiv:hep-th/9409089].
4. A. G. Cohen, D. B. Kaplan and A. E. Nelson, Phys. Rev. Lett. **82**, 4971 (1999) [arXiv:hep-th/9803132].
5. C. Gao, F.Q. Wu, X. Chen, Y.G. Shen, Phys. Rev. D **79**, 043511 (2009) [arXiv: 0712.1394 [astro-ph]].
6. R. R. Caldwell, Phys. Lett. B **545**, 23 (2002) [arXiv:astro-ph/9908168]; A. A. Starobinsky, Grav. Cosmol. **6**, 157 (2000) 157 [arXiv:astro-ph/9912054].
7. R. A. Brown, R. Maartens, E. Papantonopoulos and V. Zamarias, JCAP **0511**, 008 (2005) [arXiv:gr-qc/0508116].
8. M. Bouhmadi-López, A. Errahmani and T. Ouali, Phys. Rev. D **84**, 083508 (2011) [arXiv:1104.1181 [astro-ph.CO]].
9. M. Bouhmadi-López, JCAP **0911**, 011 (2009) [arXiv:0905.1962 [hep-th]]; M. Bouhmadi-López, S. Capozziello, V. F. Cardone, Phys. Rev. **D82**, 103526 (2010) [arXiv:1010.1547].
10. M. Bouhmadi-López and P. V. Moniz, Phys. Rev. D **78**, 084019 (2008) [arXiv:0804.4484 [gr-qc]]; M. Bouhmadi-López, Y. Tavakoli and P. V. Moniz, Phys. Rev. **D84**, 063003 (2011) [arXiv:1106.4996 [astro-ph.CO]]; JCAP **1004**, 016 (2010) [arXiv:0911.1428 [gr-qc]].
11. M. -H. Belkacemi, M. Bouhmadi-López, A. Errahmani and T. Ouali, Phys. Rev. D **85**, 083503 (2012) [arXiv:1112.5836 [gr-qc]].
12. M. Bouhmadi-López, P. F. González-Díaz, P. Martín-Moruno, Phys. Lett. **B659**, 1 (2008) [gr-qc/0612135]; ibid. Int. J. Mod. Phys. **D17**, 2269 (2008) [arXiv:0707.2390 [gr-qc]].
13. P. H. Frampton, K. J. Ludwick, R. J. Scherrer, Phys. Rev. **D84**, 063003 (2011) [arXiv:1106.4996 [astro-ph.CO]].
14. M. Bouhmadi-López, Nucl. Phys. **B797**, 78 (2008) [astro-ph/0512124].

# Black-Hole Lattices

**Eloisa Bentivegna**

**Abstract** The construction of black-hole lattices, first attempted by Richard Lindquist and John Wheeler in 1957, has recently been tackled with renewed interest, as a test bed for studying the behavior of inhomogeneities in the context of the backreaction problem. In this contribution, I discuss how black-hole lattices can help shed light on two important issues, and illustrate the conclusions reached so far in the study of these systems.

## 1 Introduction

The first appearance of the concept of a periodic arrangement of black holes can be found in [1]. There, the authors discuss a strategy to stitch together patches of the Schwarzschild solution so as to construct a space with a discrete translational symmetry but some degree of spatial inhomogeneity.

In their work, the stitching prescription does not lead to a global solution of Einstein's equation. Accepting the constraint violations, however, buys one some freedom in the specification of such prescription, which the authors use to impose that the time evolution of a suitably-defined scale factor in this space follows that of a universe filled with dust of the same total mass. One then has a simple, analytical test bed in which to measure the effect of inhomogeneities in, say, the optical properties of a cosmological model. In this work and in subsequent ones [2], it was pointed out how an exact initial-data construction could be obtained.

A few years ago, Clifton and Ferreira extended this model, originally limited to the positive-curvature case, to zero and negative curvature [3]. Again, the junction

E. Bentivegna (✉)
Max-Planck-Institut für Gravitationsphysik (Albert-Einstein-Institut), Am Mühlenberg 1, D-14476 Golm, Germany
e-mail: eloisa.bentivegna@aei.mpg.de

A. García-Parrado et al. (eds.), *Progress in Mathematical Relativity, Gravitation and Cosmology*, Springer Proceedings in Mathematics & Statistics 60,
DOI 10.1007/978-3-642-40157-2_13, 

conditions were designed to reproduce an assigned time evolution, and the models were used to explore the propagation of null rays in an inhomogeneous universe.

Recently, the first exact initial data describing a black-hole lattice have been analyzed [4] and evolved in full numerical relativity [5]. This has helped make progress on two fronts:

1. From a conceptual point of view, it has clarified some of the conditions under which black-hole solutions can be glued together; this gives some insight into the requirements for constructing a metric tensor for the universe starting from the basic building block of a spherically-symmetric, isolated object. It turns out that these conditions are remarkably close to the conditions for the existence of homogeneous, periodic solutions of Einstein's equation. The requirements that periodic boundary conditions impose on the Hamiltonian constraint are likely at the root of this correspondence.
2. From a practical standpoint, the time evolution of a lattice gives one example of the behavior of inhomogeneities in a cosmological setting and in the non-linear regime, thereby serving as a nice complement to perturbative studies and the averaging framework. Surprisingly, even the time development of these lattices remains in some sense close to the counterpart model in the dust Friedmann–Lemaître–Robertson–Walker (FLRW) class.

In the following two sections, I will discuss the initial-data construction and illustrate the time evolution of a black-hole lattice with positive conformal curvature.

## 2 The Construction of Exact Black-Hole-Lattice Initial Data

As pointed out in [1], in order to construct an exact black-hole lattice one should directly tackle the Einstein constraints. Working in the *conformal transverse-traceless* decomposition, these read:

$$\tilde{\Delta}\psi - \frac{\tilde{R}}{8}\,\psi - \frac{K^2}{12}\,\psi^5 + \frac{1}{8}\tilde{A}_{ij}\tilde{A}^{ij}\psi^{-7} = -2\pi\,\psi^5\,\rho \tag{1}$$

$$\tilde{D}_i\,\tilde{A}^{ij} - \frac{2}{3}\psi^6\tilde{\gamma}^{ij}\tilde{D}_i\,K = 0 \tag{2}$$

Let us focus on the hamiltonian constraint first. If one integrates this equation over one of the cells of the black-hole lattice, the following condition is obtained:

$$\int_D \left(\frac{\tilde{R}}{8}\,\psi + \frac{1}{12}\,K^2\,\psi^5 - \frac{1}{8}\psi^{-7}\,\tilde{A}^{ij}\,\tilde{A}_{ij}\right)\sqrt{\tilde{\gamma}}\,d^3x = 2\pi\Sigma_{i=1}^{N} m_i \tag{3}$$

where $m_i$ represent the masses of the black holes contained in the cell. This condition implies that $\tilde{R}$ and $K_{ij}$ cannot both be zero. In other words, conformally-flat lattices do not admit a time-symmetric spatial hypersurface; vice versa, lattices with

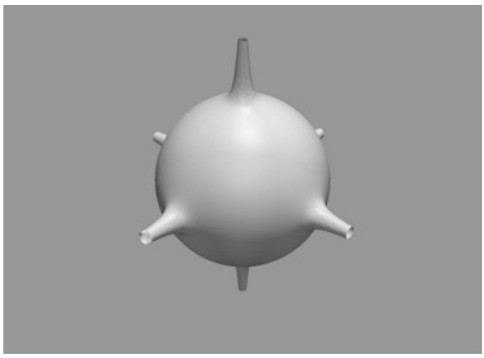

**Fig. 1** A two-dimensional section of the $N = 8$ $S^3$ black-hole lattice, embedded in three dimensions

a $K = 0$ spatial hypersurface must be conformally curved. This mirrors the identical property of the FLRW class.

The two simplest roads to the construction of a periodic black-hole lattice are thus the following:

- Choosing $K = 0$, and solving:

$$\tilde{\Delta}\psi - \frac{\tilde{R}}{8}\psi = 0 \tag{4}$$

  Equation (3) implies that $R > 0$, so that the spacetime can be foliated by conformally-$S^3$ hypersurfaces. As shown in [2], this equation can be solved exactly. Furthermore, it is linear, so one can simply superimpose known solutions to generate new ones. Notice, however, that if one is interested in regular lattices, only six possible arrangements of black holes are possible, corresponding to the six regular tessellations of $S^3$, which consist of $N = 5, 8, 16, 24, 120$ and 600 cells.
- Choosing $\tilde{R} = 0$, and solving:

$$\tilde{\Delta}\psi - \frac{K^2}{12}\psi^5 + \frac{1}{8}\tilde{A}_{ij}\tilde{A}^{ij}\psi^{-7} = 0 \tag{5}$$

$$\tilde{D}_i\tilde{A}^{ij} - \frac{2}{3}\psi^6\tilde{\gamma}^{ij}\tilde{D}_i K = 0 \tag{6}$$

  This system is more difficult to solve, as the Hamiltonian constraint is non-linear and the momentum constraint is not an identity as in the previous case. For a numerical approach to the problem, see [6].

## 3 The Evolution of an $S^3$ Lattice of Eight Black Holes

In [5], the initial data for the $N = 8$ $S^3$ lattice (a section of which is shown in Fig. 1) has been evolved in time for approximately one third of the corresponding FLRW recollapse time. A scale factor can be defined via the proper length of one of

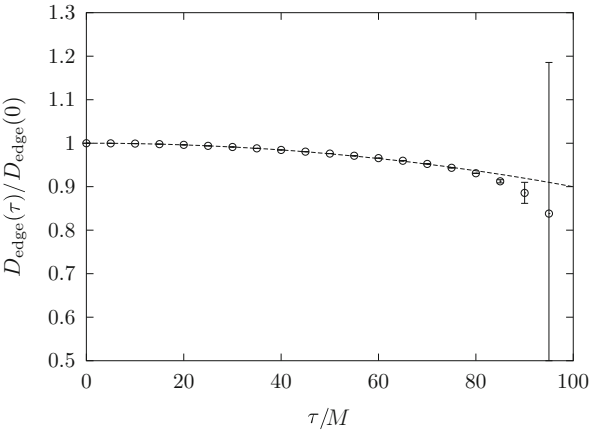


**Fig. 2** Proper length of the edge of a lattice cell as a function of proper time $\tau$. The *dashed line* represents a closed FLRW model in which the edge of a cell of the $N = 8$ tessellation is equal to $D_{\rm edge}(0)$ initially

the cell edges; its evolution is shown in Fig. 2. This scale factor is compatible with the FLRW result in this entire time window; eventually, though, due to the gauge condition used to evolve this system, reaching later and later values of the proper time is subject to an increasing numerical error, and eventually becomes impossible.

**Acknowledgement** I acknowledge the financial support from a Marie Curie International Reintegration Grant (PIRG05-GA-2009-249290).

## References

1. Lindquist, R.W., Wheeler, J.A.: Dynamics of a Lattice Universe by the Schwarzschild-Cell Method. Rev. Mod. Phys. **29**(3), 432–443 (1957). doi: 10.1103/RevModPhys.29.432
2. Wheeler, J.A.: The geometrostatic lattice cell. Foundations of Physics **13**, 161–173 (1983). doi: 10.1007/BF01889418
3. Clifton, T., Ferreira, P.G.: Archipelagian Cosmology: Dynamics and observables in a universe with discretized matter content. Phys. Rev. **D80**, 103503 (2009). doi: 10.1103/PhysRevD.80.103503
4. Clifton, T., Rosquist, K., Tavakol, R.: An exact quantification of backreaction in relativistic cosmology. Phys.Rev. **D86**, 043506 (2012). doi: 10.1103/PhysRevD.86.043506
5. Bentivegna, E., Korzynski, M.: Evolution of a periodic eight-black-hole lattice in numerical relativity. Class.Quant.Grav. **29**, 165007 (2012). doi: 10.1088/0264-9381/29/16/165007
6. Yoo, C., Abe, H., Nakao, K., Takamori, Y.: Black hole universe: Construction and analysis of initial data. Phys.Rev. **D86**, 044027 (2012). doi: 10.1103/PhysRevD.86.044027

# Axial Quasi-normal Modes of Neutron Stars with Exotic Matter

**J.L. Blázquez-Salcedo, L.M. González-Romero, and F. Navarro-Lérida**

**Abstract** We investigate the axial w quasi-normal modes of neutron stars for 18 realistic equations of state in order to study the influence of hyperons and quarks on the modes. The study has been developed with a new method based on Exterior Complex Scaling with variable angle, which allow us to generate pure outgoing quasi-normal modes. A complete study of the junction conditions has been done. We have obtained that w-modes can be used to distinguish between neutron stars with exotic matter and without exotic matter for compact enough stars.

## 1 Quasi-normal Modes Formalism and Numerical Method

We will consider a spherical and static star. The matter inside of it is considered to be a perfect fluid. Following the original papers (see reviews [1, 2]), we make perturbations over the spherical static metric and the stress–energy tensor, taking into account only the axial perturbations. After some algebra, it can be seen that the perturbations satisfy the well-known Regge–Wheeler equation [3], both inside and outside the star. The eigen-frequency of the axial mode is a complex number $\omega = \omega_{\Re} + i\,\omega_{\Im}$. Inside the star an equation of state must be provided, so in general also the static configuration must be solved numerically. Outside the star the metric is known (Schwarszchild) and only the perturbation must be integrated.

J.L. Blázquez-Salcedo (✉) · L.M. González-Romero
Depto. Física Teórica II, Facultad de Ciencias Físicas, Universidad Complutense de Madrid, 28040-Madrid, Spain
e-mail: joseluis.blazquez@fis.ucm.es; mgromero@fis.ucm.es

F. Navarro-Lérida
Depto. Física Átomica, Molecular y Nuclear, Facultad de Ciencias Fí sicas, Universidad Complutense de Madrid, 28040-Madrid, Spain
e-mail: fnavarro@fis.ucm.es

A. García-Parrado et al. (eds.), *Progress in Mathematical Relativity, Gravitation and Cosmology*, Springer Proceedings in Mathematics & Statistics 60,
DOI 10.1007/978-3-642-40157-2_14, 

We are only interested in purely outgoing waves. In general a solution of the Regge–Wheeler equation will be a composition of incoming and outgoing oscillating waves. Because the outgoing wave diverges towards infinity, the purely outgoing quasi-normal mode condition could only be imposed as a behavior far enough from the star, but every small numerical error in the imposition of this behavior will be amplified as we approach the border of the star, resulting in a mixture of outgoing with ingoing waves. Note also that in general the exterior solution will oscillate infinitely towards infinity. We have developed the following method, based on the Colsys package [4], to deal with these difficulties. We make use of previously well known techniques and new ones.

*Exterior solution:* We study the phase function (logarithmic derivative of the Regge–Wheeler function), which does not oscillate. Hence, the differential equation outside the star is reduced to a Riccati equation and we can compactify the radial variable. The boundary condition must grant the outgoing wave behavior. In order to impose a constringent enough condition, we make use of Exterior Complex Scaling method [5] with variable angle, where the integration coordinate is considered to be a complex variable. The principal advantage with respect other methods is that in principle no assumption on the imaginary part (i.e. damping time) of the quasi-normal mode is done.

*Interior solution:* The interior part of the solution is integrated numerically. As we want to obtain realistic configurations, we implement the equations of state in two different ways: (1) A piece-wise polytrope approximation, done by Read et al. [6], in which the equation of state is approximated by a polytrope in different density–pressure intervals. (2) A piece-wise monotone cubic Hermite interpolation satisfying local thermodynamic conditions.

We generate two independent solutions inside of the star for the same static configuration. These two solutions must be combined to match the exterior solution with the appropriate junction conditions. We use Darmois conditions (continuity of the fundamental forms of the matching hypersurface). This formulation allow us to introduce surface layers of energy density on the border of the star, that allow us to approximate the exterior *crust* as a thin layer enveloping the core.

*Determinant method:* The junction conditions can be used to construct what we call the *determinant method*: We construct a matrix in terms of the derivatives of the Regge–Wheeler function whose determinant must be zero only if the matching conditions are fulfilled, i.e., when $\omega$ corresponds to a quasi-normal mode for the static configuration integrated. The matrix is calculated using both independent solutions in the interior of the star together with the exterior phase function.

This method has been successfully extended to study polar modes of realistic neutron stars. These results will be presented elsewhere.

## 2 Numerical Results

We have made several tests on our method successfully reproducing data from previous works for axial modes. As an example, we reproduce the results from [7] with a precision of $10^{-7}$. In this section we will present our results for new realistic EOS. Using the parametrization presented by Read et al. [6], we can study the 34 equations of state they considered. We have used, following their notation, SLy, APR4, BGN1H1, GNH3, H1, H4, ALF2, ALF4. After the recent measurement of the $1.97M_{\odot}$ for the pulsar PSR J164-2230 [8], several exotic matter EOS have been proposed satisfying this condition. We have considered the following ones using the cubic Hermite interpolation: two EOS presented by Weissenborn et al. with hyperons in [9], we call them WCS1 y WCS2; three EOS presented by Weissenborn et al. with quark matter in [10], we call them WSPHS1, WSPHS2, WSPHS3; four EOS presented by L. Bonanno and A. Sedrakian in [11]; we call them BS1, BS2, BS3, BS4; and one EOS presented by Bednarek et al. in [12], we call it BHZBM.

Empirical relations between the frequency and damping time of quasi-normal modes and the compactness of the star can be useful in order to use future observations of gravitational waves to estimate the mass and the radius of the neutron star, as well as to discriminate between different families of equations of state. In top of Fig. 1 we present the frequency of the fundamental mode scaled to the radius of each configuration. The softest equations of state that include hyperon matter, H1 and BGN1H1, present a quite different behavior than the rest of EOS considered. Nevertheless, as the detection of the recent $2M_{\odot}$ pulsar suggest, these two particular EOS cannot be realized in nature.

Another exception is found in pure quark matter stars (WSPHS1-2 EOS). Their behavior is clearly differentiated from the rest because of the different layer structure found at the exterior of the star.

In general, for hyperon matter EOS and hybrid stars, we obtain linear relations between the scaled frequency and the compactness. These relations could be used, applying the technique from [13], to measure the radius of the neutron star and constrain the equation of state.

We plot at the bottom left of Fig. 1 a new phenomenological relation between the real part and the imaginary part of the frequency of the w quasi-normal modes valid for all the EOS. We plot $\bar{\omega}_R = 2\pi \frac{1}{\sqrt{p_c(cm^{-2})}} \frac{10^3}{c} \omega(Khz)$ and $\bar{\omega}_I = \frac{1}{\sqrt{p_c(cm^{-2})}} \frac{10^6}{c} \frac{1}{\tau(\mu s)}$. Although the empirical relation between $\bar{\omega}_R$ and $\bar{\omega}_I$ is quite independent of the EOS, the parametrization of the curve is EOS dependent. So a possible application of this empirical relation is the following. If the frequency $\omega(Khz)$ and the damping time $\tau(\mu s)$ are known, we can parametrize a line defining $\bar{\omega}_R$ and $\bar{\omega}_I$ with parameter $p_c$ using the observed frequency and damping time. The crossing point of this line with the empirical relation presented in the bottom left of Fig. 1 gives us an estimation of the central pressure $p_c$ independent of the EOS. Now, we can check which EOS is compatible with this $p_c$, i.e., which one have

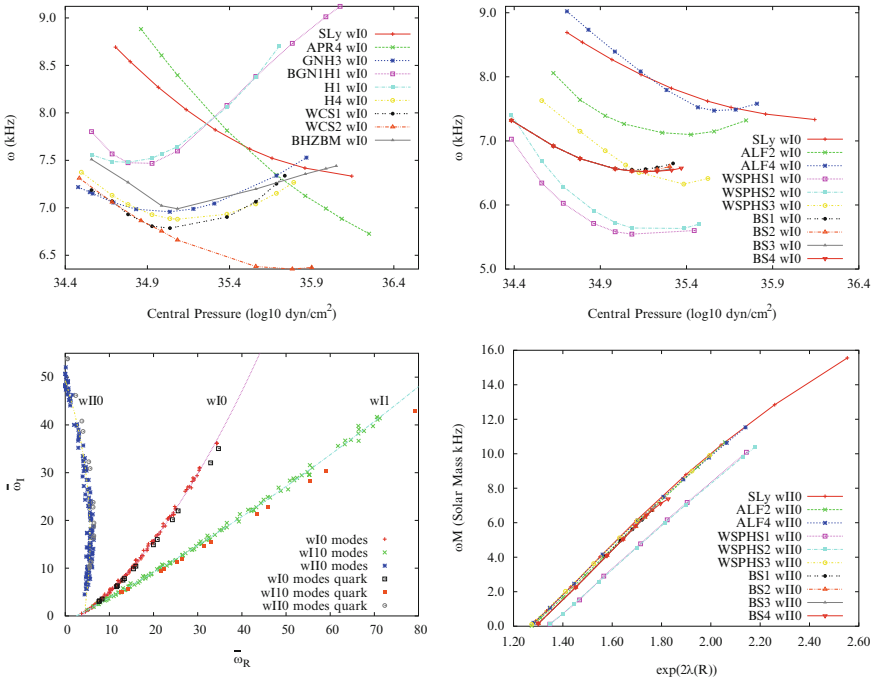


**Fig. 1** *Top*: scaled frequency of the fundamental wI mode vs M/R for stars with hyperon (*left*) and quark matter (*right*). *Bottom left*: all w-modes in units of the central pressure for all EOS and different central pressures. *Bottom right*: scaled frequency of the fundamental wII mode vs $e^{2\lambda(R)}$

the measured wI0 mode near the crossing point for the estimated central pressure. Hence, this method could be used to constrain the equation of state. Note that if mass and radius are already measured, we would have another filter to impose to the EOS.

Also, the precision of our algorithm allows us to construct explicitly the universal low compactness limiting configuration for fundamental wII modes (bottom right of Fig. 1) around $M/R = 0.106$ for which the fundamental wII mode vanishes [14].

We also study the impact of the core-*crust* transition pressure on the quasi-normal mode spectrum. We obtain that variations of the transition pressure from $10^{32} dyn/cm^2$ to $10^{33} dyn/cm^2$ affect the frequency and damping time order 0.1 %.

## References

1. K.D. Kokkotas, B. Schmidt, Living Reviews in Relativity **2**(2) (1999)
2. H.P. Nollert, Classical and Quantum Gravity **16**(12), R159 (1999)
3. F.J. Zerilli, Phys. Rev. Lett. **24**, 737 (1970)
4. U. Ascher, J. Christiansen, R.D. Russell, Mathematics of Computation **33**(146), pp. 659 (1979)

5. J.L. Blázquez-Salcedo, L.M. González-Romero, F. Navarro-Lérida, ArXiv:1207.4651 (2012)
6. J.S. Read, B.D. Lackey, B.J. Owen, J.L. Friedman, Phys. Rev. D **79**, 124032 (2009)
7. L. Samuelsson, N. Andersson, A. Maniopoulou, Classical and Quantum Gravity **24**(16), 4147 (2007)
8. P. Demorest, T. Pennucci, S. Ransom, M. Roberts, J. Hessels, Nature **467**, 1081 (2010)
9. S. Weissenborn, D. Chatterjee, J. Schaffner-Bielich, Phys. Rev. C **85**, 065802 (2012)
10. S. Weissenborn, et al., APJ Letters **740**(1), L14 (2011)
11. Bonanno, Luca, Sedrakian, Armen, A&A **539**, A16 (2012)
12. Bednarek, I., Haensel, P., Zdunik, J. L., Bejger, M., Ma´nka, R., A&A **543**, A157 (2012)
13. N. Andersson, K.D. Kokkotas, MNRAS **299**(4), 1059 (1998). DOI 10.1046/j.1365-8711.1998.01840.x
14. D.H. Wen, B.A. Li, P.G. Krastev, Phys.Rev. **C80**, 025801 (2009)

# The Quantum Scalar Field in Spherically Symmetric Loop Quantum Gravity

**Enrique F. Borja, Iñaki Garay, and Eckhard Strobel**

**Abstract** We consider the quantization of a spherically symmetric gravitational system coupled to a massless scalar field within the loop quantum gravity framework. Our results rely on the uniform discretizations method developed during the last years. We minimize the associated discrete "master constraint" using a trial state whose gravitational part is peaked around the classical Schwarzschild solution.

## 1 Introduction

Loop Quantum Gravity (LQG) presents a framework towards a canonical quantization of general relativity. It provides a rigorous, well defined and non-perturbative mathematical formulation of the kinematical sector of the theory, with a suitably

E.F. Borja
Laboratoire de Physique, ENS Lyon, CNRS-UMR 5672, 46 Allée d'Italie, Lyon 69007, France

Departamento de Física Teórica and IFIC, Centro Mixto Universidad de Valencia-CSIC. Facultad de Física, Universidad de Valencia, Burjassot-46100, Valencia, Spain
e-mail: enrique.fernandez@uv.es

I. Garay (✉)
Departamento de Física Teórica, Universidad del País Vasco, Apartado 644, 48080 Bilbao, Spain

Programa de Pós-Graduação em Física, Universidade Federal do Pará, 66075-110, Belém, PA, Brazil
e-mail: i.garay.elizondo@gmail.com

E. Strobel
ICRA, Piazzale della Repubblica 10, 65122 Pescara, Italy

Dipartimento di Fisica, Università di Roma "La Sapienza", Piazzale Aldo Moro 5, 00185 Rome, Italy

ICRANet, University of Nice-Sophia Antipolis, 28 Av. de Valrose, 06103 Nice Cedex 2, France
e-mail: Eckhard.Strobel@irap-phd.eu

A. García-Parrado et al. (eds.), *Progress in Mathematical Relativity, Gravitation and Cosmology*, Springer Proceedings in Mathematics & Statistics 60,
DOI 10.1007/978-3-642-40157-2_15, 

built Hilbert space and rigorous definitions for quantum operators with a clear geometrical meaning (areas and volumes) [1].

Although LQG showed remarkable results, especially concerning microscopic pictures of the early universe and black holes, the dynamics of the full theory still faces problems. The method of uniform discretizations is a promising approach to obtain a deeper understanding on the LQG dynamics [2]. Here, we consider a gravitational system with spherical symmetry coupled to a massless scalar field, and we proceed to minimize the expectation value of the "Master Constraint" (that plays the role of the Hamiltonian in the discrete theory) over a trial state built as a tensor product of a quantum state for the gravitational part that corresponds to a Gaussian peaked around the classical Schwarzschild metric, and the Fock vacuum of the matter sector of the theory [3–5].

## 2 Uniform Discretizations

The uniform discretizations method introduced in [2] is a method to quantize totally constrained systems. As the master constraint program [6], it is an approach to find an alternative for the Dirac quantization used in canonical LQG. In general, discretization of constraints and evolution equations does not preserve the original constraint algebra and the systems become second class constrained systems. The objective is to construct discretized theories with a well defined continuum limit.

We choose a discretization such that it satisfies the following time evolution for a discrete variable $A_n$

$$A_{n+1} = e^{\{\cdot,\mathbb{H}^\epsilon\}} A_n := A_n + \{A_n, \mathbb{H}^\epsilon\} + \frac{1}{2}\{\{A_n, \mathbb{H}^\epsilon\}, \mathbb{H}^\epsilon\} + \dots \tag{1}$$

where $\mathbb{H}^\epsilon$ is the discrete "master constraint", $\mathbb{H}^\epsilon = \frac{1}{2}\sum_j^M (\phi_j^\epsilon)^2$, given in terms of the discretized constraints $\phi_j^\epsilon$, with $\epsilon$ an abstract discretization parameter that will be, in our context, a spatial lattice separation. Notice that the master constraint generates no time flow (there is no evolution if the constraints are fulfilled exactly). As $\mathbb{H}^\epsilon$ is a constant of motion, we can fix its value to $\mathbb{H}^\epsilon =: \delta^2/2$, where $\delta$ can be interpreted as the size of the discrete time step of the evolution (1).

In the continuum limit we recover the constraint algebra of the continuum theory, the usual evolution equations for the constraints and, in our case, the Master constraint of LQG for our system.

## 3 Trial States and Expectation Value of the Master Constraint for Spherically Symmetric Systems

We use the invariant connection formulation developed in [7] in order to consider the constraints of a gravitational system with spherical symmetry coupled to a massless scalar field. We take into account the "energy of the vacuum", necessary to obtain

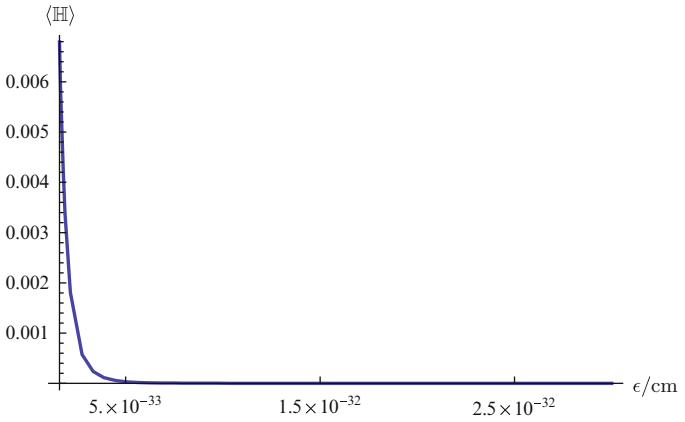


**Fig. 1** Expectation value of the integrand of the master constraint for $\sigma_0 = 10, n = 2$ and $\rho = 1$ as a function of the lattice spacing $\epsilon$ in the region near $\ell_p$ (because of the independence of $\sigma$ with respect to the position we set $\sigma = \sigma_0 \frac{\epsilon^n}{\ell_p^n}$ )

a zero value of the expectation value of the matter constraint in the semiclassical limit, by introducing an additional term in our Hamiltonian constraint [3, 4].

After gauge fixing, solving the diffeomorphism constraint $\mathscr{C}_r$ and applying the uniform discretization method to the Hamiltonian constraint $H(i)$; we construct the discrete master constraint $\mathbb{H}^\epsilon = \sum_i (H(i))^2$.

Now, in order to compute the expectation value of the master constraint, we construct a trial state. We consider a polymeric Hilbert space for the gravitational part (analogous to the one in Loop Quantum Cosmology [8]) and a Fock Hilbert space for the matter part. Then we write the trial state as

$$|\Psi_\sigma^{\text{trial}}\rangle = |\Psi_\sigma^{\text{grav}}\rangle \otimes |0\rangle;$$

where $|\Psi_\sigma^{grav}\rangle$ is a Gaussian with width $\sigma$ centered around the Schwarzschild metric, and $|0\rangle$ is the Fock vacuum state of the scalar field. Notice that this decomposition is only possible for the vacuum state; for higher excitation one would expect backreaction.

The Fock vacuum is constructed using the matter part of the Hamiltonian constraint $\hat{H}_{\text{matt}}(i)$. It contains operators acting both on the gravitational part and on the matter part, so we obtain the effective matter Hamiltonian as

$$\hat{H}^{\text{eff}}_{\text{matt}} = \langle \Psi_\sigma^{\text{grav}} | \hat{H}_{\text{matt}} | \Psi_\sigma^{\text{grav}} \rangle.$$

Going back to the continuum limit (it is easier to solve the differential equations of motion) and performing a Fourier-like transformation, we construct the creation and annihilation operators for the matter sector. Finally we define the Fock vacuum as usual (the state annihilated by the annihilation operator).

At this point, the expectation value of the Master constraint $\langle \Psi_\sigma^{trial} | \hat{\mathbb{H}} | \Psi_\sigma^{trial} \rangle$ can be computed. In the Fig. 1 we plot this expectation value. We observe that the master

constraint drops very fast for lattice spacings larger than the Planck scale. As in the Minkowski case [4], we expect the master constraint to increase again because of the break down of the approximation for $\epsilon > 10^{-23}$ cm. So we can conclude that there is a minimum around $\epsilon \approx 10^{-23}$ cm. Therefore, we can construct the vacuum state for our minimally coupled system also in the Schwarzschild case [3].

## 4 Conclusions

We explored an approximation for the vacuum state of a scalar field coupled to gravity with spherical symmetry within a Loop Quantum Gravity framework. We focused on the Schwarzschild spacetime for the gravitational sector and we employed the method presented in [4] for the Minkowski case. The fact that the techniques already used there are also valid for the Schwarzschild case, provides a consistency proof of the method.

The vacuum for the coupled system is constructed as the direct product of the Fock vacuum state for the scalar field and a Gaussian centered around the classical Schwarzschild solution for the gravitational sector. In order to deal with the dynamics, the uniform discretization technique is used. This setting allows us to develop a minimization of the expectation value of the (discrete) master constraint of the system, after the construction of the Fock vacuum of the matter sector.

There are several ways to extend the results presented here. For example, performing a polymeric quantization for the coupled system, or trying to work out this computation avoiding the gauge fixing of the diffeomorphism constraint. Although these options would clearly rise the technical complexity of the problem, a deeper understanding of this setting would provide us with a suitable vacuum state in this context, opening the possibility of performing a detailed study of the Hawking radiation within the LQG framework.

**Acknowledgements** This work was in part supported by the Spanish MICINN research grant FIS2009-11893. IG is supported by the CNPq-Brasil. ES is supported by the Erasmus Mundus Joint Doctorate Program by Grant Number 2012-1710 from the EACEA of the European Commission.

## References

1. T. Thiemann. *Modern Canonical Quantum General Relativity*. Cambridge University Press, 2007.
2. M. Campiglia, C. Di Bartolo, R. Gambini, and J. Pullin. *Phys. Rev.* D74, 124012 (2006).
3. E. F. Borja, I. Garay and E. Strobel. *Class. Quant. Grav.* 29, 145012 (2012).
4. R. Gambini, J. Pullin and S. Rastgoo. *Class. Quant. Grav.* 26, 215011 (2009).
5. M. Campiglia, R. Gambini, and J. Pullin. *Class. Quant. Grav.* 24, 3649 (2007).
6. T. Thiemann. *Class. Quant. Grav.* 23, 2211 (2006).
7. M. Bojowald and H. A. Kastrup. *Class. Quant. Grav.* 17, 3009 (2000).
8. M. Bojowald. Loop quantum cosmology. *Living Rev. Rel.*, 11 (2008).

# The Spectrum of Gravitational Waves in an $f(R)$ Model with a Bounce

**Mariam Bouhmadi-López, João Morais, and Alfredo B. Henriques**

**Abstract** We present an inflationary model preceded by a bounce in a metric $f(R)$ theory. In this model, modified gravity affects only the early stages of the universe. We analyse the predicted spectrum of the gravitational waves in this scenario using the method of the Bogoliubov coefficients. We show that there are distinctive (oscillatory) signals on the spectrum for very low frequencies; i.e., corresponding to modes that are currently entering the horizon.

## 1 Introduction

We propose a bouncing scenario [1] within the context of a metric $f(R)$ theory [2]:

$$S = \frac{1}{2\kappa^2}\int d^4x\sqrt{-g}\,f(R) + S^{(m)}. \tag{1}$$

The bounce we will consider in our model is followed by an inflationary era which is asymptotically de Sitter where, in addition, the gravitational action approaches the Hilbert–Einstein action on that regime, such that the modification to Einstein's General Relativity (GR) affects exclusively the very early universe, around the bounce and a few e-folds after that. We will constrain the model obtaining the spectrum of the stochastic gravitational fossil as would be measured today.

M. Bouhmadi-López (✉)
Instituto de Estructura de la Materia, IEM-CSIC, Serrano 121, 28006 Madrid, Spain
e-mail: mariam.bouhmadi@iem.cfmac.csic.es

J. Morais · A.B. Henriques
CENTRA, Dept. de Física, Instituto Superior Técnico, Av. Rovisco Pais 1, 1049 Lisboa, Portugal
e-mail: joao.morais@ist.utl.pt; alfredo.henriques@fisica.ist.utl.pt

A. García-Parrado et al. (eds.), *Progress in Mathematical Relativity, Gravitation and Cosmology*, Springer Proceedings in Mathematics & Statistics 60,
DOI 10.1007/978-3-642-40157-2_16, 

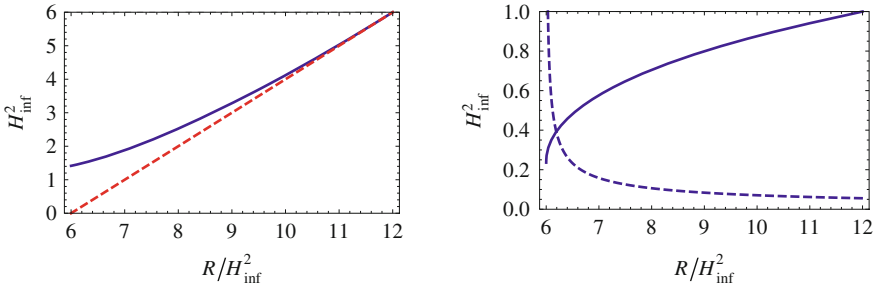


**Fig. 1** These plots show: (*left*) the behaviour of $f(R)$ as a function of $R/H^2_{\rm inf}$ (see the *blue curve*) and linear approximation $R-6H^2_{\rm inf}$, well during inflation (see the *red curve*); (*right*) the behaviour of $f_R$ (see the *continuous curve*) and $f_{RR}$ (see the *dashed curve*) as functions of $R/H^2_{\rm inf}$

## 2 Model for the Early Universe

Inspired on the de Sitter solution for a closed space-time, we define the scale factor around the bounce as:

$$a(t) = a_b \cosh\left(H_{\rm inf} t\right), \tag{2}$$

where $a(t)$ is the scale factor, $a_b$ is a constant quantifying the size of the universe at the bounce. The parameter $H_{\rm inf}$ is related to the energy scale of inflation just after the bounce.

In a Friedmann–Lemaître–Robertson–Walker (FLRW) universe with a spatially flat metric and the scale factor defined as in (2), the minimization of the $f(R)$ action (1) leads to a second order differential equation for the function $f$. Solving this equation in conjunction with appropriate physical constraints gives [3]:

$$f(r) = 2H^2_{\rm inf}\sqrt{r-3}\cos\left[\frac{\sqrt{3}}{2}\left(\pi - \arccos\frac{9-r}{3}\right) - \arccos\sqrt{\frac{3}{2}\frac{r-6}{r-3}}\right]. \tag{3}$$

In the above equation $r \equiv R/H^2_{\rm inf}$.

## 3 Energy Spectrum of the Gravitational Waves

The spectrum of the gravitational waves is determined using the method of the continuous Bogoliubov coefficients $\alpha$ and $\beta$, as in [4]. The graviton density of the universe is given by $|\beta|^2$, while the dimensionless logarithmic energy spectrum of the gravitational waves (GW) of angular frequency $\omega$ is defined at the present time $\eta_0$ as [5]:

$$\Omega_{GW}(\omega, \eta_0) = \frac{\hbar\kappa^2}{3\pi^2 c^5 H^2(\eta_0)}\omega^4 |\beta(\eta_0)|^2 \tag{4}$$

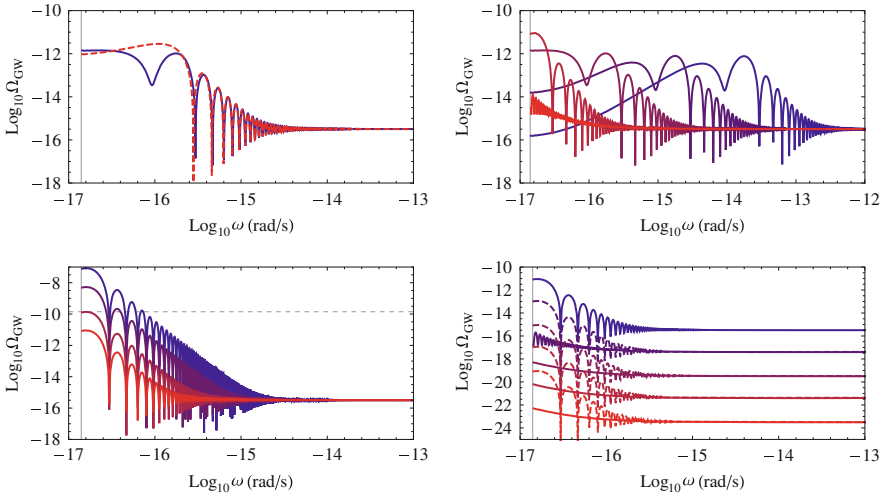


**Fig. 2** These plots show the spectra of the energy density of GW at present time: (*top left*) obtained with an $f(R)$ treatment for the perturbations (*blue continuous curve*) and a GR treatment for the perturbations (*red dashed curve*). $E_{\rm inf} = 1.5\times10^{16}$ GeV. $t_{\rm ini} = -\text{arccosh}(10)H_{\rm inf}^{-1}$. $a_b = 2\times10^3$. (*Top right*) obtained in an $f(R)$ treatment for different values of $a_b$. The value of $a_b$ increases from the *red curve* to the *blue curve* as: $a_b = 2\times10^2$; $a_b = 2\times10^3$; $a_b = 2\times10^4$; $a_b = 10\times10^5$. $a_b = 10\times10^6$. $E_{\rm inf} = 1.5\times10^{16}$ GeV. $t_{\rm ini} = -\text{arccosh}(10)H_{\rm inf}^{-1}$. (*Bottom left*) obtained in an $f(R)$ treatment for different values of $t_{\rm ini}$. The value of $t_{\rm ini}$ increases in absolute value from the *red curve* to the *blue curve* as: $t_{\rm ini} = -\text{arccosh}(10)H_{\rm inf}^{-1}$; $t_{\rm ini} = -\text{arccosh}(20)H_{\rm inf}^{-1}$; $t_{\rm ini} = -\text{arccosh}(50)H_{\rm inf}^{-1}$; $t_{\rm ini} = -\text{arccosh}(100)H_{\rm inf}^{-1}$. $E_{\rm inf} = 1.5\times10^{16}$ GeV. $a_b = 2\times10^3$. (*Bottom right*) obtained in an $f(R)$ treatment for different values of $E_{\rm inf}$. A comparison is made between the results obtained with a fixed value of $a_b$ (*continuous curves*) and a fixed value of $a_b H_{\rm ini}$ (*discontinuous curves*). The value of $E_{\rm inf}$ increases from the *red curve* to the *blue curve*: $E_{\rm inf} = 1.5\times10^{14}$ GeV; $E_{\rm inf} = 0.5\times10^{15}$ GeV; $E_{\rm inf} = 1.5\times10^{15}$ GeV; $E_{\rm inf} = 0.5\times10^{16}$ GeV; $E_{\rm inf} = 1.5\times10^{16}$ GeV. ($a_{\rm ini} = 10a_b$. $a_b = 2\times10^3$)

To calculate the evolution of the gravitational waves, we express the continuous Bogoliubov coefficients in terms of the variables $X$ and $Y$, see [6, 7], which obey the set of differential equations:

$$X'' = \left(k^2 - \frac{z''}{z}\right)X, \qquad \text{and} \qquad X' = -ikX. \tag{5}$$

Here, $k$ is the wave-number, a prime indicates a derivative with respect to the conformal time $\eta$ ($a = dt/d\eta$) and $z \equiv a\sqrt{f_R}$. The differential equations (5) are integrated from an initial time $t_{\rm ini}$, set before the bounce, until the present time. We describe the late time evolution of the universe in a GR setup, using the $\Lambda$CDM model [8] complemented with a radiation phase and making the connection between the $f(R)$ driven early inflation and the radiation phase with a model of a modified Generalized Chaplygin Gas suitable for the early universe [7]. The results obtained for the GW spectra are shown in Fig. 2.

## 4 Conclusions

The existence of the bounce in the early universe affects the spectrum of GWs only in the low frequency range, $\lesssim 10^{-12}$ Hz, where various peaks appear whose position and intensity depend on the parameters of the mode. The fact that the oscillatory structure appears in the spectra of (a) the GR treatment and (b) the $f(R)$ treatment suggests it is not a consequence of the effects of $f(R)$-gravity. Similar oscillations have been obtained in works of loop quantum cosmology first pointed out by Afonso et al. [9]. Due to the low energy density of the cosmological GW's, the results obtained in this work are hard to be detected in the near future (see Fig. 2 of [10] and Fig. 6 of [11]). The detection of the B-mode polarization of the CMB radiation seems to be the best candidate to obtain information about the cosmological GW's [12].

**Acknowledgements** M.B.L. is supported by the Spanish Agency "Consejo Superior de Investigaciones Científicas" through JAEDOC064. This work was supported by the Portuguese Agency "Fundção para a Ciência e Tecnologia" through PTDC/FIS/111032/2009.

## References

1. M. Novello and S. E. P. Bergliaffa, Phys. Rept. **463**, 127 (2008) arXiv:0802.1634v1 [astro-ph]; S. Carloni, P. K. S. Dunsby and D. M. Solomons, Class. Quant. Grav. **23**, 1913 (2006) arXiv:gr-qc/0510130v1; C. Barragan, G. J. Olmo and H. Sanchis-Alepuz, Phys. Rev. D **80**, 024016 (2009) arXiv:0907.0318v2 [gr-qc].
2. S. Capozziello and M. De Laurentis, Phys. Rept. **509**, 167 (2011) arXiv:1108.6266 [gr-qc]; T. P. Sotiriou and V. Faraoni, Rev. Mod. Phys. **82**, 451 (2010) arXiv:0805.1726v4 [gr-qc].
3. M. Bouhmadi-Lopez, J. Morais and A. B. Henriques, arXiv:1210.1761 [astro-ph.CO].
4. L. Parker, Phys. Rev. 183, 1057 (1969).
5. B. Allen, Phys. Rev. D **37**, 2078 (1988).
6. P. M. Sá and A. B. Henriques, Phys. Rev. D **77**, 064002 (2008) arXiv:0712.2697 [astro-ph]; P. M. Sá and A. B. Henriques, Gen. Rel. Grav. **41**, 2345 (2009) arXiv:0804.3278v2 [astro-ph].
7. M. Bouhmadi-López, P. Frazão and A. B. Henriques, Phys. Rev. D **81**, 063504 (2010) arXiv:0910.5134v2 [astro-ph.CO].
8. E. Komatsu *et al.* [WMAP Collaboration], Astrophys. J. Suppl. **192**, 18 (2011) arXiv:1001.4538v3 [astro-ph.CO].
9. C. M. Afonso, A. B. Henriques and P. V. Moniz, arXiv:1005.3666v1 [gr-qc]; P. M. Sá and A. B. Henriques, Phys. Rev. D **85**, 024034 (2012) arXiv:1108.0079v1 [gr-qc].
10. T. L. Smith, M. Kamionkowski and A. Cooray, Phys. Rev. D **73**, 023504 (2006) arXiv:astro-ph/0506422v2.
11. M. Kawasaki, K. 'i. Saikawa and N. Takeda, arXiv:1208.4160 [astro-ph.CO].
12. H. Bourhrous, A. de la Cruz-Dombriz and P. Dunsby, AIP Conf. Proc. **1458**, 343 (2011) arXiv:1202.3862 [gr-qc]; G. Efstathiou and S. Gratton, JCAP **0906**, 011 (2009); A. Bonaldi and S. Ricciardi, arXiv:1101.4876 [astro-ph.CO].

# On the Isotropization of a 3-Brane in an Extra-Dimensional Tolman–Bondi Universe

**Philippe Brax, José Pedro Mimoso, and Nelson Nunes**

**Abstract** We report here on the results of Brax et al. (Phys. Rev. D 85:123516, 2012) where we consider the dynamics of a 3-brane embedded in an extra-dimensional Tolman–Bondi Universe where the origin of space plays a special role. We study the mirage cosmology on the probe brane, resulting in an inhomogeneous and anisotropic four dimensional cosmology where the origin of space is also special. We show that the induced geometry, which is initially inhomogeneous and anisotropic, converges to an isotropic and homogeneous Friedmann–Lemaitre 4d space-time around the origin of the spatial geometry. For example, when a 3-brane is embedded in a 5d matter dominated model, the 4d dynamics around the origin converge to a Friedmann–Lemaitre Universe in a radiation dominated epoch. We analyse this isotropisation process and show that it is a late time attractor.

## 1 Introduction

In the last 15 years and in particular after the discovery of fundamental branes and the building of phenomenological brane-world models [1] such as the one constructed by Randall and Sundrum [2, 3], the emerging possibility of extra

P. Brax
Institut de Physique Theorique, CEA, IPhT, CNRS, URA 2306, F-91191Gif/Yvette Cedex, France
e-mail: philippe.brax@cea.fr

J.P. Mimoso (✉)
Departamento de Física and Centro de Astronomia e Astrofísica da Universidade de Lisboa, Faculdade de Ciências, Ed. C8, Campo Grande, 1769-016 Lisboa, Portugal
e-mail: jpmimoso@fc.ul.pt

N. Nunes
Centro de Astronomia e Astrofísica da Universidade de Lisboa, Faculdade de Ciências, Ed. C8, Campo Grande, 1769-016 Lisboa, Portugal
e-mail: njnunes@fc.ul.pt

A. García-Parrado et al. (eds.), *Progress in Mathematical Relativity, Gravitation and Cosmology*, Springer Proceedings in Mathematics & Statistics 60,
DOI 10.1007/978-3-642-40157-2_17, 

dimensional cosmology has been considered thoroughly. Recently, the discovery of the acceleration of the Universe [4] has led to a reappraisal of the underlying assumptions of cosmology. In particular, the cosmological principle, which states that the Universe is homogeneous and isotropic on large scales, has been under scrutiny [5]. As a result, Tolman–Bondi models of the Universe where the earth would lie close to the centre of an inhomogeneous Universe have been considered [6–8]. Along these lines, it seems to be timely to question the usual hypothesis that extra dimensions should be a symmetric space.

Here we report on the results of [9] where we consider that the Universe is a 3-brane embedded in an extra dimensional space with no homogeneity at all. We study the dynamics of the brane as it responds to the extra-dimensional cosmology. We assume that the brane is a probe and as a result we only investigate the mirage cosmology on the brane.

We envisage a $(d+4)$-dimensional TB universe with a pressureless fluid and metric

$$ds^2 = -dt^2 + e^{\lambda(r,t)}dr^2 + R^2(r,t)d\Omega_{d+2}^2 \,. \tag{1}$$

where $d\Omega_{d+2}^2 = (\mathrm{d}\theta^1)^2 + \Pi_{i=1}^{d+1} \sin^2\theta^i \, (\mathrm{d}\theta^{i+1})^2$ is the metric on the $(d+2)$-sphere.

Our choice of embedding corresponds to a two dimensional cross-section of the $(d+2)$-sphere. Our 3-brane consists of the cone defined by the angles $\theta^3, \ldots, \theta^n =$ constant and the free angles $\theta^1$ and $\theta^2$. We consider a single uncharged 3-brane described by its world-volume action

$$S_b = -T_3 \int d^4x \sqrt{-\tilde{g}}, \tag{2}$$

where $T_3$ is the brane tension and $\tilde{g}_{\mu\nu}$ is the induced metric on the brane related to the extra dimensional metric $G_{AB}$ by $\tilde{g}_{\mu\nu} = G_{AB}\frac{\partial X^A}{\partial x^\mu}\frac{\partial X^B}{\partial x^\nu}$ where $x^\mu$ are the brane coordinates and $X^A(x^\mu)$ the brane embedding.

The Lagrangian is $\mathscr{L} = -T_3\left[-(\tilde{g}_{tt}\tilde{g}_{rr} - \tilde{g}_{tr}^2)(\tilde{g}_{\phi\phi}\tilde{g}_{\chi\chi} - \tilde{g}_{\phi\chi}^2)\right]^{1/2}$. We expand this Lagrangian to second order in the time and radial derivatives as we are interested in low energy modes

$$\begin{aligned}\mathscr{L} = -T_3 R^2 e^{\lambda/2} |\sin\theta^1| \Bigg(&\frac{\partial\theta^1}{\partial\phi}\frac{\partial\theta^2}{\partial\chi} - \frac{\partial\theta^1}{\partial\chi}\frac{\partial\theta^2}{\partial\phi}\Bigg) \\ &\Bigg\{1 + \frac{1}{2}R^2 e^{-\lambda}\left[\left(\frac{\partial\theta^1}{\partial r}\right)^2 + \sin^2\theta^1\left(\frac{\partial\theta^2}{\partial r}\right)^2\right] \\ &-\frac{1}{2}R^2\left[\left(\frac{\partial\theta^1}{\partial t}\right)^2 - \sin^2\theta^1\left(\frac{\partial\theta^2}{\partial t}\right)^2\right]\Bigg\}\end{aligned} \tag{3}$$

We concentrate on the case of a 3-brane embedding in a TB Universe where the curvature effects measured by $f(r)$ can be neglected in the neighbourhood of the origin. In this case, the extra-dimensional dynamics in a local patch becomes:

$$R(t,r) = r\left(\frac{t}{t_0}\right)^{2/(n+1)}, \qquad e^{\lambda} = \left(\frac{t}{t_0}\right)^{4/(n+1)}, \tag{4}$$

and we focus on the induced metric on the brane, noticing that $\theta^2$ is cyclic, so that $\partial_\mu A^\mu = 0$, where $A^\mu = \frac{\partial \mathscr{L}}{\partial(\partial_\mu \theta^2)}$, and adopting the simplifying assumptions: $A^r = A^\chi = 0$ implying that $\theta^2_{,r} = \theta^1_{,\phi} = 0$, $e^{-\lambda/2}\theta^1_{,r}\ell^2\dot{\theta^1}$, and $A^t$ constant in time. Then the induced metric takes the form

$$\tilde{g}_{tt} = -1 + R^2(\dot{\theta}^1)^2 + R^2\sin^2\theta^1(\dot{\theta}^2)^2\ ,\ \tilde{g}_{rr} = e^{\lambda}\ ,\ \tilde{g}_{\phi\phi} = R^2\sin^2\theta^1(\theta^2_{,\phi})^2\ , \tag{5}$$

$$\tilde{g}_{\chi\chi} = R^2(\theta^1_{,\chi})^2 + R^2\sin^2\theta^1(\theta^2_{,\chi})^2\ , \qquad \tilde{g}_{\phi\chi} = R^2\sin^2\theta^1\theta^2_{,\chi}\theta^2_{,\phi}. \tag{6}$$

and we must solve

$$\ddot{\theta}^1 - \left(4\frac{\dot{R}}{R} + \frac{1}{2}\dot{\lambda} + 2\frac{\dot{A}^\phi}{A^\phi}\right)\dot{\theta}^1 - 5\frac{\cos\theta^1}{\sin\theta^1}(\dot{\theta}^1)^2 = \sin^2\theta^1\,\frac{\dot{\theta}^2\,\dot{\theta}^2_{,\chi}}{\theta^1_{,\chi}}. \tag{7}$$

We look for a solution for $\theta^1$ locally such that $\theta^1 \approx \theta_0$ and we write

$$\theta^1 = \theta_0 - \frac{(A^t)^2}{2T_3 s\sin^3\theta_0 M_0^6 c_0^2 r^4 g e^{\lambda/2} R^4}\int \frac{1}{f}\,d\chi + \alpha(t), \tag{8}$$

where $\theta_0$ is a fixed angle arising as an integrating constant, $\alpha(t)$ an unknown function yet to be determined and we have introduced $A^\phi(r,t,\chi) = M_0^6 r^4 f(\chi)g(t)$, in order to separate the time and $\chi$-dependent contributions that make up $A^\phi$. Here, $M_0$ is an unspecified energy scale. Notice that the $r$-dependence cancels if and only if $A^t$ varies in $r^4$ as required by $\theta^2_{,r} = 0$. This leads to identify the constant of motion $A^t$ as $(A^t)^2 = 2T_3 M_0^6 c_0^2 s\sin^3\theta_0 r^8 g_0$, and write the solution for $\theta^1$ as

$$\theta^1 = \theta_0 - \frac{g_0}{g}e^{-\lambda/2}\left(\frac{r}{R}\right)^4\chi + \alpha(t), \tag{9}$$

which is $r$-independent, hence satisfying our assumption on the small $r$ variations of $\theta^1$. At $t = t_0$ we have that $\theta^1 = \theta_0 - \chi$, and $\theta^2 = c_0\phi$ . Separating the terms in $\chi$ from the ones of order zero in $\chi$, we obtain two second order differential equations for $\alpha$ and $g$

$$\ddot{\alpha} - \left(4\frac{\dot{R}}{R} + \frac{1}{2}\dot{\lambda} + 2\frac{\dot{g}}{g}\right)\dot{\alpha} = I_\alpha, \tag{10}$$

where $I_\alpha = -(2f_1 g_0 M_0^6/T_3)e^{\lambda/2}(g/g_0)^3(R/r)^4$, and

$$\frac{\ddot{g}}{g} - \left(\frac{\dot{g}}{g}\right)^2 + 4\frac{\ddot{R}}{R} - 4\left(\frac{\dot{R}}{R}\right)^2 + \frac{1}{2}\ddot{\lambda} - \left(\frac{\dot{g}}{g} + 4\frac{\dot{R}}{R} + \frac{1}{2}\dot{\lambda}\right)^2 - \left(2\frac{\dot{g}}{g} + 4\frac{\dot{R}}{R} + \frac{1}{2}\dot{\lambda}\right)\left(\frac{\dot{g}}{g} + 4\frac{\dot{R}}{R} + \frac{1}{2}\dot{\lambda}\right) = I_g, \tag{11}$$

where $I_g = -(4f_1^2 g_0 M_0^6/T_3)e^{\lambda}(g/g_0)^4(R/r)^8$

We find that the solution of the homogeneous $g$-equation is

$$g = g_0\left(\frac{t_0}{t}\right)^{10/(n+1)}\left|1 + c_3\left[\left(\frac{t_0}{t}\right)^{(9-n)/(n+1)} - 1\right]\right|^{-1/3}, \tag{12}$$

where $c_3$ is a constant. As long as the term within the power $-1/3$ does not vanish (which only depends on the initial conditions), the asymptotic behaviour of the homogeneous solution is

$$g \approx \gamma_g t^{-10/(n+1)}, \tag{13}$$

where $\gamma_g$ is a constant. Using this result one finds that the asymptotic behaviour of $\alpha$ is

$$\alpha \approx \gamma_\alpha t^{(n-9)/(n+1)} + \alpha_\infty, \tag{14}$$

where $\gamma_\alpha$ and $\alpha_\infty$ are constants, i.e., for $n < 9$, $\alpha$ converges to a constant at infinity. Hence we find that the asymptotic metric is isotropic.

In [9] it is shown that this solution is also a global attractor. The global solution is valid at infinity and around each $\theta_0$ it is identical to the one obtained from (12) with $c_3 = 0$. (For more details the reader is kindly referred to [9]).

Summing up our results, the mirage cosmology on the brane reveals that the late time behaviour metric on the brane becomes isotropic and homogeneous in the vicinity of the origin, where the effects of curvature in the bulk can be neglected, even though the initial condition were not so. In this work we have only analysed the mirage case where matter on the brane is subdominant and the dynamics are governed by the embedding of the brane in the time-dependent extra dimensional background. The coupling between matter on the brane and outside the brane in an inhomogeneous context is left for future work.

**Acknowledgements** This work was carried out in the context of the Portugal-France Programa Pessoa bilateral agreement. The work of NJN is supported by a Ciência 2008 research contract funded by FCT. JPM and NJN also acknowledge the support from FCT through the projects PEst-OE/FIS/UI2751/2011, CERN/FP/123618/2011 and CERN/FP/123615/2011.

## References

1. P. Brax and C. van de Bruck, Class. Quant. Grav. **20**, R201 (2003) [hep-th/0303095].
2. L. Randall and R. Sundrum, Phys. Rev. Lett. **83**, 3370 (1999) [hep-ph/9905221].
3. L. Randall and R. Sundrum, Phys. Rev. Lett. **83**, 4690 (1999) [hep-th/9906064].
4. S. Perlmutter *et al.* [Supernova Cosmology Project Collaboration], Astrophys. J. **517**, 565 (1999) [astro-ph/9812133].
5. For a short discussion see P. Brax and references therein, arXiv:0912.3610 [astro-ph.CO].
6. I. Zehavi, A. G. Riess, R. P. Kirshner and A. Dekel, Astrophys. J. **503**, 483 (1998) [astro-ph/9802252].
7. K. Tomita, Mon. Not. Roy. Astron. Soc. **326**, 287 (2001)[astro-ph/0011484].
8. R. R. Caldwell and A. Stebbins, Phys. Rev. Lett. **100**, 191302 (2008) [arXiv:0711.3459 [astro-ph]].
9. P. Brax, J. P. Mimoso and N. J. Nunes, Phys. Rev. D **85**, 123516 (2012) [arXiv:1203.5687 [hep-th]].

# Phase Transitions in General Gravity Theories

**Xián O. Camanho**

**Abstract** Phase transitions between two competing vacua of a given theory are quite common in physics. We discuss how to construct the space-time solutions that allow the description of phase transitions between different branches (or asymptotics) of a given higher curvature gravity theory at finite temperature.

## 1 Introduction

Higher-curvature corrections to the Einstein–Hilbert (EH) action appear in any sensible theory of quantum gravity as next-to-leading orders in the low energy effective action and some, e.g. the Lanczos–Gauss–Bonnet (LGB) action [1], also appear in realizations of string theory [2]. This particular quadratic combination is specially important as any quadratic term can be brought to the LGB form, $\mathscr{R}^2 = R_{\mu\nu\alpha\beta}R^{\mu\nu\alpha\beta} - R_{\mu\nu}R^{\mu\nu} + R^2$, via field redefinitions.

Non-perturbatively in the couplings and due to the non-linearity of the equations of motion, these theories generally admit more than one maximally symmetric solution, $R_{\mu\nu\alpha\beta} = \Lambda_i (g_{\mu\alpha}g_{\nu\beta} - g_{\mu\beta}g_{\nu\alpha})$; (A)dS vacua with effective cosmological constants $\Lambda_i$, whose values are determined by a polynomial equation [3],

$$\Upsilon[\Lambda] \equiv \sum_{k=0}^{K} c_k \, \Lambda^k = c_K \prod_{i=1}^{K} (\Lambda - \Lambda_i) = 0. \tag{1}$$

X.O. Camanho (✉)
Department of Particle Physics and IGFAE, University of Santiago de Compostela, E-15782 Santiago de Compostela, Spain
e-mail: xian.otero@usc.es

A. García-Parrado et al. (eds.), *Progress in Mathematical Relativity, Gravitation and Cosmology*, Springer Proceedings in Mathematics & Statistics 60,
DOI 10.1007/978-3-642-40157-2_18, 

$K$ being the highest power of curvature (without derivatives) in the field equations. $c_0 = 1/L^2$ and $c_1 = 1$ give canonically normalized cosmological and EH terms, $c_{k\geq 2}$ are the LGB and higher order couplings (see [4] for details).

Any vacua is a priori suitable in order to define boundary conditions for the gravity theory we are interested in; i.e. we can define sectors of the theory as classes of solutions that asymptote to a given vacuum [5]. In that way, each branch has associated static solutions, representing either black holes or naked singularities,

$$ds^2 = -f(r)\,dt^2 + \frac{dr^2}{g(r)} + r^2\,d\Omega_{d-2}^2, \qquad f, g \xrightarrow{r\to\infty} -\Lambda_i r^2, \tag{2}$$

and other metrics with the same asymptotics. The main aim of the present work is that of studying transitions between the different branches. This is important to determine whether a new non-perturbative instability occurs in the theory, some branches *decaying* by bubble nucleation. This new kind of phase transitions have been recently investigated in the context of LGB [6] and Lovelock gravities [7].

## 2 Higher Order Free Particle

The existence of branch transitions in higher curvature gravity theories is a concrete expression of the multivaluedness problem of these theories. In general the canonical momenta, $\pi_{ij}$, are not invertible functions of the velocities, $\dot{g}^{ij}$ [8]. An analogous situation may be illustrated by means of a simple one-dimensional example [9]. Consider a free particle lagrangian containing higher powers of velocities,

$$L(\dot{x}) = \frac{1}{2}\dot{x}^2 - \frac{1}{3}\dot{x}^3 + \frac{1}{17}\dot{x}^4 \tag{3}$$

In the hamiltonian formulation the equation of motion just implies the constancy of the conjugate momentum, $\frac{d}{dt}p = 0$. However, being this multivalued (also the hamiltonian), the solution is not unique. Fixing boundary conditions $x(t_{1,2}) = x_{1,2}$, an obvious solution would be constant speed $\dot{x} = (x_2 - x_1)/(t_2 - t_1) \equiv v$ but we may also have jumping solutions with constant momentum and the same mean velocity.

In our example, for mean velocities corresponding to multivalued momentum (see Fig. 1) solutions are infinitely degenerate as the jumps may occur at any time and unboundedly in number as long as the mean velocity is the same. Nevertheless, this degeneracy is lifted once the value of the action is taken into account. The minimal action path is the naive one for mean velocities outside the range covered by the dashed line whereas in that interval it corresponds to arbitrary jumps between the velocities of the two extrema. The *effective* Lagrangian (dashed line) is a convex function of the velocities and the effective momentum dependence corresponds to the analogous of the Maxwell construction from thermodynamics (see [7] for a detailed explanation of this one-dimensional example).

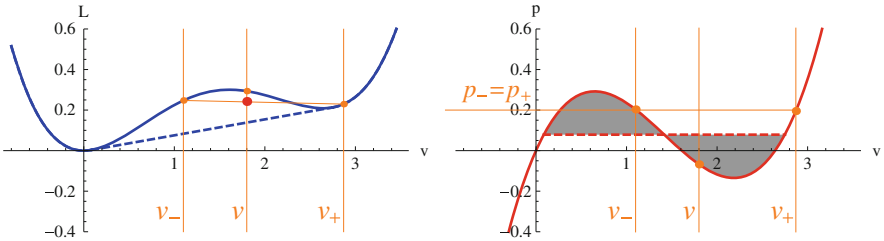


**Fig. 1** Lagrangian and momentum for the action (3). For the same mean velocity $v$, the action is lower for jumps between $v_\pm$ (*big dot*) than for constant speed, the minimum action corresponding to the value on the *dashed line* (*effective* Lagrangian)

## 3 Generalized Hawking–Page Transitions

In the context of General Relativity in asymptotically AdS spacetimes, the Hawking–Page phase transition [10] is the realization that above certain temperature the dominant saddle in the gravitational partition function comes from a black hole, whereas for lower temperatures it corresponds to the thermal vacuum. The *classical* solution is the one with least Euclidean action among those with a smooth Euclidean section.

When one deals with higher curvature gravity there is a crucial difference that has been overlooked in the literature. In addition to the usual continuous and differentiable metrics (2), one may construct distributional metrics by gluing two solutions corresponding to different branches across a spherical shell or *bubble* [11,12]. The resulting solution will be continuous at the bubble—with discontinuous derivatives, even in absence of matter. The higher curvature terms can be thought of as a sort of matter source for the Einstein tensor. The existence of such *jump* metrics, as for the one-dimensional example, is due to the multivaluedness of momenta in the theory.

In the gravitational context, continuity of momenta is equivalent to the junction conditions that need to be imposed on the bubble. In the EH case, Israel junction conditions [13], being linear in velocities, also imply the continuity of derivatives of the metric. The generalization of these conditions for higher curvature gravity contain higher powers of velocities, thus allowing for more general situations.

Static bubble configurations, when they exist, have a smooth Euclidean continuation. It is then possible to calculate the value of the action and compare it to all other solutions with the same asymptotics and temperature. This analysis has been performed for the LGB action [6] for unstable boundary conditions [3]. The result suggests a possible resolution of the instability through bubble nucleation.

In the case of LGB gravity there are just two possible static spacetimes to be considered in the analysis for the chosen boundary conditions; the thermal vacuum and the static bubble metric, the usual spherically symmetric solution (2) displaying a naked singularity. For low temperatures the thermal vacuum is the preferred

solution whereas at high temperatures the bubble will form, as indicated by the change of sign on the relative free energy. The bubble pops out in an unstable position and may expand reaching the boundary in a finite time thus changing the asymptotics and charges of the solution, from the initial to the inner ones.

Still, if the free energy is positive the system is metastable. It decays by nucleating bubbles with a probability given, in the semiclassical approximation, by $e^{-F/T}$. Therefore, after enough time, the system will always end up in the stable horizonful branch of solutions, the only one usually considered as relevant. This is then a natural mechanism that selects the general relativistic vacuum among all the possible ones, the stable branch being the endpoint of the initial instability.

## 4 Discussion

The phenomenon described here is quite general. It occurs also for general Lovelock gravities [7] and presumably for more general classes of theories. In the generic case, however, the possible situations one may encounter are much more diverse. We may have for instance stable bubble configurations as opposed to the unstable ones discussed above or even bubbles that being unstable cannot reach the boundary of the spacetime. Other generalizations may include transitions between positive and negative values of $\Lambda_i$ and even non-static bubble configurations.

Another situation one may think of is that of having different gravity theories on different sides of the bubble. This has a straightforward physical interpretation if we consider the higher order terms as sourced by other fields that vary across the bubble. For masses above $m^2 > \|\Lambda_\pm\|$ a bubble made of these fields will be well approximated by a thin wall and we may integrate out the fields for the purpose of discussing the thermodynamics. If those fields have several possible vacuum expectation values leading to different theories we may construct interpolating solutions in essentially the same way discussed above. In this case the energy carried by the bubble can be interpreted as the energy of the fields we have integrated out.

**Acknowledgements** The author thanks A. Gomberoff for most interesting discussions, and the Front of pro-Galician Scientists for encouragement. He is supported by a spanish FPU fellowship. This work is supported in part by MICINN and FEDER (grant FPA2011-22594), by Xunta de Galicia (Consellería de Educación and grant PGIDIT10PXIB206075PR), and by the Spanish Consolider-Ingenio 2010 Programme CPAN (CSD2007-00042).

## References

1. C. Lanczos, Annals Math. **39**, 842 (1938).
2. B. Zwiebach, Phys. Lett. B **156**, 315 (1985).
3. D. Boulware and S. Deser, Phys. Rev. Lett. **55**, 2656 (1985).
4. J. D. Edelstein, these proceedings (and references therein), arXiv:1303.6213 [hep-th]

5. X. O. Camanho and J. D. Edelstein, Class. Quantum Grav. **30**, 035009 (2013).
6. X. O. Camanho, J. D. Edelstein, G. Giribet, A. Gomberoff, Phys. Rev. D **86**, 124048 (2012)
7. X. O. Camanho *et al*., to appear.
8. C. Teitelboim and J. Zanelli, Class. Quantum Grav., **4**, 125 (1987).
9. M. Henneaux, C. Teitelboim, and J. Zanelli, Phys. Rev. A, **36**, 4417 (1987).
10. S. W. Hawking and D. N. Page, Commun. Math. Phys. **87**, 577 (1983).
11. E. Gravanis and S. Willison, Phys. Rev. D **75**, 084025 (2007).
12. C. Garraffo, G. Giribet, E. Gravanis and S. Willison, J. Math. Phys. **49**, 042502 (2008).
13. W. Israel, Nuovo Cimento B **48**, 463 (1967).

# Concordance Cosmology with Particle Creation

**Saulo Carneiro**

**Abstract** A constant-rate creation of dark particles in the late-time FLRW spacetime provides a cosmological model in accordance with precise observational tests. The matter creation backreaction implies in this context a vacuum energy density scaling linearly with the Hubble parameter, which is consistent with the vacuum expectation value of the QCD condensate in a low-energy expanding spacetime. Both the cosmological constant and coincidence problems are alleviated in this scenario. We discuss the cosmological model that arises in this context and present a joint analysis of observations of the first acoustic peak in the cosmic microwave background (CMB) anisotropy spectrum, the Hubble diagram for supernovas of type Ia (SNIa), the distance scale of baryonic acoustic oscillations (BAO) and the distribution of large scale structures (LSS). We show that a good concordance is obtained, albeit with a higher value of the present matter abundance than in the standard model.

The gravitation of vacuum fluctuations is in general a difficult problem, since their energy density usually depends on the renormalization procedure and on an adequate definition of the vacuum state in the curved background. In the case of conformal fields in de Sitter spacetime, the renormalized vacuum density is $\Lambda \approx H^4$ [1–4], which in a low-energy universe leads to a too tiny cosmological term.

In the case we consider the vacuum energy of interacting fields, it has been suggested that in a low energy, approximately de Sitter background the vacuum condensate originated from the QCD phase transition leads to $\Lambda \approx m^3 H$, where $m \approx 150\,\mathrm{MeV}$ is the energy scale of the transition [5–11]. These results are in fact intuitive. In a de Sitter background the energy per observable degree of freedom is given by the temperature of the horizon, $E \approx H$. For a massless free field this

S. Carneiro (✉)
Instituto de Física, Universidade Federal da Bahia, Salvador, BA, Brazil
e-mail: saulo.carneiro@pq.cnpq.br

A. García-Parrado et al. (eds.), *Progress in Mathematical Relativity, Gravitation and Cosmology*, Springer Proceedings in Mathematics & Statistics 60,
DOI 10.1007/978-3-642-40157-2_19, 

energy is distributed in a volume $1/H^3$, leading to a density $\Lambda \approx H^4$, as above. For a strongly interacting field in a low energy space-time, on the other hand, the occupied volume is $1/m^3$, owing to confinement, and the expected density is $\Lambda \approx m^3 H$.

Such a late-time variation law for the vacuum term can also be derived as a backreaction of the creation of non-relativistic dark particles in the expanding spacetime [12]. The Boltzmann equation for this process is

$$\frac{1}{a^3}\frac{d}{dt}\left(a^3 n\right) = \Gamma n, \tag{1}$$

where $n$ is the particle number density and $\Gamma$ is a constant creation rate. By taking $\rho_m = nM$, it can also be written as

$$\dot{\rho}_m + 3H\rho_m = \Gamma\rho_m, \tag{2}$$

where $M$ is the mass of the created particle.

Let us take, in addition to (2), the Friedmann equation

$$\rho_m + \Lambda = 3H^2, \tag{3}$$

with the vacuum term satisfying the equation of state $p_\Lambda = -\Lambda$. Using (2) and (3) we obtain the conservation equation for the total energy,

$$\dot{\rho} + 3H(\rho + p) = 0, \tag{4}$$

provided we take

$$\Lambda = 2\Gamma H + \lambda_0, \tag{5}$$

where $\lambda_0$ is a constant of integration.[1] Since there is no natural scale for this constant, let us make it zero. Then we have $\Lambda = 2\Gamma H$. This is the time-variation law predicted for the vacuum density of the QCD condensate, with $\Gamma \approx m^3$. Dividing it by $3H^2$, we obtain

$$\Gamma = \frac{3}{2}\left(1 - \Omega_m\right) H, \tag{6}$$

where $\Omega_m = 1 - \Omega_\Lambda \equiv \rho_m/(3H^2)$ is the relative matter density (for simplicity, we are considering only the spatially flat case).

[1] Strictly speaking, this result is only exact if we neglect the conserved baryons in the balance equations. Since baryons represent only about 5 % of the total energy content, this can be considered a good approximation.

In the de Sitter limit ($\Omega_m = 0$), we have $\Gamma = 3H/2$, that is, the creation rate is equal (apart from a numerical factor) to the thermal bath temperature predicted by Gibbons and Hawking in the de Sitter spacetime [13]. It also means that the scale of the future de Sitter horizon is determined, through $\Gamma$, by the energy scale of the QCD phase transition, the last cosmological transition we have. For the present time we have, from (6) (with $\Omega_m \approx 1/3$), $H_0 \approx \Gamma \approx m^3$, and hence $\Lambda \approx m^6$, where $H_0$ is the current Hubble parameter. The former result is an expression of the Eddington–Dirac large number coincidence [14]. The later—also known as Zeldovich's relation [15]—gives the correct order of magnitude for $\Lambda$.

The corresponding cosmological model has a simple analytical solution, which reduces to the CDM model for early times and to a de Sitter universe for $t \to \infty$ [16]. It has the same free parameters of the standard model and presents good concordance when tested against type Ia supernovas, baryonic acoustic oscillations, the position of the first peak of CMB and the matter power spectrum [12, 17–21]. Furthermore, the coincidence problem is alleviated, because the matter density contrast is suppressed in the asymptotic future, owing to the matter production [12, 20].

With $\Lambda = 2\Gamma H$ we obtain, from the Friedmann equations, the solution [16–19]

$$\frac{H}{H_0} \approx \left\{\left[1 - \Omega_{m0} + \Omega_{m0}(1+z)^{3/2}\right]^2 + \Omega_{r0}(1+z)^4\right\}^{1/2}, \tag{7}$$

where $\Omega_{m0}$ is the present relative matter density, and we have added conserved radiation with present density parameter $\Omega_{r0}$. As discussed in [17–19], for non-zero $\Omega_{r0}$ the expression (7) is an approximate solution, differing only 1 % from the exact one, since $\Omega_{r0} \approx 8 \times 10^{-5}\ell^2 1$. For $\Omega_{r0} = 0$, the solution (7) is exact.

For early times we obtain $H^2(z) = H_0^2\Omega_{r0}z^4$, and the radiation era is indistinguishable from the standard one. On the other hand, for high redshifts the matter density scales as $\rho_m(z) = 3H_0^2\Omega_{m0}^2 z^3$. The extra factor $\Omega_{m0}$—as compared to the $\Lambda$CDM model—is owing to the late-time process of matter production. In order to have nowadays the same amount of matter, we need less matter in the past. Or, in other words, if we have the same amount of matter in the past (say, at the time of matter-radiation equality), this will lead to more matter today. We can also see from (7) that, in the asymptotic limit $z \to -1$, the solution tends to the de Sitter solution. Note that, like the $\Lambda$CDM model, the above model has only two free parameters, namely $\Omega_{m0}$ and $H_0$. On the other hand, it can not be reduced to the $\Lambda$CDM case except for $z \to -1$. In this sense, it is falsifiable, that is, it may be ruled out by observations.

The Hubble function (7) can be used to test the model against background observations like SNIa, BAO and the position of the first peak in the CMB spectrum [17–19]. The analysis of the matter power spectrum was performed in [20], where, for simplicity, baryons were not included and the cosmological term was not perturbed. In a subsequent publication a gauge-invariant analysis, explicitly considering the presence of late-time non-adiabatic perturbations, has shown that the vacuum perturbations are indeed negligible, except for scales near the horizon [21].

**Table 1** $2\sigma$ limits to $\Omega_{m0}$ (SNe + CMB + BAO + LSS)

| | $\Lambda(t)$CDM | | $\Lambda$CDM | |
|---|---|---|---|---|
| Test | $\Omega_{m0}$ | $\chi^2_{min}/\nu$ | ${\Omega_{m0}}^a$ | $\chi^2_{min}/\nu$ |
| Union2 (SALT2) | $0.420^{+0.009}_{-0.010}$ | 1.063 | $0.235 \pm 0.011$ | 1.027 |
| SDSS (MLCS2k2) | $0.450^{+0.014}_{-0.010}$ | 0.842 | $0.260^{+0.013}_{-0.016}$ | 1.231 |
| Constitution (MLCS2k2-17) | $0.450^{+0.008}_{-0.014}$ | 1.057 | $0.270 \pm 0.013$ | 1.384 |

We show in Table 1 the best-fit results for $\Omega_{m0}$ (with $H_0$ marginalized) with three samples of supernovas: the SDSS and Constitution compilations calibrated with the MLCS2k2 fitter, and the Union2 sample. For the sake of comparison, we also show the best-fit results for the spatially flat $\Lambda$CDM model. We should have in mind that the Union2 dataset is calibrated with the Salt2 fitter, which makes use of a fiducial $\Lambda$CDM model for including high-$z$ supernovas in the calibration. Therefore, that sample is not model-independent and, in the case of the standard model, the test should be viewed as rather a test of consistence. From the table we can see that for the model with particle creation the concordance is quite good. For the samples calibrated with the MLCS2k2 fitter it is actually better than in the $\Lambda$CDM case. As anticipated above, the present matter density is higher than in the standard case.

With the concordance values of $\Omega_{m0}$ in hand, we can obtain the age parameter of the Universe. It is given by [16–19]

$$H_0 t_0 = \frac{2 \ln \Omega_{m0}}{3(\Omega_{m0} - 1)}. \tag{8}$$

In the case of the SDSS and Constitution samples, this leads to $H_0 t_0 = 0.97$, in good agreement with standard predictions and astronomical limits. For $H_0 \approx 70$ Km/(s.Mpc), we have $t_0 \approx 13.5$ Gyr.

Article note presented in *Relativity and Gravitation: 100 years after Einstein in Prague* (Prague, June 2012). It is dedicated to the memory of Prof. Pedro Félix González-Díaz.

## References

1. L. Ford, Phys.Rev. **D11**, 3370 (1975)
2. J. Dowker, R. Critchley, Phys.Rev. **D13**, 3224 (1976)
3. P. Davies, Phys.Lett. **B68**, 402 (1977)
4. A.A. Starobinsky, Phys.Lett. **B91**, 99 (1980)
5. R. Schutzhold, Phys.Rev.Lett. **89**, 081302 (2002)
6. F. Klinkhamer, G. Volovik, Phys.Rev. **D79**, 063527 (2009)
7. F.R. Urban, A.R. Zhitnitsky, Phys.Rev. **D80**, 063001 (2009)
8. F.R. Urban, A.R. Zhitnitsky, Phys.Lett. **B688**, 9 (2010)
9. F.R. Urban, A.R. Zhitnitsky, Nucl.Phys. **B835**, 135 (2010)
10. N. Ohta, Phys.Lett. **B695**, 41 (2011)

11. B. Holdom, Phys.Lett. **B697**, 351 (2011)
12. J. Alcaniz, H. Borges, S. Carneiro, J. Fabris, C. Pigozzo, et al., Phys.Lett. **B716**, 165 (2012)
13. G. Gibbons, S. Hawking, Phys.Rev. **D15**, 2738 (1977)
14. G.A. Mena Marugan, S. Carneiro, Phys.Rev. **D65**, 087303 (2002)
15. J. Bjorken, (2010)
16. H. Borges, S. Carneiro, Gen.Rel.Grav. **37**, 1385 (2005)
17. C. Pigozzo, M. Dantas, S. Carneiro, J. Alcaniz, JCAP **1108**, 022 (2011)
18. S. Carneiro, M. Dantas, C. Pigozzo, J. Alcaniz, Phys.Rev. **D77**, 083504 (2008)
19. S. Carneiro, C. Pigozzo, H. Borges, J. Alcaniz, Phys.Rev. **D74**, 023532 (2006)
20. H. Borges, S. Carneiro, J. Fabris, C. Pigozzo, Phys.Rev. **D77**, 043513 (2008)
21. W. Zimdahl, H. Borges, S. Carneiro, J. Fabris, W. Hipolito-Ricaldi, JCAP **1104**, 028 (2011)

# Quasinormal Modes from a Naked Singularity

**Cecilia Chirenti, Alberto Saa, and Jozef Skákala**

**Abstract** What should be the quasinormal modes associated with a spacetime that contains a naked singularity instead of a black hole? In the present work we address this problem by studying the scattering of scalar fields on a curved background described by a Reissner–Nordström spacetime with $q > m$. We discuss the necessary conditions for the well-posedness of the problem, and give some numerical results for low $l$. The talk "Quasinormal modes from a naked singularity" was presented at the Spanish Relativity Meeting 2012 and was based on the results presented in Chirenti et al. (Phys. Rev. D 86:124008, 2012).

## 1 Introduction

The naked Reissner–Nordström (R–N) singularity is a classical general relativistic solution in electrovacuum. It was discovered that the scalar field scattering problem on such a singular background can be still well defined [2,3,5,7–9], since the waves remain regular at the origin. Despite this nice property of the scattering problem, the spacetime is non-globally hyperbolic and the time evolution of the fields is not unique [4, 6]. This means one has to specify additional boundary condition at the singularity to obtain a fully unique time evolution. (One "preferred" way in which such a self-adjoint extension can be always realized is through the so called Friedrich's extension [9], which will also be the case of this paper.) After uniquely specifying the dynamics, one should be able to characterize the scattering by a set

C. Chirenti (✉) · J. Skákala
Centro de Matemática, Computação, e Cognição, UFABC, 09210-170 Santo André, SP, Brazil
e-mail: cecilia.chirenti@ufabc.edu.br; jozef.skakala@ufabc.edu.br

A. Saa
Departamento de Matemática Aplicada, Universidade Estadual de Campinas, 13083-859 Campinas, SP, Brazil
e-mail: asaa@ime.unicamp.br

A. García-Parrado et al. (eds.), *Progress in Mathematical Relativity, Gravitation and Cosmology*, Springer Proceedings in Mathematics & Statistics 60,
DOI 10.1007/978-3-642-40157-2_20, 

of characteristic oscillations, the quasi-normal modes. One of the questions that we want to answer in the present paper is what will be the behaviour of the *low* damped quasinormal modes when departing from the R–N black hole to the R–N naked singularity.

## 2 The Scalar Wave Scattering on a R–N Naked Singularity

Take the Klein–Gordon equation for the complex (charged) scalar field:

$$\frac{1}{\sqrt{-g}}\partial_\mu(\sqrt{-g}\, g^{\mu\nu}\partial_\nu\Psi) = 0, \tag{1}$$

with the metric line element given as

$$g_{\mu\nu}dx^\mu dx^\nu = -f(r)dt^2 + f(r)^{-1}dr^2 + r^2 d\Omega^2. \tag{2}$$

For the Reissner–Nordström (R–N) singularity the function $f(r)$ is in Planck units given as:

$$f(r) = 1 - \frac{2m}{r} + \frac{q^2}{r^2}, \quad (q^2 > m^2). \tag{3}$$

Take the decomposition of the field into the spherical harmonics

$$\Psi(t, r, \theta, \phi) = \sum_{l,m} \psi_l(t, r) Y_{ml}(\theta, \phi). \tag{4}$$

After we separate the variables we obtain the following reduced equation

$$\frac{d^2\psi_l(t,r)}{dt^2} = \frac{f(r)}{r^2}\frac{d}{dr}\left[r^2 f(r)\frac{d\psi_l(t,r)}{dr}\right] - \frac{l(l+1)f(r)}{r^2}\psi_l(t,r). \tag{5}$$

Using $\phi_l$ defined as $\phi_l(r,t) = r\psi_l(r,t)$ and $x$ the tortoise coordinate given by the condition:

$$\frac{dr}{dx} = f(r), \tag{6}$$

one can rewrite the equation (5) into the following form

$$\frac{\partial^2\phi_l(x,t)}{\partial t^2} - \frac{\partial^2\phi_l(x,t)}{\partial x^2} = V(m,q,l,x)\phi_l(x,t), \tag{7}$$

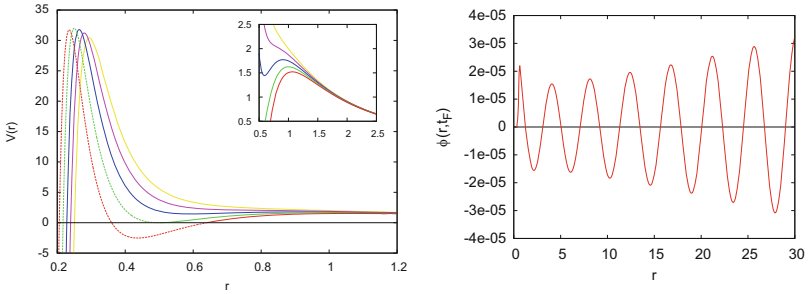


**Fig. 1** *Left*: potential $V(r)$ given by (8) with $l = 2$, $m = 0.5$ for $q = 0.48, 0.5, 0.52, 0.54$ and 0.56. (The *curves* from *left* to *right* correspond to the increase of charge.) Note that the *dashed part* of the potential (for $q = 0.48$ and 0.5) is inside the black hole horizon. *Right*: behavior of $\phi$ with $l = 2$ as a function of $r$ near the center $r = 0$ for a late time $t_F = 350$, shown here in order to exemplify the effect of conditions (10) and (11) in the numerical integration, for a spacetime with $m = 0.5$ and $q = 0.52$

with

$$V(m,q,l,x) = \left[\frac{l(l+1)}{r^2(x)} + \frac{2m}{r^3(x)} - \frac{2q^2}{r^4(x)}\right] f\big(r(x)\big). \tag{8}$$

We want to solve Eq. (7) with potential (8) numerically, in the case where $q > m$ (see the left plot of Fig. 1). To do this, we rewrite Eq. (7) in terms of the light-cone variables $u = t - x$ and $v = t + x$, where $x$ corresponds to the tortoise coordinate (6), as

$$\frac{\partial^2\phi}{\partial t^2} - \frac{\partial^2\phi}{\partial x^2} = -4\frac{\partial^2\phi}{\partial u \partial v} = V(r)\phi, \tag{9}$$

that can be integrated with the boundary conditions

$$\phi(r = 0, t) = \phi(u, v = u + 2x_0) = 0, \tag{10}$$

$$\phi(u = 0, v) = e^{-\frac{(v-v_c)^2}{2\sigma^2}}, \tag{11}$$

where condition (10) is a necessary condition on the field $\phi$ near the origin (see the discussion on Fig. 1 below) and condition (11) defines an "arbitrary" relevant initial signal to be propagated.

As we can see in the right plot of Fig. 1, the boundary conditions (10) and (11) ensure the necessary conditions on the fields $\phi$ and $\psi$ near the center. The physically correct boundary condition for $\psi$ is $\psi(0,t) = 0$. From this we must have for $\phi(r,t) = r\psi(r,t)$ that $\phi(0,t) = 0$ and $\phi'(0,t) = 0$ [1]. In Fig. 2 we can see some examples of the time evolution of the scalar field, and the behavior of the fundamental quasinormal modes as we increase the $q/m$ ratio.

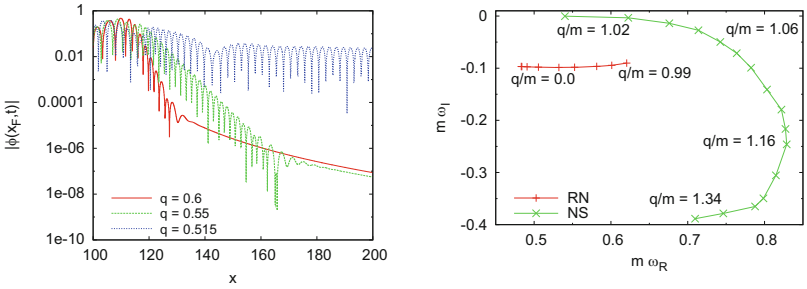


**Fig. 2** *Left*: $\phi(x_F, t)$ with $l = 2$ at $x_F = 100$ for a spacetime with $m = 0.5$ and different values of $q > m$. *Right*: frequencies of the fundamental mode with $l = 2$ in the $\omega_R \times \omega_I$ plane, parametrized by the $q/m$ ration

## 3 Conclusions

The basic results can be summarized as follows: for the large $l$ there is a continuous transition in the low damped quasinormal modes between the R–N black hole and the R–N naked singularity (see [1]). However, when the ratio $q^2/m^2$ becomes larger than approximately $9/8$ then the picture becomes significantly different and the low damped modes do *not* exist for large $l$-s [1]. (This is a very different picture from the BH based intuition.) For the small $l$ numbers the modes face a discontinuous transition when transiting from the black hole to the naked singularity. Furthermore, the $l$ dependence $|\omega_I|$ (for small $l$) changes as $q^2/m^2$ becomes larger than approximately $9/8$: $|\omega_I|$ decreases for $q^2/m^2 \lesssim 9/8$ and increases for $q^2/m^2 \gtrsim 9/8$. It might be interesting to notice that for $q^2/m^2 \gtrsim 9/8$ the increase of $|\omega_I|$ as a function of $l$ (for small $l$-s) matches the behaviour of $|\omega_I|$ for large $l$-s. In the case of large $l$-s and $q^2/m^2 \gtrsim 9/8$ we have shown that $|\omega_I|$ of the fundamental mode grows at least cubically with $l$ and thus, as we already mentioned, the low damped modes do not exist [1].

**Acknowledgements** This work was supported by FAPESP, CNPq and the Max Planck Society.

## References

1. Chirenti, C., Saa, A., Skakala, J.: Quasinormal modes for the scattering on a naked Reissner-Nordstrom singularity. Phys. Rev. D **86**, 124008 (2012)
2. Gibbons, G.: Quantized fields propagating in plane wave spacetimes. Comm. Math. Phys **45**, 191–202 (1975)
3. Horowitz, G. T., Marolf, D: Quantum Probes of Spacetime Singularities. Phys. Rev. D **52**, 5670–5675 (1995)
4. Ishibashi, A., Hosoya, A.: Who's afraid of naked singularities? Phys. Rev. D. **60**, 104028 (1999)

5. Ishibashi, A., Wald, R.M.: Dynamics in Non-Globally-Hyperbolic Static Spacetimes II: General Analysis of Prescriptions for Dynamics. Class. Quant. Grav. **20**, 3815–3826 (2003)
6. Martellini, M., Reina, C., Treves, A.: Klein-Gordon field in a naked singularity background. Phys. Rev. D **17**, 2573–2578 (1978)
7. Pitelli, J.P.M., Letelier, P.S.: Quantum Singularities in Static Spacetimes. Int. J. Mod. Phys. D **20**, 729–743 (2011)
8. Sandberg, V.D.: Light scattering properties of naked singularities. Phys. Rev. D **12**, 2226–2229 (1975)
9. Wald, R.M.: Dynamics in nonglobally hyperbolic, static spacetimes. J. Math. Phys **21**, 2802–2805 (1980)

# *n*-DBI Gravity: A Short Overview

**Flávio S. Coelho, Carlos Herdeiro, Shinji Hirano, and Yuki Sato**

**Abstract** We present a model of gravity motivated by the Dirac–Born–Infeld type conformal scalar theory it yields when the Universe is conformally flat. We show that, if the Universe is permeated by a perfect fluid of radiation, the theory naturally predicts two eras of accelerated expansion mediated by a radiation dominated epoch, with a large hierarchy between the two effective cosmological constants, thus providing an alternative inflation scenario. This theory, dubbed *n*-DBI gravity, contains a preferred unit vector field, everywhere time-like, which breaks diffeomorphism invariance and gives rise to an extra scalar degree of freedom. We analyze the dynamics of this mode and conclude that it is free from some of the pathologies found in similar models, namely the issues of vanishing lapse short distance instability and strong coupling. We also show that the standard black holes of General Relativity are solutions of this theory.

## 1 Motivation: Scale Invariance and Inflation

Observations suggest that the Universe is nearly scale invariant at early and late times, when it is believed to be approximately de Sitter space. At the present epoch, the accelerating expansion is thought to be driven by a nearly constant vacuum energy. To explain the inflation phase after the Big Bang, most current models involve a scalar field, the *inflaton*, which acts as the agent of the nearly exponential expansion of the Universe. However, the nature of such a field is far from clear

F.S. Coelho (✉) · C. Herdeiro
Departamento de Física da Universidade de Aveiro and I3N, Campus de Santiago, 3810-183 Aveiro, Portugal
e-mail: flavio@physics.org

S. Hirano · Y. Sato
Department of Physics, Nagoya University, Nagoya 464-8602, Japan
e-mail: hirano@eken.phys.nagoya-u.ac.jp

A. García-Parrado et al. (eds.), *Progress in Mathematical Relativity, Gravitation and Cosmology*, Springer Proceedings in Mathematics & Statistics 60,
DOI 10.1007/978-3-642-40157-2_21, 

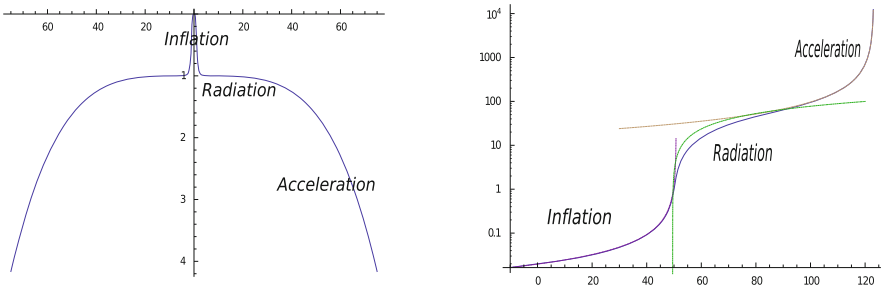


**Fig. 1** *Left:* the effective potential $V(\phi)$. *Right:* time evolution of the conformal factor $\phi(\tau)$

from the particle physics point of view, which means there is room for alternative explanations of inflation.

With these issues in mind, some of us proposed a new model for the gravitational field [6], which yields a Dirac–Born–Infeld type conformal scalar theory when the Universe is conformally flat. It is defined by the action

$$S = -\frac{3\lambda}{4\pi G_N^2}\int d^4x\sqrt{-g}\left\{\sqrt{1+\frac{G_N}{6\lambda}\left(R+\mathscr{K}\right)}-q\right\}+S_m, \tag{1}$$

where $S_m$ is the matter action, $\lambda$ and $q$ are arbitrary constants, $G_N$ is Newton's constant, $R$ is the Ricci scalar and $\mathscr{K}$ is defined through a unit, everywhere time-like, vector field $n^\mu$ as $\mathscr{K} = -2\nabla_\mu(n^\mu\nabla_\nu n^\nu)$.

Concretely, for the Friedmann–Robertson–Walker ansatz

$$ds^2 = l_P^2\phi^2\left(-d\tau^2+\delta_{ij}dx^i dx^j\right), \tag{2}$$

where $l_P$ is the Planck length, the conformal factor $\phi$ is governed by

$$\frac{1}{2}\dot{\phi}^2+V(\phi)=0, \qquad V(\phi)=-\frac{1}{2}\lambda\phi^4\left[1-\left(q+\frac{\epsilon}{\lambda\phi^4}\right)^{-2}\right]. \tag{3}$$

The integration constant $\epsilon$ can be shown to be the energy density of radiation, so we are actually dealing with a Universe permeated by a perfect fluid obeying $\rho = 3p$.

As we can see from Fig. 1, this model naturally results in primordial inflation, followed by a radiation dominated epoch and subsequent accelerated expansion at late times. Matter can also be included in this picture without significant qualitative changes. The current value of the cosmological constant, approximately $10^{-12}$ GeV, and an energy scale of inflation of the order $10^{15}$ GeV constrain the free parameters $\lambda \sim 10^{-8}$, $q-1 \sim 10^{-110}$. The required fine-tuning is of the same order as in standard cosmology, and generates a large hierarchy between the two effective cosmological constants, $1/\sqrt{1-q^{-2}}$.

## 2 Breaking Diffeomorphism Invariance: The Emergence of a Scalar Graviton

The introduction of the vector field $n^\mu$ in the action (1) allows the field equations to remain second order in time derivatives, while becoming higher order in spatial derivatives. Furthermore, it breaks the general diffeomorphisms group of General Relativity down to the subgroup of *foliation-preserving diffeomorphisms*:

$$t \to t + \xi^0(t), \qquad x^i \to x^i + \xi^i(t, x)\,. \tag{4}$$

This gives rise to a scalar degree of freedom in addition to the two tensor modes of General Relativity, very much alike Hořava–Lifshitz gravity. Its existence was firmly established through Dirac's theory of constrained systems [4]. Whereas in General Relativity the Hamiltonian constraint is automatically preserved, here its time evolution gives an equation for the scalar mode. By studying perturbations around flat space, we concluded that this mode is *non propagating* and carries no energy. We further argued that it is free from the pathologies that afflict some versions of Hořava–Lifshitz gravity, namely the issues of vanishing lapse [5], short-distance instability and strong coupling [1]. This good behaviour stems from the non-linear lapse terms in the action. Concretely, working in the Arnowitt–Deser–Misner (ADM) formalism, i.e. foliating space-time by spatial hypersurfaces orthogonal to $n^\mu$, we can write

$$R + \mathscr{K} =^{(3)} R + K_{ij}K^{ij} - K^2 - 2N^{-1}\Delta N, \tag{5}$$

where ${}^{(3)}R$ is the Ricci scalar of the hypersurface metric, $K_{ij}$ is the extrinsic curvature or second fundamental form and $N$ is the lapse function. Terms like $N^{-1}\partial_i N$ where introduced in healthy extensions of Hořava–Lifshitz gravity [2].

## 3 Einstein's Gravity Limit and Black Holes

General Relativity is recovered by taking the double limit $\lambda \to \infty, q \to 1$ while keeping the product $\lambda(q-1)$ fixed, which yields Einstein's equations with a cosmological constant $\Lambda_C = 6\lambda(q-1)/G_N^2$. Indeed, for weak curvature, the leading order term in (1) is the Einstein–Hilbert action with the Gibbons–Hawking–York boundary term.

The field equations of $n$-DBI simplify tremendously if we restrict to solutions with constant $R + \mathscr{K}$, in which case one can prove the following theorem and corollary [7]:

**Theorem 3.1.** *Any solution of Einstein's gravity with cosmological constant plus matter, admitting a foliation with constant $R + \mathscr{K}$, is a solution of $n$-DBI gravity.*

**Corollary 3.2.** *Any Einstein space admitting a foliation with constant* ${}^{(3)}R - N^{-1}\Delta N$ *(where* $N$ *is the lapse and* ${}^{(3)}R$ *the Ricci scalar of the three-dimensional hypersurfaces), is a solution of n-DBI gravity.*

By requiring spherical symmetry, one can explicitly obtain the Schwarzschild, Reissner–Nordström and (anti) de Sitter black hole solutions, albeit in an unusual set of coordinates. Unlike General Relativity, however, the cosmological constant is not determined at the level of the action but appears instead as an integration constant. Corollary 3.2 can be interpreted as the *maximal slicing* gauge condition common in Numerical Relativity, and it is then straightforward to show that the Kerr metric in Boyer–Lindquist coordinates is also a solution of $n$-DBI gravity [3].

## 4 Conclusion

We have presented a model of gravity with interesting cosmological properties, studied some of its exact solutions and answered most of the doubts on the stability and self-consistency of the extra scalar degree of freedom. However, its true nature and possible observational consequences remain to be understood. Maybe the scalar mode is in fact acting as an inflaton. We anticipate that it could source scalar perturbations in the Cosmic Microwave Background, which will be the subject of future work. We believe that models such as $n$-DBI gravity are interesting learning grounds for deepening our understanding of (non-) relativistic gravity. Hurdles are high to self-consistently modify Einstein's elegant theory of general relativity.

**Acknowledgements** F.C. is funded by FCT through the grants SFRH/BD/60272/2009. This work was partially supported by the Grant-in-Aid for Nagoya University Global COE Program (G07), by FCT (Portugal) through the project PTDC/FIS/116625/2010 and by the Marie Curie Action NRHEP295189-FP7-PEOPLE-2011-IRSES.

## References

1. D. Blas, O. Pujolas and S. Sibiryakov, "On the Extra Mode and Inconsistency of Hořava Gravity," JHEP **0910**, 029 (2009).
2. D. Blas, O. Pujolas and S. Sibiryakov, "Consistent Extension of Horava Gravity," Phys. Rev. Lett. **104** 181302 (2010).
3. F. S. Coelho, C. Herdeiro and M. Wang, "n-DBI gravity, maximal slicing and the Kerr geometry," arXiv:1301.1070 (2012).
4. F. S. Coelho, C. Herdeiro, S. Hirano and Y. Sato, "Scalar graviton in n-DBI gravity," Phys. Rev. D **86** 064009 (2012).
5. M. Henneaux, A. Kleinschmidt and G. Lucena Gomez, "A dynamical inconsistency of Hořava gravity," Phys. Rev. D **81**, 064002 (2010).
6. C. Herdeiro and S. Hirano, "Scale invariance and a gravitational model with non-eternal inflation," JCAP **1205** 031 (2012).
7. C. Herdeiro, S. Hirano and Y. Sato, "n-DBI gravity," Phys. Rev. D **84** 124048 (2011).

# Radiation from a D-Dimensional Collision of Shock Waves: A Summary of the First Order Results

**Flávio S. Coelho, Carlos Herdeiro, Carmen Rebelo, and Marco O.P. Sampaio**

**Abstract** We describe how to set up a perturbative framework to compute the metric in the future of a D-dimensional collision of two high speed black holes, by superimposing two equal Aichelburg–Sexl shock waves traveling, head-on, in opposite directions. We then estimate the radiation emitted in the collision using a D-dimensional generalisation of the Landau–Lifschitz pseudo-tensor—workable in a first order approach—and compute the percentage of the initial centre of mass energy emitted as gravitational waves. We shall see that our first order results are always within the bound obtained from apparent horizons computations.

## 1 D-Dimensional Head-On Black Holes Collision

The discovery of different vacuum black hole solutions in five dimensions (for a review see [1]) unveiled that the physics of higher-dimensional black holes can be markedly different, and much richer, than in four dimensions. In particular, this motivates the study of General Relativity in higher dimensions in order to clarify its special behaviour in four dimensions. A relevant question, also taking into account the ongoing physics runs at the LHC concerning the production of higher dimensional black holes, is to understand how much energy is lost in gravitational radiation, in a D-dimensional black hole collision.

To addressed the previous question we should start by considering the simplest scenario: the head-on collision of two high speed Tangherlini black holes. In this particular case, the gravitational field of each black hole reduces to a shock wave solution described by the Aichelburg–Sexl metric [2], and therefore the black holes

F.S. Coelho · C. Herdeiro · C. Rebelo (✉) · M.O.P. Sampaio
Departamento de Física da Universidade de Aveiro and I3N Campus de Santiago, 3810-183 Aveiro, Portugal
e-mail: flavio@physics.org; herdeiro@ua.pt; carmenrebelo@ua.pt; msampaio@ua.pt

A. García-Parrado et al. (eds.), *Progress in Mathematical Relativity, Gravitation and Cosmology*, Springer Proceedings in Mathematics & Statistics 60,
DOI 10.1007/978-3-642-40157-2_22, 

collision can be modelled by the collision of shock waves. By causality, the space-time where two shock waves travel in opposite directions, is well known everywhere by superimposing the two shock wave metrics, except in the future light cone of the collision. In [3] we have generalized a technique first developed in D = 4 by D'Eath and Payne [4–6] to compute the geometry of the D-dimensional space-time to the future of the collision using a perturbative approach.

## 2 Perturbative Metric in the Future of the Shock Waves Collision

The D-dimensional Aichelburg–Sexl shock wave solution is obtained by boosting the Tangherlini black hole to the limit of infinite boost and vanishing mass, keeping the total energy $\mu$ fixed. Using a coordinate system $(u, v, x^i)$, where the retarded and advanced times $(u, v)$ are $(t - z, t + z)$ in terms of Minkowski coordinates, and $x^i$ are the remaining Cartesian coordinates on the plane of the shock, $i = 1 \ldots D - 2$, such that the transverse radius is $\rho = \sqrt{x^i x_i}$; the resulting geometry for a shock wave travelling in the $+z$ direction is

$$ds^2 = -du dv + d\rho^2 + \rho^2 d\Omega^2_{D-3} + \kappa \Phi(\rho)\delta(u) du^2, \tag{1}$$

where $\kappa \equiv 8\pi G_D \mu / \Omega_{D-3}$ and the function $\Phi$ depends only on $\rho$.

The geometry for an identical shock wave travelling in the $-z$ direction is obtained by changing $z \to -z$ in (1). Following [4] it is simple to see that in a boosted frame (moving with respect to the $(u, v)$ chart with velocity $\beta$ in the $-z$ direction), the oppositely directed shock waves keep their form, but with new energy parameters, respectively,

$$\kappa \to e^{\alpha} \kappa \equiv \nu, \qquad \kappa \to e^{-\alpha} \kappa \equiv \lambda, \tag{2}$$

where $e^{\alpha} = \sqrt{(1 + \beta)/(1 - \beta)}$.

The main point is that in this boosted frame one may face the wave traveling in the $-z$ direction as a small perturbation of the wave traveling in the $+z$ direction, since

$$\lim_{\beta \to 1} \frac{\lambda}{\nu} << 1. \tag{3}$$

Since the geometry of the latter is flat for $u > 0$, we make a perturbative expansion of the Einstein equations around flat space, in order to compute the metric in the future of the collision $(v, u > 0)$.

In [3], a perturbative ansatz was assumed such that, to the future of $u = 0$ the metric has an expansion of the type

$$g_{\mu\nu} = \nu^{\frac{2}{D-3}} \left[ \eta_{\mu\nu} + \sum_{i=1}^{\infty} \left( \frac{\lambda}{\nu} \right)^i h^{(i)}_{\mu\nu} \right], \tag{4}$$

where $\eta_{\mu\nu}$ is the flat metric. To compute the metric to first order one needs to solve the linearised Einstein equations around flat Minkowski space-time, subject to a boundary condition induced by the superposition of the two shock waves on $u = 0^+$, in order to determine $h^{(1)}_{\mu\nu}(u, v, \rho)$.

In short, imposing the de Donder gauge condition on the trace-reversed metric perturbation $\bar{h}^{(1)}_{\mu\nu}$, the linearised Einstein equations become simply a set of decoupled wave equations in Minkowski space for each component:

$$\left(-2\partial_u\partial_v + \partial_i^2\right) \bar{h}^{N(1)}_{\mu\nu} = 0, \tag{5}$$

the corresponding solution has the form

$$\bar{h}^{N(1)}_{\mu\nu}(u, v, x_i) = \frac{1}{(2\pi u)^{\frac{D-2}{2}}} \int d^{D-2}x' \partial_{v'}^{\frac{D-2}{2}} \bar{h}^{N(1)}_{\mu\nu}(0, v', x'_i), \tag{6}$$

where for each $x'$, $v'$ defines points at the $u = 0$ hypersurface, which are *on* the past light cone of the event $(u, v, x_i)$.

## 3 Gravitational Radiation

To extract the gravitational radiation produced in the collision we used the Landau–Lifshitz pseudo-tensor—$t^{\mu\nu}_{LL}$, which was generalised to higher dimensions in [7] and is fully determined by our perturbations $h^{N(1)}_{\mu\nu}(u, v, x_i)$.

Despite not being unique or gauge-invariant it is well known that the integral

$$E_{\text{radiated}} = \int t^{0i}_{LL} n_i \, dS dt, \tag{7}$$

computed on a "distant" surface with area element $dS$ outward unit normal $n^i$, is a gauge-invariant well defined energy.

The total radiation emitted will be computed, to first order, under the assumption that $dE/d\cos\theta$ is isotropic. Thus we integrate the power emitted inside the narrow cone around the $\hat{\theta} \equiv \pi - \theta = 0$ axis. Using $dS = r^{D-2} d\Omega_{D-2}$, taking the limit close to the axis and multiplying by the area of the sphere of radius $r$, this energy is

$$E_{\text{radiated}} = \frac{\Omega_{D-3}}{32\pi G_D} \lim_{\hat{\theta}\to 0, r\to\infty} \left( r^2 \rho^{D-4} \int h^{N(1)ij}_{,v} h^{N(1)}_{ij,v} dt \right). \tag{8}$$

The results we obtain for the percentage of energy lost in gravitational radiation are summarised in the following table [3, 8], where the apparent horizon bounds obtained in [9], are also given for comparison:

| Spacetime dimension | 4 | 5 | 6 | 7 | 8 | 9 | 10 | 11 |
|---|---|---|---|---|---|---|---|---|
| First order perturbation theory (%) | 25.0 | 30.0 | 33.3 | 35.7 | 37.5 | 38.9 | 40.0 | 40.9 |
| Apparent horizon bound (%) | 29.3 | 33.5 | 36.1 | 37.9 | 39.3 | 40.4 | 41.2 | 41.9 |

Like the apparent horizon bound, which is determined by the area of the apparent horizon found on the past light cone of the collision between two shock waves, our results indicate that the energy radiated increases monotonically with $D$. If this reduction trend is verified by higher order perturbation theory (or other methods, such as numerical black hole collisions) this result has important phenomenological implications. Moreover, our result is always below the bound, as expected. This suggests that the final black hole will be more massive than previously estimated, making it more consistent with the semi-classical analysis used for estimating the potentially observable Hawking radiation. Finally, most remarkably, we have found a perfect numerical agreement between the percentage of radiated energy compute at first order, and the simple formula $1/2 - 1/D$.

The next step in this analytical treatment is to consider second order perturbation theory. This is challenging since it involves solving the second order Einstein equations. Moreover, the Landau–Lifschitz method used to extract the gravitational radiation has to be adapted, since to second order one must consider the angular dependence for the radiation emitted.

**Acknowledgements** This work was supported by the grants *NRHEP-295189*, FP7-PEOPLE-2011-IRSES and PTDC/FIS/116625/2010. F.C., C.R and M.S. are funded respectively by the grants SFRH/BD/60272/2009, SFRH/BPD/77223/2011 and SFRH/BPD/69971/2010.

## References

1. R. Emparan and H. S. Reall, Living Rev. Rel. **11** 6 (2008) [arXiv:0801.3471 [hep-th]].
2. P. C. Aichelburg and R. U. Sexl, Gen. Rel. Grav. **2** 303 (1971)
3. C. Herdeiro, M. O. P. Sampaio and C. Rebelo, JHEP **1107** 121 (2011) [arXiv:1105.2298 [hep-th]].
4. P. D. D'Eath and P. N. Payne, Phys. Rev. D **46** 658 (1992)
5. P. D. D'Eath and P. N. Payne, Phys. Rev. D **46** 675 (1992)
6. P. D. D'Eath and P. N. Payne, Phys. Rev. D **46** 694 (1992)
7. H. Yoshino and M. Shibata, Phys. Rev. D **80** 084025 (2009) [arXiv:0907.2760 [gr-qc]].
8. F. S. Coelho, C. Herdeiro and M. O. P. Sampaio, Phys. Rev. Lett. **108** 181102 (2012) [arXiv:1203.5355 [hep-th]].
9. D. M. Eardley and S. B. Giddings, Phys. Rev. D **66** 044011 (2002) [gr-qc/0201034].

# Radiation from a D-Dimensional Collision of Shock Waves: Numerics and a Charged Case

**Flávio. S. Coelho, Carlos Herdeiro, Carmen Rebelo, and Marco O.P. Sampaio**

**Abstract** We describe the generalisation to higher orders, of a perturbative framework to find the metric after the collision of two Aichelburg–Sexl gravitational shock waves in D-dimensions. A central challenge is to estimate the amount of gravitational radiation emitted in the collision, at higher orders. We present an adaptation of the Bondi mass loss formula in $D$-dimensions which is valid non-perturbatively, for axially symmetric asymptotically flat space-times. This is shown to coincide with the Landau–Lifshitz pseudo tensor result at first order in perturbation theory. We also discuss the validity of the method with a collision of charged shocks.

## 1 Transplanckian Collisions

In recent studies [3, 4, 9] we have analysed transplanckian collisions at the speed of light in $D$-dimensional general relativity (GR), using Aichelburg–Sexl (AS) gravitational shock waves [1] and a $D = 4$ method by D'Eath and Payne [5–7]. Transplanckian collisions have attracted a lot of attention for reasons such as TeV gravity at the LHC, $AdS/CFT$ (for a review see [2]), or to understand GR by varying $D$. We found the remarkable result that the *inelasticity* (fraction of radiated energy) agrees numerically with

$$\epsilon_{\text{1st order}} = \frac{1}{2} - \frac{1}{D}, \tag{1}$$

F.S. Coelho · C. Herdeiro · C. Rebelo · M.O.P. Sampaio (✉)
Departamento de Física da Universidade de Aveiro and I3N Campus de Santiago, 3810-183 Aveiro, Portugal
e-mail: flavio@physics.org; herdeiro@ua.pt; carmenrebelo@ua.pt; msampaio@ua.pt

A. García-Parrado et al. (eds.), *Progress in Mathematical Relativity, Gravitation and Cosmology*, Springer Proceedings in Mathematics & Statistics 60,
DOI 10.1007/978-3-642-40157-2_23, 

within the apparent horizon bound for colliding AS shocks [8] (Fig. 2 right). Some interesting questions arise which we discuss in the remainder: (a) is there a simple generalisation of (1) at higher orders? (strikingly the second order $D = 4$ estimate of D'Eath and Payne agrees with numerical GR [11]); (b) what is the validity of the method? Can we use this method for a collision of charged shock waves.

## 2 The Collision and the Perturbative Framework

To investigate the general formulation with or without charge we consider a charged shock wave obtained by boosting the $D$-dimensional Reissner–Nordström solution with mass $M$ and charge $Q$ to the limit of infinite boost $\gamma$ and vanishing mass and charge, keeping fixed the following energy and charge parameters [10]

$$\kappa \equiv \frac{8\pi G_D \gamma M}{\Omega_{D-3}}, \qquad a \equiv \frac{8\pi^2 G_D \gamma Q^2}{D-3}\frac{(2D-5)!!}{(2D-4)!!}. \tag{2}$$

The resulting geometry is flat space with a moving impulsive plane in the $+z$ direction with a radial profile on the plane (transverse radius $\rho$)

$$\Phi(\rho, a/\kappa) = -\frac{2a/\kappa}{(2D-7)\rho^{2D-7}} + \begin{cases} -2\ln(\rho), & D = 4 \\ \dfrac{2}{(D-4)\rho^{D-4}}, & D > 4 \end{cases}. \tag{3}$$

Such a geometry describes the gravitational field of a pointlike particle moving at the speed of light with fixed energy and, when $a \neq 0$, a charge parameter. Due to causality, we can superpose two shock waves moving in opposite directions and the space-time metric is known everywhere except inside the future light cone of the collision. Furthermore, in [9] we have shown that, in a boosted frame, the metric on the future light cone of the collision is expanded perturbatively as

$$g_{\mu\nu} = \nu^{\frac{2}{D-3}}\left[\eta_{\mu\nu} + h_{\mu\nu}\right] = \nu^{\frac{2}{D-3}}\left[\eta_{\mu\nu} + \sum_{i=1}^{\infty}\left(\frac{\lambda}{\nu}\right)^i h^{(i)}_{\mu\nu}\right], \tag{4}$$

where, $\lambda, \nu$ are the energy parameters of the weak/strong shock in the boosted frame, respectively, and the background flat metric is written in null coordinates. The retarded/advanced times are ($\sqrt{2}u = t - z$, $\sqrt{2}v = t + z$) in terms of Minkowski time $t$, $z$ coordinates, and $\{x^i\}$ are Cartesian coordinates on the plane of the shocks, $i = 1 \ldots D-2$, such that the transverse radius is $\rho = \sqrt{x^i x_i}$. The superposition of two shock waves induces boundary conditions on $u = 0$ (the location of the strong shock) that at second order are exact. This may be the source of the good agreement of the $D = 4$ second order calculation with numerical GR, for $a = 0$.

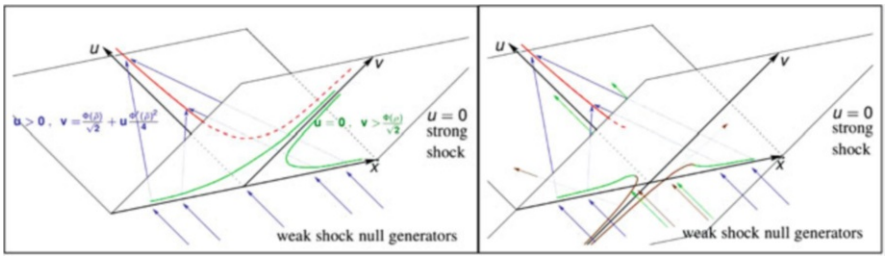


**Fig. 1** Evolution of the weak shock null generators (incident *blue*, *green* and *brown arrows*) for $D > 4$ (*left*: neutral case, *right*: charged case). For $u < 0$ they are at $v = 0$; then the generators undergo a discontinuity in $v$ at $u = 0$. They jump to the collision surface (*green* and *brown lines*). Generically, the rays gain shear and: (a) for large $\rho$ (*green part* of the *curve*) focus along the caustic (*red line*); (b) for small $\rho$ (*brown part* of the *curve*) diverge. Undeflected rays are drawn in *green*

The general perturbative method at higher orders is obtained as follows [4]. The generic ansatz (4) together with a choice of de Donder gauge order by order, are used in Einstein's equations to obtain a tower of decoupled wave equations

$$\Box h_{\mu\nu}^{(i)} = T_{\mu\nu}^{(i-1)}\left[h_{\alpha\beta}^{(j<i)}\right], \tag{5}$$

$$h_{\mu\nu}^{(i)} = F.P.\int_{u'>0} d^D y'\, G(y,y')\left[T_{\mu\nu}^{(i-1)}(y') + 2\delta(u')\partial_{v'}h_{\mu\nu}^{(i)}(y')\right], \tag{6}$$

where the source on the right hand side is generated by lower order perturbations and we have written the general solution of the decoupled wave equations (5) in flat space as an integral solution using the flat space Green function $G(y, y')$ ($F.P.$ denotes the finite part of the integral and $y = \{u, v, x_i\}$). The axial symmetry, allows to show that the radiative components are written in terms of two functions $E, H$:

$$h_{ij} \equiv E(u,v,\rho)\,\Delta_{ij} + H(u,v,\rho)\,\delta_{ij} \qquad \Delta_{ij} \equiv \delta_{ij} - (D-2)\Gamma_i\Gamma_j \quad , \quad \Gamma_i \equiv \frac{x_i}{\rho}\,. \tag{7}$$

A physical understanding of the problem, is achieved by looking at the rays of the weak shock wave before and after the collision. In Fig. 1, we have space-time diagrams for a collision of neutral shock waves (left) and charged shock waves (right). Focusing on the left neutral case, the weak shock null generators travelling along $v = 0$, hit the strong shock at $u = 0$ jumping to the green collision surface (corresponding to the shock profile $\Phi$) and are deflected as to converge towards the axis (blue arrows). On the other hand, the right panel (charged) shows that null generators which are incident close to the axis, the deflection diverges the rays away from the axis (brown arrows emerging from the brown line of the profile $\Phi$). This is qualitatively different from the neutral case (left) where all rays are convergent; the divergent behaviour is caused by the repulsive gravitational effect of the charge.

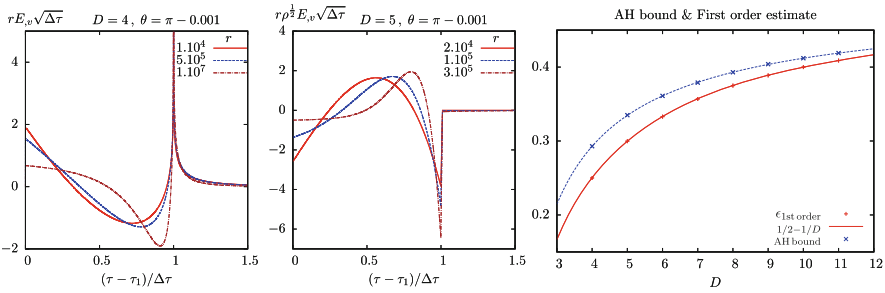


**Fig. 2** *Wave Forms (left) & Extracted inelasticity (right) for* $a = 0$*:* the two *left panels* contain wave form curves for the radiation signal observed close to the axis for various (large) $r$. The horizontal axis time has been rescaled and shifted according to two geometrical optics rays

To compute the radiated energy from (6), we derived a higher $D$ generalisation of the Bondi news function [4,12]. The final result for the inelasticity at all orders is

$$\epsilon_{\text{radiated}} \equiv -\frac{1}{E_{CM}} \int d\tau \frac{dM_B}{d\hat{\tau}} = \int_{-1}^{1} \frac{d\cos\theta}{2} \lim_{r\to+\infty} \int d\tau W(\tau, r, \theta)^2, \tag{8}$$

with $E_{CM}$ the centre of mass energy and

$$W(\tau, r, \theta) \equiv \sqrt{\frac{(D-2)(D-3)}{8}}\, r\rho^{\frac{D-4}{2}} \left(E_{,v} + H_{,v} + E_{,u} + H_{,u}\right). \tag{9}$$

This (more general) result can be used to compute the second order estimate in higher $D$. We have checked numerically that it reduces to the result obtained in [9] using the Landau–Lifschitz method.

Figure 2 summarises the important results for the neutral case. We observe that the wave forms for all $D$ start at a first leading optical ray ($\tau = 0$) and peak at the second optical ray. The right plot shows the perfect agreement of the first order estimate for the inelasticity as a function of $D$ with the formula (1).

In the charged case, we found [4] that the wave signal contains two distinct wave forms, corresponding to pairs of convergent rays, the second pair being due to the divergent (brown) rays that are now allowed from the repulsive region at the centre. The result for the inelasticity in this case is expected to be unreliable, since it receives contributions from rays which cross a region inside the apparent horizon. This is observed when we compute $\epsilon_{1\text{st order}}$ with $a \neq 0$, which actually becomes independent of $a$. This interesting example shows a limitation of the perturbative method when a repulsive core is present.

**Acknowledgements** This work was supported by the grants *NRHEP–295189*, FP7-PEOPLE-2011-IRSES and PTDC/FIS/116625/2010. F.C., C.R and M.S. are funded respectively by the grants SFRH/BD/60272/2009, SFRH/BPD/77223/2011 and SFRH/BPD/69971/2010.

## References

1. P. C. Aichelburg and R. U. Sexl, Gen. Rel. Grav. **2**, 303 (1971).
2. V. Cardoso et al, Class. Quant. Grav. **29**, p. 244001 (2012).
3. F. S. Coelho, C. Herdeiro and M. O. P. Sampaio, Phys. Rev. Lett. **108** 181102 (2012).
4. F. S. Coelho, C. Herdeiro, C. Rebelo and M. O. P. Sampaio (2012).
5. P. D. D'Eath, P. N. Payne, Phys. Rev. **D46** 658–674 (1992).
6. P. D. D'Eath, P. N. Payne, Phys. Rev. **D46** 675–693 (1992).
7. P. D. D'Eath, P. N. Payne, Phys. Rev. **D46** 694–701 (1992).
8. D. M. Eardley, S. B. Giddings, Phys. Rev. **D66** 044011 (2002).
9. C. Herdeiro, M. O. P. Sampaio and C. Rebelo, JHEP **1107** 121 (2011).
10. C. O. Lousto and N. G. Sanchez, Int. J. Mod. Phys. A **5** 915 (1990).
11. U. Sperhake et al, Phys. Rev. Lett. **101** 161101 (2008).
12. K. Tanabe, S. Kinoshita and T. Shiromizu, Phys. Rev. D **84** 044055 (2011).

# Relativistic Positioning Systems in Flat Space-Time: The Location Problem

**Bartolomé Coll, Joan Josep Ferrando, and Juan Antonio Morales-Lladosa**

**Abstract** The location problem in relativistic positioning is considered in flat space-time. When two formal solutions are possible for a user (receiver) of the system, its true location may be obtained from a standard set of emission data extended with an observational rule. The covariant expression giving the location of the user in inertial coordinates is decomposed with respect to an inertial observer.

## 1 Relativistic Positioning Systems

Basically, a *relativistic positioning system* (RPS) is a set of four clocks or emitters $A$ ($A = 1, 2, 3, 4$), of world-lines $\gamma_A(\tau^A)$, broadcasting their respective proper times $\tau^A$ by means of electromagnetic signals. The set $\mathscr{R}$ of events reached by the broadcast signals is called the emission region of the RPS. The *characteristic emission function* $\Theta$ of the RPS assigns to each event $P$ in $\mathscr{R}$ its four proper times received by it, $\{\tau^A\}$, $\Theta(P) = \{\tau^A\}$. The region $\mathscr{C}$ where $\Theta$ is invertible is called the *emission coordinate region* of the RPS, and the four proper times $\{\tau^A\}$ received at every event $P$ are the *emission coordinates of* $P$.

The *orientation of a RPS* at the event $P$ is the orientation of the emission coordinates at $P$, $\hat{\epsilon} \equiv sgn[*(d\tau^1 \wedge d\tau^2 \wedge d\tau^3 \wedge d\tau^4)]$, and it coincides with the sign of the Jacobian determinant of $\Theta$, $\hat{\epsilon}(P) = sgn\, j_\Theta(P)$. The zero Jacobian hypersurface, $\mathscr{J} \equiv \{P \mid j_\Theta(P) = 0\}$, is of relevant interest in relativistic positioning, according to the following result by Coll and Pozo [3]: $\mathscr{J}$ *consists in those events for which any user at them can see the four emitters on a circle on its celestial sphere*.

B. Coll · J.J. Ferrando · J.A. Morales-Lladosa (✉)
Departament d'Astronomia i Astrofísica, Universitat de València, 46100 Burjassot, València, Spain
e-mail: bartolome.coll@uv.es; joan.ferrando@uv.es; antonio.morales@uv.es

A. García-Parrado et al. (eds.), *Progress in Mathematical Relativity, Gravitation and Cosmology*, Springer Proceedings in Mathematics & Statistics 60,
DOI 10.1007/978-3-642-40157-2_24, 

This result (being Lorentz invariant) suggests that at any event of the emission coordinate region $\mathscr{C} = \mathscr{R} - \mathscr{J}$, the orientation $\hat{\epsilon}$ could be obtained from the relative positions of the emitters on the celestial sphere of the user at this event. Let us denote by $\vec{\nu}_A$ the unit vectors ($\vec{\nu}_A^2 = 1$) along the line of sight from the user to the emitter $A$, so that the future pointing null vectors $m_A = (u \cdot m_A)(-u + \vec{\nu}_A)$ describe the propagation of the signals, $u$ being the unit user velocity ($u^2 = -1$). The following *observational rule* to determine $\hat{\epsilon}$ has been proved in [5][1]:

▷ *Consider the circle of the celestial sphere defined by three emitters a (say $a = 1, 2, 3$). Their unit directions $\vec{\nu}_1$, $\vec{\nu}_2$ and $\vec{\nu}_3$ are contained in the cone confined by this circle. Accordingly, if the fourth emitter is in the interior of the circle, $\vec{\nu}_4$ is in the interior of the cone and $\hat{\epsilon}$ is given by $\hat{\epsilon} = sgn[(\vec{\nu}_1, \vec{\nu}_2, \vec{\nu}_3)]$. Otherwise, $\hat{\epsilon} = -sgn[(\vec{\nu}_1, \vec{\nu}_2, \vec{\nu}_3)]$*

Let $\{x^\alpha\}$ be any given specific coordinate system covering $\mathscr{R}$. In relativistic positioning, the *location problem* consists in determining the coordinates $\{x^\alpha\}$ of a user from its emission coordinates $\{\tau^A\}$ and a given set of suitable data. Equation (1) (see below) provides the solution in terms of the emitter trajectories and the orientation $\hat{\epsilon}$. The set of the emitter world-lines referred to the coordinates $\{x^\alpha\}$, and the values of the emission coordinates received by a user, $E \equiv \{\gamma_A(\tau^A), \{\tau^A\}\}$, is called the *standard emission data set*. This set $E$ allows solving the location problem only in a part of the emission region $\mathscr{R}$, called the central region of the RPS (see [4] or footnote 3 below). Out of this region, the set $E$ is unable to determine the orientation $\hat{\epsilon}$ so that it must be extended with, for example, the above observational rule in order to solve the location problem. This problem and the zero Jacobian points have been recently studied by using numerical codes (see [6,7]).

An extended version of this contribution has been presented at the workshop *Relativistic Positioning Systems and their Scientific Applications*.

## 2 The Location Problem in Minkowski Space-Time

In Minkowski space-time, the location problem is formally solved by finding the coordinate transformation, $x^\alpha(\tau^A)$, from emission $\{\tau^A\}$ to inertial $\{x^\alpha\}$ coordinates.[2] The *configuration of the emitters for an event $P$* is the set of the four events

[1] We use the following notation: $(-,+,+,+)$ is the signature of the Minkowski metric $g$; $i()$ denotes the interior product (if $x$ is a vector and $T$ a covariant 2-tensor, $[i(x)T]_\nu = x^\mu T_{\mu\nu}$); $\wedge$ stands for the exterior product; the asterisk $*$ denotes the Hodge dual operator associated to the metric volume element $\eta$, $\eta_{\alpha\beta\gamma\delta} = -\sqrt{-det\, g}\, \epsilon_{\alpha\beta\gamma\delta}$, where $\epsilon_{\alpha\beta\gamma\delta}$ is Levi–Civita permutation symbol, $\epsilon_{0123} = 1$. For a given inertial observer of unit velocity $u$, $u^2 = -1$, any vector $x$ splits as $x = x^0 u + \vec{x}$ where $x^0 = -x \cdot u$ and $\vec{x} \in E_\perp$ with $E_\perp$ the three-space of $u$. For vectors $\vec{x}$, $\vec{y} \in E_\perp$, the vector product is given by $\vec{x} \times \vec{y} = *(u \wedge \vec{x} \wedge \vec{y})$ and $(\vec{x}, \vec{y}, \vec{z}) \equiv (\vec{x} \times \vec{y}) \cdot \vec{z}$ (with $\vec{z} \in E_\perp$) is the scalar triple product.

[2] It seems that Abel and Chaffee [1,2] were the first authors in considering the location problem in connection with Global Positioning System (GPS) by using Lorentzian algebra.

$\{\gamma_A(\tau^A)\}$ of the emitters at the emission times $\{\tau^A\}$ received at $P$. Let us denote by $x \equiv OP$ the position vector with respect to the origin $O$ of a specific inertial coordinate system. If a user at $P$ receives the broadcast times $\{\tau^A\}$, $\gamma_A$ denote the position vectors of the emitters at the emission times, $\gamma_A \equiv O\gamma_A(\tau^A)$. Let us choose the fourth emitter as the *reference emitter* and name the other emitters the *referred emitters*, whose relative position vectors with respect the reference emitter are given by $e_a = \gamma_a - \gamma_4$ $(a = 1, 2, 3)$. The vectors $m_A \equiv x - \gamma_A$ represent the trajectories followed by the light signals from the emitters $\gamma_A(\tau^A)$ to the reception event $P$. The configuration of the emitters has associated the following quantities: the *configuration scalars* $\Omega_a = \frac{1}{2}(e_a)^2$, which are the world function of the pairs of emitters $\{\gamma_a, \gamma_4\}$, the *configuration vector* $\chi \equiv *(e_1 \wedge e_2 \wedge e_3)$ which is orthogonal to the hyperplane containing the four configuration events, and the *configuration bivector* $H \equiv *(\Omega_1 e_2 \wedge e_3 + \Omega_2 e_3 \wedge e_1 + \Omega_3 e_1 \wedge e_2)$. All these quantities are computable from the sole standard data set $E$ because they are defined from $e_a$. Here, we assume that $\chi \neq 0$, that is, the four emission events $\{\gamma_A(\tau^A)\}$ determine a hyperplane, the *configuration hyperplane* for $P$. Emitter configurations, with $\chi = 0$, can occur in current GPS as it was stressed in [1, 2].

## 2.1 Covariant Expression of the Solution

In flat space-time, the coordinate transformation $x^\alpha(\tau^A)$ is given by:

$$x = \gamma_4 + y_* - \lambda\chi, \quad y_* = \frac{1}{\xi \cdot \chi}\, i(\xi)H, \quad \lambda = \frac{y_*^2}{(y_* \cdot \chi) + \hat{\epsilon}\sqrt{\Delta}}, \tag{1}$$

$\xi$ being any vector transversal to the configuration, $\xi \cdot \chi \neq 0$, and $\Delta$ being the following quadratic invariant of $H$, $\Delta \equiv -\frac{1}{2}H_{\mu\nu}H^{\mu\nu} = (y_* \cdot \chi)^2 - y_*^2\chi^2$, which is non-negative, $\Delta \geq 0$ (see [4, 5]). Note that $y_*$ and $\Delta$ are both computable from the sole standard data set $E$. The orientation $\hat{\epsilon}$ depends on $x$ and it *is not always* computable from the sole set $E$. In fact, we have: (a) if $\chi^2 \leq 0$ there is a sole emission solution $x$, and there is no bifurcation. To obtain the solution, take $\hat{\epsilon} = sgn(u \cdot \chi)$, where $u$ is any future pointing time-like vector. (b) If $\chi^2 > 0$ there are two emission solutions, $x$ and $x'$, which only differ by their orientation $\hat{\epsilon}$ (bifurcation problem). In this case, the sole standard data set $E$ is insufficient to solve the location problem but our observational rule allows to determine $\hat{\epsilon}$ and to solve it.[3]

[3]The region $\mathscr{C}^C \equiv \{x \in \mathscr{C} \mid \chi^2 \leq 0\}$ is called the *central region* of the RPS. The orientation $\hat{\epsilon}$ is constant on $\mathscr{C}^C$, and may be evaluated from the sole standard data set $E$. The bifurcation problem always appears in the time-like configuration region $\mathscr{C}_t \equiv \{x \in \mathscr{C} \mid \chi^2 > 0\} = \mathscr{C} - \mathscr{C}^C$.

## 2.2 Splitting of the Solution for an Inertial Observer

Consider the inertial observer associated to the specific inertial coordinate system $\{x^\alpha\}$, of unit velocity $u$, $u^2 = -1$. Next, we decompose respect to this inertial observer the quantities appearing in the transformation (1) from emission to inertial coordinates. The position vector of the emitter $A$ becomes $\gamma_A = t_A u + \bar{\gamma}_A$, $t_A \equiv \gamma_A^0$ being the value of the inertial time of the observer $u$ at the event $\gamma_A(\tau^A)$; then $m_A = (x^0 - t_A)u + \vec{x} - \bar{\gamma}_A$ and $(x^0 - t_A)^2 = (\vec{x} - \bar{\gamma}_A)^2$ with $x^0 > t_A$, because each $m_A$ is null and future pointing.

The position vector of the emitter $a$ with respect to the reference emitter splits as $e_a = \sigma_a u + \vec{e}_a, a = 1, 2, 3$, with $\sigma_a = t_a - t_4$ and $\vec{e}_a = \bar{\gamma}_a - \bar{\gamma}_4$ and then the configuration scalars are given by $\Omega_a = \frac{1}{2}((\vec{e}_a)^2 - \sigma_a^2)$. The configuration vector splits as $\chi = \chi^0 u + \bar{\chi}$, with $\chi^0 = (\vec{e}_1, \vec{e}_2, \vec{e}_3)$ and $\bar{\chi} = \sigma_1 \vec{e}_2 \times \vec{e}_3 + \sigma_2 \vec{e}_3 \times \vec{e}_1 + \sigma_3 \vec{e}_1 \times \vec{e}_2$, and the configuration bivector is written as $H = u \wedge \vec{S} - *(u \wedge \vec{B})$, where the electric-like $\vec{S} \equiv -i(u)H$ and the magnetic-like $\vec{B} \equiv -i(u) * H$ parts of $H$ are expressed as:

$$\vec{S} = \Omega_1 \vec{e}_2 \times \vec{e}_3 + \Omega_2 \vec{e}_3 \times \vec{e}_1 + \Omega_3 \vec{e}_1 \times \vec{e}_2, \tag{2}$$

$$\vec{B} = (\sigma_2 \Omega_3 - \sigma_3 \Omega_2)\vec{e}_1 + (\sigma_3 \Omega_1 - \sigma_1 \Omega_3)\vec{e}_2 + (\sigma_1 \Omega_2 - \sigma_2 \Omega_1)\vec{e}_3, \tag{3}$$

and satisfy $\vec{S}^2 \geq \vec{B}^2$ and $\vec{S} \cdot \vec{B} = 0$. By choosing $\xi^0 = 1$, $\xi = u + \bar{\xi}$, one has $i(\xi)H = -(\bar{\xi} \cdot \vec{S})u - \vec{S} - \bar{\xi} \times \vec{B}$, and $y_* = y_*^0 u + \vec{y}_*$ is provided by:

$$y_*^0 = -\frac{\bar{\xi} \cdot \vec{S}}{D}, \quad \vec{y}_* = -\frac{\vec{S} + \bar{\xi} \times \vec{B}}{D}, \quad D \equiv \bar{\xi} \cdot \bar{\chi} - (\vec{e}_1, \vec{e}_2, \vec{e}_3) \neq 0, \tag{4}$$

with $\vec{S}$ and $\vec{B}$ given by (2) and (3). Substituting $\lambda$ in (1) by:

$$\lambda = \frac{-(y_*^0)^2 + \vec{y}_*^{\,2}}{-y_*^0 \chi^0 + \vec{y}_* \cdot \bar{\chi} + \hat{\epsilon}\sqrt{\vec{S}^2 - \vec{B}^2}}, \tag{5}$$

the user location is expressed in terms of the orientation $\hat{\epsilon}$ (which is obtainable from the observational rule) and $\gamma_4 = \{t_4, \bar{\gamma}_4\}$, $\chi = \{\chi^0, \bar{\chi}\}$, $H = \{\vec{S}, \vec{B}\}$ and $y_* = \{y_*^0, \vec{y}_*\}$ (which are obtainable from the sole standard data $E$). When $(\vec{e}_1, \vec{e}_2, \vec{e}_3) \neq 0$, one may take $\bar{\xi} = 0$ to simplify the above expressions.

**Acknowledgements** This work has been supported by the Spanish ministries of "Ciencia e Innovación" and "Economía y Competitividad" MICINN-FEDER projects FIS2009-07705 and FIS2012-33582.

## References

1. Abel, J. S., Chaffee, J. W.: IEEE Trans. Aerosp. Electron. Syst. **27**, 952 (1991)
2. Chaffee, J. W., Abel, J. S.: IEEE Trans. Aerosp. Electron. Syst. **30**, 1021 (1994)
3. Coll, B., Pozo, J. M.: *Constuction in 4D: Algebraic properties and special observers.* Lecture delivered at the School on Relativistic Coordinates, Reference and Positioning Systems, (Salamanca 2005). See also arXiv: gr-qc/0601125
4. Coll, B., Ferrando, J. J., Morales-Lladosa, J. A.: Class. Quantum Grav **27**, 065013 (2010)
5. Coll, B., Ferrando, J. J., Morales-Lladosa, J. A.: Phys. Rev. D **86**, 084036 (2012)
6. Puchades, N., Sáez, D.: Astrophys. Space. Sci. **341**, 631 (2012). See also arXiv:11126054
7. Sáez, D., Puchades, N.: *Locating objects away from Earth surface: positioning accuracy.* In these proceedings.

# BSSN Equations in Spherical Coordinates Without Regularization

**Isabel Cordero-Carrión and Pedro J. Montero**

**Abstract** Brown introduced a covariant formulation of the BSSN equations well suited for curvilinear coordinate systems. We solve the BSSN equations in spherical symmetry and the general relativistic hydrodynamic equations written in flux-conservative form using a second-order partially implicit Runge–Kutta method to integrate the evolution equations without any regularization algorithm. Some tests assess the accuracy, numerical stability and expected convergence of the code.

## 1 Introduction

The BSSN formulation of Einstein equations [1–3] is one of the most used in numerical simulations. It is particularly tuned for Cartesian coordinates. Brown [4] introduced a covariant formulation well suited for curvilinear coordinates. The singularities associated with curvilinear coordinates are a known source of numerical problems (e.g., $1/r$ terms near $r = 0$) and special care should be taken to avoid numerical instabilities. A regularization procedure [5] has been explored (see, e.g., [6]) in spherical and axial symmetry. However, it is not easy to implement numerically and requires auxiliary variables as well as their evolution equations.

Implicit methods are used to deal with equations that require a special numerical treatment to achieve stable evolutions. Stiff source terms in the equations can lead to the development of numerical instabilities. Some coordinate systems may introduce factors which can be numerically interpreted as stiff terms (e.g., $1/r$ factors due to spherical coordinates near $r = 0$ even when regular data is evolved).

Partially implicit Runge–Kutta (PIRK) methods (see [7] for details and applications in wave equations) have been applied [8] to the hyperbolic part of Einstein

I. Cordero-Carrión (✉) · P.J. Montero
Max-Planck Institute für Astrophysik, Karl-Schwarzschild-Str. 1, D-85748, Garching bei München, Germany
e-mail: chabela,pmontero@mpa-garching.mpg.de

A. García-Parrado et al. (eds.), *Progress in Mathematical Relativity, Gravitation and Cosmology*, Springer Proceedings in Mathematics & Statistics 60,
DOI 10.1007/978-3-642-40157-2_25, 

equations in the Fully Constrained Formulation [9]. A second-order PIRK method was used in [10] to the BSSN equations in spherical coordinates, assuming spherical symmetry, without any regularization at the origin. We use $c = G = M_\odot = 1$.

## 2 Basic Equations

We solve the BSSN equations in spherical symmetry [6, 10], following the description in [6]. The spatial line element is written as $dl^2 = e^{4\chi}[a(r,t)dr^2 + r^2 b(r,t)d\Omega^2]$, where $d\Omega^2 = d\theta^2 + \sin^2\theta d\varphi^2$, $a$ and $b$ are the metric functions, and $\chi$ is the conformal factor, $\chi := \frac{\ln(\gamma/\hat{\gamma})}{12}$, $\hat{\gamma}$ being the determinant of the conformal metric. We consider $\hat{\gamma} = r^4 sin^2\theta$. The evolution equations for $X \equiv e^{-2\chi}$ and $a$ are

$$\partial_t X = \beta^r \partial_r X - \frac{1}{3} X(\alpha K - \hat{\nabla}_m \beta^m), \tag{1}$$

$$\partial_t a = \beta^r \partial_r a + 2a\partial_r \beta^r - \frac{2}{3} a \hat{\nabla}_m \beta^m - 2\alpha a A_a, \tag{2}$$

$K$ being the trace of the extrinsic curvature, $\alpha$ the lapse function, $\hat{\nabla}_m \beta^m$ the conformal divergence of the shift vector $\beta^i$ and $\hat{A}_{ij}$ the traceless part of the conformal extrinsic curvature. Note that $A_a + 2A_b = 0$, where $A_a \equiv \hat{A}^r_r$ and $A_b \equiv \hat{A}^\theta_\theta$. Due to length restrictions, we refer to [10] for the explicit form of the evolution equations for $b$, $A_a$, $K$ and the radial component of the additional BSSN variable, $\hat{\Delta}^r$. The non-advective 1+log condition [11] and the Gamma-driver condition [6, 12] are given by

$$\partial_t \alpha = -2\alpha K, \quad \partial_t B^r = \frac{3}{4}\partial_t \hat{\Delta}^r, \quad \partial_t \beta^r = B^r. \tag{3}$$

The Hamiltonian constraint, $\mathscr{H} \equiv R - (A_a^2 + 2A_b^2) + \frac{2}{3}K^2 - 16\pi E = 0$, is used as diagnostics of the accuracy. The general relativistic hydrodynamic equations, $\nabla_\mu T^{\mu\nu} = 0$ and $\nabla_\mu (\rho u^\mu) = 0$, $T^{\mu\nu}$ being the stress–energy tensor for a perfect fluid and $\rho$ the density, are written in a conservative form in spherical coordinates following [13]. We use the $\Gamma$-law equation of state. A second-order PIRK method [7] is applied to all the evolution equations as it is described in [10].

## 3 Numerical Results

Spatial derivatives are computed using fourth-order finite differences. We use Kreiss–Oliger dissipation [14], a second-order slope limiter reconstruction scheme and a HLLE approximate Riemann solver [15, 16]. Spherical symmetry is imposed

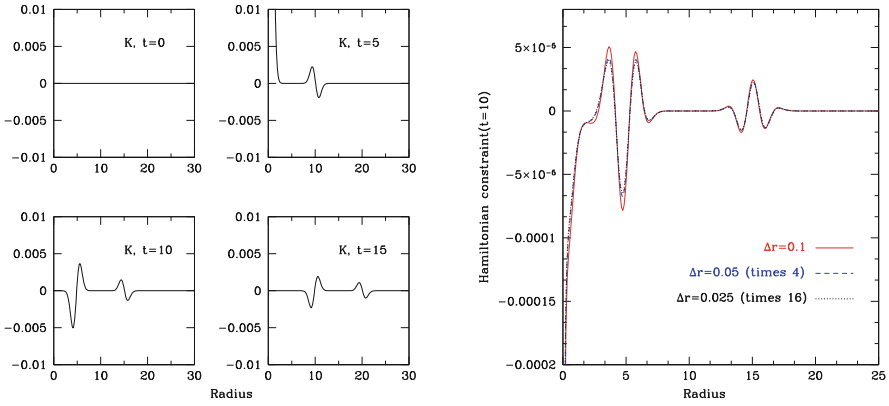


**Fig. 1** *Left panel* shows radial profile of $K$ for a pure gauge pulse at different times; *right panel* shows the (rescaled) Hamiltonian constraint at $t = 10$ for different resolutions

at the origin and radiative conditions [12] at the outer boundary for the metric variables.

We first consider the propagation of a pure gauge pulse using the same initial data as in [6], without regularization at the origin but using a PIRK scheme to achieve numerical stability. Initially, $\chi = A_a = A_b = K = \hat{\Delta}^r = 0$, $a = b = 1$, $\alpha = 1 + \alpha_0 r^2(1 + r^2)^{-1}[e^{-(r-r_0)^2} + e^{-(r+r_0)^2}]$, $\alpha_0 = 0.01$, $r_0 = 5$. We use zero shift and harmonic slicing, $\partial_t \alpha = -\alpha^2 K$. In the left panel of Fig. 1, radial profiles of $K$ for several times are displayed. The evolution remains well behaved everywhere. At $t = 5$, $K \sim 0.1$ at the origin but later returns to zero, as shown by [6]. Hamiltonian constraint shows the expected second-order convergence (right panel of Fig. 1).

Schwarzschild metric in isotropic coordinates, $dl^2 = \psi^4(dr^2 + r^2 d\Omega^2)$, $\psi = (1 + M/2r)$, $M = 1$, is evolved within the moving puncture approach with a precollapsed lapse and initially $\beta^i = 0$. Gauge conditions are given by (3). Our results agree with previous ones (see, e.g., [17]). A stationary state is reached after $t \sim 20$. The maximum value of the shift settles to $\sim$0.15. The time evolution of the mass of the apparent horizon (AH) is conserved during the evolution (error $<$0.2 % at $t = 2,500$).

We focus now on a relativistic star with polytropic index $N = 1$, polytropic constant $\kappa = 100$ and central density $\rho_c = 1.28 \times 10^{-3}$. Truncation errors excite small periodic radial oscillations, visible as periodic variations of the central density. The frequency peaks of the power spectrum of the time evolution of the central density agree with the fundamental frequency and the first two overtones computed by [18] (relative error $<$0.1 %). We obtain stable long-term simulations of non-vacuum regular spacetimes in spherical coordinates without any regularization at the origin.

We finally test the gravitational collapse to a black hole of a spherical relativistic $\kappa = 100$, $N = 1$ polytropic star with central density $\rho_c = 3.15 \times 10^{-3}$; initially,

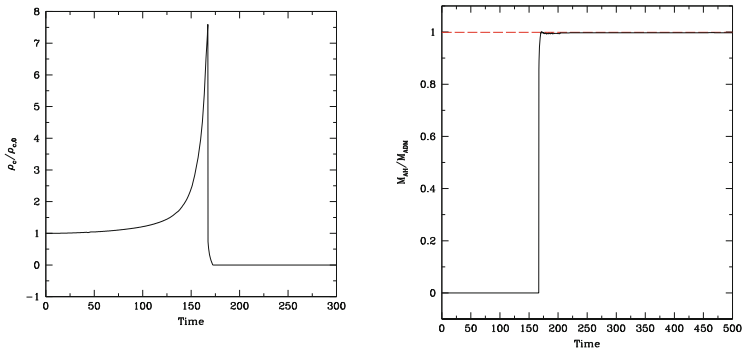


**Fig. 2** Evolution in time of the central density (*left panel*) and of the AH mass (*right panel*) in the gravitational collapse to a black hole

density is increased by 0.5 %. Gauge conditions are given by (3). The star increases its compactness with time and an AH is formed ($t \sim 167$). We plot in Fig. 2 the time evolution of $\rho_c$, and of the mass of the AH which relaxes to the ADM mass of the system (difference about 0.2 % at $t = 500$). The numerical scheme can handle accurately the transition between a regular spacetime (that of the star) and a singular one containing a puncture singularity at $r = 0$.

## 4 Summary

We have reviewed the work presented in [10], which solves numerically the BSSN equations in spherical symmetry and the relativistic hydrodynamic equations, using a second-order PIRK method without any regularization algorithm. Some tests assess the accuracy and expected convergence. We refer to [19] for details on the implementation without any symmetry assumptions in three spatial dimensions.

**Acknowledgements** I. C.-C. acknowledges support from Alexander von Humboldt Foundation and AYA2010-21097-C03-01 (Spanish MICINN). P.M. acknowledges support by the Deutsche Forschungsgesellschaft (DFG) through its SFB/TR 7 “Gravitational Wave Astronomy”.

## References

1. Nakamura, T., Oohara, K., Kojima, Y. Prog. Theor. Phys. Suppl. **90**, 1 (1987)
2. Shibata, M., Nakamura, T. Phys. Rev. D **52**, 5428 (1995)
3. Baumgarte, T.W., Shapiro, S.L. Phys. Rev. D **59**, 024007 (1999)
4. Brown, J.D. Phys. Rev. D **79**, 1004029 (2009)
5. Rinne, O., Stewart, J.M. Class. Quant. Grav. **22**, 1143 (2005)
6. Alcubierre, M., Mendez, M.D. Gen. Rel. Grav. **43**, 2769 (2011)

7. Cordero-Carrión, I., Cerdá-Durán, P. *arXiv:1211.5930 [math-ph]*
8. Cordero-Carrión, I., Cerdá-Durán, P., Ibáñez, J.M. Phys. Rev. D **85**, 044023 (2012)
9. Bonazzola, S., Gourgoulhon, E., Grandclément, P., Novak, J. Phys. Rev. D **70**, 104007 (2004)
10. Montero, P.J., Cordero-Carrión, I. Phys. Rev. D **85**, 124037 (2012)
11. Bona, C., Massó, J., Seidel, E., Stela, J. Phys. Rev. D **56**, 3405 (1997)
12. Alcubierre, M., et al. Phys. Rev. D **67**, 084023 (2003)
13. Banyuls, F., Font, J.A., Ibánez, J.M., Martí, J.M., Miralles, J.A. Astrophys. J. **476**, 221 (1997)
14. Kreiss, H.-O., Oliger, J. In: Methods for the Approximate Solution of the Time Dependent Problems, GARP Publ. Ser., Geneva (1973)
15. Harten, A., Lax, P.D., van Leer, B. SIAM Rev. **25**, 35 (1983)
16. Einfeldt, B. SIAM J. Numer. Anal. **25**, 294 (1988)
17. Hannam, M., et al. Phys. Rev. Lett. **99**, 241102 (2007)
18. Font, J.A., et al. Phys. Rev. D **65**, 084024 (2002)
19. Baumgarte, T.W., Montero, P.J., Cordero-Carrión, I., Müller, E. *arXiv:1211.6632 [gr-qc]*

# Hidden Momentum in the Framework of Gravitoelectromagnetism

**L. Filipe O. Costa**

**Abstract** A still not well understood feature of extended bodies in general relativity is the fact that their momentum is not, in general, parallel to the center of mass 4-velocity—the body is said to have "hidden momentum". It can be split in two main types, a physical one that is gauge invariant, and the pure gauge hidden momentum that arises from the spin supplementary condition. In this paper I focus on the latter, using the formalism of gravitoelectromagnetism, which yields an easy way of understanding it, and under which conditions it arises.

## 1 Introduction: Two Main Types of Hidden Momentum

Extended test bodies in General Relativity can be described through a set of moments of its energy momentum tensor $T^{\alpha\beta}$ and of its charge current density 4-vector $j^{\alpha}$, see e.g. [5, 6]. Herein we are interested in pole–dipole particles, which amounts to consider only two moments of $T^{\alpha\beta}$, the momentum $P^{\alpha}$ and the angular momentum $S^{\alpha\beta}$, defined by

$$P^{\alpha} \equiv \int_{\Sigma(\tau,U)} T^{\alpha\beta} d\Sigma_{\beta} \; ; \qquad S^{\alpha\beta} \equiv 2 \int_{\Sigma(\tau,U)} r^{[\alpha} T^{\beta]\gamma} d\Sigma_{\gamma},$$

($r^{\alpha} \equiv x^{\alpha} - z^{\alpha}(\tau)$) and three moments of $j^{\alpha}$: the charge $q$ and the electric and magnetic dipole moments $d^{\alpha}$ and $\mu^{\alpha}$,

L.F.O. Costa (✉)
Centro de Física do Porto — CFP, Departamento de Física e Astronomia, Universidade do Porto — FCUP, Rua do Campo Alegre, 4169-007 Porto, Portugal
e-mail: filipezola@fc.up.pt

A. García-Parrado et al. (eds.), *Progress in Mathematical Relativity, Gravitation and Cosmology*, Springer Proceedings in Mathematics & Statistics 60,
DOI 10.1007/978-3-642-40157-2_26, 

$$q \equiv \int_{\Sigma} j^{\alpha} d\Sigma_{\alpha}; \qquad d^{\alpha} \equiv \int_{\Sigma(\tau,U)} r^{\alpha} j^{\sigma} d\Sigma_{\sigma};$$
$$\mu^{\alpha} \equiv \frac{1}{2}\epsilon^{\alpha}{}_{\beta\gamma\delta} U^{\delta} \int_{\Sigma(\tau,U)} r^{\beta} j^{\gamma} U^{\sigma} d\Sigma_{\sigma}.$$

These moments are taken with respect to a reference worldline $z^{\alpha}(\tau)$, of proper time $\tau$ and tangent vector $U^{\alpha} \equiv dz^{\alpha}/d\tau$, and a hypersurface of integration $\Sigma(\tau, U) \equiv \Sigma(z(\tau), U)$, orthogonal to $U^{\alpha}$ at $z^{\alpha}(\tau)$. From the conservation equations $j^{\alpha}_{;\alpha} = 0$ and $(T_{\text{tot}})^{\alpha\beta}_{\ \ ;\beta} = 0 \Leftrightarrow T^{\alpha\beta}_{\ \ ;\beta} = F^{\alpha\beta} j_{\beta}$, follow the evolution equations [5,6]

$$\frac{DP^{\alpha}}{d\tau} = qF^{\alpha}_{\ \beta} U^{\beta} + \star F_{\beta\gamma}{}^{;\alpha} U^{\gamma} \mu^{\beta} + F^{\alpha}_{\ \gamma;\beta} U^{\gamma} d^{\beta} + F^{\alpha}_{\ \beta} \frac{Dd^{\beta}}{d\tau} - \frac{1}{2} R^{\alpha}_{\ \beta\mu\nu} S^{\mu\nu} U^{\beta}, \tag{1}$$

$$\frac{DS^{\alpha\beta}}{d\tau} = 2P^{[\alpha} U^{\beta]} + 2\epsilon_{\lambda\nu}{}^{\theta[\beta} F^{\alpha]}_{\ \ \theta} \mu^{\lambda} U^{\nu} + 2d^{[\alpha} F^{\beta]}_{\ \ \gamma} U^{\gamma}. \tag{2}$$

These are equations of motion provided that $z^{\alpha}(\tau)$ is some representative point of the body. The natural choice is the center of mass (CM); the latter however, for a spinning body, depends on the observer (see [4] and Fig. 1 therein). The so called spin supplementary condition, $S^{\alpha\beta} u_{\beta} = 0$, for some time-like unit vector field $u^{\alpha}$, amounts to require $z^{\alpha}$ to be the CM *as measured by some observer of 4-velocity* $u^{\alpha}$. Contracting Eq. (2) with some time-like vector (for instance $U_{\beta}$), we see that the momentum $P^{\alpha}$ is not parallel to the center of mass 4-velocity $U^{\alpha}$. We can decompose $P^{\alpha}$ in its projections parallel ($P^{\alpha}_{\text{kin}}$) and orthogonal ($P^{\alpha}_{\text{hid}}$) to $U^{\alpha}$,

$$P^{\alpha} = P^{\alpha}_{\text{kin}} + P^{\alpha}_{\text{hid}}; \qquad P^{\alpha}_{\text{kin}} = mU^{\alpha}; \qquad P^{\alpha}_{\text{hid}} = (h^{U})^{\alpha}_{\ \beta} P^{\beta} \tag{3}$$

where $m = -P^{\alpha} U_{\alpha}$ and $(h^{U})^{\alpha}_{\ \beta} \equiv U^{\alpha} U_{\beta} + g^{\alpha}_{\ \beta}$ denotes the projector orthogonal to $U^{\alpha}$. The "kinetic momentum" $P^{\alpha}_{\text{kin}}$ is the familiar momentum associated with the center of mass motion. $P^{\alpha}_{\text{hid}}$ is the so-called hidden momentum; the reason for denomination is seen taking the perspective of the center of mass frame, where the particle is by definition at rest, but at the same time the 3-momentum is in general not zero: $\vec{P} = \vec{P}_{\text{hid}} \neq 0$; hence $\vec{P}$ must be somehow hidden in the particle.

$P^{\alpha}_{\text{hid}}$ consists of two terms. One induced by the electromagnetic field [1], $P^{\alpha}_{\text{hidEM}} = \epsilon^{\alpha}_{\ \beta\gamma\delta} U^{\delta} \mu^{\beta} E^{\gamma}$, which is gauge independent, and causes a magnetic dipole to accelerate without force, leading e.g. to the bobbing effects studied in [7] (see also Fig. 1 of [3]), or in opposite direction to the force, as shown in [5] (for a particle initially in radial motion in a Coulomb field). And a pure gauge one [7] that we dub "inertial" ($P^{\alpha}_{\text{hidI}}$), due to its relation with inertial forces, which is the subject of next section.

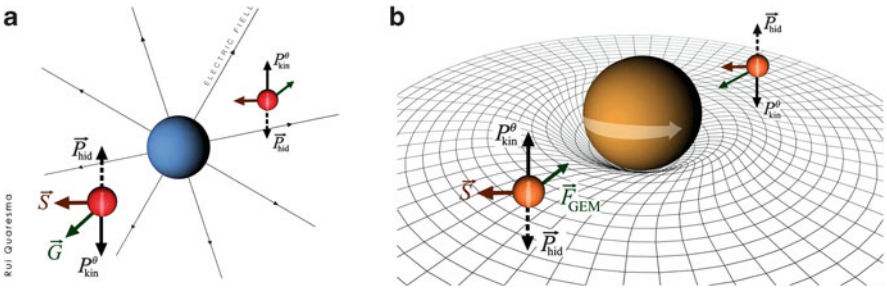


**Fig. 1** (**a**) A spinning charged particle (with $\vec{\mu} = 0$) orbiting a Coulomb charge. When the center of mass (CM) is computed in the "laboratory" frame (which is an inertial frame, so $F^{\alpha}_{\text{GEM}} = 0$), $P^{\alpha}_{\text{hid}} = 0$ and the trajectory is an ellipse. When the CM is computed in the comoving frame ($F^{\alpha}_{\text{GEM}} = G^{\alpha}$), there is a hidden momentum $\vec{P}_{\text{hid}} = \vec{S} \times_U \vec{G}$ along the $\mathbf{e}_\theta$ direction, which oscillates along the orbit; the total momentum along $\mathbf{e}_\theta$ however must be constant, $P^{\theta} = P^{\theta}_{\text{kin}} + P^{\theta}_{\text{hid}} = 0$ (as the Coulomb force is radial); this means that the CM bobs up and down in order for $P^{\theta}_{\text{kin}} = mU^{\theta}_{\text{kin}}$ to cancel out $P^{\theta}_{\text{hid}}$. (**b**) A spinning body in the Kerr spacetime; the situation is *opposite*: there are inertial forces in the laboratory frame ($\vec{F}_{\text{GEM}} = \gamma\left[\gamma\vec{G} + \vec{U} \times_u \vec{H}\right]$), thus there is hidden momentum $\vec{P}_{\text{hid}} \sim \vec{S} \times \vec{F}_{\text{GEM}}$ and bobbings when the CM is computed therein, whilst in the comoving frame these are negligible

## 2 GEM Formulation of the "Inertial" Hidden Momentum

Let $u^{\alpha}$ be the 4-velocity field relative to which the CM is evaluated; that is, $S^{\alpha\beta}u_{\beta} = 0$. Contracting (2) with $u^{\alpha}$, we have ($\gamma \equiv -U^{\beta}u_{\beta}$)

$$P^{\alpha}_{\text{hidI}} = \frac{1}{\gamma}(h^U)^{\alpha}_{\ \sigma} S^{\sigma\beta}\frac{Du_{\beta}}{d\tau} = \frac{1}{\gamma}(h^U)^{\alpha}_{\ \sigma} S^{\sigma\beta}u_{\beta;\lambda}U^{\lambda}, \tag{4}$$

telling us that this form of hidden momentum arises when $u^{\alpha}$ varies along the center of mass worldline $z^{\alpha}$. Taking $u^{\alpha}$ to be the tangent vector (i.e., the 4-velocity) of some congruence of observers $\mathscr{O}(u)$, we can decompose

$$u_{\alpha;\beta} = -a(u)_{\alpha}u_{\beta} - \epsilon_{\alpha\beta\gamma\delta}\omega^{\gamma}u^{\delta} + K_{(\alpha\beta)}$$

where $a(u)^{\alpha} \equiv u^{\alpha}_{\ ;\beta}u^{\beta}$ is the observers' acceleration (*not* the particle's!); $\omega^{\alpha} = \frac{1}{2}\epsilon^{\alpha\lambda\sigma\tau}u_{\tau}u_{[\sigma;\lambda]}$ their vorticity, and $K_{(\alpha\beta)} \equiv (h^u)^{\lambda}_{\alpha}(h^u)^{\nu}_{\beta}u_{(\lambda;\nu)}$ the shear/expansion tensor. We can thus write

$$P^{\alpha}_{\text{hidI}} = -\frac{1}{\gamma^2}(h^U)^{\alpha}_{\ \sigma}S^{\sigma}_{\ \beta}F^{\beta}_{\text{GEM}}; \quad F^{\alpha}_{\text{GEM}} = \gamma\left[\gamma G^{\alpha} + \epsilon^{\alpha}_{\ \beta\gamma\delta}u^{\delta}U^{\beta}H^{\gamma} - K^{(\alpha\beta)}U_{\beta}\right], \tag{5}$$

where $F^{\alpha}_{\text{GEM}}$ is the *gravitoelectromagnetic force* (resembling the Lorentz force), describing the inertial "forces" associated with the observer congruence. $G^{\alpha} \equiv -a(u)^{\alpha}$ is the "gravitoelectric field", $H^{\alpha} = \omega^{\alpha}$ is the so-called "Fermi–Walker

gravitomagnetic[1] field" [8]. As discussed in [2], in a general formulation $H^\alpha$ consists on the sum of two terms: the vorticity $\omega^\alpha$ of the congruence, plus the rotation $\Omega^\alpha$ of the spatial triads $\mathbf{e}_i$ carried by each observer $\mathscr{O}(u)$ relative to Fermi–Walker transport. Hence $F^\alpha_{\text{GEM}}$ above yields the inertial forces of a frame $\mathbf{e}_\alpha$ whose time axis is $\mathbf{e}_0 \propto u^\alpha$, and the spatial triads $\mathbf{e}_i$ undergo Fermi–Walker transport along $\mathscr{O}(u)$ (i.e., $\Omega^\alpha = 0$).

The important statement encoded in (5) is that one has inertial hidden momentum ($P^\alpha_{\text{hidI}} \neq 0$) only when there are inertial forces *in the frame where the center of mass* of the particle is evaluated (note that this is *not* about the frame where the motion is being described; they are not in general the same).

## 3 Hidden Momentum Arising in the Different Spin Conditions

We shall now compare, in simple examples in flat and curved spacetime, the inertial hidden momentum arising from two types of spin condition: one requiring the center of mass to be evaluated in a frame comoving with it, which corresponds to the Mathisson–Pirani (MP) spin condition $S^{\alpha\beta}U_\beta = 0$ (and usually to a good approximation also to the Tulczyjew–Dixon condition $S^{\alpha\beta}P_\beta = 0$, which chooses the CM as measured in the $P^i = 0$ frame), and other choosing the center of mass as measured in the "laboratory frame", that is, $S^{\alpha\beta}u_\beta = 0$, where $u^\alpha$, in the case of a stationary asymptotically flat spacetime, are the "static" observers[2] $u^\alpha \propto \partial/\partial t$.

Consider first the situation in Fig. 1a, a spinning charged particle (but with $\vec{\mu} = 0$, so that $P^\alpha_{\text{hid}} = P^\alpha_{\text{hidI}}$, and the only force acting on the particle is the Lorentz force) in flat spacetime orbiting a Coulomb charge. Consider first the CM as measured by the static observers; this is an inertial frame, thus there is no hidden momentum: $F^\alpha_{GEM} = 0 \Rightarrow P^\alpha_{\text{hidI}} = 0$, and the CM trajectory is an ellipse. Now consider the CM measured in the comoving frame (MP condition, $u^\alpha = U^\alpha$); the hidden momentum takes in this case the simple form $P^\alpha_{\text{hidI}} = S^{\alpha\beta}a_\beta = (\vec{S} \times_U \vec{G})^\alpha$, where $a^\alpha = -G^\alpha$ coincides with *the particle's acceleration*. Since $a^\alpha \neq 0$, $P^\alpha_{\text{hidI}} \neq 0$; it oscillates along the orbit, as depicted in Fig. 1a, leading to a bobbing motion of the CM.

Consider now a gravitational system such as the one depicted in Fig. 1b, a spinning test particle orbiting a spinning mass (e.g., a Kerr black hole). Take the CM measured by the static observers (CP condition); such congruence is accelerated and has vorticity; that is, according to these observers, an inertial "force" acts on

[1]This gravitomagnetic field differs by a factor of 2 from the most usual one in the context of experimental gravitomagnetism, $H^\alpha_{(\Omega=\omega)} = 2\omega^\alpha$, obtained by demanding the triads $\mathbf{e}_i$ to co-rotate with the congruence ($\Omega^\alpha = \omega^\alpha$). The frame of "the distant stars", relative to which gyroscope and orbital precessions are measured, is set up in this way, see [2] for details.

[2]This is a generalization of the condition introduced by Corinaldesi–Papapetrou (CP) for the Schwarzschild spacetime (see in [4]).

the particle, cf. (5), and thus $P^{\alpha}_{\text{hidI}} \neq 0$ and there are bobbings. Now take the CM as measured by the comoving observer; the motion is nearly geodesic (apart from the spin-curvature force, last term of (1)); such observer is thus nearly inertial, and $\vec{P}_{\text{hid}} \sim \mathcal{O}(S^2)$ is negligible in a pole–dipole approximation, see [5].

We have thus contrasting effects: for a spinning particle under a force in flat spacetime, there is hidden momentum and bobbings when the CM is computed in the comoving frame, which vanish when one evaluates it in the "laboratory" frame; for a spinning particle in a gravitational field, it is the other way around.

Concluding, the GEM formalism is useful for understanding the hidden momentum that arises in a given system under the different spin conditions; and to chose the most convenient one for each application. It is important to bear in mind that, whenever $P^{\alpha}_{\text{hid}} \neq 0$, force does *not* equal mass times acceleration; the contribution $DP^{\alpha}_{\text{hid}}/d\tau$ is in principle not negligible to dipole order, for instance in the application of Fig. 1b (for the *laboratory frame*) is of the same order of magnitude ($\sim MSv/r^3$) of the-spin curvature force.

## References

1. Babson, D., Reynolds, S., Bjorquist, R., Griffiths, D. J., Am. J. Phys. **77**, 826 (2009)
2. Costa, L. F., Natário J., [arXiv:1207.0465] (2012)
3. Costa, L. F., Natário, J., Zilhão, M., AIP Conf. Proc. 1458 (2011) 367–370 [arXiv:1206.7093]
4. Costa, L. F., Herdeiro C., Natário J., Zilhão, M., Phys. Rev. D **85**, 024001 (2012)
5. Costa, L. F., Natário J., Zilhão, M., [arXiv:1207.0470] (2012)
6. Dixon, W. G., Il Nuovo Cimento **34**, 317 (1964)
7. Gralla, S. E., Harte, A. I., Wald, R. M., Phys. Rev. D **81,** 104012 (2010)
8. Jantzen R. T., Carini, P., Bini, D., Ann. Phys. **215**(1) (1992) [arXiv:gr-qc/0106043]

# Comparing Results for a Global Metric from Analytical Perturbation Theory and a Numerical Code

**J.E. Cuchí, A. Molina, and E. Ruiz**

**Abstract** We compare the results obtained from analytical perturbation theory and the AKM numerical code for an axistationary spacetime built from a rotating perfect fluid interior with the equation of state $\epsilon - 3p = 4B$ of the simple MIT bag model matched to an asymptotically flat exterior. We discuss the behaviour of the error in the metric components of the analytical approximation going to higher orders. Additionally, we check and comment the errors in multipole moments, central pressure and some other physical properties of the spacetime.

## 1 Introduction

The lack of stellar models in General Relativity—i.e. a stationary and axisymmetric perfect fluid interior matched with an asymptotically flat vacuum exterior—is in direct contrast with the importance they could have for the astrophysics of compact stars and in particular the determination of their possible compositions. One of such possibilities is the interesting case of strange matter. A versatile model for strange matter is a simple MIT bag model with equation of state (EOS) $\epsilon - 3p = 4B$. We will study this stellar model with the results provided by the CMMR post-Minkowskian and slow rotation approximation scheme [3] and its behaviour when we go to higher orders of approximation. Also, we will give the relative error in these functions and quantities when compared with very precise numerical results obtained with the AKM code [1, 2].

J.E. Cuchí (✉) · E. Ruiz
Departamento de Física Fundamental, Universidad de Salamanca, Salamanca, Spain
e-mail: jecuchi@gmail.com; eruiz@usal.es

A. Molina
Departamento de Física Fonamental, Universitat de Barcelona, 08014 Barcelona, Spain
e-mail: alfred.molina@ub.edu

A. García-Parrado et al. (eds.), *Progress in Mathematical Relativity, Gravitation and Cosmology*, Springer Proceedings in Mathematics & Statistics 60,
DOI 10.1007/978-3-642-40157-2_27, 

## 2 The Analytical and Numerical Metrics

The stationary and axisymmetric spacetime we study is the following. The interior $\mathscr{V}^-$ is filled with a perfect fluid with the EOS $\epsilon - 3p = \epsilon_0$ and in rigid rotation so that, if $\boldsymbol{\xi}$, $\boldsymbol{\chi}$ are the Killing vectors, its velocity is $\boldsymbol{u} = \psi(\boldsymbol{\xi} + \omega\boldsymbol{\chi})$, with $\psi$ a normalization factor and $\omega$ a constant corresponding to the angular velocity of the fluid as seen by a distant observer. The exterior $\mathscr{V}^+$ is asymptotically flat vacuum and is matched with the interior imposing continuity of the metrics and their first derivatives on the $p = 0$ surface.

In CMMR, we solve the Einstein equations using a truncated multipolar post-Minkowskian approximation in spherical-like coordinates associated to harmonic ones. The post-Minkowskian parameter is $\lambda = m/r_s$, which $m$ the Newtonian mass of the source and $r_s$ the coordinate radius of the static fluid; a different parameter $\Omega^2 = \omega^2 r_s^3/m$ (the ratio between Newtonian centrifugal and gravitational forces), gives the truncation point of the expansion in spherical harmonics, in this case preserving terms up to $\mathscr{O}(\Omega^3)$. The metric in each spacetime $\boldsymbol{g}^{\pm}(\lambda, \Omega)$ is decomposed in Minkowski $\boldsymbol{\eta}$ plus the deviation $\boldsymbol{h}^{\pm}(\lambda, \Omega)$ and then Einstein's equations can be solved iteratively. The spacetimes are matched on the $p = 0$ surface which can be expanded as $r_\Sigma = r_s\left[1 + \sigma\Omega^2 P_2(\cos\theta)\right] + \mathscr{O}(\Omega^4)$ with $\sigma$ constant. Finally, the global metric depends only on $\epsilon_0$, $\omega$ and $r_s$. In [4] (CGMR) we obtained the $\mathscr{O}(\lambda^{5/2}, \Omega^3)$ metric for the EOS $\epsilon + (1-k)p = \epsilon_0$. Here we use its ($k = 4$, $\epsilon_0 = 4B$) subcase corresponding to the simple MIT bag model but now including terms up to $\mathscr{O}(\lambda^{9/2}, \Omega^3)$.

AKM is a multi-domain spectral code that gives the matched metric on a grid over a quadrant of finite size. The grid coordinates are $\{\rho, \zeta\}$, cylindrical associated to quasi-isotropic coordinates and the resolution is customizable. It also gives some physical properties, like the first mass and angular momentum multipole moments $M_0$ and $J_1$, baryon rest mass $M_\mathrm{b}$, circumpherential radius $R_\mathrm{circ}$, binding energy $E_\mathrm{b}$, polar and equatorial coordinate radii $r_\mathrm{p}$, $r_\mathrm{e}$, polar redshift $z_\mathrm{p}$ and central pressure and specific enthalpy $p_\mathrm{c}$, $h_\mathrm{c}$. To build a stellar model, it needs goal values for any pair of these quantities as well as to fix some parameters to specify the EOS and provide an initial data file. The code is able to obtain initial data for different EOS if one manages to avoid unphysical configurations in the process. The precision it gets depends on the number $n$ of Chebyshev polynomials used, and can reach machine accuracy for high enough $n$ when the deformation of the source is not extreme. We fix it here to $n = 20$.

## 3 Comparison and Results

We build stellar models for different values of $(M_\mathrm{b}, \omega)$ and compare the metrics on the cylindrical-like coordinate grid of AKM. Working in units where ($c = G = B = 1$), the $k = 4$ CGMR has only $(r_s, \omega)$ as free parameters. Unlike $\omega$, $r_s$ has no equivalent in AKM, so we must adjust its value. Hence, for each model we

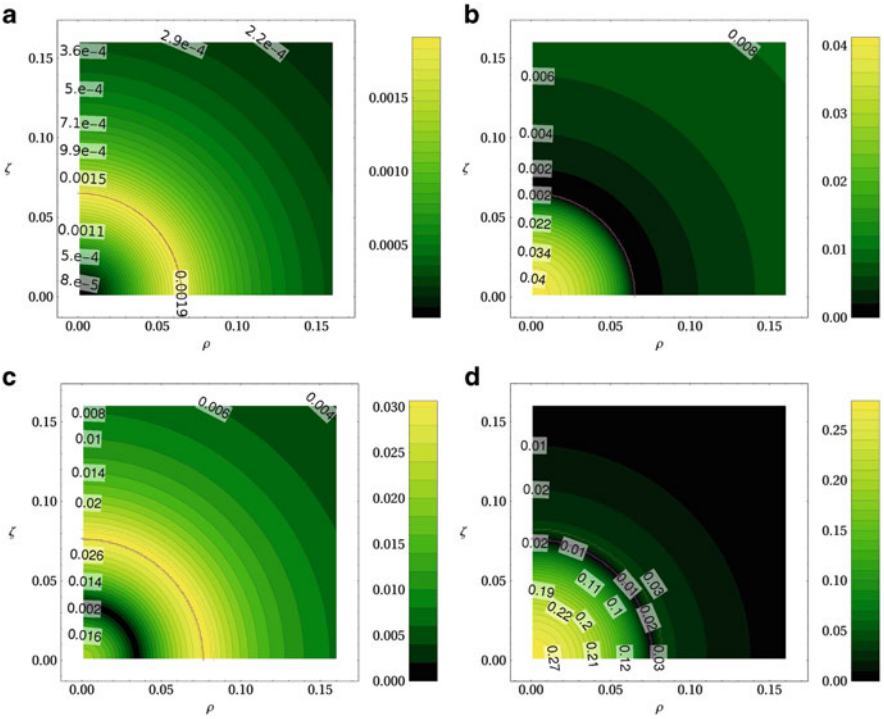


**Fig. 1** Relative error between $\mathcal{O}(\lambda^{9/2}, \Omega^3)$ CMMR and $n = 20$ AKM in (**a**, **b**) $g_{tt}$ and $g_{t\varphi}$ for $M_0 = 8 \times 10^{-3}$, $\omega = 0.24$ ($\lambda \approx 0.077$, $\Omega \approx 0.059$); (**c**, **d**) $g_{tt}$ and $g_{t\varphi}$ for $M_0 = 0.0184$, $\omega = 0.24$ ($\lambda \approx 0.12$, $\Omega \approx 0.059$). The *thin dotted lines* represent the AKM and CMMR surfaces

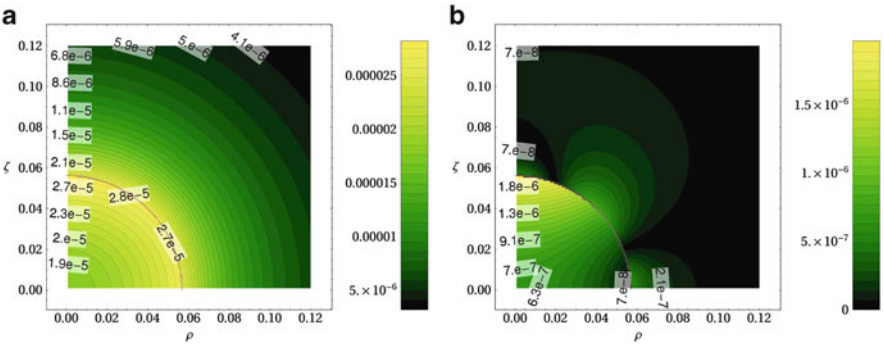


**Fig. 2** Relative error for constant density in $g_{tt}$ using $M_0 = 8 \times 10^{-4}$, $\omega = 0.2$ using CMMR up to: (**a**) $\mathcal{O}(\lambda^{5/2}, \Omega^3)$; (**b**) $\mathcal{O}(\lambda^{9/2}, \Omega^3)$. The *thin dotted lines* represent the AKM and CMMR surfaces (indistinguishable in this picture size)

**Table 1** Some CMMR values and relative error with respect to AKM in ($c = G = B = 1$) units. In other units, the three models rotate at $\nu = 102$ Hz and their masses in $M_\odot$ appear in the first row

| | $M_0 = 0.054,\ M_\mathrm{b} = 0.06$ | | $M_0 = 0.51,\ M_\mathrm{b} = 0.6$ | | $M_0 = 1.39,\ M_\mathrm{b} = 1.7$ | |
|---|---|---|---|---|---|---|
| $M_\odot$ | CMMR | Error | CMMR | Error | CMMR | Error |
| $\omega$ | 0.24 | | 0.24 | | 0.24 | |
| $M_\mathrm{b}$ | 7.9997e−4 | 3.2e−5 | 7.95e−3 | 6.1e−3 | 0.02241 | 0.0406 |
| $M_0$ | 7.104e−4 | | 6.772e−3 | | 0.0184 | |
| $J_1$ | 8.3609e−8 | 1e−4 | 3.586e−6 | 0.012 | 1.82e−5 | 0.034 |
| $R_\mathrm{circ}$ | 0.034769 | 3.6e−5 | 0.07287 | 8.6e−3 | 0.102 | 0.068 |
| $E_\mathrm{bind}$ | 8.8730e−6 | 2.8e−4 | 3.766e−4 | 0.040 | 1.75e−3 | 0.19 |
| $z_\mathrm{p}$ | 0.021133 | 7.6e−5 | 0.1079 | 0.016 | 0.24 | 0.13 |
| $V_0$ | −0.020913 | 4.6e−5 | −0.103 | 0.010 | −0.221 | 0.087 |
| $r_\mathrm{p}$ | 0.033914 | 4.7e−5 | 0.0657 | 9.8e−3 | 0.0831 | 0.09 |
| $r_\mathrm{e}$ | 0.034055 | 3.8e−5 | 0.06593 | 9.8e−3 | 0.0834 | 0.091 |
| $r_\mathrm{ratio}$ | 0.995862 | 9.4e−6 | 0.9964 | 2.4e−5 | 0.997 | 3e−4 |
| $\epsilon_\mathrm{c}$ | 4.5935 | 6.8e−5 | 4.712 | 0.019 | 5.56 | 0.21 |
| $p_\mathrm{c}$ | 0.043679 | 2.4–4 | 0.254 | 0.052 | 0.631 | 0.37 |
| $h_\mathrm{c}$ | 0.908786 | 1.7e−6 | 0.9522 | 2e−3 | 1.025 | 0.042 |

take the value of one of the AKM physical quantities and equating it to its CMMR counterpart we get $r_s$. Using $M_0$, $p_\mathrm{c}$, and $J_1$ for this gives similar results. Here we use $M_0$.

The results of Fig. 1 show the relative error in the metric $(g_{tt}, g_{t\phi})$ components for $M_0 = 0.51\,M_\odot$ and the typical $M_0 = 1.39\,M_\odot$ for a moderately fast rotation frequency $\nu = 102$ Hz near the source. The first case has a reasonable error (higher in $g_{t\phi}$) and the second must be improved (Table 1). Going to higher orders in the $\lambda$ approximation is now automatic with the help of our *Mathematica* subroutines, but improving the slow-rotation approximation is more cumbersome. Nevertheless, Fig. 2 shows the improvement for a $\epsilon = \epsilon_0$ EOS moving from $\mathscr{O}(\lambda^{5/2}, \Omega^3)$ to $\mathscr{O}(\lambda^{9/2}, \Omega^3)$. It makes us confident that, since our current error graphics do not show the lobular aspect of Fig. 2b, which means that the truncation of the multipolar expansion is an important error source, our results can be improved very easily even in the case of the strong gravitational field of a compact source of realistic mass.

**Acknowledgements** JEC thanks Junta de Castilla y León for grant EDU/1165/2007. This work was supported by grant FIS2009-07238 (MICINN).

## References

1. Ansorg, M., Kleinwächter, A., Meinel, R. Highly accurate calculation of rotating neutron stars. Astron. & Astrophys. **381**(3), L49–L52 (2002)
2. Ansorg, M., Kleinwächter, A., Meinel, R. Highly accurate calculation of rotating neutron stars. Detailed description of the numerical methods. Astron. & Astrophys. **405**, 711–721 (2003)

3. Cabezas, J.A., Martín, J., Molina, A., Ruiz, E. An approximate global solution of Einstein's equations for a rotating finite body. Gen. Relativ. Gravit. **39**(6), 707–736 (2007)
4. Cuchí, J.E., Gil-Rivero, A., Molina, A., Ruiz, E. An approximate global solution of Einstein's equations for a rotating compact source with linear equation of state. Gen. Relativ. Gravit. (2013). doi:10.1007/s10714-013-1528-7. Published Online First: 4 April 2013

# Thick Dirac–Nambu–Goto Branes on Black Hole Backgrounds

**Viktor G. Czinner**

**Abstract** Thickness corrections to static, axisymmetric Dirac–Nambu–Goto branes embedded into spherically symmetric black hole spacetimes with arbitrary number of dimensions are studied. First, by applying a perturbative approximation, it is found that the thick solutions deviate significantly in their analytic properties from the thin ones near the axis of the system, and perturbative approaches around the thin configurations can not provide regular thick solutions above a certain dimension. For the general case, a non-perturbative, numerical approach is applied and regular solutions are obtained for arbitrary brane and bulk dimensions. As a special case, it has been found that two-dimensional branes are exceptional, as they share their analytic properties with the thin branes rather than the thick solutions of all other dimensions.

## 1 Introduction

The study of higher dimensional black holes, branes and their interactions is an active field of research in several different areas of modern theoretical physics. One interesting direction, which has been first introduced by Frolov [1], is to consider a brane—black hole toy model for studying merger and topology changing transitions in higher dimensional classical general relativity [2], or in certain strongly coupled gauge theories [3] through the gauge/gravity correspondence. The model consists of a bulk $N$-dimensional black hole and a test $D$-dimensional brane in it ($D \leq N - 1$),

V.G. Czinner (✉)
Centro de Matemática, Universidade do Minho, Campus de Gualtar, 4710-057 Braga, Portugal

HAS Wigner Research Centre for Physics, Institute for Particle and Nuclear Physics, H-1525 Budapest, P.O. Box 49, Hungary
e-mail: czinner.viktor@wigner.mta.hu

A. García-Parrado et al. (eds.), *Progress in Mathematical Relativity, Gravitation and Cosmology*, Springer Proceedings in Mathematics & Statistics 60,
DOI 10.1007/978-3-642-40157-2_28, 

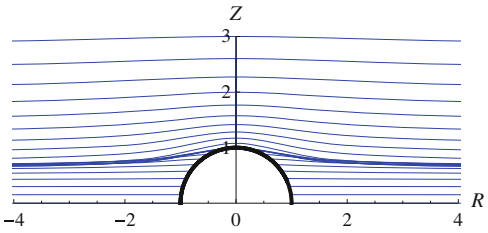


**Fig. 1** A sequence of thin brane equilibrium configurations on Schwarzschild background. The different configurations belong to different boundary conditions. For simplicity, the horizon radius is put to be 1, and $R$ and $Z$ are standard cylindrical coordinates

called *brane-black hole* (BBH) system. The brane is infinitely thin, and it is described by the Dirac–Nambu–Goto [4] action.

Due to the gravitational attraction of the black hole, the brane is deformed and there are two types of equilibrium configurations. The brane either crosses the black hole horizon (supercritical), or it lies totally outside of the black hole (subcritical), see Fig. 1.

Generalizations of the BBH model by studying the effects of thickness corrections obtained from higher order curvature terms in the effective brane action, have also been studied by Frolov and Gorbonos [5] within a perturbative approach, near the critical solution and restricted to the Rindler zone. As an interesting result they found that when the spatial dimension of the brane is greater than 2, supercritical solutions behave quite differently from subcritical ones, and according to their numerical analysis, they did not find evidence for the existence of such solutions. They suggested that quantum corrections may cure this pathological behaviour.

As a different approach, in three consecutive papers [6–8], we have re-considered the problem of thickness corrections to the BBH system within a more general framework than that of [5]. We did not restrict ourselves to work neither in the Rindler zone, nor in the near-critical solution region, and we also chose to follow a different path in obtaining the brane Euler–Lagrange equation. As a result we were able to provide the complete set of regular solutions of the thick-BBH problem for arbitrary brane and bulk dimensions, and also to clarify the question of phase transition in the system.

In this paper we present very briefly the outline of our main findings, and refer the reader to the works [6–8] for details and the complete results.

## 2 Perturbative Approach

In [6], we applied a linear perturbation method to the thick BBH problem obtained from the curvature corrected Dirac–Nambu–Goto action:

$$S = \int d^D\zeta \sqrt{-\det\gamma_{\mu\nu}} \left[ -\frac{8\mu^2}{3\ell}(1 + C_1 R + C_2 K^2) \right],$$

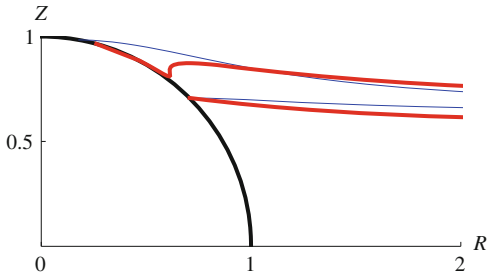


**Fig. 2** The picture shows two thick (*red*) brane configurations together with their thin (*blue*) counterparts in the case of an $N = 5$, $D = 4$ black hole embedding. The boundary conditions are $\theta_0 = \frac{\pi}{4}$ (*bottom curves*) and $\frac{\pi}{17}$ (*top curves*)

and derived the general form of the perturbation equation for the thick branes. From the asymptotic behaviour of the perturbation equation, in accordance with the results of [5], we found that there is no regular solution of the perturbed problem in the Minkowski embedding case, unless the brane is a string, or a two-dimensional sheet. This restriction, however does not hold for the black hole embedding solutions, which are always regular within our perturbative approach.

From these results we concluded that the absence of regular solutions above the dimension $D = 3$ implies, that the problem can not be solved within perturbative approaches around the thin solutions which are *not smooth* on the axis of the system. For a general discussion, one needs to find a new, non-perturbative solution of the problem, that is expected to behave differently from the thin solutions by being *smooth* on the axis.

After these conclusions, we provided the solution of the perturbation equation for various brane ($D$) and bulk ($N$) dimensions. The far distance equations were integrated analytically, while the near horizon solutions were obtained by numerical computations. The deformations of the perturbed brane configurations were plotted (see e.g. Fig. 2) and a comparison was made with the corresponding thin brane configurations with identical boundary conditions.

## 3 Non-perturbative Solutions

In [7] we further studied the effects of curvature corrections to the BBH system. Since the results of [6] clearly showed that perturbative approaches fail to provide regular solutions near the axis of the system in Minkowski type topologies, we considered a different, exact, numerical approach to the problem. We analysed the asymptotic properties of the complete, fourth-order, highly non-linear Euler–Lagrange equation of the thick BBH system, presented its asymptotic solution for far distances, and obtained regularity conditions in the near horizon region for both Minkowski and black hole embeddings. We showed that the requirement of regularity for the thick solution defines almost completely the boundary conditions for the Euler–Lagrange equation in the Minkowski embedding case. The only exceptions are the brane configurations with 1, 2 and 3 spacelike dimensions.

In the cases of 1 and 3, regular solutions of the problem could be found, however, which was an unexpected result, the problem could not be solved with the applied, non-perturbative method for the case of 2 spacelike dimensions.

## 4 The Two-Dimensional Case

In [8] we further studied the problem of a topologically flat 2-brane in the thickness corrected BBH system. Despite the previously mentioned difficulties, we were able to find a regular, non-perturbative, numerical solution for this special case also, based on earlier perturbative considerations [6]. The main result here was the observation that the two-dimensional case is special as being *non-analytic* at the axis of the system, just like the thin solutions. This property makes it unique in the family of thick solutions, as in all other dimensions both the Minkowski and black hole embedding solutions are *analytic* in their entire domain.

**Acknowledgements** The research leading to these results was supported in part by the Japan Society for the Promotion of Science contract No. P06816, the Hungarian National Research Fund, OTKA No. K67790 grant, and by the National Research Foundation of South Africa. It has also received funding from the European Union Seventh Framework Programme (FP7/2007–2013) under grant agreement n° PCOFUND-GA-2009-246542 and from the Foundation for Science and Technology of Portugal.

## References

1. Frolov, V. P.: Merger transitions in brane black-hole systems: Criticality, scaling, and self-similarity. Phys. Rev. D **74** 044006 (2006)
2. Kol, B.: Topology change in general relativity, and the black-hole black-string transition. J. High Energy Phys. **10** 049 (2005); Kol, B.: The phase transition between caged black holes and black strings. Phys. Rep. **422** 119 (2006)
3. Mateos, D., Myers R. C. and Thomson R. M.: Holographic Phase Transitions with Fundamental Matter. Phys. Rev. Lett. **97** 091601 (2006); Mateos, D., Myers R. C. and Thomson R. M.: Thermodynamics of the brane. J. High Energy Phys. **05** 067 (2007)
4. Dirac, P. A. M.: An Extensible Model of the Electron. Proc. R. Soc. A. **268** 57 (1962); Nambu, J.: Lectures at the Copenhagen Summer Symposium (1970), unpublished; Goto, T.: Relativistic Quantum Mechanics of One-Dimensional Mechanical Continuum and Subsidiary Condition of Dual Resonance Model. Prog. Theor. Phys. **46** 1560 (1971)
5. Frolov, V. P. and Gorbonos, D.: Toy model for topology change transitions: Role of curvature corrections. Phys. Rev. D **79** 024006 (2009).
6. Czinner, V. G. and Flachi, A.: Curvature corrections and topology change transition in brane-black hole systems: A perturbative approach. Phys. Rev. D **80** 104017 (2009)
7. Czinner, V. G.: Thick-brane solutions and topology change transition on black hole backgrounds. Phys. Rev. D **82** 024035 (2010)
8. Czinner, V. G.: A topologically flat thick 2-brane on higher dimensional black hole backgrounds. Phys. Rev. D **83** 064026 (2011)

# Cosmological Applications of Extended Electromagnetism

**Roberto Dale and Diego Sáez**

**Abstract** Extended electromagnetism (EE) has been applied to cosmology in various papers. In all of them, the zero order energy density of the EE vector field plays the same role as vacuum energy. Perturbations of this field have been studied by using different approaches. Firstly, some basic equations and ideas are summarized and, then, the CMBFAST code is used to calculate the cosmic microwave background angular power spectrum for appropriate values of the EE parameters. Comparisons of the resulting spectra with a good observational one compatible with WMAP7 (Wilkinson map anisotropy probe 7 years data) seem to be promising. We are currently looking for a set of parameters leading to the best fitting between the WMAP7 and EE spectra. Results will be presented elsewhere.

## 1 Generalities

Some vector tensor (VT) theories were proposed four decades ago [1] as theories of gravitation. Recent papers [2–4] have developed a VT theory which is a generalization of the Einstein–Maxwell (EM) one. The vector field, $A^{\mu}$, is coupled to the electrical currents and, consequently, it plays the role of the electromagnetic field. Cosmological perturbations in this theory—which is named extended electromagnetism (EE)—were studied in [3,4] by using different methods. In [3], some simplifying assumptions were assumed to compute the CMB angular

R. Dale (✉)
Departament d'estadística, matemàtiques i informàtica, Universitat Miguel Hernàndez, 03202, Elx, Alacant, Spain
e-mail: rdale@umh.es

D. Sáez
Departamento de Astronomía y Astrofísica, Universidad de Valencia, 46100 Burjassot, Valencia, Spain
e-mail: diego.saez@uv.es

A. García-Parrado et al. (eds.), *Progress in Mathematical Relativity, Gravitation and Cosmology*, Springer Proceedings in Mathematics & Statistics 60,
DOI 10.1007/978-3-642-40157-2_29, 

power spectrum. As it is discussed in [4], this spectrum must be estimated again without simplifying hypothesis. This estimation is studied, for the first time, in this preliminary paper.

Our signature is $(-,+,+,+)$. Greek indices run from 0 to 3. The symbol $\nabla$ stands for a covariant derivative. The tensor $F_{\mu\nu} = \nabla_\mu A_\nu - \nabla_\nu A_\mu$ may be then defined from the vector field $A^\mu$ of EE. Whatever quantity $N$ may be, $\dot{N}$ and $N_B$ are the time derivative with respect to the conformal time and the background value of $N$, respectively. Units are chosen in such a way that the speed of light is $c = 1$. In the framework of EE, the field and motion equations of a charged isentropic perfect fluid may be obtained from the following Lagrangian (see [4] for details):

$$I = \int \left[ \frac{R}{16\pi G} - \frac{1}{4} F_{\mu\nu} F^{\mu\nu} + \gamma (\nabla \cdot A)^2 + J^\mu A_\mu - \rho\,(1+\epsilon) \right] \sqrt{-g}\, d^4x, \quad (1)$$

where $\gamma$, $G$, $R$, $\rho$, $\epsilon$, and $g$ are an arbitrary coupling constant, the gravitational constant, the scalar curvature, a conserved energy density, the internal energy density, and the determinant of the metric matrix $g_{\mu\nu}$.

In [4], the following equations were derived from the Lagrangian (1):

$$\nabla^\nu F_{\mu\nu} = J_\mu + J^A_\mu, \quad (2)$$

$$T^{\mu\nu}(\gamma, A) = 2\gamma[\{A^\alpha \nabla_\alpha (\nabla \cdot A) + \frac{1}{2}(\nabla \cdot A)^2\} g^{\mu\nu} - A^\mu \nabla^\nu (\nabla \cdot A) - A^\nu \nabla^\mu (\nabla \cdot A)], \quad (3)$$

where $T^{\mu\nu}(\gamma, A)$ is the part of the energy momentum tensor of field $A^\mu$ which does not appear in EM theory, $\nabla \cdot A \equiv \nabla_\mu A^\mu$, and $J^A_\mu = -2\gamma \nabla_\mu (\nabla \cdot A)$. From the field equations (2) it follows that $J^T_\mu = J_\mu + J^A_\mu$ is the conserved current of the theory.

## 2 Basic EE Cosmological Equations and Results

Our background universe is homogeneous, isotropic, neutral, and flat. The metric has the Robertson Walker form with scale factor $a$. The covariant components of the EE vector field and the four-velocity are $[A_{0B}(\tau), 0, 0, 0]$ and $[a(\tau), 0, 0, 0]$, respectively. There are no charges $[\rho_q(\tau) = 0]$ and currents $[J_\mu = 0]$. In this case, (2) reduces to

$$\Xi_B \equiv (\nabla \cdot A)_B = -\frac{1}{a^2}[\dot{A}_{0B} + 2\frac{\dot{a}}{a} A_{0B}] = constant \quad (4)$$

and, from (3), the energy density and pressure of the field $A^\mu$ are found to be $\rho^A_B = -P^A_B = -\gamma \Xi^2_B = constant$; hence, constant $\gamma$ must be negative to have a positive energy density and, then, $\rho^A_B$ may play the role of the vacuum

energy density. The remaining cosmological equations are identical to those of the standard GR model with cosmological constant ($\rho_\Lambda = \rho_A$).

Let us now use the Bardeen formalism [5] to evolve background perturbations in momentum space. These perturbations are expanded in terms of scalar ($Q^{(0)}$), vector, and tensor harmonics. Since vector and tensor modes evolve as in Einstein–Maxwell (EM) theory [3,4], only scalar modes are considered. A possible scalar mode associated to the EE vector $J^\mu$ is assumed to be zero. Under this assumption, it was proved [4] that the mode $\Xi^{(0)}$, involved in the expansion $\nabla \cdot A = \Xi_B(1 + \Xi^{(0)} Q^{(0)})$, is the most suitable one to write the equations of the theory. This mode satisfies the following differential equation:

$$\ddot{\Xi}^{(0)} + 2\frac{\dot{a}}{a}\dot{\Xi}^{(0)} + k^2 \Xi^{(0)} = 0, \tag{5}$$

which is fully decoupled from any other equation of this Bardeen first order approximation. The initial conditions necessary to solve this equation are the values of $\Xi^{(0)}$ and $\dot{\Xi}^{(0)}$ at a certain initial time ($z = 10^8$). Since one can always take $\dot{\Xi}^{(0)}_{in} \simeq 0$ [4], only the initial value $\Xi^{(0)}_{in}$ may be varied. This is the unique free cosmological parameter characteristic of EE.

The code CMBFAST [6] may be used to calculate the CMB angular power spectrum in standard cosmology. The equations and initial conditions of this code may be found in [7]. They may be easily extended to EE if the following elements are used: (a) the Bardeen formalism with the particular modes appearing in [7], and (b) the synchronous gauge. In this way, the evolution equations for the standard modes of GR cosmology may be written as follows:

$$k^2\eta - \frac{1}{2}\frac{\dot{a}}{a}\dot{h} = 4\pi G[-a^2\rho_B\delta - 2|\gamma|\Xi_B(a^2\Xi_B\Xi^{(0)} + A_{0B}\xi^{(0)})] \tag{6}$$

$$k^2\dot{\eta} = 4\pi G[a^2(\rho_B + P_B)\theta + 2|\gamma|k^2 A_{0B}\Xi_B\Xi^{(0)}] \tag{7}$$

$$\ddot{h} + 2\frac{\dot{a}}{a}\dot{h} - 2k^2\eta = -24\pi G[a^2 P_B \pi_L - 2|\gamma|\Xi_B(a^2\Xi_B\Xi^{(0)} - A_{0B}\xi^{(0)})] \tag{8}$$

$$\ddot{h} + 6\ddot{\eta} + 2\frac{\dot{a}}{a}(\dot{h} + 6\dot{\eta}) - 2k^2\eta = -24\pi G a^2(\rho_B + P_B)\sigma. \tag{9}$$

In these equations $\eta$, $h$, $\delta$, $\theta$, $\sigma$ and $\pi_L$ are modes of the standard cosmological model defined in [7], whereas $\Xi^{(0)}$ and $\xi^{(0)} = \dot{\Xi}^{(0)}$ are new EE modes (see above). Moreover, $\rho_B$ and $P_B$ are the background energy density and pressure of the cosmological fluid, respectively. The correcting terms—with respect to the standard GR model—are those involving the constant $|\gamma|$. These terms and the new equations describing the evolution of the electromagnetic field $A^\mu$ must be included in CMBFAST for applications to EE. The modified code has been used to get the CMB angular power spectrum in four cases, and the resulting spectra are shown in Fig. 1. The four cases correspond to the same standard parameters of the concordance model (given in [8]), but to distinct values of $\Xi^{(0)}$. Solid line

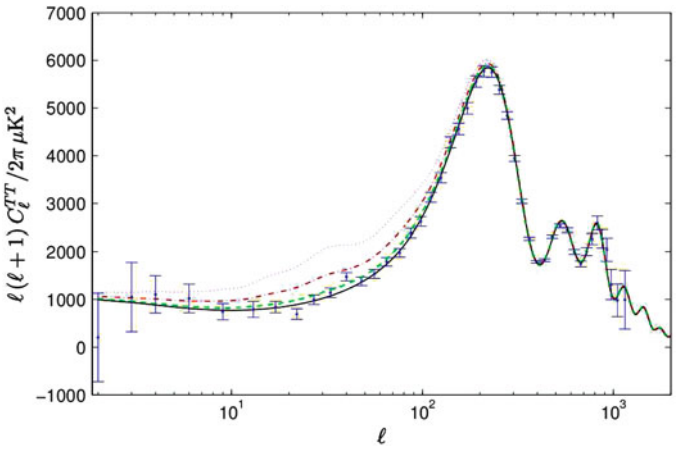


**Fig. 1** Lines display the CMB angular power spectrum corresponding to four realizations (see text) of the EE cosmological model. Points with error bars are WMAP7 measurements

has been obtained for $\Xi^{(0)} = 0$, whereas the dashed, point-dashed, and dotted lines correspond to three increasing values of $\Xi_{in}^{(0)}$. From Fig. 1 it follows that the deviations with respect to the solid line—which are EE deviations associated to the value of $\Xi_{in}^{(0)}$—are only relevant for $\ell$ values smaller than $\sim$250 (angular scales greater than $\sim 0.7°$). If $\Xi_{in}^{(0)}$ is too big (dotted line) the resulting spectrum does not fit the WMAP7 observations; however, for appropriate $\Xi_{in}^{(0)}$ values, the deviations are small, but likely significant in a fitting to WMAP7 spectra based on various parameters and Markov chains. Results on this subject will be presented elsewhere.

**Acknowledgements** This work has been supported by the Spanish Ministries of *Ciencia e Innovación* and *Economía y Competitividad*, MICINN-FEDER projects FIS2009-07705 and FIS2012-33582.

## References

1. Will, C. M.: *Theory and Experiment in gravitational Physics*, Cambridge University Press, New York (1993).
2. Beltrán Jiménez, J., Maroto, A. L.: J. Cosmol. Astropart. Phys. **03**, 016 (2009)
3. Beltrán Jiménez, J., Koivisto, T.S., Maroto, A.L., Mota, D.F.: J. Cosmol. Astropart. Phys. **10** 029 (2009).
4. Dale, R., Sáez, D.: Phys. Rev. D **85**, 124047 (2012).
5. Bardeen, J.M.: Phys. Rev. D **22**, 1882 (1980).
6. Seljak, U., Zaldarriaga, M.: Astrophys. J. **469**, 437 (1996).
7. Ma, C.P., Bertschinger, E.: Astrophys. J. **455**, 7 (1995).
8. Dale, R., Sáez, D.: Astrophys. Space Sci. **337**, 439 (2012).

# General Relativistic Simulations of the Collapsar Scenario

**Nicolas de Brye, Pablo Cerdá-Durán, Miguel Ángel Aloy, and José Antonio Font**

**Abstract** We are exploring the viability of the collapsar model for long-soft gamma-ray bursts. For this we perform state-of-the-art general relativistic hydrodynamic simulations in a dynamically evolving space-time with the CoCoNuT code. We start from massive low metallicity stellar models evolved up to core gravitational instability, and then follow the subsequent evolution until the system collapses forming a compact remnant. A preliminary study of the collapse outcome is performed by varying the typical parameters of the scenario, such as the initial stellar mass, metallicity, and rotational profile of the stellar progenitor. 1D models (without rotation) have been used to test our newly developed neutrino leakage scheme. This is a fundamental piece of our approach as it allows the central remnant (in all cases considered, a metastable high-mass neutron star) to cool down, eventually collapsing to a black hole (BH). In two dimensions, we show that sufficiently fast rotating cores lead to the formation of Kerr BHs, due to the fall-back of matter surrounding the compact remnant, which has not been successfully unbounded by a precedent supernova shock.

## 1 Introduction

Gamma-ray bursts (GRBs), routinely discovered by means of onboard satellite observatories, are one of the most luminous astrophysical events known. As they do not repeat, they must be catastrophic events. The tremendous energy and high variability at stake hint at the long GRBs to be sequels of the formation process of hyper-accreting stellar mass BHs. Thus we will focus on modelling massive rotating

N. de Brye (✉) · P. Cerdá-Durán · M.Á. Aloy · J.A. Font
Departamento de Astronomía y Astrofísica, Universidad de Valencia, 46100 Burjassot (Valencia), Spain
e-mail: nicolas.de-brye@uv.es

A. García-Parrado et al. (eds.), *Progress in Mathematical Relativity, Gravitation and Cosmology*, Springer Proceedings in Mathematics & Statistics 60,
DOI 10.1007/978-3-642-40157-2_30, 

progenitor stars collapsing to BH and developing a thick accretion disk in their vicinity.

The art of creating a collapsar model is based on selecting the physics playing an allegedly key part in the process. Still, it has to be simplified with approximations to be able to simulate it on reasonable CPU times. The final fate of a massive star is a quite complex process, whose prevailing conditions involve the fundamental interactions of nature. These are (a) gravity, modelled with general relativity (GR), approximated by the conformally flat condition [1,3,11], which is exact for spherical symmetry; (b) the weak interaction between baryonic matter and leptons, modelled with selected deleptonization processes, that are approximated with a parametric fit [5] for the collapse phase, and an energy-gray leakage scheme for the post-bounce evolution; (c) the strong nuclear interaction between baryonic particles, for which we employ a microphysical equation of state (EoS) [4]; and (d) electromagnetism, not included in this work, that would be modelled with the MHD theory in the GR framework, and whose implications are promising for explaining the stellar matter accretion energy transformation into the GRB jet kinetic energy.

Technically, as the central singularity *begins* to form, one need to prescribe a procedure to follow the space-time hypervolume which will end up inside of the event horizon. Thus, we need to implement an apparent horizon (AH) finder.

Finally, we perform a number of 2D simulations with CoCoNuT [2], in order to include rotation (breaking the initial spherical symmetry). We will show that rotating models naturally develop convective motions as well as a handful of hydrodynamic instabilities, such as the standing accretion shock instability (SASI). Hereafter, we briefly describe the deleptonization schemes employed and discuss some preliminary spherical symmetry and 2D equatorial symmetry results.

## 2 Deleptonization Schemes

The deleptonization schemes employed make the neutrino physics enter the local hydrodynamics conservation equations in the form of source terms: the nuclear composition change rate, and the energy-momentum exchange between the fluid and the radiative neutrino field.

The pre-supernova (SN) initial model starts collapsing due to its baryon self-gravity. In this hot dense matter, the weak interaction processes timescale becomes smaller than the dynamical timescale, and the core begins deleptonizing mainly by electron captures, which yields a copious amount of neutrinos that escape out of the core. As the collapse proceeds and the density rises ($\sim 4\,10^{11}\,\mathrm{g\,cm^{-3}}$), these neutrinos become trapped, forming a neutrinosphere a few milliseconds before core bounce. In the trapped core region, neutrinos thermalize by scattering, and diffuse out, a process that we include with the Liebendörfer prescription [5] that reproduces the consequences of the delicate neutrino thermalization-diffusion process. A fit of the electron fraction as a function of the density (obtained in spherical symmetry simulations including full neutrino transport) permits deleptonizing in a reasonably

realistic way up to bounce. The electron fraction loss and entropy changes are deduced from this fit.

Once the saturation density ($2\,10^{14}\,\mathrm{g\,cm^{-3}}$) of nuclear matter is reached, the strong nuclear interaction suddenly turns matter more incompressible, and a shock wave forms. In this post-bounce phase, the previous Liebendörfer fit cannot reproduce the deleptonization, and a neutrino leakage scheme based on [7, 9, 10] serves as another neutrino cooling approximation. It relies upon splitting up the stellar core interior in two regions: one denser, where the neutrino diffusion timescale is longer than the dynamical timescale (neutrinos are trapped and reach β-equilibrium at center, e.g. $\dot{Y}_e = \partial_t Y_e = 0$), and another less dense beyond the neutrinosphere where neutrinos stream out freely. In the intermediate semi-transparent region, an empirical opacity-based interpolation allows us approximating the neutrino transport. Of course, this approximation to the true (much more costly) neutrino radiative transport shall be regarded as a first step towards implementing more elaborated schemes.

The neutrino interactions treated in this leakage, exchanging energy and/or lepton number, are charged current β-processes on nucleons and nuclei, neutral current elastic scattering on nucleons and nuclei, and thermal neutrino-pair production-absorption with electron–positron pair and transversal plasmon decay. The neutral current neutrino-electron inelastic scattering cannot be properly included in this energy-gray leakage scheme. However, this process is only important before the shock breaks through the neutrinosphere, i.e. in a dynamical phase where we are using the Liebendörfer prescription, where the aforementioned microphysics is properly included. The opacity is mainly due to scattering in this first phase, and then due to absorption-emission in the second phase.

## 3 Results and Discussion

We have improved the leakage scheme of [7] to match GR simulations of the G15 model [6] with full Boltzmann transport up to 250 ms after bounce. We have performed simulations of several progenitor models of [12] to test for mass and metallicity effects. Models with initial iron core mass just above the Chandrasekhar mass form an AH very late (between 3 and 5 s after core bounce). The reason is the very small accretion rate onto the newly formed proto-neutron star (PNS). Nevertheless, over such long periods, the validity of our neutrino transport approximation is doubtful, since a proper transport scheme may well yield a successful SN explosion. Thus our models predictions regarding late BH formation shall be taken with special care. We have checked that, in agreement with previous studies [8], the heavier the core, the faster the AH forms. In the sample of initial models at hand, the heaviest cores correspond to stars with the lower metallicity. Indeed, the observed trend confirms that the most likely progenitor stars producing collapsars are the low metallicity ones, which correlate with those having the most massive iron cores. It is also worth mentioning that our simulations did not lead to direct collapse

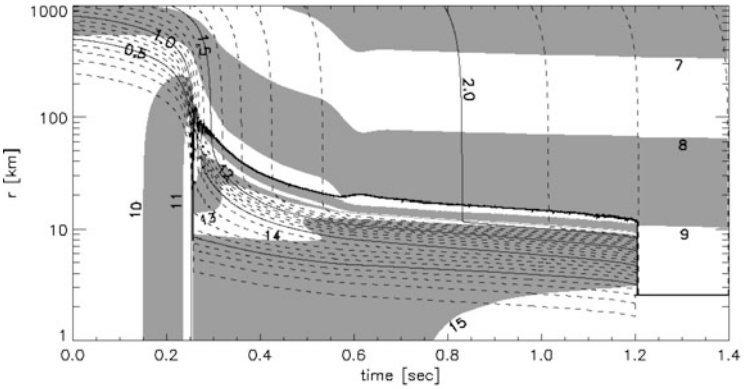


**Fig. 1** Time evolution, for model s40 on the first 1,000 km, of the shock radius (*thick solid line*), the isopycnal positions of $10^7$–$10^{15}$ g cm$^{-3}$ (*grey strip contours*), and the equal enclosed mass positions of 0.1–2.0 $M_\odot$ in steps of 0.1 $M_\odot$, and 2.0–2.15 $M_\odot$ in steps of 0.05 $M_\odot$ (*solid* and *dashed lines*). The *bottom-right corner* corresponds to the excised region within the AH

to a BH even for the most massive models of 75 $M_\odot$; all BH formation happened by post-bounce accretion, and driven by neutrino-cooling. Figure 1 shows the 1D space-time evolution of the pre-SN initial model s40, employing the LS180 EoS during the collapse phase up to 0.257 s, the PNS phase to 1.206 s, and the BH phase.

After having optimized our leakage scheme, we are currently obtaining a grid of numerical models with an ad hoc rotational profile on top of 1D stellar progenitors. Preliminary results show that convection and SASI develop in the stellar cores, delaying the AH formation. However, a Kerr BH eventually forms, and the centrifugal barrier halts the accretion onto it, yielding the formation of a thick accretion disk. More detailed results of this process will be subject of a future publication.

**Acknowledgements** This work was supported by the Spanish Ministry of Education (AYA2010-21097-C03-01), the European Research Council (STG-ERC-259276-CAMAP) and the Generalitat Valenciana (PROMETEO-2009-103).

## References

1. Cordero-Carrión, I., Ibáñez, J. M., & Morales-Lladosa, J. A., J. Math. Phys. **52**, 112501 (2011)
2. Dimmelmeier, H., Novak, J., Font, J. A., Ibáñez, J. M., Müller, E., Phys. Rev. D **71**, 064023 (2005)
3. Isenberg J. A., Int. J. Modern Phys. D **17**, 265 (2008)
4. Lattimer, J. M., & Douglas Swesty, F., Nuclear Physics A **535**, 331 (1991)
5. Liebendörfer, M., ApJ **633**, 1042 (2005)
6. Liebendörfer, M., Rampp, M., Janka, H.-T., & Mezzacappa, A., ApJ **620**, 840 (2005)
7. O'Connor, E., & Ott, C. D., Classical and Quantum Gravity **27**, 114103 (2010)

8. O'Connor, E., & Ott, C. D., ApJ **730**, 70 (2011)
9. Rosswog, S., & Liebendörfer, M., MNRAS **342**, 673 (2003)
10. Ruffert, M., Janka, H.-T., & Schäfer, G., A&A **311**, 532 (1996)
11. Wilson, J. R., Mathews, G. J., & Marronetti, P., Phys. Rev. D **54**, 1317 (1996)
12. Woosley, S. E., Heger, A., & Weaver, T. A., Reviews of Modern Physics **74**, 1015 (2002)

# Cleaning Up a Tiny Part of the Exact Solution's Augean Stable

**Liselotte De Groote**

**Abstract** In the past century many exact solutions of Einstein's field equations have been found and published. Some of these publications contain metrics which are *not* solutions of the Einstein field equations. This is due to typing errors in the one-forms or metrics, to the introduction of mysterious new coordinates after having carried out calculations in a different coordinate system or to the presentation of incorrect or incomplete solutions of some non-linear differential equations, etc. Also, many publications contain sets of supposedly different solutions to a given problem, which at a closer look can be seen to be special cases of others. As examples we look at the Newman Tamburino vacuum solutions and at the twisting type $D$ solutions published by Frolov and Khlebnicov.

## 1 Introduction

Publications of exact solutions often contain redundancies in the sense that line-elements are presented which are special cases of others, or that they contain non-distinguishing free functions or constants. As an example we look at the Robinson Trautman pure radiation metrics of Petrov type $D$, published by Frolov and Khlebnicov [3]. Eight of their metrics can be shown to be special cases of one single form. This form, in [5], contains five free functions, where we only expect four.

Apart from redundancy some publications also contain mistakes. Often this is due to typing errors, but sometimes more fundamental errors are made: non-linear differential equations are not given their most general solution, coordinate transformations are not performed in a correct way, etc.

L. De Groote (✉)
Department of Mathematical Analysis, Ghent University, Galglaan 2, S22, 9000 Ghent, Belgium
e-mail: ldgroote@cage.ugent.be

A. García-Parrado et al. (eds.), *Progress in Mathematical Relativity, Gravitation and Cosmology*, Springer Proceedings in Mathematics & Statistics 60,
DOI 10.1007/978-3-642-40157-2_31, 

Why is that a problem? First of all, publications are often cited or referred to. Solutions are copied in reference works, such as [5]. If the original papers or the formulae and expressions in the reference works contain errors or redundancy, this creates a puzzle for authors trying to construct a generalisation of these solutions, as it becomes (nearly) impossible to obtain the old metrics as limiting cases of any new one. Therefore it would be necessary for those who are looking for new exact solutions to first check the results that were published before. A second occasion where redundancy causes problems, is in the context of equivalence of metrics: do two metrics, in different coordinate systems, describe the same geometry, and are in fact the same? Particularly when a former publication presents a solution with *more* free functions than a later one, the second author might think his solution is less general than the first one, where actually his solution, with fewer free functions or constants, is equivalent to the previous. This will become more clear in Sect. 3.

## 2 Frolov and Klebnicov

In 1975 Frolov and Khlebnicov investigated non-twisting Petrov type $D$ pure radiation fields. These solutions belong to the Robinson Trautman class, and together with the solutions in [2] they give all aligned Petrov type $D$ pure radiation metrics. In the original paper [3], the solutions are divided into three classes: A, B and C, of which the A and B-classes are further subdivided into three and five subclasses, respectively. As shown in [5], the C-class in the original paper is incorrect. It is also shown there that both A- and B-classes can be combined into one form for the line-element:

$$\mathrm{d}s^2 = \frac{2r^2\mathrm{d}\zeta\mathrm{d}\bar{\zeta}}{P^2} - 2\mathrm{d}u\mathrm{d}r - \left[\Delta \log P - 2r(\log P)_{,u} - \frac{2m(u)}{r}\right]\mathrm{d}u^2, \quad \Delta \equiv 2P^2\partial_\zeta\partial_{\bar{\zeta}} \tag{1}$$

where $P = a(u)\zeta\bar{\zeta} + b(u)\zeta + \bar{b}(u)\bar{\zeta} + e(u)$, with $a(u)$, $e(u)$ and $m(u)$ real functions of $u$ and $b(u)$ a complex function of $u$.

One important remark remains: in (1) five free real functions of $u$ appear, while a GHP-analysis [1] shows that one would only expect four distinguishing functions. Therefore a coordinate transformation should exist, which eliminates one of them. Indeed, if $e(u) \neq 0$, one can easily make it equal to one by replacing $a(u)$, $b(u)$ and $r$ by $\tilde{a}(u)\,e(u)$, $\tilde{b}(u)\,e(u)$ and $\tilde{r}\,e(u)$ and by next introducing a new coordinate $u$ for which $\mathrm{d}u = \mathrm{d}\tilde{u}/e(u)$. Absorbing a factor $(e(\tilde{u}))^{-3}$ in $m(\tilde{u})$ then eliminates $e(\tilde{u})$.

## 3 Newman Tamburino Solutions

In 1961 Newman and Tamburino investigated vacuum solutions for metrics which have non-vanishing shear and divergence, and are further characterised by the existence of a hypersurface orthogonal and geodesic principal null direction [4].

They tried to generalise the Robinson Trautman solutions to the shearing case. However, insisting that the shear is non-zero leads to extra conditions, not present in the shearfree case, thus preventing the finding of the Robinson Trautman solutions as a limit.

The Newman Tamburino solutions are divided into two classes, called cylindrical or spherical,[1] according to whether $\rho^2 = \sigma\overline{\sigma}$ or $\rho^2 \neq \sigma\overline{\sigma}$. In the original paper there is redundancy in the spherical class, which, as far as the author is aware, was not noticed before. On the other hand, there are mistakes in the cylindrical class, as was shown by A. Barnes (private communication) independently from the author's calculations. Furthermore it is possible to write the cylindrical metric in a nicer form, without elliptic functions.

Let us first consider the spherical solutions, published in [4] as follows:

$$g^{22} = \frac{2rL}{A} - \frac{2r^2\sqrt{\zeta\overline{\zeta}}}{r^2-a^2} + \frac{2r^2A\left(r\left(\zeta^2+\overline{\zeta}^2\right) - 2A\left(\zeta\overline{\zeta}\right)^{3/2}\right)}{\left(r^2-a^2\right)^2}, \quad g^{12} = 1, \tag{2}$$

$$g^{23} = 4A^2x\left(\zeta\overline{\zeta}\right)^{3/2}\left(\frac{L}{2a^3} - \frac{r-2a}{2a^2\left(r^2-a^2\right)} - \frac{r-a}{\left(r^2-a^2\right)^2}\right), \quad g^{33} = \frac{-2\left(\zeta\overline{\zeta}\right)^{3/2}}{(r+a)^2}$$

$$g^{24} = 4A^2y\left(\zeta\overline{\zeta}\right)^{3/2}\left(\frac{L}{2a^3} - \frac{r+2a}{2a^2\left(r^2-a^2\right)} - \frac{r+a}{\left(r^2-a^2\right)^2}\right), \quad g^{44} = \frac{-2\left(\zeta\overline{\zeta}\right)^{3/2}}{(r-a)^2}$$

where $A$ is either a real constant or proportional to $u$ and

$$a = A(\zeta\overline{\zeta})^{1/2}, \qquad \zeta = x + \mathrm{i}y, \qquad 2L = \log\left((r+a)/(r-a)\right). \tag{3}$$

We show that both forms can be written in one single form:

$$\mathrm{d}s^2 = \frac{c-2L}{2\sqrt{x^2+y^2}}\Big[2r(x^2+y^2) + (c-2L)\Big((r+1)^2x^2 + (r-1)^2y^2\Big)\Big]\mathrm{d}u^2 + \frac{1}{2}\frac{(r+1)^2}{\sqrt{x^2+y^2}}\mathrm{d}x^2 \tag{4}$$

$$-\left[2\sqrt{x^2+y^2}\mathrm{d}r - \frac{(r+1)^2x}{\sqrt{x^2+y^2}}(c-2L)\,\mathrm{d}x - \frac{(r-1)^2\,y}{\sqrt{x^2+y^2}}(c-2L)\mathrm{d}y\right]\mathrm{d}u + \frac{1}{2}\frac{(r-1)^2}{\sqrt{x^2+y^2}}\mathrm{d}y^2.$$

To see this, first apply the coordinate transformation $r \to a\tilde{r}$ to the original metric (2)–(3). If $A$ is proportional to $u$ also apply a coordinate transformation

$$x \longrightarrow 64(\tilde{x}u^2c^2)^{-1}, \qquad y \longrightarrow 64(\tilde{y}u^2c^2)^{-1}.$$

[1] The terminology refers to the geometry of the $u$ = *constant*, $r$ = *constant* surfaces (using the original coordinates), which admit a single Killing vector in the "cylindrical" class and which resemble distorted spheres in the "spherical" class.

Next, replace $u$ by $\exp(-3\tilde{u}/64)$ and $c = 3\tilde{c}/2$. The corresponding line-element is then identical to (4).

If $A$ is a constant scale $x$ and $y$ by a factor $A^{-2}$ and $u$ by a factor $A$ in order to put $A = B$ equal to one. The corresponding line-element is then precisely (4) for $c = 0$.

This shows that both spherical metrics can be written in a single form (4).

An even more interesting result can be found when considering the cylindrical metric. First of all, this metric is wrong in [4], as well as in both editions of [5]. In all three publications different mistakes occur, leading to metrics which are not vacuum solutions of the Einstein field equations. The correct version of the general cylindrical vacuum metric is the following:

$$\begin{aligned} \mathrm{d}s^2 = &\left[\left(4 + cn^4\left(\log r^2\right)^2 + \log(r^2 cn^4)\right) b^2 + c\right]/cn^2 \mathrm{d}u^2 - 2\mathrm{d}r\,\mathrm{d}u \\ &+ \left(r^2/2 + 8u^2 b^4\left(1 - cn^4\right)\right)\mathrm{d}x^2 + 4cn\sqrt{2}u\sqrt{1-cn^4}b^2\mathrm{d}x\mathrm{d}y + cn^2\mathrm{d}y^2 \\ &+ 2\sqrt{2}b\left(2u\,cn^2 b^2\log r^2 + r\right)\sqrt{1-cn^4}/cn\mathrm{d}x\mathrm{d}u + 2cn^2 b\log r^2\mathrm{d}y\mathrm{d}u, \end{aligned} \tag{5}$$

where $b, c \in \mathbb{R}$, and where $cn = cn(bx)$ is a Jacobi elliptic function for which

$$\mathrm{d}cn/\mathrm{d}x = -b\sqrt{(1-cn^4)/2}, \qquad \mathrm{d}^2 cn/\mathrm{d}x^2 = -b^2 cn^3. \tag{6}$$

The misprint in the original paper is to be found in the coefficient of $\mathrm{d}x^2$. In [4] the authors also determine the Sachs metric as a limiting case of (5)[2]:

$$\mathrm{d}s^2 = \left(\log\left(r^2x^4\right) - g\right)/x^2\mathrm{d}u^2 - (2\mathrm{d}r + 4r/x\mathrm{d}x)\,\mathrm{d}u + x^2\mathrm{d}y^2 + r^2\mathrm{d}x^2, \qquad g \in \mathbb{R}$$

Now look at the general cylindrical vacuum metric (5) which contains two constants, $b$ and $c$, and is written out by making use of an elliptic function $cn(bx)$. We show that one of the constants is redundant, and that it is possible to write the line-element without elliptic functions. Apply the coordinate transformation

$$y \to \sqrt{2}\tilde{y}/2 + b\,u\log(2cn^4/b^2), \qquad r \to -\sqrt{2}b\tilde{r}/(2cn^2),$$

use $cn$ as coordinate $x$ (taking into account (6)), replace $u = \sqrt{2}\tilde{u}/(2b)$, introduce a new constant $c = b^2(-a - 4 - \log(b^2/2))$, and drop the tildes:

$$\mathrm{d}s^2 = \frac{x^4\left(\log r^2\right)^2 - \log r^2 - a}{2x^2}\mathrm{d}u^2 + \frac{\mathrm{d}u\mathrm{d}r}{x^2} + x^2\log r^2\mathrm{d}u\mathrm{d}y + \frac{x^2\mathrm{d}y^2}{2} + \frac{r^2\mathrm{d}x^2}{2x^4(1-x^4)}.$$

[2]Note that $g$ can always be put equal to zero, and is therefore redundant. To see this, scale $r$ and $y$ by a factor $\exp(-g/2)$ and $x$ and $u$ by a factor $\exp(g/2)$.

This metric is easier to use than the original one, for example in the context of equivalence of metrics or to find it as a limiting case of charged metrics [1].

## References

1. De Groote, L.: Einstein Maxwell solutions of Newman Tamburino class and Aligned pure radiation Kundt solutions. Ugent PhD thesis (2012)
2. De Groote, L., Van den Bergh, N., Wylleman, L.: Petrov type *D* pure radiation fields of Kundt's class. J. Math. Phys. **51**, 102501 (2010)
3. Frolov, V.P., Khlebnikov, V.I.: Gravitational field of radiating systems. I. Twisting free type D metrics. Preprint no. 27, Lebedev Phys. Inst. Ak ad. Nauk. Moscow (1975)
4. Newman, E., Tamburino, I.: Empty space metrics containing hypersurface orthogonal geodesic rays. J. Math. Phys. **3**, 902–907 (1962)
5. Stephani, H., Kramer, D., MacCallum, M.A.H, Hoenselaers, C. and Herlt, E.: Exact solutions of Einstein's field equations. Cambridge : Cambridge University Press (2003)

# Towards Degeneracy Problem Breaking by Large Scale Structures Methods

**Álvaro de la Cruz Dombriz**

**Abstract** An arguable aspect of the modified gravity theories is that many of them present the so-called *degeneracy problem*. For instance, the cosmological evolution, gravitational collapse and the main features of standard black-hole configurations, can be mimicked by many of those theories. In this communication we revise briefly the appropriate observable quantities to be measured in order to discard alternative theories to $\Lambda$CDM, such as the observed growth of scalar perturbations with Sloan data and the CMB tensor perturbations evolution.

## 1 Introduction

Modified gravity [1] has been shown to be able to mimic both the dark energy (DE) and the inflationary eras [2]. However the use of large scale observations, such as Ia type supernova, baryon acoustic oscillations, or the cosmic microwave background (CMB), which only depend upon the expansion history of the Universe is not enough to determine uniquely the nature and the origin of DE. Let us rephrase the argument: identical cosmological background evolutions can be explained by a pleiad of theories. This is the so-called *degeneracy problem*, whose breaking requires measurements not only sensitive to the cosmological expansion but, for instance, the evolution of scalar perturbations [3], the stability of cosmological solutions when subjected to small perturbations [4] and the existence of General Relativity (GR)-predicted astrophysical objects such as black holes [5]. Finally, the study of CMB tensor perturbations may also shed some light about the viability of modified gravity theories [6–11].

Á. de la Cruz Dombriz (✉)
Astronomy, Cosmology and Gravity Center (ACGC) and Department of Mathematics—Applied Mathematics, University of Cape Town, Rondebosch 7700, South Africa
e-mail: alvaro.delacruzdombriz@uct.ac.za

A. García-Parrado et al. (eds.), *Progress in Mathematical Relativity, Gravitation and Cosmology*, Springer Proceedings in Mathematics & Statistics 60,
DOI 10.1007/978-3-642-40157-2_32, 

In this realm, the simplest and in fact the most studied modification of the Hilbert–Einstein action is generalized to a general function of the Ricci scalar $R$, dubbed $f(R)$ gravity theories [12, 13] whose action can be written as >

$$\mathscr{A} = \frac{1}{16\pi G}\int \mathrm{d}^4x\sqrt{-g}\,(R + f(R) + 2\mathscr{L}_m), \tag{1}$$

where the symbols hold their usual meanings. In addition to reproducing the entire cosmological history [14] and despite some shortcomings [13], these theories may behave quite well on local scales, where the GR limit must be recovered [15]. As for any alternative theory of gravity, in $f(R)$ theories, the density contrast evolution, the CMB perturbations and the backreaction mechanism [16], if the latter is assumed to be true, need to be studied in order to unveil the potential distinct features of these scenarios. In the present investigation we sketch the main features and steps to study the two first issues in $f(R)$ theories.

## 2 Scalar Perturbations in $f(R)$ Theories

The density contrast evolution for $f(R)$ theories obeys a fourth-order differential equation [17]. The resulting equation for the density contrast $\delta$ can be written as follows:

$$\begin{aligned}&\beta_{4,f}\delta^{iv} + \beta_{3,f}\delta''' + (\alpha_{2,EH} + \beta_{2,f})\delta'' + (\alpha_{1,EH} + \beta_{1,f})\delta' \\ &\quad +(\alpha_{0,EH} + \beta_{0,f})\delta = 0\end{aligned} \tag{2}$$

where the coefficients $\beta_{i,f}$ $(i = 1,\ldots,4)$ involve terms that disappear for $f(R)$ functions linear in $R$ (i.e., GR) whereas $\alpha_{i,EH}$ $(i = 0,1,2)$ involve the linear part in $R$ of $f(R)$. Thus, the quasi-static limit ($k >> \mathscr{H}$) of (2) becomes [17]

$$\begin{aligned}&\delta'' + \mathscr{H}\delta' + \frac{(1+f_R)^5\mathscr{H}^2(-1+\kappa_1)(2\kappa_1-\kappa_2) - \frac{16}{a^8}f_{RR}^4(\kappa_2-2)k^8 8\pi G\rho_0 a^2}{(1+f_R)^5(-1+\kappa_1) + \frac{24}{a^8}f_{RR}^4(1+f_R)(\kappa_2-2)k^8} \\ &\quad \delta = 0\end{aligned} \tag{3}$$

Contrarily to its counterpart for $\Lambda$CDM, the coefficients in (2) depend both upon the model under consideration and the wavenumber $k$. This fact gives rise to $k$-dependent transfer functions that may alter dramatically the matter power spectra [17–19]. Available data [20] using luminous red galaxies in the Sloan Digital Sky Survey (SDSS) were able to measure the large-scale real-space power spectrum. These measurements were used to sharpen the constraints on cosmological parameters [21] and may be straightforwardly compared with the predictions made by gravity theories [18, 22]. Very recently a full study for the $R^n$ models [19] have stressed the importance of the initial conditions in the perturbed equations which

determine the evolution of the transfer function. Consequently, this method provides an excellent arena to impose tight constraints for modified gravity models that are claimed to be valid once compared with existing and future data [23].

## 3 CMB Perturbations in $f(R)$ Theories

The study of the CMB tensor perturbations in modified gravity theories has not received much interest in comparison with the scalar counterpart. This fact has laid in the difficulty of obtaining the required tensor perturbed equations which are in general of higher order. An alternative route in order to circumvent this difficulty consists of tackling the problem by using the simulations performed by several codes available such as CAMB [24] based upon modifications of CMBFast [25].

Different attempts were made for several modified gravity scenarios [8] but most of the attention was devoted to the study of the tensor perturbations evolution in the brane-world theories context [9, 10]. Finally, with regard to $f(R)$ fourth order gravity theories, the only attempts to encapsulate the main features of tensor perturbation were made in [11] and more recently in [6, 7]. The authors of the first investigation analyzed the tensor perturbations of flat thick domain wall branes in $f(R)$ gravity. They showed that under the transverse and traceless gauge, the metric perturbations decouple from the perturbation of the background scalar field which generates the brane. Authors in [6, 7] addressed for the first time in literature the tensor perturbations full calculations for the $f(R)$ gravity theories in the metric formalism and Jordan frame. These general results were applied to $R^n$ models for different values of $n$ describing the features that may distinguish those models from Concordance model predictions. This implementation proved the importance of considering the correct background when alternative theories of gravity are subjected to this kind of analyses since a relevant contribution to the $c_l^{\mathrm{TT}}$ and $c_l^{\mathrm{EE}}$ CMB coefficients comes from the background implementation.

Thus, exclusions tests for $f(R)$ models can be performed since data for $c_l^{\mathrm{TT}}$ are already available from WMAP [26] once the scalar contribution are also included. With respect to $c_l^{\mathrm{EE}}$ once Planck [27] measurements are ready, some data may be compared with theoretical predictions.

**Acknowledgements** The author acknowledges financial support from URC and NRF (South Africa), MICINN (Spain) project numbers FIS2011-23000, FPA2011-27853-C02-01 and Consolider—Ingenio MULTIDARK CSD2009-00064.

## References

1. S. Nojiri and S. D. Odintsov, Int. J. Geom. Meth. Mod. Phys. **4**, 115 (2007); T. P. Sotiriou and V. Faraoni, Rev. Mod. Phys. **82** 451 (2010); F. S. N. Lobo, arXiv:0807.1640 [gr-qc]; S. Capozziello and V. Faraoni, *Beyond Einstein Gravity*, Springer Ed., Dordrecht (2011). A. Dobado and A. L. Maroto *Phys. Rev.* **D 52** 1895 (1995). G. Dvali, G. Gabadadze and

M. Porrati *Phys. Lett.* **B 485** 208 (2000). J. Beltrán and A. L. Maroto *Phys. Rev.* **D 78** 063005 (2008); *JCAP* **0903** 016 (2009) ; *Phys. Rev.* **D 80** 063512 (2009); *Int. J. Mod. Phys.* **D 18** 2243–2248 (2009).
2. S. Nojiri and S. D. Odintsov, Phys. Rev. D **74** 086005 (2006); E. Elizalde and D. Sáez-Gómez, Phys. Rev. D **80**, 044030 (2009); S. Nojiri, S. D. Odintsov and D. Sáez-Gómez, Phys. Lett. B **681**, 74 (2009); S. A. Appleby, R. A. Battye and A. A. Starobinsky, JCAP **1006**, 005 (2010);
3. J. M. Bardeen, Phys. Rev. D22 1882 (1980); S. M. Carroll, I. Sawicki, A. Silvestri and M. Trodden, New J. Phys. 8 323, (2006); Y. S. Song, W. Hu and I. Sawicki, Phys. Rev. D 75 044004, (2007); A. A. Starobinsky, JETP Lett. 86, 157 (2007); S. Carloni, P. K. S. Dunsby and A. Troisi, Phys. Rev. D 77 024024, (2008); A. Abebe, M. Abdelwahab, A. de la Cruz-Dombriz and P. K. S. Dunsby, Class. Quant. Grav. **29** 135011 (2012).
4. A. de la Cruz-Dombriz and D. Sáez-Gómez, Class. Quant. Grav., **29** 245014, 2012.
5. G. J. Olmo, Phys. Rev. D 75, 023511 (2007); A. M. Nzioki, S. Carloni, R. Goswami and P. K. S. Dunsby, Phys. Rev. D81 084028 (2010); A. de la Cruz-Dombriz, A. Dobado and A. L. Maroto, Phys. Rev. D 80, 124011 (2009) [Erratum: Phys. Rev. D 83, 029903(E) (2011)]; J. Phys. Conf. Ser. **229** (2010) 012033; J. A. R. Cembranos, A. de la Cruz-Dombriz and P. Jimeno Romero, e-Print: arXiv:1109.4519 [gr-qc]; AIP Conf. Proc. 1458, 439 (2012).
6. H. Bourhrous, A. de la Cruz-Dombriz, and P. K. S. Dunsby, AIP Conf. Proc. **1458**, 343 (2012).
7. M. Abdelwahab, H. Bourhrous, A. de la Cruz-Dombriz, and P. K. S. Dunsby, in preparation.
8. N. Bevis, M. Hindmarsh, M. Kunz and J. Urrestilla, Phys. Rev. D **75**, 065015 (2007); S. Foreman, A. Moss and D. Scott, Phys. Rev. D **84**, 043522 (2011); J. Urrestilla, N. Bevis, M. Hindmarsh and M. Kunz, JCAP **1112**, 021 (2011); Phys. Rev. D **82**, 065004 (2010); C. Ringeval, Adv. Astron. **2010**, 380507 (2010); C. Ringeval and F. R. Bouchet, Phys. Rev. D **86**, 023513 (2012).
9. R. A. Battye, C. Van de Bruck and A. Mennim, Phys. Rev. D **69** 064040 (2004); R. Easther, D. Langlois, R. Maartens and D. Wands, JCAP **0310** 014 (2003).
10. B. Leong, A. Challinor, R. Maartens and A. Lasenby, Phys. Rev. D **66** 104010 (2002).
11. Y. Zhong, Y. -X. Liu and K. Yang, Phys. Lett. B **699**, 398 (2011)
12. A. A. Starobinsky *Phys. Lett.* **91B** 99 (1980); S. Nojiri and S. Odintsov *Phys. Rev.* **D 68** 123512 (2003); *Gen. Rel. Grav.* **36** 1765 (2004); S. M. Carroll *et al*, *Phys. Rev.* **D71** 063513 (2005); S. Carloni, P. K. S. Dunsby, S. Capozziello and A. Troisi *Class. Quant. Grav.* **22** 4839 (2005). J. A. R. Cembranos *Phys. Rev.* **D 73** 064029 (2006); Phys. Rev. Lett. **102** 141301 (2009); T. Clifton and J. D. Barrow *Phys. Rev.* **D 72** 103005 (2005); D. Sáez-Gómez, Gen. Rel. Grav. **41**, 1527 (2009); P. K. S. Dunsby it et al., Phys. Rev. D **82**, 023519 (2010).
13. T. Clifton *et al.*, Phys. Rept. **513**, 1 (2012).
14. A. de la Cruz-Dombriz and A. Dobado, Phys. Rev. D **74**, 087501 (2006)
15. W. Hu and I. Sawicki, Phys. Rev. D **76**, 064004 (2007); L. Pogosian and A. Silvestri, Phys. Rev. D **77**, 023503 (2008); S. Capozziello and S. Tsujikawa, Phys. Rev. D **77**, 107501 (2008).
16. A. de la Cruz-Dombriz, in preparation.
17. A. de la Cruz-Dombriz, A. Dobado and A. L. Maroto, Phys. Rev. D 77 123515 (2008).
18. A. de la Cruz-Dombriz, A. Dobado and A. L. Maroto, Phys. Rev. Lett. D 103, 179001 (2009).
19. A. Abebe, M. Abdelwahab, A. de la Cruz-Dombriz and P. K. S. Dunsby, Class. Quantum Grav. **29**, 135011 (2012).
20. http://space.mit.edu/home/tegmark/sdss.html
21. M. Tegmark *et al.* [SDSS Collaboration], Phys. Rev. D **74**, 123507 (2006).
22. H. Okada, T. Totani, S. Tsujikawa, arXiv:1208.4681 [astro-ph.CO].
23. G. -B. Zhao, H. Li, E. V. Linder, K. Koyama, D. J. Bacon and X. Zhang, Phys. Rev. D **85**, 123546 (2012); A. J. Ross *et al.*, arXiv:1208.1491 [astro-ph.CO]; S. E. Nuza *et al.*, arXiv:1202.6057 [astro-ph.CO]; L. Anderson *et al.*, arXiv:1203.6594 [astro-ph.CO]; A. J. Ross *et al.*, arXiv:1203.6499 [astro-ph.CO]. C. G. Scoccola *et al.*, arXiv:1209.1394 [astro-ph.CO].
24. A. Lewis, A. Challinor, and A. Lasenby, Astrophys. J. 538, 473 (2000); A. Lewis, PhD Thesis, University of Cambridge (2000).

25. U. Seljak and M. Zaldarriaga, 1996 ApJ, 469, 437; M. Zaldarriaga, U. Seljak and E. Bertschinger, 1998 ApJ, 494, 491; M. Zaldarriaga and U. Seljak, 2000 ApJS, 129, pp 431–434.
26. N. Jarosik, C. L. Bennett, J. Dunkley, B. Gold, M. R. Greason, M. Halpern, R. S. Hill and G. Hinshaw *et al.*, Astrophys. J. Suppl. **192**, 14 (2011); E. Komatsu *et al.* [WMAP Collaboration], Astrophys. J. Suppl. **192**, 18 (2011).
27. Planck Collaboration, ESA-SCI-2005-1, arXiv: astro-ph/0604069.

# Geometric and Thermodynamic Aspects of Charged Black Holes in Nonlinear Electrodynamics

**Joaquín Díaz-Alonso and Diego Rubiera-García**

**Abstract** A brief summary of the new features and properties of four-dimensional charged black holes supported by general nonlinear models of electrodynamics minimally coupled to gravity, as compared to the usual Reissner–Nordström solution, is provided. These models are chosen as arbitrary function of the two field invariants and constrained by several physical admissibility requirements.

## 1 Introduction

It is well known that the theorems on singularities in General Relativity (GR) [1] lead to the Reissner–Nordström (RN) solution of the Einstein–Maxwell field equations as the final outcome of (nonrotating) charged matter. This solution describes the gravitational and electromagnetic fields of a collapsed spherically symmetric charged object of mass $M$ and charge $Q$, to which a system of Schwarzschild-like coordinates is adapted. Depending on whether the constraint $M^2 \geq Q^2$ is satisfied or not, the solution corresponds to a black hole (BH) with two horizons (Cauchy and event) or a naked singularity (NS) (to be ruled out from the spectrum of physically meaningful solutions by the cosmic censorship conjecture), with an extreme black hole (EBH) (defined by a single degenerate horizon) in between these two states. Deep inside the event horizon of the BH, a (timelike) singularity always dwells. However, the RN solution is not taking into account the expected effects of the quantum vacuum close to the singularity, that should modify the charge distribution

J. Díaz-Alonso · D. Rubiera-García (✉)
LUTH, Observatoire de Paris, CNRS, Université Paris Diderot. 5 Place Jules Janssen, 92190 Meudon, France

Departamento de Física, Universidad de Oviedo. Avenida Calvo Sotelo 18, 33007 Oviedo, Asturias, Spain
e-mail: joaquin.diaz@obspm.fr; rubieradiego@gmail.com

A. García-Parrado et al. (eds.), *Progress in Mathematical Relativity, Gravitation and Cosmology*, Springer Proceedings in Mathematics & Statistics 60,
DOI 10.1007/978-3-642-40157-2_33, 

of the Maxwell lagrangian leading to nonlinear electrodynamics (NED) as a more realistic description of the configuration [2]. Moreover, other NEDs (as the Born–Infeld-like ones [3]) also arise in other contexts, such as in the low-energy regime of string/D-Brane physics [4]. Thus, a definitive answer to the question of which is most appropriate NED lagrangian in describing the final state of the BH collapse is not available yet. According to this, in this work we make a short review of the new BH configurations and features that may arise when elementary solutions of general physically reasonable NEDs are considered as sources of the gravitational field.

## 2 Geometry, Singularities and Thermodynamics of NEDs

In four space-time dimensions a NED is defined by a function $\varphi(X, Y)$ of the two field invariants $X = -\frac{1}{2} F_{\mu\nu} F^{\mu\nu}$ and $Y = -\frac{1}{2} F_{\mu\nu} F^{*\mu\nu}$, which are constructed with the field strength tensor $F_{\mu\nu} = \partial_\mu A_\nu - \partial_\nu A_\mu$ and its dual $F^{*\mu\nu} = \frac{1}{2}\varepsilon^{\mu\nu\alpha\beta} F_{\alpha\beta}$. The Einstein–Maxwell action is thus modified as

$$\begin{aligned} S_{MAXWELL} &= \int d^4x \sqrt{-g} \left( \frac{1}{16\pi G} - X \right) \rightarrow S_{NED} \\ &= \int d^4x \sqrt{-g} \left( \frac{1}{16\pi G} - \varphi(X, Y) \right) \end{aligned} \tag{1}$$

so $\varphi(X, Y)_{Maxwell} = X$. The function $\varphi(X, Y)$ is assumed to be continuous and differentiable on its domain of definition, satisfy the parity invariance condition ($\varphi(X, Y) = \varphi(X, -Y)$), and fulfil the weak energy condition, requirements defining the set of *admissible* models considered here. The Einstein-NED equations for electrostatic spherically symmetric (ESS) solutions can be solved as [5]

$$ds^2 = \lambda(r) dt^2 - \lambda^{-1}(r) dr^2 - r^2 d\Omega^2 \quad ; \quad \lambda(r) = 1 - \frac{2M}{r} + \frac{2}{r}\varepsilon_{ex}(r, Q) \tag{2}$$

$$r^2 \varphi_X E(r) = Q \tag{3}$$

where $d\Omega^2 = d\theta^2 + r^2 \sin^2\theta d\phi^2$, $M$ is the ADM mass and $\varepsilon_{ex}(r, Q) = 4\pi \int_r^\infty R^2 T_t^t(R, Q) dR$, dubbed as the *external energy function*, is a monotonically decreasing function of $r$ for admissible models [6]. Restricting to NED models modifying the Coulomb behaviour near the center, we can distinguish three *admissible* ESS behaviours, namely, **UVD**, when $E(r) \sim 1/r^p$, with $p > 1$ ($p = 2$: Maxwell), **A1**, when $E(r) \sim 1/r^p$, with $0 < p < 1$ ($p = 2/3$: Euler–Heisenberg [2]), and **A2**, with $E(r) \sim a + br^q$ ($q = 4$: Born–Infeld [3]). The last two cases lead to finite energy solutions $\varepsilon(Q) = 4\pi \int_0^\infty r^2 T_t^t(r, Q) dr < \infty$ if the large-$r$ behaviour is Coulombian.

From (2) the horizons $r_h$ can be found as $M - r/2 = \varepsilon_{ex}(r, Q)$ and thus are given by the cut points between the function $\varepsilon_{ex}(r, Q)$ and the beam of straight lines $M - r/2$. Its analysis for admissible models leads to the full classification of all the available gravitating structures [6], which we summarize here.

The family **UVD** leads always to a similar BH structure as the RN solution: two-horizon BHs, EBHs or NS. A timelike singularity is always found at the center.

For the case of family **A1** there are new configurations depending on the sign of $C = M - \varepsilon(Q)$. When $C > 0$ the structure is similar as the RN one (and again a timelike singularity). But when $C < 0$ we always have a single-horizon BH, and a spacelike singularity. The case $C = 0$ requires an expansion of the metric around the center, but leads again to a spacelike singularity cloaked by a single (event) horizon.

In case **A2**, for $C \neq 0$, when $Q > Q_c = 16\pi qa$ we have either two-horizon BHs, EBHs or NS, while for $Q < Q_c$ only single-horizon BHs or NS exist. And for $C = 0$ an expansion around $r = 0$ reveals that the metric is finite everywhere, but the curvature invariants diverge also in that case (as $\sim 1/r^4$). When $Q > Q_c$ we have $g_{tt}(r = 0) < 0$, revealing the existence of a single (nondegenerate) horizon, while for $Q < Q_c$ then $g_{tt}(r = 0) > 0$ and we have a NS. The case $Q = Q_c$ leads to the so-called *"black points"* [7], which possess a rich thermodynamic behaviour [5].

Focusing now on the thermodynamics, the first law of BH thermodynamics

$$dM = T(r_h, Q)dS + \Phi(r_h, Q)dQ = T(S, Q)dS + \Phi(S, Q)dQ, \tag{4}$$

where the temperature $T$, entropy $S$, and electric potential $\Phi$, are given by

$$T = \frac{\kappa}{2\pi} = \frac{1 - 8\pi r_h^2 T_0^0}{4\pi r_h} \; ; \; S = \frac{A}{4} = \pi r_h^2 \; ; \; \Phi(r, Q) = 8\pi A_0(r, Q), \tag{5}$$

hold for asymptotically fast enough damping ($E(r \to \infty, Q) \sim r^p$), $p < -1$ [8] (see [9] for proof of the Coulombian case). Moreover, a generalized Smarr law ($M = 2TS + Q\Phi$ for Maxwell) can be obtained for any NED model as

$$M = \sqrt{S/(9\pi)} + 2(TS + Q\Phi)/3. \tag{6}$$

From the field equations for general NEDs in flat space it can be proven the existence of a multiplicative group of scale transformations between the thermodynamic variables associated to the corresponding black hole solutions. The structure of this group is the same for all NEDs and leads to new relations between these variables [5]. An example of these renormalization group-like equations is

$$\frac{\partial z}{\partial x} + \frac{\partial z}{\partial y} - 1 = 0. \tag{7}$$

where $x = \ln(Q); y = \ln(S); z = \ln(\Phi^2)$. This is a first-order, linear, partial differential equation whose system of ESS BH solutions associated to a given NED are represented by ruled surfaces generated by the beam of characteristics of these equations (here, straight lines parallel to the vector $(1, 1, -1)$ in the $(x, y, z)$ space [5]).

For the behaviour of some state variables, let us consider the case of the temperature-horizon radius $T(r_h)$. In the RN case this function begins from zero at finite $r_h = r_{hEBH}$ (corresponding to an EBH), grows up to a maximum $T_{max}(r_{hmax})$ and then it decreases as $\sim 1/r_h$ (Schwarzschild behaviour) as $r_h \to \infty$. The specific heat $C_Q = (\partial M)/(\partial T)|_Q$ splits into two phases, the first one comprised between $r_{hEBH}$ and $r_{hmax}$ with a positive value for $C_Q$, and a second one $r_h > r_{hmax}$ for which $C_Q < 0$. This behaviour is qualitatively similar for the families **UVD** and **A1**.

In case **A2**, however, the behaviour splits in three branches. When $Q < Q_c$ the behaviour is similar as in the previous case. However, when $Q > Q_c$, we have $T(r_h = 0) \to +\infty$ and either $T(r_h)$ decreases monotonically, thus $C_Q$ showing a single negative phase (similar as the Schwarzschild solution) or there is both a minimum and a maximum in $T(r_h)$, thus corresponding to three phases in $C_Q$ (negative, positive and negative, as $r_h$ grows). Finally, when $Q = Q_c$ then $T(r_h = 0) \to 0$ and $C_Q$ has a similar behaviour as the RN solution with $r_{hEBH} \to 0$.

In more general cases the sign of $dT(r_h)/dr_h$ at constant $Q$ can change many times as $r_h$ increases, leading to several minima/maxima of $T(r_h)$ and thus to more phases for $C_Q$. This behaviour can be illustrated with a family of NEDs whose ESS solutions are of the form $E(r, Q) = \frac{1}{R^2} + \frac{\alpha R^n}{(\beta + R^n)^2}$, where $R = r/\sqrt{Q}$ and $\alpha > 0$, $\beta > 0$ and the integer $n \geq 2$ being fixed constants for a given model of the family, which must satisfy $\alpha < \frac{6}{n+2}\beta^{(1-\frac{1}{n})}$ for positive definiteness of the energy density. For some combinations of the parameters (e.g. $n = 4, \alpha = 1/\beta = 1/5.2$) the temperature $T(r_h)$ exhibits three extrema, and thus $C_Q$ has four phases $(+, -, +, -)$ [5].

In summary, in RN solutions one finds BHs with either two horizons, a single (degenerate) one or a NS. The strength of this (timelike) singularity in all cases runs at $\sim 1/r^8$. The zeroth and first laws of thermodynamics, as well as the Smarr law, hold. For other physically admissible NEDs there exist, in addition, BHs with a single (nondegenerate) horizon, black points, and metrics which are finite everywhere. There is always a curvature singularity at $r = 0$ (timelike, spacelike, or null) running at a minimum divergence of $\sim 1/r^4$. The zeroth and first laws always hold, and there exists a generalized Smarr law, besides other finite relations. More involved behaviours for the temperature exist, with the possibility of many phases for $C_Q$ depending on the existence of a ESS field satisfying $E''(r) = 0$ several times [5]. As a conclusion, the problem of singularities cannot be avoided in physically reasonable NED models within GR, which motivates the stufy of generalizations of GR, such as $f(R)$ and beyond, or to consider nonabelian gauge fields.

## References

1. B. Carter, Phys. Rev. Lett. **26**, 331 (1971); R. Penrose, Riv. Nuovo Cim. Numero Speciale **1**, 252 (1969) [Gen. Rel. Grav. **34**, 1141 (2002)] S. W. Hawking and G. F. R. Ellis, *The large scale structure of space-time*; Cambridge University Press, Cambridge, UK, 1973).
2. W. Heisenberg and H. Euler, Z. Phys. **120**, 714 (1936); J. Schwinger, Phys. Rev. **82**, 664 (1951); A. Dobado, A. Gómez-Nicola, A. L. Maroto, and J. R. Peláez, *Effective Lagrangians for the Standard Model* (Springer, Berlin, 1997);
3. M. Born and L. Infeld, Proc. Roy. Soc. London. A **144**, 425 (1934).
4. E. Fradkin and A. A. Tseytlin, Phys. Lett. B **163**, 123 (1985); D. Brecher, Phys. Lett. B **442**, 117 (1998); D. Brecher and M. J. Perry, Nucl. Phys. B **527**, 121 (1998).
5. J. Diaz-Alonso and D. Rubiera-Garcia, arXiv:1204.2506 [gr-qc].
6. J. Diaz-Alonso and D. Rubiera-Garcia, Phys. Rev. D **81**, 064021 (2010).
7. H. H. Soleng, Phys. Rev. D **52**, 6178 (1995).
8. J. Diaz-Alonso and D. Rubiera-Garcia, Phys. Rev. D **82**, 085024 (2010).
9. D. A. Rasheed, hep-th/9702087.

# Properties of Holographic Dark Energy at the Hubble Length

**Ivan Duran and Luca Parisi**

**Abstract** We consider holographic cosmological models of dark energy in which the infrared cutoff is set by the Hubble's radius. We show that any interacting dark energy model, regardless of its detailed form, can be recast as a non interacting model in which the holographic parameter $c^2$ evolves slowly with time. Two specific cases are analyzed. We constrain the parameters of both models with observational data, and show that they can be told apart at the perturbative level.

## 1 Introduction

Whatever the nature of DE it seems reasonable that it fulfills the holographic principle [1]. Based on this, Li [2] proposed for the density of DE the expression

$$\rho_X = \frac{3M_P^2\, c^2}{L^2}\,. \tag{1}$$

where $c^2$ is a dimensionless parameter and $L$ the IR cutoff.

We will take $L$ as the Hubble radius, $L = H^{-1}$, see e.g. [3]. See e.g.[2, 4–7] for other choices. It has been argued that an IR cutoff defined by $H^{-1}$ cannot lead to an accelerated Universe. However, if DM and DE interact according to

$$\dot{\rho}_M + 3H\rho_M = Q \qquad \text{and} \qquad \dot{\rho}_X + 3H(1+w)\rho_X = -Q\,, \tag{2}$$

where $Q > 0$ is the interaction term, an accelerated expansion can be achieved [8].

I. Duran (✉)
Universitat Autònoma de Barcelona, Cerdanyola del Vallès, Catalonia, Spain
e-mail: ivan.duran@uab.cat

L. Parisi
Università di Salerno, 84084 Fisciano Salerno, Italy
e-mail: parisi@sa.infn.it

A. García-Parrado et al. (eds.), *Progress in Mathematical Relativity, Gravitation and Cosmology*, Springer Proceedings in Mathematics & Statistics 60,
DOI 10.1007/978-3-642-40157-2_34, 

In [9] the $c^2$ parameter was considered to increase slowly with time in such a way that $0 < \left(c^2\right)^{\cdot} \leq H$. In what follows, quantities referring to models with variable $c^2$ will be noted by a tilde. By assumption their energy densities conserve separately,

$$\dot{\tilde{\rho}}_M = -3H\tilde{\rho}_M \qquad \text{and} \qquad \dot{\tilde{\rho}}_X = -3H(1+\tilde{w})\tilde{\rho}_X \,. \tag{3}$$

By considering both points of view it was demonstrated that identical backgrounds evolutions can be described by an interacting holographic DE model, with $c^2$ strictly fixed, or by a non-interacting holographic DE model in which $\tilde{c}^2$ depends weakly on time [10]. In spite that the global evolution is identical in both scenarios, the energy densities and the EoS parameters can behave rather differently.

## 2 Proposed Models: Model 1 and Model 2

Here we consider the holographic interacting model studied in [11] in order to construct its equivalent $\tilde{c}^2(t)$ model. In the former the IR cutoff was also set by the Hubble's length and the interaction term was $Q \equiv 3AH_0\rho_M$, with $A$ a semipositive definite constant, related to the constant decay rate of DE into DM, $\Gamma$, by $A \equiv \frac{\Gamma}{3H_0 r}$, with $r \equiv \rho_M/\rho_X$. Thus, the Hubble function takes the form

$$H = H_0\left(A + (1-A)(1+z)^{\frac{3}{2}}\right), \tag{4}$$

We expand $H^2(z)$ assuming that the $(1+z)^3$ term corresponds to DM and identify the remainder of the expression as the DE energy density. Thus,

$$\frac{M_P^{-2}}{3H_0^2}\tilde{\rho}_M = (1-A)^2(1+z)^3 \qquad \textit{and} \qquad \frac{M_P^{-2}}{3H_0^2}\tilde{\rho}_X = A^2 + 2A(1-A)(1+z)^{\frac{3}{2}}, \tag{5}$$

alongside with

$$\tilde{c}^2 = \frac{2A(1-A)(1+z)^{\frac{3}{2}} + A^2}{\left(A + (1-A)(1+z)^{\frac{3}{2}}\right)^2}\,. \tag{6}$$

The best fit values are found to be $H_0 = 69.4 \pm 1.7$ and $A = 0.588 \pm 0.004$, while $\chi^2/dof = 1.00$. For details see [10]. As the top right panel of Fig. 1 shows, the coincidence problem (i.e., "why the densities of DM and DE are of the same order precisely today?") gets solved ($r$ stays constant) in the interacting case (solid green line). In the $\tilde{c}^2$ model (thin dot-dashed red lines) it is not solved but results much less severe than in $\Lambda$CDM (thick short dashed blue line).

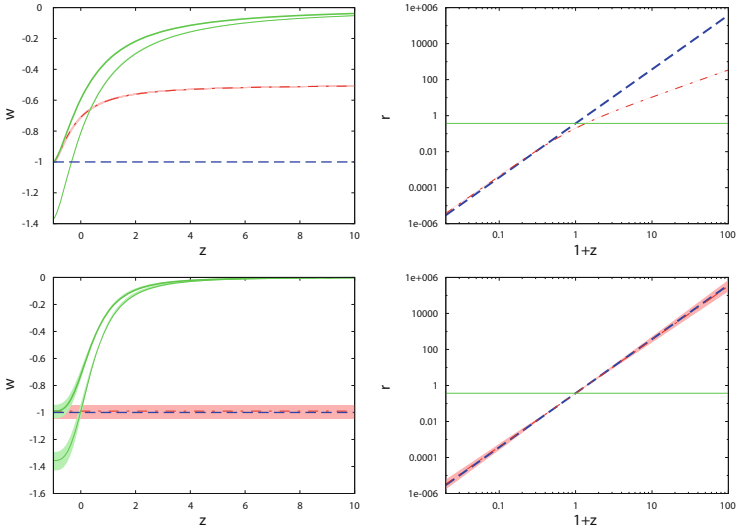


**Fig. 1** *Top panels* are for model 1 and *bottom panels* for model 2. *Left panels*: EoS parameter for the interacting (*w thin line*, and $w_{eff}$ *thick line*), the $\tilde{c}^2$ and $\Lambda$CDM models. *Right panels*: energy densities ratios, $r \equiv \rho_M/\rho_X$, versus $1+z$ for the $\Lambda$CDM, the interacting and the $\tilde{c}^2$ models. *Solid (green) lines* are used for the interacting case, *thin dot dashed (red) lines* for the $\tilde{c}^2$ model, and *thick short dashed (blue)* for $\Lambda$CDM

We next propose model 2. In this model DM and DE evolve separately but $\tilde{c}^2$ varies slowly with time. In order to have $0 \leq \tilde{c}^2 \leq 1$, and $\left(\tilde{c}^2\right)^{\cdot} \geq 0$ we define

$$\tilde{c}^2 = \frac{1}{1 + \tilde{r}_0(1+z)^{\epsilon}} \tag{7}$$

where $\tilde{r}_0 \equiv \frac{\tilde{\Omega}_{M0}}{\tilde{\Omega}_{X0}}$ and $\epsilon$ a semipositive definite constant. In this case

$$H = H_0\sqrt{\tilde{\Omega}_{M0}(1+z)^3 + \tilde{\Omega}_{X0}(1+z)^{3-\epsilon}} \tag{8}$$

is identical to a spatially flat $w$CDM model with $\tilde{w} = -\frac{\epsilon}{3}$. If we consider Eq. (8) as resulting from some interaction between DE and DM, the interacting term would be

$$Q = -3\,c^2\,w\rho_M\,H, \tag{9}$$

Detailed calculations can be found in [10]. The best fit values are $\Omega_{X\,0} = 0.73 \pm 0.007$, $H_0 = 71.5 \pm 2.6$ and $\epsilon = 2.97^{+0.16}_{-0.14}$, being $\chi^2/dof = 0.97$. As the bottom right panel of Fig. 1 shows the interacting model (solid green line) solves the coincidence problem.

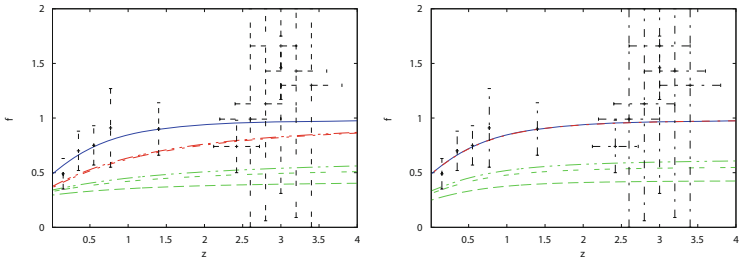


**Fig. 2** *Left panel*: evolution of the growth function, $f$, versus redshift for model 1. *Right panel*: the same for model 2. The *dashed (green) lines* describe the interacting scenario, the *dot-dashed (red) lines* the $\tilde{c}^2$, and the *solid (blue) line* the $\Lambda$CDM. The observational data were borrowed from [13]

## 3 Evolution of the Subhorizon Perturbations

In the interacting case, the energy-momentum tensors of DM and DE are not independently conserved, $T_i^{\mu\,\nu}{}_{;\mu} = Q_i^{\nu}$. For subhorizon scales, i.e., $k \gg aH$, the density and energy and momentum conservation equations simplify to

$$\dot{\delta}_M = -\frac{\theta_M}{a} \qquad and \qquad \dot{\theta}_M = -H\theta_M + \frac{k^2}{a}\phi \tag{10}$$

$$\dot{\delta}_X = -(1+w)\frac{\theta_X}{a} - 3H(1-w)\delta_X + \frac{1}{\rho_X}(Q\delta_X - \delta Q), \tag{11}$$

$$\dot{\theta}_X = \frac{1}{(1+w)}\frac{k^2}{a}\delta_X - \frac{Q}{(1+w)\rho_X}(\theta_M - 2\theta_X), \tag{12}$$

See [10] for the description of the $\delta Q$ in each model. To confront it with observations, we resort to the growth function, $f \equiv d\ln\delta_M/d\ln a$ [12]. We can see in Fig. 2, that matter density perturbations clearly different in the interacting and the $\tilde{c}^2$ scenarios.

**Acknowledgements** We are indebted to Diego Pavón, Gaetano Vilasi, Ninfa Radicella and Fernando Atrio-Barandela for fruitful discussions. ID was supported by the Spanish MICINN under Grant No. FIS2009-13370-C02-01, by the Generalitat de Catalunya under Grant No. 2009SGR-00164. LP was partially supported by the Italian MIUR through the PRIN 2008 grant.

## References

1. G. 't Hooft, "Dimensional reduction in quantum gravity", preprint gr-qc/9310026; L. Susskind, J. Math. Phys. (N.Y.) *36*, 6377 (1995).
2. M. Li, Phys. Lett. B *603*, 1 (2004).

3. S. D. H. Hsu, Phys. Lett. B *594*, 13 (2004); D. Pavón and W. Zimdahl, Phys. Lett. B *628*, 206 (2005).
4. C. Gao, F. Wu, X. Chen, and Y.G. Shen, Phys. Rev. D *79*, 043511 (2009).
5. L. Xu, W. Li, and J. Lu, Mod. Phys. Lett. A *24*, 1355 (2009).
6. M. Suwa, T. Nihei, Phys. Rev. D *81*, 023519 (2010).
7. I. Duran and D. Pavón, Phys. Rev. D *83*, 023504 (2011).
8. W. Zimdahl and D. Pavón, Class. Quantum Grav. *24*, 5461 (2007).
9. D. Pavón, W. Zimdahl,Phys. Lett. B *628*, 206 (2005).
10. I. Duran and L. Parisi, Phys. Rev. D *85*, 123538 (2012).
11. I. Duran, D. Pavón and W. Zimdahl, JCAP *07*, 018 (2010).
12. L. Wang and P. J. Steinhardt, Astrophys. J. *508*, 483 (1998).
13. Y. Gong, Phys. Rev. D *78* 123010 (2008).

# Complete Quantization of Scalar Cosmological Perturbations

**Mikel Fernández-Méndez, Guillermo A. Mena Marugán, and Javier Olmedo**

**Abstract** We quantize a perturbed Friedmann–Lemaître–Robertson–Walker model coupled to a massive scalar field. We consider only scalar perturbations, in a universe whose spatial sections have the topology of a three-sphere. The local gauge freedom is fixed at the classical level. We choose a preferred parametrization of the system by adapting uniqueness criteria for the quantization of scalar fields with time-dependent mass. The Hilbert space of the theory is constructed combining a polymer representation for the homogeneous background and the preferred Fock quantization for the perturbations. Finally, we propose a prescription to promote the Hamiltonian constraint to a quantum operator, and characterize the states annihilated by it in terms of their initial data at the minimum-volume section.

## 1 Introduction

The lack of a quantum theory of gravity has prevented a complete quantum description of cosmological inflation. Even so, one expects that quantum field theory in a suitable curved spacetime can provide a good approximation to the full theory in a certain regime. On the other hand, the application of the techniques of Loop Quantum Gravity (LQG) [8] to cosmological models such as the Friedmann–Lemaître–Robertson–Walker (FLRW) universe has proven very successful, giving rise to the field known as Loop Quantum Cosmology (LQC) [3]. The treatment of anisotropic or inhomogeneous models has also received considerable attention.

M. Fernández-Méndez (✉) · G.A. Mena Marugán
Instituto de Estructura de la Materia, IEM-CSIC, Serrano 121, 28006 Madrid, Spain
e-mail: m.fernandez@iem.cfmac.csic.es; mena@iem.cfmac.csic.es

J. Olmedo
Instituto de Física, Facultad de Ciencias, Iguá 4225, esq. Mataojo, Montevideo, Uruguay
e-mail: jolmedo@fisica.edu.uy

A. García-Parrado et al. (eds.), *Progress in Mathematical Relativity, Gravitation and Cosmology*, Springer Proceedings in Mathematics & Statistics 60,
DOI 10.1007/978-3-642-40157-2_35, 

In particular, the combination of the loop quantization of the global degrees of freedom and a standard Fock quantization of the local ones has allowed one to attain a complete hybrid quantization of Gowdy models [7]. In this work, this hybrid quantization approach is applied to scalar perturbations of a FLWR model coupled to a massive scalar field. We consider the case of spatial sections with the topology of the three-sphere.

## 2 The Classical System

The Arnowitt–Deser–Misner metric variables and the scalar field can be expanded using the hyperspherical harmonics $\{Q_{\vec{n}}\}$. The mode $Q_{\vec{n}}$ is an eigenfunction of the Laplace–Beltrami operator, with eigenvalue $-\omega_n^2$. The zero modes must satisfy Friedmann equations, so we treat them as the FLRW background in which the perturbations propagate ($e^\alpha$ and $\varphi$ being proportional to the scale factor and the homogenous part of the field, respectively). Up to quadratic order in the inhomogeneities, the modes are decoupled and the Hamiltonian is a linear combination of constraints of different nature. The homogeneous Hamiltonian constraint, multiplied by the homogeneous lapse $N_0$, is corrected with quadratic terms, while the diffeomorphism and the linear Hamiltonian constraint, which appear with local Lagrange multipliers, are of first order in the perturbations. By fixing the local gauge freedom, we can remove all the constraints except for the one related to the homogeneous lapse. However, care must be taken that the gauge fixing conditions are well-posed and consistent with the dynamics. Here, we consider the longitudinal gauge, in which the shift vector vanishes and the three-metric of the spatial sections is conformal to the round metric. After the reduction of the system, the Hamiltonian takes the form $H = N_0(H_0 + \sum_{\vec{n}} H_2^{\vec{n}})$, where $H_0$ and $H_2^{\vec{n}}$ are, respectively, of zeroth and second order in the perturbations. The inhomogeneous sector can be parametrized by the coefficients of the mode decomposition of the scalar-field perturbation, $f_{\vec{n}}$, and their momenta $\pi_{f_{\vec{n}}}$. In terms of them, the second-order Hamiltonian reads $H_2^{\vec{n}} = \frac{1}{2}e^{-\alpha}\left(E_{\pi\pi}\pi_{f_{\vec{n}}}^2 + 2E_{f\pi}f_{\vec{n}}\pi_{f_{\vec{n}}} + E_{ff}^n f_{\vec{n}}^2\right)$, where the coefficients $E_{\pi\pi}$, $E_{f\pi}$, and $E_{ff}$ depend exclusively on the homogeneous variables. We must bear in mind that our aim is to carry out a Fock quantization of the perturbation. However, it is known that there is an infinite ambiguity in doing this: firstly, in the choice of fundamental variables (as we can scale the field configuration with background functions, and change the canonical momentum), and also in the choice of representation for them. Nevertheless, we can appeal to some uniqueness results for the quantization of a scalar field with time-dependent mass in a compact manifold. The requirements of (a) invariance of the vacuum state under the spatial symmetries of the field equations, and (b) unitarily implementable field dynamics, select a preferred scaling of the field, its momentum, and a unique

unitary equivalence class of Fock representations for this canonical pair [4]. We can apply these results to our case and attain a unitary quantization in the limit in which the background behaves effectively in a classical way. Since the uniqueness results depend only in the ultraviolet behavior, it proves sufficient to reach a Klein–Gordon Hamiltonian with subdominant corrections in the large-$\omega_n$ limit [6]. This can be done with the change of variables: $\bar{f}_{\vec{n}} = e^{\alpha} f_{\vec{n}}$, $\pi_{f_{\vec{n}}} = e^{-\alpha}(\pi_{f_{\vec{n}}} - 3\pi_{\alpha} f_{\vec{n}} - 3\pi_{\varphi} a_{\vec{n}})$; $\bar{\varphi} = \varphi + 3\sum_{\vec{n}} a_{\vec{n}} f_{\vec{n}}$, with momentum $\pi_{\bar{\varphi}} = \pi_{\varphi}$; and $\bar{\alpha} = \alpha + \frac{1}{2}\sum_{\vec{n}}(f_{\vec{n}}^2 + a_{\vec{n}}^2)$, with momentum $\pi_{\bar{\alpha}} = \pi_{\alpha} - \sum_{\vec{n}}(f_{\vec{n}}\pi_{f_{\vec{n}}} - \pi_{\alpha} f_{\vec{n}}^2 - 3\pi_{\varphi} a_{\vec{n}} f_{\vec{n}})$. Here $a_{\vec{n}} = 3[\pi_{\varphi}\pi_{f_{\vec{n}}} + (e^{6\alpha}\tilde{m}^2\varphi - 3\pi_{\alpha}\pi_{\varphi}) f_{\vec{n}}]/[9\pi_{\varphi}^2 + (\omega_n^2 - 3)e^{4\alpha}]$, $\tilde{m}$ being proportional to the inflaton mass $m$. These new variables are canonical with respect to the reduced symplectic structure up to the considered perturbative order.

## 3 Hybrid Quantization

The hybrid quantization that we employ combines a polymer representation for the homogeneous degrees of freedom of the geometry, a standard Schrödinger representation for the homogeneous matter field $\phi \propto \varphi$, and a Fock representation for the inhomogeneities. The polymer approach starts with the variables $N_{\mu} = \exp(i\mu c/2)$ and $p$, which parametrize the holonomies of the Ashtekar–Barbero connection along straight edges of length $\mu l_0$ in the directions of a fiducial triad ($l_0^3$ being the fiducial volume of the three-sphere) and the fluxes of the densitized triad through "square surfaces" of geodesic edges, respectively. In the improved dynamics scheme [1], one considers edges of length $\bar{\mu} l_0$, related to the minimum non-zero area eigenvalue allowed in LQG, $\Delta$, by the expression $\bar{\mu} = \sqrt{\Delta/p}$. These new variables parametrize the homogeneous sector and are canonical up to a constant, $\{c, p\} = 8\pi G\gamma$, $G$ being the Newton constant and $\gamma$ the Barbero–Immirzi parameter. They are to be represented in the space of square-integrable functions in the Bohr compactification of the real line with respect to the corresponding Haar measure, $L^2(\mathbf{R}_{\mathrm{B}}, d\mu_{\mathrm{B}})$. It is convenient to adopt the orthonormal basis $\{|v\rangle | v \in \mathbf{R}\}$ in which $\hat{N}_{\bar{\mu}}|v\rangle = |v+1\rangle$ and $\hat{p}|v\rangle = p(v)|v\rangle$, with $p(v) \propto \mathrm{sgn}(v)|v|^{2/3}$. As for the inhomogeneities, we choose the quantization selected by the uniqueness results mentioned above. In particular, we adopt the massless representation, which can be constructed from the annihilation-like variables $a_{f_{\vec{n}}} = (\omega_n f_{\vec{n}} + i\pi_{f_{\vec{n}}})/\sqrt{2\omega_n}$ and their creation-like counterpart $a^*_{f_{\vec{n}}}$. We denote by $\mathscr{F}$ the corresponding Fock space.

The total kinematical Hilbert space is then $L^2(\mathbf{R}_{\mathrm{B}}, d\mu_{\mathrm{B}}) \otimes L^2(\mathbf{R}, d\phi) \otimes \mathscr{F}$. This is the space in which the Hamiltonian constraint must now be represented. The homogeneous part of the constraint, $\hat{C}_0$, can be regularized as in the unperturbed case [2]. With a suitable factor ordering:

$$\hat{C}_0 = \widehat{\left(\frac{1}{|p|}\right)^{\frac{3}{4}}} \left[ 8\pi G(\hat{\pi}_\phi^2 + m^2|\hat{p}|^3\hat{\phi}^2) - \frac{6\left(\hat{\Omega}^2 + (1+\gamma^2)l_0^2\hat{p}^2 - |\hat{p}|^3 \sin^2(\hat{\bar{\mu}}l_0)/\Delta\right)}{\gamma^2} \right] \widehat{\left(\frac{1}{|p|}\right)^{\frac{3}{4}}}, \quad (1)$$

$$\hat{\Omega} = \frac{1}{4i\sqrt{\Delta}} |\hat{p}|^{\frac{3}{4}} \left[ \widehat{\mathrm{sgn}(p)}, e^{-i\hat{\bar{\mu}}l_0/2} \hat{N}_{2\bar{\mu}} e^{-i\hat{\bar{\mu}}l_0/2} - e^{i\hat{\bar{\mu}}l_0/2} \hat{N}_{-2\bar{\mu}} e^{i\hat{\bar{\mu}}l_0/2} \right]_+ |\hat{p}|^{\frac{3}{4}}. \quad (2)$$

Here, $[\cdot,\cdot]_+$ is the anticommutator and the inverse powers of $p$ are regularized in the usual way [1]. The (second-order) difference operator $\hat{\Omega}^2$ connects only states $|v\rangle$ with $v \in \mathscr{L}_\varepsilon^\pm = \{\pm(\varepsilon + 4n) | n \in \mathbf{N}\}$. Therefore, the Hilbert spaces $\mathscr{H}_\varepsilon^\pm$ of states with support in the semilattices $\mathscr{L}_\varepsilon^\pm$ are superselection sectors. Now we need a prescription to quantize the part of the Hamiltonian constraint quadratic in the perturbations [5], $\hat{C}_2^{\vec{n}}$. Since the variable $c$ has no corresponding operator in the quantum theory, we promote the even powers $(cp)^{2k}$ to operators $\hat{\Omega}^{2k}$, and the odd powers $(cp)^{2k+1}$ to $|\hat{\Omega}|^k \hat{\Lambda} |\hat{\Omega}|^k$. The operator $\hat{\Lambda}$ is introduced so as to preserve the superselection sectors, and is defined like $\hat{\Omega}$ but with a $1/2$ factor and steps of $4\bar{\mu}$ instead of $2\bar{\mu}$. The complete Hamiltonian constraint $\hat{C} = \hat{C}_0 + \sum_{\vec{n}} \hat{C}_2^{\vec{n}}$ is thus a difference operator whose solutions are characterized in each sector $\mathscr{H}_\varepsilon^\pm$ by their "initial data" at the minimum volume sector $v = \varepsilon$. Endowing this space with an inner product (e.g., by imposing reality conditions on a complete set of observables), we can provide it with the structure of a Hilbert space—the physical Hilbert space $L^2(\mathbf{R}, d\phi) \otimes \mathscr{F}$.

## 4 Conclusions

We have presented a complete hybrid quantization of the scalar perturbations of a closed FLRW universe filled with a scalar field. The local gauge freedom has been fixed classically (nonetheless, the physical degrees of freedom of the perturbations can equivalently be described in terms of gauge invariants [5]). The combination of polymer and Fock techniques has allowed us to construct a rigorous quantum theory. Criteria of symmetry and unitary dynamics have been used to select a preferred Fock representation for the inhomogeneities. A quantum representation of the Hamiltonian constraint has been proposed, and it has been noted that its solutions can be identified with the space of initial data in the minimum volume section.

**Acknowledgement** This work was supported by the research grant MICINN/MINECO FIS2011-30145-C03-02 from Spain.

## References

1. Ashtekar, A., Pawlowski, T., Singh, P.: Quantum nature of the big bang: Improved dynamics. Phys. Rev. D **74**, 084003 (2006)
2. Ashtekar, A., Pawlowski, T., Singh, P., Vandersloot, K.: Loop quantum cosmology of $k = 1$ FRW models. Phys. Rev. D **75**, 024035 (2007)
3. Ashtekar, A., Singh, P.: Loop quantum cosmology: a status report. Class. Quantum Grav. **28**, 213001 (2011)
4. Cortez, J., Mena Marugán, G.A., Olmedo, J., Velhinho, J.M.: Criteria for the determination of time dependent scalings in the Fock quantization of scalar fields with a time dependent mass in ultrastatic spacetimes. Phys. Rev. D **86**, 104003 (2012)
5. Fernández-Méndez, M., Mena Marugán, G.A., Olmedo, J.: Hybrid quantization of an inflationary universe. Phys. Rev. D **86**, 024003 (2012)
6. Fernández-Méndez, M., Mena Marugán, G.A., Olmedo, J., Velhinho, J.M.: Unique Fock quantization of scalar cosmological perturbations. Phys. Rev. D **85**, 103525 (2012)
7. Martín-Benito, M., Garay, L.J., Mena Marugán, G.A.: Hybrid quantum Gowdy cosmology: Combining loop and Fock quantizations. Phys. Rev. D **78**, 083516 (2008)
8. Thiemann, T.: Modern Canonical Quantum General Relativity. Cambridge University Press, Cambridge, England (2007)

# Null Geodesics of Black Holes in String Theory

**Sharmanthie Fernando**

**Abstract** In this talk, we presented the null geodesics of the static charged black hole in heterotic string theory. The talk is based on a paper published in Physical Review D (Fernando, Phys. Rev. D 85:02403, 2012). In this paper, a detailed analysis of the geodesics are done in the Einstein frame as well as in the string frame. In the Einstein frame, the geodesics are solved exactly in terms of the Jacobi-elliptic integrals for all possible energy levels and angular momentum of the photons. In the string frame, the geodesics are presented for the circular orbits. As a physical application of the null geodesics, we have obtained the angle of deflection for the photons and the quasinormal modes of a massless scalar field in the eikonal limit.

## 1 Introduction to GMGHS Charged Black Holes in String Theory

In this paper we studied null geodesics of the GMGHS charged black hole in the string theory. Let us first give an introduction to the theory and the resulting black hole solution.

The action corresponding to the GMGHS black hole is given by,

$$S = \frac{1}{16\pi}\int d^4x\sqrt{-g}\left[R - 2(\bigtriangledown\Phi)^2 - e^{-2\Phi}F_{\mu\nu}F^{\mu\nu}\right] \tag{1}$$

Here $\Phi$ is the dilaton field, $R$ is the scalar curvature and $F_{\mu\nu}$ is the Maxwell's field strength. The static charged black hole solutions to the above action were found first

S. Fernando (✉)
Northern Kentucky University, Highland Heights, KY 41099, USA
e-mail: fernando@nku.edu

A. García-Parrado et al. (eds.), *Progress in Mathematical Relativity, Gravitation and Cosmology*, Springer Proceedings in Mathematics & Statistics 60,
DOI 10.1007/978-3-642-40157-2_36, 

by Gibbons and Maeda[2]. It was also independently found by Garfinkle, Horowitz and Strominger [3] few years later.

The GMGHS black hole solution to the action in Eq. (1) is given by,

$$ds_E^2 = -\left(1 - \frac{2M}{r}\right) dt^2 + \frac{1}{\left(1 - \frac{2M}{r}\right)} dr^2 + r\,(r-a)\,(d\theta^2 + sin^2(\theta) d\phi^2) \tag{2}$$

Here, the electric field strength and the dilaton field are given by,

$$F_{rt} = \frac{Q}{r^2}; \qquad e^{2\Phi} = 1 - \frac{Q^2}{Mr}; \;\; a = \frac{Q^2}{M} \tag{3}$$

There is an event horizon at $r = 2M$. How ever, the area of the sphere of the string black hole is smaller and the area approaches zero when $r = Q^2/M$. Therefore, $r = Q^2/M$ surface is singular. For $Q^2 \leq 2M^2$, the singular surface is inside the event horizon and the Penrose diagram is identical to the one of the Schwarzschild black hole. When $Q^2 = 2M^2$, the singular surface coincides with the horizon. This is the extremal limit where a transition between the black hole and the naked singularity occurs.

## 2 Null Geodesics

The null geodesics for the above black hole are given by the following three equations.

$$R(r)^2 \dot{\phi} = L \tag{4}$$

$$f(r)\dot{t} = E \tag{5}$$

$$\dot{r}^2 + f(r)\frac{L^2}{R(r)^2} = E^2 \tag{6}$$

Here $f(r) = 1 - \frac{2M}{r}$. One can do a change of variable as $u = \frac{1}{r}$ and combine the above Eqs. (4), (5) and (6) to obtain an equation,

$$\left(\frac{du}{d\phi}\right)^2 = g(u) \tag{7}$$

where,

$$g(u) = -2aMu^4 + (a + 2M)u^3 + u^2\left(a^2\frac{E^2}{L^2} - 1\right) - 2a\frac{E^2}{L^2}u + \frac{E^2}{L^2} \tag{8}$$

When $a \to 0$, $g(u) \to 2Mu^3 - u^2 + \frac{E^2}{L^2}$ as expected for the Schwarzschild black hole [4]. When $a \to 0$, $g(u)$ has maximum three real roots as described in the book by Chandrasekhar[4].

## 3 Bending of Light

Once the null geodesics are analyzed in detail for various parameters in the theory such as $E, L, M$ and $Q$, it is possible to apply that knowledge to study important properties of the black hole geometry. One of them is the gravitational lensing or bending of light by the black hole. We obtained explicit expressions for the closest approach $r_o$ of the light ray in terms of the impact parameter $D$ given in Eqs. (9), (10) and (11). There after, we compared the deflection angle of light as a function of $D$ for the GMGHS black hole and the Schwarzschild black hole.

$$r_o^{string} = 2\sqrt{-\frac{p}{3}}cos\left(\frac{1}{3}cos^{-1}\left(\frac{3q}{2p}\sqrt{-\frac{3}{p}}\right)\right) + \frac{a}{3} \tag{9}$$

Here, $p$ and $q$ are given by,

$$p = \frac{a^2 - 3D^2}{3} \tag{10}$$

$$q = \frac{54MD^2 - 9aD^2 - 2a^3}{27} \tag{11}$$

## 4 Unstable Null Geodesics and Quasinormal Modes of the Massless Scalar Field in the Eikonal Limit

When a black hole is perturbed, it undergoes damped oscillations; the frequencies of oscillations are called quasinormal modes. Perturbations of a black hole with a scalar field are given by the equation,

$$\frac{d^2\eta}{dr_*^2} + \left(\omega^2 - \left(\frac{l(l+1)}{R^2} + \frac{ff'R'}{R} + \frac{f^2R''}{R}\right)\right)\eta = 0 \tag{12}$$

Here, $l$ is the spherical harmonic index and $r_*$ is the tortoise coordinate. The computation of quasinormal modes at the eikonal limit and the unstable null geodesics are related [5]. In the eikonal limit, the quasinormal modes are given as,

$$\omega_{QNM} = \Omega_c l - i(n + \frac{1}{2})|\lambda| \tag{13}$$

Here, the value $n$ is a nonnegative integer. $\Omega_c$ is the coordinate angular velocity given by $\frac{\dot{\phi}}{\dot{t}}$ computed at unstable circular radius of the null geodesics which is given in Eq. (14). $\lambda$ is the Lyapunov exponent which gives the instability timescale of the unstable circular null geodesics, given in Eq. (15)

$$\Omega_c = \frac{\dot{\phi(r_c)}}{\dot{t}(r_c)} = \sqrt{\frac{f(r_c)}{R(r_c)^2}} = \sqrt{\frac{r_c - 2M}{r_c^2(r_c - a)}} \tag{14}$$

$$\lambda = \sqrt{\frac{(2M - r_c)(3r_c^3 - 12Mr_c^2 - 3ar_c^2 + 16aMr_c + a^2r_c - 6a^2M)}{r_c^4(r_c - a)^2}} \tag{15}$$

## 5 Conclusions

We have studied the null geodesics of the GMHHS black hole. The equations for the geodesics were solved exactly for various values of energy and angular momentum of the photons.

As physical applications of the properties of the null geodesics obtained here, we have studied light bending and quasinormal modes of massless scalar field. The closest approach of the photons bending around the black hole is computed as a function of the impact parameter. The deflection angle $\alpha$ is computed as a function of the impact parameter. A comparison is done with the deflection angle of the Schwarzschild black hole. It was observed that the photons with the same impact parameter bend less around the string black hole compared to the Schwarzschild black hole. These results would be beneficial in computations of gravitational lensing of string black holes.

The unstable circular null geodesics of the black hole are used to compute the quasinormal modes of the black hole in the eikonal limit. We have followed an important result by Cardoso et al. [5] in deriving these results. The Lyapunov exponent $\lambda$, which gives the instability time scale is also computed. It was noted that there is a maximum value for $\lambda$ at $a = 6M(2 - \sqrt{3})$.

## References

1. S. Fernando, *Null geodesics of charged black holes in string theory*, Physical Review **D 85** 02403 (2012)
2. G.W. Gibbons & K. Maeda, *Black holes and membranes in higher dimensional theories with dilaton fields*, Nucl. Phys. **B298** 741 (1988)
3. D. Garfinkle, G.T. Horowitz & A. Strominger, *Charged black holes in string theory*, Phys. Rev. **D43** 3140 (1991)
4. S. Chandrasekhar, *The Mathematical Theory of Black holes*, Oxford, UK (1983)
5. V. Cardoso, A.S. Miranda, E. Berti, H. Witeck & V.T. Zanchin, *Geodesics stability, Lyapunov exponents and quasinormal modes*, Phys.Rev. **D79** 064016 (2009)

# The Causal Boundary of Spacetimes Isocausal to Standard Stationary Ones

**José L. Flores**

**Abstract** We present some recent results in Flores et al. (ArXiv:1011.1154) about the relation between the causal boundary of standard stationary spacetimes (previously studied in Flores et al. (Memoirs A.M.S. ArXiv:1011.1154)) and that of a wide class of spacetimes which are isocausal to them.

## 1 Introduction

In the last years the causal boundary has been computed for some well-known classes of spacetimes, as standard stationary ones [4]. In order to extend these results to other spacetimes of interest, it is natural to argue that spacetimes with similar causal structure will present similar causal boundaries. This is the case of conformally equivalent spacetimes, which trivially have the same causal boundary. The notion of isocausality, introduced by García-Parrado and Senovilla in [7], provides a relation of equivalence between spacetimes which is more flexible than the conformal one. So, it is natural to ask if isocausal spacetimes will also present the same causal boundary. Here, we will see that, even if the answer to this question is negative in general [2], it is possible to relate the causal boundary of standard stationary spacetimes with that of a wide class of spacetimes isocausal to them [5].

J.L. Flores (✉)
Departamento de Álgebra, Geometría y Topología, Facultad de Ciencias, Universidad de Málaga, Campus Teatinos, 29071 Málaga, Spain
e-mail: floresj@uma.es

A. García-Parrado et al. (eds.), *Progress in Mathematical Relativity, Gravitation and Cosmology*, Springer Proceedings in Mathematics & Statistics 60,
DOI 10.1007/978-3-642-40157-2_37, 

## 2 C-Boundary of Spacetimes

The causal boundary of a strongly causal spacetime $(V, g)$ was introduced in [8] (see, e.g., [1] for an outline and terminology). In this paper we will consider the most recent redefinition of the causal boundary developed in [3], called *c-boundary*.

Denote by $\hat{V}$ ($\check{V}$) the *future (past) c-completion* of a strongly causal spacetime $(V, g)$, i.e. the set of IPs (IFs) in $(V, g)$ endowed with the topology associated to the limit operator $\hat{L}$ ($\check{L}$), where $P \in \hat{L}(P_n)$ iff $P \subset \liminf(P_n)$ and $P$ maximal in $\limsup(P_n)$ ($\check{L}$ is defined analogously). The *c-completion* $\overline{V}$ and the *c-boundary* $\partial V$ of $(V, g)$ are defined as follows:

$$\overline{V} := \{(P, F) \in (\hat{V} \cup \emptyset) \times (\check{V} \cup \emptyset), P \sim_S F\} \setminus \{(\emptyset, \emptyset)\}, \qquad \partial V := \overline{V} \setminus V,$$

where $P \sim_S F$ iff $P$ is a maximal IP in $\downarrow F := I^-(\{q \in V : q\ell^2 p, \forall p \in F\})$ and $F$ is a maximal IF in $\uparrow P := I^+(\{p \in V : q\ell^2 p, \forall q \in P\})$. If $P$ (F) does not satisfy previous property for any $F$ ($P$), we assume $P \sim_S \emptyset$ ($\emptyset \sim_S F$). The c-completion $\overline{V}$ is endowed with the following chronological relation:

$$(P, F)\overline{\ell^2}(P', F') \quad \text{iff} \quad F \cap P' \neq \emptyset.$$

The c-completion is also endowed with a structure of topological space just by considering the topology associated to the limit operator $L$, where

$$(P, F) \in L(\{(P_n, F_n)\}) \Leftrightarrow \begin{cases} P \in \hat{L}(P_n) \text{ if } P \neq \emptyset \\ F \in \check{L}(F_n) \text{ if } F \neq \emptyset. \end{cases}$$

## 3 Isocausal Comparison

The isocausal comparison between spacetimes was introduced by García-Parrado and Senovilla in [7]. First, $V$ is said to be *causally related* with $V'$, denoted $V \prec V'$, if there exists a diffeomorphism $\phi : V \to V'$ mapping causal vectors to causal vectors (preserving time-orientation). Then, $V$ and $V'$ are *isocausal* if they are causally related in both directions (perhaps by using different diffeomorphisms). Note that isocausality is more flexible than conformal equivalence. Moreover, it preserves some relevant global properties associated to the conformal structure of the spacetime (but not all of them, as remarked in [6]).

In [2] the authors showed the existence of two isocausal spacetimes with different future c-boundaries.

## 4 Standard Stationary Framework

A *standard stationary spacetime* $(V, g)$ is a product manifold $V = \mathbb{R} \times M$ endowed with a metric $g = -dt^2 + \omega \otimes dt + dt \otimes \omega + h$, where $\omega$ is a one-form on $M$ and $(M, h)$ a Riemannian manifold. For every standard stationary spacetime, there exist two *Finsler metrics* of *Randers type* over $M$:

$$F^{\pm}(v) = \sqrt{h(v,v) + \omega^2(v)} \pm \omega(v), \qquad v \in TM.$$

The Finsler metric $F = F^+$ defines a distance map $d : M \times M \to \mathbb{R}$ in the natural way. As $F$ is only positively homogeneous, $d$ may not be symmetric, and so, it may not be a real distance, but a *generalized distance*, that is, $d$ satisfies the three properties of a *quasi-distance* (a distance which is not necessarily symmetric) plus this other one: $\lim_n d(x_n, x) = 0$ iff $\lim_n d(x, x_n) = 0$. The possible non-symmetry of $d$ provides two possible Cauchy completions $M_C^{\pm}$ for the generalized metric space $(M, d)$, whose corresponding Cauchy boundaries $\partial_C^{\pm} M$ satisfy the relation $\partial_C^s M = \partial_C^+ M \cap \partial_C^- M$, being $\partial_C^s M$ the Cauchy boundary for the *symmetrized distance* $d^s(x, y) := 1/2(d(x, y) + d(y, x))$. The *(forward)* Cauchy completion $M_C^+$ is endowed with the natural extension $d_Q^+$ of $d$, which becomes a quasi-distance. In order to get good topological properties, $M_C^+$ is endowed with the topology induced by the *backward* $d_Q^+$-balls, instead of that induced by the forward ones.

## 5 Main Results

We are now in conditions to state the main results. We want to study the c-boundary of spacetimes $(V, g)$ of the form

$$V = \mathbb{R} \times M \quad \text{and} \quad g = -dt^2 + \omega_t \otimes dt + dt \otimes \omega_t + h_t,$$

where now $\omega_t$ and $h_t$ depend on $t$. To this aim, we will assume

$$g_{cl} \prec_0 g \prec_0 g_{op}, \quad \text{being} \quad \begin{cases} g_{cl} = -dt^2 + \omega \otimes dt + dt \otimes \omega + h \\ g_{op} = -dt^2 + \alpha(t)\omega \otimes dt + \alpha(t) dt \otimes \omega + \alpha^2(t) h, \end{cases}$$

for some positive function $\alpha : \mathbb{R} \to \mathbb{R}$ ($\prec_0$ means causally related by using $\phi \equiv Id$). Under these conditions $g_{op}$ is conformal to $g_{cl}$, and the metrics $g$, $g_{cl}$ (and $g_{op}$) are isocausal. In order to relate the future c-completions $\hat{V}$ and $\hat{V}_{cl}$ of $(V, g)$ and $(V, g_{cl})$, resp., first consider the following relation: $P^1, P^2 \in \hat{\partial} V$ are *st-related*, $P^1 \sim_{st} P^2$, if there exists a TIP $P_{cl}$ for $g_{cl}$ such that $P_{cl} \subset P^1 \cap P^2$ and $I_{op}^-(P^1) = I_{op}^-(P_{cl}) = I_{op}^-(P^2)$ (where $I_{op}^-(\cdot)$ means $I^-(\cdot)$ computed with metric $g_{op}$).

**Theorem 5.1.** *Let $(V, g)$ be a spacetime as above. If the integral condition*

$$\int_0^{\infty} \left( \frac{1}{\alpha(s)} - 1 \right) ds < \infty$$

*holds, $d_Q^+$ is a generalized distance and $M_C^+$ is locally compact then the map*

$$\hat{\mathscr{J}} = \hat{\Pi} \circ \hat{j} : \hat{V}_{cl} \to \hat{V}/\sim_{st}, \quad \text{with } \hat{j}(P_{cl}) := I^-(P_{cl}) \text{ and } \hat{\Pi} : \hat{V} \to \hat{V}/\sim_{st}$$

*is bijective and continuous.*

*If, in addition, $\hat{V}/\sim_{st}$ is Hausdorff, then $\hat{\mathscr{J}}$ is an homeomorphism.*

An analogous result can be established for the past c-completions $\check{V}$ and $\check{V}_{cl}$.

Finally, in order to relate the c-completions $\overline{V}$ and $\overline{V}_{cl}$ of $(V, g)$ and $(V, g_{cl})$, resp., we consider a map $\overline{j} : \overline{V}_{cl} \to \overline{V}$ satisfying

$$(P_{cl}, F_{cl}) \mapsto \overline{j}((P_{cl}, F_{cl})) := \begin{cases} (I^-(P_{cl}), \emptyset) & \text{if } F_{cl} = \emptyset \\ (\emptyset, I^+(F_{cl})) & \text{if } P_{cl} = \emptyset \\ (P_0, F_0) & \text{otherwise,} \end{cases}$$

for some $P_0 \in \hat{\Pi}^{-1}(\hat{\mathscr{J}}(P_{cl}))$, $F_0 \in \check{\Pi}^{-1}(\check{\mathscr{J}}(F_{cl}))$ such that $P_0 \sim_S F_0$. Such a map exists and is injective. Then, consider the relation $\sim_{st}$ on $\overline{V}$ defined by

$$(P, F) \sim_{st} (P', F') \iff (P, F), (P', F') \in ST((P_{cl}, F_{cl})) \text{ for some } (P_{cl}, F_{cl}) \in \overline{V}_{cl},$$

$$\text{where } (P, F) \in ST((P_{cl}, F_{cl})) \iff \begin{cases} P \neq \emptyset \neq P_{cl} \Rightarrow P \in \hat{\Pi}^{-1}(\hat{\mathscr{J}}(P_{cl})) \\ F \neq \emptyset \neq F_{cl} \Rightarrow F \in \check{\Pi}^{-1}(\check{\mathscr{J}}(F_{cl})) \\ P_{cl} = \emptyset \Rightarrow P = \emptyset \\ F_{cl} = \emptyset \Rightarrow F = \emptyset. \end{cases}$$

**Theorem 5.2.** *Let $(V, g)$ be a spacetime as above. If the integral conditions*

$$\int_{-\infty}^{0} \left( \frac{1}{\alpha(s)} - 1 \right) ds < \infty, \qquad \int_0^{\infty} \left( \frac{1}{\alpha(s)} - 1 \right) ds < \infty$$

*hold, $d_Q^+$ is a generalized distance and $M_C^s = M \cup \partial_C^s M$ is locally compact, then*

$$\mathscr{J} = \Pi \circ \overline{j} : \overline{V}_{cl} \to \overline{V}/\sim_{st}, \qquad \text{with } \Pi : \overline{V} \to \overline{V}/\sim_{st}$$

*is injective and continuous.*

*If, in addition, $\overline{V}/\sim_{st}$ is Hausdorff, then $\mathscr{J}$ is an homeomorphism.*

**Acknowledgements** The author is partially supported by the Spanish MICINN Grant MTM2010-18099 and Regional J. Andalucía Grant P09-FQM-4496, both with FEDER funds.

## References

1. Beem J.K., Ehrlich P.E., Easley K.L., *Global Lorentzian geometry*, Monographs Textbooks Pure Appl. Math. **202** (Dekker Inc., New York, 1996).
2. Flores J.L., Herrera J., Sánchez M., Class. Quant. Grav. **28**, 175016 (2011).
3. Flores J.L., Herrera J., Sánchez M., Adv. Theor. Math. Phys. **15**, 991–1058 (2011).
4. Flores J.L., Herrera J., Sánchez M., to appear in Memoirs A.M.S. ArXiv:1011.1154.
5. Flores J.L., Herrera J., Sánchez M., ArXiv:1011.1154.
6. García-Parrado A., Sánchez M., Class. Quant. Grav. **22**, 4589–4619 (2005).
7. García-Parrado A., Senovilla J.M.M., Class. Quant. Grav. **22**, 625–664 (2003).
8. Geroch R.P., Kronheimer E.H. and Penrose R., Proc. Roy. Soc. Lond. A **237**, 545–567 (1972).

# A New Numerical Approach to Estimate the Sunyaev–Zel'dovich Effect

**Màrius Josep Fullana i Alfonso, Josep Vicent Arnau i Córdoba, Robert J. Thacker, Hugh M.P. Couchman, and Diego P. Sáez Milán**

**Abstract** Several years ago, we designed a particular ray tracing method. Combined with a Hydra parallel code (without baryons), it may compute some CMB anisotropies: weak lensing (WL) and Rees–Sciama (RS) effects. Only dark matter is fully necessary to estimate these effects. For very small angular scales, we made an exhaustive study leading to a lensing contribution slightly—but significantly—greater than previous ones. Afterwards, the same ray tracing procedure was included in a parallel Hydra code with baryons. The resulting code was then tested. This code is being currently applied to the study of the thermal and kinetic Sunyaev–Zel'dovich (SZ) contributions to the CMB anisotropies. We present here our first results.

## 1 Introduction

In order to improve on previous estimates of CMB anisotropies based on PM methods (see [1] and [2]), *AP3M codes* are used. First, a Hydra AP3M *sequential* code [3] was used. Only dark matter was taken into account to evolve structures and

M.J. Fullana i Alfonso (✉)
IMM, Universitat Politècnica València, C. Vera, s/n 46022 València
e-mail: mfullana@mat.upv.es

J.V. Arnau i Córdoba
DMA, Universitat de València, Dr. Moliner 50, 46100 Burjassot, Spain

R.J. Thacker
DAP, St. Mary's University, Halifax, Nova Scotia, B3H 3C3 Canada

H.M.P. Couchman
DPA, McMaster University, 1280 Main St. West, Hamilton, Ontario, L8S 4M1 Canada

D.P.S. Milán
DAA, Universitat de València, Dr. Moliner 50, 46100 Burjassot, Spain

A. García-Parrado et al. (eds.), *Progress in Mathematical Relativity, Gravitation and Cosmology*, Springer Proceedings in Mathematics & Statistics 60,
DOI 10.1007/978-3-642-40157-2_38, © Springer-Verlag Berlin Heidelberg 2014

compute gravitational CMB anisotropies. Afterwards, a Hydra AP3M *parallel* code was used, which allowed us to get a higher resolution [4]. Now, we are moving CMB photons along the simulation boxes of a Hydra AP3M *parallel code with baryons*. RS and WL CMB anisotropies have been calculated again—with similar boxes and resolution—. Comparisons with previous computations give consistent results. Now, calculation of SZ effect is being performed by using appropriate resolutions and our ray-tracing techniques (designed to move CMB photons thorough the simulated boxes while running the code). The peculiar gravitational potential, its gradients, the electron number density $n_e$, the electron temperature $T_e$, and other necessary quantities are calculated and used at every time step of the Hydra simulation. More details about previous work may be found in other publications [1, 3–6]

## 2 On the Computation of Thermal and Kinetic SZ Effects

In order to estimate the relative temperature variation $(\Delta T/T)$, in the $\vec{n}$ direction, due to the thermal and kinetic SZ effects, the integrals involved in the following equations [7]:

$$\frac{\Delta T}{T}(\vec{n}) = -2\,\frac{\sigma_T}{m_e c^2}\int_{l_i}^{l_0} n_e\; k\; (T_e - T_{CMB})\; dl, \tag{1}$$

$$\frac{\Delta T}{T}(\vec{n}) = -\,\frac{\sigma_T}{c}\int_{l_i}^{l_0} n_e\; v_r\; dl \tag{2}$$

must be numerically computed. In these equations, $T_{CMB}$, $v_r$, $\sigma_T$, $k$, $m_e$ and $c$ are the CMB average temperature, the radial peculiar velocity, the Thompson cross section, the Boltzmann constant, the electron mass and the speed of light, respectively. The integrals in (1) and (2) are performed along background null geodesics (Born approximation) using the following method:

1. Select the propagation directions of the CMB photons (ray-tracing).
2. Use the photon spatial step to determine all the evaluation events (positions and times) on the background null geodesics, from the initial to the final redshift. Then, localize each of these positions inside one of the simulation boxes and place there a test particle.
3. At each time step of the simulation (while running), try to calculate $n_e$, $T_e$ and $v_r$ at the test particle position as it is done in the Hydra algorithm for the positions of the baryon particles. Alternatively, use an appropriate approximating method to get a good enough estimate of $n_e$, $T_e$ and $v_r$. Our approximation involves 3 quantities: the distance $R$ ($R_{max}$) from the position of the test particle to the nearest baryon (the 32nd baryon), and the Hydra effective spatial resolution $R_{min}$.
4. Multiply the integrands of Eqs. (1) and (2)—evaluated at the position of the nearest baryon—by a factor $f(R)$ defined as follows:

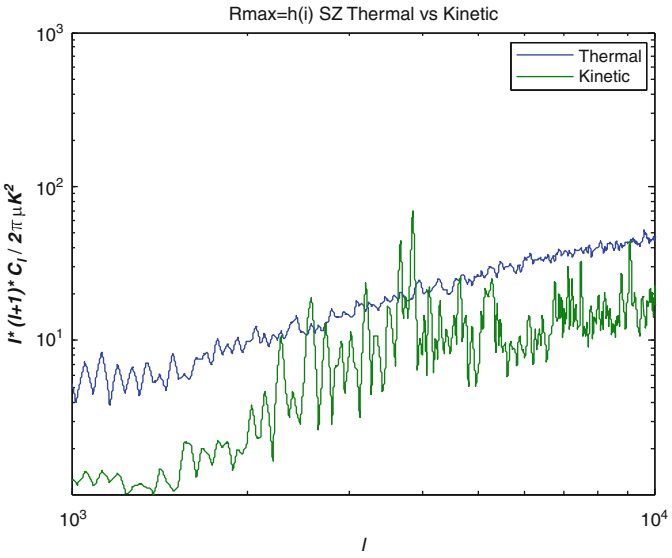


**Fig. 1** Thermal and Kinetic SZ contributions computed with one test simulation

(a) For $R \leq R_{min} : f(R) = 1$. The integrand is then evaluated at the position of the nearest baryon.
(b) For, $R_{min} \leq R \leq R_{max}$:

$$f(R) = 1 - \left[ \left( \frac{R - R_{min}}{R_{max} - R_{min}} \right)^2 \left( 1 - 2 \frac{R - R_{max}}{R_{max} - R_{min}} \right) \right] \tag{3}$$

Therefore $f(R_{min}) = 1$ and $f(R_{max}) = 0$. This is a Hermite interpolation with null derivatives at $R$ extremes, i.e. a cubic kernel of spline type.
(c) For $R > R_{max} : f(R) = 0$. The integrand is taken to be zero since the nearest baryon is too far away.

## 3 Current Work and Projects

A version of Hydra code with baryons has been modified to include CMB photons. Some subroutines and the computational load allocation configuration of the initial code have been remodeled. The resulting code has been tested. We are computing RS, WL and SZ contributions together. In this way, we can also compute the coupling of all contributions to the CMB spectrum. One of the most powerful tests is based on the comparison of the WL and RS power spectra obtained by using simulations with and without baryons, which have given very similar results [6].

We have started SZ computation using test simulations. The main parameters of such simulations are: box size $L_{box} = 512h^{-1}Mpc$, number of particles $N_p = 2\times256^3$, number of cells $N_c = 512^3$, number of photon directions $N_{dir} = 512\times512$ and initial redshift for computation of SZ contribution at $Z_{in} = 6$, see Fig. 1. We obtain acceptable values (compare with Fig. 5 of [7]).

We are running by now higher resolution simulations based on the following main parameters: box size $L_{box} = 200h^{-1}Mpc$, number of particles $N_p = 2\times640^3$, number of cells $N_c = 1024^3$, number of photon directions $N_{dir} = 512 \times 512$ and initial redshift for computation of SZ contribution at $Z_{in} = 6$. The angular resolution of these simulations is $D_{ang} \approx 0.12'$, and the map size is $\sim 1° \times 1°$. We think these simulations will improve on previous results allowing us: (i) a better estimate of the SZ effect by using our ray-tracing procedure, (ii) the simultaneous calculation of the total anisotropy produced by the RS, WL, and SZ effects, whose superposition may be nonlinear, and (iii) the comparison of the resulting total anisotropy with recent observations at very small angular scales [8, 9].

**Acknowledgements** This work has been supported by the Spanish Ministries of *Ciencia e Innovación* and *Economía y Competitividad*, MICINN-FEDER projects FIS2009-07705 and FIS2012-33582. Calculations have been made using the Lluis Vives Computer of UV. We are grateful to the working team of the Servei d'Informàtica de la Universitat de València for their useful help.

## References

1. Fullana, M.J., Sáez D.: Making Maps of the Rees-Sciama Effect. Sidharth, B.G., Honsell, F., de Angelis, A. (eds). Frontiers of Fundamental Physics: Proceedings of the Sixth International Symposium "Frontiers of Fundamental and Computational Physics". Udine, Italy, September 26–29, 2004. Springer, The Netherlands, 115–122 (2006)
2. Puchades, N., Fullana, M.J., Arnau, J.V., Sáez, D.: On the Rees-Sciama effect: maps and statistics. Mon. Not. R. Astron. Soc. **370**, 1849–1858 (2006)
3. Fullana, M.J., Arnau, J.V., Sáez, D.: Weak Lensing on the CMB: Estimations Based on AP3M Simulations. Sidharth, B.G., Honsell, F., Mansutti, O., Sreenivasan, K.R., Angelis, A. de (eds.) Frontiers of Fundamental and Computational Physics: 9th International Symposium. Udine and Trieste, Italy, January 7–9, 2008. AIP Conference Proceedings **1018**, 80–85 (2008)
4. Fullana, M.J., Arnau, J.V., Thacker R.J., Couchman H.M.P., Sáez D.: Estimating small angular scale Cosmic Microwave Background anisotropy with high-resolution $N$-body simulations: weak lensing. Astrophys. J. **712**, 367–379 (2010)
5. Fullana, M.J., Arnau, J.V., Thacker R.J., Couchman H.M.P., Sáez D.: Observations and simulations of the CMB temperature anisotropy at very small angular scales. Kouneiher, J., Barbachoux, C., Masson, T., Vey, D. (eds.) Frontiers of Fundamental Physics: The Eleventh International Symposium. Paris, France, July 6–9, 2010. AIP Conference Proceedings **1446**, 252–260 (2012)
6. Fullana, M.J., Arnau, J.V., Thacker R.J., Couchman H.M.P., Sáez D.: CMB anisotropy computations using Hydra gas code. Sidharth, B.G. et al. (eds.) Frontiers of Fundamental and Computational Physics: 12th International Symposium (*in press*). Udine Italy, November 21–23, 2011.
7. Scannapieco, E., Thacker, R. J., Couchman, H. M. P.: Measuring AGN Feedback with the Sunyaev-Zel'dovich Effect. Astrophys. J. **678**, 674 (2008)

8. Lueker M. et al.: Measurements of Secondary Cosmic Microwave Background Anisotropies with the South Pole Telescope. Astrophys. J. **719**, 1045–1066 (2010)
9. Fowler, J.W. et al.: The Atacama Cosmology Telescope: A Measurement of the $600 < \ell < 8000$ Cosmic Microwave Background Power Spectrum at 148 GHz. Astrophys. J. **722**, 1148–1161 (2010)

# Hawking Radiation for a Proca Field: Numerical Strategy

**Carlos Herdeiro, Marco O. P. Sampaio, and Mengjie Wang**

**Abstract** We compute the Hawking radiation for a Proca field in the D-dimensional Schwarzschild background. We construct a numerical strategy to solve the coupled system which describes a coupling between two physical degrees of freedom of the field due to the mass term. We show how to define the transmission factors for the coupled system from an S matrix and compute them to generate the Hawking fluxes.

## 1 Introduction

Hawking radiation [1] is black body like radiation emitted by black holes when one considers quantum fields near the event horizon. An intuitive way to understand this effect is to consider vacuum fluctuations near the event horizon, which create virtual particle/anti-particle pairs. When the virtual particles with negative energy are absorbed by the hole while the corresponding anti-particles become real outside of the hole, Hawking radiation appears.

In brane-world scenarios, it has been argued that miniature black holes may be produced in colliders if the true fundamental Planck scale is as low as the TeV scale [2–5]. The miniature black holes should decay promptly due to Hawking radiation, so in principle we can search for black hole events via Hawking radiation. Event generators such as CHARYBDIS2 and BLACKMAX are currently in use at the LHC. In such event generators, the longitudinal modes of Proca fields are modeled by scalar fields. In [6] we show that the longitudinal modes couple with a transverse mode. This implies that for Proca fields we have to solve coupled equations as well as decoupled single equations, rather han just solve decoupled single equations. In the remainder, we will present the method we have used and some main results.

C. Herdeiro · M.O.P. Sampaio · M. Wang (✉)
Departamento de Física da Universidade de Aveiro and I3N
Campus de Santiago, 3810-183 Aveiro, Portugal
e-mail: herdeiro@ua.pt; msampaio@ua.pt; mengjie.wang@ua.pt

A. García-Parrado et al. (eds.), *Progress in Mathematical Relativity, Gravitation and Cosmology*, Springer Proceedings in Mathematics & Statistics 60,
DOI 10.1007/978-3-642-40157-2_39, 

## 2 Numerical Strategies and Results

We start from the Lagrangian which describes the $Z$ particle in the Standard Model

$$\mathscr{L} = -\frac{1}{2} W^{\dagger}_{\mu\nu} W^{\mu\nu} + M^2 W^{\dagger}_{\mu} W^{\mu}, \tag{1}$$

where $W_{\mu\nu} = \partial_\mu W_\nu - \partial_\nu W_\mu$, and $M$ is the field mass. Then the equations of motion can be derived directly when the background is fixed. For the gravitational background, we consider Einstein symmetric spaces of the form [7]

$$ds^2 = h_{ab}(y) dy^a dy^b - r(y)^2 d\sigma_n^2 \,, \qquad d\sigma_n^2 = \sigma_{ij}(x) dx^i dx^j \,, \tag{2}$$

where $\sigma_n$ is an $n$-dimensional Einstein space with metric $\sigma_{ij}$.

In the equations of motion we decompose the vector field in tensorial types [7]. $W_a$ are $m$-scalars, with respect to $\sigma_n$, so they obey ($\kappa_0^2$ is the spin-0 eigenvalue)

$$\left(\hat{\Delta} + \kappa_0^2\right) W_a = 0, \tag{3}$$

$W_i$ is a vector field which is decomposed as a scalar $\Phi$, and a transverse vector $W_i^T$

$$W_i = \hat{D}_i \Phi + W_i^T, \qquad \hat{D}_i \hat{W}^{Ti} = 0, \tag{4}$$

where $\hat{D}_i$ is the covariant derivative on $\sigma_n$. Since $\Phi$ is a scalar, it obeys (3). The transverse vector obeys ($\kappa_1^2$ is the spin-1 eigenvalue)

$$\left(\hat{\Delta} + \kappa_1^2\right) W_i^T = 0, \tag{5}$$

Specifying our background geometry to be Schwarzschild–Tangherlini case and expanding the field equations with the decomposition (4), using conditions (3) and (5), we obtain coupled equations for two modes ($\psi$, $\chi$) when $\kappa_0^2 \neq 0$

$$\left[V^2 \frac{d}{dr}\left(\frac{1}{r^{n-2}} \frac{d}{dr} r^{n-2}\right) + \omega^2 - \left(\frac{\kappa_0^2}{r^2} + M^2\right) V\right] \chi - i\omega V' \psi = 0, \tag{6}$$

$$\left[\frac{V^2}{r^n} \frac{d}{dr}\left(r^n \frac{d}{dr}\right) + \omega^2 - \left(\frac{\kappa_0^2}{r^2} + M^2\right) V\right] \psi + i\omega \left(\frac{2V}{r} - V'\right) \chi = 0, \tag{7}$$

with $V = 1 - \mu/r^{n-1}$, $\kappa_0^2 = \ell(\ell + n - 1)$ and a set of decoupled single equations. There are a lot of studies on decoupled case, so here we focus on the coupled case.

In order to solve Eqs. (6) and (7), firstly we expand $\psi$ and $\chi$ at the horizon as

$$\psi = y^\rho \sum_{j=0}^{\infty} \mu_j y^j, \qquad \chi = y^\rho \sum_{j=0}^{\infty} \nu_j y^j, \tag{8}$$

to initialize the coupled system numerically ($y = r - r_H$ and $r_H$ is the horizon radius). Then integrating them up to large $r$, we can factor out the coefficients for outgoing/ingoing waves at infinity through far field expansions

$$\psi \to \frac{1}{r^{\frac{n}{2}-1}}\left[\left(a_0^+ + \frac{a_1^+}{r} + \dots\right)e^{i\Phi} + \left(a_0^- + \frac{a_1^-}{r} + \dots\right)e^{-i\Phi}\right],$$
$$\chi \to \frac{1}{r^{\frac{n}{2}-1}}\left[\left(\left(-\frac{k}{\omega} + \frac{c^+}{r}\right)a_0^+ + \dots\right)e^{i\Phi} + \left(\left(\frac{k}{\omega} + \frac{c^-}{r}\right)a_0^- + \dots\right)e^{-i\Phi}\right]. \tag{9}$$

In one of the asymptotic regions (either at the horizon or at infinity), we need 4 independent coefficients to parameterize these two fields. Let us denote the ingoing and outgoing wave coefficients ($-/+$ respectively) at the horizon and at infinity by

$$\vec{\mathbf{h}} = (\mathbf{h}^+, \mathbf{h}^-) = (h_i^+, h_i^-), \quad \vec{\mathbf{y}} = (\mathbf{y}^+, \mathbf{y}^-) = (y_i^+, y_i^-),$$

where $i = 1, 2$. Due to linearity, we can define a scattering matrix

$$\vec{\mathbf{y}} = \mathbf{S}\vec{\mathbf{h}} \;\Leftrightarrow\; \begin{pmatrix}\mathbf{y}^+\\ \mathbf{y}^-\end{pmatrix} = \left(\begin{array}{c|c}\mathbf{S}^{++} & \mathbf{S}^{+-}\\ \hline \mathbf{S}^{-+} & \mathbf{S}^{--}\end{array}\right)\begin{pmatrix}\mathbf{h}^+\\ \mathbf{h}^-\end{pmatrix} \;\Leftrightarrow\; \begin{pmatrix}y_i^+\\ y_i^-\end{pmatrix}$$
$$= \sum_j \left(\begin{array}{c|c}S_{ij}^{++} & S_{ij}^{+-}\\ \hline S_{ij}^{-+} & S_{ij}^{--}\end{array}\right)\begin{pmatrix}h_j^+\\ h_j^-\end{pmatrix},$$

which contains all the information on the scattering process. At the horizon we impose an ingoing boundary condition $\mathbf{h}^+ = 0$. We can define a reflection matrix

$$\mathbf{y}^+ = \mathbf{S}^{+-}(\mathbf{S}^{--})^{-1}\mathbf{y}^- \equiv \mathbf{R}\,\mathbf{y}^-, \tag{10}$$

and fix the freedom of this definition by computing the energy flux

$$\mathscr{F}|_r = -\int_{S^n} d\Sigma\, T_t{}^r, \tag{11}$$

where $d\Sigma$ is the volume element on the Einstein space. At infinity we get

$$\mathscr{F}_\infty^{\text{coupled}} = (\mathbf{y}^-)^\dagger\left(\mathbf{1} - \mathbf{R}^\dagger\mathbf{R}\right)\mathbf{y}^- \equiv (\mathbf{y}^-)^\dagger\mathbf{T}\,\mathbf{y}^-, \tag{12}$$

where we have defined a (hermitian) transmission matrix $\mathbf{T}$. Using energy flux conservation, one obtains an alternative definition of $\mathbf{T}$ at the horizon

$$\mathbf{T} = (\mathbf{S}^{--}\mathbf{S}^{\dagger--})^{-1}\,. \tag{13}$$

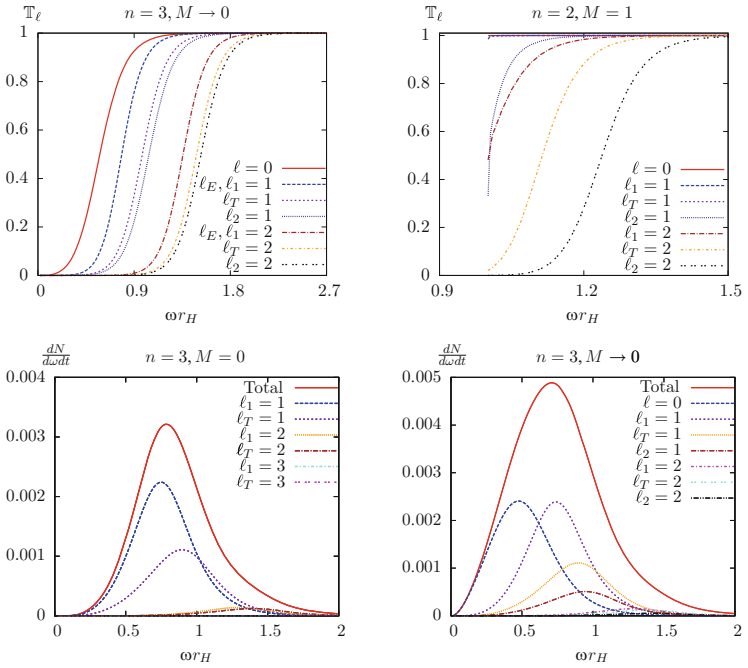


**Fig. 1** *Transmission factors and Number fluxes:* the first row shows transmission factors of coupled modes $(\ell_1, \ell_2)$, transverse vector mode $\ell_T$ and electromagnetic mode $\ell_E$; the second row shows number fluxes for a Maxwell field (*left panel*) and the small $M$ limit of a Proca field (*right panel*)

Through the standard Hawking formulas [6], the number and energy fluxes can be computed after obtaining the transmission factors.

As a summary of our results, we present plots showing transmission factors in the first row and the number fluxes in the second row in Fig. 1. The left panel of the first row shows that in the small mass limit one of the coupled modes $(\ell_1)$ coincides with the electromagnetic mode $(\ell_E)$, which can be used to check the coupled results because the transmission factor of the decoupled mode is easier to define and calculate. The right panel of the first row shows that in the large mass limit the transmission factors start from a non-zero value at the threshold $\omega = M$ for small $\ell$. Since the mass term of Proca theory introduces a longitudinal mode, from the second row we find that this extra mode contributes considerably.

Our results have been extended to charged Proca fields in [8], and they can be used to improve the black hole event generators currently used at the LHC.

**Acknowledgements** The work in this paper is supported by the grants PTDC/FIS/116625/2010 and NRHEP–295189-FP7-PEOPLE-2011-IRSES. M.S. and M.W. are funded by FCT through the grants SFRH/BPD/69971/2010 and SFRH/BD/51648/2011.

## References

1. S. W. Hawking, Commun. Math. Phys **43** (1975) 199–220.
2. I. Antoniadis, Phys. Lett. B **246** (1990) 377.
3. N. Arkani-Hamed, S. Dimopoulos and G. R. Dvali Phys. Lett. B **429** (1998) 263.
4. I. Antoniadis, et al Phys. Lett. B **436** (1998) 257.
5. N. Arkani-Hamed, S. Dimopoulos and G. R. Dvali Phys. Rev. D **59** (1999) 086004.
6. C. Herdeiro, M. O. P. Sampaio and M. Wang Phys. Rev. D **85** (2012) 024005.
7. H. Kodama, A. Ishibashi and O. Seto Phys. Rev. D **62** (2000) 064022.
8. M. Wang, M. O. P. Sampaio and C. Herdeiro, arXiv:1212.2197 [gr-qc].

# Perturbations of Kantowski–Sachs Models with a Cosmological Constant

**Z. Keresztes, M. Forsberg, M. Bradley, P.K.S. Dunsby, and L.Á. Gergely**

**Abstract** We investigate perturbations of Kantowski–Sachs models with a positive cosmological constant, using the gauge invariant $1+3$ and $1+1+2$ covariant splits of spacetime together with a harmonic decomposition. The perturbations are assumed to be vorticity-free and of perfect fluid type, but otherwise include general scalar, vector and tensor modes. In this case the set of equations can be reduced to six evolution equations for six harmonic coefficients.

## 1 Introduction

In this work we consider perturbations of Kantowski–Sachs models with a positive cosmological constant. Some of these models can undergo an anisotropic bounce where the universe changes from a contracting to an expanding phase. A simple argument used by Börner and Ehlers, [1], to show that an isotropic bouncing universe is excluded by observations does not hold for the Kantowski–Sachs models [2]. Hence it is of interest to study the evolution and propagation of perturbations in these models and their possible effects on observables, like the Sachs–Wolfe effect [8]. To do this we use the $1+3$ and $1+1+2$ covariant splits of

Z. Keresztes · L.Á. Gergely
Department of Theoretical Physics and Department of Experimental Physics, University of Szeged, Szeged, Hungary
e-mail: zkeresztes@titan.physx.u-szeged.hu; gergely@physx.u-szeged.hu

M. Forsberg · M. Bradley (✉)
Department of Physics, Umeå University, Sweden
e-mail: mats.forsberg@physics.umu.se; michael.bradley@physics.umu.se

P.K.S. Dunsby
Department of Mathematics and Applied Mathematics, University of Cape Town, South Africa
e-mail: peter.dunsby@uct.ac.za

A. García-Parrado et al. (eds.), *Progress in Mathematical Relativity, Gravitation and Cosmology*, Springer Proceedings in Mathematics & Statistics 60,
DOI 10.1007/978-3-642-40157-2_40, 

spacetime, [3–6], that are suitable for perturbation theory, as they employ variables that vanish on the background and hence their perturbations are gauge invariant [9]. The perturbations are assumed to be vorticity-free and of perfect fluid type, but otherwise include general scalar, vector and tensor modes. The evolution equations for the perturbative variables are then derived in terms of harmonics.

## 2 The 1 + 3 and 1 + 1 + 2 Covariant Formalisms

A covariant formalism for the $1+3$ split of spacetimes with a preferred timelike vector, $u^a$, was developed in [5, 6]. The projection operator onto the perpendicular 3-space is given by $h^b_a = g^b_a + u_a u^b$. With the help of this vectors and tensors can be covariantly decomposed into "spatial" and "timelike" parts. The covariant time derivative and projected spatial derivative are given by

$$\dot{\psi}_{a..b} \equiv u^c \nabla_c \psi_{a...b} \quad \text{and} \quad D_c \psi_{a...b} \equiv h^f_c h^d_a \dots h^e_b \nabla_f \psi_{d...e} \tag{1}$$

respectively. The covariant derivative of the 4-velocity, $u^a$, can be decomposed as

$$\nabla_a u_b = -u_a A_b + D_a u_b = -u_a A_b + \frac{1}{3}\theta h_{ab} + \omega_{ab} + \sigma_{ab} \tag{2}$$

where the kinematic quantities of $u^a$, acceleration, expansion,vorticity and shear are defined by $A_a \equiv u^b \nabla_b u_a$, $\theta \equiv D_a u^a$, $\omega_{ab} \equiv D_{[a} u_{b]}$, and $\sigma_{ab} \equiv D_{<a} u_{b>}$ respectively. These quantities, together with the Ricci tensor (expressed via the Einstein equations by energy density $\mu$ and pressure $p$ for a perfect fluid) and the electric, $E_{ab} \equiv C_{acbd} u^c u^d$, and magnetic, $H_{ab} \equiv \frac{1}{2}\eta_{ade} C^{de}_{\ bc} u^c$, parts of the Weyl tensor, are then used as dependent variables. From the Ricci and Bianchi identities one obtains evolution equations in the $u^a$ direction and constraints.

A formalism for a further split $(1+2)$ with respect to a spatial vector $n^a$ (with $u^a n_a = 0$) was developed in [3, 4]. Projections perpendicular to $n^a$ are made with $N^b_a = h^b_a - n_a n^b$, and in an analogous way to above "spatial" vectors and tensors may be decomposed into scalars along $n^a$ and perpendicular two-vectors and symmetric, trace-free two-tensors as $A^a = \mathscr{A} n^a + \mathscr{A}^a$, $\omega^a = \Omega n^a + \Omega^a$, $\sigma_{ab} = \Sigma(n^a n^b - \frac{1}{2} N_{ab}) + 2\Sigma_{(a} n_{b)} + \Sigma_{ab}$ and similarly for $E_{ab}$ and $H_{ab}$ in terms of $\mathscr{E}$, $\mathscr{E}_a$, $\mathscr{E}_{ab}$ and $\mathscr{H}$, $\mathscr{H}_a$, $\mathscr{H}_{ab}$ respectively. Derivatives along and perpendicular to $n^a$ are

$$\hat{\psi}_{a...b} \equiv n^c D_c \psi_{a...b} = n^c h^f_c h^d_a \dots h^e_b \nabla_f \psi_{d...e} \ \text{ and } \ \delta_c \psi_{a...b} \equiv N^f_c N^d_a \dots N^e_b D_f \psi_{d...e} \tag{3}$$

respectively. Similarly to the decomposition of $\nabla_a u_b$, $D_a n_b$ and $\dot{n}_a$ can be decomposed into further "kinematical" quantities of $n^a$ as

$$D_a n_b = n_a a_b + \frac{1}{2}\phi N_{ab} + \xi\epsilon_{ab} + \zeta_{ab} \quad \text{and} \quad \dot{n}_a = \mathscr{A} u_a + \alpha_a \tag{4}$$

where $a_a \equiv \hat{n}_a$, $\phi \equiv \delta_a n^a$, $\xi \equiv \frac{1}{2}\epsilon^{cabd}\delta_a n_b u_c n_d$, $\zeta_{ab} \equiv \delta_{\{a}n_{b\}}$, $\mathscr{A} \equiv n^a A_a$, $\alpha_a \equiv N_a^b \dot{n}_b$.

The Ricci and Bianchi identities are then written as evolution and propagation equations in the $u^a$ and $n^a$ directions and constraints.

## 3 Perturbations of Kantowski–Sachs

As backgrounds we take the Locally Rotationally Symmetric (LRS) Kantowski–Sachs cosmologies [7]

$$ds^2 = -dt^2 + a_1^2(t)dz^2 + a_2^2(t)\left(d\vartheta^2 + \sin^2\theta d\varphi^2\right) \tag{5}$$

with cosmological constant $\Lambda > 0$ and matter given by a perfect fluid with barytropic equation $p = p(\mu)$. The shear $\Sigma$, energy density $\mu$ and the expansion $\theta$ evolve as

$$\dot{\Sigma} = -\frac{1}{2}\Sigma^2 - \frac{2}{3}\Sigma\theta - \mathscr{E}, \quad \dot{\mu} = -\theta(\mu + p), \quad \dot{\theta} = (\Lambda - \frac{1}{2}\mu - \frac{3}{2}p) - \frac{1}{3}\theta^2 - \frac{3}{2}\Sigma^2 \tag{6}$$

where the electric part of the Weyl tensor is $\mathscr{E} = -\frac{2}{3}\mu - \frac{2}{3}\Lambda - \Sigma^2 + \frac{2}{9}\theta^2 + \frac{1}{3}\Sigma\theta$.

Instead of the background variables $\theta, \Sigma, \mathscr{E}, \mu$ we use their gradients

$$W_a \equiv \delta_a\theta, \quad V_a \equiv \delta_a\Sigma, \quad X_a \equiv \delta_a\mathscr{E}, \quad \mu_a \equiv \delta_a\mu, \tag{7}$$

which vanish on the background and hence are gauge invariant (the derivatives $\hat{\theta} \equiv n^a D_a\theta$ etc. can be given in terms of the $\delta_a$ derivatives due to commutation relations in the case of no vorticity). Similar variables vanishing on the background are $a_a, \phi, \xi, \zeta_{ab}, \alpha_a, \mathscr{A}, \mathscr{A}_a, \Sigma_a, \Sigma_{ab}, \mathscr{E}_a, \mathscr{E}_{ab}, \mathscr{H}, \mathscr{H}_a, \mathscr{H}_{ab}$ where $a_a$ can be put to zero by choice of frame.

The scalar, vector and tensor variables are expanded in harmonics according to

$$\Psi = \sum_{k_\parallel, k_\perp} \Psi_{k_\parallel k_\perp} P_{k_\parallel} Q_{k_\perp}, \quad \Psi_a = \sum_{k_\parallel, k_\perp} P_{k_\parallel}\left(\Psi^V_{k_\parallel k_\perp} Q_a^{k_\perp} + \overline{\Psi}^V_{k_\parallel k_\perp}\overline{Q}_a^{k_\perp}\right),$$
$$\Psi_{ab} = \sum_{k_\parallel, k_\perp} P_{k_\parallel}\left(\Psi^T_{k_\parallel, k_\perp} Q_{ab}^{k_\perp} + \overline{\Psi}^T_{k_\parallel, k_\perp}\overline{Q}_{ab}^{k_\perp}\right) \tag{8}$$

where $Q_{k_\perp}$, $Q_a^{k_\perp}$, $\overline{Q}_a^{k_\perp}$, $Q_{ab}^{k_\perp}$ and $\overline{Q}_{ab}^{k_\perp}$ are harmonics on the 2-spheres of constant $z$ and $P_{k_\parallel}$ the corresponding expansion functions in the $z$-direction.

All coefficients can be given in terms of $\mu^V_{k_\parallel,k_\perp}$, $\Sigma^T_{k_\parallel,k_\perp}$, $\mathscr{E}^T_{k_\parallel,k_\perp}$, $\overline{\mathscr{H}}^T_{k_\parallel,k_\perp}$ and $\overline{\mathscr{E}}^T_{k_\parallel,k_\perp}$, $\mathscr{H}^T_{k_\parallel,k_\perp}$, so the system has six degrees of freedom. The first four coefficients form a closed system of evolution equations coupled to the density gradient, in agreement with the results for scalar perturbations in [2]. This reads

$$\dot{\mu}^V_{k_\parallel,k_\perp}=\left[\frac{\Sigma}{2}\left(1-6\frac{\mu+p}{B}\right)-\frac{4\theta}{3}\right]\mu^V_{k_\parallel,k_\perp}+ \frac{a_2}{2}(\mu+p)\left[(1-C)\left(B\Sigma^T_{k_\parallel,k_\perp}+\mathscr{E}^T_{k_\parallel,k_\perp}\right)-P\overline{\mathscr{H}}^T_{k_\parallel,k_\perp}\right], \tag{9}$$

$$\dot{\Sigma}^T_{k_\parallel,k_\perp}=-\frac{1}{a_2(\mu+p)}\frac{dp}{d\mu}\mu^V_{k_\parallel,k_\perp}+\left(\Sigma-\frac{2\theta}{3}\right)\Sigma^T_{k_\parallel,k_\perp}-\mathscr{E}^T_{k_\parallel,k_\perp}, \tag{10}$$

$$\dot{\mathscr{E}}^T_{k_\parallel,k_\perp}=-\frac{3\Sigma}{2a_2B}\mu^V_{k_\parallel,k_\perp}-\frac{\mu+p}{2}\Sigma^T_{k_\parallel,k_\perp}-\frac{3}{2}(F+\Sigma C)\mathscr{E}^T_{k_\parallel,k_\perp}+\frac{P}{2}\overline{\mathscr{H}}^T_{k_\parallel,k_\perp},$$

$$\dot{\overline{\mathscr{H}}}^T_{k_\parallel,k_\perp}=-\frac{ik_\parallel}{a_1a_2B}\mu^V_{k_\parallel,k_\perp}-R\overline{\mathscr{H}}^T_{k_\parallel,k_\perp}-\frac{ik_\parallel}{a_1}\left[1-\frac{3}{2}\left(C-\frac{\mathscr{E}}{B}\right)\right]\mathscr{E}^T_{k_\parallel,k_\perp}, \tag{11}$$

where we have introduced the notations $B=\frac{2k_\parallel^2}{a_1^2}+\frac{k_\perp^2}{a_2^2}+\frac{9}{2}\Sigma^2+3\mathscr{E}$, $C=B^{-1}\left(\frac{2-k_\perp^2}{a_2^2}+3\mathscr{E}\right)$, $D=C+\frac{\mu+p}{B}$, $E=\frac{\Sigma}{2}\left(C-\frac{\mathscr{E}}{B}\right)+\frac{\theta\mathscr{E}}{3B}$, $F=\Sigma+\frac{2\theta}{3}$, $P=\frac{a_1}{ik_\parallel}\left[\frac{2k_\parallel^2}{a_1^2}(1-C)-\frac{k_\perp^2}{a_2^2}\frac{2-k_\perp^2}{a_2^2B}\right]$ and $R=\frac{3}{2}F-\left(\Sigma+\frac{\theta}{3}\right)\frac{k_\perp^2}{a_2^2B}-\frac{1}{2B}\left(\Sigma-\frac{2\theta}{3}\right)\left(D-\frac{2k_\parallel^2}{a_1^2}\right)$. The two last coefficients form a closed system for free waves

$$\dot{\overline{\mathscr{E}}}^T_{k_\parallel,k_\perp}=-\frac{3}{2}(F+\Sigma D)\overline{\mathscr{E}}^T_{k_\parallel,k_\perp}+\frac{ik_\parallel}{a_1}(1-D)\mathscr{H}^T_{k_\parallel,k_\perp},$$

$$\dot{\mathscr{H}}^T_{k_\parallel,k_\perp}=-\frac{a_1}{2ik_\parallel}\left(\frac{2k_\parallel^2}{a_1^2}-BC+9\Sigma E\right)\overline{\mathscr{E}}^T_{k_\parallel,k_\perp}-\frac{3}{2}(2E+F)\mathscr{H}^T_{k_\parallel,k_\perp}. \tag{12}$$

These sets of equations can be used to study the propagation of gravitational waves and the coupling between scalar and tensor perturbations. Furthermore, from the null geodesics of photons, equations for the redshift in different directions can be given completely in terms of the $1+1+2$ quantities. From their solutions the Sachs–Wolfe effect and the corresponding variations in the CMB temperature can be calculated.

**Acknowledgements** ZK was supported by OTKA grant no. 100216.

## References

1. G. Börner and J. Ehlers, Astron. Astrophys., **204**, 1 (1988)
2. M. Bradley, P. K. S. Dunsby, M. Forsberg, and Z. Keresztes, Class. Quantum Grav. **29**, 095023 (2012).
3. C.A. Clarkson, Phys. Rev. D, **76**, 104034 (2007).
4. C. A. Clarkson and R. Barrett, Class. Quantum Grav. **20**, 3855 (2003).
5. G.F.R Ellis and M. Bruni, Phys. Rev. D, **40**, 1804 (1989).
6. G.F.R Ellis and H. van Elst, in M. Lachieze-Rey (ed.), *Theoretical and Observational Cosmology*, NATO Science Series, Kluwer Academic Publishers (1998), arXiv:gr-qc/9812046v5.
7. R. Kantowski and R.K. Sachs, J. Math. Phys. **7**, 443 (1967).
8. R. K. Sachs, and A. M. Wolfe, Astrophys. J. **147**, 73 (1967)
9. J.M. Stewart and M. Walker, Proc. R. Soc. London, **A341**, 49 (1974).

# On the Uniqueness of the Energy and Momenta of an Asymptotically Minkowskian Space-Time: The Case of the Schwarzschild Metric

**Ramon Lapiedra and Juan Antonio Morales-Lladosa**

**Abstract** Some theorems about the uniqueness of the energy of asymptotically Minkowskian spaces are recalled. The suitability of almost everywhere Gauss coordinates to define some kind of physical energy in these spaces is commented. Schwarzschild metric, when its source radius is larger than the Schwarzschild radius and in the case of a black hole, is considered. In both cases, by using a specific almost everywhere Gaussian coordinate system, a vanishing energy results. We explain why this result is not in contradiction with the quoted theorems. Finally we conclude that this metric is a particular case of what we have called elsewhere a *creatable universe*.

## 1 Introduction

Let it be an asymptotically flat space-time, $V_4$. Choose a symmetric complex to allow for a definition of the angular 4-moment of $V_4$. More precisely, let us take the Weinberg complex [1]. As it is well known, the energy of $V_4$ associated to this complex is just the Arnowitt, Deser, Misner energy [2]. Now, refer $V_4$ to coordinates $\{x^\alpha\}$ which are rectilinear ones at the spatial infinity $r \to \infty$, such that $g_{\alpha\beta} - \eta_{\alpha\beta} = O(1/r)$, where $g_{\alpha\beta}$ is the $V_4$ metric and $\eta_{\alpha\beta}$ is the Minkowski metric. Then, well-known theorems (cf. [3,4]) state that the corresponding energy, $P^0$, of $V_4$ is positive and vanishes if and only if $V_4$ becomes the Minkowski space, $M_4$.

R. Lapiedra (✉) · J.A. Morales-Lladosa
Departament d'Astronomia i Astrofísica, Universitat de València, 46100 Burjassot, València, Spain
e-mail: ramon.lapiedra@uv.es; antonio.morales@uv.es

A. García-Parrado et al. (eds.), *Progress in Mathematical Relativity, Gravitation and Cosmology*, Springer Proceedings in Mathematics & Statistics 60,
DOI 10.1007/978-3-642-40157-2_41, 

## 2 Gauss Coordinates and $V_4$ 4-Momenta

In some previous papers [5–7], the present authors and others have explained why in order to define consistent linear, $P^\alpha$, and angular, $J^{\alpha\beta}$, 4-momenta of $V_4$, we should use, at least in the infinity $r \to \infty$, Gaussian coordinate systems. These coordinate systems can always be implemented *almost* everywhere in the present case of Schwarzschild metric and can be defined as the ones where $g_{00} = -1$ and $g_{0i} = 0$. They correspond to families of free falling observers and the coordinate time corresponds to a *universal* (see [8]) and, at the same time, proper time. Because of this property, the different elementary contributions to $P^\alpha$ and $J^{\alpha\beta}$, when these 4-momenta are expressed as 3-space volume integrals at a given time, are calculated in simultaneous physical times in a natural way; the same happens when we express these 4-momenta as 2-surface integrals on the boundary $r \to \infty$.

Starting from $P^\alpha$ and $J^{\alpha\beta}$ written as 3-space volume integrals, we can write these 4-momenta as 2-surface integrals on the boundary $r \to \infty$ by applying Gauss theorem, provided that the first 3-space derivatives of the metric be continuous everywhere. Notice, by the way, that rectilinear coordinates at this boundary are trivially a particular kind of Gaussian coordinates on it.

## 3 The Case of the Schwarzschild Metric

Let us consider the metric of an ideal spherical, static, non rotating star, whose source radius $a$ (the star radius) is larger than the Schwarzschild radius, $r_0 \equiv 2m$, where $m$ is the star mass, and we have taken the gravitational constant and the speed of light equal to 1. This metric is regular everywhere when $a > r_0$. For $r > a$, using the standard static coordinates, it can be written

$$ds^2 = -\left(1 - \frac{r_0}{r}\right) dt^2 + \frac{dr^2}{1 - \frac{r_0}{r}} + r^2 d\sigma^2, \tag{1}$$

where $d\sigma^2 \equiv d\theta^2 + \sin^2\theta\, d\phi^2$ is the metric on the unit 2-sphere. These coordinates are manifestly Gaussian for $r \to \infty$, but not everywhere since $g_{00} = -1 + r_0/r \neq -1$.

Imagine that we want to calculate the energy, $P^0$, of this metric with respect to Gauss coordinates everywhere and not only at the infinity $r \to \infty$. For instance, with respect to the new coordinates $(T, \rho)$ defined as

$$T = t + 2\sqrt{r_0 r} + r_0 \ln\left|\frac{\sqrt{r} - \sqrt{r_0}}{\sqrt{r} + \sqrt{r_0}}\right|, \quad r^{3/2} = \rho^{3/2} - 3\sqrt{r_0}\, T/2 + C, \tag{2}$$

with $C$ an arbitrary constant.

In these coordinates we have for the metric (1),

$$ds^2 = -dT^2 + \frac{\rho}{r}d\rho^2 + r^2 d\sigma^2, \tag{3}$$

showing that the new coordinates with $(T, \rho)$ are Gauss coordinates *almost* everywhere for $r > a$. Further, it can be easily seen that for each constant value, $T_0$ of $T$, they are rectilinear coordinates for $\rho \to \infty$. More precisely, for $g_{\alpha\beta}$ in the metric (3) we have $g_{\alpha\beta} - \eta_{\alpha\beta} = O(1/\rho^{3/2}) = O(1/r^{3/2})$.

Since this metric, when completed with its inner $(r < a)$ part, is regular everywhere, starting from the expression of $P^0$ as a 3-space volume integral, and using Gauss theorem, we can write $P^0$ as a 2-surface integral over the boundary $r \to \infty$:

$$16\pi P^0 = \int \partial_i(\partial_j g_{ij} - \partial_i g_{jj})dx^1 dx^2 dx^3 = \lim_{r\to\infty} \int (\partial_j g_{ij} - \partial_i g_{jj})x^i r \sin\theta d\theta d\phi, \tag{4}$$

where the contractions are performed with the Kronecker $\delta_{ij}$, and $r^2 = \delta_{ij}x^i x^j$. Then, using the metric (3) in (4), taking into account the above asymptotic behaviour for $g_{\alpha\beta}$, straightforwardly produces the result $P^0 = 0$, to be compared with the well-known result $P^0 = m$, for the standard static coordinates. The new result is not in contradiction with the positiveness of $P^0$, quoted in the Introduction, since the ancient condition $g_{\alpha\beta} - \eta_{\alpha\beta} = O(1/r)$ has now been replaced by $g_{\alpha\beta} - \eta_{\alpha\beta} = O(1/r^{3/2})$.

On the other hand, it can be easily seen that coordinates $(T, \rho)$ are associated to free falling observers, which are asymptotically at rest since for $\rho \to \infty$, we have $\rho \to r$. So, $P^0 = 0$ could be considered as the *intrinsic* energy of the Schwarzschild metric [9].

## 4 The Energy of a Black Hole

Imagine that differently to the precedent section we have a black hole, i.e., $a < r_0$. Then, the above standard static coordinates $(t, r)$ in (1) can no longer be used to calculate $P^0$. This happens that way because, when expressing $P^0$ as a 3-space volume integral, the contribution of the interval $(r > r_0, \infty)$ to this integral goes to infinite when $r \to r_0$, which means in particular that we cannot apply Gauss theorem in order to transform this volume integral in the corresponding 2-surface integral. Thus, if we want to calculate some physical value of $P^0$ for a black hole, we have to leave the standard, and now no more static everywhere coordinates $(t, r)$. This leaving was an avoidable option that we took in the precedent section when going to the new coordinates $(T, \rho)$, but now this is actually a need. Thus, let us fulfill this need by taking the Gauss coordinates $(T, \rho)$. In order to calculate the $P^0$ value associated to these Gauss coordinates, let us fix a given time value, $T_0$, of $T$.

Then, in (2), let us take the particular $C$ value, $C = 3\sqrt{r_0}\,T_0/2$. Therefore, we are left with the instantaneous equality $\rho = r$, which means that the Schwarzschild metric (3) becomes $M_4$ for $T = T_0$ (discarding the value $r = 0$ from this slice since the intrinsic singularity at $r = 0$ did not belong to the original space-time manifold, $V_4$), which is in itself a very remarkable result. Then, trivially, the corresponding value of $P^0$, defined in a natural way as the corresponding integral limit when we approach $r = 0$, vanishes, whatever be the selected $T_0$ value (each time, of course, selecting as explained a suitable different $C$ value). Notice that this result is in accordance with the above vanishing of $P^0$ for the ideal star of the precedent section. Actually, we could imagine an ideal star having enough mass to undergo an ideal collapse preserving the spherical symmetry and without expelling any mass (of course, without radiating any gravitational energy too). Thus, if initially it was $P^0 = 0$, according to the precedent section, this should be the remaining value when the collapse has been completed, which is just the result we have obtained in the present section for the resulting black hole.

## 5 The *Creatable* Character of the Schwarzschild Metric

We have seen that the energy, $P^0$, of the Schwarzschild metric in Gaussian coordinates $(T, \rho)$ vanishes. But, these coordinates are adapted to the spherical symmetry of the metric. Thus, the linear 3-momentum, $P^i$, the angular 3-momentum, $J^{ij}$, and also the $J^{0i}$ components of the 4-angular momentum, vanish too. In all, the two 4-momenta of Schwarzschild metric vanish. In [5–7, 9] we have called such an space-time with vanishing 4-momenta a *creatable universe*. The name comes from the speculation [10] that our Universe could have raised as a vacuum quantum fluctuation, in which case one could expect that these momenta would vanish. But, $P^0$, for instance, does not vanish for the Schwarzschild metric when we use standard static coordinates. This seems to remove any intrinsic meaning to the concept of *creatable universe*. However, our point of view is that we have a *creatable universe* each time we have at least a coordinate system where all two 4-momenta vanish, assuming that other coordinate systems where we have not such a vanishing simply are breaking some symmetry of the metric. Which one? Just some of the ones that allow to obtain the above vanishing in the above singled out coordinate system.

**Acknowledgements** Work supported by the Spanish ministries of "Ciencia e Innovación" and "Economía y Competitividad", MICINN-FEDER projects FIS2009-07705 and FIS2012-33582.

## References

1. Weinberg, S.: Gravitation and Cosmology, John Wiley and Sons (1972)
2. Arnowitt, R., Deser, S., Misner, C. W.: Phys. Rev. D **122**, 997 (1961)

3. Schoen R., Yau, S-T.: Commun. Math. Phys., **65**, 45 (1979); ibid. **79**, 231 (1981)
4. Parker, T., Taubes, C. H.: Commun. Math. Phys., **84**, 223 (1982).
5. Lapiedra, R., Morales–Lladosa, J. A.: Gen. Relativ. Gravit. **44**, 367 (2012)
6. Lapiedra, R., Sáez, D.: Phys. Rev. D **77**, 104011 (2008)
7. Ferrando, J. J., Lapiedra, R., Morales, J. A.: Phys. Rev. D **75**, 124003 (2007)
8. Landau, L., Lifchitz, E. M.: The Classical Theory of Fields, epigraph 84, Elsevier, Amsterdam, Fourth ed., 1975. Reprinted (2007)
9. Lapiedra, R., Morales–Lladosa, J. A.: Gen. Relativ. Gravit. 10.1007/s10714-013-1515-z
10. Tryon, E. P.: Nature **246**, 396 (1973)

# Matter and Ricci Collineations

**Josep Llosa**

**Abstract** The infinitesimal transformations that leave invariant a two-covariant symmetric tensor are studied. The interest of these symmetry transformations lies in the fact that this class of tensors includes the energy-momentum and Ricci tensors. Moreover, all curvature collineations are necessarily Ricci collineations. We find that in most cases the class of infinitesimal generators of these transformations is a finite dimensional Lie algebra but also, in some cases exhibiting a higher degree of degeneracy, this class is infinite dimensional and may fail to be a Lie algebra.

## 1 Introduction

The interest in the study of symmetries in General Relativity is long-standing. Some of them, namely isometries and affine transformations and their infinitesimal counterparts, Killing vector fields and affine vector fields, are well understood since long ago [1]. In the last 20 years, there has been an steady interest in curvature collineations, Ricci collineations and even matter (Einstein) collineations [2, 3]. Their infinitesimal counterparts, namely collineation fields, are characterized by the vanishing of the Lie derivative of the curvature tensor (resp., the Ricci or the energy-momentum tensor). Collineation fields are thus an extension of the aforementioned Killing fields and affine fields in that every Killing vector field is an affine vector filed which in turn is a curvature collineation field and also a Ricci and a matter collineation field. However it is well known that collineation fields present new features and, contrarily to the case of Killing and affine fields, the class $\mathscr{C}$ of curvature (resp., Ricci and matter) collineation fields is a real vector space which may be infinite dimensional; this is due to the dependence on arbitrary functions, which

J. Llosa (✉)
Dept. Física Fonamental and Institut de Ciències del Cosmos (ICCUB),
Universitat de Barcelona, Spain
e-mail: pitu.llosa@ub.edu

A. García-Parrado et al. (eds.), *Progress in Mathematical Relativity, Gravitation and Cosmology*, Springer Proceedings in Mathematics & Statistics 60,
DOI 10.1007/978-3-642-40157-2_42, 

also results in the fact that a collineation field needs not to be smooth and, as a consequence, $\mathscr{C}$ may not be a Lie algebra [3].

Given a 4-manifold $\mathscr{M}$ and a smooth field of symmetric 2-covariant tensors $T$, we shall concentrate on finding the class $\mathscr{C}$ of vector fields $\mathbf{X}$ such that $\mathscr{L}_{\mathbf{X}} T = 0$ and try to answer the questions of whether the number of dimensions of $\mathscr{C}$ is finite, $\mathbf{X}$ is smooth or $\mathscr{C}$ is a Lie algebra.

The answers to these questions depend, but not exclusively, on the rank of $T$. Particularly, if rank $T = 4$, $T$ itself can be taken as a non-degenerate metric tensor and the collineation equation is actually a Killing equation, $\mathbf{X}$ is a smooth vector field, $\mathscr{C}$ is a Lie algebra and $\dim \mathscr{C} \leq 10$.

For rank $T < 4$, we come across an assorted casuistry which depends not only on the rank of $T$ but also on the derivatives of $T$. In many instances $\mathbf{X}$ is a solution of a complete partial differential system that gives all derivatives up a certain order of $X^a$ as functions of lower order derivatives. In these cases, $\mathbf{X}$ is smooth and depends on a finite number of real parameters, and $\mathscr{C}$ is a finite dimensional Lie algebra. In what follows we list a classification of the tensor fields $T$ according to its class $\mathscr{C}$ of collineation fields (the reader can find the details in [4]).

Let $T$ be a 2-covariant symmetric smooth tensor field on a 4-manifold $\mathscr{M}$, with constant rank $T = m < 4$. At each $p \in \mathscr{M}$ it exists a base, $\{\phi^a\}_{a=1\ldots4}$, of $\Lambda^1\mathscr{M}$ such that

$$T = \eta_{\alpha\beta}\phi^\alpha \otimes \phi^\beta, \qquad \text{with} \qquad \eta_{\alpha\beta} = \text{diag}(+1 \overset{r}{\ldots} +1, -1 \overset{s}{\ldots} -1) \tag{1}$$

and $r + s = m$ ($\alpha, \beta = 1 \ldots m$; $A, B = m + 1 \ldots 4$; $a, b = 1 \ldots 4$ and the summation convention is always understood).

The set of 1-forms $\{\phi^\alpha\}_{\alpha=1\ldots m}$ is called a *$T$-frame* and is determined up to a $T$-rotation:

$$\tilde{\phi}^\alpha := R^\alpha_{\ \beta}\phi^\beta, \qquad \text{where} \qquad R^\mu_{\ \alpha} R^\nu_{\ \beta}\eta_{\mu\nu} = \eta_{\alpha\beta} \tag{2}$$

i.e. $R^\alpha_{\ \beta}$ is a field of $\eta$-orthogonal matrices.

## 2 Rank 3 Tensors

The $T$-frame $\{\phi^\alpha\}_{\alpha=1\ldots3}$ determines an integrable Pfaff system and local charts exist such that $T = T_{\alpha\beta}(y^a)\, dy^\alpha \otimes dy^\beta$. Let us now write

$$\mathbf{X} = \mathbf{Z} + f\, \partial_4 \qquad \text{and consider} \qquad K_{\alpha\beta} := \frac{1}{2}\, \partial_4 T_{\alpha\beta}$$

- If $K_{\alpha\beta} = 0$, then $\mathbf{Z}$ is a Killing vector of the 3-metric $T_{\alpha\beta}(y^\nu)$ on the submanifolds $y^4 =$ constant and $f$ is an arbitrary function.
- If $\partial_4 K_{\alpha\beta}$ is not proportional to $K_{\alpha\beta}$, then $\mathscr{C}$ is a Lie algebra and $\dim\mathscr{C} \leq 6$.

- If $\partial_4 K_{\alpha\beta} \propto K_{\alpha\beta}$, but $K^{\alpha\beta}K_{\beta\mu} \neq 0$ and $K_{\alpha\beta}$ is not proportional to $T_{\alpha\beta}$, then $\mathscr{C}$ is a Lie algebra and $\dim\mathscr{C} \leq 7$.

In the nongeneric cases that one of the above inequalities fails, our analysis has been left incomplete and they probably involve arbitrary functions, i.e. $\mathscr{C}$ is infinite dimensional.

## 3 Rank 1 Tensors

We write $T = \phi \otimes \phi$ and $\mathscr{L}_{\mathbf{X}} T = 0$ amounts to $\mathscr{L}_{\mathbf{X}}\phi = 0$. Several possibilities arise, depending on the class of $\phi$ [5].

*Class 4* $d\phi$ is simplectic and, in canonical coordinates $(q^i, p_j)$, we have that

$$\mathbf{X} = f^{|i}\partial_i - f_{|j}\partial^j, \qquad \text{with} \quad f^{|i} := \frac{\partial f}{\partial p_i}, \quad f_{|i} := \frac{\partial f}{\partial q^i}$$

where $f(q^i, p_j)$ is homogeneous and of first degree on the "momenta" $p_j$.

*Class 3* Coordinates $(q^i, p_j)$ exist such that

$$\mathbf{X} = f^{|1}\partial_1 - f_{|1}\partial^1 + (f - p_1 f^{|1})\,\partial_2 + X_2\partial^2, \qquad f(p_1, q^1), \text{ and } X_2 \text{ arbitrary}$$

*Class 2* Coordinates $(q^i, p_j)$ exist such that

$$\mathbf{X} = F\,\partial_1 - p_1 F'\partial^1 + X^2\partial_2 + X_2\partial^2, \qquad F(q^1), X^2 \text{ and } X_2 \text{ arbitrary}$$

*Class 1* In this case coordinates $x^a$, $a = 1 \ldots 4$ exist such that $\phi = dx^1$ and

$$\mathbf{X} = C\,\partial_1 + \sum_{i=2}^{4} X^i\partial_i, \qquad C \text{ constant and } X^i(q^j, p_l) \text{ arbitrary}$$

## 4 Rank 2 Tensors

We take the canonical expression, $T = \eta_{\mu\nu}\phi^\mu \otimes \phi^\nu$, $\mu, \nu = 1, 2$, and classify $T$ on the basis of the volume forms $\Sigma^{\mu\nu} = d\phi^\mu \otimes d\phi^\nu$ and $\Upsilon^\mu = d\phi^\mu \otimes \phi^1 \otimes \phi^2$.

*Type 2.I.a* There is a $T$-frame in which $\Sigma^{11} \neq 0$, $\Upsilon^1 = 0$ and $\Upsilon^2 \neq 0$ and a canonical base $\{\phi^a\}_{a=1\ldots4}$ exists such that $\mathscr{L}_{\mathbf{X}}\phi^a = 0$. In this case $\dim\mathscr{C} \leq 4$.

*Type 2.I.b* There is a $T$-frame in which $\Sigma^{11} = \Upsilon^1 = 0$ and $\Upsilon^2 \neq 0$. Then it exists a base, $\{\phi^a\}_{a=1\ldots4}$, in which

$$d\phi^2 = \frac{s}{2}\,\phi^1 \wedge \phi^2 + \phi^3 \wedge \phi^4, \qquad d\phi^1 = r\,\phi^1 \wedge \phi^2 + v_\alpha\phi^\alpha \wedge \phi^3$$

- If $v_\alpha = 0$, then $\mathbf{X}$ contains arbitrary functions and
- if $v_\alpha \neq 0$ and $\phi^3 \wedge d\phi^3 \neq 0$, then $\dim \mathscr{C} \leq 4$.

*Type 2.N* This case, $\Upsilon^1 = \Upsilon^2 \neq 0$, only occurs if the tensor $T$ has no definite sign, and a canonical base $\{\phi^a\}_{a=1\ldots4}$ exists such that

$$d\phi^1 = \frac{t}{2}\,\phi^1\wedge\phi^2+\phi^3\wedge\phi^4, \qquad d(\phi^2-\phi^1) = \frac{r}{2}\,\phi^1\wedge\phi^2+\left[w(\phi^2-\phi^1)+u\phi^2\right]\wedge\phi^3$$

with either $u \neq 0$ or $u = r = 0$.

*Subtype 2.N.1* If $u \neq 0$ and $\phi^3\wedge d\phi^3 \neq 0$, then $\dim \mathscr{C} \leq 5$ but, if $\phi^3\wedge d\phi^3 = 0$, $\mathbf{X}$ might contain arbitrary functions, and

*Subtype 2.N.0* if $u = r = 0$, then $\mathbf{X}$ might depend on arbitrary functions.

*Type 2.H* If $\Upsilon^1 = \Upsilon^2 = 0$, local charts exist such that $T = T_{\alpha\beta}dx^\alpha \otimes dx^\beta$. Writing then $\mathbf{X} = \mathbf{Z} + f^A\partial_A$, with $\mathbf{Z} = Z^\nu\partial_\nu$, and $K_{A|\alpha\beta} := \frac{1}{2}\,\partial_A T_{\alpha\beta}$, we have that

*Case 2.H.0* If $K_{A|\alpha\beta} = 0$, then $\mathbf{Z}$ is a Killing vector of the 2-metric $T_{\alpha\beta}(x^\nu)$ and $f^A$ are arbitrary functions.

*Case 2.H.2* If $K_{A|\alpha\beta} \neq 0$, $A = 3, 4$, then there is a linear system connecting $f^A$ and $\partial_B f^A$ and another one connecting the derivatives $\partial_b f^A$.

- If the first of these is a Cramer's system, then $\dim \mathscr{C} \leq 3$ and,
- if it is not, but the second system is, then $\dim \mathscr{C} \leq 5$.

We have left unsolved the highly nongeneric case when none of the above mentioned systems is a Cramer's systems. This might involve arbitrary functions.

*Case 2.H.1* $K_{4|\alpha\beta} = 0$ but $K_{3|\alpha\beta} \neq 0$, then $\mathbf{X}$ involves one arbitrary function at least.

## References

1. Stefani H, Kramer D, MacCallum M, Hoenselaers C and Herlt E, *Exact Solutions of Einstein's Field Equations* (Cambridge, Cambridge University Press) 2003; Yano K, *The theory of Lie derivatives and its applications*, (Amsterdam, North-Holland) 1955; Hall, G S, *J Math Phys* **31** 1198 (1990); Hall, G S and Lonie, D P, *Class Quantum Grav* **12** 1007 (1995)
2. Bokhari A H and Qadir A, *J Math Phys* **34** 3543 (1993); Melfo A, Nuñez L, Percoco U and Villalba V M, *J Math Phys* **33** 2258 (1992); Carot, J, da Costa J and Vaz E G L R, *J Math Phys* **35** 4832 (1994)
3. Hall, G S and da Costa, J, *J Math Phys* **32** 2848 and 2854 (1991)
4. Llosa J, " Matter and Ricci collineations", arXiv:1302.3048
5. Godbillon C, *Géometrie Différentielle et Mécanique analytique*, (Paris; Hermann) 1969

# Self-Gravitating Newtonian Disks Revisited

**Patryk Mach, Edward Malec, and Walter Simon**

**Abstract** Recent analytic results concerning stationary, self-gravitating fluids in Newtonian theory are discussed. We give a theorem that forbids infinitely extended fluids, depending on the assumed equation of state and the rotation law. This part extends previous results that have been obtained for static configurations. The second part discusses a Sobolev bound on the mass of the fluid and a rigorous Jeans-type inequality that is valid in the stationary case.

## 1 Introduction

In a series of papers [1–3] we deal with the properties of self-gravitating, stationary configurations of barotropic fluids. In the Newtonian theory, the underlying set of equations consist of the continuity equation

$$\nabla \cdot (\rho \mathbf{U}) = 0, \tag{1}$$

the Euler equation

$$\nabla \cdot (\rho \mathbf{U} \otimes \mathbf{U}) + \nabla p + \rho \nabla \Phi = 0, \tag{2}$$

and the Poisson equation for the gravitational potential

P. Mach (✉) · E. Malec
M. Smoluchowski Institute of Physics, Jagiellonian University, Reymonta 4, 30-059 Kraków, Poland
e-mail: patryk.mach@uj.edu.pl; malec@th.if.uj.edu.pl

W. Simon
Gravitational Physics, Faculty of Physics, Vienna University, Boltzmanngasse 5, 1090 Vienna, Austria
e-mail: walter.simon@univie.ac.at

A. García-Parrado et al. (eds.), *Progress in Mathematical Relativity, Gravitation and Cosmology*, Springer Proceedings in Mathematics & Statistics 60,
DOI 10.1007/978-3-642-40157-2_43, 

$$\Delta\Phi = 4\pi G\rho. \tag{3}$$

Here $\rho$ denotes the mass density, $p$ is the pressure, $\mathbf{U}$ the velocity of the fluid, and $\Phi$ the gravitational potential. The above system is closed by the barotropic equation of state $p = p(\rho)$ and the rotation law.

From the physical point of view solutions of Eqs. (1)–(3) serve as simple models of rotating stars, or self-gravitating accretion disks (note that a disk-like or toroidal shape of the fluid region is allowed). The key mathematical questions include the existence of solutions, their uniqueness, possible parametrization and stability.

In the following we will restrict ourselves to configurations for which the term $(\mathbf{U}\cdot\nabla)\mathbf{U}$ can be expressed as a gradient of a potential, i.e., $(\mathbf{U}\cdot\nabla)\mathbf{U} = \nabla\Phi_{\mathrm{c}}$. In this case the Euler equations can be integrated, yielding

$$h + \Phi_{\mathrm{c}} + \Phi = C, \tag{4}$$

where $h$ denotes the specific enthalpy $dh = dp/\rho$, and $C$ is an integration constant. Equation (4) is only valid in the closure of a region where $\rho \neq 0$. In what follows, this region will be denoted by $\Omega$.

## 2 Finite or Infinite?

In this section we formulate simple criteria on the equation of state $p = p(\rho)$ and the rotation law $\Phi_{\mathrm{c}} = \Phi_{\mathrm{c}}(\mathbf{x})$ that guarantee finite spatial extent of a stationary configuration of the rotating fluid. The detailed discussion can be found in [3]. It extends previous results that have been obtained for the static case, both in General Relativity and in Newtonian Theory [4–6].

The argument is based on the suitable form of the virial theorem. Consider a vector field $\mathbf{w} = \left((\mathbf{x}\cdot\nabla)\Phi + \frac{1}{2}\Phi\right)\nabla\Phi - \frac{1}{2}|\nabla\Phi|^2\mathbf{x} + 4\pi G p\mathbf{x}$. A simple calculation making use of Eqs. (1)–(3) shows that $\nabla\cdot\mathbf{w} = 4\pi G\left(\frac{1}{2}\rho\Phi - \rho\mathbf{x}\cdot\nabla\Phi_{\mathrm{c}} + 3p\right)$. Integrating the above equation over $\mathbb{R}^3$ one obtains

$$\frac{1}{2}\int_{\mathbb{R}^3} d^3x\rho\Phi - \int_{\mathbb{R}^3} d^3x\rho\mathbf{x}\cdot\nabla\Phi_{\mathrm{c}} + 3\int_{\mathbb{R}^3} d^3xp = 0, \tag{5}$$

provided that the surface integral of $\mathbf{w}$ vanishes at infinity. This is assured by requiring that $\rho \in W^{0,2}_{-3-\epsilon}$, $0 < \epsilon < 1$. Then $\Phi \in W^{2,2}_{\mathrm{loc}}$, and $\Phi - M/\sigma \in W^{2,2}_{-1-\epsilon}$. Here we are using weighted Sobolev spaces $W^{k,p}_{\delta}$ $(1 \leq p \in \mathbb{R}, \delta \in \mathbb{R}, k \in \mathbb{N}_0)$ based on weighted Lebesgue norms

$$\|u\|_{k,p,\delta} = \sum_{0\leq|\alpha|\leq k} \|D^\alpha u\|_{p,\delta-|\alpha|}, \quad \|u\|_{p,\delta} = \left(\int_{\mathbb{R}^3} d^3x|u|^p\sigma^{-\delta p-3}\right)^{1/p}$$

with $\sigma = (1 + |\mathbf{x}|)^{1/2}$. The total mass of the fluid $M = \int_{\mathbb{R}^3} d^3x\rho$ is assumed to be finite. We also require that $p \in W^{1,1}_{-4-\epsilon}$.

The integrated Euler equation (4) and Eq. (5) yield $MC = \int_{\mathbb{R}^3} d^3x\,(F + 2\rho D)$, where $F = \rho h - 6p$, $D = \mathbf{x} \cdot \nabla\Phi_c + \frac{1}{2}\Phi_c$. The key observation, following from Eq. (4), is that an infinite configuration with a finite mass requires $C = 0$. Thus if $F > 0$ and $D > 0$, or $F < 0$ and $D < 0$, the fluid must be finite.

We would like to point out the role of the assumed rotation law $D = D(\mathbf{x})$. Former results on the finiteness of configurations were basically amendments to existence theorems [7], and finiteness was assured by imposing stringent conditions on the equation of state only.

The limiting-case conditions $F \equiv 0$ and $D \equiv 0$ lead to a polytropic equation of state $p = K\rho^{1+1/n}$ with $n = 5$, and $\Phi_c = z^{-1/2}\tau(x/z, y/z)$, where $\tau$ is an arbitrary function, and $(x, y, z)$ denote Cartesian coordinates. Remarkably, the resulting equation for $h$ is invariant under the scaling transformation $h(\mathbf{x}) \mapsto h(\mathbf{x}/\lambda)/\sqrt{\lambda}$, $\lambda \in \mathbb{R}_+$.

Another result can be obtained for axially symmetric systems. Let $(r, \phi, z)$ denote the cylindrical coordinates. A classic theorem due to Poincaré and Wavre [8] states that for barotropic fluids with $\mathbf{U} = \omega(r, z)\partial_\phi$ one has in fact $\omega = \omega(r)$, and $\Phi_c = -\int^r dr' r' \omega^2(r')$. In this case the fluid cannot extend to infinity in the $z$ direction, unless it is static. This follows by contradiction from Eq. (4).

Systems with a central point mass $M_c$, that resemble disk-like configurations around compact objects, should be discussed separately. The suitable form of the virial theorem for such systems was formulated in [2], and the reasoning concerning finite extent of stationary configurations was done in [5, 9].

## 3 Mass Estimates

In the following, we give a strict derivation of a new mass estimate valid for a class of stationary configurations of perfect fluids. The discussion is based on a paper by Mach and Malec [1]. We specialize to polytropic equations of state $p = K\rho^{1+1/n}$, where $K$ and $n$ are constant, and assume that the fluid is finite. From Eqs. (1) and (2) one obtains

$$\Delta h = -Ah^n - \Delta\Phi_c, \tag{6}$$

where $A = 4\pi G/(K(1 + n))^n$. Assume now that $\Delta\Phi_c \leq 0$. Multiplying Eq. (6) by $h$ and integrating over $\Omega$ we get

$$-\int_\Omega d^3xh\Delta h = \int_\Omega d^3x|\nabla h|^2 = A\int_\Omega d^3xh^{n+1} + \int_\Omega d^3xh\Delta\Phi_c \leq A\int_\Omega d^3xh^{n+1},$$

because $h = 0$ on $\partial\Omega$. The last integral in the above expression can be estimated making use of the Hölder inequality. For $n > 1$, we have

$$\int_\Omega d^3x h^{n+1} = \int_\Omega d^3x h^{n-1} h^2 \leq \|h^{n-1}\|_{L^{3/2}(\Omega)} \|h^2\|_{L^3(\Omega)}.$$

The Sobolev inequality yields $\|h\|_{L^6(\Omega)} \leq C(3,2)\|\nabla h\|_{L^2(\Omega)}$, where the constant $C(3,2) = 4^{1/3}/(\sqrt{3}\pi^{2/3})$ is a universal number in $\mathbb{R}^3$. This gives

$$\|h^{n-1}\|_{L^{3/2}(\Omega)} = \left(\int d^3x h^{3(n-1)/2}\right)^{2/3} \geq \frac{1}{AC^2(3,2)}.$$

The remaining steps are simple. Introducing the mass of the fluid $M = \int_\Omega d^3x\rho = A/(4\pi G)\int_\Omega d^3x h^n$ we get

$$M > \left(4\pi G\sqrt{A}C^3(3,2)h_{\max}^{(n-3)/2}\right)^{-1} \tag{7}$$

for $n \geq 3$. Here $h_{\max}$ denotes the maximum value of the specific enthalpy. For the ideal gas the temperature is given by $T = p\mu m_{\mathrm{p}}/(\rho k_{\mathrm{B}})$, where $\mu$ is the mean molecular weight, $m_{\mathrm{p}}$ denotes the proton mass, and $k_{\mathrm{B}}$ is the Boltzmann constant. In this case the inequality (7) can be written as

$$M > \frac{3\sqrt{3\pi}}{32}\left(\frac{(1+n)k_{\mathrm{B}}}{G\mu m_{\mathrm{p}}}\right)^{3/2}\frac{T_{\max}^{3/2}}{\sqrt{\rho_{\max}}}.$$

An interesting corollary follows from the above discussion for $n = 3$. Let $\bar{\rho}$ and $\bar{T}$ denote volume averaged mass density and temperature, respectively. A simple calculation involving Hölder's inequality yields $\bar{T} \leq (K\mu m_{\mathrm{p}}/k_{\mathrm{B}})\bar{\rho}^{1/n}$. The mass estimate can be now written as

$$M > \frac{3\sqrt{3\pi}}{4}\left(\frac{k_{\mathrm{B}}}{G\mu m_{\mathrm{p}}}\right)^{3/2}\frac{\bar{T}^{3/2}}{\sqrt{\bar{\rho}}},$$

i.e., in a form of a Jeans inequality for a bound system.

## References

1. P. Mach, E. Malec, Mon. Not. R. Astron. Soc. 411, 1313 (2011)
2. P. Mach, Mon. Not. R. Astron. Soc. 422, 772 (2012)
3. P. Mach, W. Simon, Ann. Henri Poincaré 14, 159 (2013)
4. W. Simon, Class. Quantum Grav. 10, 177 (1993)
5. J.M. Heinzle, Class. Quantum Grav. 19, 2835 (2002)

6. J.M. Heinzle, C. Uggla, Ann. Phys. 308, 18 (2003)
7. J.F.G. Auchmuty, R. Beals, Arch. Rat. Mech. Anal. 43, 255 (1971)
8. J.L. Tassoul, Theory of Rotating Stars, Princeton Univ. Press, Princeton (1978)
9. P. Mach, E. Malec, M. Piróg, Acta Phys. Pol. B 44, 107 (2013)

# Weyl Curvature Hypothesis in Terms of Spacetime Thermodynamics

**Takuya Maki and Masaaki Morita**

**Abstract** We formulate Penrose's Weyl curvature hypothesis from an aspect of spacetime thermodynamics, which has been proposed by Jacobson. Using the evolution equation for the shear tensor of a null congruence in a local Rindler frame, we show that the entropy variation can be expressed in terms of the Weyl curvature. This result supports Penrose's hypothesis, which claims that entropy of the gravitational field is somehow linked to the Weyl curvature. We point out that Penrose's hypothesis corresponds to Clausius' relation for a quasi-equilibrium state in spacetime thermodynamics.

Recent cosmological observations have revealed that a standard cosmological model called a $\Lambda$-CDM model successfully explains the evolution of large-scale structure of the universe [1,2]. This fact leads us to describe the universe as a physical system with the following property: it has an almost homogeneous initial state and a present state with highly inhomogeneous structures of the spacetime due to cosmological structure formation. Considering the second law of thermodynamics as a fundamental law, it is even a natural idea that an entropy increases through the evolution of the universe. Penrose [3,4] has proposed that the gravitational field itself should carry an entropy, and it may be related to the Weyl tensor $C_{\alpha\beta\gamma\delta}$. This proposal is known as *Penrose's Weyl curvature hypothesis* (or *conjecture*), which has been explored by several authors, employing specific models [5–8]. In this article, we

T. Maki
Japan Women's College of Physical Education, Nikaido-gakuen, Setagaya, Tokyo 157-8565, Japan
e-mail: maki@jwcpe.ac.jp

M. Morita (✉)
Okinawa National College of Technology, 905 Henoko, Nago, Okinawa 905-2192, Japan
e-mail: morita@okinawa-ct.ac.jp

A. García-Parrado et al. (eds.), *Progress in Mathematical Relativity, Gravitation and Cosmology*, Springer Proceedings in Mathematics & Statistics 60,
DOI 10.1007/978-3-642-40157-2_44, 

point out that a natural formulation of Penrose's Weyl curvature hypothesis arises, from an aspect of Jacobson's spacetime thermodynamics.

First we give an outline of Jacobson's spacetime thermodynamics and the derivation of the Einstein equation as an "equation of state of spacetime" [9–11]. Let $P$ be a point in a spacetime, and consider an infinitesimal region around $P$ as a local inertial frame (local Minkowski spacetime) with coordinates $X^\mu$. This is always possible because of the Equivalence Principle. The line element of the neighborhood of $P$ is then written as

$$g_{\mu\nu}(X)\mathrm{d}X^\mu \mathrm{d}X^\nu = \left[\eta_{\mu\nu} + O(\ell^2)\right]\mathrm{d}X^\mu \mathrm{d}X^\nu, \tag{1}$$

where $\ell$ denotes the size of the region considered. The local Rindler frame can be obtained by the transformation $X^0 = \chi \sinh(\kappa\eta)$, $X^1 = \chi\cosh(\kappa\eta)$, where $\kappa$ is a constant. The line element near $P$ is transformed as

$$\mathrm{d}s^2 = -\kappa^2\chi^2\mathrm{d}\eta^2 + \mathrm{d}\chi^2 + \mathrm{d}\ell_\perp^2, \tag{2}$$

where $\mathrm{d}\ell_\perp^2$ is the line element of the transverse space. The null geodesics $X^0 \pm X^1 = 0$ correspond to the trajectories of light. We consider an observer near $P$ accelerating uniformly to the direction of $X^1$, and the observer in the front of null geodesic of the $X^0 - X^1 = 0$ plane looks on the null geodesic as a causal horizon (named 'local Rindler horizon'). The trajectory of the observer is a hyperbolic curve which asymptotically approaches the $X^0 - X^1 = 0$ plane. The null geodesic is parameterized by an affine parameter $\lambda$, so that $\lambda = 0$ at $P$. The observer sees that the light wavefront behind him approaches him, and an energy flow $\delta Q$ into the horizon behind him is measured by $\lambda$. Note that $\lambda < 0$ on the local Rindler horizon. We introduce a vector $\xi^\mu$ tangent to the observer's trajectory. When the observer's trajectory is close enough to the causal horizon, we have $\xi^\mu \approx -\kappa\lambda k^\mu$, and

$$\delta Q = \int \mathrm{d}\eta \int_{\bar{\mathscr{S}}} T_{\mu\nu}\xi^\mu k^\nu \mathrm{d}A \approx -\kappa \int \lambda\,\mathrm{d}\lambda \int_{\mathscr{S}} T_{\mu\nu}k^\mu k^\nu\,\mathrm{d}A, \tag{3}$$

where $k^\mu$ denotes a unit null vector, and $T_{\mu\nu}$ an energy-momentum tensor of a matter field. The $\bar{\mathscr{S}}$ denotes an infinitesimal two-dimensional spatial area of the timelike surface near the causal horizon, and $\mathscr{S}$ is that of the causal horizon. We assume the following:

1. The observer measures the Unruh temperature $T_\mathrm{U} = \hbar a/(2\pi)$ ($a$ denotes the acceleration) [12] from the wavefront, and the local Rindler horizon is regarded as a heat bath of the temperature $T = T_\mathrm{U}\sqrt{-g_{00}} = \hbar\kappa/(2\pi)$.
2. Clausius' relation $\delta Q = T\delta S$ for an equilibrium state holds.
3. The entropy $S$ is proportional to horizon area $A$ with a constant $\alpha$ and hence $\delta S = \alpha\delta A$.

The change of the horizon area is given as

$$\delta A = \int_{\mathscr{S}} \theta \, \mathrm{d}\lambda \, \mathrm{d}A, \tag{4}$$

where the expansion $\theta := (\kappa\chi)^2 h^{\mu\nu}\nabla_\mu k_\nu$ with $h_{\mu\nu} := g_{\mu\nu} + \xi_\mu k_\nu + \xi_\nu k_\mu$, and $\nabla_\mu$ denoting the covariant derivative associated with $g_{\mu\nu}$. The expansion $\theta$ in Eq. (4) is approximated for small $\lambda$ as

$$\theta \approx \theta_P + \lambda \left.\frac{\mathrm{d}\theta}{\mathrm{d}\lambda}\right|_P + O(\lambda^2). \tag{5}$$

The second term of the right-hand side of Eq. (5) can be evaluated by the Raychaudhuri equation:

$$\frac{\mathrm{d}\theta}{\mathrm{d}\lambda} = -\frac{1}{2}\theta^2 - \sigma_{\mu\nu}\sigma^{\mu\nu} - R_{\mu\nu}k^\mu k^\nu, \tag{6}$$

where the shear tensor $\sigma_{\mu\nu} := \nabla_\mu k_\nu + \nabla_\nu k_\mu - (1/2)\theta h_{\mu\nu}$. Thus the change of area $\delta A$ is expressed by substituting Eqs. (5) and (6) into Eq. (4) as

$$\delta A = \int \mathrm{d}\lambda \int_{\mathscr{S}} \mathrm{d}A \left[\theta - \lambda\left(\frac{1}{2}\theta^2 + \sigma_{\mu\nu}\sigma^{\mu\nu} + R_{\mu\nu}k^\mu k^\nu\right)\right]_P. \tag{7}$$

Using Eqs. (3) and (7), and choosing the null congruence so that $\theta = 0$ and $\sigma_{\mu\nu} = 0$ at $P$, we obtain

$$T\delta S - \delta Q = \kappa \int \lambda \, \mathrm{d}\lambda \int_{\mathscr{S}} \mathrm{d}A \left(T_{\mu\nu}k^\mu k^\nu - \alpha\frac{\hbar}{2\pi}R_{\mu\nu}k^\mu k^\nu\right) = 0. \tag{8}$$

To hold Eq. (8) for an arbitrary null vector $k^\mu$, we have $(2\pi/\hbar\alpha)T_{\mu\nu} = R_{\mu\nu} + \Phi g_{\mu\nu}$, where $\Phi$ is an integration function. From equation of motion for the matter field, $\nabla^\nu T_{\mu\nu} = 0$, and the Bianchi identity $\nabla^\nu R_{\mu\nu} = \frac{1}{2}\nabla_\mu R$, we find $\Phi = -(1/2)R + \Lambda$, where $\Lambda$ is a constant. Imposing the relation $\alpha = 1/(4G\hbar)$, where $G$ is Newton's gravitational constant, the Einstein equation is shown to be reproduced.

Next we explore the way to describe a quasi-equilibrium state, taking the shear term into account as the effect of next order with respect to the affine parameter $\lambda$. For this purpose, we alter the assumptions of Clausius' relation as $\delta Q \leq T\delta S$. The evolution equation for the shear tensor is [13]

$$\frac{\mathrm{d}\sigma_{\mu\nu}}{\mathrm{d}\lambda} = -\theta\sigma_{\mu\nu} + C_{\alpha\nu\mu\beta}k^\alpha k^\beta. \tag{9}$$

If we choose the null congruence so that $\theta = 0$ and $\sigma_{\mu\nu} = 0$ at $P$ again, Eq. (9) is integrated for small $\lambda$ as

$$\sigma_{\mu\nu} = \lambda\hat{E}_{\mu\nu} + O(\lambda^2), \tag{10}$$

where $\hat{E}_{\mu\nu} := C_{\alpha\nu\mu\beta}k^\alpha k^\beta$, and with the method of iteration, Eq. (6) is integrated to obtain

$$\theta = -\lambda R_{\mu\nu}k^\mu k^\nu - \frac{\lambda^3}{6}\left(R_{\mu\nu}k^\mu k^\nu\right)^2 - \frac{\lambda^3}{3}\hat{E}_{\mu\nu}\hat{E}^{\mu\nu} + O(\lambda^4). \tag{11}$$

Therefore we can write the entropy variation up to $O(\lambda^3)$ as

$$\delta S = -\alpha \int \mathrm{d}\lambda \int_{\mathscr{S}} \mathrm{d}A \left[\lambda R_{\mu\nu}k^\mu k^\nu + \frac{\lambda^3}{6}\left(R_{\mu\nu}k^\mu k^\nu\right)^2 + \frac{\lambda^3}{3}\hat{E}_{\mu\nu}\hat{E}^{\mu\nu}\right], \tag{12}$$

and Clausius' relation for a quasi-equilibrium state becomes

$$T\delta S - \delta Q = \kappa \int \lambda\, \mathrm{d}\lambda \int_{\mathscr{S}} \mathrm{d}A \Bigg[T_{\mu\nu}k^\mu k^\nu - \frac{\hbar\alpha}{2\pi}\Big(R_{\mu\nu}k^\mu k^\nu + \frac{\lambda^2}{6}\left(R_{\mu\nu}k^\mu k^\nu\right)^2 + \frac{\lambda^2}{3}\hat{E}_{\mu\nu}\hat{E}^{\mu\nu}\Big)\Bigg] \geq 0. \tag{13}$$

If the Einstein equation holds, Eq. (13) is reduced to

$$T\delta S - \delta Q = -\frac{\kappa}{8\pi G}\int \frac{\lambda^3}{6}\,\mathrm{d}\lambda \int_{\mathscr{S}} \mathrm{d}A \left[\left(R_{\mu\nu}k^\mu k^\nu\right)^2 + 2\hat{E}_{\mu\nu}\hat{E}^{\mu\nu}\right] \geq 0. \tag{14}$$

Note that the integration with respect to $\lambda$ is performed on the interval $[-|\lambda|, 0]$, and hence Eq. (14) implies that the integral over the two-dimensional area $\mathscr{S}$ should be non-negative for an arbitrary null vector $k^\mu$. The term $(R_{\mu\nu}k^\mu k^\nu)^2$ in Eq. (14) can be rewritten in terms of the energy-momentum tensor $T_{\mu\nu}$ by using the Einstein equation, and thus this term corresponds to the entropy variation associated with the matter field. On the other hand, the term $2\hat{E}_{\mu\nu}\hat{E}^{\mu\nu}$, which contains the Weyl curvature, can be regarded as "intrinsic" entropy variation that comes from the gravitational field. Thus we can say that Eq. (14) is compatible with Penrose's Weyl curvature hypothesis.

We have elaborated spacetime thermodynamics, which have been originally proposed by Jacobson, taking the shear effect into account. Approximating the expansion and the shear tensor of a null congruence perturbatively with respect to the affine parameter $\lambda$, we have confirmed that the Einstein equation is reproduced at the lowest order, and have found that the shear term naturally generates the Weyl tensor at the next order. We have written a formula of gravitational entropy in terms of the Weyl tensor, and have shown that it does not decrease if Clausius' relation for a quasi-equilibrium state holds in the sense of spacetime thermodynamics. We hope that the entropy formula presented in this article plays an important role in exploring the problem of time asymmetry in gravitational dynamics.

## References


1. F. Bernardeau, S. Colombi, E. Gaztanaga and R. Scoccimarro, Phys. Rep. **367**, 1 (2002).
2. C. G. Tsagas, A. Challinor and R. Maartens, Phys. Rep. **465**, 61 (2008).
3. R. Penrose, in *General Relativity: An Einstein Centenary Survey*, ed. by S.W. Hawking and W. Israel (Cambridge University Press, Cambridge, 1979), p. 581.
4. R. Penrose, J. Stat. Phys. **77**, 217 (1994).
5. Ø. Grøn and S. Hervik, arXiv:gr-qc/0205026.
6. J. D. Barrow and S. Hervik, Class. Quantum Grav. **19**, 5173 (2002).
7. F. C. Mena and P. Tod, Class. Quantum Grav. **24**, 1733 (2007).
8. Ø. Rudjord, Ø. Grøn and S. Hervik, Phys. Scr. **77**, 055901 (2008).
9. T. Jacobson, Phys. Rev. Lett. **75**, 1260 (1995).
10. C. Eling, R. Guedens and T. Jacobson, Phys. Rev. Lett. **96**, 121301 (2006).
11. G. Chirco and S. Liberati, Phys. Rev. D **81**, 024016 (2010).
12. W. G. Unruh, Phys. Rev. D **14**, 870 (1976).
13. R. M. Wald, *General Relativity* (The University of Chicago Press, Chicago, 1984), p. 222.

# On the Properties of Exact Solutions Endowed with Negative Mass

**Vladimir S. Manko**

**Abstract** It is shown that various pathological properties of spacetimes can be explained by the presence of negative mass, including the cases when the total mass of the solution is a positive quantity. As an illustration, we consider several well-known stationary axisymmetric vacuum and electrovac solutions of the Einstein–Maxwell equations. Our investigation naturally leads to a critique of the known maximal extensions of the Kerr and Kerr–Newman spacetimes which turn out to be neither analytic nor physically meaningful.

## 1 Introduction

The study of equilibrium configurations in the original and extended double-Kerr solutions [1, 2] revealed a close connection between negative mass and pathologies of a spacetime: a source carrying a negative mass necessarily develops a massless ring singularity off the symmetry axis [3, 4], even in the situations when the total mass of the equilibrium configuration is positive. Negative mass could be also responsible for the formation of the regions with closed timelike curves (CTC), as in the case of the NUT solution where negative mass has been shown to be distributed along a part of the semi-infinite massive source [5]. Since many other stationary axisymmetric spacetimes with positive total mass are known to have massless ring singularities outside the symmetry axis and regions with CTCs, it is of interest to find out whether these pathologies are also due to the presence of some negative mass distributions. In the present communication several recent results demonstrating the relation that exists between negative mass and space-time

V.S. Manko (✉)
Departamento de Física, Centro de Investigación y de Estudios Avanzados del IPN, A.P. 14-740, 07000 México D.F.
e-mail: vsmanko@fis.cinvestav.mx

A. García-Parrado et al. (eds.), *Progress in Mathematical Relativity, Gravitation and Cosmology*, Springer Proceedings in Mathematics & Statistics 60,
DOI 10.1007/978-3-642-40157-2_45, 

pathologies will be discussed. These results suggest in particular that the known maximal extensions of the Kerr and Kerr–Newman spacetimes need a critical reconsideration.

## 2 Negative Mass in $\delta = 2$ Tomimatsu-Sato, Kerr and Kerr–Newman Solutions

The well-known $\delta = 2$ Tomimatsu-Sato (TS2) solution for a spinning mass was discovered in 1972 and is defined by an Ernst complex potential [6] of the form [7]

$$\begin{aligned} &\mathscr{E} = (A - B)/(A + B), \\ &A = p^2(x^4 - 1) + q^2(y^4 - 1) - 2ipqxy(x^2 - y^2), \\ &B = 2px(x^2 - 1) + 2iqy(y^2 - 1), \end{aligned} \tag{1}$$

where the real parameters $p$ and $q$ are subject to the constraint $p^2 + q^2 = 1$, while the prolate spheroidal coordinates $(x, y)$ are related to the cylindrical Weyl-Papapetrou coordinates $(\rho, z)$ by the formulae

$$x = \frac{1}{2\kappa}(r_+ + r_-), \quad y = \frac{1}{2\kappa}(r_+ - r_-), \quad r_\pm = \sqrt{\rho^2 + (z \pm \kappa)^2}, \tag{2}$$

$\kappa$ being a positive constant.

The total mass $M_T$ of the TS2 solution is given by the expression $M_T = 2\kappa/p$, so it is a positive quantity for $p > 0$. However, this solution has both a massless ring singularity outside the symmetry axis [7] and a region with CTCs [8]. In a recent paper [9] the exact analytic formulae defining the negative mass distribution in the TS2 spacetime have been obtained with the aid of Komar integrals [10], and evidence relating negative mass to the pathologies of this spacetime has been provided. Moreover, the analysis of the TS2 solution with total negative mass ($p < 0$) carried out in [9] shows that the case $M_T < 0$ is characterized by appearance of new pathological features: the ring singularity changes its location, passing from the inner to the outer stationary limit surface (SLS), while the region with CTCs, now located outside the outer SLS, becomes visible to a distant observer. It is of interest to compare the latter case with the Kerr [11] and Kerr–Newman [12] spacetimes endowed with negative mass.

### *2.1 The Kerr Solution with $M < 0$*

Due to the simple form of the Kerr solution, the corresponding negative-mass case permits a purely analytic investigation to be carried out in [9]. Quite

interestingly, the ring singularity of the Kerr metric with $M < 0$ lies in the equatorial plane ($z = 0$) off the symmetry axis (at $\rho = |a|$, $a$ being the angular momentum per unit mass). It is massless and thus reminiscent of the case of the TS2 spacetime. The ring singularity is a locus of points where the SLS touches the region with CTCs, the latter region having a toroidal topology.

### 2.2 The Kerr–Newman Solution with $M < 0$

According to a recent study [13], the presence of an electromagnetic field in the Kerr–Newman (KN) solution slightly affects the location of the singularity developed by the negative mass compared with the vacuum Kerr case. In particular, the ergoregion and the region with CTCs do not intersect, neither do they touch each other, and the massless ring singularity is located entirely inside the latter region of the causality violation.

## 3 Some Remarks on the Maximal Extensions of the Kerr and KN Spacetimes

A thorough analysis of the Kerr and KN solutions with negative mass by García-Compeán and Manko [14] leads to the conclusion that the known maximal analytic extensions of the stationary black-hole spacetimes proposed by Boyer and Lindquist [15] and by Carter [16] are erroneous. As a matter of fact, the known extensions are physically inconsistent because each of them represents an artificial unification of two different spacetimes corresponding to masses of opposite signs (the region $r < 0, M > 0$ is similar to the region $r > 0, M < 0$ via the invariance of the Kerr and KN metrics under the change $r \to -r$, $M \to -M$). As a consequence, these extensions are not analytic on the disk joining the two asymptotically flat regions. A correct extension of $r$ into negative values must be accompanied by the simultaneous extension of $M$ into negative values too. Then the region $r < 0$, $M < 0$ will be identical (up to the change $\theta \to -\theta$) with the region $r > 0$, $M > 0$, and thus the gluing of two identical spacetimes on the disk encircled by the ring singularity will be analytic.

## References

1. Kramer, D., Neugebauer, G.: The superposition of two Kerr solutions. Phys. Lett. A **75**, 259–261 (1980)
2. Manko, V.S., Ruiz, E.: Exact solution of the double–Kerr equilibrium problem. Class. Quantum Grav. **18**, L11–L15 (2001)

3. Hoenselaers, C.: Remarks on the double–Kerr solution. Prog. Theor. Phys. **72**, 761–767 (1984)
4. Manko, V.S., Ruiz, E., Sanabria–Gómez, J.D.: Extended multi–soliton solutions of the Einstein field equation: II. Two comments on the existence of equilibrium states. Class. Quantum Grav. **17**, 3881–3898 (2000)
5. Manko, V.S., Ruiz, E.: Physical interpretation of the NUT family of solutions. Class. Quantum Grav. **22**, 3555–3560 (2005)
6. Ernst, F.J.: New formulation of the axially symmetric gravitational field problem. Phys. Rev. **167**, 1175–1178 (1968)
7. Tomimatsu, A., Sato, H.: New exact solution for the gravitational field of a spinning mass. Prog. Theor. Phys. **29**, 1344–1345 (1972)
8. Gibbons, G.W., Russell-Clark, R.A.: Note on the Sato-Tomimatsu solution of Einstein's equations. Phys. Rev. Lett. **30**, 398–399 (1973)
9. Manko, V.S.: On the physical interpretation of $\delta = 2$ Tomimatsu-Sato solution. Prog. Theor. Phys. **127**, 1057–1075 (2012)
10. Komar, A.: Covariant conservation laws in general relativity. Phys. Rev. **113**, 934–936 (1959)
11. Kerr, R.P.: Gravitational field of a spinning mass as an example of algebraically special metrics. Phys. Rev. Lett. **11**, 237–238 (1963)
12. Newman, E.T., Couch, E., Chinnapared, K., Exton, A., Prakash, A., Torrence, R.: Metric of a rotating charged mass. J. Math. Phys. **6**, 918–919 (1965)
13. Manko, V.S.: Singularity in Kerr–Newman spacetimes endowed with negative mass. ArXiv:1110.6764 (2011)
14. García-Compeán, H., Manko, V.S.: Are known maximal extensions of the Kerr and Kerr–Newman spacetimes physically meaningful and analytic? ArXiv:1205.5848, (2012)
15. Boyer, R.H., Lindquist, R.W.: Maximal analytic extension of the Kerr metric. J. Math. Phys. **8**, 265–281 (1967)
16. Carter, B.: Global structure of the Kerr family of gravitational fields. Phys. Rev. **174**, 1559–1571 (1968)

# On the Bergqvist Approach to the Penrose Inequality

**Marc Mars and Alberto Soria**

**Abstract** The Penrose inequality in terms of the Bondi mass at past null infinity can be approached with a method due to Ludvigsen and Vickers and clarified later on by Bergqvist (Ludvigsen and Vickers, J. Phys. A: Math. Gen. 16:3349–3353, 1983; Bergqvist, Class. Quantum Grav. 14:2577–2583, 1997). In this work, we apply the method to the special case of null shells of dust collapsing in a four-dimensional Minkowski background (Penrose construction, 1973). Our main conclusion is that the class of surfaces covered by the method is severely restricted. We provide afterwards a wide family of surfaces satisfying the Penrose inequality which includes the ones determined by the Bergqvist method.

## 1 Introduction

The Penrose inequality [3] bounds from below the total mass of a spacetime in terms of the area of suitable surfaces that represent black holes. There are several versions of the Penrose inequality (see [4] for a relatively recent review). For asymptotically flat four-dimensional spacetimes with a regular past null infinity, the inequality reads $16\pi M_B^2 \geq |S_0|$, where $|S_0|$ is the area of any marginally outer trapped surface $|S_0|$ whose outer directed past null cone is smooth and $M_B$ is the Bondi mass on the cut defined by the intersection of the outer past null cone of $S_0$ and past null infinity. Ludvigsen and Vickers [1] proposed an argument to prove this inequality which used an implicit assumption that does not hold in general [2]. Moreover, it is not easy to write down conditions directly on $S_0$ which ensure that this extra assumption holds true. Therefore the Penrose inequality for the Bondi mass is still an open problem. The Penrose inequality was originally put forward by Penrose in 1973 [3].

M. Mars (✉) · A. Soria
Dept. Física Fundamental, Univ. de Salamanca, Pl. de la Merced s/n, 37008 Salamanca, Spain
e-mail: marc@usal.es

A. García-Parrado et al. (eds.), *Progress in Mathematical Relativity, Gravitation and Cosmology*, Springer Proceedings in Mathematics & Statistics 60,
DOI 10.1007/978-3-642-40157-2_46, 

His strategy consisted of arranging incoming null shells of dust in the Minkowski spacetime. After the shell has passed, there are two well-differenciated regions with different geometries separated by a null hypersurface and the energy on the shell can be arranged so that a trapped surface $S_0$ forms with respect to the exterior geometry. One of the beauties of the construction is that the Penrose inequality becomes a geometric inequality in the Minkowski spacetime, with no reference to the shell construction (see [3,5] for details).

## 2 Bergqvist Method

Let $M$ be a four-dimensional asymptotically flat spacetime at past null infinity satisfying the dominant energy condition. Consider a spacelike two-surface $S_0$ of spherical topology. The normal bundle $NS_0$ of $S_0$ admits a global basis of future null vectors $k$ and $\ell$. Consider the normalization $\langle k, \ell\rangle = -1$. As usual, the null extrinsic curvatures are defined by $K^\ell(X,Y) = -\langle \ell, \nabla_X Y\rangle$, with $X, Y$ tangent vectors to $S_0$, and similarly for $K^k$. The traces of these tensors define the null expansions $\theta_\ell$, $\theta_k$.

Assume $S_0$ to be a marginally outer trapped surface (MOTS), i.e. $\theta_\ell = 0$. If we choose any real number $r_0$, we can consider the unique past directed null geodesics $\alpha_p(r)$ starting at $\alpha_p(r = r_0) = p \in S_0$, with tangent vector $\alpha_p' = -k|_p$ and $\nabla_k k = 0$. Let $\Omega$ be the null hypersurface generated by these geodesics. We will refer to $k$ as the inner future null direction. In general $\Omega$ will become singular due to the development of caustics. However, for suitable $S_0$ and appropriate choice of inner direction, $\Omega$ will be regular everywhere, with no caustics developing even at past null infinity. Any such $S_0$ will be called *spacetime convex*.

Let $S_r$ be the surfaces obtained by dragging the initial surface $S_0$ along the null geodesics after a parameter "$r$". Let $\eta_{S_r}$ be the volume form of $S_r$. The method used by Ludvigsen and Vickers [1] and later on by Bergqvist [2] uses as hypothesis the following conditions at infinity:

$$\lim_{r\to\infty} \frac{\eta_{S_r}}{r^2} = \eta_{\mathbb{S}^2}, \qquad \theta_k = \frac{-2}{r} + O(r^{-3}), \qquad \theta_\ell = \frac{1}{r} + \frac{a}{r^2} + O(r^{-2}), \tag{1}$$

where $\eta_{\mathbb{S}^2}$ is the volume form of a limiting metric of Gauss curvature one (which may be defined on any of the $S_r$ as they are all diffeomorphic to each other via the geodesics). Let $E_B$ be the Bondi energy on the cut defined by the intersection of $\Omega$ and past null infinity with respect to the reference frame defined by the flow of the surfaces $S_r$. With a suitable choice of scaling in $k$ and a choice of $r_0$ the form for $\theta_k$ given above can always be accomplished. However imposing the rest of the conditions does in general restrict the original surface $S_0$. The Bondi energy can be expressed as $-8\pi E_B = \int_{\mathbb{S}^2} a\eta_{\mathbb{S}^2}$. The method involves two functions of $r$:

$$M_b(r) := 8\pi E_B + \int_{S_r} \theta_\ell(r)\eta_{S_r} - 4\pi r, \qquad D(r) := \sqrt{4\pi|S_r|} - 4\pi r.$$

The Penrose inequality takes the form $M_b(r_0) \geq D(r_0)$ and the method proves this by showing $M_b \geq 0$ and $D \leq 0$ for all $r$. The function $M_b$ (often called Bergqvist mass) is nonincreasing as a consequence of the spherical topology of $S_0$ and the dominant energy condition. The asymptotic conditions (1) imply that $M_b$ approaches zero and that $D$ is nowhere positive, which establishes the inequality (under assumptions (1)).

## 3 Bergqvist Method in $\mathscr{M}^{1,3}$

We focus now on the Penrose construction of null shells in the four-dimensional Minkowski spacetime $\mathscr{M}^{1,3}$. Let $S_0$ be any embedded spacetime convex surface in $\mathscr{M}^{1,3}$. Let $\xi'$ be the future directed, unit generator of a time translation and $\{k', \ell'\}$ the future null basis of the normal bundle of $S_0$ satisfying $\langle k', \xi' \rangle = -1$ and $\langle k', \ell' \rangle = -1$, with $k'$ inner. Objects defined with respect to the geometry exterior and interior to the shell will be distinguished with signs $+$ and $-$ respectively. The energy density $\rho'$ of the shell satisfies the equation $k'(\rho') = -\theta_{k'}\rho'$ and is adjusted so that $S_0$ is a MOTS with respect to the outer geometry. The jump of $\theta_{\ell'}$ across the shell satisfies (see e.g. [4]) $\theta^+_{\ell'} - \theta^-_{\ell'} = -8\pi\rho'_0$ (we use $'$ for all objects depending on $\xi'$). The integral of the energy density on any spatial section of $\Omega$ equals the Bondi energy $E'_B$ with respect to the reference frame determined by the flow of surfaces generated by $k'$. The Penrose inequality can be rewritten [3, 5] as

$$\int_{S_0} \theta^-_{\ell'} \eta_{S_0} \geq \sqrt{4\pi |S_0|}.$$

For any other inner future null section $k$ of $NS_0$, let $f := -\langle k, \xi' \rangle$. Define $\ell$ as the null normal vector satisfying $\langle k, \ell \rangle = -1$. $S_0$ being spacetime convex, the intersection of $\Omega$ with a constant time hyperplane $\Sigma'_0$ orthogonal to $\xi'$ and completely to the past of $S_0$ is a (strictly) convex hypersurface of Euclidean space, which we will denote by $\widehat{S}_0{}'$. We define also $\tau'_r$ ('time height' to $\Sigma'_0$) as the orthogonal distance of any point of each $S_r$ to $\Sigma'_0$. Since $\widehat{S}_0{}'$ is convex, we can endow it with the standard two-sphere metric $\overline{\gamma}'$ via the Gauss map and introduce the support function $h'$, which measures the signed distance from the euclidean origin to each tangent plane of $\widehat{S}_0{}'$. All geometric objects on $S_r$ can be expressed in terms of the geometry of the standard two sphere $(\mathbb{S}^2, \overline{\gamma}')$, and in terms of $h'$, $f$, $\tau'_0 = \tau'_r|_{r=r_0}$ and $r_0$. A straightforward calculation shows that the asymptotic behaviour at $r = +\infty$ of the null expansions is

$$\theta_k = \frac{-2}{r} + \frac{C}{r^2} + O(r^{-3}), \qquad \theta^-_\ell = \frac{-1}{f^3}(\triangle_{\overline{\gamma}'} f - f(1 + \frac{1}{f^2}|Df|^2_{\overline{\gamma}'}))\frac{1}{r} + O(r^{-2}),$$

$C = u'/f - 2r_0$ with $u' = \triangle_{\overline{\gamma}'} h' + 2(h' - \tau'_0)$. A fundamental input of the Bergqvist method is that $\theta_\ell^+ = \frac{1}{r} + O(r^{-2})$. It can be checked that the leading term of $\theta_\ell$ does not jump across the shell, and hence the leading coefficient of $\theta_\ell^-$ must equal 1 for the method to apply. This happens if and only if $f$ satisfies $\triangle_{\overline{\gamma}'} \log f + f^2 = 1$. We can characterize the solutions of this equation as follows:

**Theorem 1 (Choice of the Killing).** *$f$ satisfies $\triangle_{\overline{\gamma}'} \log f + f^2 = 1$ if and only if there is a new unit time translation $\xi$ satisfying $\langle k, \xi \rangle = -1$.*

In terms of the new Killing $\xi$, the explicit expressions for $\theta_k$ and $\theta_\ell$ simplify notably, even though the objects themselves remain unaltered (note that neither $k$, nor the parametrization of the geodesics has been changed). From $\langle k, \xi \rangle = -1$ and using the jump equation for $\theta_\ell$ and $\int_S \rho \eta_S = E_B$, the expression for $M_b$ becomes $M_b(r) = \int_{S_r} \theta_\ell^-(r) \eta_{S_r} - 4\pi r$. It is easy to see that the limits of $M_b$ and $D$ as $r \to \infty$ coincide and are equal to $L_{r_0} := \frac{1}{2} \int_{\mathbb{S}^2} C \eta_{\mathbb{S}^2}$, where $C$ (which, recall, has not changed) can now be written in the form $u - 2r_0$, with $u = \triangle_{\overline{\gamma}} h + 2(h - \tau_0)$ and all quantities are determined with respect to the geometry of the plane $\Sigma_0$ orthogonal to $\xi$. Comparing with Sect. 2 the Bergqvist approach requires setting $C = 0$, i.e. $u = 2r_0$. This is equivalent to $\tau_0 = \frac{H(\widehat{S}_0)}{\mathrm{Scal}(\widehat{S}_0)} - \beta$, $\beta > 0$, where $\tau_0$ is the 'time height' from $S_0$ to $\Sigma_0$, and $H(\widehat{S}_0)$ and $\mathrm{Scal}(\widehat{S}_0)$ are, respectively, the mean and the scalar curvature of the projected surface $\widehat{S}_0$ in $\Sigma_0$. It follows that the class of surfaces for which the method applies depends on a single parameter for each choice of convex $\widehat{S}_0$ and hence it is severely restricted, as claimed.

If we completely relax the condition $C = 0$ we can still apply a suitable modification of the method. Recall that $M_b \geq L_{r_0}$. A different way of obtaining $M_b \geq D$ is imposing conditions so that $D \leq L_{r_0}$. Since $\lim_{r \to \infty} D(r) = L_{r_0}$, we can ask $D$ to satisfy $\frac{dD}{dr}(r) \geq 0$. This leads to the following condition (see Theorem 6 in [6]):

$$4\pi \int_{\mathbb{S}^2} \left( (\triangle_{\overline{\gamma}} h)^2 + 2h \triangle_{\overline{\gamma}} h \right) \eta_{\mathbb{S}^2} \geq 4\pi \int_{\mathbb{S}^2} u^2 \eta_{\mathbb{S}^2} - \left( \int_{\mathbb{S}^2} u \eta_{\mathbb{S}^2} \right)^2 .$$

The class of surfaces satisfying this inequality is quite large as it depends on arbitrary functions for each choice of $\widehat{S}_0$. It is also immediate to check that it includes the class covered by the Bergqvist method.

**Acknowledgements** Financial support under the projects FIS2009-07238, FIS2012-30926 (MICINN) and P09-FQM-4496 (Junta de Andalucía and FEDER funds) are acknowledged. AS acknowledges the Ph.D. grant AP2009-0063 (MEC).

## References

1. Ludvigsen, M., Vickers J.A.G.: An inequality relating the total mass and the area of a trapped surface in general relativity. J. Phys. A: Math. Gen. **16**, 3349–3353 (1983)
2. Bergqvist, G.: On the Penrose inequality and the role of auxiliary spinor fields. Class. Quantum Grav. **14**, 2577–2583 (1997)
3. Penrose R.: Naked singularities. Ann, N. Y. Acad. Sci. **224**, 125–134 (1973)
4. Mars M.: Present status of the Penrose inequality. Class. Quantum Grav. **26**, 193001 (2009)
5. Gibbons G. W.: Collapsing shells and the isoperimetric inequality for black holes. Class. Quantum Grav. **14**, 2905–15 (1997)
6. Mars M., Soria A.: On the Penrose inequality for dust null shells in the Minkowski spacetime of arbitrary dimension. Class. Quantum Grav. **29** 135005 (2012)

# Inhomogeneous Loop Quantum Cosmology: Hybrid Quantization and Approximated Solutions

**Daniel Martín-de Blas, Mercedes Martín-Benito, and Guillermo A. Mena Marugán**

**Abstract** We study approximation methods to construct physical solutions for the hybrid quantization of the Gowdy model with linear polarization and a massless scalar field. The loop quantization of the Bianchi I background and the presence of inhomogeneities lead to a very complicated Hamiltonian constraint. Therefore, the extraction of physical predictions calls for the introduction of well justified approximations. We show that, for specific regimes of physical interest, one can approximate the Hamiltonian constraint by a more simple one and obtain its solutions.

## 1 Introduction and Motivation

Loop quantum cosmology (LQC) [2, 4] is the application of the quantization techniques and methods of loop quantum gravity (LQG) [9] to symmetry reduced gravitational systems in cosmology. The quantization within LQC of simple cosmological models, such as the Friedmann–Robertson–Walker (FRW) model coupled to a massless scalar, leads to a remarkable result: the resolution of the initial Big-Bang singularity by means of a quantum bounce [1].

In order to study inhomogeneous systems in the context of LQC, one can use a hybrid quantization, combining a LQC quantization of the homogeneous degrees of freedom with a Fock quantization of the inhomogeneities [6]. This hybrid quantization allows one to deal with the field complexity, and in particular

D. Martín-de Blas (✉) · G.A. Mena Marugán
Instituto de Estructura de la Materia, IEM-CSIC, Serrano 121, Madrid 28006, Spain
e-mail: daniel.martin@iem.cfmac.csic.es; mena@iem.cfmac.csic.es

M. Martín-Benito
Perimeter Institute, 31 Caroline St N, Waterloo ON, Canada N2L 2Y5
e-mail: mmartinbenito@perimeterinstitute.ca

A. García-Parrado et al. (eds.), *Progress in Mathematical Relativity, Gravitation and Cosmology*, Springer Proceedings in Mathematics & Statistics 60,
DOI 10.1007/978-3-642-40157-2_47, 

to construct operators representing the quantum constraints that are well defined. Nevertheless, these quantum constraints are typically very complicated and it seems necessary to develop approximation methods and perturbative approaches to solve them. With this aim, we study the hybrid quantization of the Gowdy model with three-torus spatial topology, linear polarization, and a minimally coupled massless scalar field [7]. We focus our study in the subsystem with local rotational symmetry (LRS).

## 2 Hybrid Gowdy Model

Gowdy cosmologies are globally hyperbolic spacetimes with two axial and hypersurface orthogonal Killing vectors. For the model with three torus topology, after a partial gauge fixing, the reduced system can be seen as a Bianchi I background coupled to a homogeneous massless scalar $\phi$ and coupled to two kind of inhomogeneities that propagate in one of the cyclic directions of the three torus. These are linear gravitational waves and matter inhomogeneities.

The hybrid quantization of this system is given in [7]. We briefly summarize it. The Bianchi I (LRS) background geometry is quantized using LQC techniques. Hence, the basic operators are densitized triad components constructed out of the scale factors in each of the three directions, and the holonomies of their conjugate variables. The prescription used for quantization, known as *improved dynamics* [3], is such that the volume is discretized and the holonomies cause a constant shift in the volume, but with a complicated action in the variable measuring the anisotropy. An orthonormal basis of the Hilbert space is given by states $|v, \Lambda\rangle$, where $v \in R^+$ is proportional to the Bianchi I volume and $\Lambda \in R$ is (essentially) the logarithm of the scale factor in the homogeneous direction. The massless scalar $\phi$ is quantized using a standard Schrödinger representation such that $p_\phi = -i\hbar\partial_\phi$.

Concerning the inhomogeneities, both kinds can be treated in the very same way, owing to the fact that, mathematically speaking, they are two copies of the same field and they take part identically in the system. They are quantized adopting the privileged Fock quantization that is obtained by demanding unitary evolution and invariance under the spatial symmetries of the system [5]. These criteria select a time dependent scaling for the fields and a unique Fock representation for the corresponding canonical commutation relations. An orthonormal basis of the Fock spaces is that given by the corresponding n-particle states. The kinematical Hilbert space is just the tensor product of the Hilbert spaces mentioned above.

The resulting reduced model is subject to two global constraints: a momentum constraint and a Hamiltonian one. Once one has defined the quantum representation, one can build the operators that correspond to these constraints. The momentum constraint operator only acts on the Fock spaces, imposing a mild condition in the occupation numbers of the n-particle states [7].

On the other hand, the (densitized) Hamiltonian constraint operator can be written (up to a constant factor) as

$$\hat{C} = \frac{4\hat{p}_\phi^2}{\pi G\hbar^2} - \frac{3}{\kappa^2}\hat{\Omega}^2 - \frac{1}{\kappa^2}(\hat{\Omega}\hat{\Theta} + \hat{\Theta}\hat{\Omega}) + \frac{16}{\beta}\widehat{e^{2\Lambda}}\hat{H}_0 + \frac{2\beta}{\kappa^2}\widehat{e^{-2\Lambda}}\hat{D}\hat{\Omega}^2\hat{D}\hat{H}_I, \quad (1)$$

where $\kappa$ is some constant involving parameters of the quantization. The two first terms in Eq. (1) correspond to the FRW Hamiltonian constraint in LQC [1]. The third term is the anisotropy term. The last two terms couple the background with the inhomogeneities, and contain respectively the free contribution of the inhomogeneities ($\hat{H}_0$), an interaction term ($\hat{H}_I$), and a regularization of the inverse of the volume ($\hat{D}$) (see [7] for more details).

The action of the Hamiltonian constraint does not relate all the states with different labels $v$ and $\Lambda$ but it *superselects* them: $v$ is superselected in semilattices of step four, labeled by $\epsilon \in (0, 4]$, and $\Lambda$ is superselected in a numerable dense set of the real line that depends on $\epsilon$ [6].

When looking for quantum solutions of this Hamiltonian constraint, the problematic terms are (1) the anisotropy term, because $\hat{\Omega}$ and $\hat{\Theta}$ do not commute, (2) the interaction term that creates and annihilates infinite pairs of particles and that goes multiplied by $\hat{D}$, whose action in $v$ is complicated.

## 3 Approximations

With the aim of dealing with such a complicated Hamiltonian constraint, one can introduce approximations to reach a simpler constraint. In order to do that, we make use of the behavior of the (generalized) eigenfunctions $e_\rho(v)$ of the FRW operator $\hat{\Omega}^2$ with eigenvalue $\rho^2$. This behavior is well known [8], with an oscillating Wheeler-De Witt limit for large $v$'s, and highly suppressed wavefunctions for $v < \rho/2\kappa$.

One can then show that, for eigenstates such that $\rho \gg 8\kappa$, the contributions of the $\hat{D}$ operators can be disregarded in the interaction term and, more importantly, the anisotropy term "factorizes", so that $(\hat{\Omega}\hat{\Theta} + \hat{\Theta}\hat{\Omega}) \approx 2\hat{\Omega}'\hat{\Theta}_\Lambda$, whenever smooth profiles $f(\Lambda)$ are considered. Here, the operator $\hat{\Omega}'$ is the counterpart of $\hat{\Omega}$, but defined in semilattices of step four in $v$, instead of step two [8]. Besides, the operator $\hat{\Theta}_\Lambda$ is given by

$$\hat{\Theta}_\Lambda|\Lambda\rangle = -i\frac{2\kappa}{q_\epsilon}\left[|\Lambda - q_\epsilon\rangle - |\Lambda + q_\epsilon\rangle\right]. \quad (2)$$

This is essentially the discretization with step $q_\epsilon$ of the derivative with respect to $\Lambda$. The spectral properties of this self-adjoint operator are well known. It has a bounded, doubly degenerated absolutely continuous spectrum equal to $[-4\kappa/q_\epsilon, 4\kappa/q_\epsilon]$. Given an eigenvalue $p$, the eigenstates are given (up to normalization factors) by $e_p^{(1)}(\Lambda) = e^{i\Lambda x/q_\epsilon}$ and $e_p^{(2)}(\Lambda) = e^{i\Lambda(\pi-x)/q_\epsilon}$, where $q_\epsilon p = 4\kappa \sin x$. The step $q_\epsilon$ can be chosen by demanding that the superselection

sectors in $\Lambda$ are preserved (therefore, $q_\epsilon$ depends on $\epsilon$) and such that the "best possible approximation" is obtained. It is worth noting that the operators $\hat{\Omega}^2$ and $\hat{\Theta}_\Lambda$ commute.

In this situation, one can consider (Gaussian) profiles $\psi(p)$ in the eigenvalues of $\hat{\Theta}_\Lambda$ peaked on $p = 0$ and such that the profiles in $\Lambda$,

$$\bar{\psi}(\Lambda) = \int dp \psi(p) e_p^{(1)}(\Lambda), \tag{3}$$

are peaked on large values of $\Lambda$. For such profiles, the expectation values of both the anisotropy term and the interaction term in the Hamiltonian constraint (with reasonable inhomogeneities content) are negligible. Therefore, approximate solutions to the Hamiltonian constraint would be provided by the solutions of the solvable constraint obtained by disregarding these two terms and considering the above mentioned profiles.

## 4 Conclusions

We have studied approximation methods in the context of LQC in order to construct physical solutions of inhomogeneous and anisotropic systems. We have applied such methods to the hybrid quantization of the Gowdy $T^3$ model with linear polarization and a massless scalar field. Taking into account the behavior of the eigenstates of the FRW operator, we have obtained that, on the one hand, one can disregard the contributions coming from the regularization of the inverse volume operator and, on the other hand, the anisotropy term can be approximated by a tensor product of one operator that only acts in the label $v$ and another operator that only acts in the label $\Lambda$. In addition, the latter is a well known operator that commutes with the FRW one, being possible to find states whose profiles in $\Lambda$ allow one to disregard both the interaction and the anisotropy terms. By considering such profiles, one would obtain approximate solutions to the original constraint.

**Acknowledgements** This work was supported by the Spanish MICINN Project No. FIS2011-30145-C03-02. D M-dB is supported by CSIC and the European Social Fund under the Grant No. JAEPre-09-01796.

## References

1. Ashtekar, A., Pawłowski T., Singh P.: Quantum nature of the big bang: improved dynamics. Phys. Rev. D **74**, 084003 (2006).
2. Ashtekar, A., Singh, P.: Loop quantum cosmology: a status report Class. Quant. Grav. **28**, 213001 (2011).

3. Ashtekar, A., Wilson-Ewing, E.: Loop quantum cosmology of Bianchi I models Phys. Rev. D **79**, 083535 (2009).
4. Bojowald, M.: Loop quantum cosmology Living Rev. Rel. **11**, 4 (2008).
5. Cortez, J., Mena Marugán, G. A., Velhinho, J. M.: Uniqueness of the Fock quantization of the Gowdy $T^3$ model Phys. Rev. D **75**, 084027 (2007).
6. Garay, L. J., Martín-Benito, M., Mena Marugán, G. A.: Inhomogeneous Loop Quantum Cosmology: Hybrid Quantization of the Gowdy Model Phys. Rev. D **82**, 044048 (2010).
7. Martín-Benito, M., Martín-de Blas, D., Mena Marugán, G. A.: Matter in inhomogeneous loop quantum cosmology: the Gowdy $T^3$ model Phys. Rev. D **83**, 084050 (2011).
8. Martín-Benito, M., Mena Marugán, G. A., Olmedo, J.: Further Improvenments in the Understanding of Isotropic Loop Quantum Cosmology Phys. Rev. D **80**, 104015 (2009).
9. Thiemann, T.: Modern canonical quantum general relativity. (Cambridge: Cambridge University Press, 2007).

# Black Holes in Extended Gravity Theories in Palatini Formalism

**Jesús Martínez-Asencio, Gonzalo J. Olmo, and Diego Rubiera-García**

**Abstract** We consider several physical scenarios where black holes within classical gravity theories including $R^2$ and Ricci-squared corrections and formulated à la Palatini can be analytically studied.

## 1 Palatini Approach and Black Holes

In General Relativity (GR) the field equations are obtained by assuming a Riemannian geometry and performing variations of the action with respect to the metric. If the Riemannian condition is relaxed and the connection is allowed to vary independently of the metric (Palatini formalism) the resulting field equations for GR turn out to be equivalent to those obtained under the Riemannian assumption though, in general, they are different. This is so because in the case of GR the connection field equation can be solved in terms of the Christoffel symbols of the metric (Levi–Civita connection). This compatibility between metric and connection and thus the identification between both approaches has mostly become implicitly assumed in any extension of GR that includes curvature corrections to the Einstein–Hilbert action. We note that, in particular, quadratic curvature terms are required for a high-energy completion of the theory and indeed arise in the quantization of fields in curved spacetime [1] and in several approaches to quantum gravity such as those based on string theory [2]. However, the physical and

G.J. Olmo · J. Martínez-Asencio
Departamento de Física Teórica and IFIC, Universidad de Valencia-CSIC, Facultad de Física, C/ Dr. Moliner 50, Burjassot-46100, Valencia, Spain
e-mail: gonzalo.olmo@csic.es

D. Rubiera-García (✉)
Departamento de Física, Universidad de Oviedo. Avenida Calvo Sotelo 18, 33007 Oviedo, Asturias, Spain
e-mail: rubieradiego@gmail.com

A. García-Parrado et al. (eds.), *Progress in Mathematical Relativity, Gravitation and Cosmology*, Springer Proceedings in Mathematics & Statistics 60,
DOI 10.1007/978-3-642-40157-2_48, © Springer-Verlag Berlin Heidelberg 2014

mathematical properties of extended gravity theories formulated in the metric or Palatini approaches are very different. While the former is affected by a number of problems such as higher-order field equations or the existence of ghosts and other perturbative instabilities, the latter provides always second-order field equations and absence of ghosts. In the particular case of Lovelock gravities [3], metric and Palatini formulations yield the same field equations [4]. Here we briefly summarize some scenarios concerning black holes in quadratic (Palatini) extensions of GR, where the connection equation can be algebraically solved and the properties of the theories formulated in this way are physically appealing.

For a theory $f(R, Q)$ depending on the invariants $R = g_{\mu\nu}R^{\mu\nu}$ and $Q = R_{\mu\nu}R^{\mu\nu}$ the variation with respect to the connection $\Gamma^{\gamma}_{\alpha\beta}$ leads, in the most general case (admitting both nonvanishing torsion $\Gamma^{\gamma}_{[\alpha\beta]}$ and antisymmetric-Ricci $R_{[\mu\nu]}$), to [5]

$$\frac{1}{\sqrt{-g}}\tilde{\nabla}_{\alpha}[\sqrt{-g}M^{(\beta\nu)}] = \Xi^{(+)\beta\nu\kappa\rho}_{\alpha}M_{[\kappa\rho]} \tag{1}$$

$$\frac{1}{\sqrt{-g}}\tilde{\nabla}_{\alpha}[\sqrt{-g}M^{[\beta\nu]}] = \Xi^{(-)\beta\nu\kappa\rho}_{\alpha}M_{(\kappa\rho)} \tag{2}$$

where $M^{(\beta\nu)} = f_R g^{\beta\nu} + 2f_Q R^{(\beta\nu)}(\Gamma)$, $M^{[\beta\nu]} = 2f_Q R^{[\beta\nu]}(\Gamma)$ and $\Xi^{(\pm)\beta\nu\kappa\rho}_{\alpha} = [\tilde{S}^{\nu}_{\alpha\lambda}g^{\beta\kappa} \pm \tilde{S}^{\beta}_{\alpha\lambda}g^{\nu\kappa}]g^{\lambda\rho}$. The symmetric connection $\tilde{C}^{\beta}_{\alpha\lambda}$ in the covariant derivative $\tilde{\nabla}_{\alpha}$ in (1) and (2) has been introduced by convenience, and is related to the original connection $\Gamma^{\beta}_{\alpha\lambda} = C^{\beta}_{\alpha\lambda} + S^{\beta}_{\alpha\lambda}$ (with $C^{\beta}_{\alpha\lambda}$ and $S^{\beta}_{\alpha\lambda}$ its symmetric and antisymmetric components, respectively) as (with $S_{\mu} = S^{\lambda}_{\mu\lambda}$)

$$C^{\lambda}_{\mu\nu} = \tilde{C}^{\lambda}_{\mu\nu} - \frac{1}{3}(\delta^{\lambda}_{\nu}S_{\mu} + \delta^{\lambda}_{\mu}S_{\nu})\ ;\ S^{\lambda}_{\mu\nu} = \tilde{S}^{\lambda}_{\mu\nu} - \frac{1}{3}(\delta^{\lambda}_{\nu}S_{\mu} - \delta^{\lambda}_{\mu}S_{\nu}). \tag{3}$$

Equations (1) and (2) constitute a system such that the symmetric and antisymmetric parts of $M^{\mu\nu}$ are coupled to each other through the torsion tensor $\tilde{S}^{\beta}_{\alpha\lambda}$. The simplest solutions to this system of equations correspond to putting both $\tilde{S}^{\beta}_{\alpha\lambda}$ and $R_{[\mu\nu]}$ to zero, so that (2) becomes trivially satisfied and (1) reads simply

$$\frac{1}{\sqrt{-g}}\nabla_{\alpha}[\sqrt{-g}(f_R g^{\mu\nu} + 2f_Q R^{(\beta\nu)})] = 0. \tag{4}$$

On the other hand, the variation of the action with respect to metric leads to

$$f_R R_{\mu\nu} - \frac{f}{2}g_{\mu\nu} + 2f_Q R_{\mu\alpha}R^{\alpha}{}_{\nu} = \kappa^2 T_{\mu\nu}, \tag{5}$$

where $T_{\mu\nu}$ is the energy-momentum tensor of the matter. If $f_Q$ =constant, taking the trace in this equation one gets an algebraic equation implying that $R = R(T)$, with

$T$ the trace of $T_{\mu\nu}$. Because in Palatini $f(R)$ theories the modifications with respect to GR lie in a number of $T$-dependent terms on the right-hand-side of the field equations [6], it follows that for traceless matter-energy sources the dynamics in Palatini theories is exactly the same as in the case of GR (+ a cosmological constant term, depending on the Lagrangian chosen). However, nonlinear electrodynamics (NED) are able to yield $T \neq 0$ and thus provide modified dynamics. In such a case the connection equation (4) may be solved by defining a rank-two tensor $h_{\mu\nu} = f_R g_{\mu\nu}$ such that $\nabla_\mu(\sqrt{-h}h^{\mu\nu}) = 0$ and thus $\Gamma^\gamma_{\alpha\beta}$ becomes the Levi–Civita connection of $h^{\mu\nu}$. In terms of $h_{\mu\nu}$, the field equations of pure $f(R)$ theories read

$$R_\mu{}^\nu(h) = \frac{1}{f_R^2}\left(\kappa^2 T_\mu{}^\nu + \frac{f}{2}\delta^\nu_\mu\right). \tag{6}$$

Dealing with this equation for a given gravity and matter Lagrangians, and putting the result in terms of the physical metric $g_{\mu\nu}$, provides a full solution. In [6] the particular case of $f(R) = R \pm R^2/R_P$ ($R_P \equiv$ Planck curvature) coupled to Born-Infeld electrodynamics [7] was analyzed, finding the existence of black holes with up to three horizons, and a singularity of minimum divergence $\sim 1/r^2$, which is milder than in GR ($\sim 1/r^4$ for Schwarzschild and $\sim 1/r^8$ for Reissner–Nordström).

This procedure also works for the general $f(R, Q)$ case. Now there is deviance from GR even for traceless matter-energy sources. The connection equation (4) leads to the following relation between the auxiliary $h_{\mu\nu}$ and physical $g_{\mu\nu}$ metrics

$$h^{\mu\nu} = \frac{g^{\mu\alpha}\Sigma_\alpha{}^\nu}{\sqrt{\det\hat{\Sigma}}}, \quad h_{\mu\nu} = (\sqrt{\det\hat{\Sigma}})\Sigma_\mu{}^\alpha g_{\alpha\nu}. \tag{7}$$

where $\Sigma_\mu{}^\nu = (f_R\delta^\nu_\mu + 2f_Q P_\mu{}^\nu)$ with $P_\mu{}^\nu \equiv R_{\mu\alpha}g^{\alpha\nu}$. In terms of $h_{\mu\nu}$ the field equations read as (6) with the replacement $f_R^2 \to \sqrt{\det(\hat{\Sigma})}$. When $T_{\mu\nu}$ represents a monopolar Maxwell field, a generalization of the Reissner–Nordström solution is obtained [8]. Taking the Lagrangian density $f(R, Q) = R + l_P^2(R^2 + bQ)$ where $l_P \equiv$ Planck's length and $b$ a constant, solving (6) and writing the final result for a static, spherically symmetric metric $ds^2 = g_{tt}c^2dt^2 + g_{rr}dr^2 + r^2d\Omega^2$ leads to

$$g_{tt} = -\frac{A(z)}{\sigma_+}, \; g_{rr} = \frac{\sigma_+}{\sigma_- A(z)}, \; A(z) = 1 - \frac{[1 + \delta_1 G(z)]}{\delta_2 z \sigma_-^{1/2}}, \tag{8}$$

where $z \equiv r/r_c$, $r_c \equiv \sqrt{r_q l_P}$, $\sigma_\pm = 1 \pm 1/z^4$, $r_q^2 = \kappa^2 q^2/4\pi$ and the parameters

$$\delta_1 = \frac{1}{2r_S}\sqrt{r_q^3/l_P}, \; \delta_2 = \frac{\sqrt{r_q l_P}}{r_S}. \tag{9}$$

where $r_S = 2GM/c^2$ and the function $\frac{dG}{dz} = \frac{z^4+1}{z^4\sqrt{z^4-1}}$. These equations define black holes that recover their GR counterparts for $r \gg l_P$ but which undergo relevant

non-perturbative changes near $z = 1$. Indeed when $\delta_1 = \delta_1^* \simeq 0.5720$ an expansion of the curvature invariants about $z = 1$ reveals that the spacetime is nonsingular. Moreover, the metric can be extended beyond $z = 1$ revealing a wormhole structure whose properties are currently under investigation. When $r_q < 2l_P$ the event horizon of these objects disappears, making them stable against Hawking decay and with a mass spectrum $M \approx 1.23605 \left(N_q/N_q^c\right)^{3/2} m_P$, where $N_q < N_q^c \simeq 16.55$ is the number of charges and $m_P$ the Planck mass.

The Palatini approach also allows to study the black hole formation process from a null fluid [9] in exact analytical form. Consider an ingoing stream of neutral particles with an energy-momentum tensor $T_{\mu\nu} = \rho_{in} l_\mu l_\nu$, where $\rho_{in}$ is the energy density of the stream and $l_\mu$ a null radial vector, $l_\mu l^\mu = 0$. In this case, the matrix $\Sigma_\mu{}^\nu$ relating the metrics $h_{\mu\nu}$ and $g_{\mu\nu}$ is given by $\Sigma_\mu{}^\nu = \delta_\mu^\nu + 2l_P^2 \kappa^2 \rho_{in} l_\mu l^\nu$. Considering a Vaidya-type metric $ds^2 = -Be^{2\Psi} dv^2 + 2e^\Psi dv dr + r^2 d\Omega^2$ the field equations lead to $\Psi = 0$ and

$$B = 1 - \frac{2\int^v L(v')dv'}{r} - \frac{4L(v)}{\rho_P r^2}, \tag{10}$$

where $\rho_P = \frac{c^2}{l_P^2 G} \sim 10^{96} kg/m^3$ is Planck's density and $L(v) = \kappa^2 r^2 \rho_{in}/2$ is the luminosity function. Equation (10) describes a Reissner–Nordström solution with a *wrong-sign* charge term, that interpolates between two Schwarzschild solutions of masses $M$ and $M'$ through a transient (charge-term) contribution to the mass function.

## 2 Concluding Remarks

Palatini theories containing $R$ and $R_{\mu\nu} R^{\mu\nu}$ terms have a rich structure in terms of black hole solutions. In these theories the connection can be algebraically determined and the field equations cast in terms of the metric $h_{\mu\nu}$ associated to a Levi–Civita connection. Transforming back to the physical metric $g_{\mu\nu}$ provides a full solution to a given problem. More results on this line will be presented elsewhere.

Work supported by the Spanish grant FIS2011-29813-C02-02 and the JAE-doc program of the Spanish Research Council (CSIC).

## References


1. L. Parker, D. J. Toms, in *Quantum field theory in curved spacetime: quantized fields and gravity* (Cambridge University Press, 2009); N. D. Birrell, P. C. W. Davies, in *Quantum fields in curved space* (Cambridge University Press, 1982).
2. M. Green, J. Schwarz, E. Witten, in *Superstring Theory* (Cambridge University Press, Cambridge, 1987); T. Ortin, in *Gravity and strings* (Cambridge Monographs on Mathematical Physics, Cambridge University Press, 2004).
3. D. Lovelock, J. Math. Phys. **12**, 498 (1971); C. Garraffo, G. Giribet, Mod. Phys. Lett. A**23**, 1801 (2008).
4. M. Borunda, B. Janssen, M. Bastero-Gil, JCAP **0811**, 008 (2008).
5. G. J. Olmo, D. Rubiera-García, work in progress.
6. G. J. Olmo, D. Rubiera-García, Phys. Rev. D **84**, 124059 (2011);
7. M. Born, L. Infeld, Proc. R. Soc. London A **144**, 425 (1934).
8. G. J. Olmo, D. Rubiera-García, Phys. Rev. D **86**, 044014 (2012); Eur. Phys. J. C **72**, 2098 (2012); Int. J. Mod. Phys. D **21**, 1250067 (2012).
9. J. Martinez-Asencio, G. J. Olmo, D. Rubiera-García, Phys. Rev. D **86**, 104010 (2012).

# What Is a Reasonable Spacetime? Some Remarks on the Hole-Free Condition

**Ettore Minguzzi**

**Abstract** The notion of hole-free spacetime, initially introduced by Geroch, is reformulated, improved and commented. It is argued that any reasonable spacetime should satisfy it.

## 1 Introduction

As today, the best definition of spacetime has been provided by the General Theory of Relativity, according to which the physical spacetime is best mathematically modeled as a

**Definition 1.1 (Spacetime).** A connected Hausdorff (paracompact) time-oriented Lorentzian four-dimensional ($C^r$, $r \geq 2$) manifold.

It is usually denoted $(M, g)$ where $g$ is the Lorentzian metric.

It is easy to forget that the concept of spacetime appears already in Aristotelian mechanics and that it passed through successive, very interesting, revolutions which had the effect of refining its formulation and enriching its properties. Indeed, with the development of Galilean Mechanics we understood that it was meaningless to speak of events happening "at the same place". Analogously, with the the advent of Special Relativity we understood that it was meaningless to speak of events happening "at the same time". Following these type of conceptual revolutions we finally arrived at the above definition of spacetime. In this work I wish to comment on some of its limits, taking the move from some criticisms by Robert Geroch [4].

E. Minguzzi
Dipartimento di Matematica e Informatica "U. Dini", Università degli Studi di Firenze,
Via S. Marta 3, I-50139 Firenze, Italy
e-mail: ettore.minguzzi@unifi.it

A. García-Parrado et al. (eds.), *Progress in Mathematical Relativity, Gravitation and Cosmology*, Springer Proceedings in Mathematics & Statistics 60,
DOI 10.1007/978-3-642-40157-2_49, 

The spacetime of General Relativity has a distinguished feature with respect to all previous formulations, including that of Special Relativity, namely, while the former definitions involved a static mathematical entity (think at the direct product $M = \mathbb{R} \times S$ of Aristotelian Mechanics, at the fiber bundle structure $\pi : M \to \mathbb{R}$ of Newtonian Mechanics, or at the Minkowskian spacetime of Special Relativity) the latter becomes a dynamical entity controlled by some partial differential equations: the Einstein equations. Here we might take the view that Definition 1.1 really defines the *extended configuration space* of an evolution problem determined by Einsten's equation.

In this work we shall not be interested in the details of the dynamics, as we shall focus instead on the nature of the extended configuration space. Indeed, whatever the dynamics, our definition of spacetime suffers already some problems connected to its evolution. In order to make an example, let us observe that if we remove a point or a set from a spacetime we still get a spacetime. The dynamics cannot determine a single object, as removing points outside the (partial Cauchy) hypersurface where we put the initial data, still returns a solution to the problem. Similarly, imagine to remove a point from an observer's (i.e. timelike) worldline. The initial segment of the curve could still represent an observer who, however, cannot tell that he will disappear in the next instants without any warning. In this situation it seems impossible to use this type of configuration space to make any kind of prediction. The conclusion is that Definition 1.1 gives really a too broad definition of spacetime.

As a first attempt, we can try to improve the definition introducing an inextendibility condition. Let us recall that an isometry is an imbedding $\varphi : M \to M'$, from $(M, g)$ to $(M', g')$ such that $g = \varphi^* g'$. A spacetime $(M, g)$ *inextendible* if it is not a proper subset of another spacetime. In other words, every isometry $\varphi : M \to M'$ is surjective.

Intuitively, in an inextendible spacetime no observer will see or experience a spacetime singularity if there is the possibility of removing it by enlarging the manifold. The inextendibilty condition allows us to discard as unreasonable those spacetimes which are obtained from proper subsets of other spacetimes. Null or timelike geodesically complete spacetimes are necessarily inextendible, for any extension would allow one to extended a geodesic with this causal type which, as a consequence, had to be incomplete in the original spacetime.

The condition of *inextendibility*, as that of geodesic completeness, is a *metric* concept. Thus, a spacetime can be conformally extendible but inextendible. Indeed, every conformally extendible non-total imprisoning spacetime can be made geodesically complete and hence inextendible [1].

Unfortunately, the inclusion of the inextendibility condition does not lead to a satisfactory definition. Let us consider the inextendible examples of Fig. 1 which are obtained from Minkowski $1 + 1$ spacetime, by removing a set and making some identifications (following the integral lines of a Killing vector field $k = t\partial_x + x\partial_t$).

While true that we do not fix the dynamics, we expect $D^+(S)$ to be determined by the dynamics and by the initial conditions on $S$, whatever they could be. In these inextendible examples, instead, it depends on the spacetime as a whole, whether

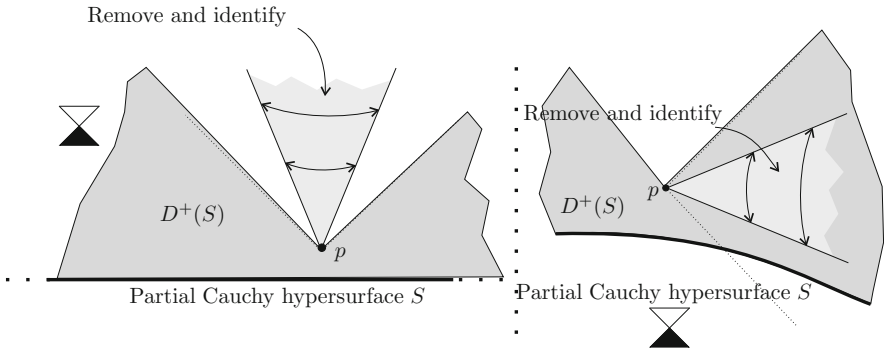


**Fig. 1** Two spacetimes obtained by making some identifications in a subset of Minkowski spacetime. The domain of dependence of $S$ depends on the already fully developed spacetime, whether it is that depicted in the figure or Minkowski

it is $1+1$ Minkowski spacetime or a just locally so version obtained from cut and paste.

We might consider two types of evolutions depending on the development $D^+(S)$ which follows from the initial data. There is a conceptual difference as to whether it is *maximal* or *maximum*, where these terms are used in their usual partial order sense.

(i) If we demand that for every initial data, there should be a *maximum* development, then we demand *determinism*.
(ii) If we demand that there should be just a maximal development then we allow for random ingredients in the spacetime dynamics. We cannot tell which development we will get from the initial condition, but we want it to be maximal. This means that *the dynamics, deterministic or not, shapes spacetime as far as possible*.

The Choquet–Bruhat–Geroch theorem

**Theorem 1.2.** *For every sufficiently smooth vacuum initial data* $(S, h, K)$*, there exists a unique, up to isometric diffeomorphism, vacuum development* $(M, g)$*, which is globally hyperbolic and contains any other globally hyperbolic development (in particular it is maximal).*

implies that if the dynamics is determined by the vacuum Einstein's equation, then the restrictive condition (i) applies. However, there is no fundamental reason for this to be the case for say, general matter fields, and option (ii) might be expected to apply instead. The precise formulation of the term *maximal* in (ii) is given by the hole-free condition. Roughly speaking a spacetime is not holed if for every hypersurface $S$ its Cauchy development $D(S)$ is maximal, that is, we cannot modify the spacetime outside $D(S)$ so as to extend the Cauchy development. It turns out that making this idea precise presents several difficulties. There is not enough

space here to make a full account of the history of the various definitions that have been proposed [2–6]. A completely satisfactory one is [7] (here $\tilde{D}(S) = \overline{D(S)}$, and a *partial Cauchy hypersurface* is an acausal edgeless set).

**Definition 1.3.** A spacetime $(M, g)$ has a *future Cauchy hole* (or simply a future hole) if there is a partial Cauchy hypersurface $S$ and an isometry $\varphi : \tilde{D}(S) \to N$, on a spacetime $(N, \sigma)$, such that $\varphi(S)$ is acausal and

$$\varphi(H^+(S)) \cap D^+(\varphi(S)) \neq \emptyset.$$

The definition of *past Cauchy hole* is given dually. A spacetime is *Cauchy holed* if it has a future or a past hole.

The main idea is that there is a hole if the initial Cauchy development can be attached to a different spacetime in such a way that, not only the Cauchy development gets enlarged, but also, the previous horizon gets at least in part canceled by the new Cauchy development. That is: *we can extend prediction passing through the former horizon*.

Let us now recall that a spacetime is *causally simple* if it is causal (no closed causal curves) and if it has a closed causal relation $J^+$. Globally hyperbolic spacetimes are causally simple. An inspection of available examples of causally simple spacetimes shows, rather intuitively, that they have no holes. I was indeed able to prove this fact, obtaining the next result [7].

**Theorem 1.4.** *Every inextendible causally simple spacetime is hole-free.*

If the spacetime is holed we can also infer the existence of singularities [7]

**Theorem 1.5.** *Every inextendible future holed spacetime admits a future lightlike incomplete geodesic and a future timelike incomplete geodesic. These geodesics are contained in D(S) and the Riemann tensor, and its covariant derivatives at any order, evaluated on a parallely transported base over them have a finite limit.*

In conclusion, the hole-free condition should be included in the very definition of spacetime. Hopefully, it will lead to new physically interesting results.

**Acknowledgements** This work has been partially supported by GNFM of INDAM

## References

1. Beem, J. K.: Conformal changes and geodesic completeness. Commun. Math. Phys. **49**, 179–186 (1976)
2. Clarke, C. J. S.: *The analysis of space-time singularities*. Cambridge: Cambridge University Press (1993)
3. Earman, J.: *Bangs, crunches, whimpers, and shrieks: singularities and acausalities in relativistic spacetimes*. Oxford: Oxford University Press (1995)

4. Geroch, R.: *Prediction in general relativity*, Minneapolis: University of Minnesota Press, vol. Foundations of Space-Time Theories of *Minnesota Studies in the Philosophy of Science, vol. VIII,*, pages 81–93 (1977)
5. Krasnikov, S.: Even Minkowski spacetime is holed. Phys. Rev. D **79**, 124041 (2009)
6. Manchak, J. B.: Is spacetime hole-free? Gen. Relativ. Gravit. **41**, 1639–1643 (2009)
7. Minguzzi, E.: Causally simple inextendible spacetimes are hole-free. J. Math. Phys. **53**, 062501 (2012)

# Optimal Time Travel in the Gödel Universe

**José Natário**

**Abstract** Using the theory of optimal rocket trajectories in general relativity, we present a candidate for the minimum total integrated acceleration closed timelike curve in the Godel universe, and give evidence for its minimality. The total integrated acceleration of this curve is lower than Malament's conjectured value (Malament, 1984); however, Malament's conjecture does seem to hold for periodic closed timelike curves.

## 1 The Gödel Universe

Recall that the Gödel universe is given in appropriate units by the line element

$$ds^2 = -\left[dt - \sqrt{2}(\cosh(r) - 1)d\varphi\right]^2 + dr^2 + \sinh^2(r)d\varphi^2 + dz^2. \qquad (1)$$

It is a solution of the Einstein equations with cosmological constant $\Lambda = -1/2$, sourced by a dust of density $1/8\pi$ and four-velocity $\partial/\partial t$. Ignoring the trivial $z$-direction, we notice that this metric can be written as $ds^2 = -(dt + \sqrt{2}\theta)^2 + dl^2$, where $dl^2$ is the metric for the unit hyperbolic plane and $\theta$ is the Liouville form (that is, $d\theta$ is the area form). From this, it is easy to obtain the geodesics, whose projections on the hyperbolic plane are circles, represented in Fig. 1. Famously, the Gödel universe contains closed timelike curves (CTCs), whose projections can also be circles, as depicted in Fig. 1. Note that these CTCs are *never* geodesics.

The endpoints of the lift of a closed curve $\gamma$ in the hyperbolic plane to the Gödel universe have a coordinate time difference

J. Natário (✉)
Departamento de Matemática, Instituto Superior Técnico, 1049-001 Lisboa, Portugal
e-mail: jnatar@math.ist.utl.pt

A. García-Parrado et al. (eds.), *Progress in Mathematical Relativity, Gravitation and Cosmology*, Springer Proceedings in Mathematics & Statistics 60,
DOI 10.1007/978-3-642-40157-2_50, 

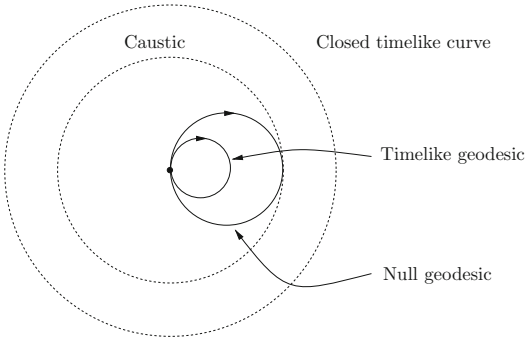


**Fig. 1** Projections on the hyperbolic plane of timelike and null geodesics, and of closed timelike curves

$$\Delta t = \oint_\gamma dt = \oint_\gamma \sqrt{2}\,\theta + \sqrt{d\tau^2 + dl^2} = \sqrt{2}\,A + \oint_\gamma \frac{dl}{v}, \tag{2}$$

where $A$ is the signed area enclosed by $\gamma$ and $v$ is the velocity with respect to the dust. From this and the isoperimetric inequality in the hyperbolic plane one can deduce that the projections of closed timelike curves must be traversed *clockwise*, enclose an area $|A| > 4\pi$, have length $l > 4\pi\sqrt{2}$ and attain a maximum velocity $v_{max} > \sqrt{2}/2$.

## 2 Total Integrated Acceleration

The initial and final masses of a rocket exhausting matter with constant velocity $v_e$ are related by

$$\frac{m_1}{m_0} = \exp\left(-\frac{1}{v_e}\int_{\tau_0}^{\tau_1} a(\tau)d\tau\right), \tag{3}$$

where $a$ is the magnitude of the proper acceleration [1]. The *total integrated acceleration* $TA = \int_{\tau_0}^{\tau_1} a(\tau)d\tau$ is therefore an interesting measure of the failure of a CTC to be a geodesic.

Malament [2] proved that $TA \geq \ln(2+\sqrt{5}) \simeq 1.4436$ for any CTC in the Gödel universe, and conjectured that in fact $TA \geq 2\pi\sqrt{9+6\sqrt{3}} \simeq 27.6691$ (corresponding to a certain circle in the hyperbolic plane). This would mean that $m_0/m_1 > 10^{12}$ for any rocket traversing a CTC, a calculation performed by Gödel himself [3] when arguing for the physical plausibility of his universe.

However, Manchak [4] recently gave a counter-example to Malament's conjecture. This counter-example is a *non-periodic* CTC, that is, the initial and final four-velocities are different.

## 3 Rocket Theory

The problem of finding the curve that minimizes $TA = \int_{\tau_0}^{\tau_1} a(\tau) d\tau$ is a difficult problem in the Calculus of Variations, because the second order Lagrangian $L = a = |\nabla_U U|$ is not differentiable at zero, while one can expect the optimal curve to contain portions where $a = 0$ (geodesics). A closely related issue is the occurrence of instantaneous accelerations, unlike for, say, $L = a^2$ (the Lorentzian equivalent of the Lagrangian for Bernoulli's elastic curves). In fact, if we consider Lagrangians of the form $L = a^p$, it is easy to see that instantaneous accelerations have infinite cost for $p > 1$ (and so do not occur in the minimizing curve), and zero cost for $p < 1$ (so that the minimum is trivially zero). The case $p = 1$ is the borderline case, where instantaneous accelerations have a finite nonzero cost. It can be treated using Optimal Control Theory with a restriction $a \leq \bar{a}$ and taking the limit as $\bar{a} \to +\infty$. The resulting optimality conditions were recently obtained in [1]:

$$\begin{cases} \nabla_U U^\mu = a P^\mu \\ \nabla_U P^\mu = -q^\mu + a U^\mu \\ \nabla_U q_\mu = R_{\mu\alpha\beta\gamma} U^\alpha P^\beta U^\gamma \end{cases} \tag{4}$$

Here $U$ is the optimal curve's four-velocity, $P$ is the vector of Lagrange multipliers, and $R_{\alpha\beta\gamma\delta}$ is the Riemann tensor. Note that for geodesic arcs ($a = 0$) these equation reduce to the geodesic and Jacobi (geodesic deviation) equations. The optimality conditions also require that $|P| \leq 1$, with $|P| = 1$ if $a \neq 0$ and at instantaneous accelerations. If the initial (final) value of $U$ is not specified, then we must have $P = 0$ at the beginning (end) of the curve.

## 4 Optimal Time Travel

Since we are looking for the CTC that minimizes *TA*, we do not want to fix the initial and final values of $U$, and so $P = 0$ at the endpoints of the optimal curve. This means that the optimal curve must begin and end with a geodesic arc. The simplest arrangement of this type is depicted in Fig. 2: an initial geodesic arc, followed by an accelerated circle, followed by a final geodesic arc identical to the initial arc (possibly with instantaneous accelerations at the junction points). This type of curve depends on a finite number of parameters $R, r, x, y, \alpha, \beta, \varepsilon, \theta, \varphi, \psi$, which we can (numerically) adjust so as to minimize *TA*. It can then be checked that the curve thus obtained satisfies the optimality conditions, and is therefore a candidate to be the CTC with minimum *TA* in the Gödel universe (see [5] for details). The optimality conditions, however, are necessary but not sufficient, and there is no guarantee that this curve is indeed the minimum. A conclusive answer would require searching over all possible arrangements of geodesic and accelerated arcs with instantaneous accelerations at the junction points, clearly not a feasible task.

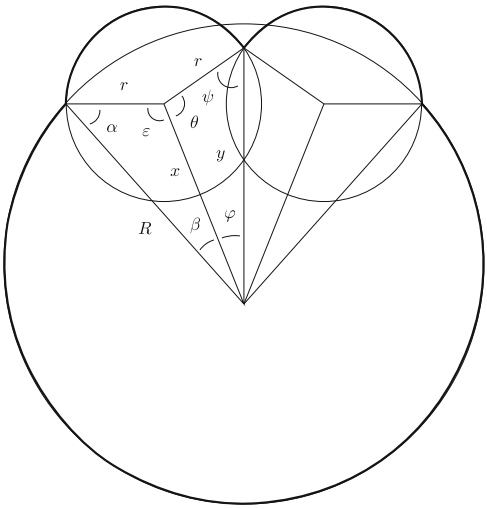


**Fig. 2** Projection of the candidate optimal trajectory on the hyperbolic plane (*circles and lines* represent circles and geodesics of the hyperbolic plane)

Our candidate curve satisfies $TA \simeq 24.9927$, substantially less than the value $TA \simeq 27.6691$ given by Malament's conjecture. However, if we include the instantaneous acceleration necessary to boost the final four-velocity to the initial four-velocity we obtain $TA \simeq 28.6085 > 27.6691$. It is therefore conceivable that Malament's conjecture still hold for *periodic* CTCs.

## References

1. Henriques, P., Natário, J.: The rocket problem in general relativity. J. Optim. Theory Appl. **154**, 500–524 (2012)
2. Malament, D.: Minimal acceleration requirements for "time travel" in Gödel space-time. J. Math. Phys. **26**, 774–777 (1985)
3. Gödel, K.: A remark about the relationship between relativity theory and idealistic philosophy. In: Schilpp, P. (ed.) Albert Einstein: Philosopher-Scientist, pp. 560–561. Open Court, Illinois (1949)
4. Manchak, J.: On efficient "time travel" in Gödel spacetime. Gen. Rel. Grav. **43**, 51–60 (2011)
5. Natário, J.: Optimal time travel in the Gödel universe. Gen. Rel. Grav. **44**, 855–874 (2012)

# Diagonal Future of Some Non-diagonal Bianchi A Spacetimes with Matter of Vlasov Type

**Ernesto Nungesser**

**Abstract** We have been able to show that after a possible basis change the future of the non-diagonal Bianchi II and $VI_0$ spacetimes with collisionless matter is asymptotically diagonal assuming small data. More precisely these solutions are asymptotic to the Collins-Stewart solution with dust and the Ellis–MacCallum solution respectively.

## 1 Introduction

In presence of a cosmological constant *isotropization* has been shown for a wide class of different matter models. This no longer can be expected in absence of this constant and it for different Bianchi types the asymptotic behaviour towards the future has been established to a large extend in the case that the Universe is modelled by a perfect fluid with linear equation of state. For a non-tilted single fluid in a homogeneous spacetimes if the initial data, i.e. metric, second fundamental form and energy momentum tensor are diagonal initially, they will remain diagonal. The same happens if one assumes extra symmetries. In the case of Bianchi spacetimes which are locally rotationally symmetric the problem is also diagonal for matter of Vlasov type. For the latest result on these spacetimes we refer to [2]. The diagonal assumption is not possible without these restrictions for collisionless matter. However we have been able to show that after a possible basis change the future of the non-diagonal Bianchi II and $VI_0$ spacetimes with collisionless matter is asymptotically diagonal. That these basis changes are possible is probably related to the existence of a hierarchical structure of conserved quantities and monotonic functions (see [1] for details).

E. Nungesser (✉)
KTH Royal Institute of Technology, SE-100 44 Stockholm, Sweden

A. García-Parrado et al. (eds.), *Progress in Mathematical Relativity, Gravitation and Cosmology*, Springer Proceedings in Mathematics & Statistics 60,
DOI 10.1007/978-3-642-40157-2_51, © Springer-Verlag Berlin Heidelberg 2014

Without going into the details which can be found in [3] we want to present its main results. It is a small data result where we assume that certain quantities are close to the ones corresponding to special solutions. In the case of Bianchi II, we assume that we are close to the Collins-Stewart solution with dust and the case of Bianchi $\mathrm{VI}_0$ we are close to the Ellis–MacCallum solution. In order to be more specific let us introduce some notation. We can decompose the second fundamental form introducing $\sigma_{ab}$ as the trace-free part

$$k_{ab} = \sigma_{ab} - Hg_{ab}$$

and using the Hubble parameter

$$H = -\frac{1}{3}k$$

we define

$$\Sigma_a^b = \frac{\sigma_a^b}{H}$$

and

$$\Sigma_+ = -\frac{1}{2}(\Sigma_2^2 + \Sigma_3^3);\ \Sigma_- = -\frac{1}{2\sqrt{3}}(\Sigma_2^2 - \Sigma_3^3)$$

We will also need some curvature quantities scaled by the Hubble parameter as $N = R/H^2$ and

$$N_i^j = \frac{R_i^j}{H^2}$$

where $R$ and $R_i^j$ are the Ricci scalar and tensor respectively. In the Bianchi II case we also use the notation $(N_1)^2 = -2N$ and for Bianchi $\mathrm{VI}_0$ we also use the following notation

$$n_{ij} = \frac{g_{ij}}{\sqrt{g}H}$$

where $g$ is the determinant of the 3-metric. The smallness assumption then means that the difference of these quantities with respect to the quantities in the model case is small. In addition to that, there is also a smallness assumption concerning the dispersion of the velocities which can be described by $P$. This quantity

$$P(t) = \Sigma\{|p| = (g^{ab}p_a p_b)^{\frac{1}{2}}|f(t,p) \neq 0\}$$

is assumed to be small, i.e. the spacetime is close to dust.

## 2 Main Results

### 2.1 Bianchi II

With the following transformation of the basis vector

$$\tilde{e}_1 = e_1$$
$$\tilde{e}_2 = e_2 + ae_1$$
$$\tilde{e}_3 = e_3 + be_1$$

which preserves the Lie-algebra, i.e. the Bianchi type, we obtain the same asymptotics as in the diagonal case, in fact we are able to conclude

**Theorem 1.** *Consider any $C^\infty$ solution of the Einstein-Vlasov system with Bianchi II symmetry and with $C^\infty$ initial data. Assume that $|\Sigma_+(t_0) - \frac{1}{8}|$, $|\Sigma_-(t_0)|$, $|\Sigma_2^1(t_0)|$, $|\Sigma_3^1(t_0)|$, $|\Sigma_3^2(t_0)|$, $|\Sigma_2^3(t_0)|$, $|\Sigma_1^2(t_0)|$, $|\Sigma_1^3(t_0)|$, $|N_1(t_0) - \frac{3}{4}|$, $|N_2^1(t_0)|$, $|N_3^1(t_0)|$ and $P(t_0)$ are sufficiently small. Then at late times, after possibly a basis change, the following estimates hold:*

$$H(t) = \frac{2}{3}t^{-1}(1 + O(t^{-\frac{1}{2}})),\ P(t) = O(t^{-\frac{1}{2}})$$
$$\Sigma_+ - \frac{1}{8} = O(t^{-\frac{1}{2}});\ \Sigma_- = O(t^{-1})$$
$$\Sigma_2^1 = O(t^{-\frac{1}{2}});\ \Sigma_3^1 = O(t^{-\frac{1}{2}})$$
$$\Sigma_3^2 = O(t^{-1});\ \Sigma_2^3 = O(t^{-1})$$
$$\Sigma_1^2 = O(t^{-1});\ \Sigma_1^3 = O(t^{-1})$$
$$N_1 - \frac{3}{4} = O(t^{-\frac{1}{2}})$$
$$N_2^1 = O(t^{-\frac{1}{2}});\ N_3^1 = O(t^{-\frac{1}{2}})$$

### 2.2 Bianchi $VI_0$

This time we can make the following basis change

$$\tilde{e}_1 = e_1 + ae_2 + be_3$$
$$\tilde{e}_2 = e_2$$
$$\tilde{e}_3 = e_3$$

such that we obtain the following result:

**Theorem 2.** *Consider any $C^\infty$ solution of the Einstein-Vlasov system with Bianchi $VI_0$ symmetry and with $C^\infty$ initial data. Assume that $|\Sigma_+(t_0) + \frac{1}{4}|$, $|\Sigma_-(t_0)|$, $|\Sigma_2^1(t_0)|$, $|\Sigma_3^1(t_0)|$, $|\Sigma_3^2(t_0)|$, $|\Sigma_2^3(t_0)|$, $|\Sigma_1^2(t_0)|$, $|\Sigma_1^3(t_0)|$, $|N(t_0) + \frac{9}{8}|$, $|N_2^2(t_0)|$, $|n_{23}(t_0)|$, $|n_{12}(t_0)|$,$|n_{13}(t_0)|$ and $P(t_0)$ are sufficiently small. Then at late times, after possibly a basis change, the following estimates hold:*

$$
\begin{aligned}
&H(t) = \frac{2}{3}t^{-1}(1 + O(t^{-\frac{1}{2}}));\ P(t) = O(t^{-\frac{1}{2}})\\
&\Sigma_+ - \frac{1}{4} = O(t^{-\frac{1}{2}});\ \Sigma_- = O(t^{-\frac{1}{2}})\\
&\Sigma_2^1 = O(t^{-1});\ \Sigma_3^1 = O(t^{-1})\\
&\Sigma_3^2 = O(t^{-1});\ \Sigma_2^3 = O(t^{-1})\\
&\Sigma_1^3 = O(t^{-\frac{1}{2}});\ \Sigma_1^2 = O(t^{-\frac{1}{2}})\\
&n_{12} = O(t^{-\frac{1}{2}});\ n_{13} = O(t^{-\frac{1}{2}})\\
&n_{23} = O(t^{-\frac{1}{2}});\ N_2^2 = O(t^{-\frac{1}{2}})\\
&N + \frac{9}{8} = O(t^{-\frac{1}{2}})
\end{aligned}
$$

Apart from that the spacetimes become asymptotically diagonal, they become asymptotically dust-like since the ratio between the trace of the spatial part of the energy-momentum tensor and the energy-density can be bounded by $P^2$ which tends to zero. In fact one can show that the distribution function becomes a Dirac delta with respect to the momentum variable asymptotically.

## 3 Outlook

There is a correspondence between the Bianchi types and Thurstons classification of 3-manifolds. It is thus of interest to explore possible links to results of dynamical nature, like for instance results concerning the Einstein flow. We refer the interested reader to [4] and references therein.

## References

1. Heinzle, J. M. and Uggla, C. Monotonic functions in Bianchi models: why they exist and how to find them. *Class. Quant. Grav.*, 27: 015009, 2010.
2. Heißel, G. Dynamics of locally rotationally symmetric Bianchi type VIII cosmologies with anisotropic matter. *arXiv:1203.2852v1 [gr-qc]*, 2012.
3. Nungesser, E. Future non-linear stability for solutions of the Einstein-Vlasov system of Bianchi types II and $VI_0$. *J. Math. Phys.*, 53: 102503, 2012.
4. Reiris, M. The ground state and the long-time evolution in the CMC Einstein flow. *Annales Henri Poincaré*, 10: 1559–1604,2010.

# Stability of the Einstein Static Universe in Massive Gravity

**Luca Parisi, Ninfa Radicella, and Gaetano Vilasi**

**Abstract** We discuss the stability of static cosmological solutions in the framework of the dRGT theory of massive gravity (de Rham and Gabadadze, Phys. Rev. D82:044020, 2010). These solutions, only sourced by a perfect fluid, are either neutrally stable or unstable against spatially homogeneous and isotropic perturbations thus generalizing the Einstein static universe found in General Relativity. This paper summarises the results presented in (Phys Rev D 86:024035, 2012).

## 1 Introduction

The Einstein Static (ES) Universe is the simplest closed Friedmann–Robertson–Walker model i.e. a static cosmological solution of the Einstein equations sourced by a perfect fluid and a cosmological constant (see [5]). The renewed interest in the ES Universe, besides its historical importance, comes from the Emergent Universe scenario [4], an inflationary cosmological model in which it plays a crucial role as initial state.

The stability properties of this cosmological model and those of some analogous solutions in modified gravity and quantum gravity have been widely investigated (see [1,9] and references therein). Indeed, when dealing with modified cosmological equations, many new static solutions are present whose stability properties are substantially different from those of the classical ES solution of General Relativity (GR). In particular, neutrally stable solutions are present thus ameliorating the fine-tuning problem of the emergent Universe scenario [7].

Here we study static cosmological solutions in the framework of a covariant Massive Gravity (MG) model recently proposed in [3]. In contrast with GR where,

L. Parisi (✉) · N. Radicella · G. Vilasi
Dipartimento di Fisica "E.R.Caianiello", Università degli Studi di Salerno,
I-84084 Fisciano (Sa), Italy
e-mail: parisi@sa.infn.it

A. García-Parrado et al. (eds.), *Progress in Mathematical Relativity, Gravitation and Cosmology*, Springer Proceedings in Mathematics & Statistics 60,
DOI 10.1007/978-3-642-40157-2_52, 

in order to have static solutions, a cosmological constant term and a positive curvature term are needed in addition to a suitable perfect fluid source term, we find that in the considered MG theory it is possible to have static cosmological solutions only sourced by a perfect fluid. These solutions can be either unstable or neutrally stable and they exist even for spatially flat (i.e. $\mathscr{K} = 0$) cosmological models.

## 2 Cosmological Equations

In the considered theory [3] the Friedmann equations for a Robertson-Walker Universe with three-dimensional spatial curvature $\mathscr{K} = 0, \pm 1$ read

$$H^2 = \frac{\kappa}{3}\rho - \frac{\mathscr{K}}{a^2} + \frac{m^2}{3}\left(A_1 + \frac{A_2}{a} + \frac{A_3}{a^2}\right) \tag{1}$$

$$\dot{H} = -\frac{\kappa}{2}\rho(1+w) + \frac{\mathscr{K}}{a^2} - \frac{m^2}{6}\left(\frac{A_2}{a} + 2\frac{A_3}{a^2}\right). \tag{2}$$

where $H = \dot{a}/a, \kappa = 8\pi G$, and the coefficients $A_1 = -3c_4 - 6$, $A_2 = 3(3 + 2c_4)$, $A_3 = -3(1 + c_4)$ depend on the arbitrary dimensionless real constants $c_3$ and $c_4$ arising from the theory. In the following analysis we assume a constant equation of state parameter $w$ thus $p = w\rho$. Moreover, the parameter space is reduced imposing $c_3 = -c_4$ since, this is the simplest choice that presents a successful Vainshtein effect in the weak field limit [6].[1]

Matter couples minimally to gravity thus its equation of motion is

$$\dot{\rho} + 3H(\rho + p) = 0. \tag{3}$$

Making use of the Friedmann constraint Eq. (1) one can recast Eq. (2) as a second order nonlinear differential equation in $a$ and its first and second derivatives which, in turn, can be easily recast as a proper two-dimensional autonomous dynamical system by introducing the variables:

$$q = a, \qquad p = \dot{a}. \tag{4}$$

Thus, the system to be considered is the following:

$$\dot{q} = p, \tag{5}$$

$$\dot{p} = \frac{m^2}{2}\left[A_1(1+w)q + A_2\frac{2+3w}{3}\right] + \frac{-1}{2q}(1+3w)\left[\frac{A_3}{3}m^2 + (\mathscr{K} + p^2)\right]. \tag{6}$$

[1] For a full-fledged analysis of the spatially flat case where the model parameters are constrained using cosmological data, see [2].

The dynamics described by the above equations is globally Hamiltonian with respect to the symplectic structure $\omega = q^{1+3w} dq \wedge dp$ which is singular in $q = 0$. Indeed $i_X \omega = -d\mathscr{H}$ where

$$\mathscr{H} = \frac{q^{3(1+w)}}{2}\left[\left(\frac{p}{q}\right)^2 + \frac{\mathscr{K}}{q^2} - \frac{m^2}{3}\left(A_1 + \frac{A_2}{q} + \frac{A_3}{q^2}\right)\right], \tag{7}$$

and $i_X$ is the contraction operator with respect to the vector field

$$X = p\frac{\partial}{\partial q} + \left(\frac{m^2}{2}\left(A_1(w+1)q + A_2\frac{2+3w}{3}\right) + \frac{-1}{2q}(3w+1)\left(\frac{A_3}{3}m^2 + (\mathscr{K} + p^2)\right)\right)\frac{\partial}{\partial p},$$

which is singular in $q = 0$ and $p = 0$. The Hamilton's equations read

$$\dot{q} = q^{-(1+3w)}\frac{\partial \mathscr{H}}{\partial p}, \qquad \dot{p} = -q^{-(1+3w)}\frac{\partial \mathscr{H}}{\partial q}. \tag{8}$$

## 3 Static Solutions and Their Stability

The system of Eqs. (1)–(3) admits the following static solutions

$$a_\pm = -\frac{mA_2(2+3w) \pm \sqrt{\Omega}}{6m(1+w)A_1}; \qquad \rho_\pm = \frac{3}{\kappa}\left[\frac{\mathscr{K}}{a_\pm^2} - \frac{m^2}{3}\left(A_1 + \frac{A_2}{a_\pm} + \frac{A_3}{a_\pm^2}\right)\right] \tag{9}$$

with

$$\Omega = m^2(2+3w)^2A_2^2 + 12(3\mathscr{K} - m^2A_3)(1 + 4w + 3w^2)A_1. \tag{10}$$

Two kinds of solutions are present: neutrally stable solutions and unstable solutions (of the saddle type). The stability properties have been characterized considering the dynamical system in Eqs. (5)–(6) and performing a linearised stability analysis, some numerical integrations and, for the non-hyperbolic fixed points, applying Lyapunov's second criterion using the function $\mathscr{H}$ in Eq. (7) (after a suitable rescaling) as Lyapunov function. The results can be summarized as follows.

*Spatially closed ($\mathscr{K} = 1$) models*

- both the unstable and the neutrally stable solutions are admitted;
- neither the unstable solution or the neutrally stable solution is admitted;
- no static solutions are admitted.

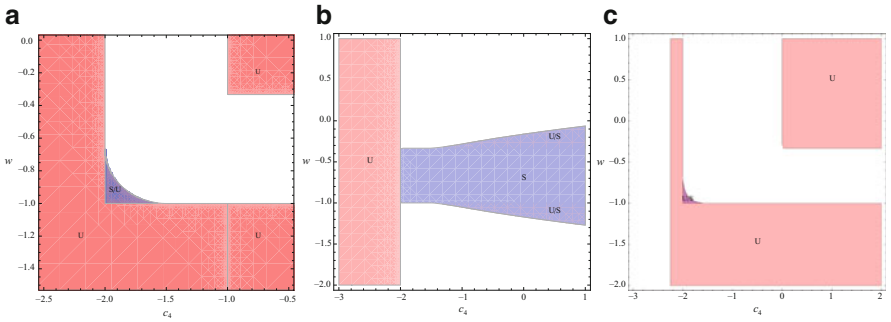


**Fig. 1** $(w, c_4)$-plane for (**a**) the $\mathscr{K} = 0$ case, (**b**) the $\mathscr{K} = -1$ case and (**c**) the $\mathscr{K} = 1$ case. In the considered subset of the parameter space, $-3 < c_4 < 1$ and $-2 < w < 1$, the two solutions behave differently, one being unstable (U, *red*), the second being stable (S, *blue*), their stability regions overlapping only partially

*Spatially flat ($\mathscr{K} = 0$) and open ($\mathscr{K} = -1$) models*

- both the unstable and the neutrally stable solutions are admitted;
- only the unstable solution is admitted;
- no static solutions are admitted.

In the considered region of the parameter space, the neutrally stable solution requires a negative equation of state parameter $w$; in particular it must be $-1 < w < -2/3$ in the $\mathscr{K} = 0, -1$ cases and $-1.2 < w < 0$ in the $\mathscr{K} = 1$ case (Fig. 1).

The effect of a massive graviton is to enrich the phase space of the cosmological equations modifying its global structure, enlarging the ranges of existence of static solutions and affecting their stability properties. In particular, it is possible to construct models in which the Universe oscillates indefinitely about an initial static state, thus the fine-tuning problem suffered by the emergent Universe scenario in GR [4] is ameliorated. On the other hand, in order to break the regime of infinite oscillations and enter the current expanding phase undergone by the Universe [7] a mechanism is needed whose description is beside the scope of our work.

**Acknowledgements** This work is partially supported by the Italian Ministero Istruzione Università e Ricerca (MIUR) through the PRIN 2008 grant, by the INFN/MICINN collaboration, Grant No.AIC10-D-000581 and by Agenzia Spaziale Italiana (ASI).

## References

1. R. Canonico and L. Parisi, Phys. Rev. D **82**, 064005 (2010).
2. V. F. Cardone, N. Radicella, L. Parisi Phys. Rev. **D85** , 124005 (2012).
3. C. de Rham, G. Gabadadze, Phys. Rev. **D82** 044020 (2010); C. de Rham, G. Gabadadze and A. J. Tolley, Phys. Rev. Lett. **106** 231101 (2011).

4. G. F. R. Ellis and R. Maartens, Class. Quant. Grav. **21** 223–232 (2004); G. F. R. Ellis, J. Murugan and C. G. Tsagas, Class. Quant. Grav. **21** 233–249 (2004); S. Mukherjee, B. C. Paul, N. K. Dadhich, S. D. Maharaj and A. Beesham, Class. Quant. Grav. **23** 6927–6933 (2006).
5. S. W. Hawking and G. F. R. Ellis, *The Large scale structure of space-time*, *Cambridge University Press, Cambridge, 1973*.
6. K. Koyama, G. Niz, G. Tasinato, Phys. Rev. **D84** 064033 (2011).
7. J. E. Lidsey and D. J. Mulryne, Phys. Rev. D **73** 083508 (2006); J. E. Lidsey, D. J. Mulryne, N. J. Nunes and R. Tavakol, Phys. Rev. D **70** 063521 (2004).
8. L. Parisi, N. Radicella and G. Vilasi, Phys. Rev. D **86** 024035 (2012).
9. L. Parisi, M. Bruni, R. Maartens and K. Vandersloot, Class. Quant. Grav. **24** 6243 (2007).

# Tilted Lemaître Model and the Dark Flow

**Julio J. Fernández and José-F. Pascual-Sánchez**

**Abstract** In the last years, the peculiar velocities of many X-ray galaxies clusters with respect to the distance have been measured directly in the rest frame of the cosmic microwave background radiation (CBR), using the kinematic Sunyaev–Zeldovich (kSZ) effect. These measures prove that exists a highly coherent motion, extending out to at least to 1 *Gpc*, of the matter rest frame with respect to the CBR rest frame. This global motion was named "dark flow". By using an inhomogeneous spherically symmetric "tilted" Lemaître model, we could explain the dark flow if we assume a linear increase with distance of the peculiar velocities, which is in principle allowed by these observations. This linear increase of the dark flow with the distance has the same behavior that the intrinsic dipole, due to the kinematic acceleration, which appears in the Hubble law of the Lemaître model. In the "tilted" Lemaître model considered, we consider that the radiation orthogonal congruence is a perfect fluid and the matter "tilted" congruence is an imperfect fluid with heat flux.

## 1 Tilted Cosmological Models

In cosmology it is essential to specify the set of observers, or rather, the congruences of world-lines from which observations are made.

Cosmological quantities depend on the choice of these congruences, specified by 4-velocities fields. For instance, with the same spacetime metric, one can have two

J.J. Fernández
Dept. Fisica Teórica, Facultad de Ciencias, Universidad de Valladolid, Valladolid, 47011, Spain
e-mail: julio.j.fernandez@hotmail.es

J.-F. Pascual-Sánchez (✉)
IMUVA and Dept. Matemática Aplicada, E.I.I., Universidad de Valladolid, 47011, Spain
e-mail: jfpascua@maf.uva.es

A. García-Parrado et al. (eds.), *Progress in Mathematical Relativity, Gravitation and Cosmology*, Springer Proceedings in Mathematics & Statistics 60,
DOI 10.1007/978-3-642-40157-2_53, 

different stress-energy-momentum tensors, corresponding to two different congruences, both satisfying the Einstein equations. The interpretation of the universe of two observers, associated with two different congruences, can be radically different. These models are named "tilted" in the literature, which begins with [1].

If $\Sigma$ is a global 3D spacelike space, which exists assuming zero vorticity, $n^{*\alpha}$ is the four velocity of the normal or orthogonal congruence to $\Sigma$ and $u^\alpha$ the four velocity of the tilted one.

The relationship between both velocities is, at low speed, a galilean transformation: $u^\alpha = n^{*\alpha} + v^\alpha$. The relative ("tilting") peculiar velocity $v^\alpha$ between the two congruences may be related to a physical phenomenon such as the observed motion of our galaxy relative to the cosmic microwave background radiation, the CBR dipole, which is usually interpreted as a Doppler effect.

Previous works on tilted models have been realized by using FLRW [2], Bianchi [1] and, recently, Lemaître–Tolman–Bondi (LTB) [3] and Szekeres metrics [4].

In this work and in the more detailed article [5], we will consider a different case: the Lemaître model. This is the generalization of the LTB model to the case of non-dust matter with a non-null pressure gradient, which gives rise to a kinematic acceleration. This can explain the acceleration of the expansion obtained by the SN1a supernovae distance measures, without considering dark energy, see [6].

## 2 The Tilted Lemaître Model

The metric of the Lemaître model in comoving coordinates is:

$$ds^2 = -N(r,t)^2\,dt^2 + B(r,t)^2\,dr^2 + R(r,t)^2\,(d\theta^2 + sin^2\theta d\phi^2), \qquad (1)$$

Where $N(r,t)$ is the lapse and $R(r,t)$ is the areal radius (or warp factor). It is spherically symmetric, with three Killing vectors. Its symmetry group is a $G_3/S^2$. and it has a "local" preferred radial spatial direction at each point. Also, it belongs to Petrov type D and it has null magnetic Weyl tensor.

This metric is compatible with a general non-perfect (with heat flux and anisotropic pressures) comoving fluid, as Lemaître first pointed out in [7].

The comoving congruence is normal to a foliation of global 3D spacelike hypersurfaces, $n^*{}_\alpha = N^{-1}\delta^t_\alpha$.

The kinematical quantities, expansion, shear tensor and acceleration four-vector of the Lemaître spacetime are all non-null and can be reduced to scalars. Moreover, as the vorticity $\omega^*{}_{\alpha\beta} = 0$, it admits a global $1+3$ splitting. Also, as a LRSIIb model, it admits a $1+1+2$ threading.

Choosing the radially "tilted" non-comoving congruence $u^\alpha$ as

$$u^\alpha = \left(\frac{1}{N}, \frac{v_r}{B}, 0, 0\right), \qquad (2)$$

where $v_r$ means the radial peculiar velocity w.r.t. the normal $n^{*\alpha}$ frame. Due the spherical symmetry of the Lemaître model, $v_r$ is a spherical average.

All the kinematical quantities of the "tilted" Lemaître spacetime w.r.t. the "tilted" congruence $u^\alpha$ can be computed and related to the non-tilted ones.

Consider the Lemaître metric $g_{\alpha\beta}$ as the solution of the Einstein equations for the two different fluid congruences. Where the two stress-energy-momentum tensors $T^*_{\alpha\beta}$ and $T_{\alpha\beta}$ are:

$$T^*_{\alpha\beta} = \frac{4}{3}\mu^* n^*_\alpha n^*_\beta + \frac{1}{3}\mu^*\, g_{\alpha\beta}, \tag{3}$$

which corresponds to an inhomogeneous radiation fluid with energy density $\mu^*(r,t)$ and

$$T_{\alpha\beta} = (\mu + p)u_\alpha u_\beta + p\, g_{\alpha\beta} + q_\alpha u_\beta + u_\alpha q_\beta, \tag{4}$$

which corresponds to an inhomogeneous imperfect matter fluid, with heat flux, $q_\alpha = q\, s_\alpha(r,t)$, in the radial direction of the observer.

Since the Einstein tensor is the same for the tilted (matter) and orthogonal (radiation) congruences, imposing

$$T_{\alpha\beta} = T^*_{\alpha\beta},$$

we should have the following relations between dynamical quantities:

$$\mu = \mu^* + \frac{1}{3}\mu^* v_r^2\,;\ p = \frac{1}{3}(\mu^* + \mu^* v_r^2)\,;\ q = \frac{4}{3}v_r. \tag{5}$$

## 3 The CBR Dipole and the Dark Flow

In the $\Lambda CDM$ model the Hubble expansion is assumed to be uniform, so that the differences between peculiar velocities of galaxies (or clusters) $v_r$ and the observer velocity, are deviations from the isotropy of the usual Hubble law of the FLRW models. In the concordance $\Lambda CDM$ model, the spherically averaged peculiar bulk velocity has a hyperbolic $1/r$ dependence with distance.

On the other hand, the kinematic Sunyaev–Zeldovich (kSZ) effect, which measures the dipole anisotropy of the CBR through a tiny temperature shift (of the order of $\mu K$) in the spectrum of CMB photons scattered from hot gas in clusters of galaxies, gives us the peculiar velocity of any cluster directly in the rest frame of the CMB. By using the kSZ effect, the authors in the review [8] claim to have detected a highly significant CBR dipole for $\sim$ 1200 clusters with redshift $z \leq 0.12$ up to $z = 0.6$.

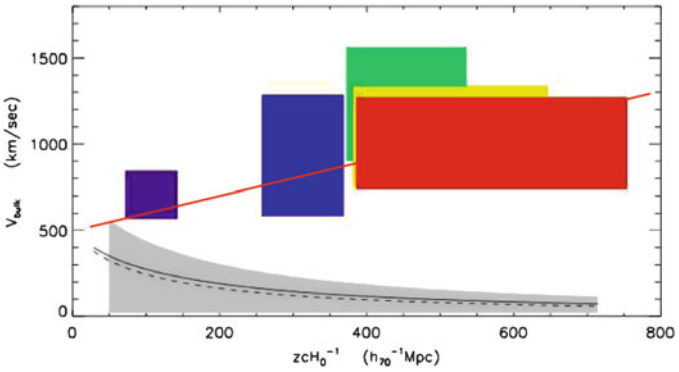


**Fig. 1** In *colored rectangles*, the kSZ measured peculiar velocities as a function of the distance. *Shaded grey region* shows the peculiar velocity in the concordance $\Lambda CDM$ model. The *red line* is our hypothesis of linear increasing with the distance of the kinematic dipole of the dark flow. Figure taken, without the *red line*, from A. Kashlinsky et al. [8]

This detection proves that exists a highly coherent motion, extending out to at least to $1\,Gpc$, of the matter rest frame with respect to the CBR rest frame congruence. This global motion was named "dark flow" by the authors of [8] and supposed by them to be approximately constant, but see Fig. 1. This dark flow do not has the $1/r$ dependence with distance, so is in contradiction with the result of the $\Lambda CDM$ model. Also, it appears that the dark flow may extend across the entire observable Universe horizon. This can be considered as an evidence for a "tilted" Universe. In [9] it was shown that, in the Lemaître model, the following generalized Hubble law is verified:

$$c\,z = \left(\frac{\dot{R}}{R} - A\cos\Psi + \sqrt{3}\,\sigma\cos^2\Psi\right)_0 r_a. \tag{6}$$

This law shows an intrinsic dipole, due to the acceleration, increasing linearly with the distance as in our hypothesis. Where, $\Psi$ is the angle between the direction of observation of a light ray and the preferred radial vector $e_r$ of the Lemaître model, $\sigma$ is the scalar shear, $A$ is the kinematic acceleration and $r_a$ is the angular diameter distance. However, up to now, there is not the necessary accuracy to obtain the possible shear using the kSZ effect. Note that in the pure dust Lemaître–Tolman–Bondi model the intrinsic dipole, due to the acceleration, is absent.

In conclusion, accepting that the dark flow is real and that it increases linearly with the distance, the tilted Lemaître model could be considered as a candidate to explain it. Then there exists a preferred radial spatial direction in the Universe, given by the matter dark flow. Is this "the axis of evil" or better "the rebel or guerrillero axis", because it reappears when the dark flow is considered?.

## References

1. A.R. King and G.F.R. Ellis, Comm. Math. Phys. **31**, 209 (1973)
2. A. A. Coley and B. O. J. Tupper, Ap. J., **271**, 1 (1983)
3. L. Herrera, A. Di Prisco and J. Ibañez, Phys. Rev. **D84**, 064036 (2011)
4. L. Herrera, A. Di Prisco, J. Ibañez and J. Carot, Phys. Rev. **D86**, 044003 (2012)
5. J. J. Fernández and J.-F. Pascual-Sánchez, in submission
6. J.-F. Pascual-Sánchez, Mod. Phys. Lett. A **14**, 1539 (1999)
7. G. Lemaître, Ann. Soc. Sci. Brux. **53**, 51 (1933); reprinted in Gen. Rel. Grav. **29**, 641 (1997)
8. A. Kashlinsky, F. Atrio-Barandela, H. Ebeling, arXiv:1202.0717
9. J.-F. Pascual-Sánchez, Class. Quantum Grav. **17**, 4913, (2000)

# Accelerating $f(T)$ Gravity Models Constrained by Recent Cosmological Data

**Ninfa Radicella, Vincenzo F. Cardone, and Stefano Camera**

**Abstract** Generalised Teleparallel gravity, also referred to as $f(T)$ gravity, has been recently proposed as an extended theory of gravitation able to give rise to an accelerated expansion in a matter only universe. We focus on two particular choices for $f(T)$ and we check their viability contrasting the predicted background dynamics to the Hubble diagram as traced by both Type Ia Supernovae (SNeIa) and Gamma Ray Bursts (GRBs), the measurement of the rate expansion $H(z)$, the Baryon Acoustic Oscillations (BAOs) at different redshifts, and the Cosmic Microwave Background Radiation (CMBR) distance priors. Both $f(T)$ models turn out to be in very good agreement with this large dataset so that we also investigate whether it is possible to discriminate among them relying on the different growth factors.

## 1 Introduction

The discovery of the acceleration of the universe through the SNeIa Hubble diagram has been latter confirmed by wide range of data, from more recent SNeIa data to BAOs and CMBR anisotropies. On the other hand, such overwhelming abundance of observational evidences in favour of the cosmic speed up does not fit in the

N. Radicella (✉)
Dipartimento di Fisica, Università degli Studi di Salerno, INFN sez. Napoli
e-mail: ninfa.radicella@sa.infn.it

V.F. Cardone
I.N.A.F.-Osservatorio Astronomico di Roma, via Frascati 33, 00040—Monte Porzio Catone (Roma), Italy
e-mail: winnyenodrac@gmail.com

S. Camera
CENTRA, Instituto Superior Técnico, Universidade Técnica de Lisboa, Av. Rovisco Pais 1, 1049-001 Lisboa, Portugal
e-mail: stefano.camera@ist.utl.pt

A. García-Parrado et al. (eds.), *Progress in Mathematical Relativity, Gravitation and Cosmology*, Springer Proceedings in Mathematics & Statistics 60,
DOI 10.1007/978-3-642-40157-2_54, 

framework of General Relativity (GR) making clear that out theoretical background is seriously flawed.

In as much the same way as for $f(R)$ theories, one can obtain a generalised teleparallel gravity replacing $T$ with a generic function $f(T)$ thus opening the way to a rich phenomenology. A particular important consequence is the breakdown of the equivalence with the classical GR with the two theories now predicting a radically different dynamics [1]. Modified teleparallel gravity preserves the advantage of giving equations that are still second order in field derivatives opposite to the fourth order equations deduced in $f(R)$ gravity thus avoiding unpleasant pathologies. On the other hand, it suffers from the lack of Local Lorentz Invariance (LLI) so that all the 16 components of the vierbien are independent and one cannot simply fix 6 of them by a gauge choice [2].

A critical role in generalised teleparallel theories is played by the choice of the functional expression for $f(T)$. The lack of firmly established theoretical constraints leaves open the way to a wide range of possibilities which can only be validated a posteriori, i.e. by contrasting their predictions with the observational data. This is the aim of the present work where we focus our attention on two particular classes able to give rise to a phantom-like behaviour of the effective torsion fluid.

There are actually almost no theoretical hints on the functional form of $f(T)$ with, on the contrary, many possible expressions leading to an accelerated expansion.Two recently proposed model of this kind can be obtained setting [3]

$$f(T) = \begin{cases} \alpha(-T)^n \tanh\left(\dfrac{T_0}{T}\right) \\ \\ \alpha(-T)^n \left[1 - \exp\left(-p\dfrac{T_0}{T}\right)\right] \end{cases}, \tag{1}$$

where the subscript 0 denotes present day quantities.

We then test these two models against SNeIa + GRB Hubble diagram, $H(z)$ measurements from cosmic chronometers, BAOs data and the CMBR distance priors. Although wide, the present dataset only traces the background expansion so that we will also investigate whether further insight into the properties of these models can be obtained by the analysis of the growth factor being this latter a quick way to look at how perturbations evolve in the proposed modified teleparallel scenarios.

## 2 $f(T)$ Models Versus Data

In order to answer the question whether $f(T)$ gravity can reproduce the observed Universe, we will explore the model parameter spaces by investigating the following likelihood function

$$\mathscr{L}(\mathbf{p}) = \mathscr{L}_{\mu}(\mathbf{p}) \times \mathscr{L}_{H}(\mathbf{p}) \times \mathscr{L}_{BAO}(\mathbf{p}) \times \mathscr{L}_{CMB}(\mathbf{p}). \tag{2}$$

**Table 1** Constraints on the parameters for the tanh model. Columns are as follows: (1.) id parameter, (2.) best fit, (3.) mean, (4.) median, (5.), (6.) 68% and 95% confidence levels

| Id | $x_{BF}$ | $\langle x \rangle$ | $\tilde{x}$ | 68% CL | 95% CL |
|---|---|---|---|---|---|
| $\Omega_M$ | 0.286 | 0.286 | 0.287 | (0.274, 0.299) | (0.264, 0.311) |
| $h$ | 0.719 | 0.722 | 0.722 | (0.712, 0.734) | (0.702, 0.745) |
| $n$ | 1.616 | 1.610 | 1.615 | (1.581, 1.636) | (1.547, 1.667) |

The first term refers to the Hubble diagram, i.e. the distance modulus $\mu$ as function of the redshift $z$. While SNeIa and GRBs probe the distance-redshift relation as standardizeable candles, Baryon Acoustic Oscillations (BAOs) work as standard rulers. We therefore add the term $\mathscr{L}_{BAO}$ to the full likelihood following the method detailed in [4]. The last term in the likelihood finally refers to the WMAP7 distance priors which have been recommended as a quick and efficient way to include the CMBR constraints without computing the full anisotropy spectrum. The observable quantities are the redshift $z_\star$ to the last scattering surface the acoustic scale $\ell_A = \pi r(z_\star)/r_s(z_\star)$ and the shift parameter $\mathscr{R}$.

In order to efficiently explore the parameter space, we use a Markov Chain Monte Carlo (MCMC) code running multiple chains and checking the convergence through the Gelman–Rubin criterium. The best fit parameters will be the ones maximizing the full likelihood, but the most reliable constraints on each single parameter $p_i$ are obtained by marginalizing over all the parameters but the $i$-th one.

## 3 Results and Conclusions

The best fit parameters and marginalized constraints for the tanh and exp model are given in Tables 1 and 2, while Fig. 1 shows the remarkable agreement among the best fit models predictions and the SNeIa + GRB Hubble diagram and $H(z)$ data. The overall good quality of the fit may be further appreciated by comparing the model predictions for the BAO and CMB quantities with the observed values.

Having been designed to give an accelerated expansion, the parameter space of both models collapses into a region giving rise to a background dynamics similar to the $\Lambda$CDM one. As a consequence, the two models can be hardly discriminated based on the dataset we have used. It is worth stressing that this is not a limitation of the data, but rather an intrinsic feature of how the models have been worked out. As such, improving the precision of the measurements or increasing the statistics does not help in discriminating among the $f(T)$ models and the $\Lambda$CDM one. On the contrary, one has to resort to different tracers which are related to the evolution of the perturbations, the simplest one being the growth factor $g(z)$. On small scales, the impact of torsion only introduces a redshift dependent rescaling of the gravitational constant which now becomes $G_{eff} = G/(1 + f_T)$. On the largest scales, the torsion field modifies the growth of perturbations by altering

**Table 2** Same as Table 1 but for the exp model

| Id | $x_{BF}$ | $\langle x \rangle$ | $\tilde{x}$ | 68% CL | 95% CL |
|---|---|---|---|---|---|
| $\Omega_M$ | 0.284 | 0.286 | 0.287 | (0.276, 0.297) | (0.265, 0.308) |
| $h$ | 0.724 | 0.731 | 0.731 | (0.723, 0.740) | (0.713, 0.749) |
| $n$ | 1.152 | 0.757 | 0.736 | (0.577, 0.939) | (0.514, 1.103) |
| $p$ | 0.814 | -0.110 | -0.100 | (-0.263, 0.046) | (-0.395, 0.131) |

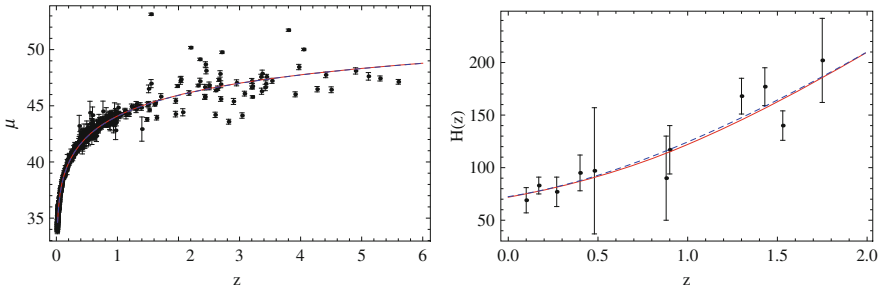


**Fig. 1** Best fit curves superimposed to the SNeIa + GRB Hubble diagram (*left*) and $H(z)$ data (*right*) for the tanh (*red solid*) and exp (*blue dashed*) models. Note that the $\mu(z)$ curves are almost perfectly superimposed so no difference is seen in the plot

both the gravitational constant and the friction term. As a consequence a richer phenomenology is achieved possibly leading to other ways to discriminate among $f(T)$ models and dark energy ones. Two candidate probes are the matter power spectrum $P(k)$ and cosmic shear and deserve a detailed analysis to a forthcoming publication.

This contribution is based on [5].

## References

1. R. Ferraro, F. Fiorini, Phys. Rev. D 75, 081031, 2007; R. Ferraro, F. Fiorini, Phys. Rev. D 78, 124019, 2008; F. Fiorini, R. Ferraro, Int. J. Mod. Phys. A 24, 1686, 2009
2. B. Li, T.P. Sotiriou, J.D. Barrow, Phys. Rev. D 83, 064035, 2011
3. P. Wu, H. Yu, Eur. Phys. J. C 71, 1552, 2011
4. C. Blake, E.A. Kazin, F. Beutler, T.M. Davis, D. Parkinson, et al., MNRAS 418, 1707, 2011
5. V.F. Cardone, N. Radicella and S. Camera, Phys. Rev. D 85, 124007, 2012

# Kasner Solution in Brans–Dicke Theory and Its Corresponding Reduced Cosmology

**Seyed M.M. Rasouli**

**Abstract** We present a brief review of the modified Brans–Dicke theory (MBDT) in arbitrary dimensions, whereby the $(N+1)$-dimensional field equations reduce to the $N$-dimensional ($ND$) configuration with sources and an effective induced scalar potential. We then investigate a generalized Bianchi type I anisotropic cosmology in $5D$ BD theory that leads to an extended Kasner solution. By employing the original equations of MBDT, we probe the reduced Kasner cosmology on the hypersurface with proceeding the investigations for a few cosmological quantities, explaining their properties for some cosmological models.

## 1 Dimensional Reduction of Brans–Dicke Theory in Arbitrary Dimensions

The original motivation of the induced-matter theory (IMT) [1] was to achieve the unification of matter and geometry. Recently, the idea of the IMT has been employed for generalizing BD theory, as a fundamental underlying theory, in four [2] and arbitrary dimensions [3]. In the following, we present only a brief review of the latter.

The variation of the $(N+1)D$ BD action in vacuum with respect to metric and BD scalar field, $\phi$, give the equations

$$G_{ab}^{(N+1)} = \frac{\omega}{\phi^2}\left[(\nabla_a\phi)(\nabla_b\phi) - \frac{1}{2}\gamma_{ab}(\nabla^c\phi)(\nabla_c\phi)\right] + \frac{1}{\phi}\Big(\nabla_a\nabla_b\phi - \gamma_{ab}\nabla^2\phi\Big), \quad (1)$$

$$\nabla^2\phi = 0, \quad (2)$$

S.M.M. Rasouli (✉)
Departamento de Física, Universidade da Beira Interior, 6200 Covilhã, Portugal
e-mail: mrasouli@ubi.pt

A. García-Parrado et al. (eds.), *Progress in Mathematical Relativity, Gravitation and Cosmology*, Springer Proceedings in Mathematics & Statistics 60,
DOI 10.1007/978-3-642-40157-2_55, 

where the Latin indices run from 0 to $N$; $\gamma_{ab}$ is the metric associated to the $(N+1)D$ space-time, $\nabla^2 \equiv \nabla_a \nabla^a$ and $\omega$ is a dimensionless parameter. Here, we have chosen $c = 1$.

In the following, we only employ the equations of the MBDT in arbitrary dimensions, which convey relations between the $(N+1)D$ field equations to the corresponding ones with sources in $ND$ space-time in the context of BD theory [3].

We can find the reduced field equations on the $ND$ hypersurface by employing the BD field Eqs. (1), (2) and a $(N+1)D$ space-time with a line element

$$dS^2 = \gamma_{ab}(x^c)dx^a dx^b = g_{\mu\nu}(x^\alpha, l)dx^\mu dx^\nu + \epsilon\psi^2(x^\alpha, l)\, dl^2, \tag{3}$$

where the Greek indices run from zero to $(N-1)$, $l$ is a non-compact coordinate associated to $(N+1)$th dimension, the parameter $\epsilon = \pm 1$ allows we to choose the extra dimension to be either time-like or space-like, and $\psi$ is the another scalar field taken as a function of all the coordinates.

Here, we only present some of the reduced equations on the $ND$ hypersurface. These equations will be described in two separated parts with a short interpretation.

**1.** We can construct the Einstein tensor on the hypersurface as

$$G^{(N)}_{\mu\nu} = \frac{8\pi}{\phi}T^{(\mathrm{BD})}_{\mu\nu} + \frac{\omega}{\phi^2}\left[(\mathscr{D}_\mu\phi)(\mathscr{D}_\nu\phi) - \frac{1}{2}g_{\mu\nu}(\mathscr{D}_\alpha\phi)(\mathscr{D}^\alpha\phi)\right] + \frac{1}{\phi}\left[\mathscr{D}_\mu\mathscr{D}_\nu\phi - g_{\mu\nu}\mathscr{D}^2\phi\right] - g_{\mu\nu}\frac{V(\phi)}{2\phi}, \tag{4}$$

where $\mathscr{D}_\alpha$ is the covariant derivative on $ND$ hypersurface, which is calculated with $g_{\alpha\beta}$, and $\mathscr{D}^2 \equiv \mathscr{D}^\alpha\mathscr{D}_\alpha$.

The above equations correspond to the BD equations, obtained from the standard BD action containing a scalar potential, but here there are some differences which we clarify them in the following

- The quantity introduced by $V(\phi)$ is actually the effective induced scalar potential on the hypersurface which will be determined by a relation in part 2.
- The quantity $T^{(\mathrm{BD})}_{\mu\nu}$, can be interpreted as an induced energy-momentum tensor (EMT) for a BD theory in $N$-dimensions and it, in turn, contains three components as

$$T^{(\mathrm{BD})}_{\mu\nu} \equiv T^{(\mathrm{I})}_{\mu\nu} + T^{(\phi)}_{\mu\nu} + \frac{1}{16\pi}g_{\mu\nu}V(\phi), \tag{5}$$

where $8\pi/\phi T^{(\mathrm{I})}_{\mu\nu}$ is the same as the induced EMT appearing in IMT, while

$$\frac{8\pi}{\phi}T^{(\phi)}_{\mu\nu} \equiv \frac{\epsilon\phi_{,N}}{2\psi^2\phi}\left[g_{\mu\nu,N} + g_{\mu\nu}\left(\frac{\omega\phi_{,N}}{\phi} - g^{\alpha\beta}g_{\alpha\beta,N}\right)\right], \tag{6}$$

where $A_{,N}$ is the partial derivative of the quantity $A$ with respect to $l$.

**2.** The wave equation on the hypersurface is given by

$$\mathscr{D}^2\phi = \frac{8\pi T^{(\mathrm{BD})}}{(N-2)\omega+(N-1)} + \frac{1}{(N-2)\omega+(N-1)}\left[\phi\frac{dV(\phi)}{d\phi} - \frac{N}{2}V(\phi)\right], \quad (7)$$

where

$$\phi\frac{dV(\phi)}{d\phi} \equiv -(N-2)(\omega+1)\left[\frac{(\mathscr{D}_\alpha\psi)(\mathscr{D}^\alpha\phi)}{\psi} + \frac{\epsilon}{\psi^2}\left(\phi_{,NN} - \frac{\psi_{,N}\phi_{,N}}{\psi}\right)\right] \quad (8)$$
$$-\frac{(N-2)\epsilon\omega\phi_{,N}}{2\psi^2}\left[\frac{\phi_{,N}}{\phi} + g^{\mu\nu}g_{\mu\nu,N}\right] + \frac{(N-2)\epsilon\phi}{8\psi^2}\left[g^{\alpha\beta}{}_{,N}g_{\alpha\beta,N} + (g^{\alpha\beta}g_{\alpha\beta,N})^2\right].$$

Actually in this approach, the $(N+1)D$ field equations (1) and (2) split naturally into four sets of equations on every $ND$ hypersurface, in which we only have introduced the two sets (4) and (7). Regarding the geometrical interpretation of the other two sets, we will not discuss them and leave them for next paper in this series.

In the following, we investigate the Kasner solution in BD theory in a $5D$ space-time; then, as an application of the MBDT in cosmology, we present the properties of a the reduced cosmology on the hypersurface.

## 2 Kasner Solution in Brans–Dicke Theory and Its Corresponding Reduced Cosmology

We start with the generalized Bianchi type I anisotropic model in a $5D$ space-time as

$$dS^2 = -dt^2 + \sum_{i=1}^{3} a_i^2(t,l)dx_i^2 + h^2(t,l)dl^2, \quad (9)$$

where $t$ is the cosmic time, $(x_1, x_2, x_3)$ are the Cartesian coordinates, $l$ is the non-compactified extra dimension, and $a_i(t,l)$, $h(t,l)$ are different cosmological scale factors in each of the four directions. We assume that there is no matter in $5D$ space-time and $\phi = \phi(t,l)$. In addition, based on the usual spatial homogeneity, we solve the field equations (1) and (2) by assuming separation of variables as

$$\phi(t,l) = \phi_0 t^{p_0} l^{s_0}, \qquad a_i(t,l) \propto t^{p_i} l^{s_i}, \qquad h(t,l) = h_o t^{p_4} l^{s_4}, \quad (10)$$

where $h_0$ and $\phi_0$ are constants, and the $p_a$'s and $s_a$'s ($a = 0, 2, 3, 4$ ) are parameters satisfying field equations. By replacing the *ansatz* (10) into Eq. (2) and using (9), we get five classes of solutions. In the following, we are interested to investigate just

the solutions that leads to a generalized Kasner relations in five dimensions. Also, we then apply the MBDT to obtain the corresponding reduced cosmology on a $4D$ hypersurface.

In order to have consistency and ignoring the trivial solutions we set $p_4 \neq 1$ and $s_4 \neq -1$. Also for simplicity, we assume $h_o = 1$ in *ansatz* (10). Hence after a little manipulation, we can obtain the following relations among the generalized Kasner parameters [4]

$$\sum_{a=0}^{4} p_a = 1, \qquad (\omega+1)p_0^2 + \sum_{m=1}^{4} p_m^2 = 1, \qquad \sum_{\mu=0}^{3} s_\mu = 1 + s_4, \tag{11}$$

$$(\omega+1)s_0^2 + \sum_{i=1}^{3} s_i^2 = (1+s_4)^2, \qquad (\omega+1)p_0 s_0 + \sum_{i=1}^{3} p_i s_i = p_4(1+s_4)\,.$$

Equation (11) lead to a few constrains, so that there are only five independent relations among the Kasner parameters, designated as the generalized Kasner relations in $5D$ BD theory.

In what follows, for the sake of brevity, we would like to present a brief review of the results of the reduced Kasner cosmology on the $4D$ hypersurface [4]: the pressure and energy density of the specified induced matter on any $4D$ hypersurface can be derived from (5). These results show that, in general, we cannot consider it as a perfect fluid. By applying (8), (10) and (11), the induced scalar potential is obtained to be either in the power law or in the logarithmic form, in which we only investigate the properties of the former. The properties of a few cosmological quantities as well as physical quantities such as the average scale factor, the mean Hubble parameter, the expansion scalar, the shear scalar and the deceleration parameter have been studied. First, these quantities have been derived in terms of the generalized Kasner parameters. Then, we find that the induced EMT satisfies the barotropic equation of state, where the equation of state parameter, $w$, is a function of the Kasner parameters. And thus, the evolution of all the quantities has been represented with respect to $w$, $\omega$ and the deceleration parameter, $q$. We then probe the quantities, in the general case, versus $q$, $t$ and $\omega$ for the stiff fluid and the radiation-dominated universe. We have shown that, for both of the fluids, there is an expanding universe commenced with a big bang, and there is a horizon for each of them. Also, we have shown that the rate of expansion slows down by time. By employing the weak energy condition, the allowed (or the well-behaved) ranges of the deceleration and the BD coupling parameters have been obtained for each of the fluids. The behavior of the quantities, in the very early universe and the very large time show that the models yield empty universes when the cosmic time tends to infinity. However, both of the models, in general, do not approach isotropy for large values of the cosmic time.

**Acknowledgements** I sincerely appreciate to Prof. Paulo Vargas Moniz for a critical reading of the letter. I am supported by the Portuguese Agency Fundação para a Ciência e Tecnologia through the fellowship SFRH/BPD/82479/2011.

## References

1. P. S. Wesson and J. Ponce de Leon, *J. Math. Phys.* **33**, 3883 (1992).
2. J. Ponce de Leon, *JCAP* **03**, 030 (2010).
3. S. M. M. Rasouli, M. Farhoudi and P. V. Moniz "Modified Brans-Dicke Theory in Arbitrary Dimensions", work in progress.
4. S. M. M. Rasouli, M. Farhoudi and H. R. Sepangi, *Class. Quantum Grav.* **28**, 155004 (2011).

# Revisiting Hartle's Model for Relativistic Rotating Stars

**Borja Reina and Raül Vera**

**Abstract** The key paper that has served as the basis for the models describing the equilibrium configuration of a rotating isolated compact body using perturbation theory in General Relativity is due to Hartle (Astrophys J 150:1005–1029, 1967). Apart from a number of very restrictive explicit assumptions on the interior, the construction of the perturbed configuration hides some seemingly important implicit assumptions. In this work we focus on the study of these implicit assumptions, and therefore, on the rigorousness of the model. In order to do that we use a relatively recent framework following a proper theoretical analysis of a completely general perturbative approach to second order around static configurations of the exterior (asymptotically flat) vacuum problem of stationary and axisymmetric bodies with arbitrary matter content.

## 1 Hartle's Model in Brief

The search for global models in General Relativity to describe rotating isolated self-gravitating bodies in equilibrium has proven to be very difficult. In particular, there are no exact solutions suitable to describe the global gravitational field of such a situation so far. In contrast, some approximate solutions are known, as the recent CMMR [1], where the perturbative approach is based on two parameters, controlling a post-Minkowskian expansion and a slow rotation respectively. But it is Hartle's model [3] which is considered the basis for the perturbation theory of rotating stars. In this model the interior of the body is a perfect fluid which satisfies a barotropic equation of state, does not have convective motions and rotates rigidly. This is matched to a stationary and axisymmetric asymptotically flat vacuum

B. Reina (✉) · R. Vera
Física Teórica e Hist. de la Ciencia, UPV/EHU, Apt. 644, Bilbao 48080,
Basque Country, Spain

A. García-Parrado et al. (eds.), *Progress in Mathematical Relativity, Gravitation and Cosmology*, Springer Proceedings in Mathematics & Statistics 60,
DOI 10.1007/978-3-642-40157-2_56, 

exterior region across a timelike hypersurface, and the whole model is assumed to have an equatorial symmetry. This analytic approach makes use of a perturbative method for slow rotation around a spherically symmetric static configuration, driven by a parameter $\Omega_H$ defined as the ratio of the angular and time components of the velocity of the fluid. The metric is taken up to order $\Omega_H^2$, and it is written as [3]

$$\begin{aligned} \mathrm{d}s^2 = &-e^{\nu(r)}\left(1+2h(r,\theta)\right)dt^2 + e^{\lambda(r)}\left(1+\frac{2m(r,\theta)}{r-2M}\right)dr^2 \\ &+r^2(1+2k(r,\theta))\left[d\theta^2+\sin^2\theta(d\varphi-\omega(r,\theta)dt)^2\right], \qquad r\in(0,\infty). \end{aligned} \tag{1}$$

The first order perturbation only appears in the crossed term $\omega$, and it accounts for the rotational dragging of inertial frames, but it does not change the shape of the surface of the star. The second order perturbation, in contrast, does affect the original spherical shape of the body, since this must be independent of the sense of rotation. The metric second order terms are $h$, $m$ and $k$. In addition to the deformation of the star, these terms give the relation between the central density of the star, which is kept unperturbed, and the excess of mass between the perturbed and the static background configuration, in analogy to the Newtonian approach [2].

Both the first and the second order perturbations are solved assuming that the coordinates chosen are (Lichnerowicz) admissible, in which the metric is of class $C^1$. Thus, boundary conditions are taken both at the origin (regularity) and at infinity (asymptotic flatness) using the same radial coordinate $r$, for which continuity of the relevant functions (and first derivatives) across the surface is taken for granted.

The existence of admissible coordinates once the matching of spacetimes is performed is known (c.f. [5]), but the a priori explicit choice of coordinates in which the metric is $C^1$ constitutes an implicit assumption that, in principle, could subtract generality to the model. To study the rigorousness of this generality we plan to study the whole problem independently of the coordinates used.

## 2 Existence of the Exterior for Slowly Rotating Interior Candidates

The problem of a slowly rotating stationary and axisymmetric isolated object can be studied within the framework described in [4], which is coordinate independent and does not assume any particular matter model for the interior. The exterior, being a stationary and axisymmetric asymptotically flat vacuum region, is fully determined by two potentials $\Omega$ and $U$, that depend on two of the Weyl coordinates $\{\rho, z\}$ spanning the surfaces orthogonal to the orbits of the Killing vector fields [8]. These potentials satisfy an elliptic system of PDEs, known as the Ernst equations [8], with boundary data consisting in the values of the potentials at infinity (asymptotic flatness) and the data on the matching hypersurface $\Sigma$ arising from the Darmois

matching conditions with the interior. These data involve the values and the normal derivatives of the potentials on $\Sigma$: $U|_\Sigma$, $\vec{n}(U)|_\Sigma$, $\Omega|_\Sigma$, $\vec{n}(\Omega)|_\Sigma$, where $\vec{n}$ is the unit normal to $\Sigma$ pointing towards the exterior. Since the elliptic problem is overdetermined, there will be some compatibility conditions to be satisfied by the boundary data to ensure the existence of a regular exterior solution [4].

The perturbative approach is built by considering the family of exterior spacetimes $(\succeq_\epsilon, g_\epsilon)$ using the Weyl gauge. The metric and hence the potentials depend on the parameter $\epsilon$, and the perturbation fields (denoted with $'_0$) correspond to their derivatives with respect to $\epsilon$ evaluated at $\epsilon = 0$. The Ernst equations are found to each order, as well as the expressions of the boundary data in terms of the interior geometry on $\Sigma_0$ (the matching hypersurface of the static configuration). Since $\Sigma_0$ is axisymmetric, its projection onto the space $\{\rho, z\}$ is a curve $\{\rho_0(\mu), z_0(\mu)\}$ where the parameter $\mu$ runs from the south (S, $\mu = 0$) to the north (N, $\mu = \pi$) pole of $\Sigma_0$. Although this framework contemplates any stationary and axisymmetric perturbation around any static and axisymmetric configuration, we need to focus only on Hartle's problem, for which, firstly, $U_0$ corresponds to the Schwarzschild geometry (with mass $M$ given by the interior spherical static configuration) and, secondly, $U_0' = \Omega_0'' = 0$ are compatible with the interior due to symmetry reasons.

The problems for $\Omega_0'$ and $U_0''$ can be written in terms of the metric $\gamma = d\rho^2 + dz^2 + \rho^2 d\phi^2$, and $\tilde{\gamma} = e^{-8U_0}\gamma$, as follows [4]

$$(i) \quad \triangle_{\tilde{\gamma}}\Omega_0' - 4\left(\mathrm{d}\Omega_0', \mathrm{d}U_0\right)_{\tilde{\gamma}} = 0, \qquad \text{given } \Omega_0'|_{\Sigma_0} = f_0,\ \vec{n}(\Omega_0')|_{\Sigma_0} = f_1,$$

$$(ii)\ \triangle_\gamma U_0'' + e^{-4U_0}\left(\mathrm{d}\Omega_0', \mathrm{d}\Omega_0'\right)_\gamma = 0, \ \text{given } U_0''|_{\Sigma_0} = g_0,\ \vec{n}(U_0'')|_{\Sigma_0} = g_1,$$

recalling $lim_{\rho^2+z^2\to\infty}\Omega_0' = 0$, $lim_{\rho^2+z^2\to\infty}U_0'' = 0$. We refer to [4] for the explicit expressions of the data $f_0(\mu), \ldots$ in terms of the interior geometry. Corresponding necessary and sufficient conditions on the first and second order boundary data $\{f_0, f_1\}, \{g_0, g_1\}$ for the existence of a solution are found to be [4]

$$\int_0^\pi \left[\Psi_y\, f_1 - f_0\, \vec{n}(\Psi_y)\right] \rho e^{-4U_0}|_{\Sigma_0}\mathrm{d}\mu = 0, \int_0^\pi \left[\psi_y\, g_1 - g_0\, \vec{n}(\psi_y) - \boldsymbol{T_1}\left(\vec{n}\right)\right] \rho|_{\Sigma_0}\mathrm{d}\mu = 0,$$

where $\psi_y$ and $\Psi_y$ are families of regular axially symmetric harmonic functions: they solve the Laplace equation for $\gamma$ and $\tilde{\gamma}$ respectively, admit a $C^1$ extension to $\Sigma_0$ and decay at infinity at least as $(\rho^2 + z^2)^{-1/2}$. The former reads explicitly $\psi_y(\rho, z) \equiv \frac{1}{\sqrt{\rho^2+(z-y)^2}}$, while the latter is more complicated. Since the above integrals depend on the parameter $y \in (z_S, z_N)$, each one gives an infinite set of conditions. The vector $T_1$ is used to transform volume integrals into surface integrals and its explicit expression is too long to be included here, but for more details about the derivation and the exact meaning of each term, see [4].

## 3 Application to Hartle's Model for the Interior

We can apply the framework introduced in the previous section to Hartle's model, but strictly *restricted to his analysis of the interior*. Now $\Sigma_0$ is spherically symmetric, and from the interior, and in terms of Hartle's coordinates, it reads, $\Sigma_0 : \{t = \tau, \varphi = \Phi, r = R_0, \theta = \pi - \mu \equiv \vartheta\}$. The boundary data for $\Omega_0'$ is computed in terms of the first order perturbation for the interior, $\omega(r,\theta)|_{\Sigma_0} = \omega(R_0, \vartheta)$. It reads [7]

$$\Omega_0'|_{\Sigma_0} = M \sin\vartheta \left[ 2(b_1 - \omega(R_0,\vartheta)) \left(3 - \frac{R_0}{M}\right) + R_0 \left(\frac{R_0}{M} - 2\right) \partial_r \omega|_{r=R_0,\theta=\vartheta} \right],$$

$$\vec{n}(\Omega_0')|_{\Sigma_0} = \sqrt{R_0(R_0 - 2M)}\, [2\cos\vartheta\,(b_1 - \omega(R_0,\vartheta)) - \sin\vartheta\,\partial_\vartheta\,(\omega(R_0,\vartheta))]\,.$$

The first order constant $b_1$ comes from the freedom in the choice of the interior timelike Killing vector [6]. Performing the change $\omega = \tilde{\Omega} - \tilde{\omega}$, where $\tilde{\Omega}$ is defined in analogy to $\Omega_H$, and expanding $\tilde{\omega}(r,\theta) = \sum_{l=1}^{\infty} \tilde{\omega}_l(r) \left(-\frac{1}{\sin\theta} \frac{dP_l}{d\theta}\right)$, restrictions for each $\tilde{\omega}_l(R_0)$ are found:

- There is a relation for $\tilde{\omega}_1$ and its derivative: $\partial_r \tilde{\omega}_1(R_0) = \frac{3}{R_0} \left[(\tilde{\Omega} - b_1) - \tilde{\omega}_1(R_0)\right]$.
- The ratios between $\tilde{\omega}_l$ and $\partial_r \tilde{\omega}_l$ on $R_0$ $\forall\ l > 1$ are negative.

But given the interior ODE for $\tilde{\omega}_l$, regularity at the origin requires those ratios to be positive for any $r$ [7]. Therefore, the only possibility compatible with the disagreement of the signs of the ratios at $r = R_0$ is that $\tilde{\omega}_l(r) = 0$ for $l > 1$. As a result $\omega$ is a function of $r$ alone, and satisfies the aforementioned constraint at $R_0$ between the function and its derivative. This result on $\tilde{\omega}$ coincides with that in [3] once the constant $b_1$ is reabsorbed in the interior after a redefinition of $\Omega_H$ (c.f. [6]).

The previous result simplifies a lot the expressions for the boundary data of the second order perturbation $U_0''$ and also for the vector $T_1$, which carries explicitly the boundary data for $\Omega_0'$, but they are still rather lengthy to be written here. However, the compatibility condition has already been evaluated and we find relations between $h$, $m$ and $k$ and their normal derivatives at $\Sigma_0$, but the latter can be removed by using the field equations for the interior. The $l = 0$ and $l = 2$ sectors do not get mixed since they are splitted by independent polynomials in $y$. The whole analysis of the second order is work in progress [7].

**Acknowledgements** BR and RV thanks support from project IT-221-07 of the Basque Government, and FIS2010-15492 from the MICINN. BR also holds a PhD fellowship of the Basque Government.

## References

1. Cabezas, J., Martin-Martin, J., Molina, A., Ruiz, E.: An Approximate global solution of Einstein's equations for a finite body. Gen.Rel.Grav. **39**, 707–736 (2007)
2. Chandrasekhar, S.: The equilibrium of distorted polytropes I. MNRAS **93**, 390–406 (1933)
3. Hartle, J.B.: Slowly rotating relativistic stars. 1. Astrophys.J. **150**, 1005–1029 (1967)
4. MacCallum, M.A., Mars, M., Vera, R.: Stationary axisymmetric exteriors for perturbations of isolated bodies in general relativity, to second order. Phys.Rev. **D75**, 024,017 (2007)
5. Mars, M., Senovilla, J.M.M.: Geometry of general hypersurfaces in spacetime: junction conditions. Classical and Quantum Gravity **10**(9), 1865–1897 (1993)
6. Mars, M., Senovilla, J.M.M.: On the construction of global models describing rotating bodies: Uniqueness of the exterior gravitational field. Mod.Phys.Lett. **A13**, 1509–1519 (1998)
7. Reina, B., Vera, R.: In preparation
8. Stephani, H., Krämer, D., MacCallum, M., Hoenselaers, C., Herlt, E.: Exact solutions of Einstein's field equations; 2nd ed. Cambridge Univ. Press, Cambridge (2003)

# Is General Relativity a $v/c \to 0$ Limit of a Finsler Geometry?

**Martin Rivas**

**Abstract** Gravity is understood as a geometrization of spacetime. But spacetime is also the manifold of the boundary values of the spinless point particle in a variational approach. The manifold of the boundary variables for any mechanical system, instead of being a Riemannian space it is a Finsler metric space such that the variational formalism can always be interpreted as a geodesic problem on this manifold. This manifold is just the flat Minkowski spacetime for the free relativistic point particle. Any interaction modifies its flat Finsler metric. In the spirit of unification of all forces, gravity cannot produce, in principle, a different and simpler geometrization than any other interaction. This implies that the basic assumption that what gravity produces is a Riemannian metric instead of a Finslerian one is a strong restriction so that general relativity can be considered as a low velocity limit of a more general gravitational theory.

## 1 The Geodesic Interpretation of the Variational Formalism

Let us consider any mechanical system of $n$ degrees of freedom described by a Lagrangian, $L(t, q_i, q_i^{(1)})$. The variational approach means that the path followed by the system makes stationary the action functional

$$\mathscr{A}[q(t)] = \int_{t_1}^{t_2} L(t, q_i, q_i^{(1)}) dt,$$

between the initial state $x_1 \equiv (t_1, q_i(t_1))$ and final state $x_2 \equiv (t_2, q_i(t_2))$. If the evolution is described in parametric form $t(\tau)$, $q_i(\tau)$ in terms of some arbitrary parameter $\tau$, then $q_i^{(1)}(\tau) = \dot{q}_i/\dot{t}$, the variational approach will be written as [1]

M. Rivas (✉)
Theoretical Physics Department, University of the Basque Country, Bilbao, Spain
e-mail: martin.rivas@ehu.es

A. García-Parrado et al. (eds.), *Progress in Mathematical Relativity, Gravitation and Cosmology*, Springer Proceedings in Mathematics & Statistics 60,
DOI 10.1007/978-3-642-40157-2_57, © Springer-Verlag Berlin Heidelberg 2014

$$\int_{\tau_1}^{\tau_2} L(t, q_i, \dot{q}_i/\dot{t})\dot{t}\, d\tau = \int_{\tau_1}^{\tau_2} \tilde{L}(x, \dot{x}) d\tau, \quad \tilde{L} = L\dot{t},$$

$\tilde{L}$ is independent of $\tau$ and is a homogeneous function of first degree of the derivatives $\dot{x}$. $\tilde{L}^2$ is a positive definite homogeneous function of second degree of $\dot{x}$. Therefore $\tilde{L}^2 = g_{ij}(x, \dot{x})\dot{x}^i \dot{x}^j$, and the definite positive metric $g_{ij}$ are computed as [2, 3]

$$g_{ij}(x, \dot{x}) = \frac{1}{2} \frac{\partial^2 \tilde{L}^2}{\partial \dot{x}^i \partial \dot{x}^j} = g_{ji}. \tag{1}$$

The variational formalism looks now

$$\int_{\tau_1}^{\tau_2} \tilde{L}(x, \dot{x}) d\tau = \int_{\tau_1}^{\tau_2} \sqrt{\tilde{L}^2(x, \dot{x})} d\tau = \int_{\tau_1}^{\tau_2} \sqrt{g_{ij}(x, \dot{x})\dot{x}^i \dot{x}^j}\, d\tau = \int_{x_1}^{x_2} ds,$$

where $ds$ is the arc length on the $X$ manifold w.r.t. the metric $g_{ij}$. The variational statement has been transformed into a geodesic problem with a Finsler metric.

The relativistic point particle of mass $m$ has a kinematical space spanned by time $t$ and the position of the point $\mathbf{r}$, so that the free Lagrangian $\tilde{L}_0 = \pm mc\sqrt{c^2\dot{t}^2 - \dot{\mathbf{r}}^2}$, is a homogeneous function of first degree of the derivatives $\dot{t}$ and $\dot{\mathbf{r}}$.

## 2 Examples of Finsler Spaces

In the case of a uniform gravitational field $\mathbf{g}$, the dynamical equations $d\mathbf{p}/dt = m\mathbf{g}$, come from the Lagrangian

$$\tilde{L}_g = \tilde{L}_0 + m\mathbf{g} \cdot \mathbf{r}\dot{t}. \tag{2}$$

It corresponds from (1) to an evolution in a spacetime with the Finsler metric:

$$g_{00} = m^2c^2 + m^2(\mathbf{g} \cdot \mathbf{r})^2/c^2 - \frac{m^2 c(\mathbf{g} \cdot \mathbf{r})}{(c^2 - u^2)^{3/2}}(2c^2 - 3u^2),$$

$$g_{11} = -m^2c^2 + \frac{m^2 c(\mathbf{g} \cdot \mathbf{r})}{(c^2 - u^2)^{3/2}}(c^2 - u_y^2 - u_z^2), \quad g_{22} = -m^2c^2 + \frac{m^2 c(\mathbf{g} \cdot \mathbf{r})}{(c^2 - u^2)^{3/2}}(c^2 - u_x^2 - u_z^2),$$

$$g_{33} = -m^2c^2 + \frac{m^2 c(\mathbf{g} \cdot \mathbf{r})}{(c^2 - u^2)^{3/2}}(c^2 - u_x^2 - u_y^2),$$

$$g_{01} = -\frac{m^2 u^2(\mathbf{g} \cdot \mathbf{r})}{(c^2 - u^2)^{3/2}} u_x, \quad g_{02} = -\frac{m^2 u^2(\mathbf{g} \cdot \mathbf{r})}{(c^2 - u^2)^{3/2}} u_y, \quad g_{03} = -\frac{m^2 u^2(\mathbf{g} \cdot \mathbf{r})}{(c^2 - u^2)^{3/2}} u_z,$$

$$g_{12} = \frac{m^2 c(\mathbf{g} \cdot \mathbf{r})}{(c^2 - u^2)^{3/2}} u_x u_y, \quad g_{23} = \frac{m^2 c(\mathbf{g} \cdot \mathbf{r})}{(c^2 - u^2)^{3/2}} u_y u_z, \quad g_{13} = \frac{m^2 c(\mathbf{g} \cdot \mathbf{r})}{(c^2 - u^2)^{3/2}} u_x u_z.$$

If the velocity is negligible with respect to $c$, the nonvanishing coefficients are

$$g_{00} = m^2c^2\left(1 - \frac{\mathbf{g}\cdot\mathbf{r}}{c^2}\right)^2, \quad g_{ii} = -m^2c^2\left(1 - \frac{\mathbf{g}\cdot\mathbf{r}}{c^2}\right), \quad i = 1,2,3,$$

where $g_{00}$ is the same as the component of the Rindler metric.

The dynamics of a point particle in a Newtonian potential and its Lagrangian

$$\frac{d\mathbf{p}}{dt} = -\frac{GmM}{r^3}\mathbf{r}, \quad \tilde{L}_N = \tilde{L}_0 + \frac{GmM}{cr}c\dot{t}.$$

and from (1) the metric coefficients are

$$g_{00} = m^2c^2 + \frac{G^2m^2M^2}{c^2r^2} - \frac{Gm^2Mc}{r(c^2-u^2)^{3/2}}(2c^2 - 3u^2),$$

$$g_{11} = -m^2c^2 + \frac{Gm^2Mc^3}{r(c^2-u^2)^{3/2}} - \frac{Gm^2Mc(u_y^2+u_z^2)}{r(c^2-u^2)^{3/2}},$$

$$g_{22} = -m^2c^2 + \frac{Gm^2Mc^3}{r(c^2-u^2)^{3/2}} - \frac{Gm^2Mc(u_x^2+u_z^2)}{r(c^2-u^2)^{3/2}},$$

$$g_{33} = -m^2c^2 + \frac{Gm^2Mc^3}{r(c^2-u^2)^{3/2}} - \frac{Gm^2Mc(u_x^2+u_y^2)}{r(c^2-u^2)^{3/2}},$$

$$g_{01} = -\frac{Gm^2Mu^2u_x}{r(c^2-u^2)^{3/2}}, \quad g_{02} = -\frac{Gm^2Mu^2u_y}{r(c^2-u^2)^{3/2}}, \quad g_{03} = -\frac{Gm^2Mu^2u_z}{r(c^2-u^2)^{3/2}},$$

$$g_{12} = \frac{Gm^2Mcu_xu_y}{r(c^2-u^2)^{3/2}}, \quad g_{23} = \frac{Gm^2Mcu_yu_z}{r(c^2-u^2)^{3/2}}, \quad g_{31} = \frac{Gm^2Mcu_zu_x}{r(c^2-u^2)^{3/2}},$$

It is a Finsler metric, which in the case of low velocities it becomes

$$g_{00} = m^2c^2\left(1 - \frac{GM}{c^2r}\right)^2, \quad g_{ii} = -m^2c^2\left(1 - \frac{GM}{c^2r}\right), \quad i = 1,2,3.$$

This corresponds to the static and spherically symmetric Riemannian metric

$$\left(1 - \frac{GM}{c^2r}\right)^2 c^2dt^2 - \left(1 - \frac{GM}{c^2r}\right)(dr^2 + r^2d\Omega^2).$$

This metric is not a vacuum solution of Einstein's equations, so that it cannot be transformed into the Schwarzschild metric in isotropic coordinates.

In all the examples, the free Lagrangian $\tilde{L}_0$ of the spinless particle, has been transformed by the interactions in the Finsler metric

$$\tilde{L}_0^2 = m^2c^2\eta_{\mu\nu}\dot{x}^\mu\dot{x}^\nu \quad \Rightarrow \quad \tilde{L}^2 = g_{\mu\nu}(x,\dot{x})\dot{x}^\mu\dot{x}^\nu. \tag{3}$$

The low velocity limit produces a Riemannian approximation which does not give rise to the usual dynamical equations.

However, General Relativity states that gravity modifies the metric of spacetime producing a new (pseudo-)Riemannian metric $g_{\mu\nu}(x)$, which is related through Einstein's equations to the energy momentum distribution $T^{\mu\nu}$. The motion of a point particle is a geodesic on spacetime, and therefore can be treated as a Lagrangian dynamical problem with a Lagrangian

$$\tilde{L}_g^2 = g_{\mu\nu}(x)\dot{x}^\mu \dot{x}^\nu. \tag{4}$$

In the spirit of unification of all interactions, one is tempted to extend the formulation of gravity (4) to (3) by allowing the metric to be also a function of the derivatives. Otherwise, to assume only a Riemannian metric is to consider that gravity produces a different geometrization than any other interaction. In a region of a uniform gravitational field, the Lagrangian dynamics is equivalent to a geodesic problem where the metric is necessarily a Finsler metric. The elimination of the velocities in the metric coefficients could be interpreted as a low velocity limit of a more general gravitational theory.

## 3 Conclusions

The manifold of the boundary variables of any Lagrangian system is a Finsler space. Any variational approach is equivalent to a geodesic statement on this manifold. The metric, is a function of the $x \in X$ and $\dot{x}$, depends on the interaction, and to assume that gravitation only produces a modification of the metric which is only a function of the $x$, is a restriction of a more general formalism.

In all examples we have seen the Finsler structure of spacetime under different gravitational interactions, although the metrics are obtained by pure Lagrangian statements and not by any field equations. The new metrics are true Finsler metrics which in the case of $v/c \to 0$, resemble the metrics obtained in a general relativity formalism but they are not strict vacuum solutions of Einstein's equations. This could suggest some relationship between general relativity and the low velocity limit of the corresponding Finsler structure of the gravitational problems.

**Acknowledgements** This work has been partially supported by Universidad del País Vasco/Euskal Herriko Unibertsitatea grant 9/UPV00172.310-14456/2002.

## References

1. Rivas M *Kinematical theory of spinning particles*, (Dordrecht: Kluwer), Chapter 6 2001.
2. Asanov GS *Finsler geometry, Relativity and Gauge theories*, (Reidel Pub. Co, Dordrecht) 1985.
3. Rund H *The Hamilton-Jacobi theory in the calculus of variations*, (Krieger Pub. Co., N.Y) 1973.

# Phenomenology of Unified Dark Matter Models with Fast Transition

**Alberto Rozas-Fernández, Marco Bruni, and Ruth Lazkoz**

**Abstract** A fast transition between a standard matter-like era and a late $\Lambda$CDM-like epoch generated by a single Unified Dark Matter component can explain the observed acceleration of the Universe. UDM models with a fast transition should be clearly distinguishable from $\Lambda$CDM (and alternatives) through observations. Here we focus on a particularly simple model and analyse its viability by studying features of the background model and properties of the adiabatic UDM perturbations.

## 1 Introduction

A possible framework explaining the acceleration of the Universe is provided by models of Unified Dark Matter (UDM) where a single matter component is supposed to source the acceleration and structure formation at the same time (see e.g. [1], for a recent review).

UDM models with fast transition were introduced in [2] and show interesting features [2, 3]. The single UDM component must accelerate the Universe and provide acceptable perturbations which evolve in a scale-dependent fashion. In view of testing models against observations this may become computationally expensive. It is therefore essential to consider simple phenomenological models of the fast-transition paradigm for which as much theoretical progress as possible can be made

A. Rozas-Fernández (✉) · M. Bruni
ICG, University of Portsmouth, UK
e-mail: alberto.rozas@port.ac.uk; marco.bruni@port.ac.uk

R. Lazkoz
Dpto. de Física Teórica, Universidad del País Vasco UPV/EHU, Apdo. 644,
E-48080 Bilbao, Spain
e-mail: ruth.lazkoz@ehu.es

A. García-Parrado et al. (eds.), *Progress in Mathematical Relativity, Gravitation and Cosmology*, Springer Proceedings in Mathematics & Statistics 60,
DOI 10.1007/978-3-642-40157-2_58, 

from analytical calculations. This then can be used to increase the efficiency of numerical codes in dealing with these models.

It turns out that the best receipt to proceed analytically is to prescribe the evolution of the energy density of UDM.

## 2 Generalities of UDM Models

### 2.1 The Background and the Perturbations

We assume a flat Friedmann–Lemaître–Robertson–Walker (FLRW) cosmology where $w = p/\rho$ characterises the background of our UDM model.

We assume adiabatic perturbations. The squared Jeans wave number plays a crucial role in determining the viability of a UDM model, because of its effect on perturbations, which is then revealed in observables such as the CMB and matter power spectrum [2, 4]. The explicit form of the Jeans wave number is [2]

$$k_{\mathrm{J}}^2 = \frac{3}{2}\rho a^2 \frac{(1+w)}{c_{\mathrm{s}}^2}\left|\frac{1}{2}(c_{\mathrm{s}}^2 - w) - \rho\frac{dc_{\mathrm{s}}^2}{d\rho} + \frac{3(c_{\mathrm{s}}^2 - w)^2 - 2(c_{\mathrm{s}}^2 - w)}{6(1+w)} + \frac{1}{3}\right|, \quad (1)$$

where $c_{\mathrm{s}}^2$ is the effective speed of sound. So if we want an analytic expression for $k_{\mathrm{J}}^2$ in order to obtain some insight on the behaviour of perturbations in a given UDM model, we need to be able to obtain analytic expressions for $\rho$, $p$, $w$ and $c_{\mathrm{s}}^2$.

## 3 Prescribing $\rho(a)$

Given a function (at least of class $C^3$) $\rho = \rho(a)$, we can obtain the following expressions for the quantities that enter into $k_{\mathrm{J}}^2$ (1):

$$w = -\frac{a}{3}\frac{\rho'}{\rho} - 1, \quad (2)$$

$$c_{\mathrm{s}}^2 = -\frac{a}{3}\frac{\rho''}{\rho'} - \frac{4}{3}, \quad (3)$$

$$\frac{dc_{\mathrm{s}}^2}{d\rho} = -\frac{1}{3\rho'^2}\left[a\rho''' + \rho'' - a\frac{\rho''^2}{\rho'}\right]. \quad (4)$$

where a prime indicates derivative with respect to $a$.

# 4 Phenomenological UDM Models with Fast Transition

## 4.1 A Simple Model for the Background

We introduce an "affine" model [4]:

$$\rho = \rho_{\rm t}\left(\frac{a_{\rm t}}{a}\right)^3 + \left[\rho_\Lambda + (\rho_{\rm t} - \rho_\Lambda)\left(\frac{a_{\rm t}}{a}\right)^{3(1+\alpha)} - \rho_{\rm t}\left(\frac{a_{\rm t}}{a}\right)^3\right] H_t(a - a_{\rm t})\ . \quad (5)$$

$H_{\rm t}$ is compatible with having $c_{\rm s}^2 > 0$:

$$H_{\rm t}(a - a_{\rm t}) = \frac{1}{2} + \frac{1}{\pi}\arctan(\beta(a - a_{\rm t})), \quad (6)$$

where the parameter $\beta$ represents the rapidity of the transition. For $\alpha = 0$, Eq. (5) reduces to

$$\rho = \rho_{\rm t}\left(\frac{a_{\rm t}}{a}\right)^3 + \rho_\Lambda\left[1 - \left(\frac{a_{\rm t}}{a}\right)^3\right] H_t(a - a_{\rm t}), \quad (7)$$

representing a sudden transition to $\Lambda$CDM. In the following, we shall restrict our attention to this sub-class of models. Here $\rho_{\rm t}$ is the energy scale at the transition, $\rho_\Lambda$ is the effective cosmological constant and the redshift for the transition $z_{\rm t} = a_{\rm t}^{-1} - 1$.

# 5 The Jeans Scale and the Gravitational Potential

## 5.1 The Jeans Wave Number

We require $k^2\ell^2 k_{\rm J}^2$ for all scales of cosmological interest to which the linear perturbation theory applies. A large $k_{\rm J}^2$ can be obtained not only when $c_{\rm s}^2 \to 0$, but when Eq. (1) is dominated by the $\rho\, dc_{\rm s}^2/d\rho$ term.

Thus, viable adiabatic UDM models can be constructed which do not require $c_{\rm s}^2\ell^2 1$ at all times if the speed of sound goes through a rapid change, a fast transition period during which $k_{\rm J}^2$ can remain large, in the sense that $k^2\ell^2 k_{\rm J}^2$.

In general $k_{\rm J}^2$ becomes larger, with a vanishingly small Jeans length (its inverse) before and after the transition. Although it becomes vanishingly small for extremely short times, the effects caused by its vanishing are negligible (see the behaviour of the gravitational potential $\Phi$ below).

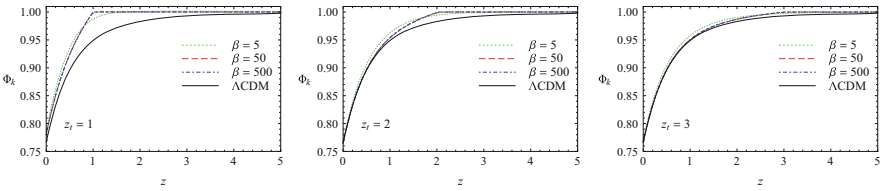


**Fig. 1** Illustrative plots of the gravitational potential $\Phi(\mathbf{k}; z)$ as a function of the redshift $z$ for $\Lambda$CDM and for our UDM model for $k = 0.2\ h\ \mathrm{Mpc}^{-1}$ and different values of $\beta$ and $z_\mathrm{t}$. The *black solid line* corresponds to the gravitational potential in the $\Lambda$CDM model with $\Omega_{\Lambda,0} = 0.72$

## 5.2 The Gravitational Potential

The equation that governs the behaviour of the gravitational potential $\Phi$ is [5]:

$$\frac{d^2\Phi(\mathbf{k},a)}{da^2} + \left(\frac{1}{\mathscr{H}}\frac{d\mathscr{H}}{da} + \frac{4}{a} + 3\frac{c_\mathrm{s}^2}{a}\right)\frac{d\Phi(\mathbf{k},a)}{da} + \left[\frac{2}{a\mathscr{H}}\frac{d\mathscr{H}}{da} + \frac{1}{a^2}(1+3c_\mathrm{s}^2) + \frac{c_\mathrm{s}^2k^2}{a^2\mathscr{H}^2}\right]\Phi(\mathbf{k},a) = 0, \quad (8)$$

where $\mathscr{H} = \frac{da}{d\eta}/a$ is the conformal time Hubble function. Also, $\mathscr{H} = aH$.

From Fig. 1 we see that for an early enough fast transition with $\beta > 500$ and $z_\mathrm{t} > 2$ our UDM model should be compatible with observations. On the other hand, a study of the matter and CMB power spectra is needed to study the viability of models with $10 \lesssim \beta < 500$, and those with $\beta > 500$ and $z_\mathrm{t} < 2$.

**Acknowledgements** MB is supported by the STFC (grant no. ST/H002774/1), RL by the Spanish Ministry of Economy and Competitiveness through research projects FIS2010-15492 and Consolider EPI CSD2010-00064, the University of the Basque Country UPV/EHU under program UFI 11/55 and also by the ETORKOSMO special research action. ARF is supported by the 'Fundación Ramón Areces'.

## References

1. D. Bertacca, N. Bartolo and S. Matarrese, Adv. Astron. **2010** 904379 (2010) [arXiv:1008.0614 [astro-ph.CO]].
2. O. F. Piattella, D. Bertacca, M. Bruni and D. Pietrobon, JCAP **1001** 014 (2010) [arXiv:0911.2664 [astro-ph.CO]].
3. D. Bertacca, M. Bruni, O. F. Piattella and D. Pietrobon, JCAP **1102** 018 (2011) [arXiv:1011.6669 [astro-ph.CO]].
4. D. Pietrobon, A. Balbi, M. Bruni and C. Quercellini, Phys. Rev. D **78** 083510 (2008) [arXiv:0807.5077 [astro-ph]].
5. D. Bertacca and N. Bartolo, JCAP **0711** 026 (2007) [arXiv:0707.4247 [astro-ph]].

# Locating Objects Away from Earth Surface: Positioning Accuracy

**Diego Sáez and Neus Puchades**

**Abstract** The motion of the Galileo and GPS satellite constellations is simulated in Schwarzschild space-time, whereas photons travel in Minkowski space-time. This is a good enough approach to deal with the main goal of this paper: the study of positioning accuracy in the framework of the so-called relativistic positioning. Our study is based on numerical 4D simulations. In this meeting, the contribution of J.A. Morales-Lladosa contains some basic ideas which have been important to perform our numerical calculations. For four chosen emitters (satellites) of a certain constellation, many receivers located at different distances from Earth surface and in distinct directions are considered. Thus, we verify that, in some space-time regions, the Jacobian of the transformation giving the emission coordinate in terms of the inertial ones vanishes. For receivers placed close to these regions, positioning errors due to uncertainties in the satellite trajectories are too great. Our results suggest that, given a receiver, the 4-tuple of satellites used for location must be carefully chosen to minimize positioning errors (large enough Jacobian values).

## 1 Positioning Accuracy: Basic Ideas, Calculations and Results

In an ideal relativistic positioning system (RPS), there is a well defined inertial reference, in which, the equations of the satellite world lines are known; however, in a realistic RPS, there are uncertainties in the satellite world lines which lead to positioning errors. Some aspects of the error analysis are numerically considered here. In order to define our ideal RPS, it is assumed that the Earth gravitational

D. Sáez (✉) · N. Puchades
Departamento de Astronomía y Astrofísica, Universidad de Valencia, 46100 Burjassot, Valencia, Spain
e-mail: Diego.Saez@uv.es; Neus.Puchades@uv.es

A. García-Parrado et al. (eds.), *Progress in Mathematical Relativity, Gravitation and Cosmology*, Springer Proceedings in Mathematics & Statistics 60,
DOI 10.1007/978-3-642-40157-2_59, © Springer-Verlag Berlin Heidelberg 2014

field is well described by the Schwarzschild space-time, which asymptotically tends to a Minkowski geometry allowing us to define the inertial references of the RPS. In this spherically symmetric space-time, it is assumed that free satellites are moving along circular orbits with a well known angular velocity (other orbits exist). In reference [1], the equations of the satellite world lines were given to first order in the small parameter $GM_\oplus/R$, where $G$, $M_\oplus$, and $R$ are the gravitational constant, the Earth mass, and the orbit radius, respectively. The explicit form of these equations –unnecessary in this paper– was given in terms of asymptotic inertial coordinates. In these coordinates the metric is diagonal, and its non vanishing components are $\eta_{11} = \eta_{22} = \eta_{33} = 1$, and $\eta_{44} = -c^2$. Photons are moved in this asymptotic Minkowski space-time by using the same coordinates (corrections to first order in $GM_\oplus/R$ are negligible in our calculations). The effects of the gravitational field on the clocks attached to the satellites is taken into account in our ideal RPS. Units are taken in such a way that the speed of light is $c = 1$. Times are given in hours.

In any RPS, there are four satellites broadcasting their proper times by mean of codified signals. The inertial coordinates of an user, $x^\alpha$, are related to the emission ones, which are the four proper times, $\tau^A$, simultaneously received by the user at time $x^4$. Index $A$ labels the four satellites. The equations of the satellite world lines are known. Their generic form is $y^\alpha = x^\alpha_A(\tau^A)$. These equations give the satellite inertial coordinates $x^\alpha_A$ in terms of the proper times $\tau^A$ (see [1]). A well known formula derived in [2] and discussed in [3, 4] gives the inertial coordinates (user position) in terms of the emission ones. Moreover, given the inertial coordinates of an user, the emission ones may be calculated by solving the system

$$\eta_{\alpha\beta}[x^\alpha - x^\alpha_A(\tau^A)][x^\beta - x^\beta_A(\tau^A)] = 0. \tag{1}$$

These four equation may be numerically solved by using the Newton-Rhapson method (see [1, 5]) to get the unknowns $\tau^A$. Let us now suppose a real RPS. The equations of the satellite world lines may be written as follows: $y^\alpha = x^\alpha_A(\tau^A) + \xi^\alpha_A(\tau^A)$, where $\xi^\alpha_A$ are deviations with respect to the world lines of the ideal RPS. The subsequent discussion is independent from the origin of the deviations. In the real RPS, the following equations must be solved to find the emission coordinates from the inertial ones:

$$\eta_{\alpha\beta}[x^\alpha - x^\alpha_A(\tau^A) - \xi^\alpha_A][x^\beta - x^\beta_A(\tau^A) - \xi^\beta_A] = 0. \tag{2}$$

In conclusion, for ideal orbits in Schwarzschild space-time as well as for real ones with $\xi^\alpha_A$ deviations, we may find the inertial (emission) coordinates from the emission (inertial) ones. Therefore, in order to study the positioning errors we may proceeds as follows. First of all, we take inertial coordinates $x^\alpha$ and, then, we use the Newton-Raphson method to solve Eqs. (1) and (2). In the first case, the resulting emission coordinates are $\tau^A$, whereas in the second case we get new emission coordinates $\tau^A + \Delta\tau^A$. Let us now use the analytical formula giving the

inertial coordinates from the emission ones (see [2]), to find the inertial coordinates in the ideal case (circular orbits in Schwarzschild geometry), and also in the real one (with deviations $\xi_A^\alpha$). In the ideal case, this process must recover the chosen initial $x^\alpha$ coordinates with small errors which are strictly numerical, since we use multiple precision codes these errors have been proved to be fully negligible (accuracy test for our codes). In the real case –with deviations $\xi_A^\alpha$– the resulting inertial coordinates are $x^\alpha + \Delta x^\alpha$. Quantities $\Delta x^\alpha$ measure the positioning errors due to the satellite world line uncertainties $\xi_A^\alpha$. A good estimator of these errors is the quantity $\Delta_d = [(\Delta x^1)^2 + (\Delta x^2)^2 + (\Delta x^3)^2]^{1/2}$. It is worthwhile to notice that quantities $\xi_A^\alpha(\tau^A)$ may be assumed to be constant in the small intervals $\Delta\tau^A$ defined above, in which, the real and ideal satellite world lines do not have enough time to undergo significant deviations.

Positioning errors strongly depend on the Jacobian $J$ of the transformation giving the emission coordinates in terms of the inertial ones. These errors tend to infinity as $J$ tends to zero and, consequently, they are expected to be uncomfortably large close to Minkowski events (users) with vanishing $J$. This is verified in this paper, whereas a more detailed study of positioning errors –related to the so-called dilution problem [6]– will be presented elsewhere. It has been shown that $J$ vanishes at a certain user position (see [3,4] and references cited therein) if and only if the user sees the four satellites –at emission times– along generatrices of a certain cone. Equivalently, let us consider the cone generated by the lines of sight of satellites $A = 1, 2, 3$, and the angle $\alpha_1$ ($\alpha_4$) formed by the cone axis and any generatrix (and the line of sight of the satellite $A = 4$). Then, the Jacobian vanishes if and only if $\alpha_1 = \alpha_4$.

In the technical literature about RPS [2, 3], the reader may find the definition of functions $\chi^2$ and $\Delta$, which may be calculated at any user position by using: its emission coordinates, and the world line equations of the four satellites used for relativistic positioning. Moreover, in the same articles, it is proved that the Jacobian $J$ vanishes if and only if function $\Delta$ takes on the zero value. This fact may be used to find users with $J \simeq 0$, which have too small positioning accuracy. In order to get these users, sections $x^4 = constant$ of the Minkowski space-time – surrounding a point $E$ located on Earth surface– are systematically covered by points $(x^1, x^2, x^3)$, which are placed along a large number of segments starting from $E$ and having appropriate directions; thus, we define users with inertial coordinates $(x^1, x^2, x^3, x^4)$. The corresponding emission coordinates $\tau^A$ may be found by solving Eq. (1) and, then, functions $\chi^2$ and $\Delta$ may be evaluated. In some segments there are pairs of neighbouring points where the continuous function $\Delta$ has different signs. So, function $\Delta$ and, consequently, the Jacobian $J$ must vanish between these pairs of points. Representations of the regions of vanishing Jacobian will be shown elsewhere. Here, a point $P$, with vanishing $J$ and located in a certain direction on section $x^4 = 17$, has been chosen. Many points have been placed –in the same section and direction– along a segment of length $\Delta L = 200\ Km$, which has the point $P$ at the centre. Finally, the estimator $\Delta_d$ of positioning errors and the angle $\alpha_1 - \alpha_4$ have been calculated in each of the points placed on the segment. Results are shown in Fig. 1. From the bottom panel it follows that $J$ vanishes at a point, $P$, where $\alpha_1 - \alpha_4 = 0$, and in the top panels it is shown that positioning

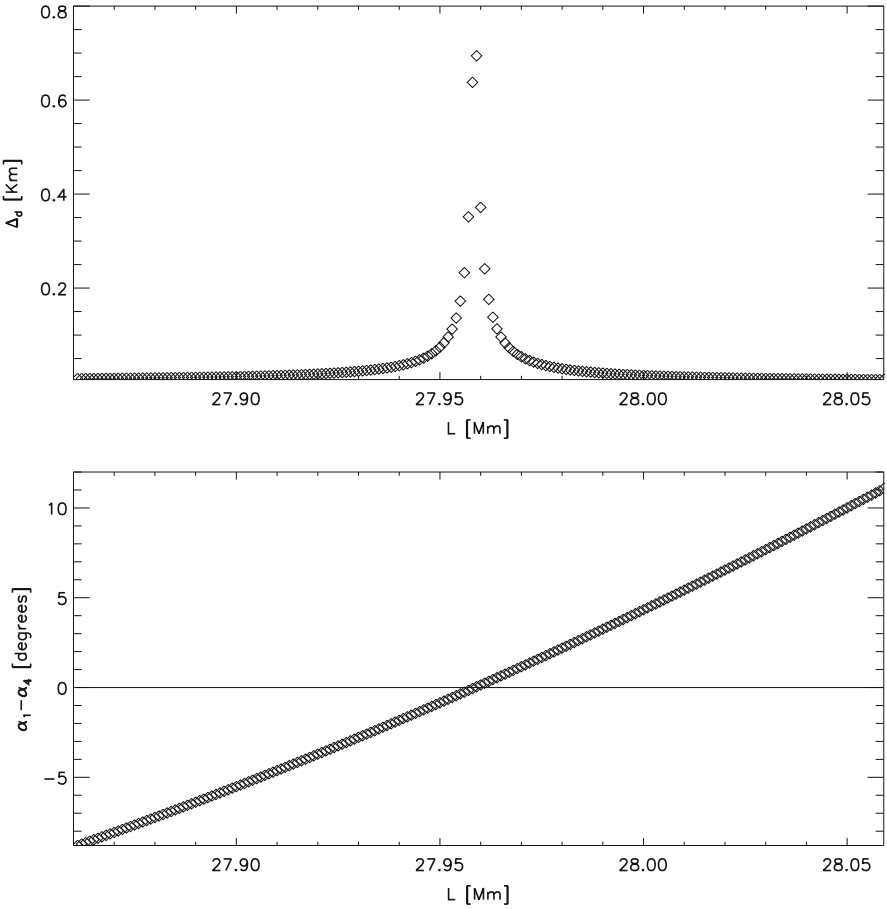


**Fig. 1** *Top*: Quantity $\Delta_d$ v.s. the distance $L$ to point $E$ in a segment of length $\Delta L = 200\ Km$. *Bottom*: Angle $\alpha_1 - \alpha_4$ in terms of $L$

errors are very big close to $P$. In a certain zone around $P$, these errors become too large.

**Acknowledgements** This work has been supported by the Spanish Ministries of *Ciencia e Innovación* and *Economía y Competitividad*, MICINN-FEDER projects FIS2009-07705 and FIS2012-33582.

## References

1. Puchades, N., Sáez, D.: Astrophys. Space Sci., **341**, 631 (2012)
2. Coll, B., Ferrando, J. J., Morales-Lladosa, J. A.: Class. Quantum Grav **27**, 065013 (2010)

3. Coll, B., Ferrando, J. J., Morales-Lladosa, J. A.: Phys. Rev. D **86**, 084036 (2012)
4. Coll, B., Ferrando, J. J., Morales-Lladosa, J. A.: *Relativistic positioning systems in flat spacetime: the location problem*. (In these proceedings).
5. Puchades, N., Sáez, D.: J. Phys. Conf. Ser., **314**, 012107 (2011)
6. Langley, R. B.: GPS World, **10**, 52 (1999)

# SN and BAO Constraints on (New) Polynomial Dark Energy Parametrizations

**Irene Sendra and Ruth Lazkoz**

**Abstract** In this work we introduce two new polynomial parametrizations of dark energy equation of state, $w$, and explore their correlation properties. The parameters to fit are the equation of state values at $z = 0$ and $z = 0.5$, which have naturally low correlation and have already been shown to improve the popular Chevallier–Polarski–Linder (CPL) parametrization. We test our models with Type Ia Supernovae (SNeIa) and Baryon Acoustic Oscillations (BAO), in the form of both current and synthetic data. On one hand, we investigate the degree of improvement in dark energy constraints that can be achieved with future data. On the other hand, according to the Bayesian deviance information criterion (DIC), which penalizes large errors and correlations, we show that our models perform better than the CPL re-parametrization proposed by Wang (in terms of $z = 0$ and $z = 0.5$). This is due to the combination of a lower correlation and smaller relative errors. The same holds for a frequentist perspective: our Figure-of-Merit is larger for our parametrizations.

## 1 Dark Energy EoS Parametrizations

The two new polynomial parametrizations we propose are inspired by the CPL parametrization, $w(z) = w_0 + w_a z/(1+z)$, and represent a small departure from the $\Lambda$CDM case ($w = -1$).

- **Conventional Polynomial parametrization**

The first parametrization we present is expressed in terms of conventional polynomial and has the form: $w(z) = -1 + c_1\,(1 + z/(1+z)) + c_2\,(1 + z/(1+z))^2$. However, it is desirable to fit parameters which are physically transparent and

I. Sendra (✉) · R. Lazkoz
Fisika Teorikoa, Zientzia eta Teknologia Fakultatea, Euskal Herriko Unibertsitatea UPV/EHU, 644 Posta Kutxatila, 48080 Bilbao, Spain
e-mail: irene.sendra@ehu.es; ruth.lazkoz@ehu.es

A. García-Parrado et al. (eds.), *Progress in Mathematical Relativity, Gravitation and Cosmology*, Springer Proceedings in Mathematics & Statistics 60,
DOI 10.1007/978-3-642-40157-2_60, 

lightly correlated. In [7], a new parametrization for the dark energy EoS in terms of its value at present, $w_0$, and at redshift $z = 0.5$, $w_{0.5}$, was given: $w(z) = 3w_{0.5} - 2w_0 + 3(w_0 - w_{0.5})/(1+z)$ (Wang's parametrization). It is shown that this reformulation of the classic CPL minorates the correlation between the parameters. Thus, we follow the same procedure and we move on to a scenario in which $w_0$ and $w_{0.5}$ are the parameters subject to estimation:

$$w(z) = (4\left(1-4z^2\right)w_0 + 9z\,(1+2z)\,w_{0.5} + z(1-2z))/(4(1+z)^2). \tag{1}$$

- **Chebychev polynomial parametrization**

In the second parametrization we propose, we want to make a further generalisation by considering a bit more involved functions. In this case we make use of Chebychev polynomials, which have a significant role in most areas of numerical analysis, as well as in other areas of Mathematics. Specifically, we propose $w(z) = -1 + c_1 T_1(1 + z/(1+z)) + c_2 T_2(1 + z/(1+z))$, with $T_n$ being the first kind Chebyshev polynomial of degree $n$. As before, we switch to the less correlated set of parameters $\{w_0, w_{0.5}\}$, having:

$$w(z) = (w_0(11 - z(38z+3)) + z(9w_{0.5}(5z+3) - 4z + 2))/(11(z+1)^2). \tag{2}$$

## 2 Observational Data and Results

We test these new models with low redshift astronomical probes: Type Ia Supernovae and Baryon Acoustic Oscillations (BAO). However, for this analysis we consider not only currently available datasets, but also mock data of forthcoming surveys. Specifically, we have used the BAO data presented in [5] and the largest SNeIa data sample up to date, the Union2 [2]. At the same time and making use of the iCosmo software, we have carried out simulations of measurements of the radial and transversal BAO scales similar to those expected in a BAO high precision spectroscopic redshift survey [4] and pre-WFIRST supernovae data following the specifications reported in [1].

Following Bayesian Statistics, we have inferred the values $\Omega_m$ and the dark energy parameters for the models considered. We report our findings in two main ways: on the one hand we present our best fits, errors and derived quantities in Table 1; on the other hand we present credible contours obtained after a numerical marginalization over $\Omega_m$. As mentioned, we have considered the combination of real and mock SN and BAO data, and in addition we have introduced in all cases a Gaussian prior on $\Omega_m$ and $\Omega_b$ deduced in [3] with $h = 0.742$ as is given by [6].

As a general trend, we see that choosing $w_0$ and $w_{0.5}$ as the parameters to constrain is worthy as percentual errors are low. However, another interesting point

**Table 1** Constraints on dark energy parameters and derived quantities from current and mock data

| Data Set | Model | $\chi^2_{min}$ | $\Omega_m$ | Dark energy parameters | $\text{FoM}_{\text{Wang}}$ | $\rho_{1,2}$ | DIC |
|---|---|---|---|---|---|---|---|
| Current Data | CPL | 544.91 | $0.315 \pm 0.033$ | $w_0 = -1.033 \pm 0.180$<br>$w_a = -0.742 \pm 1.520$ | 14.16 | −0.930 | 10.30 |
| | Wang | 544.91 | $0.315 \pm 0.033$ | $w_0 = -1.033 \pm 0.180$<br>$w_{0.5} = -1.281 \pm 0.361$ | 42.47 | −0.792 | 8.11 |
| | Chebychev Pol. | 544.96 | $0.314 \pm 0.032$ | $w_0 = -1.049 \pm 0.163$<br>$w_{0.5} = -1.268 \pm 0.373$ | 43.63 | −0.785 | 8.02 |
| | Conventional Pol. | 544.98 | $0.314 \pm 0.032$ | $w_0 = -1.055 \pm 0.157$<br>$w_{0.5} = -1.263 \pm 0.377$ | 44.11 | −0.780 | 7.98 |
| Mock Data | CPL | 5320.38 | $0.269 \pm 0.005$ | $w_0 = -1.151 \pm 0.041$<br>$w_a = 0.244 \pm 0.207$ | 616.25 | −0.946 | 21.44 |
| | Wang | 5320.38 | $0.269 \pm 0.005$ | $w_0 = -1.151 \pm 0.041$<br>$w_{0.5} = -1.069 \pm 0.031$ | 1848.70 | −0.712 | 11.69 |
| | Chebychev Pol. | 5320.43 | $0.269 \pm 0.005$ | $w_0 = -1.140 \pm 0.035$<br>$w_{0.5} = -1.073 \pm 0.029$ | 2065.28 | −0.666 | 11.38 |
| | Conventional Pol. | 5320.45 | $0.269 \pm 0.005$ | $w_0 = -1.137 \pm 0.033$<br>$w_{0.5} = -1.075 \pm 0.028$ | 2147.57 | −0.648 | 11.29 |

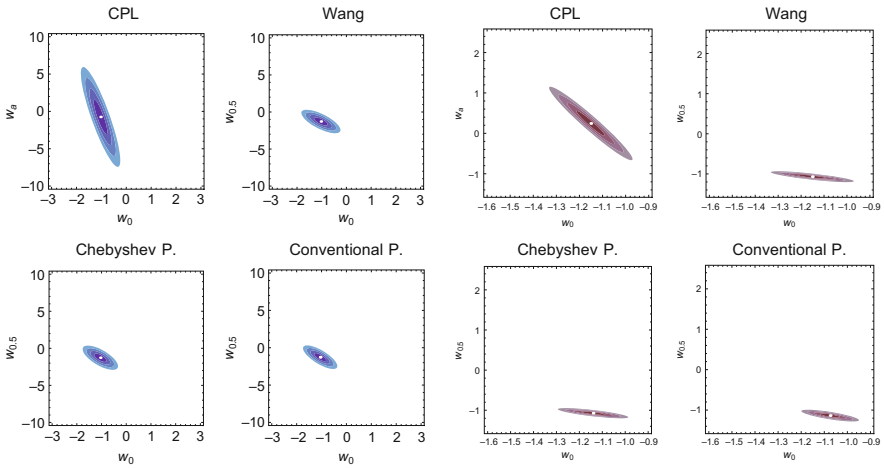


**Fig. 1** Credible contours for the four parametrizations using current and mock data

of view to interpret our results is Pearson's correlation coefficient, $\rho_{1,2} = \sigma_{12}^2/\sigma_1\sigma_2$ which can be used to study the lineal correlation between the two dark energy parameters. Here $\sigma_{12}$ is the non-diagonal element of the covariance matrix for the parameters 1 and 2. A related magnitude is the (frequentist) Figure-of-Merit (FoM), which has been defined [7] as $\mathrm{FoM}_{\mathrm{Wang}} = 1/\sqrt{\det \mathbf{C}(c_1, c_2, c_3, \ldots)}$, where $\mathbf{C}(c_1, c_2, c_3, \ldots)$ is the covariance matrix of the corresponding $c_i$ dark energy parameters. Results on the FoM get summarized very simply: the conventional polynomial has the largest value of the $\mathrm{FoM}_{\mathrm{Wang}}$.

For both sorts of data the conventional polynomial parametrization is naturally less correlated than all three others. The second best is the Chebyshev one, and all three are considerably less correlated than CPL. In agreement with our discussion the degree of correlation at a certain low redshift in our two new parametrizations immediately drives to very narrow errors on the total $w$ at that location (Fig. 1).

The last criterion we resort to is the Bayesian deviance information criterion (DIC). When applied for model selection the setting with the lowest DIC is in principle the best. The behaviour of the DIC follows the same pattern as the FoM. Basically, the conventional polynomial model is the best one, then we have the Chebyshev polynomial model, then Wang's scenario, and finally, the CPL model closes the ranking with the highest DIC by far.

Finally, we can see that the FoM values obtained with the mock data are typically better than those for currently available data. This fact proves the capability of the forthcoming surveys to describe the evolutionary features of dark energy.

## 3 Conclusions

The conclusions that emerge from our analysis is that our new parametrizations perform better in the sense that they allow to obtain tighter constraints on the dark energy EOS at present and its derivative, and they are also favoured by the statistical indicator we mention above (DIC). The main reason why we feel they fare better than their competitors is that they represent rather flexible perturbations of the $\Lambda$CDM scenario, which in many respects still remains the best description of the accelerated universe, and not surprisingly is often referred to as the concordance model. In contrast, either CPL or Wang are models which when taken as perturbations of $\Lambda$CDM are left with one free parameter only, and then one could expect less ability to accommodate themselves to the data.

**Acknowledgements** The authors are supported by the Spanish Ministry of Science and Innovation through research projects FIS2010-15492, Consolider EPI CSD2010- 00064 and also by the Basque Government through the special research action KAFEA.

## References

1. Albrecht, A.J., et al.: Findings of the joint dark energy mission figure of merit science working group (2009)
2. Amanullah, R., et al.: Spectra and light curves of six type ia supernovae at $0.511 < z < 1.12$ and the union2 compilation. ApJ **716**, 712–738 (2010)
3. Burigana, C., et al.: Forecast for the Planck precision on the tensor to scalar ratio and other cosmological parameters. ApJ **724**, 588–607 (2010)
4. Percival, W.: Geometrical constraints from galaxy clustering measurements based on euclid spectroscopy. http://sci.esa.int/science-e/www/object/doc.cfm?fobjectid=46450 (2010)
5. Percival W., W.J., et al.: Baryon Acoustic Oscillations in the Sloan Digital Sky Survey Data Release 7 Galaxy Sample. MNRAS **401**, 2148–2168 (2010)
6. Riess, A.G., et al.: A Redetermination of the Hubble Constant with the Hubble Space Telescope from a Differential Distance Ladder. ApJ **699**, 539–563 (2009)
7. Wang, Y.: Figure of merit for dark energy constraints from current observational data. Phys. Rev. D **77**(12), 123,525 (2008)

# Remarks on the Stability Operator for MOTS

**José M.M. Senovilla**

**Abstract** Deformations of marginally outer trapped surfaces (MOTS) and tubes (MOTT) are studied by using the stability operator introduced by Andersson–Mars–Simon. Novel formulae for the principal eigenvalue are presented. The possibility of selecting a privileged MOTT is discussed. This is related to the concept of 'core' of black holes. In spherical symmetry the spherical MOTT is the boundary of a core. I argue how similar results may hold in general black-hole spacetimes.

## 1 Basic Concepts and the Stability Operator

Let $S$ be a closed *marginally outer trapped surface* (MOTS): its outer null expansion vanishes $\theta_{\vec{k}} = 0$ [4, 5]. Here, the two future-pointing null vector fields orthogonal to $S$ are denoted by $\vec{l}$ and $\vec{k}$ with $l^\mu k_\mu = -1$. I will also use the concept of outer trapped surface (OTS, $\theta_{\vec{k}} < 0$ ). A *marginally outer trapped tube* (MOTT) is a hypersurface foliated by MOTS.

As proven in [1], the variation $\delta_{f\vec{n}}\theta_{\vec{k}}$ of the vanishing expansion along any normal direction $f\vec{n}$ such that $k_\mu n^\mu = 1$ reads

$$\delta_{f\vec{n}}\theta_{\vec{k}} = -\Delta_S f + 2s^B\overline{\nabla}_B f + f\left(K_S - s^B s_B + \overline{\nabla}_B s^B - G_{\mu\nu}k^\mu l^\nu\big|_S - \frac{n^\rho n_\rho}{2}W\right) \tag{1}$$

where $K_S$ is the Gaussian curvature on $S$, $\Delta_S$ its Laplacian, $G_{\mu\nu}$ the Einstein tensor, $\overline{\nabla}$ the covariant derivative on $S$, $s_B = k_\mu e^\sigma_B \nabla_\sigma l^\rho$ (with $\vec{e}_B$ the tangent vector fields on $S$), and $W \equiv G_{\mu\nu}k^\mu k^\nu\big|_S + \sigma^2$ with $\sigma^2$ the shear of $\vec{k}$ at $S$. Note that $\vec{n}$ is selected

J.M.M. Senovilla (✉)
Física Teórica, Universidad del País Vasco, Apartado 644, 48080 Bilbao, Spain
e-mail: josemm.senovilla@ehu.es

A. García-Parrado et al. (eds.), *Progress in Mathematical Relativity, Gravitation and Cosmology*, Springer Proceedings in Mathematics & Statistics 60,
DOI 10.1007/978-3-642-40157-2_61, 

by fixing its norm $\vec{n} = -\vec{l} + \frac{n_\mu n^\mu}{2}\vec{k}$ and that its causal character is unrestricted. Due to energy conditions [4, 5] $W \geq 0$ and $W = 0$ requires $G_{\mu\nu}k^\mu k^\nu\big|_S = \sigma^2 = 0$ leading to Isolated Horizons [2]. I shall assume $W > 0$ throughout, $W \geq 0$ being more involved.

The righthand side in (1) defines a linear differential operator $L_{\vec{n}}$ acting on $f$: $\delta_{f\vec{n}}\theta_{\vec{k}} \equiv L_{\vec{n}} f$. $L_{\vec{n}}$ is an elliptic operator on $S$, called the stability operator for $S$ in the normal direction $\vec{n}$. $L_{\vec{n}}$ is not self-adjoint in general (with respect to the $L^2$-product on $S$). Nevertheless, it has a real principal eigenvalue $\lambda_{\vec{n}}$, and the corresponding (real) eigenfunction $\phi_{\vec{n}}$ can be chosen to be positive on $S$. The (strict) stability of the MOTS $S$ along a spacelike $\vec{n}$ is ruled by the (positivity) non-negativity of $\lambda_{\vec{n}}$.

The formal adjoint operator with respect to the $L^2$-product on $S$ is given by

$$L^\dagger_{\vec{n}} \equiv -\Delta_S - 2s^B\overline{\nabla}_B + \left(K_S - s^B s_B - \overline{\nabla}_B s^B - G_{\mu\nu}k^\mu l^\nu\big|_S - \frac{n^\rho n_\rho}{2}W\right)$$

and has the same principal eigenvalue $\lambda_{\vec{n}}$ as $L_{\vec{n}}$ [1]. I denote by $\phi^\dagger_{\vec{n}}$ the corresponding principal (real and positive) eigenfunctions.

## 2 Possible MOTTs Through a Single MOTS

For each normal vector field $\vec{n}$, the operator $L_{\vec{n}} - \lambda_{\vec{n}}$ has a vanishing principal eigenvalue and $\phi_{\vec{n}}$ as principal eigenfunction: $L_{\vec{n}} - \lambda_{\vec{n}}$ corresponds to the stability operator $L_{\vec{n}'}$ along another normal direction $\vec{n}'$ given by $n'^\mu n'_\mu = n^\mu n_\mu + (2/W)\lambda_{\vec{n}}$, so that $\delta_{\phi_{\vec{n}}\vec{n}'}\theta_{\vec{k}} = 0$. If $\vec{n}$ is spacelike and $S$ is strictly stable along $\vec{n}$ ($\lambda_{\vec{n}} > 0$), then $\vec{n}'$ points "above" $\vec{n}$ (as $n'^\mu n'_\mu > n^\mu n_\mu$). The directions tangent to MOTTs through $S$ *belong* to (but may not exhaust!) the set $\{\phi_{\vec{n}}\vec{n}'\}$. These MOTTs are generically different: given two normal vector fields $\vec{n}_1$ and $\vec{n}_2$ the corresponding "primed" directions are equal if and only if $\vec{n}_1 - \vec{n}_2 = \frac{\text{const.}}{W}\vec{k}$. On the other hand, for any such two $\vec{n}_1$ and $\vec{n}_2$

$$(W/2)\, f\left(n_1^\rho n_{1\rho} - n_2^\rho n_{2\rho}\right) = \left(L_{\vec{n}_2} - L_{\vec{n}_1}\right) f \tag{2}$$

providing the relation between two deformation directions pointwise.

For any given $\vec{n}$ one easily gets

$$\oint_S L_{\vec{n}} f = \oint_S \left(K_S - s^B s_B - \overline{\nabla}_B s^B - G_{\mu\nu}k^\mu l^\nu\big|_S - \frac{n^\rho n_\rho}{2}W\right) f$$

$$\oint_S L^\dagger_{\vec{n}} f = \oint_S \left(K_S - s^B s_B + \overline{\nabla}_B s^B - G_{\mu\nu}k^\mu l^\nu\big|_S - \frac{n^\rho n_\rho}{2}W\right) f$$

in particular for the principal eigenfunctions

$$\lambda_{\vec{n}} \oint_S \phi_{\vec{n}} = \oint_S \left( K_S - s^B s_B - \overline{\nabla}_B s^B - G_{\mu\nu} k^\mu l^\nu \big|_S - \frac{n^\rho n_\rho}{2} W \right) \phi_{\vec{n}}$$

$$\lambda_{\vec{n}} \oint_S \phi^\dagger_{\vec{n}} = \oint_S \left( K_S - s^B s_B + \overline{\nabla}_B s^B - G_{\mu\nu} k^\mu l^\nu \big|_S - \frac{n^\rho n_\rho}{2} W \right) \phi^\dagger_{\vec{n}}$$

which are two explicit *formulas* for the principal eigenvalue *bounding* it

$$\min_S \left( K_S - s^B s_B \pm \overline{\nabla}_B s^B - G_{\mu\nu} k^\mu l^\nu \big|_S - \frac{n^\rho n_\rho}{2} W \right) \leq \lambda_{\vec{n}}$$

$$\leq \max_S \left( K_S - s^B s_B \pm \overline{\nabla}_B s^B - G_{\mu\nu} k^\mu l^\nu \big|_S - \frac{n^\rho n_\rho}{2} W \right). \tag{3}$$

Furthermore, the two functions $\lambda_{\vec{n}} - \left( K_S - s^B s_B \pm \overline{\nabla}_B s^B - G_{\mu\nu} k^\mu l^\nu \big|_S - \frac{n^\rho n_\rho}{2} W \right)$ *must vanish* somewhere on $S$ for all $\vec{n}$.

There are two obvious simple choices $\vec{n}_\pm$ leading to a vanishing principal eigenvalue: $n^\mu_\pm n_{\pm\mu} = \frac{2}{W} \left( K_S - s^B s_B \pm \overline{\nabla}_B s^B - G_{\mu\nu} k^\mu l^\nu \big|_S \right)$. The corresponding stability operators are $L_\pm = -\Delta_S + 2s^B \overline{\nabla}_B + (1 \mp 1) \overline{\nabla}_B s^B$. The corresponding principal eigenfunctions $\phi_\pm > 0$ satisfy $L_\pm \phi_\pm = 0$. The respective formal adjoints read: $L^\dagger_\pm = -\Delta_S - 2s^B \overline{\nabla}_B - (1 \pm 1) \overline{\nabla}_B s^B$ with vanishing principal eigenvalues too. Observe that $L_-$ and $L^\dagger_+$ are gradients $L_- f = -\overline{\nabla}_B \left( \overline{\nabla}^B f - 2 f s^B \right)$, $L^\dagger_+ f = -\overline{\nabla}_B \left( \overline{\nabla}^B f + 2 f s^B \right)$.

## 3 A Distinguished MOTT

$L_-$ has special relevant properties, because (2) leads to

$$(W/2) f \left( n^\rho n_\rho - n^\rho_- n_{-\rho} \right) = L_- f - \delta_{f\vec{n}} \theta_{\vec{k}} \tag{4}$$

For any other direction $\vec{n}'$ defining a local MOTT

$$(W/2) \left( n'^\rho n'_\rho - n^\rho_- n_{-\rho} \right) = \lambda_{\vec{n}} - \left( K_S - s^B s_B - \overline{\nabla}_B s^B - G_{\mu\nu} k^\mu l^\nu \big|_S - \frac{n^\rho n_\rho}{2} W \right)$$

and, as remarked above, the righthand side must change sign on $S$.

**Theorem 3.1.** *The local MOTT defined by the direction $\vec{n}_-$ is such that any other nearby local MOTT must interweave it: the vector $\vec{n}' - \vec{n}_-(\propto \vec{k})$ changes its causal orientation on any of its MOTSs.*

From (4), deformations using $c\phi_-$ with constant $c$ lead to outer untrapped (resp. trapped) surfaces if $c\left(n^\rho n_\rho - n^\rho_- n_{-\rho}\right) < 0$ (resp. $> 0$) everywhere. Integrating (4) on $S$ one thus gets

$$\frac{1}{2}\oint_S Wf\left(n^\rho n_\rho - n^\rho_- n_{-\rho}\right) = -\oint_S \delta_{f\vec{n}}\theta_{\vec{k}}$$

hence the deformed surface can be outer trapped (untrapped) only if $f\left(n^\rho n_\rho - n^\rho_- n_{-\rho}\right)$ is positive (negative) somewhere. If the deformed surface has $f\left(n^\rho n_\rho - n^\rho_- n_{-\rho}\right) < 0$ (respectively $> 0$) everywhere then $\delta_{f\vec{n}}\theta_{\vec{k}}$ must be positive (resp. negative) somewhere.

Choose the function $f = a_0\phi_- + \tilde{f}$ for a constant $a_0 > 0$ so that, as $\phi_- > 0$ has vanishing eigenvalue, (4) becomes $(W/2)(a_0\phi_- + \tilde{f})\left(n^\rho n_\rho - n^\rho_- n_{-\rho}\right) = L_-\tilde{f} - \delta_{f\vec{n}}\theta_{\vec{k}}$. This can be split into two parts:

$$(W/2)a_0\phi_-\left(n^\rho n_\rho - n^\rho_- n_{-\rho}\right) = -\delta_{f\vec{n}}\theta_{\vec{k}}, \quad \frac{W}{2}\left(n^\rho n_\rho - n^\rho_- n_{-\rho}\right) = \frac{L_-\tilde{f}}{\tilde{f}} \tag{5}$$

The first of these tells us that $\delta_{f\vec{n}}\theta_{\vec{k}} < 0$ whenever $\vec{n}$ points "above" $\vec{n}_-$. But then the second in (5) requires finding a function $\tilde{f}$ such that $L_-\tilde{f}/\tilde{f}$ is strictly positive on $S$. This leads to the following interesting mathematical problem:

> Is there a function $\tilde{f}$ on $S$ such that (i) $L_-\tilde{f}/\tilde{f} \geq \epsilon > 0$, (ii) $\tilde{f}$ changes sign on $S$, and (iii) $\tilde{f}$ is positive in a region as small as desired?

To prove that there are OTSs penetrating both sides of the MOTT it is enough to comply with points (i) and (ii). If the operator $L_-$ has any real eigenvalue other than the vanishing principal one, then these two conditions do hold for the corresponding real eigenfunction because integration of $L_-\psi = \lambda\psi$ implies $\oint_S \psi = 0$ (as $\lambda > 0$) ergo $\psi$ changes sign on $S$. However, even if there are no other real eigenvalues the result might hold. Point (iii) would ensure, then, that the deformed OTS intersects the trapped region "above" the MOTT only in a portion that can be shrunk as much as desired. This is important for the concept of *core* and its boundary, see [3].

As illustration of the above, consider a marginally trapped round sphere $\varsigma$ in a spherically symmetric space-time, that is, any sphere with $r = 2m$ where $4\pi r^2$ is its area and $m = (r/2)(1 - r_{,\mu}r^{,\mu})$ is the "mass function". For any such $\varsigma$, $s^B = 0$ and $\sigma^2 = 0$, ergo the directions $\vec{n}_\pm$ and operators $L_\pm$ coincide: $\vec{n}_+ = \vec{n}_- \equiv \vec{m}$, $L_+ = L_- = L_{\vec{m}} = -\Delta_\varsigma$. As it happens, $\vec{m}$ is tangent to the unique spherically symmetric MOTT: $r = 2m$ [3]. Therefore, points (i) and (ii) are easily satisfied by choosing $\tilde{f}$ to be an eigenfunction of the spherical Laplacian $\Delta_\varsigma$, say $\tilde{f} = cP_l$ for a constant $c$ and $l > 0$, where $P_l$ are the Legendre polynomials. Actually, one can find an explicit function satisfying point (iii) too, proving that the region $r \leq 2m$ is a core in spherical symmetry, [3]. This is a surprising, maybe deep result, because the concept of core is global and requires full knowledge of the future, however its

boundary $r = 2m$ is a MOTT, hence defined locally. Whether or not this happens in general is an open important question.

**Acknowledgements** Supported by grants FIS2010-15492 (MICINN), GIU06/37 (UPV/EHU) and P09-FQM- 4496 (J. Andalucía–FEDER) and UFI 11/55 (UPV/EHU).

## References

1. L. Andersson, M. Mars and W. Simon, *Adv. Theor. Math. Phys.* **12**, 853–888 (2008)
2. A. Ashtekar and B. Krishnan, *Living Rev. Relativity* **7** 10 (2004).
3. I. Bengtsson and J.M.M. Senovilla, *Phys. Rev.* **D 83** 044012 (2011)
4. S.W. Hawking, G.F.R. Ellis, *The large scale structure of space-time*, (Cambridge Univ. Press, Cambridge, 1973).
5. Wald, R M *General Relativity* (The University of Chicago Press, Chicago, 1984)

# CMB Anisotropies by Collapsing Textures

**Kepa Sousa and Jon Urrestilla**

**Abstract** CMB photons passing through a collapsing texture knot receive an energy shift, creating characteristic cold and hot spots on the sky. We calculate the anisotropy pattern produced by collapsing texture knots of arbitrary shape. The texture dynamics are solved numerically on a Minkowski background.

## 1 Introduction

Textures are an unstable type of topological defect which are generically formed whenever there is a complete spontaneous breaking of a non-abelian global symmetry, what can be easily implemented in the context of Grand Unified Theories [6]. Unlike other topological defects textures are unstable, and collapse roughly at the speed of light as soon as they enter the horizon. When the defect size falls below the symmetry breaking scale the topological charge is no longer conserved and the texture decays into the vacuum (*unwinding*). The integrated Sachs–Wolfe effect causes the CMB photons passing near the texture to be typically red-shifted or blue-shifted, leaving characteristic hot and cold spots in the cosmic background. The interest on textures increased after Cruz et al. and Feeney et al. [3, 4] considered the texture model as one of the most plausible hypothesis to explain the CMB anomaly known as the *Cold Spot*.

K. Sousa (✉)
School of Engineering and Science, Jacobs University Bremen, Campus Ring 1, 28759 Bremen, Germany
e-mail: ksousa@jacobs-university.de

J. Urrestilla
Department of Theoretical Physics, University of the Basque Country UPV/EHU, Apt. 644, Bilbao 48080, Basque Country, Spain
e-mail: jon.urrestilla@ehu.es

A. García-Parrado et al. (eds.), *Progress in Mathematical Relativity, Gravitation and Cosmology*, Springer Proceedings in Mathematics & Statistics 60,
DOI 10.1007/978-3-642-40157-2_62, 

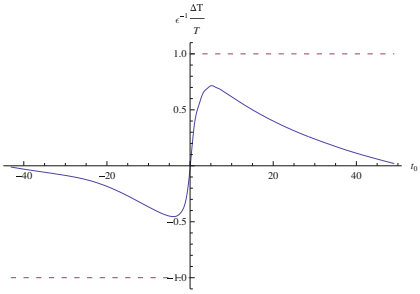


**Fig. 1** Prediction of the time evolution of the temperature fluctuation at the center of the anisotropy by different methods: field theory simulations (*solid line*), self-similar collapse (*dashed line*) (2)

These analyses rely on the existing predictions for the anisotropy pattern produced by global textures. In particular they use a very idealized analytical result obtained by Turok et al. in [6], who studied the simplest model admitting texture solutions, the O(4)-model, which is characterized by the Lagrangian

$$\mathscr{L} = \tfrac{1}{2}\partial_\mu \phi_a \, \partial^\mu \phi_a - \lambda(\phi_a \phi_a - \eta^2)^2, \qquad a = 1, \ldots, 4\,. \tag{1}$$

This model describes the dynamics of four real scalar fields $\phi_a$, with their interactions given by a Mexican-hat type potential, where $\lambda$ is the self coupling and $\eta$ the expectation value, which determines the symmetry breaking scale. The analytical solution found by Turok et al. relies on the non-$\sigma$ model approximation to solve the dynamics (i.e. $\phi_a \phi_a = \eta^2$ is assumed at all times), which breaks down at the unwinding event, and describes spherically symmetric texture collapsing in a self-similar way. The anisotropy pattern produced by such a texture is given by

$$\frac{\Delta T}{T}(r, t_0) = \frac{t_0}{(2r^2 + t_0^2)^{1/2}}\, \varepsilon, \qquad \varepsilon \equiv 8\pi^2 G \eta^2, \tag{2}$$

where $r$ is the impact parameter of the photon respect to the center of the texture, and $t_0$ the time at which it is closest to the texture, with $t_0 = 0$ being the time at unwinding. Such a solution has been known for a long time to be unlikely to occur in a cosmological context [1]. Actually, the authors of [3, 4] truncated the radial profile (2) and matched it with a Gaussian at its half-maximum because it is known not to be valid for large values of the impact parameter where it has a very slow decay as $r^{-1}$, leading to an unrealistically large spot. Moreover, the amount of red-shift or blue-shift received by the photons crossing the center of the texture is the same independently of the time of crossing $t_0$, (dashed line in Fig. 1), even at very early times when the texture size is large, and thus the energy density is very diluted.

The purpose of the present work is to provide a more realistic prediction of the anisotropy pattern left by a random texture, without making any assumption about the initial configuration of the texture, through numerical simulations of the full dynamics of a texture configuration in the O(4)-model.

## 2 Numerical Methods

In order to characterize the anisotropy produced by textures with arbitrary shape we proceed as in [2]. To simplify the dynamics it is assumed that the gravitational field produced by the texture is small, which implies that the texture can be evolved on the unperturbed background and the CMB photons travel along the unperturbed geodesics. The dynamics of the $O(4)$-model are solved evolving numerically a discretized version of the equations of motion for Minkowski background on a lattice of $96^3$ grid points. The lattice has periodic boundary conditions, and the grid spacing is $\Delta x = \sqrt{2/\lambda\eta^2}$. These results can be extended to the cosmological case as long as all the length-scales and time-scales involved in the simulation are small compared with the size of the horizon $H^{-1}$. We have evolved 1300 random initial configurations with a correlation length of 36 lattice spacings, and during a time interval of $96\Delta x \cdot c$, so that the boundary effects can be ignored. The corresponding anisotropy pattern is calculated only for those initial configurations leading to isolated unwinding events which happen away from the start and the end of the evolution (33 in total), so that photons have time enough to cross the complete texture. In a Minkowski background the Sachs–Wolfe formula can be solved explicitly in terms of the energy momentum tensor of the texture configuration. The anisotropy is calculated using an approximation of this solution valid for anisotropies covering small angular scales (see [2]).

## 3 Summary of the Results and Conclusions

In order to compare our results with the self-similar solution (2), we have measured the fractional temperature change for photons crossing the center of the texture for each of the 33 initial configurations, and then we have averaged over the whole ensemble. The result is represented by the solid line in Fig. 1. The plot shows how our numerical simulation resolves the unwinding event, which lasts about $\delta t \sim 10\,\lambda^{-1/2}\eta^{-1}$, in contrast with the analytic solution in [6] which has a step-like behavior (dashed line). Moreover, we can also see how the brightness of the spot decays at early and late times, implying that textures are only observable during a finite interval around the unwinding event. This might have important consequences for the Bayesian analyses in [3,4], which requires an estimate of the number of cold and hot spots due to textures which can be observed in the sky at a given time, and of a given angular size. In particular, as the size of the texture configuration grows with time as we go far from the unwinding event [2,6], we expect the angular scale distribution of spots to decay faster for large spots than the estimate made in [6]. We have also recovered results in [2] which show that the average cold and hot spots produced by random textures are significantly less pronounced than the Turok solution ($20-50\%$):

$$\frac{\Delta T}{T}|_{max} = (+0.77 \pm 0.21)\varepsilon, \qquad \frac{\Delta T}{T}|_{min} = (-0.49 \pm 0.13)\varepsilon, \tag{3}$$

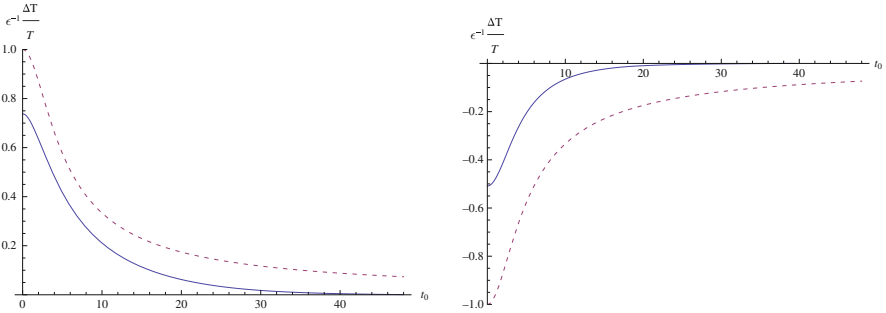


**Fig. 2** Averaged radial profiles of a *hot spot* (*left*) and a *cold spot* (*right*) at maximum brightness. The *continuous lines* represent our results and the *dashed line* corresponds to Eq. (2)

which is specially relevant in order to estimate the symmetry breaking scale, as it can be extracted from the spot brightness [3, 4].

In order to characterize the anisotropy pattern we have obtained the radial profiles of a cold and a hot spot at maximum brightness. Since textures become spherical close to the time of the unwinding [5], after averaging over the whole ensemble of initial conditions, we have also averaged the profile over the azimuth angle. The result is represented in Fig. 2 (continuous lines). In these plots we can see again the differences between the maxima and minima of the calculated profiles and the Turok solution (dashed line). In addition, it is also evident that the profiles we found are significantly more localized than the analytic solution. These results, together with the expected corrections to the angular scale distribution of observed spots suggest a revision of the analyses done by Cruz et al. and Feeney et al. [3, 4].

The present study is a first approach to improve the existing predictions for the anisotropy pattern produced by a collapsing texture. Future work involves repeating these simulations in a larger lattice in order to reduce the boundary effects, and to study the dependence of the profiles on the photon emission and reception times. In addition we intend to evolve the texture configurations in a Friedman–Robertson–Walker metric in order to characterize the effect of the expansion of the universe on the anisotropy pattern produced.

**Acknowledgements** We are grateful to M. Cruz, and E. Martinez for very useful discussions. KS acknowledges support within the framework of the Deutsche Forschungsgemeinschaft (DFG) Research Training Group 1620 Models of gravity, and thanks the Department of Theoretical Physics at the University of the Basque Country for its hospitality. JU acknowledges financial support from the Basque Government (IT-559-10), the Spanish Ministry (FPA2009-10612), and the Spanish Consolider-Ingenio 2010 Programme CPAN (CSD2007-00042).

## References

1. J. Borrill, E. J. Copeland and A. R. Liddle, Phys. Rev. D **46** , p. 524. (1992)
2. J. Borrill, E. J. Copeland, A. R. Liddle, A. Stebbins and S. Veeraraghavan, Phys. Rev. D **50**, p. 2469 (1994)
3. M. Cruz, N. Turok, P. Vielva, E. Martinez-Gonzalez and M. Hobson, Science **318**, p. 1612 (2007)
4. S. M. Feeney, M. C. Johnson, D. J. Mortlock and H. V. Peiris, Phys. Rev. Lett. **108**, p. 241301 (2012)
5. W. H. Press, B. S. Ryden and D. N. Spergel, Astrophys. J. **347**, p. 590. (1989)
6. N. Turok and D. Spergel, Phys. Rev. Lett. **64**, p. 2736. (1990)

# Relative Motions of Free Test Particles in Robinson–Trautman Spacetimes of Any Dimension

**Robert Švarc and Jiří Podolský**

**Abstract** Using the invariant form of equation of geodesic deviation we analyze the relative deformations of a congruence of free test particles in general non-twisting, shearfree and expanding geometries. In four dimensions this class of exact solutions includes important classes of expanding gravitational waves. On the other hand, higher-dimensional Robinson–Trautman spacetimes can only be of algebraic type D. We emphasize the difference between the standard four-dimensional solutions and their arbitrary-dimensional extensions from the physical point of view of a geodesic observer.

## 1 Robinson–Trautman Geometries

The optical scalars $A^2$ (twist), $\sigma^2$ (shear) and $\Theta$ (expansion) characterizing affinely parameterized null geodesic congruence $k^a$ are in arbitrary dimension $D$ given by

$$A^2 = -k_{[a;b]}k^{a;b}\,, \quad \sigma^2 = k_{(a;b)}k^{a;b} - \frac{1}{D-2}(k^a{}_{;a})^2\,, \quad \Theta = \frac{1}{D-2}k^a{}_{;a}\,. \quad (1)$$

The Robinson–Trautman class of spacetimes is defined as the geometries admitting nontwisting ($A = 0$), shearfree ($\sigma = 0$) and expanding ($\Theta \neq 0$) null geodesic congruence. The line element of a general nontwisting spacetime takes the form

R. Švarc (✉)
Department of Physics, Faculty of Science, J. E. Purkinje University in Ústí nad Labem, České mládeže 8, 400 96 Ústí nad Labem, Czech Republic
e-mail: robert.svarc@mff.cuni.cz

J. Podolský
Institute of Theoretical Physics, Faculty of Mathematics and Physics, Charles University in Prague, V Holešovičkách 2, 180 00 Prague 8, Czech Republic
e-mail: podolsky@mbox.troja.mff.cuni.cz

A. García-Parrado et al. (eds.), *Progress in Mathematical Relativity, Gravitation and Cosmology*, Springer Proceedings in Mathematics & Statistics 60,
DOI 10.1007/978-3-642-40157-2_63, 

$$\mathrm{d}s^2 = g_{ij}(r,u,x)\,\mathrm{d}x^i\mathrm{d}x^j + 2g_{ui}(r,u,x)\,\mathrm{d}x^i\mathrm{d}u - 2\mathrm{d}u\mathrm{d}r + g_{uu}(r,u,x)\,\mathrm{d}u^2\,, \quad (2)$$

where $i,\ j = 2,\ldots,\ D-1,\ u = const$ defines null hypersurfaces with normal $k^a = \partial_r$, $r$ is an affine parameter along the geodesic congruence, and $x^i$ represent $D-2$ spatial coordinates in a transverse Riemannian space. As shown in [1], the shearfree condition $\sigma = 0$ and the vacuum Einstein equations than imply $g_{ui} = 0$ in (2) and fully determine the $r$-dependence of the $D$-dimensional Robinson–Trautman metric as

$$\mathrm{d}s^2 = r^2 h_{ij}(u,x)\,\mathrm{d}x^i\mathrm{d}x^j - 2\,\mathrm{d}u\mathrm{d}r - 2H(r,u,x)\,\mathrm{d}u^2\,, \quad (3)$$

with the function $2H$ given by

$$2H = \frac{\mathscr{R}}{(D-2)(D-3)} + \frac{2(\ln\sqrt{h})_{,u}}{D-2}\,r - \frac{2\Lambda}{(D-2)(D-1)}\,r^2 - \frac{\mu}{r^{D-3}}\,, \quad (4)$$

where $\mathscr{R}(u,x)$ is the scalar curvature calculated with respect to the spatial metric $h_{ij}$,

$$h_{ij}(u,x) = P^{-2}(u,x)\,\gamma_{ij}(x) \quad \text{and} \quad \det\gamma_{ij} = 1\,, \quad (5)$$

$h(u,x)$ is defined as $h \equiv \det h_{ij} = P^{2(2-D)}$, $\Lambda$ is a cosmological constant, and $\mu(u,x)$ is an arbitrary function. For this general form of the vacuum Robinson–Trautman line element (3) the nonvanishing components of the Weyl tensor explicitly become

$$\begin{aligned}
C_{ruru} &= -(D-2)(D-3)\frac{\mu}{2r^{D-1}}\,, \qquad C_{rpuq} = -\frac{r^2 h_{pq}}{D-2}C_{ruru}\,,\\
C_{kplq} &= r^2\mathscr{R}_{kplq} - \frac{2r^2 h_{k[l}h_{q]p}}{(D-2)(D-3)}\left(2r^2 C_{ruru} + \mathscr{R}\right)\,,\\
C_{upkq} &= \frac{2r\mathscr{R}_{,[k}h_{q]p}}{(D-2)^2(D-3)}\,, \qquad C_{ruup} = \frac{\mathscr{R}_{,p}}{(D-2)^2 r}\,,\\
C_{upuq} &= 2HC_{rpuq} + W_{pq} - \frac{h_{pq}}{D-2}\,h^{ij}W_{ij}\,,
\end{aligned} \quad (6)$$

where $\mathscr{R}_{kplq}$ is the Riemann tensor of the transverse space $h_{ij}$, and $W_{pq}$ denotes

$$W_{pq} \equiv H_{,pq} - \frac{1}{2}H_{,k}\,h^{kl}\left(2h_{l(p,q)} - h_{pq,l}\right)\,. \quad (7)$$

Other restrictions on the transverse metric $h_{ij}$ and the parameters contained in the metric function $H$ (in general depending on $u$ and $x^i$ coordinates) follow from the remaining vacuum Einstein equations and significantly depend on the number of

dimensions $D$, see the detailed discussion in [1]. For our purpose here notice that in any higher dimension $D > 4$ the coordinate dependence of these metric functions is

$$\mathscr{R} = \mathscr{R}(u)\,, \qquad \mu = \mu(u)\,, \qquad P(x)\,, \qquad P(u,x) \;\text{ for }\; \mu = 0\,, \tag{8}$$

while in standard four-dimensional case we obtain

$$\mathscr{R} = \mathscr{R}(u,x)\,, \qquad \mu = \mu(u)\,, \qquad P(u,x)\,, \qquad h_{ij} = P^{-2}(u,x)\,\delta_{ij}\,. \tag{9}$$

## 2 Geodesic Deviation

In our work [2] we discussed specific influence of an arbitrary gravitational field in any dimension $D$ on relative motion of geodesic particles. In the case of vacuum spacetimes the equation of geodesic deviation takes the invariant form

$$\begin{aligned}
\ddot{Z}^{(1)} &= \frac{2\Lambda}{(D-2)(D-1)}\,Z^{(1)} + \Psi_{2S}\,Z^{(1)} + \frac{1}{\sqrt{2}}\,(\,\Psi_{1T^j} - \Psi_{3T^j}\,)\,Z^{(j)}\,,\\
\ddot{Z}^{(i)} &= \frac{2\Lambda}{(D-2)(D-1)}\,Z^{(i)} - \Psi_{2T^{(ij)}}\,Z^{(j)} + \frac{1}{\sqrt{2}}\,(\,\Psi_{1T^i} - \Psi_{3T^i}\,)\,Z^{(1)}\\
&\qquad\qquad -\frac{1}{2}\,(\,\Psi_{0^{ij}} + \Psi_{4^{ij}}\,)\,Z^{(j)}\,,
\end{aligned} \tag{10}$$

with $i,\ j = 2,\ldots,\ D-1$. Here $Z^{(1)}, Z^{(2)}, \ldots, Z^{(D-1)}$ are spatial components of the separation vector $\mathbf{Z} = Z^a\,\mathbf{e}_a$ between the test particles in a natural interpretation orthonormal frame $\{\mathbf{e}_a\}$, i.e., $\mathbf{e}_a \cdot \mathbf{e}_b = \eta_{ab}$, where $\mathbf{e}_{(0)} \equiv \mathbf{u} = \dot{r}\,\partial_r + \dot{u}\partial_u + \dot{x}^i\,\partial_i$ is the velocity vector of the fiducial test particle, $\ddot{Z}^{(1)}, \ddot{Z}^{(2)}, \ldots, \ddot{Z}^{(D-1)}$ are the corresponding relative accelerations, and the scalars $\Psi_{A\ldots}$ are defined as the components of the Weyl tensor in the null frame $\{\mathbf{k}, \mathbf{l}, \mathbf{m}_i\}$ adapted to observer's $D$-velocity $\mathbf{u}$, namely,

$$\begin{aligned}
\mathbf{k} &= \frac{1}{\sqrt{2}}(\mathbf{u} + \mathbf{e}_{(1)}) = \frac{1}{\sqrt{2}\dot{u}}\,\partial_r\,,\\
\mathbf{l} &= \frac{1}{\sqrt{2}}(\mathbf{u} - \mathbf{e}_{(1)}) = \left(\sqrt{2}\dot{r} - \frac{1}{\sqrt{2}\dot{u}}\right)\partial_r + \sqrt{2}\dot{u}\,\partial_u + \sqrt{2}\dot{x}^i\,\partial_i\,,\\
\mathbf{m}_i &= \mathbf{e}_{(i)} = \frac{1}{\dot{u}}\,g_{kl}\,\dot{x}^k m_i^l \partial_r + m_i^j\,\partial_j\,,
\end{aligned} \tag{11}$$

and the projections of the Weyl tensor (grouped by their boost weight) are

$$\begin{aligned}
\Psi_{0^{ij}} &= C_{abcd}\,k^a\,m_i^b\,k^c\,m_j^d\,,\\
\Psi_{1^{ijk}} &= C_{abcd}\,k^a\,m_i^b\,m_j^c\,m_k^d\,, \qquad\qquad \Psi_{1T^i} = C_{abcd}\,k^a\,l^b\,k^c\,m_i^d\,,
\end{aligned}$$

$$\begin{aligned}
\Psi_{2^{ijkl}} &= C_{abcd}\, m_i^a\, m_j^b\, m_k^c\, m_l^d\,, & \Psi_{2S} &= C_{abcd}\, k^a\, l^b\, l^c\, k^d\,,\\
\Psi_{2^{ij}} &= C_{abcd}\, k^a\, l^b\, m_i^c\, m_j^d\,, & \Psi_{2T^{ij}} &= C_{abcd}\, k^a\, m_i^b\, l^c\, m_j^d\,,\\
\Psi_{3^{ijk}} &= C_{abcd}\, l^a\, m_i^b\, m_j^c\, m_k^d\,, & \Psi_{3T^{i}} &= C_{abcd}\, l^a\, k^b\, l^c\, m_i^d\,,\\
\Psi_{4^{ij}} &= C_{abcd}\, l^a\, m_i^b\, l^c\, m_j^d\,,
\end{aligned} \tag{12}$$

where $i, j, k, l = 2, \ldots, D-1$.

However, for the vacuum Robinson–Trautman spacetimes using the explicit form of the Weyl tensor (6) we find that $\Psi_{0^{ij}}$, $\Psi_{1^{ijk}}$ and $\Psi_{1T^{i}}$ (which correspond to the highest boost weights $+2$ and $+1$) vanish identically. The only non-trivial Weyl scalars (12) with respect to the null frame (11) that are present in (10) take the form

$$\Psi_{2S} = -C_{ruru}\,, \qquad \Psi_{2T^{ij}} = m_i^p m_j^q\, C_{rpuq}\,, \tag{13}$$

$$\Psi_{3T^{j}} = \sqrt{2}\, m_j^p \big[\dot{x}^k (g_{kp} C_{ruru} - C_{rkup}) - \dot{u}\, C_{ruup}\big]\,, \tag{14}$$

$$\begin{aligned}
\Psi_{4^{ij}} = 2\, m_{(i}^p m_{j)}^q \big\{ & \dot{x}^k \dot{x}^l \big[g_{kl} C_{rpuq} - g_{pk}(2C_{rluq} - g_{lq} C_{ruru}) + C_{kplq}\big] \\
& + 2\dot{x}^k \dot{u}(C_{upkq} - g_{kq} C_{ruup}) + \dot{u}^2 (C_{upuq} - 2H C_{rpuq})\big\}\,,
\end{aligned} \tag{15}$$

where the Weyl tensor components are explicitly given by (6) and, due to (8) and (9), significantly depend on the number of dimensions $D$.

The Weyl scalars (13)–(15) represent specific combinations of observer's kinematics with the curvature of the spacetime. The overall relative motion measured by an arbitrary geodesic observer in any dimension $D$ with velocity $\mathbf{u}$ described by equations (10) thus, in general, consists of the isotropic influence of the cosmological constant $\Lambda$, Newton-like deformation induced by the terms $\Psi_{2S}$ and $\Psi_{2T^{(ij)}}$, the longitudinal effects encoded in $\Psi_{3T^{i}}$, and the transverse deformations corresponding to $\Psi_{4^{ij}}$, see [2] for the physical interpretation of the $\Psi_{A^{\cdots}}$ scalars.

However, the terms in (13)–(15) containing spatial components $\dot{x}^i$ of observer's velocity $\mathbf{u}$ can be (at least locally) removed by a suitable particular choice of the fiducial geodesic with $\dot{x}^i = 0$. These 'radial' observers thus measure 'pure' effects of the vacuum Robinson–Trautman gravitational field and are able to distinguish between four and a higher dimensional spacetime. To be more specific:

- The higher-dimensional constraints (8) imply than in the case $\dot{x}^i = 0$ the only nonvanishing Weyl scalars are $\Psi_{2S}$ and $\Psi_{2T^{(ij)}}$ representing Newton-like tidal deformations governed by the 'mass' parameter $\mu$, see (13) and (6).
- From (9) in four dimensions it follows that all Weyl scalars $\Psi_{2S}$, $\Psi_{2T^{(ij)}}$, $\Psi_{3T^{i}}$ and $\Psi_{4^{ij}}$ are in general nonvanishing and the test particles in vacuum Robinson–Trautman spacetimes are thus affected by Newton-like tidal deformation (13), the longitudinal effects (14), and by the transverse gravitational waves (15).

This agrees with previous results of [1, 3] that vacuum Robinson–Trautman spacetimes in $D > 4$ are only of algebraic type D, while in $D = 4$ they are of type II, or more special.

**Acknowledgements** R.Š. was supported by the grant GAČR 202/09/0772, and J.P. by the grants GAČR P203/12/0118 and MSM0021620860.

## References

1. Podolský, J., Ortaggio, M.: Robinson–Trautman spacetimes in higher dimensions. Class. Quantum Grav. **23**, 5785–5797 (2006)
2. Podolský, J., Švarc, R.: Interpreting spacetimes of any dimension using geodesic deviation. Phys. Rev. D **85**, 044057 (2012)
3. Ortaggio, M., Pravda, V., Pravdová, A.: Algebraic classification of higher dimensional spacetimes based on null alignment. Class. Quantum Grav. **30**, 013001 (2013)

# Connection Between Horizons and Algebraic Type

**Otakar Svítek**

**Abstract** We study connections between both event and quasilocal horizons and the algebraic type of the Weyl tensor. The relation regarding spacelike future outer trapping horizon is analysed in four dimensions using double-null foliation.

## 1 Introduction

We would like to, at least partially, understand how does the presence of some form of horizon restrict the possible algebraic types on it. Since algebraic type of a tensor is determined locally we need to characterize the horizon without employing global notions. We will concentrate on the Weyl tensor and Petrov types derived from it.

Event horizon is a global characteristic and the full spacetime evolution is necessary in order to localize it. In many situations this is not desirable or even attainable and therefore, over the past years different quasi-local characterizations of black hole boundary were developed. The most important ones being apparent horizon [1], trapping horizon [2] and isolated or dynamical horizon [3]. The basic *local* condition in the above mentioned horizon definitions is effectively the same: these horizons are sliced by marginally trapped surfaces with vanishing expansion of outgoing (ingoing) null congruence orthogonal to the surface. We adopt the so called spacelike future outer trapping horizon (SFOTH) which merges the properties of trapping and dynamical horizons.

Since event horizon in a static spacetime with a well-behaved matter is a Killing horizon one can use the local condition on stationary Killing field in such a situation avoiding the global nature of event horizon. This case was investigated by Pravda

O. Svítek (✉)
Institute of Theoretical Physics, Faculty of Mathematics and Physics, Charles University in Prague, V Holešovičkách 2, 180 00 Praha 8, Czech Republic
e-mail: ota@matfyz.cz

A. García-Parrado et al. (eds.), *Progress in Mathematical Relativity, Gravitation and Cosmology*, Springer Proceedings in Mathematics & Statistics 60,
DOI 10.1007/978-3-642-40157-2_64, 

and Zaslavskii [4] and we summarize their results in the next section. In the third section the relation of SFOTH to the algebraic type is derived.

## 2 Killing Horizons

Pravda and Zaslavskii [4] studied curvature scalars in a general static spacetime possessing Killing horizon (generalizing previous results of [5] on high degree of symmetry of the Einstein tensor to the non-extremal case). They assumed regularity of all polynomial invariants of the Riemann tensor on a horizon and used two naturally preferred frames for calculations—the static observer and the freely falling observer frames. Note that the static frame is singular on the null horizon.

Assuming $1+1+2$ decomposition and using the Gauss normal coordinates the metric takes the following form

$$\mathrm{d}s^2 = -M^2\mathrm{d}t^2 + \mathrm{d}n^2 + \gamma_{ab}\mathrm{d}x^a\mathrm{d}x^b \tag{1}$$

The stationary Killing field is $\xi^\mu = (1,0,0,0)$ with $M^2 \equiv \xi^\mu\xi_\mu = 0$ on the horizon. The tetrad adapted to the static observer's four-velocity and the Gaussian normal direction has the form

$$l^\mu = \frac{1}{\sqrt{2}}(\tfrac{1}{M},1,0,0),\ n^\mu = \frac{1}{\sqrt{2}}(\tfrac{1}{M},-1,0,0),\ m^\mu = (0,0,m^a) \tag{2}$$

which immediately implies $\Psi_4 = \bar{\Psi}_0$ and $\Psi_3 = -\bar{\Psi}_1$. Next, one can express the Weyl tensor, the Riemann tensor etc. using the above decomposition in terms of 2-metric $\gamma_{ab}$, extrinsic curvature $K_{ab}$, lapse $M$ and their derivatives. Upon projecting the Weyl tensor onto the tetrad and taking the horizon limit $M \to 0$ one gets the Weyl scalars on the horizon. Petrov type is then determined based on curvature invariants $I, J$ and coefficients $K, L, N$

$$I = \Psi_0\Psi_4 - 4\Psi_1\Psi_3 + 3\Psi_2^2,\ J = \det\begin{pmatrix}\Psi_4 & \Psi_3 & \Psi_2\\ \Psi_3 & \Psi_2 & \Psi_1\\ \Psi_2 & \Psi_1 & \Psi_0\end{pmatrix} \tag{3}$$

$$K = \Psi_1\Psi_4^2 - 3\Psi_4\Psi_3\Psi_2 + 2\Psi_3^3,\ L = \Psi_2\Psi_4 - \Psi_3^2,\ N = 12L^2 - \Psi_4^2 I \tag{4}$$

The resulting Petrov type is either D ($\Psi_2 \neq 0$) or O ($\Psi_2 = 0$).

In the case of the freely falling observer the adapted tetrad is given by simple transformation from (2)

$$\hat{l}^\mu = zl^\mu,\ \hat{n}^\mu = z^{-1}n^\mu \tag{5}$$

where $z = exp(-\alpha)$, $\cosh\alpha = \frac{E}{M}$, with $E$ being an energy per unit mass for radially infalling geodesic. In this frame invariants $I, J$ do not change but the coefficients are modified

$$\hat{K} = z^{-3}K,\ \hat{L} = z^{-2}L,\ \hat{N} = z^{-4}N \tag{6}$$

Since $z \to 0$ on the horizon the coefficients $\hat{K}, \hat{L}, \hat{N}$ can be nonzero in the limit (unlike for static observer). The Petrov type is either II ($\Psi_2 \neq 0$) or III ($\Psi_2 = 0$) here. Due to singular nature of the static frame on the horizon these results are more physically relevant.

## 3 Quasilocal Horizons

As mentioned in the Introduction in the general dynamical situation we use the SFOTH—spacelike future outer trapping horizon—which has the following properties:

1. spacelike submanifold foliated by closed 2-surfaces with null normal fields $l, n$
2. expansion $\Theta_l = 0$ (marginal)
3. expansion $\Theta_n < 0$ (future)
4. $\mathscr{L}_n\Theta_l < 0$ (outer)

We employ a double-null foliation developed by Hayward [2] (mainly for the characteristic initial value problem and the trapping horizon definition) and adapted by Brady and Chambers [6] to study a nonlinear stability of Kerr-type Cauchy horizons.

The procedure is based on a local foliation by closed orientable 2-surfaces $S$ with smooth embedding $\phi : S \times [0, U) \times [0, V) \to \mathscr{M}$ and induced spatial metric $h_{ab}$ on $S$ with corresponding covariant derivative $D_a$. Null vectors $l^\mu, n^\mu$ are normal to $S$ and there is a spatial two vector $s^a$ called shift (encoding freedom in identifying points on subsequent surfaces). Evolution of the induced metric is described using Lie derivatives along $l$ and $n$

$$\Sigma_{ab} = \mathscr{L}_l h_{ab} \quad , \quad \tilde{\Sigma}_{ab} = \mathscr{L}_n h_{ab} \tag{7}$$

$$\theta = \tfrac{1}{2}h^{ab}\Sigma_{ab} \quad , \quad \tilde{\theta} = \tfrac{1}{2}h^{ab}\tilde{\Sigma}_{ab} \tag{8}$$

$$\sigma_{ab} = \Sigma_{ab} - \theta h_{ab} \quad , \quad \tilde{\sigma}_{ab} = \tilde{\Sigma}_{ab} - \tilde{\theta}h_{ab} \tag{9}$$

$$\omega_a = \tfrac{1}{2}h_{ab}\mathscr{L}_l s^b \tag{10}$$

$\theta, \tilde{\theta}$ being expansions, $\sigma_{ab}, \tilde{\sigma}_{ab}$ shears and $\omega_a$ anholonomicity (related to normal fundamental form). We assume normalized null vectors thus having zero inaffinities.

From vacuum Einstein equations and contracted Bianchi identities one obtains

$$\mathscr{L}_l\theta = -\tfrac{1}{2}\theta^2 - \tfrac{1}{4}\sigma_{ab}\sigma^{ab} \tag{11}$$

$$\mathscr{L}_l h = \theta h \tag{12}$$

$$\mathscr{L}_l\omega_a = -\theta\omega_a + \tfrac{1}{2}D^b\sigma_{ab} - \tfrac{1}{2}D_a\theta \tag{13}$$

$$\mathscr{L}_l(h^{-1/2}h_{ab}) = h^{-1/2}\sigma_{ab} \tag{14}$$

After expressing curvature tensors in the given frame we get the following Weyl scalars in vacuum

$$4\Psi_0 = (2\mathscr{L}_l\Sigma_{ab} - \Sigma_{am}h^{mn}\Sigma_{bn})m^a m^b \tag{15}$$

$$4\Psi_1 = (2\omega^m\Sigma_{am} + 4\mathscr{L}_l\omega_a)m^a \tag{16}$$

$$4\Psi_2 = (2\mathscr{L}_n\Sigma_{ab} - 4D_a\omega_b - \Sigma_{am}h^{mn}\tilde{\Sigma}_{bn} - 4\omega_a\omega_b)m^a\bar{m}^b \tag{17}$$

$$4\Psi_3 = -(2\omega^m\tilde{\Sigma}_{am} + 4\mathscr{L}_n\omega_a)\bar{m}^a \tag{18}$$

$$4\Psi_4 = (2\mathscr{L}_n\tilde{\Sigma}_{ab} - \tilde{\Sigma}_{am}h^{mn}\tilde{\Sigma}_{bn})\bar{m}^a\bar{m}^b \tag{19}$$

Next, we use the vanishing of expansion and further fixing of the spatial part of the frame for simplification. We evaluate the first term on the right-hand side of equation (15) noting that

$$\mathscr{L}_l\Sigma_{ab} = \mathscr{L}_l\sigma_{ab} + \theta\Sigma_{ab} + h_{ab}\mathscr{L}_l\theta \tag{20}$$

Using the projection and the horizon condition we obtain

$$m^a m^b\mathscr{L}_l\Sigma_{ab} = m^a m^b\mathscr{L}_l\sigma_{ab} \tag{21}$$

Assuming (see [6]) the Lie-propagated spatial part of the frame and equation (14) we arrive at

$$0 = \mathscr{L}_l(h^{-1/2}h_{ab}m^a m^b) = h^{-1/2}\sigma_{ab}m^a m^b \tag{22}$$

Next, we may assume that $\omega_a = 0$ initially on $S$ and would like to have $\mathscr{L}_l\omega_a = 0$ as well. Indeed, the first and the last terms of equation (13) vanish on the horizon and by further locally fixing the spatial part of the frame we obtain $m^a D^b\sigma_{ab} = 0$. In a similar way, one can show that $\Sigma_{am}h^{mn}\Sigma_{bn}m^a m^b = 0$ on the horizon.

Then $\Psi_0 = 0$ and $\Psi_1 = 0$. Assuming regularity of $\Psi_{\{2,3,4\}}$ we have $I^3 = 27J^2$ and therefore Petrov type II. Clearly the spacetime is generically type I away from the horizon.

In the future, we would like to check whether stronger statements are possible (with additional assumptions), generalize the results to well-behaved matter fields

and nonzero cosmological constant. Also, we would like to extend the analysis to other important tensors (Ricci etc.).

**Acknowledgements** This work was supported by grant GACR 202/09/0772 and project UNCE 204020/2012.

## References

1. Hawking, S.W., Ellis, G.F.R.: The large scale structure of space-time. CUP, Cambridge (1975)
2. Hayward, S.A.:General laws of black-hole dynamics. Phys. Rev. D **49**, 6467–74 (1994)
3. Ashtekar, A., Beetle, C., Fairhurst, S.: Mechanics of isolated horizons. Class. Quant. Grav. **17**, 253–298 (2000)
   Ashtekar, A., Krishnan, B.: Dynamical horizons and their properties. Phys. Rev. D **68**, 104030 (2003)
4. Pravda, V., Zaslavskii, O.B.: Curvature tensors on distorted Killing horizons and their algebraic classification. Class. Quant. Grav. **22**, 5053–5072 (2005)
5. Medved, A.J.M., Martin, D., Visser, M.: Dirty black holes: spacetime geometry and near-horizon symmetries, Class. Quant. Grav. **21**, 3111 (2004)
6. Brady, P.R., Chambers, C.M.: Non-linear instability of Kerr-type Cauchy horizons, Phys. Rev. D **51**, 4177 (1995)

# Dynamics of Apparent Horizons in Quantum Gravitational Collapse

**Yaser Tavakoli, Andrea Dapor, and João Marto**

**Abstract** We study the gravitational collapse of a massless scalar field within the effective scenario of loop quantum gravity. Classical singularity is avoided and replaced by a quantum bounce in this model. It is shown that, quantum gravity effects predict a threshold scale bellow which no horizon can form as the collapse evolves towards the bounce.

## 1 Gravitational Collapse with a Massless Scalar Field

Loop quantum gravity (LQG) provides a fruitful ground to investigate the resolution of the classical singularities which arise in the gravitational collapse. In view of this approach, it is of interest and well motivated to further assess how LQG can affect on the evolution of the trapped surfaces and the horizon formation during the collapse. In this paper we introduce a spherically symmetric framework for the gravitational collapse. We consider the dynamical space-time inside the collapsing sphere to be *homogeneous* and is given by the flat Friedmann–Robertson–Walker (FRW) metric as [1],

$$g^{-}_{ab}dx^a dx^b = -dt^2 + a^2(t)dr^2 + R^2(t,r)d\Omega^2, \tag{1}$$

where $R(t,r) = ra(t)$ is the area radius of the collapse. In terms of the $SU(2)$ variable of LQG we introduce the phase space variables for the interior space-time

Y. Tavakoli (✉) · J. Marto
Departamento de Física, Universidade da Beira Interior, 6200 Covilhã, Portugal
e-mail: tavakoli@ubi.pt; jmarto@ubi.pt

A. Dapor
Instytut Fizyki Teoretycznej, Uniwersytet Warszawski, ul. Hoża 69, 00-681 Warsaw, Poland
e-mail: andrea.dapor@fuw.edu.pl

A. García-Parrado et al. (eds.), *Progress in Mathematical Relativity, Gravitation and Cosmology*, Springer Proceedings in Mathematics & Statistics 60,
DOI 10.1007/978-3-642-40157-2_65, 

to be $c = \gamma\dot{a}$ and $p = a^2$ [2]. Considering a *homogeneous* and *massless* scalar field for the collapsing matter source, the four dimensional phase space $(c, p; \phi, p_\phi)$ is governed by the fundamental Poisson brackets $\{c, p\} = (8\pi G/3)\gamma$, and $\{\phi, p_\phi\} = 1$. Then, the total classical Hamiltonian constraint for the system can be written as [2]

$$C = C_{\rm gr} + C_\phi = -(6/\gamma^2)c^2\sqrt{|p|} + 8\pi G p_\phi^2/|p|^{3/2} = 0, \tag{2}$$

where $p_\phi$ is a constant of motion in the classical theory. In addition, the energy density and pressure of the collapsing matter reads

$$\rho_\phi = p_\phi^2/2V^2 = p_\phi^2/2|p|^3 = -p_\phi. \tag{3}$$

The point $p = 0$ characterizes a situation where the volume $V = |p|^{3/2}$, of the collapsing matter is zero and the energy density of the matter cloud diverges. Therefore, if this point lies on any dynamical trajectory, it is an end point of that trajectory corresponding to a curvature singularity which characterizes the collapse end state.

Interior space-time should be matched at the boundary to a sufficient exterior geometry such as the generalized Vaidya metric (c.f. see [1]):

$$g^+_{ab}dx^a dx^b = -(1 - 2M/r_{\rm v})d{\rm v}^2 - 2d{\rm v}dr_{\rm v} + r_{\rm v}^2 d\Omega^2. \tag{4}$$

The formation or avoidance of a black hole in the exterior region depends on developing an apparent horizon in the interior space-time. Therefore, in this paper we are mainly concerned with whether or not horizons can form during the evolution of the interior space-time in the presence of the quantum effects (c.f. Sect. 2).

In order to study the geometry of trapped surfaces inside the star, let us introduce the radial null geodesics satisfying $g^-_{ab}dx^a dx^b = 0$, whose expansions, $\theta_\pm$, measure whether the bundle of null rays normal to the collapsing sphere is diverging ($\theta_\pm > 0$) or converging ($\theta_\pm < 0$). Let us define the useful parameter $\Theta \equiv \theta_+\theta_-$ [3]:

$$\Theta = \left(\dot{R}^2/R^2 - 1/R^2\right)/2. \tag{5}$$

So that, the space-time is referred to, respectively, as trapped, untrapped and marginally trapped if: $\Theta(t, r) > 0$, $\Theta(t, r) < 0$, and $\Theta(t, r) = 0$.

## 2 Quantum Geometry of Trapped Surfaces

The strategy here is to consider the interior space-time as a classical phase space, of the FRW model, coupled to matter that is equipped with a quantum corrected Hamiltonian constraint; the effective scenario of LQG. This constraint and its

resulting Hamilton equations of motion, provide the full set of effective Einstein's equation for the collapsing model herein. In this quantization scheme, the curvature 2-form $c^2$ is modified by $SU(2)$ holonomy along suitable loops; the leading order quantum corrections are captured in the following effective Hamiltonian [4]:

$$C_{\rm eff} = -(3/8\pi G\gamma^2\mu_o^2)\sqrt{|p|}\sin^2(\mu_o c) + B(p)p_\phi^2/2, \tag{6}$$

where $B(p)$ is the eigenvalues of operator $\widehat{|p|^{-3/2}}$ [4]. Consider a new variable $v$, given as the eigenvalue of the volume operator $\hat{V}|v\rangle = (8\pi\gamma/6)^{\frac{3}{2}}K^{-1}|v|\ell_{\rm Pl}^3|v\rangle$: then, equations of motion can be obtained by using the Hamilton's equation [4]:

$$\dot{v} = \{v, C_{\rm eff}\} = (2|v|^{1/3}/\gamma\mu_o K)(8\pi\gamma\ell_{\rm Pl}^2/6)^{1/2}\sin(\mu_o c)\cos(\mu_o c), \tag{7}$$

$$\dot{\phi} = (1/16\pi G)\{\phi, C_{\rm eff}\} = (8\pi\gamma\ell_{\rm Pl}^2/6)^{-3/2}Kp_\phi|v|^{-1}\,. \tag{8}$$

where $K = (2\sqrt{2}/3\sqrt{3\sqrt{3}})$. Using $C_{\rm eff} = 0$ in Eqs. (7) and (8), the modified Friedmann equation reads

$$\dot{a}^2/a^2 = \dot{v}^2/(9v^2) = (8\pi G/3)\rho_\phi(1-\rho_\phi/\rho_{\rm cr}), \tag{9}$$

where $\rho_{\rm cr} = \sqrt{3}/(16\pi^2\gamma^3G^2\hbar) \approx 0.82\rho_{\rm Pl}$. Notice that, in the effective scenario of LQG, the energy density $\rho_\phi = p_\phi^2/2|p|^3$ holds in the range $\rho_i < \rho_\phi < \rho_{\rm cr}$. In the limit $\rho_\phi\ell^2\rho_{\rm cr}$, the standard classical Friedmann equation, $\dot{a}^2/a^2 = (8\pi G/3)\rho_\phi$, is recovered. Equation (9) shows that, the speed of collapse $|\dot{a}|$ starts to increase initially and reaches its maximum when $\rho_\phi = 0.4\rho_{\rm cr}$:

$$|\dot{a}|_{\rm max} = \sqrt{4\pi G/5}(0.4\rho_{\rm cr})^{1/3}p_\phi\,, \tag{10}$$

at the scale $a_{\rm max}$, given by $a_{\rm max} \approx 1.16\,a_{\rm cr}$, where $a_{\rm cr} := (p_\phi^2/2\rho_{\rm cr})^{1/6}$. Hereafter, $|\dot{a}|$ decreases by time and vanishes as $\rho_\phi \to \rho_{\rm cr}$; thus, the collapsing star bounces at the minimum volume $V_{\rm min} = a_{\rm cr}^3 \approx (1.3\times10^{-33}{\rm cm}^3)p_\phi$.

To discuss the quantum geometry of the trapped region from the perspective of the effective scenario of LQG, it is convenient to rewrite $\Theta$ in Eq. (5) as [1]

$$\Theta(a) = 4\pi G/3\rho_\phi(1-\rho_\phi/\rho_{\rm cr}) - 1/(2r_{\rm b}^2a^2), \tag{11}$$

where we have replaced $\dot{a}^2/a^2$ here by the effective Hubble rate Eq. (9), and $\rho_\phi = p_\phi^2/(2a^6)$. Figure 1 shows the behavior of $\Theta$ against the scale factor $a$ for the different choices of the initial conditions for constants $r_{\rm b}$ and $p_\phi$. Equation of apparent horizon on the effective geometry can be obtained by setting $\Theta = 0$. The left plot in Fig. 1 (solid curve) indicates an untrapped interior space-time without any horizon forming, whereas two others show trapped regions; the middle and the right plots correspond to one and two horizons forming, respectively. Notice that, only one horizon would always form classically (dashed curves in Fig. 1).

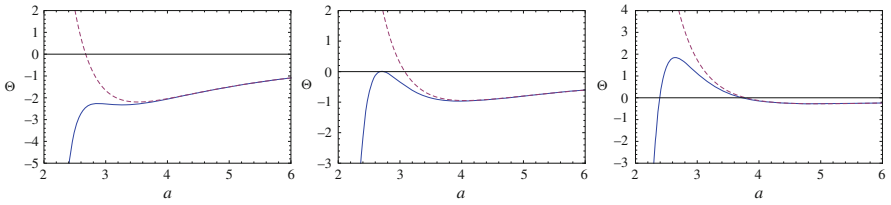


**Fig. 1** Behaviors of $\Theta(a)$ in the classical (*dashed curve*) and quantum (*solid curve*) regimes for the value of parameter $G = c_{\text{light}} = 1$, $p_\phi = 10\,000$, and the different values of $r_\text{b}$

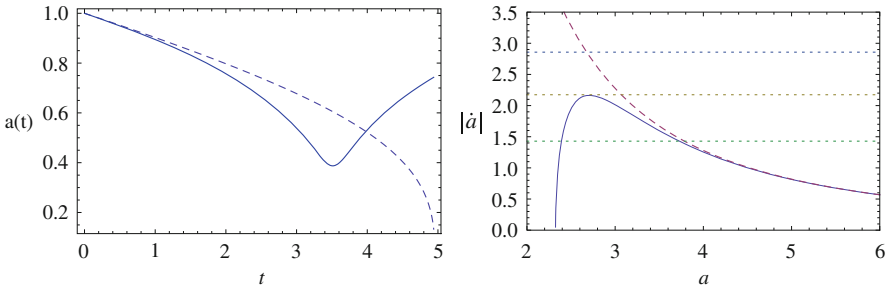


**Fig. 2** *Left figure* shows behavior of the scale factor, $a(t)$, with time in classical (*dashed curve*) and semiclassical (*solid curve*) regimes. The *right plot* shows the speed of collapse, $|\dot{a}|$, with respect to the scale factor $a$, in classical (*dashed curve*) and semiclassical (*solid curve*) regimes. The *horizontal dotted lines* correspond to different values of $r_\text{b}$; the *upper, middle and the lower lines* are, respectively, the cases $r_\text{b} < r_\text{th}$, $r_\text{b} = r_\text{th}$, and $r_\text{b} > r_\text{th}$

Using Eq. (5), we can determine the speed of the collapse at which horizon can form, where $\Theta = 0$, from which we get $\dot{R}^2 = 1$, and whence, $|\dot{a}|_\text{AH} = 1/r_\text{b}$. When the speed of collapse, $|\dot{a}|$, reaches the value $1/r_\text{b}$, apparent horizons form (Fig. 2). In other words, in order to have the horizon formation, $r_\text{b}$ must satisfy $r_\text{b} \geq |\dot{a}|^{-1}_\text{max}$. It is convenient to introduce a radius $r_\text{th}$ as,

$$r_\text{th} := |\dot{a}|^{-1}_\text{max}. \tag{12}$$

Therefore, as it is shown in Fig. 2, radius $r_\text{th}$ is a threshold radius for the horizon formation. More precisely, for the case $r_\text{b} < r_\text{th}$, no horizon would form as collapse evolves; the case $r_\text{b} = r_\text{th}$, corresponds to the formation of a dynamical horizon at the boundary of two regions; and finally, for the case $r_\text{b} > r_\text{th}$, two horizons will form, one inside and the other outside of the collapsing matter.

**Acknowledgements** The authors would like to thank R. Goswami and J. Velhinho for the useful discussion and suggestions. YT is supported by the FCT (Portugal) through the fellowship SFRH/BD/43709/2008.

## References

1. Y. Tavakoli, A. Dapor and J. Marto, in preparation.
2. A. Ashtekar, M. Bojowald, J. Lewandowski, Adv. Theor. Math. Phys. **7**, 233 (2003).
3. S. A Hayward, Phys. Rev. D **53**, 1938 (1996).
4. A. Ashtekar, T. Pawlowski, and P. Singh, Phys. Rev. D **74**, 084003 (2006).

# Thermodynamical Inequivalence of Stress-Energy and Spin Tensors

**Leonardo Tinti**

**Abstract** It is shown that different pairs of stress-energy-momentum and spin tensors of quantum relativistic fields, which are commonly believed to be equivalent in special relativity, are in fact inequivalent. Different tensors imply different mean values of physical quantities like four-momentum and angular momentum density, and, in non-equilibrium situation, entropy production and transport coefficients. This result implies that specific stress-energy-momentum and spin tensors are physically meaningful even in the absence of gravitational coupling and raises the issue of finding the right pair (or the right class of pairs) of tensors. The existence of a non-vanishing spin tensor and, especially, a non symmetric stress-energy-momentum tensor would have major consequences in hydrodynamics, gravity and cosmology.

## 1 Introduction

It is commonly known that stress-energy and spin tensors are not uniquely defined in field theory. Distinct stress-energy tensors differing by the divergence of a rank three tensor provide, once integrated in three-dimensional space, the same generators of space-time translations provided that the flux of the additional rank three tensor field vanishes at the boundary. Within quantum field theory on a flat space-time, it is possible to generate apparently equivalent stress-energy-momentum tensors which are, for instance, symmetric or non symmetric. Indeed, gravitational coupling provides an unambiguous way of defining the stress-energy tensor. Using Einstein–Hilbert action, the stress-energy-momentum tensor in Einstein field equation is symmetric by construction [1]; but, relaxing the torsion free requirement of the

L. Tinti (✉)
Università di Firenze and INFN Sezione di Firenze, Via Sansone 1, Florence, Italy
e-mail: tinti@fi.infn.it

A. García-Parrado et al. (eds.), *Progress in Mathematical Relativity, Gravitation and Cosmology*, Springer Proceedings in Mathematics & Statistics 60,
DOI 10.1007/978-3-642-40157-2_66, 

connection (for instance [2]) the Einstein tensor is no longer symmetric, and therefore the stress-energy tensor itself ought to be non symmetric in the most general case.

Studying relativistic hydrodynamics we found that, even on a flat space time, it is possible to discriminate between different microscopic (quantum) spin tensors, and, consequently, between different quantum stress-energy-momentum tensors.

## 2 Transformation of Stress-Energy and Spin Tensors

Relativistic hydrodynamics can be seen as the theory describing the dynamical behavior of the stress-energy-momentum tensor $T^{\mu\nu}$ ( the mean value of the underlying quantum stress-energy tensor $T^{\mu\nu} = \mathrm{tr}(\hat{\rho}\hat{T}^{\mu\nu})$) and the spin tensor[1] $S^{\lambda,\mu\nu}$ ($S^{\lambda,\mu\nu} = \mathrm{tr}(\hat{\rho}\hat{S}^{\lambda,\mu\nu})$), fulfilling the continuity equations:

$$\partial_\mu T^{\mu\nu} = 0 \qquad \partial_\lambda S^{\lambda,\mu\nu} = T^{\nu\mu} - T^{\mu\nu} \tag{1}$$

The total four-momentum $P^\mu$ and angular momentum $J^{\mu\nu}$ read:

$$P^\mu = \int \mathrm{d}^3\mathbf{x}\, T^{0\mu} \qquad J^{\mu\nu} = \int \mathrm{d}^3\mathbf{x}\, \left[x^\mu T^{0\nu} - x^\nu T^{0\mu} + S^{0,\mu\nu}\right] \tag{2}$$

so equations (1) ensure the conservation of energy, momentum and total angular momentum, provided that fluxes at the spatial boundary vanish.

Applying Noether's theorem to the action of a quantum field we get [3], from space time translation invariance:

$$\partial_\mu \hat{T}^{\mu\nu} = 0 \qquad \hat{P}^\mu = \int \mathrm{d}^3\mathbf{x}\, \hat{T}^{0\mu} \tag{3}$$

where $\hat{P}$ is the conserved charge, the generator of space-time translations, the four momentum operator. While from rotation and boost invariance we have:

$$\partial_\lambda \hat{S}^{\lambda,\mu\nu} = 0 \qquad \hat{J}^{\mu\nu} = \int \mathrm{d}^3\mathbf{x}\, \left[x^\mu \hat{T}^{0\nu} - x^\nu \hat{T}^{0\mu} + \hat{S}^{0,\mu\nu}\right] \tag{4}$$

If we take the average values of equations (3), (4) we recover the classical relations (1) and (2).

The canonical couple from Noether's theorem however is not the only one fulfilling (3) and (4). Once a particular couple $(\hat{T}, \hat{S})$ is found, for instance the

[1] Here the comma divides the antisymmetric indices $\mu\nu$ from the other one $\lambda$, it is not a partial derivation.

canonical one, it is possible to generate new couples $(\hat{T}', \hat{S}')$ through the following pseudo-gauge transformation:

$$\hat{T}'^{\mu\nu} = \hat{T}^{\mu\nu} - \frac{1}{2}\partial_\alpha \left(\hat{\Phi}^{\alpha,\mu\nu} - \hat{\Phi}^{\mu,\alpha\nu} - \hat{\Phi}^{\nu,\alpha\mu}\right)$$

$$\hat{S}'^{\lambda,\mu\nu} = \hat{S}^{\lambda,\mu\nu} - \hat{\Phi}^{\lambda,\mu\nu} - \partial_\alpha \hat{Z}^{\alpha\lambda,\mu\nu} \tag{5}$$

where $\hat{\Phi}$ is a rank three tensor field antisymmetric in the last two indices (often called and henceforth referred to as superpotential) and $\hat{Z}$ is a rank four tensor antisymmetric in the pairs $\alpha \leftrightarrow \lambda$ and $\mu \leftrightarrow \nu$.

The new pair $(\hat{T}', \hat{S}')$ fulfills by construction the same continuity equations of the starting couple $(\hat{T}, \hat{S})$, and the spatial integrals are still the Poincaré generators.[2] The couples $(\hat{T}, \hat{S})$ and $(\hat{T}', \hat{S}')$ are regarded as equivalent[3] in quantum field theory because they give the same total energy, momentum and angular momentum, in the operator sense.

## 3 Equilibrium Inequivalence

In classical physics we have a stronger requirement with respect to a quantum theory: we would like the energy, momentum and angular momentum of any arbitrary macroscopic spatial region to be well defined concepts. Otherwise stated, we would like to have objective values for energy, momentum and angular momentum densities.

The change that classical quantities (i.e. average values of operators) undergo as a reflection of a variation of quantum tensors crucially depends on the physical state of the system $\hat{\rho}$. The freedom of varying the stress-energy and spin tensors at a quantum level depends on the symmetry features of the physical state: a highly symmetric state allows more changes of quantum tensors than a state with little symmetry does. For instance, the familiar grand-canonical equilibrium density matrix $\hat{\rho} = 1/Z \exp[-\hat{H}/T + \mu\hat{Q}/T]$ enjoys space-time translation invariance, the average value of a gradient is then vanishing. Therefore the average value of the first equation in (5) simply is $T'^{\mu\nu} = T^{\mu\nu}$, and in general [5] any pair of quantum tensors will yield the same energy, momentum and angular momentum density.

The situation is remarkably different for a thermodynamical system having a macroscopic non-vanishing total angular momentum. Having lost space translation invariance, the mean values of gradients are not vanishing any longer. We performed

[2] Assuming suitable boundary conditions for $\hat{\Psi}$ and $\hat{Z}$.

[3] It is usually taken, among all possible stress-energy-momentum tensors, the most convenient one, based on computational considerations. For instance, the Spin 1/2 case in [4].

an explicit calculation for the simplest theory having a non vanishing canonical spin tensor, namely the free Dirac field. We compared the results for the canonical pair of tensors and the Belinfante symmetrized couple.[4] We found [5] that the linear and angular momentum density calculated from the two pairs differ, and the difference persist in the non-relativistic limit. From an experimental viewpoint, in principle, we could decide if a pair of tensor is wrong by measuring with sufficient accuracy the angular momentum density of a rotating system at full thermodynamical equilibrium.

## 4 Non-equilibrium Inequivalence

The inequivalence extends to non-equilibrium thermodynamical quantities. The use of different stress-energy-momentum tensors, related by a pseudo-gauge transformation (5), to calculate transport coefficients with the relativistic Kubo formula leads, in general, to different results.

A suitable formalism to calculate transport coefficients for relativistic quantum fields without going through kinetic theory was developed by Zubarev [6], extending to the relativistic domain a formalism already introduced by Kubo. We extended the framework of the non-equilibrium density operator to the case of a non-vanishing spin tensor [7]. We found that in general the non-equilibrium density operator is not invariant under a pseudo-gauge transformation, therefore transport coefficients are also modified. In particular we focused on the modification of the Kubo formula for shear viscosity:

$$\eta' - \eta = -\lim_{k\to 0} \mathrm{Im} \int \mathrm{d}^3\mathbf{x}\, e^{ikx^1} \langle \left[ \hat{\Xi}^{012}(\tau, \mathbf{x}), \hat{\Xi}^{012}(0, \mathbf{0}) \right] \rangle_0 + \\ - 2 \lim_{\varepsilon\to 0} \lim_{k\to 0} \mathrm{Im} \int_{-\infty}^{0} \mathrm{d}t\, e^{\varepsilon t} \int \mathrm{d}^3\mathbf{x}\, e^{ikx^1} \langle \left[ \hat{\Xi}^{012}(x), \hat{T}_S^{12}(0, \mathbf{0}) \right] \rangle_0 \qquad (6)$$

where $\hat{\Xi}^{\lambda\mu\nu} = 1/2(\hat{\Phi}^{\mu,\lambda\nu} + \hat{\Phi}^{\nu,\lambda\mu})$ and $\hat{T}_S^{\mu\nu} = 1/2(\hat{T}^{\mu\nu} + \hat{T}^{\mu\nu})$.

An important point to make is that the found dependence of the transport coefficients is indeed physically meaningful. The variation of some coefficient is not compensated by a corresponding variation of another coefficient so as to eventually leave measurable quantities unchanged. This has been proved, also in [7], where it was shown that total entropy itself undergoes a variation under a transformation of the stress-energy and spin tensor.

[4] This is the transformation using the spin tensor itself as the superpotential $\hat{S} = \hat{\Phi}$ and $\hat{Z} = 0$.

## References

1. C. W. Misner, K. S. Thorne, J. A. Wheeler, *Gravitation*, W. H. Freeman and Company (1973).
2. F. W. Hehl, P. von der Heyde, and G. D. Kerlick, Rev. Mod. Phys. **48**, 393 (1976).
3. S. Weinberg, *The Quantum Theory Of Fields* Vol. 1 Cambridge University Press (1995).
4. S. R. De Groot, W. A. van Leeuwen, Ch. G. van Weert, *Relativistic kinetic theory*, North Holland (1980).
5. F. Becattini and L. Tinti, Phys. Rev. D **84**, 025013 (2011).
6. D. N. Zubarev, Sov. Phys. Doklady **10**, 850 (1966); D. N. Zubarev and M. V. Tokarchuk, Theor. Math. Phys. **88**, 876 (1992) [Teor. Mat. Fiz. **88N2**, 286 (1992)].
7. F. Becattini and L. Tinti, arXiv:1209.6212

# Wormholes and Off-Diagonal Solutions in f(R,T), Einstein and Finsler Gravity Theories

**Sergiu I. Vacaru**

**Abstract** The aims of this work are (1) to sketch a proof that there are such parameterizations of the local frame and canonical connection structures when the gravitational field equations in f(R,T)-modified gravity, MG, can be integrated in generic off-diagonal forms with metrics depending on all spacetime coordinates and (2) to provide some examples of exact solutions.

## 1 Nonholonomic Deformations in Modified Gravity Theories

We study gravity theories formulated on a spacetime manifold $\mathbf{V}, dim\mathbf{V} = n \geq 4$ (for Finsler models, on tangent bundle $T\mathbf{V}$) endowed with metric, $\mathbf{g}$, and compatible linear connection $\mathbf{D}$, structures, $\mathbf{Dg} = 0$, see details in Refs. [1–4]. Our goal is to prove that there are such local frame and canonical connection structures when the gravitational field equations in $f(R,T)$-modified gravity, MG, see reviews [5–8], can be integrated in generic off-diagonal forms with metrics depending on all spacetime coordinates. We provide explicit examples when generalized solutions in MG can be equivalently modelled as effective Einstein spaces and determine deformations of wormhole spacetimes in general relativity (GR).

### *1.1 Geometric Preliminaries*

We consider a conventional horizontal (h) and vertical (v) splitting of the tangent space $T\mathbf{V}$, when a non-integrable (equivalently, nonholonomic, or anholonomic)

S.I. Vacaru (✉)
Alexandru Ioan Cuza University, [Rector's office], Alexandru Lapuşneanu street, nr. 14, Corpus R, UAIC, office 323; Iaşi, 700057, Romania
e-mail: sergiu.vacaru@uaic.ro; Sergiu.Vacaru@gmail.com

A. García-Parrado et al. (eds.), *Progress in Mathematical Relativity, Gravitation and Cosmology*, Springer Proceedings in Mathematics & Statistics 60,
DOI 10.1007/978-3-642-40157-2_67, 

distribution $\mathbf{N}:\ T\mathbf{V}=h\mathbf{V}\oplus v\mathbf{V}$ (for Finsler theories, $\mathbf{N}:\ TT\mathbf{V}=hT\mathbf{V}\oplus vT\mathbf{V}$). Locally, such a h–v-splitting is determined by a set of coefficients $\mathbf{N}=\{N_i^a(x,y)\}$ and coordinates parameterized: $u=(x,y)$, $u^\mu=(x^i,y^a)$, where the h–(v-)indices run $i,j,\ldots=1,2,\ldots,n$ $(a,b,\ldots=n+1,\ldots,n+n)$. There are N-adapted frames $\mathbf{e}_\nu=(\mathbf{e}_i,e_a)$, $\mathbf{e}^\mu=(e^i,\mathbf{e}^a)$,

$$\mathbf{e}_i=\partial/\partial x^i-\ N_i^a(u)\partial/\partial y^a,\ e_a=\partial_a=\partial/\partial y^a,\ e^i=dx^i,\ \mathbf{e}^a=dy^a+\ N_i^a(u)dx^i, \tag{1}$$

which satisfy the conditions $[\mathbf{e}_\alpha,\mathbf{e}_\beta]=\mathbf{e}_\alpha\mathbf{e}_\beta-\mathbf{e}_\beta\mathbf{e}_\alpha=W_{\alpha\beta}^\gamma\mathbf{e}_\gamma$, with anholonomy coefficients $W_{ia}^b=\partial_a N_i^b$, $W_{ji}^a=\Omega_{ij}^a=\mathbf{e}_j\left(N_i^a\right)-\mathbf{e}_i(N_j^a)$.

On a nonholonomic manifold $(\mathbf{V},\mathbf{N})$, and/or nonholonomic bundle $(T\mathbf{V},\mathbf{N})$, we can represent any data $(\mathbf{g},\mathbf{D})$ in N-adapted form (preserving under parallel transport a chosen h–v-splitting) parameterized as: 1) a *distinguished metric, d-metric,*

$$\mathbf{g}=g_\alpha(u)\mathbf{e}^\alpha\otimes\mathbf{e}^\beta=g_i(x)dx^i\otimes dx^i+g_a(x,y)\mathbf{e}^a\otimes\mathbf{e}^a. \tag{2}$$

and 2) a *distinguished connection, d-connection,* $\mathbf{D}=(hD,vD)$.

Any d-connection is characterized by d-torsion, nonmetricity, and d-curvature structures: $\mathcal{T}(\mathbf{X},\mathbf{Y}):=\mathbf{D}_\mathbf{X}\mathbf{Y}-\mathbf{D}_\mathbf{Y}\mathbf{X}-[\mathbf{X},\mathbf{Y}]$, $\mathcal{Q}(\mathbf{X}):=\mathbf{D}_\mathbf{X}\mathbf{g}$, $\mathcal{R}(\mathbf{X},\mathbf{Y}):=\mathbf{D}_\mathbf{X}\mathbf{D}_\mathbf{Y}-\mathbf{D}_\mathbf{Y}\mathbf{D}_\mathbf{X}-\mathbf{D}_{[\mathbf{X},\mathbf{Y}]}$, where $\mathbf{X},\mathbf{Y}\in T\mathbf{V}$ (or $\in TT\mathbf{V}$, in Finsler like theories).

There are two "preferred" linear connections which can be defined for the same data $(\mathbf{g},\mathbf{N})$: 1) the *canonical d-connection* $\widehat{\mathbf{D}}$ uniquely determined by the conditions that it is metric compatible, $\widehat{\mathbf{D}}\mathbf{g}=\mathbf{0}$, and with zero h-torsion, $h\widehat{\mathcal{T}}=\{\hat{T}^i_{jk}\}=0$, and zero v-torsion, $v\widehat{\mathcal{T}}=\{\hat{T}^a_{bc}\}=0$; 2) the Levi–Civita (LC) connection, $\nabla$, when $\mathcal{T}=0$ and $\mathcal{Q}=0$, if $\mathbf{D}\to\nabla$. Such linear connections are related via a canonical distortion relation $\widehat{\mathbf{D}}=\nabla+\widehat{\mathbf{Z}}$. We can work equivalently on $\mathbf{V}$ and $T\mathbf{V}$ using both linear connections. For any data $(\mathbf{g},\mathbf{N},\widehat{\mathbf{D}})$, we can define and compute in standard form, respectively, the Riemann, $\widehat{\mathcal{R}}=\{\widehat{\mathbf{R}}^\alpha_{\ \beta\gamma\delta}\}$, and the Ricci, $\widehat{\mathcal{R}ic}=\{\widehat{\mathbf{R}}_{\alpha\beta}:=\widehat{\mathbf{R}}^\gamma_{\ \alpha\beta\gamma}\}$ d-tensors; for $\hat{R}:=\mathbf{g}^{\alpha\beta}\widehat{\mathbf{R}}_{\alpha\beta}$, we can introduce $\widehat{\mathbf{E}}_{\alpha\beta}:=\widehat{\mathbf{R}}_{\alpha\beta}-\frac{1}{2}\mathbf{g}_{\alpha\beta}\ \hat{R}$.

## 1.2 Nonholonomically Modified Gravity

We study theories with action

$$S=\frac{1}{16\pi}\int\delta u^{n+n}\sqrt{|\mathbf{g}_{\alpha\beta}|}[f(\hat{R},T)+\ {}^mL], \tag{3}$$

generalizing the so-called modified $f(R,T)$ gravity [5–7] to the case of d-connection $\widehat{\mathbf{D}}$, which can be considered for (pseudo) Riemannian spaces (as an "auxiliary" one) [1], for Hořava–Lifshits type modifications [3, 9] and on (non)

commutative Finsler spaces [2, 4, 8]. In (3), $T$ is the trace of the stress-energy momentum tensor constructed for the matter fields Lagrangian ${}^{m}L$. It is possible to elaborate a N-adapted variational formalism for a large class of models with perfect fluid matter with ${}^{m}L = -p$, for pressure $p$, and assuming that $f(\hat{R}, T) = {}^{1}f(\hat{R}) + {}^{2}f(T)$, where ${}^{1}F(\hat{R}) := \partial\, {}^{1}f(\hat{R})/\partial\hat{R}$ and ${}^{2}F(T) := \partial\, {}^{2}f(T)/\partial T$. We obtain a model of MG with effective Einstein equations, $\hat{\mathbf{E}}_{\alpha\beta} = \Upsilon_{\beta\delta}$, for source $\Upsilon_{\beta\delta} = {}^{ef}\eta\, G\, \mathbf{T}_{\beta\delta} + {}^{ef}\mathbf{T}_{\beta\delta}$, where ${}^{ef}\eta = [1 + {}^{2}F/8\pi]/\,{}^{1}F$ is the effective polarization of cosmological constant $G$, $\mathbf{T}_{\beta\delta}$ is the usual energy-momentum tensor for matter fields and the $f$-modification of the energy-momentum tensor results in ${}^{ef}\mathbf{T}_{\beta\delta} = [\frac{1}{2}({}^{1}f - {}^{1}F\ \hat{R} + 2p\,{}^{2}F + {}^{2}f)\mathbf{g}_{\beta\delta} - (\mathbf{g}_{\beta\delta}\,\hat{\mathbf{D}}_{\alpha}\hat{\mathbf{D}}^{\alpha} - \hat{\mathbf{D}}_{\beta}\hat{\mathbf{D}}_{\delta})\,{}^{1}F]/\,{}^{1}F$.

The effective Einstein equations decouple for parameterizations of metrics (2) when the coefficients $N_i^a(u)$ in (1) are such way prescribed that the corresponding nonholonomic constraints result in $\hat{\mathbf{D}}$ with $\hat{R} = const$ and $\Upsilon_{\delta}^{\beta} = (\Lambda + \lambda)\delta_{\delta}^{\beta}$ for an effective cosmological constant $\Lambda$ for modified gravity and $\lambda$ for a possible cosmological constant in GR. This results in $\hat{\mathbf{D}}_{\delta}\,{}^{1}F_{|\Upsilon=\Lambda+\lambda} = 0$, see details in [1–3].

## 2 Ellipsoid, Solitonic and Toroid Deformations of Wormholes

The general stationary ansatz for off-diagonal solutions is

$$\mathbf{ds}^2 = e^{\tilde{\psi}(\tilde{\xi},\theta)}(d\tilde{\xi}^2 + d\vartheta^2) + \frac{[\partial_{\varphi}\varpi(\tilde{\xi},\vartheta,\varphi)]^2}{\Lambda+\lambda}\left(1 + \varepsilon\frac{\partial_{\varphi}[\chi_4(\tilde{\xi},\vartheta,\varphi)\varpi(\tilde{\xi},\vartheta,\varphi)]}{\partial_{\varphi}\varpi(\tilde{\xi},\vartheta,\varphi)}\right)$$

$$r^2(\tilde{\xi})\sin^2\theta(\tilde{\xi},\vartheta)(\delta\varphi)^2 - \frac{e^{2\varpi(\tilde{\xi},\vartheta,\varphi)]}}{|\Lambda+\lambda|}[1 + \varepsilon\chi_4(\tilde{\xi},\vartheta,\varphi)]e^{2B(\tilde{\xi})}(\delta t)^2, \quad (4)$$

$$\delta\varphi = d\varphi + \partial_{\tilde{\xi}}[{}^{\eta}\tilde{A}(\tilde{\xi},\vartheta,\varphi) + \varepsilon\overline{A}(\tilde{\xi},\vartheta,\varphi)]d\tilde{\xi} + \partial_{\vartheta}[{}^{\eta}\tilde{A}(\tilde{\xi},\vartheta,\varphi) + \varepsilon\overline{A}(\tilde{\xi},\vartheta,\varphi)]d\vartheta,$$

$$\delta t = dt + \partial_{\tilde{\xi}}[{}^{\eta}n(\tilde{\xi},\vartheta) + \varepsilon\partial_i\overline{n}(\tilde{\xi},\vartheta)]\,d\tilde{\xi} + \partial_{\vartheta}[{}^{\eta}n(\tilde{\xi},\vartheta) + \varepsilon\partial_i\overline{n}(\tilde{\xi},\vartheta)]\,d\vartheta,$$

where $\tilde{\xi} = \int dr/\sqrt{|1 - b(r)/r|}$ for $b(r)$, $B(\tilde{\xi})$ determined by a wormhole metric in GR. For 4-d theories, we consider $x^i = (\tilde{\xi}, \theta)$ and $y^a = (\varphi, t)$.

### 2.1 Rotoid-Configurations

with a small parameter (eccentricity) $\varepsilon$ are "extracted" from (4) if we take for the $f$-deformations $\chi_4 = \overline{\chi}_4(r,\varphi) := \frac{2\overline{M}(r)}{r}\left(1 - \frac{2\overline{M}(r)}{r}\right)^{-1}\underline{\zeta}\sin(\omega_0\varphi + \varphi_0)$, for $r$ considered as a function $r(\tilde{\xi})$. Let us define

$$h_3 = \tilde{\eta}_3(\tilde{\xi},\vartheta,\varphi)[1 + \varepsilon\chi_3(\tilde{\xi},\vartheta,\varphi)]\,{}^{0}\overline{h}_3(\tilde{\xi},\vartheta),\ h_4 = \tilde{\eta}_4(\tilde{\xi},\vartheta,\varphi)[1 + \varepsilon\overline{\chi}_4(\tilde{\xi},\varphi)]\,{}^{0}\overline{h}_4(\tilde{\xi}), \text{for}$$

$$ {}^0\overline{h}_3 = r^2(\tilde{\xi})\sin^2\theta(\tilde{\xi},\vartheta),\ {}^0\overline{h}_4 = q(\tilde{\xi}),\ \tilde{\eta}_3 = \frac{[\partial_\varphi \varpi(\tilde{\xi},\vartheta,\varphi)]^2}{\Lambda+\lambda}, \tilde{\eta}_4 = \frac{e^{2\varpi(\tilde{\xi},\vartheta,\varphi)]}}{|(\Lambda+\lambda)|q(\tilde{\xi})} e^{2B(\tilde{\xi})}, \tag{5} $$

where $e^{2B(\tilde{\xi})} \to q(\tilde{\xi})$ if $\tilde{\xi} \to \xi$. For a prescribed $\tilde{\varpi}(\tilde{\xi},\vartheta,\varphi)$, we compute $\tilde{\chi}_3 = \chi_3(\tilde{\xi},\vartheta,\varphi) = \partial_\varphi[\overline{\chi}_4\tilde{\varpi}]/\partial_\varphi\tilde{\varpi}$, $\overline{w}_i = \frac{\partial_i(\, r(\tilde{\xi})\sin\theta(\tilde{\xi},\vartheta)\sqrt{|q(\tilde{\xi})|}\partial_\varphi[\overline{\chi}_4\varpi])}{e^{\varpi} r(\tilde{\xi})\sin\theta(\tilde{\xi},\vartheta)\sqrt{|q(\tilde{\xi})|}\partial_\varphi\varpi} = \partial_i\overline{A}(\tilde{\xi},\vartheta,\varphi)$, for $x^i = (\tilde{\xi},\vartheta)$. We model an ellipsoid configuration with $r_+(\tilde{\xi}_+) \simeq \frac{2\,\overline{M}(\,\tilde{\xi}_+)}{1+\varepsilon\underline{\zeta}\sin(\omega_0\varphi+\varphi_0)}$, for constants $\underline{\zeta}, \omega_0, \varphi_0$ and eccentricity $\varepsilon$. We obtain

$$ \begin{aligned} \mathbf{ds}^2 = {} & e^{\tilde{\psi}(\tilde{\xi},\theta)}(d\tilde{\xi}^2 + d\vartheta^2) + \frac{[\partial_\varphi\tilde{\varpi}]^2}{\Lambda+\lambda}(1+\varepsilon\frac{\partial_\varphi[\overline{\chi}_4\tilde{\varpi}]}{\partial_\varphi\tilde{\varpi}})\,{}^0\overline{h}_3[d\varphi + \partial_{\tilde{\xi}}(\,{}^\eta\tilde{A} + \varepsilon\overline{A})d\tilde{\xi} + \partial_\vartheta(\,{}^\eta\tilde{A} + \\ & \varepsilon\overline{A})d\vartheta]^2 - \frac{e^{2\tilde{\varpi}}}{|\Lambda+\lambda|}[1+\varepsilon\overline{\chi}_4(\tilde{\xi},\varphi)]e^{2B(\tilde{\xi})}[dt + \partial_{\tilde{\xi}}(\,{}^\eta n + \varepsilon\overline{n})\,d\tilde{\xi} + \partial_\vartheta(\,{}^\eta n + \varepsilon\overline{n})\,d\vartheta]^2. \end{aligned} \tag{6} $$

If the generating functions $\tilde{\varpi}$ and effective sources are such way chosen that the polarization functions (5) can be approximated $\tilde{\eta}_a \simeq 1$ and ${}^\eta\tilde{A}$ and ${}^\eta n$ are "almost constant", the metric (6) mimics small rotoid wormhole like configurations.

## 2.2 Solitonic Waves, Wormholes and Black Ellipsoids

An interesting class of off-diagonal solutions depending on all spacetime coordinates can be constructed by designing a configuration when a 1-solitonic wave preserves an ellipsoidal wormhole configuration. Such a spacetime metric can be written in the form

$$ \mathbf{ds}^2 = e^{\tilde{\psi}(x^i)}(d\tilde{\xi}^2 + d\vartheta^2) + \omega^2\left[\tilde{\eta}_3(1+\varepsilon\frac{\partial_\varphi[\overline{\chi}_4\tilde{\varpi}]}{\partial_\varphi\tilde{\varpi}})\,{}^0\overline{h}_3(\delta\varphi)^2 - \tilde{\eta}_4[1+\varepsilon\overline{\chi}_4(\tilde{\xi},\varphi)]\,{}^0\overline{h}_4(\delta t)^2\right], \tag{7} $$

for $\delta\varphi = d\varphi + \partial_i(\,{}^\eta\tilde{A} + \varepsilon\overline{A})dx^i, \delta t = dt + {}_1n_i(\tilde{\xi},\vartheta)dx^i$, $x^i = (\tilde{\xi},\vartheta)$ and $y^a = (\varphi, t)$. The factor $\omega(\tilde{\xi},t) = 4\arctan e^{m\gamma(\tilde{\xi}-vt)+m_0}$, where $\gamma^2 = (1-v^2)^{-1}$ and constants $m, m_0, v$, defines a 1-soliton for the sine-Gordon equation, $\frac{\partial^2\omega}{\partial t^2} - \frac{\partial^2\omega}{\partial\tilde{\xi}^2} + \sin\omega = 0$.

For $\omega = 1$, the metrics (7) are of type (6). A nontrivial value $\omega$ depends on the time like coordinate $t$ and has to be constrained to certain conditions which do not change the Ricci d-tensor, which can be written for ${}_1n_2 = 0$ and ${}_1n_1 = const$ in the form $\frac{\partial\omega}{\partial\tilde{\xi}} - {}_1n_1\frac{\partial\omega}{\partial t} = 0$. A gravitational solitonic wave propagates self-consistently in a rotoid wormhole background with ${}_1n_1 = v$ which solve both the sine-Gordon and constraint equations. Re-defining the system of coordinates with $x^1 = \tilde{\xi}$ and $x^2 = \theta$, we can transform any ${}_1n_i(\tilde{\xi},\theta)$ into necessary ${}_1n_1 = v$ and ${}_1n_2 = 0$.

### *2.3 Ringed Wormholes*

We can generate a rotoid wormhole plus a torus,

$$\mathbf{ds}^2 = e^{\tilde{\psi}(x^i)}(d\tilde{\xi}^2 + d\vartheta^2) + \tilde{\eta}_3(1+\varepsilon\frac{\partial_\varphi[\overline{\chi}_4\tilde{\varpi}]}{\partial_\varphi\tilde{\varpi}})\,{}^0\overline{h}_3(\delta\varphi)^2 - f\,\tilde{\eta}_4[1+\varepsilon\overline{\chi}_4(\tilde{\xi},\varphi)]\,{}^0\overline{h}_4(\delta t)^2,$$

for $\delta\varphi = d\varphi + \partial_i(\,{}^\eta\tilde{A} + \varepsilon\overline{A})dx^i$, $\delta t = dt + \,{}_1n_i(\tilde{\xi},\vartheta)dx^i$, when $x^i = (\tilde{\xi},\vartheta)$ and $y^a = (\varphi, t)$, where the function $f(\tilde{\xi},\vartheta,\varphi)$ can be rewritten equivalently in Cartesian coordinates, $f(\tilde{x},\tilde{y},\tilde{z}) = \left(R_0 - \sqrt{\tilde{x}^2+\tilde{y}^2}\right)^2 + \tilde{z}^2 - a_0$, for $a_0 < a$, $R_0 < r_0$. We get a ring around the wormhole throat (we argue that we obtain well-defined wormholes in the limit $\varepsilon \to 0$ and for corresponding approximations $\tilde{\eta}_a \simeq 1$ and ${}^\eta\tilde{A}$ and ${}^\eta n$ to be almost constant). The ring configuration is stated by the condition $f = 0$. In above formulas, $R_0$ is the distance from the center of the tube to the center of the torus/ring and $a_0$ is the radius of the tube. If the wormhole objects exist, the variants ringed by a torus may be stable for certain nonholonomic geometry and exotic matter configurations.

**Acknowledgements** Research is supported by IDEI, PN-II-ID-PCE-2011-3-0256.

## References

1. S. Vacaru, Int. J. Geom. Meth. Mod. Phys. **8** 9 (2011)
2. S. Vacaru, Class. Quant. Grav. **27** 105003 (2010)
3. S. Vacaru, Gener. Relat. Grav. **44** 1015 (2012)
4. S. Vacaru, Int. J. Mod. Phys. D **21** 1250072 (2012)
5. S. Nojiri and S. D. Odintsov, Int. J. Geom. Meth. Mod. Phys. **4** 115–146 (2007)
6. S. Nojiri and S. D. Odintsov, Phys. Rept. **505** 59 (2011)
7. T. Harko, F. S. N. Lobo, S. Nojiri and S. D. Odintsov, Phys. Rev. D **84** 024020 (2011)
8. P. Stavrinos and S. Vacaru, accepted to: Class. Quant. Grav. **30** (2013); arXiv: 1206.3998
9. S. Vacaru, Europhysics Letters (EPL) **96** 50001 (2011)

# Conformally Reducible Perfect Fluids with 2-Spaces of Constant Curvature

**Norbert Van den Bergh**

**Abstract** I discuss conformally reducible but non-conformally flat space-times, which are solutions of the Einstein field equations with a perfect fluid source and for which the factor spaces are 2-spaces of constant curvature. These space-times are necessarily of Petrov type D. When the fluid velocity is aligned with the plane of principal null directions, they are locally rotationally symmetric of Stewart–Ellis class II and are determined up to two first order partial differential equations. When the fluid is non-aligned, the general solution can be given in terms of elementary functions.

## 1 Introduction

A space-time is called reducible if it admits a rank-2 symmetric, covariantly constant tensor field. It is then the product of two 2-dimensional manifolds, the line element being the sum of the line elements of the factor manifolds. The Petrov type is necessarily D or O [2, 3]. These space-times are likely to be of little interest, as their Ricci tensor is of Segre type $[(11),(1,1)]$ (or its degeneracies) and, with the exception of the conformally flat Bertotti–Robinson solution of the Einstein–Maxwell equations [1, 4], no physical interpretation is known. However, among the conformally reducible perfect fluids there are numerous physically relevant examples, for example all spherically symmetric space-times. As even for this simple sub-family the general solution for a perfect fluid is not known, it appears sensible to impose some extra restriction in order to obtain new classes of exact solutions. In [2] a classification was made of the perfect fluid metrics, in which the fluid's 4-velocity was aligned with the plane of real principal null directions

N. Van den Bergh (✉)
Department of Mathematical Analysis, Ghent University Galglaan 2, 9000 Gent, Belgium
e-mail: norbert.vandenbergh@ugent.be

A. García-Parrado et al. (eds.), *Progress in Mathematical Relativity, Gravitation and Cosmology*, Springer Proceedings in Mathematics & Statistics 60,
DOI 10.1007/978-3-642-40157-2_68, 

of the Weyl tensor. It was shown that, when the factor manifolds have *constant curvature*, perfect fluid solutions are necessarily conformally flat or warped. This result suggested a closer look at the non-aligned conformally 2+2-reducible perfect fluids for which both 2-spaces have constant curvature. Remarkably the non-aligned case, which at first sight looks vastly more complicated than the aligned case, can be completely solved in terms of elementary functions (see [5]). During this analysis some side-results on the aligned case were obtained, which I report here and which can shed a new light on the results obtained in [2]. Notations and sign conventions are as in [3].

## 2 Aligned Perfect Fluid

We introduce a NP tetrad $\boldsymbol{e}_1 = \delta, \boldsymbol{e}_2 = \overline{\delta}, \boldsymbol{e}_3 = \Delta, \boldsymbol{e}_4 = D$ for the reducible metric $\mathrm{d}s^2 = 2(P^{-2}\mathrm{d}\zeta\mathrm{d}\overline{\zeta} - Q^{-2}\mathrm{d}u\mathrm{d}v)$. Here $2P^{-2}\mathrm{d}\zeta\mathrm{d}\overline{\zeta}$ and $2Q^{-2}\mathrm{d}u\mathrm{d}v$ are metrics of 2-spaces of constant curvature, with signatures 2 and 0 respectively: $P = 1 + 2k\zeta\overline{\zeta}$, $Q = 1 + 2Kuv$ ($k$, $K$ constants). Defining the dual basis by

$$\boldsymbol{\omega}^1 = P^{-1}\mathrm{d}\zeta, \boldsymbol{\omega}^2 = P^{-1}\mathrm{d}\overline{\zeta}, \boldsymbol{\omega}^3 = Q^{-1}\mathrm{d}u, \boldsymbol{\omega}^4 = Q^{-1}\mathrm{d}v,$$

the non-vanishing spin coefficients are $\epsilon$, $\gamma$, $\alpha$ and $\beta = -\overline{\alpha}$, with $\alpha = \frac{1}{2}P^{-1}\overline{\delta}P = k\zeta$, $\epsilon = -\frac{1}{2}Q^{-1}DQ = -Ku$, $\gamma = \frac{1}{2}Q^{-1}\Delta Q = Kv$ being solutions of the NP equations

$$D\gamma - \Delta\epsilon + 4\epsilon\gamma = 2K, \tag{1}$$

$$\delta\alpha + \overline{\delta}\overline{\alpha} - 4\alpha\overline{\alpha} = 2k. \tag{2}$$

The non-vanishing curvature components are

$$\Psi_2 = -\frac{1}{12}R = \frac{2}{3}(K - k),\ \Phi_{11} = K + k.$$

Using the transformation formulae for the components of the Ricci tensor under a conformal transformation one can express that $\Omega^{-2}\mathrm{d}s^2$, with $\Omega = \Omega(u, v, \zeta, \overline{\zeta})$, is the metric of a perfect fluid with energy-momentum tensor $T_{ab} = (w + p)u_a u_b + pg_{ab}$ ($\boldsymbol{u}^2 = -1$). This results in an over-determined system of partial differential equations for $\Omega$.

The integrability conditions for this system are equivalent with the Bianchi equations for the perfect fluid metric $\Omega^{-2}\mathrm{d}s^2$. Assuming that $\Psi_2 = \frac{2}{3}(K - k) \neq 0$ (hence excluding the conformally flat case), one can eliminate the derivatives of $n_a = (w + p)^{1/2}u_a$ from the latter and obtain the following key equations:

$$n_4\delta\Omega + n_1 D\Omega = 0 \tag{3}$$

$$n_1(n_4\Delta\Omega - n_3 D\Omega) = 0. \tag{4}$$

A distinction should now be made between the aligned and non-aligned situation. In the following we investigate the aligned case only. One has then $n_1 = n_2 = 0$ and (3) immediately implies $\delta\Omega = 0$ and hence $\Omega = \Omega(u, v)$, in accordance with the results of [2]. From the Bianchi equations one furthermore infers that $\delta n_3 = \delta n_4 = 0$ and hence also $S \equiv w + p = 2n_3n_4 = S(u, v)$. The resulting perfect fluid space-times are then (pseudo-)spherically symmetric or plane symmetric. Substitution of $\delta\Omega = 0$ in the Bianchi equations leads to an expression for $\Lambda$:

$$\Lambda = 4\Omega^2(2k + K) - \frac{3}{4}S + 6D\Omega\Delta\Omega. \tag{5}$$

Parametrizing the velocity components by means of a boost factor $A$, $n_3 = A\sqrt{S/2}$, $n_4 = A^{-1}\sqrt{S/2}$, and using (5), the Bianchi equations reduce to the following pair of differential equations for $A$,

$$\begin{aligned} Q^2\Delta(Q^{-2}SA^{-2}\Omega^{-1}) - D[S\Omega^{-1} - 8(k - K)\Omega] = 0, \\ Q^2D(Q^{-2}SA^2\Omega^{-1}) - \Delta[S\Omega^{-1} - 8(k - K)\Omega] = 0. \end{aligned} \tag{6}$$

The integrability conditions for the latter eventually lead to a wave equation,

$$(Q^2(Q^{-2}SA^{-2}\Omega^{-1})_{,u})_{,u} + (Q^2(Q^{-2}SA^{-2}\Omega^{-1})_{,v})_{,v} = 0, \tag{7}$$

with general solution given by $S = QA^2\Omega(S_1 + S_2)$ and with $S_1$ and $S_2$ functions of $u + v$ and $u - v$ respectively. For each choice of $S_1, S_2$ one can solve (6) for $A$, after which $\Omega$ can be found from the Bianchi equations. The resulting perfect fluids form a highly restricted sub-class of the (pseudo-)spherically symmetric or plane symmetric ones, as can be seen from their kinematical quantities, $\sigma \sim (k - K)(A^{-1}\Delta + AD)\Omega$, $\dot{u} \sim (A^{-1}\Delta - AD)(S - 2(k - K)\Omega^2)$ and $\theta = \frac{1}{\sqrt{2}}(4\Omega^2(k - K) + 3S)(A^{-1}\Delta + AD)\Omega$. The vorticity is zero as a consequence of the symmetry. Non-conformally flat ($k - K \neq 0$) and shear-free members of the aligned family therefore have zero expansion, in contrast to the general aligned case, for which large classes of shear-free and expanding spherically symmetric perfect fluids are known to exist[3]. While it is not possible to write down a general solution for the system (6), special solutions can be constructed by making extra assumptions. If, for example, the fluid velocity is taken parallel to the gradient of $\Omega$,

$$(A^{-1}\Delta - AD)\Omega = 0, \tag{8}$$

one obtains a sub-family of the general *non-aligned* solution.[1] The acceleration is then zero, as acting with the $D$ and $\Delta$ operators on (8) implies that $(A^{-1}\Delta - AD)S = 0$ as well and

[1]Note that, as a consequence of (3,4) the non-aligned solutions have fewer degrees of freedom than the aligned ones.

$$A^2(D\Omega)^2 = \frac{S}{4}\frac{k+K}{k-K} \tag{9}$$

(showing that $k + K \neq 0$). It follows that $S = S(\Omega)$, which is found by integrating the integrability condition for (6): $S = 2(K^2 - k^2)K^{-1}(\Omega^2 + c\Omega^{2\frac{k-K}{k+K}})$, or, if $K = 0$, $S = (-8k \log \Omega + c)\Omega^2$, with $c$ a constant of integration. By (5, 9) and $S = S(\Omega)$ all these solutions admit a barotropic equation of state. Integrating the $D^2\Omega$ Bianchi equation one furthermore finds $D\Omega = \Omega^{\frac{k-K}{k+K}} Q^{-1} f$, with $Df = 0$ i.e. $f = f(u)$. Together with $(A^{-1}\Delta - AD)\Omega = 0$ one obtains from the $[\Delta, D]$ commutator applied to $\Omega$,

$$\Omega^{\frac{2K}{k+K}} = \frac{1}{k+K}(2Kfv Q^{-1} - \frac{1}{2} f_{,u}). \tag{10}$$

When $K \neq 0$ the function $f$ follows from integrating the $\delta^2\Omega$ Bianchi equations, leading to an ODE, $2ff'' - f'^2 - 4c(k + K)^2 = 0$, the general solution of which is given by

$$f(u) = \frac{1}{c_2}(c_1 u + c_2)^2 + 2\frac{c}{c_2}(k + K)^2 u^2, \tag{11}$$

with $c_1, c_2$ constants of integration. Using the isometries of the $(u, v)$ factor space one can put $c_1 = 0$ and assign an arbitrary (non-zero) value to $c_2$. Choosing $c_2 = k + K$ it follows that $\Omega$ is given by

$$\Omega^{\frac{2K}{k+K}} = Q^{-1}(Kv - 2cu). \tag{12}$$

Notice also that a $\gamma$-law equation of state is only possible when $c = 0$, implying $p = \Omega^2(K - k)^2/K$ and $w = \Omega^2(3k + K)(K - k))/K$. In that case (9) and the dominant energy condition require $K < 0$, which forces the pressure to be negative.

When $K = 0$ one has $[\Delta, D]\Omega = 0$ and the function $f$ is restricted to be linear in $u$. $\Omega$ can now be obtained by integrating the expressions for $D\Omega$ and $\Delta\Omega$: using the translational degree of freedom in $u$ and $v$ to eliminate two constants of integration, one finds (modulo a globally constant scale factor) $\Omega = \exp(-2kuv)$, with the boost factor, energy density and pressure given by $A^2 = v/u$, $w = 8k\Omega^2(1 + 3kuv)$, $p = -8k\Omega^2(1 + kuv)$. The latter solutions are restricted to the interior of the 2D-light cone $uv > 0$, independently of the sign of $k$. For $k > 0$ one obtains the metric (155) of [2], which satisfies the dominant energy condition in the 2D-light cone, but which again has negative pressure. For $k < 0$ on the contrary one obtains a solution with positive energy density and pressure in the region $1/3 < |k|uv < 1$.

Further examples of aligned perfect fluid solutions can be found in [2].

## References

1. Bertotti, B. : Phys. Rev. **116**, 1331 (1959) .
2. Carot, J. , Tupper, B. O. J. : Class. Quantum Grav. **19**, 4141 (2002)
3. Kramer, D. , Stephani, H. , MacCallum, M. A. H. , Hoenselaers, C. , Herlt, E. : Exact solutions of Einstein's field equations. Cambridge University Press (2003)
4. Robinson, I. : Bull. Acad. Polon. Sci. **7**, 351 (1959)
5. Van den Bergh, N. : Class. Quantum Grav. **29**, 235003 (2012)

# Head-On Collisions of Charged Black Holes from Rest

**Miguel Zilhão, Vitor Cardoso, Carlos Herdeiro, Luis Lehner, and Ulrich Sperhake**

M. Zilhão (✉)
Departamento de Física da Universidade de Aveiro and I3N, Campus de Santiago, 3810-183 Aveiro, Portugal

Perimeter Institute for Theoretical Physics, Waterloo, Ontario N2L 2Y5, Canada

Centro de Física do Porto, Departamento de Física e Astronomia, Faculdade de Ciências da Universidade do Porto, Rua do Campo Alegre, 4169-007 Porto, Portugal

Center for Computational Relativity and Gravitation, Rochester Institute of Technology, Rochester, NY 14623
e-mail: mzilhao@astro.rit.edu

C. Herdeiro
Departamento de Física da Universidade de Aveiro and I3N, Campus de Santiago, 3810-183 Aveiro, Portugal

L. Lehner
Perimeter Institute for Theoretical Physics, Waterloo, Ontario N2L 2Y5, Canada

Department of Physics, University of Guelph, Guelph, Ontario N1G 2W1, Canada

V. Cardoso
Centro Multidisciplinar de Astrofísica—CENTRA, Departamento de Física, Instituto Superior Técnico—IST, Av. Rovisco Pais 1, 1049-001 Lisboa, Portugal

Department of Physics and Astronomy, The University of Mississippi, University, MS 38677-1848, USA

U. Sperhake
Centro Multidisciplinar de Astrofísica—CENTRA, Departamento de Física, Instituto Superior Técnico—IST, Av. Rovisco Pais 1, 1049-001 Lisboa, Portugal

Department of Applied Mathematics and Theoretical Physics, Centre for Mathematical Sciences, University of Cambridge, Cambridge CB3 0WA, UK

Institut de Ciències de l'Espai (CSIC-IEEC), Facultat de Ciències, Campus UAB, E-08193 Bellaterra, Spain

California Institute of Technology, Pasadena, CA 91125, USA

A. García-Parrado et al. (eds.), *Progress in Mathematical Relativity, Gravitation and Cosmology*, Springer Proceedings in Mathematics & Statistics 60,
DOI 10.1007/978-3-642-40157-2_69, 

**Abstract** We report on head-on collisions of charged black holes. We focus on non-spinning black holes, starting from rest and with the same charge to mass ratio $Q/M$. The addition of charge to black holes introduces a new interesting channel of radiation and dynamics, most of which seem to be captured by Newtonian dynamics and flat-space intuition. The amount of gravitational-wave energy generated throughout the collision decreases by about three orders of magnitude as the charge-to-mass ratio $Q/M$ is increased from 0 to 0.98. This decrease is a consequence of the smaller accelerations present for larger values of the charge.

## 1 Introduction

We here summarize our study of non-linear dynamics of binary systems of charged black holes [1], building on previous numerical evolutions of the Einstein–Maxwell system [2–5]. For reasons of simplicity, we focus in this study on binary systems for which initial data can be constructed by purely analytic means [6]: head-on collisions, starting from rest, of non-spinning black holes with equal charge-to-mass ratio. This implies in particular that the black holes carry a charge of the *same sign* so that the electromagnetic force will always be repulsive. We will extract both gravitational and electromagnetic radiation and monitor their behaviour as the charge-to-mass-ratio parameter of the system is varied.

## 2 Numerical Setup

Following the approach outlined in [4, 7] we consider an enlarged system of the form

$$\begin{aligned} R_{\mu\nu} - \frac{R}{2} g_{\mu\nu} &= 8\pi T_{\mu\nu} \,, \\ \nabla_\mu \left( F^{\mu\nu} + g^{\mu\nu} \Psi \right) &= -\kappa n^\nu \Psi \,, \\ \nabla_\mu \left( \star F^{\mu\nu} + g^{\mu\nu} \Phi \right) &= -\kappa n^\nu \Phi \,, \end{aligned} \tag{1}$$

where $\star F^{\mu\nu}$ denotes the Hodge dual of the Maxwell–Faraday tensor $F^{\mu\nu}$, $\kappa$ is a constant and $n^\mu$ the four-velocity of the Eulerian observer. We recover the standard Einstein–Maxwell system of equations when $\Psi = 0 = \Phi$. With the scalar field $\Psi$ and pseudo-scalar $\Phi$ introduced in this way, the natural evolution of this system drives $\Psi$ and $\Phi$ to zero (for positive $\kappa$), thus ensuring the magnetic and electric constraints are controlled [2, 7]. The electromagnetic stress-energy tensor takes the usual form.

We employ a Cauchy approach so we further introduce a $3+1$ decomposition of all dynamical quantities [6]; see [1] for details. We focus on black-hole binaries with equal charge and mass colliding from rest. For these configurations, it is possible to construct initial data in an analytical fashion [6].

To extract physical information, we calculate the Newman–Penrose scalars $\Psi_4$, $\Phi_1$ and $\Phi_2$ [8]. We refer the interested reader to [9] for more details about the numerical implementation and [10] for a review of the formalism.

At a given extraction radius $R_{\rm ex}$, we perform a multipolar decomposition by projecting $\Psi_4$, $\Phi_1$ and $\Phi_2$ onto spherical harmonics of spin weight $s=-2$, 0 and $-1$ respectively. In terms of these multipoles, the radiated flux and energy is [8]

$$F_{\rm GW} = \frac{dE_{\rm GW}}{dt} = \lim_{r\to\infty} \frac{r^2}{16\pi} \sum_{l,m} \left| \int_{-\infty}^{t} dt' \psi^{lm}(t') \right|^2 , \tag{2}$$

$$F_{\rm EM} = \frac{dE_{\rm EM}}{dt} = \lim_{r\to\infty} \frac{r^2}{4\pi} \sum_{l,m} \left| \phi_2^{lm}(t) \right|^2 . \tag{3}$$

## 3 Numerical Results

The numerical integration of the Einstein–Maxwell equations has been performed using fourth-order spatial discretization with the LEAN code, originally presented in [9] for vacuum spacetimes. For further details see [1, 9].

All binaries start from rest with a coordinate distance $d/M \simeq 16$ while the charge-to-mass ratio has been varied from $Q/M=0$ to $Q/M=0.98$.

The dynamical behaviour of all our simulations is qualitatively well represented by the waveforms shown in Fig. 1 normalized with respect to $\mathscr{B} = 1 - Q^2/M^2$. The panels show the real part of the gravitational (left) and electromagnetic (right) quadrupole extracted at $R_{\rm ex} = 100\,M$ as a function of time with $\Delta t = 0$ defined as the time of the global maximum of the waveform (approximately when formation of a common apparent horizon occurs).

The electromagnetic and gravitational wave fluxes are given by Eqs. (2) and (3). We observe that the energy carried by gravitational radiation decreases with increasing $Q/M$, as the acceleration becomes smaller and quadrupole emission is suppressed. This is further illustrated in Fig. 2, which illustrates the radiated energy carried in the gravitational quadrupole and the electromagnetic quadrupole as well as their ratio as functions of the charge-to-mass ratio $Q/M$.

In contrast to the monotonically decreasing gravitational-wave energy, the electromagnetic signal reaches a local maximum around $Q/M=0.6$. The existence of such a maximum is expected as the electromagnetic radiation necessarily vanishes for $Q/M=0$ (no charge) and $Q/M=1$ (no acceleration) but takes on non-zero values in the regime in between.

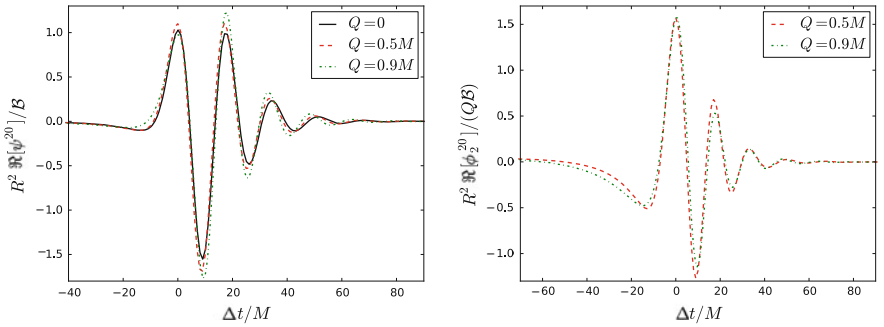


**Fig. 1** Real part of the $(2,0)$ mode of $\Psi_4$ normalized to $\mathscr{B} \equiv 1-Q^2/M^2$ (*left*) and $\Phi_2$ normalized to $Q\mathscr{B}$ (*right*) extracted at $R_{\rm ex} = 100M$, for simulations with initial (coordinate) distance $d/M \simeq 16$ and $Q/M = 0,\ 0.5,\ 0.9$

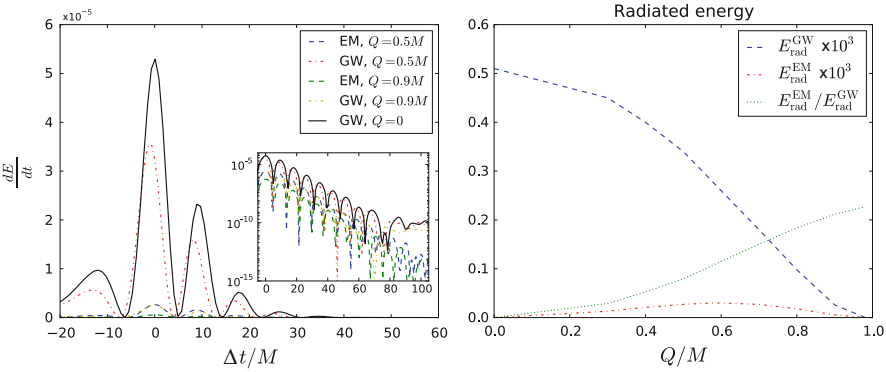


**Fig. 2** Radiated fluxes for simulations with $Q/M = 0.5$, 0.9 and 0 (*left*) and energy radiated in the gravitational and electromagnetic quadrupole as well as the ratio of the two as a function of $Q/M$ (*right*)

## 4 Final Remarks

Our present study paves the way for various future extensions. A non-zero boost, for instance, will allow us to study both binary black hole systems that will coalesce into a Kerr–Newman black hole and the impact of electric charge on the dynamics of wave emission (electromagnetic and gravitational) in high energy collisions, of interest in TeV gravity scenarios (see [11] for a review). Another extension presently under study is the case of oppositely charged black holes.

**Acknowledgements** M.Z. is funded by FCT through grant SFRH/BD/43558/2008. U.S. acknowledges support from the Ramón y Cajal Programme and Grant FIS2011-30145-C03-03 of the Ministry of Education and Science of Spain, the NSF TeraGrid and XSEDE Grant No. PHY-090003, RES Grant Nos. AECT-2012-1-0008 and AECT-2011-3-0007 through the Barcelona

Supercomputing Center and CESGA Grant Nos. ICTS-200 and ICTS-221. This work was supported by the *DyBHo–256667* ERC Starting Grant, the *CBHEO–293412* FP7-PEOPLE-2011-CIG Grant, the *NRHEP–295189* FP7-PEOPLE-2011-IRSES Grant, and by FCT—Portugal through projects PTDC/FIS/098025/2008, PTDC/FIS/098032/2008, PTDC/FIS/116625/2010 and CERN/FP/ 116341/2010, the Sherman Fairchild Foundation to Caltech as well as NSERC through a Discover Grant and CIFAR. Research at Perimeter Institute is supported through Industry Canada and by the Province of Ontario through the Ministry of Research & Innovation. Computations were performed on the Blafis cluster at Aveiro University, the Milipeia in Coimbra, the Lage cluster at Centro de Física do Porto, the Bifi Cluster of the University of Zaragoza, the CESGA Cluster Finis Terrae, NICS Kraken and the SDSC Cluster Trestles.

## References

1. M. Zilhão, V. Cardoso, C. Herdeiro, L. Lehner, U. Sperhake, Phys.Rev. **D85**, 124062 (2012). DOI 10.1103/PhysRevD.85.124062
2. C. Palenzuela, L. Lehner, O. Reula, L. Rezzolla, Mon.Not.Roy.Astron.Soc. **394**, 1727 (2009). DOI 10.1111/j.1365-2966.2009.14454.x
3. C. Palenzuela, M. Anderson, L. Lehner, S.L. Liebling, D. Neilsen, Phys.Rev.Lett. **103**, 081101 (2009). DOI 10.1103/PhysRevLett.103.081101
4. C. Palenzuela, L. Lehner, S. Yoshida, Phys.Rev. **D81**, 084007 (2010). DOI 10.1103/PhysRevD.81.084007
5. P. Mosta, C. Palenzuela, L. Rezzolla, L. Lehner, S. Yoshida, et al., Phys.Rev. **D81**, 064017 (2010). DOI 10.1103/PhysRevD.81.064017
6. M. Alcubierre, J.C. Degollado, M. Salgado, Phys.Rev. **D80**, 104022 (2009). DOI 10.1103/PhysRevD.80.104022
7. S. Komissarov, Mon.Not.Roy.Astron.Soc. (2007)
8. E. Newman, R. Penrose, J.Math.Phys. **3**, 566 (1962)
9. U. Sperhake, Phys. Rev. **D76**, 104015 (2007). DOI 10.1103/PhysRevD.76.104015
10. L. Lehner, O.M. Moreschi, Phys.Rev. **D76**, 124040 (2007). DOI 10.1103/PhysRevD.76.124040
11. V. Cardoso, L. Gualtieri, C. Herdeiro, U. Sperhake, P.M. Chesler, et al., Class.Quant.Grav. **29**, 244001 (2012). DOI 10.1088/0264-9381/29/24/244001

# Velocity-of-Light Surfaces in Kerr and Extreme Kerr

**Jan E. Åman and Helgi Freyr Rúnarsson**

**Abstract** The extreme limit of the Kerr solution has recently attracted much attention, see (Compère, arXiv:1203.3561 [hep-th]) and references therein. We have investigated hypersurfaces called velocity-of-light surfaces for extreme and near extreme Kerr.

## 1 Killing Vector Fields in Kerr

The Kerr solution possesses two linearly independent Killing vector fields, namely $\partial_t$ and $\partial_\phi$ in Boyer–Lindquist coordinates. Constant linear combinations of these are also Killing vectors. The linear combination $\chi = \partial_t + \frac{a}{2mr_+}\partial_\phi$ is known to be null at the outer horizon $r = r_+$. The norm of $\chi$ is

$$\|\chi\|^2 = \left\|\partial_t + \frac{a}{2mr_+}\partial_\phi\right\|^2 = g_{tt} + \frac{a}{mr_+}g_{t\phi} + \left(\frac{a}{2mr_+}\right)^2 g_{\phi\phi} = -\frac{r-r_+}{4m^2r_+^2\rho^2}f(r,\theta),$$

where $r_+ = m + \sqrt{m^2-a^2}$, $r_- = m - \sqrt{m^2-a^2}$, $\rho^2 = r^2 + a^2\cos^2\theta$,
$f(r,\theta) = 4m^2r_+^2(r-r_-) - a^2\sin^2\theta\left(4m^2(r-r_+) + (r-r_-)\left(\rho^2+2mr\right)\right)$.

However, an interesting fact is that there are also solutions to $f(r,\theta) = 0$ which correspond to other hypersurfaces where the Killing vector field $\chi$ becomes null; this hypersurface is called the velocity-of-light surface [1].

J.E. Åman (✉)
Department of Physics, Stockholm University, 106 91 Stockholm, Sweden
e-mail: ja@physto.se

H.F. Rúnarsson
Department of Physics, Stockholm University, 106 91 Stockholm, Sweden, Current address: Physics Department Aveiro University, Campus de Santiago, 3810-183 Aveiro, Portugal
e-mail: Helgi.Runarsson@gmail.com

A. García-Parrado et al. (eds.), *Progress in Mathematical Relativity, Gravitation and Cosmology*, Springer Proceedings in Mathematics & Statistics 60,
DOI 10.1007/978-3-642-40157-2_70, 

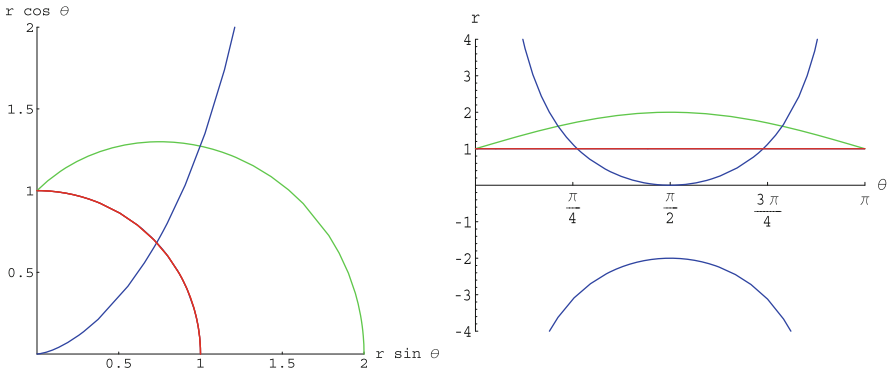


**Fig. 1** Polar and orthogonal plots for extreme Kerr, $a = m$. In our plots we take $m = 1$. The *blue line*(s) represent $f(r, \theta) = 0$. The *green line* is the outer limit of the ergosphere $r_e = m + \sqrt{m^2 - a^2 \cos^2 \theta}$. In the orthogonal plot also the solution where $r < 0$ is shown

The general solution of $f(r, \theta) = 0$ gives three roots for $r$, one of them for $r < 0$ [2]. The solutions for $r$ are somewhat long and complicated, involving third degree roots, but the solution for $\theta$ can easily be presented [3]:

$$\theta = \arcsin \sqrt{\frac{h - \sqrt{h^2 - g}}{2a^2 \Delta}},$$

where $h = (r^2 + a^2)^2 - 4m^2(a^2 + 2r_+(r - m))$, $g = 16m^2\Delta^2(2mr_+ - a^2)$,
$\Delta = r^2 + a^2 - 2mr$.

## 2 Extreme Kerr, $a = m$

For extreme Kerr $a = m$, $f(r, \theta)$ factorizes into:

$$f(r, \theta) = m^2(r-m)(m \sin\theta^2 + (r+m) \sin\theta - 2m)(m \sin\theta^2 - (r+m) \sin\theta - 2m).$$

Thus the Killing vector $\chi$ is also null when

$$r/m = \frac{2 - \sin\theta - \sin^2\theta}{\sin\theta}, \quad \text{and} \quad r/m = \frac{-2 - \sin\theta + \sin^2\theta}{\sin\theta}.$$

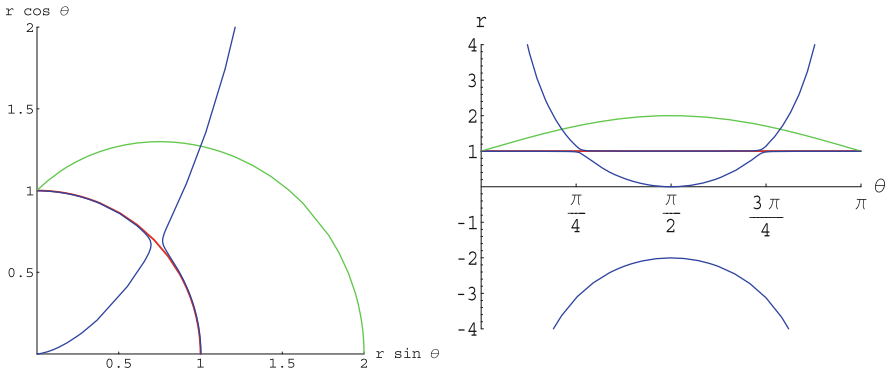


**Fig. 2** Polar plot for Kerr with $a/m = 999999/1000000$. The null hypersurfaces are close to the $a = m$ line, except near the horizons

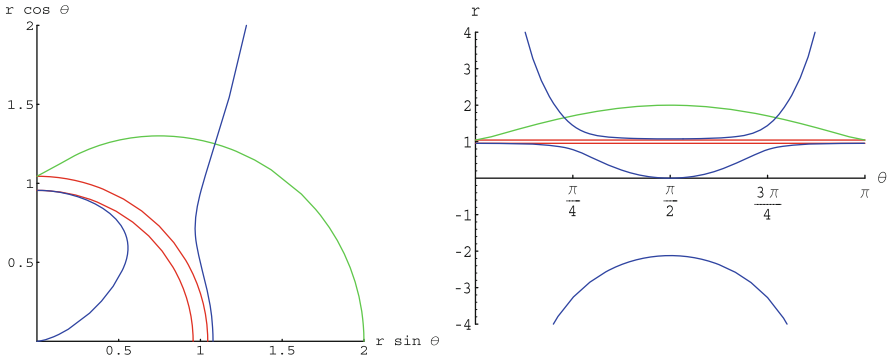


**Fig. 3** Polar and orthogonal plots for Kerr with $a/m = 999/1000$. The *red lines* represent the outer and inner horizons, $r_+$ and $r_-$. The inner velocity-of-light hypersurface (*blue*) always touches the inner horizon at the north pole

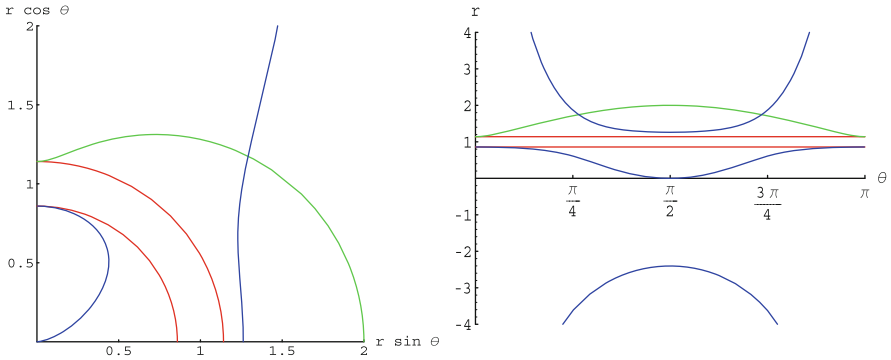


**Fig. 4** Polar and orthogonal plots for Kerr with $a/m = 99/100$

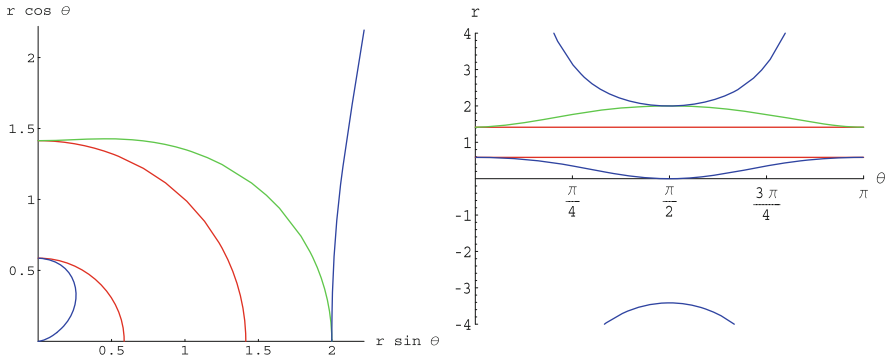


**Fig. 5** Polar and orthogonal plots where the hypersurface touches the ergosphere at the equator, $a/m = \sqrt{2(\sqrt{2}-1)} \approx 0.91018$

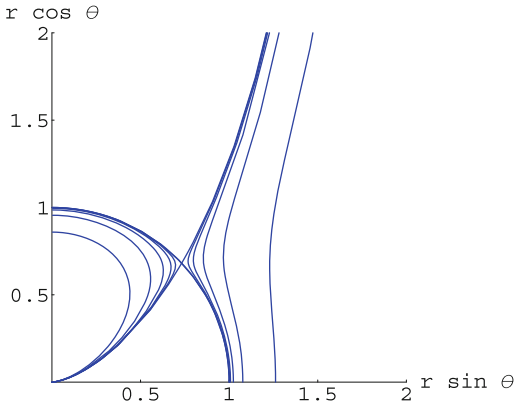


**Fig. 6** Polar plot for Kerr with $a/m = 1$ and $a/m = 1 - 10^{-\alpha}$ with $\alpha = 6, 5, 4, 3$, and 2

The latter solution is always negative. The former hits the singularity at $\theta = \pi/2$, $r = 0$ and is defined for all $r \geq 0$ and crosses the horizon, $r = m$, at $\sin\theta = \sqrt{3} - 1$ ($\theta \approx 47°$) (Figs. 1–6).

## 3 Plots

**Acknowledgements** We thank Ingemar Bengtsson for discussions.

## References

1. Amsel, A.J., Horowitz, G.T., Marolf, D., and Roberts M.M.: No dynamics in the extremal Kerr throat. JHEP **0**9 044 (2009)
2. Duffy, G., Ottewill, A.C.: Renormalized stress tensor in Kerr space-time: Numerical results for the Hartle-Hawking vacuum. Phys. Rev. D **7**7 024007 (2008)
3. Åman, J.E., Bengtsson, I., Rúnarsson, H.F.: What are extremal Killing vectors up to? Class. Quant. Grav. **2**9 215017 (2012)

# Part III
# Poster Presentations

# The Spin-2 Equation on Minkowski Background

**Florian Beyer, George Doulis, Jörg Frauendiener, and Ben Whale**

**Abstract** The linearised general conformal field equations in their first and second order form are used to study the behaviour of the spin-2 zero-rest-mass equation on Minkowski background in the vicinity of space-like infinity.

## 1 Introduction

In [5], a completely novel finite representation of space-like infinity was proposed. In this setting, space-like infinity $i^0$ "blows up" to a cylinder $I$ and, consequently, asymptotically flat initial data become regular near $i^0$ and can be prescribed on generic space-like Cauchy surfaces, i.e., the use of hyperboloidal hypersurfaces may ultimately be unnecessary [8]. It turns out that, in this representation, Friedrich's general conformal field equations (GCFE) acquire a very simple form and the cylinder becomes a total characteristic of the system in the sense that there are no radial derivatives in the equations restricted to $I$. In addition, the coordinate location of null infinity is now known beforehand and it does not have to be determined during the evolution. All these features, namely the regularity of the initial data, the a-priori fixed finite coordinate location of null infinity, the fact that in the Minkowski case the entire physical space-time can be covered by one computational domain, and the extremely simple form of the evolution equations (especially on the cylinder), make the general conformal field equations suitable for numerical manipulations. However, as expected, the intrinsic system of evolution equations on the cylinder degenerates at the interface of the cylinder $I$ with null infinity. In general, the solutions generate logarithmic singularities at these regions which are

F. Beyer (✉) · G. Doulis · J. Frauendiener · B. Whale
Department of Mathematics and Statistics, University of Otago,
P.O. Box 56, Dunedin 9010, New Zealand
e-mail: fbeyer@maths.otago.ac.nz; gdoulis@maths.otago.ac.nz; joergf@maths.otago.ac.nz;
bwhale@maths.otago.ac.nz

A. García-Parrado et al. (eds.), *Progress in Mathematical Relativity, Gravitation and Cosmology*, Springer Proceedings in Mathematics & Statistics 60,
DOI 10.1007/978-3-642-40157-2_71, 

expected to travel along null infinity and spoil its smoothness, making it impossible to read-off the gravitational radiation at $\mathscr{I}^+$. The way out of this problem is to prescribe initial data that respect the regularity conditions proposed in [5].

In this short contribution, we use Friedrich's general conformal field equations to evolve generic asymptotically flat initial data near space-like infinity. We begin our endeavour from the simplest possible case: linearised gravitational fields on a Minkowski background. Although simple, this "toy model" encapsulates most of the crucial characteristics of the full non-linear system described above. The initial data are evolved as close as possible to the ill-behaved regions $I^{\pm}$ and study the behaviour of the numerical solutions there. This procedure is carried out twice by using the linearised general conformal field equations in their first and second order form. Analytically the two approaches are equivalent, but their numerical implementation could very well differ. The latter statement is partly based on the claim made in [6] that writing the equations of general relativity as a system of second order PDE's is more advantageous numerically than writing them as a system of first order PDE's. According to [6], numerical simulations based on second order PDE's have better numerical accuracy and avoid the appearance of spurious waves travelling against the characteristic curves.

## 2 The Spin-2 Equations

We use the spin-2 zero-rest-mass equation for a totally symmetric spinor field $\phi_{ABCD}$ in the 2-spinor formulation, i.e. $\nabla_{A'}{}^{A}\phi_{ABCD} = 0$, to model linearised gravitational fields on a Minkowski background. Taking the components of the above expression, decomposing the five independent components $\phi_k$ of the spin-2 into harmonic modes $(l, m)$, introducing coordinates $(t, r, \theta, \varphi)$ and an adapted spin-frame on the cylinder, the above spin-2 equation splits into the eight coupled equations (for details see [1])

$$\begin{aligned}
(1 - t\kappa')\partial_t\phi_k + \kappa\partial_r\phi_k - (3\kappa' - (5-k)\mu)\phi_k &= \mu\, c_k\, \phi_{k-1}, \qquad k = 1:4,\\
(1 + t\kappa')\partial_t\phi_k - \kappa\partial_r\phi_k + (3\kappa' + (k+1)\mu)\phi_k &= -\mu\, c_k\, \phi_{k+1}, \quad k = 0:3,
\end{aligned} \tag{1}$$

where $\kappa(r) = r\,\mu(r)$, $\mu(0) = 1$, $c_k = \sqrt{l(l+1) - (2-k)(1-k)}$, and $'$ denotes differentiation with respect to $r$. Equations (1), when appropriately combined, split into three constraint equations and a symmetric hyperbolic (in the domain $|t| < \kappa^{-1}$) system of five evolution equations, see [1].

By differentiating the above spin-2 equation, one can derive (see [4]) the second order spin-2 wave equation $\Box\,\phi_{ABCD} = 0$. Decomposing again the components of the spin-2 field into harmonic modes and introducing coordinates $(t, r, \theta, \varphi)$, the spin-2 wave equation splits into a hyperbolic (in the domain $|t| < \kappa^{-1}$) system of five wave equations

$$
\begin{aligned}
(1-t^2\kappa'^2)\partial_{tt}\phi_k - \kappa^2\partial_{rr}\phi_k + 2\,t\kappa\kappa'\partial_{tr}\phi_k + 2\,r\kappa\mu'\partial_r\phi_k \\
+ 2\,[(2-k)\kappa' - t(\kappa'^2 + r\,\mu'\kappa' - \frac{1}{2}\kappa\,\kappa'')]\partial_t\phi_k \\
+ [(2-k)(\kappa\kappa'' + (1-k)\kappa'^2) + k(5-k)r^2\mu'^2]\phi_k \\
= -\mu^2\,c_k^2\phi_k - r\,\mu\,\mu'((4-k)c_k\,\phi_{k+1} + k\,c_{k-1}\,\phi_{k-1}).
\end{aligned}
\tag{2}
$$

Notice that the domain of hyperbolicity for both sets of equations is the same, namely $|t| < \kappa^{-1}$. Thus, as expected, in both approaches the equations degenerate at $(t, r) = (\pm 1, 0)$, i.e. at the regions $I^{\pm}$ where null like infinity $\mathscr{I}^{\pm}$ meets the cylinder.

In order to compute the same solution as with the first order system (1) we have to use all the available information from the first-order system to determine initial and boundary conditions for the second order system (2). In [4] it was shown that the two formulations are equivalent provided the initial and boundary data for the second order system are determined from the first order system.

## 3 Numerical Results

The PDE systems (1), (2) are discretised according to the method of lines. An equidistant grid on the computational domain $D = [0, 1]$ is used to discretise the spatial coordinate $r$. The spatial derivatives are approximated by summation by parts (SBP) finite difference operators [7].

The boundary conditions are implemented with a very simple, but highly efficient, simultaneous approximation term (SAT) penalty method [3]. The temporal integration is based on a standard explicit fourth order Runge–Kutta scheme. The code has been written form scratch in Python.

The comparison of the numerical properties of the two approaches is based on their ability to reproduce a specific family of exact solutions of the spin-2 equation developed in [1]. As was shown in [1, 4], the critical sets $I^+$, located at $t = 1$, can be reached in both approaches without loss of the expected 4th order accuracy; in addition, the constraint quantities are preserved to sufficient accuracy during the evolution. A comparison of the accuracy with which the two approaches numerically reproduce the exact solution is shown in Table 1. Better accuracy was achieved in the second order formulation, a result that confirms the first claim in [6]. The second claim made therein that the spurious waves disappear in the second order case is also confirmed as the high frequency features disappear in the convergence plots of the second order formulation, see [4].

**Table 1** The logarithm of the normalized $l^2$ norm of the absolute error $E$, $\log_2(||E||_2)$, between the exact solution and the solutions computed from the 1st-order system (1) and the 2nd-order system (2) at time $t = 1$

| | $\phi_0$ | | $\phi_4$ | |
|---|---|---|---|---|
| Grid | 1st order | 2nd order | 1st order | 2nd order |
| 50 | −25.2218 | −27.6006 | −11.1643 | −12.3418 |
| 100 | −29.3956 | −31.5941 | −13.9924 | −15.1743 |
| 200 | −33.7109 | −35.6075 | −16.9978 | −18.1782 |
| 400 | −38.1000 | −39.6068 | −20.1075 | −21.2850 |

## 4 Conclusion

In this work, two distinct approaches to the linearised general conformal field equations were developed and subsequently implemented numerically. In both approaches we managed to reach without loss of accuracy the ill-behaved region $I^+$. It is principally not possible to go beyond $I^\pm$ since the equations loose hyperbolicity. A possible way to resolve this problem is presented in [2]. We have also shown that the second order formulation of the spin-2 equation leads to a better accuracy by a factor of 3-4 and the spurious waves travelling against the characteristics disappear, confirming the claims made in [6].

## References

1. Beyer, F., Doulis, G., Frauendiener, J., Whale, B.: Numerical space-times near space-like and null infinity. The spin-2 system on Minkowski space. Class. Quantum Grav. **29**, 245013 (2012)
2. Beyer, F., Doulis, G., Frauendiener, J., Whale, B.: Linearized gravitational waves near space-like and null infinity. (this volume), arXiv:1302.0043 (2013)
3. Carpenter, M.H., Gottlieb, D., Abarbanel, S.: Time-stable boundary conditions for finite-difference schemes solving hyperbolic systems: methodology and application to high-order compact schemes. J. Comp. Phys. **111**, 220–236 (1994)
4. Doulis, G., Frauendiener, J.: The second order spin-2 system in flat space near space-like and null-infinity. to appear in Gen. Relativ. Gravit., arXiv:1301.4286 (2013)
5. Friedrich, H.: Gravitational fields near space-like and null infinity. J. Geom. Phys. **24**, 83–163 (1998)
6. Kreiss, H.O., Ortiz, O.E.: Some mathematical and numerical questions connected with first and second order time-dependent systems of partial differential equations. Lect. Notes Phys. 604, 359–370 (2002)
7. Mattsson, K., Nordström, J.: Summation by parts operators for finite difference approximations of second derivatives. J. Comp. Phys. **199**, 503–540 (2004)
8. Moncrief, V., Rinne, O.: Regularity of the Einstein equations at future null infinity. Class. Quantum Grav. **26**, 125010 (2012)

# Matching the Linet–Tian Spacetime with Conformally Flat Cylindrically Symmetric Sources

**Irene Brito, Maria de Fátima A. da Silva, Filipe C. Mena, and Nilton O. Santos**

**Abstract** We derive conformally flat cylindrically symmetric solutions for spacetimes with a cosmological constant and investigate the matching problem of these solutions with the exterior Linet–Tian spacetime.

## 1 Introduction

In General Relativity, cylindrical solutions have been used to study various fields such as cosmic strings, exact models of rotation matched to different sources and models for extragalactic jets and gravitational radiation. The generalization of the Levi–Civita spacetime to include a nonzero cosmological constant $\Lambda$ was obtained by Linet [1] and Tian [2]. It was shown by da Silva et al. [3] and Griffiths and

I. Brito (✉)
Centro de Matemática, Departamento de Matemática e Aplicações, Universidade do Minho, 4800-058 Guimarães, Portugal
e-mail: ireneb@math.uminho.pt

M. de Fátima A. da Silva
Departamento de Física Teórica, Instituto de Física, Universidade do Estado do Rio de Janeiro, 20550-900, Rio de Janeiro, Brazil
e-mail: mfasnic@gmail.com

F.C. Mena
Centro de Matemática, Departamento de Matemática e Aplicações, Universidade do Minho, 4710-057 Braga, Portugal
e-mail: fmena@math.uminho.pt

N.O. Santos
School of Mathematical Sciences, Queen Mary, University of London, London E1 4NS, UK; Observatoire de Paris, Université Pierre et Marie Curie, LERMA(ERGA) CNRS—UMR 8112, 94200 Ivry sur Seine, France
e-mail: n.o.santos@qmul.ac.uk

A. García-Parrado et al. (eds.), *Progress in Mathematical Relativity, Gravitation and Cosmology*, Springer Proceedings in Mathematics & Statistics 60,
DOI 10.1007/978-3-642-40157-2_72, 

Podolsky [4] that it changes the spacetime properties dramatically. The Linet–Tian (LT) solution has also been used to describe cosmic strings and, in [5], static cylindrical shell sources have been found for the LT spacetime with negative cosmological constant. Considering the extensive interest in cylindrically symmetric solutions it is worthwhile to analyse some further properties of LT spacetimes.

In this note, we summarize the results of [6], which show that it is possible to match static cylindrically symmetric conformally flat solutions of the Einstein field equations with a cosmological constant $\Lambda$ with the exterior Linet–Tian spacetime if $\Lambda > 0$.

## 2 Static Cylindrically Symmetric Anisotropic Sources with $\Lambda \neq 0$

Consider static cylindrically symmetric anisotropic matter bounded by a cylindrical surface $S$ and with energy momentum tensor given by

$$T_{ab} = (\mu + P_r)V_aV_b + P_r g_{ab} + (P_z - P_r)S_aS_b + (P_\phi - P_r)K_aK_b,$$

where $\mu$ is the energy density, $P_r$, $P_z$ and $P_\phi$ are the principal stresses and $V_a$, $S_a$ and $K_a$ satisfy $V^aV_a = -1$, $S^aS_a = K^aK_a = 1$, $V^aS_a = V^aK_a = S^aK_a = 0$. For the interior to $S$ the static cylindrically symmetric metric can be written as

$$ds^2 = -A^2dt^2 + B^2(dr^2 + dz^2) + C^2d\phi^2, \tag{1}$$

where $A$, $B$ and $C$ are functions of $r$. The non-zero components of the Einstein Field Equations $G_{ab} = T_{ab} - \Lambda g_{ab} \equiv \bar{T}_{ab}$ are

$$G_{00} = -\left(\frac{A}{B}\right)^2\left[\left(\frac{B'}{B}\right)' + \frac{C''}{C}\right] = (\mu + \Lambda)A^2 = \bar{\mu}A^2,$$

$$G_{11} = \frac{A'C'}{AC} + \left(\frac{A'}{A} + \frac{C'}{C}\right)\frac{B'}{B} = (P_r - \Lambda)B^2 = \bar{P}_rB^2,$$

$$G_{22} = \frac{A''}{A} + \frac{C''}{C} + \frac{A'}{A}\frac{C'}{C} - \left(\frac{A'}{A} + \frac{C'}{C}\right)\frac{B'}{B} = (P_z - \Lambda)B^2 = \bar{P}_zB^2,$$

$$G_{33} = \left(\frac{C}{B}\right)^2\left[\frac{A''}{A} + \left(\frac{B'}{B}\right)'\right] = (P_\phi - \Lambda)C^2 = \bar{P}_\phi C^2,$$

where the primes stand for differentiation with respect to $r$. The regularity conditions at the axis are $A'(0) = B'(0) = C''(0) = C(0) = 0$, $B(0) = C'(0) = 1$ (see [7]).

## 3 Conformally Flat Solutions

For a conformally flat interior spacetime, all Weyl tensor components vanish and one obtains the following non-linear second order ordinary differential equations for $h$ and $S$ (see [8]):

$$S' + S^2 - \frac{2h'}{h}S + \frac{h''}{h} = 0, \quad S' + S^2 + \frac{h'}{h}S - \frac{2h''}{h} = 0,$$

where $S = \frac{A'}{A} - \frac{B'}{B}$, $h = \frac{C}{B}$.

Integrating these equations and using the regularity conditions gives $h = a_1 \sinh(a_2 r)$ and $A = a_3 \cosh(a_2 r) B$; where $a_1$, $a_2$ and $a_3$ are non-zero integration constants,.

Considering the case $\bar{P}_r = \bar{P}_\phi$, it follows that the metric functions $A$, $B$ and $C$ in (1) are (see [6])

$$A = \cosh(a_2 r) B, \quad B = \frac{1}{a_4[\cosh(a_2 r) - 1] + 1}, \quad C = \frac{\sinh(a_2 r)}{a_2} B,$$

where $a_2$ and $a_4 \neq 0$ are constants. The density and pressures are given by

$$\begin{aligned}
\bar{\mu} &= 2\, a_2^2\, a_4\, [(1 - a_4)\cosh(a_2 r) + a_4 + 1] - a_2^2 \\
\bar{P}_r &= 2a_2^2 a_4[(a_4 - 1)\tanh(a_2 r)\sinh(a_2 r) - 1] + a_2^2 \\
\bar{P}_z &= 2a_2^2 a_4 \left[\frac{1 - a_4}{\cosh(a_2 r)} + a_4 - 3\right] + 3a_2^2.
\end{aligned}$$

## 4 Matching to an Exterior

Consider the exterior Linet–Tian spacetime $(M^+, g^+)$ whose metric is given by

$$\begin{aligned}
ds^{2+} = -a^2 Q^{2/3} P^{-2(1-8\sigma+4\sigma^2)/3\Sigma} dt^2 + d\rho^2 + b^2 Q^{2/3} P^{-2(1+4\sigma-8\sigma^2)/3\Sigma} dz^2 \\
+ c^2 Q^{2/3} P^{4(1-2\sigma-2\sigma^2)/3\Sigma} d\phi^2,
\end{aligned}$$

where $\Sigma = 1 - 2\sigma + 4\sigma^2$, and for $\Lambda > 0$, $Q(\rho) = \frac{1}{\sqrt{3\Lambda}} \sin(2R)$, $P(\rho) = \frac{2}{\sqrt{3\Lambda}} \tan R$, with $R = \frac{\sqrt{3\Lambda}}{2}\rho$. Matching this metric to the interior solution presented in the previous section, one obtains from the equality of the first fundamental forms:

$$\frac{\cosh(a_2 r)}{a_4[\cosh(a_2 r) - 1] + 1} \overset{S}{=} a\, Q^{1/3} P^{-(1-8\sigma+4\sigma^2)/3\Sigma}, \tag{2}$$

$$\frac{1}{a_4[\cosh(a_2 r)-1]+1} \overset{S}{=} b\, Q^{1/3} P^{-(1+4\sigma-8\sigma^2)/3\Sigma}, \tag{3}$$

$$\frac{\sinh(a_2 r)}{a_2[a_4[\cosh(a_2 r)-1]+1]} \overset{S}{=} c\, Q^{1/3} P^{2(1-2\sigma-2\sigma^2)/3\Sigma}, \tag{4}$$

and from the equality of the second fundamental forms:

$$a_2(1-a_4)\tanh(a_2 r) \overset{S}{=} \sqrt{\frac{\Lambda}{3}}\,\frac{3\sigma-\Sigma\sin^2 R}{\Sigma\sin R\cos R}, \tag{5}$$

$$a_2 a_4 \sinh(a_2 r) \overset{S}{=} \sqrt{\frac{\Lambda}{3}}\,\frac{3\sigma(1-2\sigma)+\Sigma\sin^2 R}{\Sigma\sin R\cos R}, \tag{6}$$

$$\frac{a_2[\cosh(a_2 r)(1-a_4)+a_4]}{\sinh(a_2 r)} \overset{S}{=} \sqrt{\frac{\Lambda}{3}}\,\frac{3(1-2\sigma)-2\Sigma\sin^2 R}{2\Sigma\sin R\cos R}, \tag{7}$$

where $\overset{S}{=}$ denotes equality on the matching hypersurface only. From these equations one obtains

$$\sin^2 R \overset{S}{=} \frac{3\sigma}{\Sigma}\left[1+\frac{2(a_4-1)(1-\sigma)\sqrt{1-4\sigma}}{a_4\sqrt{1-4\sigma^2}-(a_4-1)\sqrt{1-4\sigma}}\right], \tag{8}$$

$$\sinh^2(a_2 r) \overset{S}{=} \frac{4\sigma(1-\sigma)}{1-4\sigma} \tag{9}$$

and

$$a_2^2 \overset{S}{=} \Lambda\left[2a_4-1-2a_4(a_4-1)\frac{4\sigma(1-\sigma)}{\sqrt{(1-4\sigma)(1-4\sigma^2)}}\right]^{-1}. \tag{10}$$

The inequality $0 \le \sin^2 R_S \le 1$ in (8) and the positivity of the right hand side of (10), for any $0 < \sigma < 1/4$, are satisfied if $1/2 \le a_4 \le 1$.

The parameter $a_2$ is fixed by (10) whilst $\rho_S$ and $r_S$ are determined from (8) and (9); equations (2)–(4) fix the exterior parameters $a, b$ and $c$. Thus we conclude that the matching is possible for any $1/2 \le a_4 \le 1$, $0 < \sigma < 1/4$ and $\Lambda > 0$. See [6] for more details.

**Acknowledgements** IB and FM thank CMAT, Univ. Minho, for support through the FEDER Funds COMPETE and FCT Project Est-C/MAT/UI0013/2011. FM is supported by FCT projects PTDC/MAT/108921/2008 and CERN/FP/116377/2010.

## References

1. B. Linet, *J. Math. Phys.*, **27**, 1817, (1986).
2. Q. Tian, *Phys. Rev. D*, **33**, 3549, (1986).
3. M.F.A. da Silva, A. Wang, F.M. Paiva, N.O. Santos, *Phys. Rev. D*, **61**, 044003, (2000).
4. J. Griffiths, J. Podolský, *Phys. Rev. D*, **81**, 064015, (2010).
5. M. Žofka, J. Bičák, *Class. Quant. Grav.*, **25**, 015011 (2008).
6. I. Brito, M.F.A. da Silva, F.C. Mena, N.O. Santos, *Gen. Rel. Grav.*, **45**, 519, (2013).
7. T. Philbin, *Class. Quant. Grav.*, **13**, 1217, (1997).
8. L. Herrera, G. Le Denmat, G. Marcilhacy, N.O. Santos, *Int. Journ. Mod. Phys. D*, **14**, 657, (2005).

# Phase Structure of Black Di-ring in Five-Dimensional Asymptotically Flat Vacuum Gravity

**Hideo Iguchi**

**Abstract** We analyze the phase structure of five-dimensional black di-ring in asymptotically flat vacuum gravity. We numerically plot the points of black di-rings in the phase diagram to search the region covered by black di-rings. The distribution of black di-ring shows that the area of black di-ring is always less than the maximum value of black ring. The plot indicates that there are black di-ring configurations whose area parameters are close to zero.

## 1 Introduction

In five dimensions, in addition to the solutions with single horizon, there exist solutions with disconnected event horizons. Black Saturn which is a spherical black hole surrounded by a black ring was constructed by the inverse scattering method [1]. It was shown that the black rings can be superposed concentrically by using the Bäcklund transformation [4]. This black di-ring solution also can be constructed by the inverse scattering method [3].

The existence of multi-black hole configurations implies continuous non-uniqueness of five-dimensional black holes. The phase diagram of the black Saturn was investigated in [1, 2]. The plot of random sets of points in the phase diagram showed that the black Saturn covers the wide region of the phase diagram. The phases of black Saturn were investigated based on the thin and long ring approximation in which the black Saturn can be modeled as a simple superposition of an Myers–Perry black hole and a very thin black ring [1]. It was argued that

H. Iguchi (✉)
College of Science and Technology, Nihon University, Narashinodai, Funabashi, Chiba, Japan
e-mail: iguchi.h@phys.ge.cst.nihon-u.ac.jp

A. García-Parrado et al. (eds.), *Progress in Mathematical Relativity, Gravitation and Cosmology*, Springer Proceedings in Mathematics & Statistics 60,
DOI 10.1007/978-3-642-40157-2_73, 

the configurations that approach maximal entropy for fixed mass and angular momentum are black Saturns with a nearly static black hole and a very thin black ring.

The black di-ring also indicates infinite non-uniqueness [4]. It was confirmed that there are infinite number of black di-rings for same mass and same angular momentum. Distributions of black di-rings in the phase diagram have not been fully investigated. When we approximate the black di-ring as a simple superposition of two concentric black rings, we can roughly estimate the region covered by the black di-ring in the phase diagram. The maximum of the area would be smaller than the one of black Saturn for the same mass and angular momentum. Because of the strong non-linearity, however, we need rigorous analysis for the distributions of black di-ring in the phase diagram for the decisive conclusion.

## 2 Phase Structure of Black Di-ring

The physical variables of black di-ring are calculated from the exact expressions of the solution. Following [1], we normalize the ADM angular momentum and the area of horizons as

$$j^2 = \frac{27\pi}{32G}\frac{J^2}{M^3}, \quad a_h = \frac{3}{16}\sqrt{\frac{3}{\pi}}\frac{A_h}{(GM)^{3/2}}, \tag{1}$$

to compare the physical properties of black objects with same ADM mass.

The rod structure of black di-ring is composed by two semi-infinite rods and four finite rods. Two of four finite rods are timelike and the other two finite and two semi-infinite rods are spacelike. The seed solution of black di-ring has six finite rods. We define six parameters by using the lengths of these finite rods as in Fig. 1. Physical variables of black di-ring are expressed by using these six parameters.

We fix the scaling freedom by $d_1 + d_2 + d_3 + d_4 = 1$. The balance conditions impose two constraints on the parameters. As a result, the balanced black di-ring has three dimensionless parameters. In the analysis, we choose $d_2$, $d_3$ and $d_4$ as the three parameters for the balanced black di-ring. The parameter $d_1$ is determined by the scaling. The parameters $p$ and $q$ are determined by solving the balance conditions.

To investigate the region of the phase diagram covered by black di-ring, we plot the point $(j^2, a_h)$ corresponding to the sets of parameters $(d_2, d_3, d_4)$. The result is shown in Fig. 2.

The total area of black di-ring can not become larger than the maximum of black ring $a_h = 1$. There are black di-ring configurations with total area $a_h$ greater than the black ring with the same $j^2$. It can be confirmed that the black di-ring solution with $j = 0$ is possible while maintaining balance as similar as black Saturn. In the plot of Fig. 2 the low entropy black di-ring $a_h \leq 0.2$ is scarcely distributed except around $j^2 = 1$. When $d_1 = d_3 = 0$ the area of black di-ring becomes exactly zero.

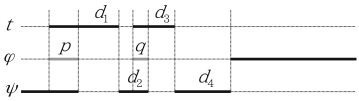


**Fig. 1** Rod structure of seed solution of black di-ring with $S^1$ rotation

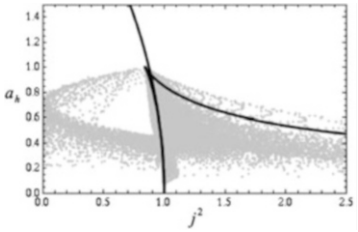


**Fig. 2** Distribution of black di-rings in the phase diagram. The *black bold curves* are the phases of the Myers–Perry black hole and the black ring

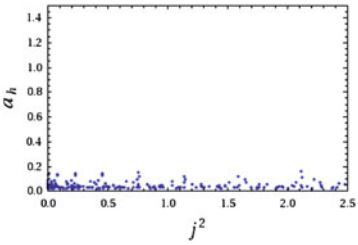


**Fig. 3** Plots for parameters which satisfy $d_1\ell^2 d_2$ and $d_3\ell^2 d_4$

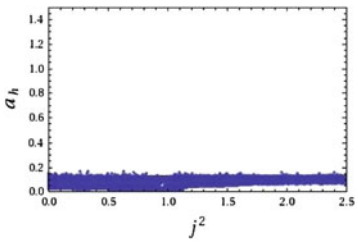


**Fig. 4** Plots for parameters which satisfy $d_1, d_3, d_4\ell^2 d_2$ and $d_3 \gg d_4$

If we simply set $d_1 = d_3 = 0$, it can be easily shown that the balance condition for spacelike rod $d_4$ is violated. Therefore we have to chose parameters such that $p$ and $q$ become very small in addition to $d_1$ and $d_3$ for the small area back di-ring.

The low entropy black di-ring would be constructed by two different configurations. One is a double thin ring and the other is a combination of a nearly extremal fat ring with large thin ring. The double thin ring configuration will be constructed by choosing the rod parameters as $d_1\ell^2 d_2$ and $d_3\ell^2 d_4$. The corresponding plot of phase diagram becomes like Fig. 3. The second configuration will be constructed by $d_1, d_3, d_4\ell^2 d_2$ and $d_3 \gg d_4$. The corresponding plot is given in Fig 4. Both plots show that the black di-rings can exit in the region $0 < a < 0.2$ of phase diagram.

## 3 Black Di-ring with Zero Length Timelike Rods

It was argued that the black di-ring rotating in the $S^1$ direction whose timelike rods are shrunk down to zero length can be constructed from $S^2$-rotating black ring [5]. We start the metric of the black ring with a rotating 2-sphere

$$ds^2 = -\frac{H(y,x)}{H(x,y)}\left[dt - \frac{20maAy(1-x^2)}{H(y,x)}d\varphi\right]^2 + \frac{H(x,y)}{A^2(x-y)^2}\left[-\frac{dy^2}{(1-y^2)F(y)} + \frac{dx^2}{(1-x^2)F(x)} - \frac{(1-y^2)F(x)}{H(x,y)}d\psi^2 + \frac{(1-x^2)F(y)}{H(y,x)}d\varphi^2\right] \tag{2}$$

where

$$F(\xi) = 1 + 2mA\xi + (aA\xi)^2, \quad H(\xi_1,\xi_2) = 1 + 2mA\xi_1 + (aA\xi_1\xi_2)^2. \tag{3}$$

At first, we construct the magnetically charged accelerating dihole solution in Kaluza–Klein theory by performing the analytic continuation and dimensionally reduction. Next we take the electric dual of the dihole solution and lift it back to five dimensions with the appropriate analytic continuation. The metric of the obtained solution is

$$ds^2 = -\frac{H(x,y)}{H(y,x)}\left[dt + \frac{2maAx(1-y^2)}{H(x,y)}d\psi\right]^2 + \frac{H(y,x)}{A^2(x-y)^2}\left[\frac{1}{K_0^2}\left(-\frac{dy^2}{(1-y^2)F(y)} + \frac{dx^2}{(1-x^2)F(x)}\right) - \frac{(1-y^2)F(x)}{H(x,y)}d\psi^2 + \frac{(1-x^2)F(y)}{H(y,x)}d\varphi^2\right], \tag{4}$$

where, now,

$$F(\xi) = 1 + 2mA\xi - (aA\xi)^2, \quad H(\xi_1,\xi_2) = 1 + 2mA\xi_1 - (aA\xi_1\xi_2)^2. \tag{5}$$

It would be important to study features of the solution in detail. It is pointed out in [5] that the rings are rotating in opposite directions to each other. It can be shown that the solution does not satisfy the balance conditions.

## 4 Summary

We analyzed the phase structure of black di-ring. The distribution of black di-rings in the phase diagram shows infinite non-uniqueness of the black di-ring. The configurations of black di-ring distribute in the open strip $0 < a_h < 1$ and $j^2 > 0$.

**Acknowledgements** This work is partially supported by Grant-in-Aid for Scientific Research (C) (No. 23540319) from Japanese Ministry of Education, Science, Sports, and Culture.

## References

1. Elvang, H. and Figueras,P.: Black Saturn, JHEP **0705**, 050 (2007)
2. Elvang, H., Emparan, R. and Figueras, P.: Phases of five-dimensional black holes, JHEP **0705**, 056 (2007)
3. Evslin, J. and Krishnan, C.: The Black Di-Ring: An Inverse Scattering Construction, Class. Quant. Grav. **26**, 125018 (2009)
4. Iguchi, H. and Mishima, T.: Black di-ring and infinite nonuniqueness, Phys. Rev. D **75**, 064018 (2007) [Erratum-ibid. D **78**, 069903 (2008)]
5. Teo, E.: Phys. Rev. D **73**, 024016 (2006)

# Spectrum from an Initially Anisotropic Universe

**Hyeong-Chan Kim and Masato Minamitsuji**

**Abstract** We revisit the issue on signatures of pre-inflationary background anisotropy by considering the quantization of a massless and minimally coupled scalar field in an axially symmetric Kasner background, mimicking cosmological perturbations. We show that the power spectrum of the scalar field fluctuation has a negligible difference from that in the standard inflation in the non-planar directions, but it has a sharp peak around the symmetry plane. This note is based on our recent paper (Kim and Minamitsuji, JCAP 1103:038, 2011).

## 1 Introduction

Inflation has become one of the paradigms of modern cosmology. First of all, inflation elegantly solves many problems which are present in the standard Big-Bang model such as the horizon and flatness problems. Secondly, inflation accounts for the origin of the large scale structure of the universe in terms of the quantum fluctuations originated from the adiabatic vacuum structure in the early universe. Remarkably, the nature of the primordial fluctuations is understood in terms of symmetries of the de Sitter spacetime. In general, we need $n$-point correlation functions to characterize the statistical nature of the primordial fluctuations. However, these symmetries lead to the power spectrum with a scale invariant form. These predictions from symmetries are robust and universal in inflationary scenarios. In fact, the above predictions have been confirmed by

H.-C. Kim
School of Liberal Arts and Sciences, Korea National University of Transportation, Chungju 380-702, Korea
e-mail: hckim@ut.ac.kr

M. Minamitsuji (✉)
Yukawa Institute for Theoretical Physics, Kyoto University, Kyoto 606-8502, Japan
e-mail: masato@yukawa.kyoto-u.ac.jp

A. García-Parrado et al. (eds.), *Progress in Mathematical Relativity, Gravitation and Cosmology*, Springer Proceedings in Mathematics & Statistics 60,
DOI 10.1007/978-3-642-40157-2_74, 

the measurements of the cosmic microwave background (CMB) [2, 3]. As the observational precision increases, we have to go beyond the power spectrum to look at the fine structures of the primordial fluctuations. Since in the realistic inflationary universe the symmetries of the de Sitter spacetime do not hold exactly, violation of them provides a measurable effect. A measurable effect may be induced by rotational symmetry breaking in the early universe [4]. Such cosmological models have been considered in e.g., [5, 6]. From the observational point of view, a lot of anomalies indicating the statistical anisotropy have been reported [7–9].

We work on the observational signatures from the preinflationary anisotropy [1]. We start from the discussion on the evolution of anisotropic universe in the Einstein gravity minimally coupled to a massive scalar field which plays the role of the inflation. Under the slow-roll approximations, the background metric can be well approximated by the Kasner de Sitter spacetime with a positive cosmological constant, $\Lambda(=3{H_i}^2)$. Among the Kasner de Sitter solutions, we are interested in the regular branch with the two dimensional axial symmetry with metric,

$$ds^2 = -d\tau^2 + \sinh^{\frac{2}{3}}(3H_i\tau)\Big[\tanh^{-\frac{2}{3}}\left(\frac{3H_i\tau}{2}\right)(dx_1^2+dx_2^2) + \tanh^{\frac{4}{3}}\left(\frac{3H_i\tau}{2}\right)dx_3^2\Big]. \tag{1}$$

This spacetime provides a good ground to test the anisotropic universes. Firstly, it bears various important features of the whole anisotropic universes including large anisotropy at $\tau = 0$. Secondly, only for this solution we can impose the adiabaticity condition and define an adiabatic vacuum state [1]. In this work, we are interested in the evolution of a massless, minimally coupled scalar field $\phi$ propagating on the background anisotropic universe (1). Note that this scalar field is not the inflation but just a *mimic of the metric perturbations*.

## 2 Quantization of the Scalar Field

The canonical quantization of a massless, minimally coupled scalar field $\phi$ is done in the standard manner:

$$\phi = \int d^3k\Big(u_{\mathbf{k}}a_{\mathbf{k}} + u^*_{\mathbf{k}}a^\dagger_{\mathbf{k}}\Big), \tag{2}$$

where the creation and annihilation operators satisfy the commutation relations $\left[a_{\mathbf{k_1}}, a^\dagger_{\mathbf{k_2}}\right] = \delta(\mathbf{k_1}-\mathbf{k_2})$ (others are zero) and $u_{\mathbf{k}} = e^{i\mathbf{kx}}\phi_{\mathbf{k}}/(2\pi)^{3/2}$. We normalize the mode function as $\phi_{\mathbf{k}}\partial_\tau\phi^*_{\mathbf{k}} - \big(\partial_\tau\phi_{\mathbf{k}}\big)\phi^*_{\mathbf{k}} = \frac{i}{e^{3\alpha}}$, where $e^\alpha = \sinh^{\frac{1}{3}}(3H_i\tau)$ is the averaged scale factor of the three-dimensional space, obtained from Eq. (1). We introduce a dimensionless time $x$ by $\sinh(\varepsilon x) = \frac{1}{\sinh(3H_i\tau)} = e^{-3\alpha}$, where $\varepsilon$ denotes a small expansion parameter. The arrow of time for $x$ is inverted since it varies from $\infty$ to $0+$ as the comoving time $\tau$ increases from $0+$ to $\infty$.

The equation of motion for the scalar field is written in the form of a time-dependent oscillator

$$\left(\frac{d^2}{dx^2}+\Omega_{\mathbf{k}}(x)^2\right)\phi_{\mathbf{k}}=0\,,\quad \Omega_{\mathbf{k}}^2(x)=\frac{2(\bar{k}\varepsilon^{2/3})^2}{9}\left(\frac{e^{\varepsilon x}}{\sinh\varepsilon x}\right)^{1/3}\left(\frac{1}{e^{2\varepsilon x}-1}+r^2\right). \tag{3}$$

Here we define a scaled wave-number and a measure of planarity of a given mode by $\bar{k}=\varepsilon^{1/3}\frac{k}{H_i}$, $r=\frac{k_3}{k}$, where $k^2:=k_1^2+k_2^2+k_3^2=k_\perp^2+k_3^2$. From now on, we omit the subscript $\mathbf{k}$ in the frequency squared $\Omega_{\mathbf{k}}^2$ for simplicity. The power spectrum is defined by

$$\langle 0|\phi^2|0\rangle:=\int d\ln k\int\frac{d\theta_{\mathbf{k}}}{2}P,\quad P=\frac{k^3}{2\pi^2}|\phi_{\mathbf{k}}|^2. \tag{4}$$

In contrast to the case of the standard inflationary models, the power spectrum would contain the direction dependence. The vacuum is chosen at the initial anisotropic era: $\tau\to+0$ to satisfy $a_{\mathbf{k}}|0\rangle=0$. We choose the solution to be purely positive frequency mode with respect to $\tau$ at the early stage.

## 3 Non-planar High-Momentum Modes

The WKB approximation is valid if $\left|\frac{d\Omega^2(x)}{dx}\right|\ell^2 1$. For the non-planar modes which are not propagating along the $(x_1,x_2)$-plane, this condition is always satisfied if $x\gg\bar{k}^{-3}$. One order higher WKB expansion improves the accuracy of the approximation by the factor $E_{\rm WKB}(x)\sim\frac{1}{\bar{k}^2x^{2/3}}$. In the asymptotic de Sitter region, $0<x<\varepsilon^{-1}$, we can consider the other approximation based on the *asymptotic approximation* in the limit $\varepsilon x\ell^2 1$. In terms of the series expansion $\Omega^2(x)=\sum_{n=0}^{\infty}\varepsilon^n V_n(x)$ in this limit, the zeroth order solution obtained from $V_0$ is the well-known mode function in the de Sitter spacetime and the higher order solutions can be obtained iteratively. One order higher order iterative solution improves the accuracy of the approximation by the factor $E_{\rm asym}(x)\sim\varepsilon\bar{k}\,x^{4/3}$.

For a given high-momentum mode $k\gg H_i$, there is a period where both approximations are valid: $\bar{k}^{-3}\ell^2x\ell^2\varepsilon^{-1}$. During this period, we can match both solutions when the accuracies of the two solution coincide, $E_{\rm WKB}=E_{\rm asym}$, which gives $x_*=(\varepsilon\bar{k}^3)^{-1}$. We set $x_*=1$, and hence $\varepsilon=\bar{k}^{-3}=\left(\frac{H_i}{k}\right)^{3/2}$, This choice is consistent with the assumptions that $\varepsilon$ is small and $\bar{k}^{-3}<x_*<\varepsilon^{-1}$.

After the matching of the solutions in these two regions, we find that the power spectrum including the corrections becomes

$$P=\frac{{H_i}^2}{4\pi^2}\left\{1+\frac{9(11-90r^2+99r^4)}{32}\left(\frac{H_i}{k}\right)^6+O\left(\left(\frac{H_i}{k}\right)^7\right)\right\}. \tag{5}$$

The correction $O((H_i/k)^6)$ is highly dependent on $k$ and the anisotropy effect is significantly suppressed.

## 4 Planar Modes

For the planar modes $r^2 \sim 0$, there appears a region where the WKB approximation may not be valid during a period in $\varepsilon x \gg 1$. This results in a large contribution of the negative frequency modes to the final power spectrum. The mode $r = 0$ behaves classically, not quantum mechanically, and will be out of scope.

Matching the solutions in the three regions yields the final amplitude and hence the power spectrum:

$$P = \left(\frac{H_i}{2\pi}\right)^2 \left(\coth \pi \bar{r} - \frac{\cos\left(2\Psi\right)}{\sinh \pi \bar{r}}\right), \tag{6}$$

where $\Psi(k) = \bar{k} x_*^{1/3} - \int_{x_1}^{x_*} \Omega(x) dx + \bar{q} e^{-\varepsilon x_1} - \frac{\pi}{4}$. In the planar limit, the deviation of the power spectrum from the ansatz in [4] is quite clear.

## 5 Discussions

We have reinvestigated the quantization of a massless and minimally coupled scalar field as a way to probe the signature of pre-inflationary background anisotropy in the spectrum of cosmological perturbations.

Firstly, we have dealt with the non-planar modes. We have shown that the power spectrum of the scalar field acquires non-vanishing corrections only when we execute the approximation up to 6$^{\text{th}}$ order. Hence, the direction dependence appears only at the order $O((H_i/k)^6)$. For the planar mode, the temporal breaking of the WKB approximation relatively enhances the effects of the primordial anisotropy in the power spectrum.

## References

1. H. -C. Kim and M. Minamitsuji, arXiv:1211.1132 [gr-qc]; JCAP 1103, 038 (2011), [arXiv:1101.0329[gr-qc]]; Phys. Rev. D **81**, 083517 (2010) [arXiv:1002.1361[gr-qc]].
2. G. Hinshaw *et al.* [WMAP Collaboration], arXiv:1212.5226 [astro-ph.CO].
3. P. A. R. Ade *et al.* [Planck Collaboration], arXiv:1303.5062 [astro-ph.CO].
4. L. Ackerman, S. M. Carroll, and M. B. Wise, Phys. Rev. D **75**, 083502 (2007), Erratum-ibid. D **80**, 069901 (2009) [arXiv:astro-ph/0701357].
5. C. Pitrou, T. S. Pereira and J. P. Uzan, JCAP **0804**, 004 (2008) [arXiv:0801.3596 [astro-ph]];

6. A. E. Gümrükçüoğlu, L. Kofman and M. Peloso, Phys. Rev. D **78**, 103525 (2008) [arXiv:0807.1335 [astro-ph]].
7. C. J. Copi, D. Huterer, D. J. Schwarz and G. D. Starkman, Adv. Astron. **2010**, 847541 (2010) [arXiv:1004.5602 [astro-ph.CO]].
8. P. A. R. Ade *et al.* [Planck Collaboration], arXiv:1303.5083 [astro-ph.CO].
9. A. E. Gumrukcuoglu, C. R. Contaldi, M. Peloso, JCAP **0711**, 005 (2007). [arXiv:0707.4179[astro-ph]].